Investigation into the Choroid Plexus Molecular Mechanisms Underlying Idiopathic Intracranial Hypertension

Thesis

School of Life, Health and Chemical Sciences

Investigation into the Choroid Plexus Molecular Mechanisms Underlying Idiopathic Intracranial Hypertension

Ester Pascual Baixauli, BSc, MSc

A thesis submitted to the Open University for the

Degree of Doctor of Philosophy

September 2020

Funded by

Sheffield Teaching Hospitals NHS Foundation Trust

Declaration

I declare that the work presented in this thesis is my own and contributions made by other researchers are acknowledged in relevant parts of the text. This work does not contain any material submitted for any award or other degree.

Abstract

Idiopathic Intracranial Hypertension (IIH) is a rare condition characterised by increased intracranial pressure for unknown reasons. It predominantly affects obese women of child-bearing age, and it has been linked to altered sex hormone levels. While the mechanisms underlying IIH are unknown, IIH is thought to be related to an impairment of cerebrospinal fluid (CSF) dynamics, including CSF hypersecretion by the choroid plexus (CP). The present study was designed to explore the effects of diet on CSF secretion in the rat with the aim to unravel possible pathogenic mechanisms underlying IIH. Other parameters, such as sex and elevated cytokines in CSF, were also studied. A high-fat diet (HFD) was able to increase both body weight and CSF secretion in male and female rats. While the differences appeared earlier in males, they were larger in females. Furthermore, elevated levels of cytokines (TNFα, CCL2, IL-6, IL-17, hydrocortisone) in CSF of HFD-fed male rats were tested, from which hydrocortisone was the only one found to potentiate HFD-induced CSF hypersecretion.

In females, weight and plasma testosterone concentration positively correlated with CSF secretion. Females under HFD supplemented with peanut butter (HFD+PB) showed the highest CSF secretion rates, body weights and testosterone levels. HFD+PB rats also had the highest deregulation in CP gene expression. In HFD+PB rats, most of the genes related to CSF secretion remained unaltered; however, two transporters, Slc4a10 and Kcna6, and several tight junction molecules (TJs), including ZO-1, were downregulated. *In vitro* tests using a CP cell model showed that testosterone was able to alter gene expression including decreased expression of TJs including ZO-1, Slc4a10, and overexpression of AQP1 and ATP1A1. Additionally, testosterone was also able to decrease barrier functionality in the *in vitro* CP model. It is hypothesised that, in IIH, obesity and elevated testosterone levels increase CP permeability, altering CSF dynamics.

Acknowledgements

This thesis is the culmination of 4 years of intense and challenging work that would not have been possible without the help and support of colleagues, friends and family members. You have all helped me greatly and for that I am very grateful.

First of all, I would like to express my deepest appreciation to my supervisors, Prof Nacho Romero, Dr Cheryl Hawkes and Dr A Jane Loughlin. Nacho, I am extremely grateful to you for giving me this opportunity and guiding me on the path to become a researcher. Your invaluable advice has helped me to grow as a scientist and as a person. I cannot begin to express my gratitude to Cheryl, whose mentorship and unparalleled support both in the lab and throughout the writing process have made this dissertation possible while also helping me become a better scientist. Your extensive knowledge and unrelenting work ethic are a real inspiration. I would also like to extend my deepest gratitude to Jane, whose support and invaluable insights have helped me greatly. The completion of this thesis would not have been possible without the support of Prof Basil Sharrack and for that I am extremely grateful.

Secondly, I would like to gratefully acknowledge the help that I received from all the department support staff, especially Karen Evans, Agata Stramek, Iwona Loza, Brett Keith, George Bryant, Igor Kraev, Radka Gromnicova, Julia Barkans, Eduardo Camacho, Dee Shaw and Jen Stefansen. I would like to thank you all for your great kindness, invaluable support and technical help. You have helped me every step of the way and for that I am eternally grateful. I would also like to recognize the help and guidance I received from other members of the LHCS department, especially Prof David Male, Dr Christopher Heath, Dr Sarah Allman, Dr Francesco Crea and Dr Zerin Alimajstorovic, whose invaluable knowledge and helpful advice have been particularly useful for the development of this project.

My time at the Open University would not have been the same without the fun moments and great times shared with my fellow students and colleagues, including Shereen, Laura, Emily C, Conor, Stephen, Tala, Ricardo, Perla, Amy, Sarah, Irene, Sophie, Marta, Sarai, Naiara, Maëva, Juan, Maurine, Marcelle and Léa. You are all great people and

I wish you all the best in your future endeavours. I am particularly thankful to Edu, Emily B and Sonia for their friendship. Your unlimited support and kindness during my time at the Open University has been extremely important for me and for that I cannot begin to express my gratitude. I would also like to thank all the friends outside of my department that I have had the pleasure of meeting during my time in Milton Keynes and that have brought so much joy to my life. You will always have a special place in my thoughts and I wish you all the best of luck in the future.

I would like to take a moment to thank my family who have supported me from the very beginning and without whom I would not be who I am. Special thanks to Margaré, Jonny and Pin, who have been by my side on the best and worst of times. Your unlimited support and nurturing have been essential to keep me going and I would not have been able to finish this thesis without you. I love you all very much.

Finally, I would like to thank the Open University and Sheffield Teaching Hospitals – NHS Foundation Trust for providing the facilities, expertise and funding that made this research project possible.

Publication List

All posters and presentations titled: Effect of High Fat Diet on Cerebrospinal Fluid Secretion in the Rat. Pascual-Baixauli E, Hawkes C, Loughlin AJ, Sharrack B, Romero IA. (Unless otherwise specified)

a) Oral presentations at scientific conferences

- CSF Disorders Day, Birmingham, UK (October 2018)

- 8th UK & Ireland Early Career BBB Symposium, Oxford, UK (November 2018)

- 9th UK & Ireland Early Career BBB Symposium, Milton Keynes, UK (November 2019)

- "Researching into rare diseases: Idiopathic Intracranial Hypertension", 3 Minute Thesis (3MT) presentation, The Open University, Milton Keynes, UK (June 2019)

b) Poster presentations at scientific conferences

- "Researching into rare diseases: Idiopathic Intracranial Hypertension", OU Postgraduate Poster Competition, Milton Keynes, UK (June 2018)

- "Researching into rare diseases: Idiopathic Intracranial Hypertension", OU Postgraduate Poster Competition, Milton Keynes, UK (June 2019)

-13th International Conference on Cerebral Vascular Biology, Miami, USA (July 2019)

c) Abstract publication

- "Effect of High Fat Diet on Cerebrospinal Fluid Secretion in the Rat" Pascual-Baixauli E, Hawkes C, Loughlin AJ, Sharrack B, Romero IA Fluids Barriers CNS 16, 16 (Suppl 1): A49 (2019). https://doi.org/10.1186/s12987-019-0135-8

d) Paper contribution

- Alimajstorovic, Z., Pascual-Baixauli, E., Hawkes, C.A. et al. Cerebrospinal fluid dynamics modulation by diet and cytokines in rats. Fluids Barriers CNS 17, 10 (2020). https://doi.org/10.1186/s12987-020-0168-z

Table of Contents

Declaration ..... **III**

Abstract ..... **IV**

Acknowledgements ..... **V**

Publication List ..... **VII**

Table of Contents ..... **IX**

List of Figures ..... **XIV**

List of Tables ..... **XIX**

List of Equations ..... **XXI**

List of Abbreviations ..... **XXII**

1. General Introduction **1**

1.1 Introduction into the Central Nervous System *1*

1.2 Overview of Central Nervous System Fluids *2*

1.2.1 The Brain Fluids 3

I. Blood 3

II. Interstitial Fluid 6

III. Cerebrospinal Fluid 7

1.2.2 The Brain Barriers 8

I. Barriers at the surface of the brain 9

II. Blood-brain barrier 10

III. Blood-cerebrospinal fluid barrier 11

1.2.3 Choroid Plexus 12

I. Choroid Plexus Morphology 12

II. Choroid Plexus Physiology 15

1.2.4 Cerebrospinal Fluid Dynamics 17

I. Composition. 17

II. Secretion. 18

III. Circulation 21

IV. Drainage 22

1.2.5 Preclinical Research on Cerebrospinal Fluid Secretion Dynamics 25

I. In vivo Assessment of Cerebrospinal Fluid Secretion....25
II. In vitro Assessment of Cerebrospinal Fluid Secretion....28

1.3 Idiopathic Intracranial Hypertension....31
1.3.1 What is Idiopathic Intracranial Hypertension?....32
1.3.2 Epidemiology....32
1.3.3 Diagnosis....33
1.3.4 Risk Factors....36
I. Obesity....36
II. Sex Hormones....37
III. Growth Hormone alteration....38
IV. Other associated conditions....39
1.3.5 Treatment....39
I. Weight loss....39
II. Drug therapies....40
III. Lumbar puncture....40
IV. Surgery....41

1.4 Cerebrospinal Fluid in Idiopathic Intracranial Hypertension....42
1.4.1 Cerebrospinal Fluid Composition in Idiopathic Intracranial Hypertension....42
1.4.2 Cerebrospinal Fluid Dynamics in Idiopathic Intracranial Hypertension....43
I. Cerebrospinal fluid hypersecretion....43
II. Cerebrospinal flow obstructions and malabsorption....44
III. Other factors....46

1.5 Hypothesis and Objectives....46

2. Effect of Diet And Cytokines On Cerebrospinal Fluid Secretion In Male Rats....49

2.1 Introduction....49

2.2 Materials and Methods....52
2.2.1 Materials....52
2.2.2 Animals....52
2.2.3 Dietary manipulation....52
2.2.4 Preparation of artificial cerebrospinal fluid....53
2.2.5 Ventriculo-cisternal perfusion....54
2.2.6 Statistical analysis....57

2.3 Results....59
2.3.1 Animal model: diet and weight....59
2.3.2 Effect of Diet on Cerebrospinal Fluid Secretion Rates....60

I. Steady state determination 60
II. Cerebrospinal fluid secretion rate....61
III. Initial Cerebrospinal Fluid Volume....63
2.3.3 Effect of diet and cytokine administration on CSF secretion. 65
I. Steady state determination 65
II. Cerebrospinal fluid secretion rate....66
III. Initial Cerebrospinal Fluid Volume....67
2.4 Discussion *68*

3. Characterisation of the Effect of High-Fat Diet on Physiological Functions and Cerebrospinal Fluid Secretion in Female Rats 73

3.1 Introduction *73*

3.2 Materials and Methods *75*
3.2.1 Materials 75
3.2.2 Animals....75
3.2.3 Dietary manipulation 76
3.2.4 Food, water and caloric intake calculations....76
3.2.5 Measurement of body parameters....78
I. Weight calculations....78
II. Oestrous cycle recordings....79
III. Hormone and cholesterol analysis....80
3.2.6 Ventriculo-cisternal perfusion....81
I. ICP monitoring 82
3.2.7 Statistical analysis 83

3.3 Results....*83*
3.3.1 Animal model: diet and weight....83
3.3.2 Food and water intake 88
3.3.3 Cholesterol levels....92
3.3.4 Oestrous cycle....94
3.3.5 Hormone levels 97
3.3.6 Effect of Diet on Cerebrospinal Fluid Secretion Rates 99
I. Steady state determination 99
II. Cerebrospinal fluid secretion rates....101
III. Cerebrospinal fluid secretion and obesity 102
IV. Cerebrospinal fluid secretion and cholesterol 103
V. Cerebrospinal fluid secretion and hormones....104

3.4 Discussion 106

4. Diet-related Changes to the mRNA and Protein Expression Profile in the Choroid Plexus of Female Rats 111

4.1 Introduction 111

4.2 Materials and Methods 113

4.2.1 Animals 113

4.2.2 Choroid plexus extraction 113

4.2.3 Gene expression analysis 114

4.2.4 Bioinformatic analysis of RNAseq-MACE results 115

4.2.5 Immunohistochemistry 116

4.2.6 Statistical analysis 117

4.3 Results 118

4.3.1 Preliminary study of gene expression profile of choroid plexus related to age and diet 118

4.3.2 Gene expression profile of choroid plexus related to diet on 15w rats. 119

I. HFD vs ND 119

II. HFD+PB vs ND 125

III. HFD+PB vs HFD 130

IV. Differences in expression of genes related to CSF secretion 135

V. Validation by qPCR 137

4.3.3 Protein expression of choroid plexus by immunohistochemistry on female rats related to diet 138

4.4 Discussion 141

5. Investigation into the Effects of Testosterone on Barrier Functionality of an *In vitro* Model of Choroid Plexus 149

5.1 Introduction 149

5.2 Materials and Methods 150

5.2.1 Cell culture 150

5.2.2 Gene expression analysis 151

5.2.3 Study of Z310 monolayer barrier functionality 153

I. Electrical resistance 154

II. Paracellular permeability 154

5.2.4 Statistical analysis 155

5.3 Results 155

5.3.1 Z310 characterisation 155
5.3.2 CP Model optimisation 158
5.3.3 Effect of testosterone on morphology of Z310 160
5.3.4 Effect of testosterone on gene expression of Z310 161
5.3.5 Effect of testosterone on Z310 barrier functionality 164

5.4 Discussion 165

6. General Discussion 170

6.1 Future Work 176

References 178

Appendix A 250

Appendix B 255

I. Deregulated genes in HFD vs ND comparison 255
II. Deregulated genes in HFD+PB vs ND comparison 308
III. Deregulated genes in the HFD+PB vs HFD comparison 495

List of Figures

Figure 1.1. Lateral and anterior view of the human brain and the ventricular system. 1

Figure 1.2. Schematic representation of molecule diffusion between the blood, ISF and CSF in the brain. 3

Figure 1.3. Anatomy of the cerebral arterial system. 5

Figure 1.4. Anatomy of the cerebral venous system. 6

Figure 1.5. Schematic representation of the brain barriers. 9

Figure 1.6. Schematic cross section of choroid plexus. 13

Figure 1.7. Intercellular junctions between choroid plexus epithelial cells. 14

Figure 1.8. Schematic representation of transporters in choroid plexus epithelial cells. 16

Figure 1.9. Model of cerebrospinal fluid secretion by the choroid plexus epithelial cell. 20

Figure 1.10. Cerebrospinal fluid dynamics in the human. 22

Figure 1.11. Glymphatic fluid drainage pathway in the brain. 24

Figure 1.12. Scheme of measurements of cerebrospinal flow rate in the human brain using MRI. 26

Figure 1.13. Schematic representation of the ventriculo-cisternal perfusion technique. 27

Figure 1.14. Blood-cerebrospinal fluid barrier *in vivo* and *in vitro.* 30

Figure 1.15. Comparation between an eye with a normal optic disc and an eye with papilledema. 34

Figure 1.16. Measurement of intracranial pressure by lumbar puncture. 35

Figure 1.17. Some of the surgery options available for IIH patients. 42

Figure 2.1. Effect of diet and cytokine administration on CSF secretion of female rats. .51

Figure 2.2 *In vivo* experiment of ventriculo-cisternal perfusion in male adult Wistar rats. 55

Figure 2.3 Weight of male rats on ND or HFD over a seven-week period. 59

Figure 2.4 Final weight comparison between ND and HFD rats. 60

Figure 2.5 Steady state determination using C_{out}/C_{in} values. 61

Figure 2.6 CSF Secretion rates in male Wistar rats. 62

Figure 2.7. Correlation between CSF secretion rate and weight in male rats. 63

Figure 2.8 Initial CSF volume in male Wistar rats. 64

Figure 2.9. Initial endogenous CSF volume versus weight......65

Figure 2.10. Mean steady state values for each cytokine treatment......66

Figure 2.11. CSF Secretion rates in male Wistar rats under HFD and different treatments using ventriculo-cisternal perfusion. 67

Figure 2.12 Initial CSF volume in male Wistar rats using ventriculo-cisternal perfusion before treatment......68

Figure 3.1. Typical cell composition of vaginal lavage samples in each stage of the oestrous cycle of the female rat. 80

Figure 3.2. Schematic representation of setup for intracranial pressure monitoring......82

Figure 3.3. Weight of female rats on ND or HFD over a seven-week period. 84

Figure 3.4. Weight of female rats on ND or HFD over an eleven-week period......85

Figure 3.5. Evaluation of overweightness level of rat model depending on diet and age. 86

Figure 3.6. Daily food (a, c) and caloric (b, d) intake in 11w rats. 88

Figure 3.7. Daily water intake for 11w rats. 89

Figure 3.8. Daily food (a, c) and caloric intake (b, d) on 15w rats. 90

Figure 3.9. Daily water intake during the experiment. 91

Figure 3.10. Cholesterol concentration in plasma of rats under different diets and at different ages. 92

Figure 3.11. Correlation between body fat composition and plasma cholesterol levels depending on diet and age. 94

Figure 3.12. Oestrous cycle of 11w rats. 95

Figure 3.13. Oestrous cycle of ND (a), HFD (b) and HFD+PB (c) 15w rats. 96

Figure 3.14. Length of oestrous cycle of rats under different diets and ages. 97

Figure 3.15. Hormone concentrations on plasma of rats under different diets and ages. 98

Figure 3.16. Hormone ratios of rats under different diets and ages. 99

Figure 3.17. Steady state determination using C_{out}/C_{in} values. 100

Figure 3.18. Cerebrospinal fluid secretion rates of rats under different diets and ages. 101

Figure 3.19. Intracranial pressures depending on diet. 102

Figure 3.20. Correlation between CSF secretion and overweightness from rats under different diets and ages. 103

Figure 3.21. Correlation between CSF secretion and cholesterol on plasma of rats under different diets and ages. 104

Figure 3.22. Correlation between hormone concentrations and CSF secretion. 105

Figure 4.1. RT-qPCR showing relative gene expression on CP of female rats depending on diet. 119

Figure 4.2. Distribution of differently expressed genes in HFD vs ND comparison. 120

Figure 4.3. Functional classification of highly deregulated genes in the HFD vs ND comparison. 122

Figure 4.4. Distribution of differently expressed genes in the HFD+PB vs ND comparison. 125

Figure 4.5. Functional classification of deregulated genes in the comparison HFD+PB vs ND. 127

Figure 4.6. Distribution of differently expressed genes in HFD+PB vs HFD comparison. 130

Figure 4.7. Functional classification of highly deregulated genes in the HFD+PB vs HFD comparison. 132

Figure 4.8. Gene expression levels on a selection of genes of the CP of rats under three different diets. 137

Figure 4.9. Immunostaining of AQP4 in choroid plexus of female rats under different diets. 139

Figure 4.10. Immunostaining of ZO-1 in choroid plexus of female rats under different diets. 140

Figure 4.11. Immunostaining of CLDN1 in choroid plexus of female rats under different diets. 141

Figure 5.1. Morphology of Z310 156

Figure 5.2. Gene expression in Z310 of genes typically expressed in CP. 157

Figure 5.3. Dependency of monolayer resistance on membrane material and coating. 159

Figure 5.4 Dependency of cell layer resistance on initial seeding number. 160

Figure 5.5. Effect of testosterone on morphology of Z310 cells. 161

Figure 5.6. Gene expression levels of Z310 cells under different treatments with testosterone (T), with and without flutamide, relative to control. 162

Figure 5.7. Changes on barrier functionality depending on testosterone treatment. ... 164

Figure 6.1. Possible pathogenic mechanisms underlying Idiopathic Intracranial Hypertension. 171

List of Tables

Table 1.1. Modified Dandy criteria for IIH diagnosis. Adapted from Friedman and Jacobson, 2002. 33

Table 2.1. Cytokine concentration in plasma and CSF of IIH patients. 50

Table 2.2. Composition of aCSF, including the molecular weight (MW) for every compound and their concentration in the aCSF solution. 53

Table 2.3 Concentration of treatment of interest in aCSF for ventriculo-cisternal perfusion. 54

Table 4.1. Sequences of primers used in qPCR analysis. 114

Table 4.2. Deregulated pathways in the HFD vs ND comparison. 123

Table 4.3. Deregulated pathways in the HFD+PB vs ND comparison. 128

Table 4.4. Deregulated pathways in the HFD+PB vs ND comparison. 133

Table 4.5. Relative gene expression in all three comparisons measured by MACE RNAseq of genes relevant to choroid plexus function related to CSF. 135

Table 4.6. Gene expression level changes depending on diet on a selection of genes as measured by MACE-RNAseq and qPCR. 138

Table 5.1. Sequences of primers used in qPCR analysis. 152

Table 5.2. Gene expression in Z310 cells and female rats. 158

Table 5.3. Gene expression in testosterone-treated Z310 cells and female rats. 163

Table 0.1. Further information about Rat and Mouse No.1 Maintenance Diet. 250

Table 0.2. Further information about Rodent Maintenance Atwater Fuel Energy High Fat Diet. 251

Table 0.3. Further information about Western Rodent Diet. 252

Table 0.4. Further information on "Grandessa Peanut Butter Crunchy". 254

Table 0.5. Highly upregulated genes in HFD rats when compared to ND and their functional classification as determined by PANTHER bioinformatics……..250

Table 0.6. Highly downregulated genes in HFD rats when compared to ND and their functional classification as determined by PANTHER bioinformatics……270

Table 0.7. Highly upregulated genes in HFD+PB rats when compared to ND and their functional classification as determined by PANTHER bioinformatics……..303

Table 0.8. Highly downregulated genes in HFD+PB rats when compared to ND and their functional classification as determined by PANTHER bioinformatics……312

Table 0.9. Highly upregulated genes in HFD+PB rats when compared to HFD and their functional classification as determined by PANTHER bioinformatics……490

Table 0.10. Highly downregulated genes in HFD+PB rats when compared to HFD and their functional classification as determined by PANTHER bioinformatics……522

List of Equations

Equation 2.1. Steady state calculation. 56

Equation 2.2. CSF Secretion rate calculation. 56

Equation 2.3.Calculations of initial CSF volume. 57

Equation 3.1. Calculation of food and caloric intake per rat 77

Equation 3.2. Calculation of adjusted food intake and adjusted water intake. 77

Equation 3.3. Calculation of absolute and adjusted water intake. 78

Equation 3.4. BMI calculation. 78

Equation 3.5. Body fat content calculation. 79

Equation 4.1. Calculation of corrected total cellular fluorescence. 117

Equation 4.2. Calculation of relative area of staining 117

Equation 5.1. Calculation of relative expression levels of gene of interest. ....**Error! Bookmark not defined.**

Equation 5.2. Permeability coefficient calculations 154

List of Abbreviations

11w	11 weeks of age
15w	15 weeks of age
ABCB1A	ATP-Dependent Phospholipid Transporter A
ABCB1B	ATP-Dependent Phospholipid Transporter B
ABCC4	Multi-Specific Organic Anion Transporter B
Actin β	Actin Beta
AJs	Adherens junctions
AF6	Afadin
AQP1	Aquaporin 1
AQP4	Aquaporin 4
AQP7	Aquaporin 7
AQP9	Aquaporin 9
AR	Androgen Receptor
ATP1 / Na^+-K^+ ATPase	Sodium-potassium adenosine triphosphatase
AvW	Average weight of the cage
BBB	Blood brain barrier
BCSFB	Blood-cerebrospinal fluid barrier
BEC	Brain endothelial cells
BMI	Body mass index

CCL2	Chemokine Ligand 2
CI	Caloric intake
CIW	Caloric intake per body weight ratio
CLDN	Claudin
CPEC	Choroid plexus epithelial cells
CSF	Cerebrospinal fluid
CV	Caloric value of diet
Cv	Coefficient of variation
D	Diestrous
DMEM	Dulbecco's Modified Eagle Medium
E2/P	Oestradiol to progesterone
ER	Oestrogen receptor
FBS	Foetal Calf Serum
FI	Food intake
FI_C	Food intake of the cage
FITC-Dextran	70kDa fluorescein isothiocyanate–Dextran
FIW	Food intake per body weight ratio
FOLR1	Folate Receptor Alpha
HC	Hydrocortisone
HDL	High-density lipoproteins

HFD	High fat diet
HFG	Hepatocyte growth factor
ICP	Intracranial pressure
IIH	Idiopathic intracranial hypertension
IL-17	Interleukin 17
IL-1β	Interleukin 1 beta
IL-2	Interleukin 2
IL-6	Interleukin 6
IL-8	Interleukin 8
ISF	interstitial fluid
JAM3	Junctional Adhesion Molecule 3
KCC4	K^+-Cl^- cotransporter 4
MRI	Magnetic resonance imaging
MS	Multiple sclerosis
NBCe2	Na^+-HCO_3^- cotransporter
ND	Normal diet
NGF	Nerve growth factor
OATP1A4	solute carrier organic anion transporter family, member 1a4
OATP2B1	Organic Anion Transporter B
Ocln	Occludin

PCOS	Polycystic Ovary Syndrome
qPCR	Real time polymerase chain reaction
RNA	Ribonucleic acid
RT	Reverse transcription
RT^{o}	Room temperature
SAS	Subarachnoid Space
Slc	solute carrier family
SLC4A2	Anion exchange 2
SLC4A5	Electrogenic Sodium Bicarbonate Cotransporter 4
SLC4A10	Na^{+}- HCO_3^{-} cotransporter
SLC9A1	ion transporters the Na^{+}-H^{+} exchanger
SLC12A2	Na^{+}-K^{+}-$2Cl^{-}$ cotransporter-1
SLC15A2	peptide transporter 2
SLC22A7	Organic Anion Transporter 2
SLC22A8	Organic Anion Transporter 3
SLC23A1	Na^{+}- dependent vitamin C transporter
T	Testosterone
T/E2	Testosterone to oestradiol
TEER	Transepithelial Electrical Resistance
TJs	Tight Junctions

TNF-α	Tumor Necrosis Factor Alpha
TTR	Transthyretin
VLDL/LDL	very low-density lipoproteins / low-density lipoproteins
WI	Water intake
WI_C	Water intake of the cage
WIW	Water intake per body weight ratio
ZO-1	Zona Occludens 1
ZO-3	Zona Occludens 3

Chapter 1. General Introduction

1.1 Introduction into the Central Nervous System

In vertebrates, the central nervous system (CNS) is a very delicate but essential organ necessary for survival. It processes and coordinates the information received from the sense organs and it controls most of the activities carried out by the body. The human brain consists of the cerebrum, divided into two cerebral hemispheres, and the cerebellum, and it is connected to the spinal cord, which is located inside the spine, forming the CNS (Figure 1.1). The brain is located inside the skull and is protected by several layers of tissue and suspended in a liquid, called the cerebrospinal fluid (CSF). The brain and spinal cord have communicating cavities filled with CSF. In the brain, four main cavities, called ventricles, can be found: two lateral ventricles, a third and a fourth ventricle. The hollow in the middle of the spinal cord is called the central canal.

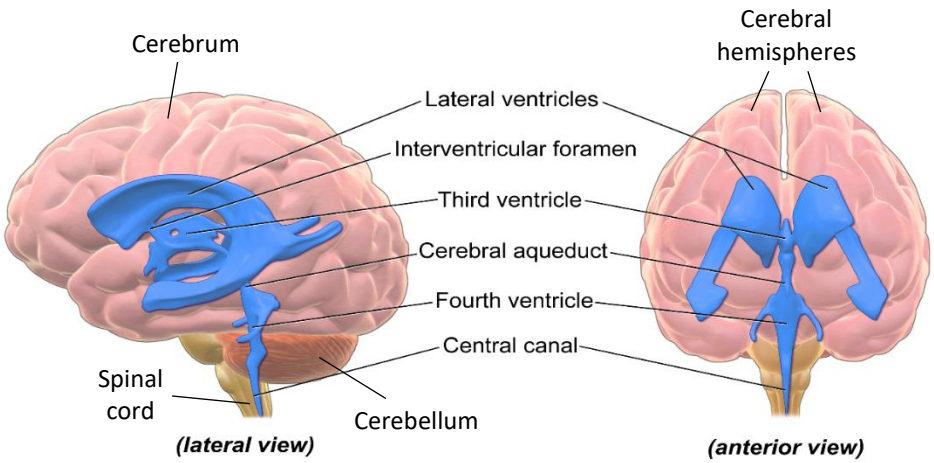

Figure 1.1. Lateral and anterior view of the human brain and the ventricular system.

The human brain consists of the cerebrum, divided into two cerebral hemispheres, and the cerebellum. The brain is connected to the spinal cord, forming the CNS. In the brain, four main cavities, called ventricles, can be found: two lateral ventricles, a third and a fourth ventricle, whereas in the spinal cord a hollow in the middle, called the central canal, is found. These cavities are connected and filled with flowing CSF (modified from Blaus, 2013).

A villous structure of vascularized layers can be found protruding from the walls of the four ventricles; this structure is called the choroid plexus (CP). The CP is formed by a monolayer of epithelial cells surrounding a stromal core of connective tissue and fenestrated capillaries and it forms an interface between the blood and the CSF (Dohrmann, 1970; Crispino and Crispino, 2015; Benarroch, 2016).

1.2 Overview of Central Nervous System Fluids

Three different types of extracellular fluid can be found in the CNS: interstitial fluid (ISF), CSF and blood. The ISF is produced by parenchyma cells and forms the microenvironment of the brain while the CSF is located in the brain ventricles, the central canal, the subarachnoid space and the channels connecting these structures. The ISF and the CSF can exchange by diffusion across the thin epithelial lining of the ventricular system called ependyma, and also across the glial layer at the surface of the brain facing the subarachnoid space (Abbott, 2004) (Figure 1.2). The blood is carried within blood vessels that perfuse the brain, deliver important substances such as nutrients and oxygen and remove waste products released as a result of normal cell function.

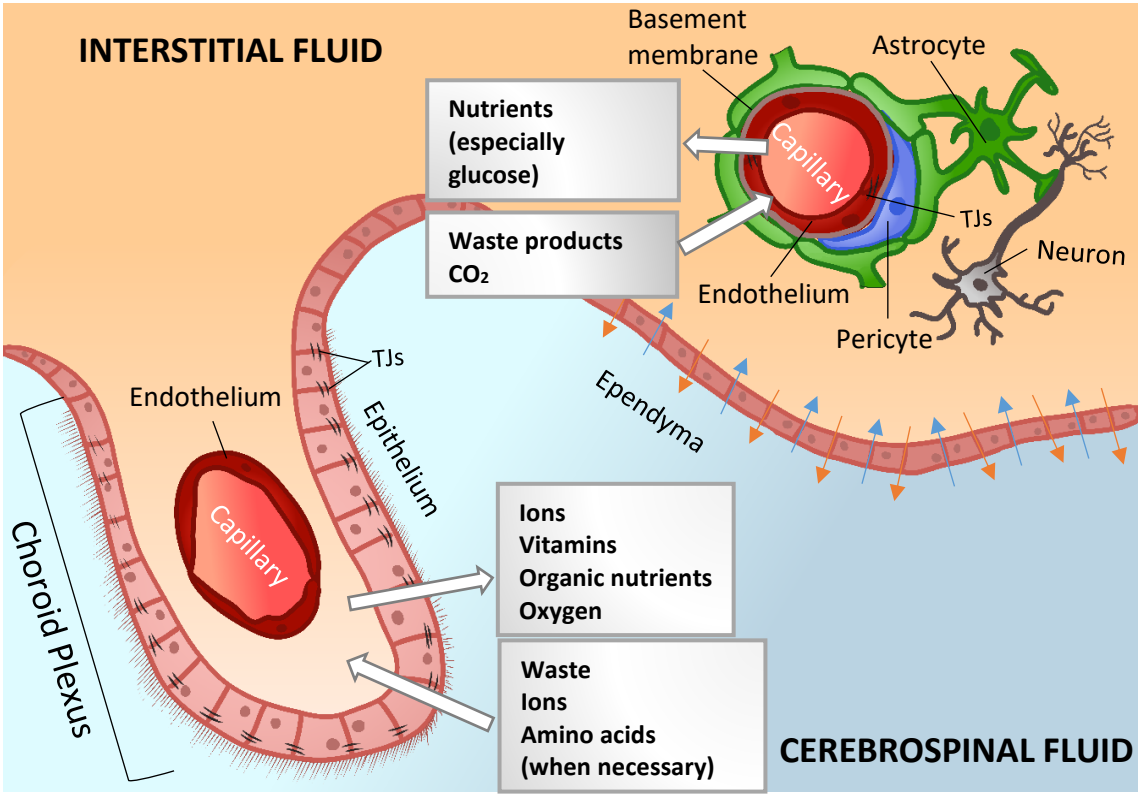

Figure 1.2. Schematic representation of molecule diffusion between the blood, ISF and CSF in the brain. Four connected cavities, called ventricles, filled with CSF can be found in the brain (left). The choroid plexus (right) is a villous structure of vascularized layers protruding from the walls of the ventricles and it is thought to be the main site of CSF secretion. The epithelial cells of the choroid plexus form a tight barrier between CSF and blood and actively controls substance trafficking between these two fluids. In the brain parenchyma, the epithelial cells surrounding the blood vessels form the blood brain barrier (BBB) and they are in charge of actively controlling and restricting the interchange of molecules between blood and ISF (Diagram by Ester Pascual Baixauli).

1.2.1 The Brain Fluids

I. Blood

The blood is an essential body fluid that delivers nutrients and oxygen to all the cells in the organism while removing metabolic waste and keeping the body at a stable temperature. In vertebrates, the blood is mainly composed of blood cells, proteins, glucose and ions in solution or suspended in plasma (Brody, 2017; Mathew and Bhimji, 2018). The most common blood cells are: erythrocytes, anucleated cells involved in transporting oxygen, facilitated by the iron-containing haemoglobin which increases oxygen binding;

leukocytes, immune cells in charge of protecting the body against infections and foreign bodies; and thrombocytes, anucleated cells whose main function is contributing to clotting (De Villota *et al.*, 1981; Hart, 2001; Sharma and Sharma, 2018).

Cerebral arteries and arterioles are formed by three distinctive concentric layers: an inner layer, the tunica intima, composed by a single layer of endothelial cells and the internal elastic membrane separating it from the next layer; the tunica media, mainly formed by smooth muscle cells, collagen and elastin fibres; and the tunica adventitia, which consists mostly of fibroblasts, associated cells such as pericytes and astrocytic end-feet, and collagen fibres. CNS arteries lack an outer elastic membrane and have thinner tunica media and adventitia containing a smaller percentage of elastic fibres than arteries in the rest of the body (Cipolla, 2009; Prince and Ahn, 2013). In humans, the blood is supplied to the brain through two pairs of large arteries, the left and right internal carotid and the left and right vertebral arteries (Figure 1.3). The internal carotids carry blood to the anterior cerebral circulation, middle and anterior cerebral arteries including the anterior choroidal artery; the vertebral arteries are connected to the posterior circulation, basilar artery and posterior cerebral arteries. The anterior and posterior cerebral circulations are connected through communicating arteries in the Circle of Willis (Alpers, 1959; Crispino and Crispino, 2015; Tanaka, 2017; Haines, 2018).

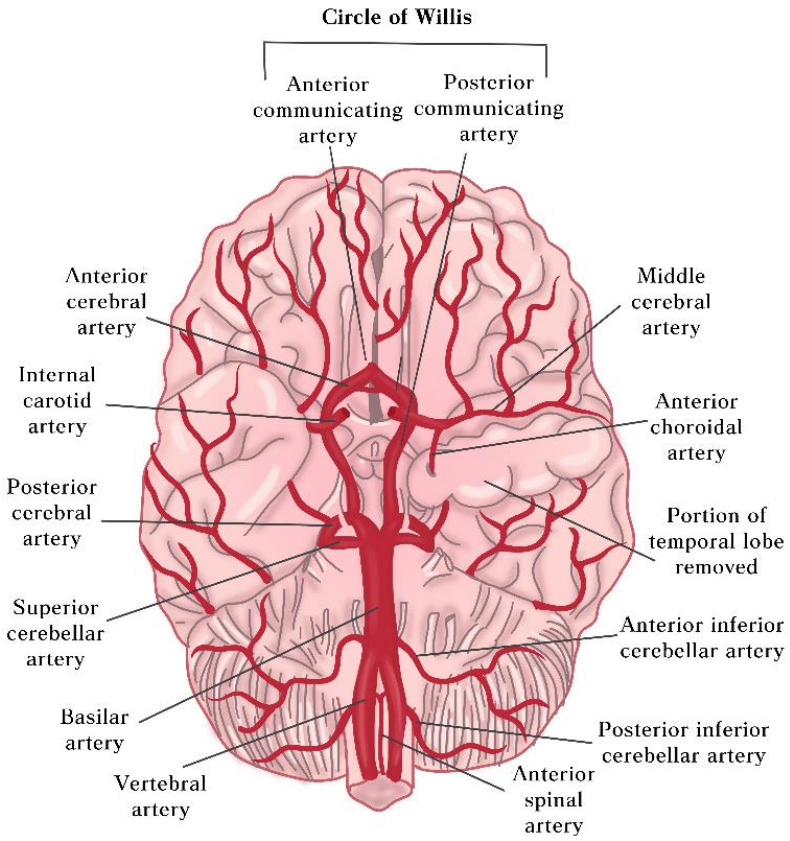

Figure 1.3. Anatomy of the cerebral arterial system.

Blood is supplied to the brain through two groups of large arteries: the internal carotids, which carry blood to the anterior cerebral circulation, middle and anterior cerebral arteries; and the vertebral arteries, which supply blood to posterior circulation, basilar artery and posterior cerebral arteries. Anterior and posterior cerebral circulations are connected through the Circle of Willis (Illustration by Ester Pascual Baixauli).

The cerebral venous circulation is comprised of cerebral veins and dural venous sinuses (**Figure 1.4**). While both types of blood vessels are valveless, cerebral veins have a thin wall lacking smooth muscle, and sinuses are larger channels lined with endothelial cells (Haines, 2018). Blood gets drained from the brain through two groups of valveless veins and sinuses: the superficial system and the deep system. The superficial system, comprising the sagittal sinuses and cortical veins, manage the venous outflow from the cerebral cortex and subcortical white matter (Cipolla, 2009; Purves *et al.*, 2018). The deep system includes the lateral, sigmoid and straight sinuses along with the deep veins, such as the great and the choroidal veins. The deep system drains the interior of the brain, white and grey matter

surrounding the lateral and third ventricles (Ono *et al.*, 1984; Uddin, Haq and Rafique, 2006). Venous blood is generally drained into the nearest venous sinus or, in the case of deeper structures, into a deep vein which will then drain into a venous sinus. Dural venous sinuses drain into the internal jugular veins (Moll and Waldron, 2014; Egemen and Solaroglu, 2017) .

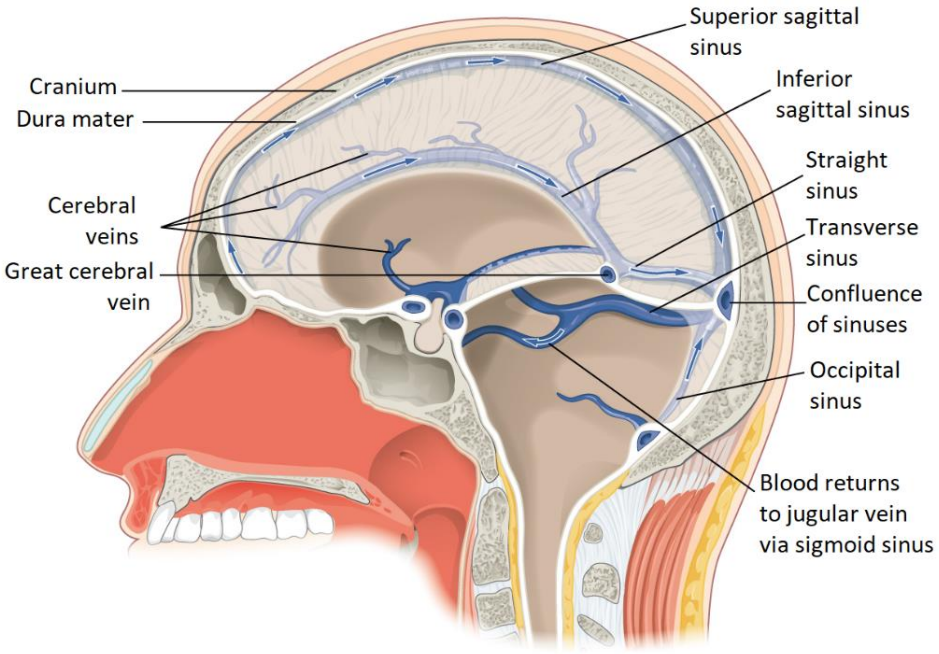

Figure 1.4. Anatomy of the cerebral venous system.

The cerebral venous system comprises cerebral veins and dural venous sinuses. Blood gets drained through two systems: the superficial system, comprising the sagittal sinuses and cortical veins, manage the venous outflow from the cerebral cortex and subcortical white matter; the deep system includes the lateral, sigmoid and straight sinuses along with the deep veins and it drains the interior of the brain. Both systems drain into internal jugular veins (OpenStax, 2016).

II. Interstitial Fluid

The ISF is a clear fluid that bathes parenchymal brain cells in the extracellular spaces of the CNS. ISF is composed of water, ions, organic molecules such as proteins, extracellular vesicles and gaseous molecules such as O_2 and CO_2 (Cserr, 1983; Hladky and Barrand, 2016; Lei *et al.*, 2017; Nakada and Kwee, 2019). Functions of the ISF include nutrient supply, intercellular communication, transport of molecules, waste removal and maintenance of

brain volume (Szentistvanyi *et al.*, 1984; Dóczi, 1993; Ueno *et al.*, 2016; Bedussi *et al.*, 2017). The ISF mainly originates from a combination of water filtered by the blood brain barrier (BBB), water produced by cellular metabolism and fluid from the CSF. Molecular exchange happens mostly with CSF via the ependyma lining the brain ventricles (Abbott, 2004; Damkier, Brown and Praetorius, 2010; Ueno *et al.*, 2016).

ISF flow along the perivascular space is driven by both diffusion and convection, which depend on pressure and homeostatic gradients. Different brain areas present different flow characteristics. In grey matter, ISF flow is mainly dependent on diffusional processes. On the other hand, in white matter, bulk flow through fluid-filled canals surrounding blood vessels delimited by the cerebrovascular basement membranes appear to be the main ISF flow motion (Healy and Vogelbaum, 2015; Boespflug and Iliff, 2018; Nakada and Kwee, 2019). Furthermore, ISF flow and volume increase during sleep, suggesting a mechanism boosting removal of waste products accumulated during wakefulness (Xie *et al.*, 2013). It has also been shown that neuronal excitation is able to reduce local ISF flow (Shi *et al.*, 2015). ISF drainage pathways include reabsorption into venous circulation, drainage into the lymphatic circulation and movement along astrocytes towards CSF compartments (Hladky and Barrand, 2016; Marchi, Banjara and Janigro, 2016; Bedussi *et al.*, 2017).

III. Cerebrospinal Fluid

The CSF is a clear colourless fluid in which the brain and spinal cord are suspended. The CSF provides essential functions for CNS protection and maintenance. The CSF acts as a protective cushion for the CNS by protecting it against accidental mechanical damage while also reducing the brain net weight from approximately 1500g to 25-50g, allowing this organ to maintain its density without being impaired by its own weight (Saladin, 2014; Tumani, Huss and Bachhuber, 2017; Adigun and Al-Dhahir, 2019). The volume and biochemical components of the CSF play vital homeostatic roles, keeping the CNS temperature stable and disposing of neural waste substances while maintaining the osmotic pressure needed for normal brain perfusion. Additionally, the CSF contains essential substances for brain nourishment, including ions, peptides, proteins and some

micronutrients such as vitamin C and folate (Spector and Johanson, 2007; Spector, 2009). Furthermore, CSF contributes to the immunologic protection of the CNS because of its high turnover, which allows for constant cleansing of the brain tissues (Emerich *et al.*, 2004; Falcão *et al.*, 2012; Spector, Snodgrass and Johanson, 2015).

1.2.2 The Brain Barriers

Brain barriers are essential to ensure the maintenance of the concentration of ions and nutrients in the CSF and the ISF within the appropriate limits for proper brain functioning. Brain barriers are formed by tight junctions (TJs) between adjacent cells that reduce their permeability to solutes. There are three main barriers in the human brain: barriers at the brain surface, the blood-brain barrier and the blood-CSF barrier (Abbott *et al.*, 2010; Engelhardt, Vajkoczy and Weller, 2017) (Figure 1.5).

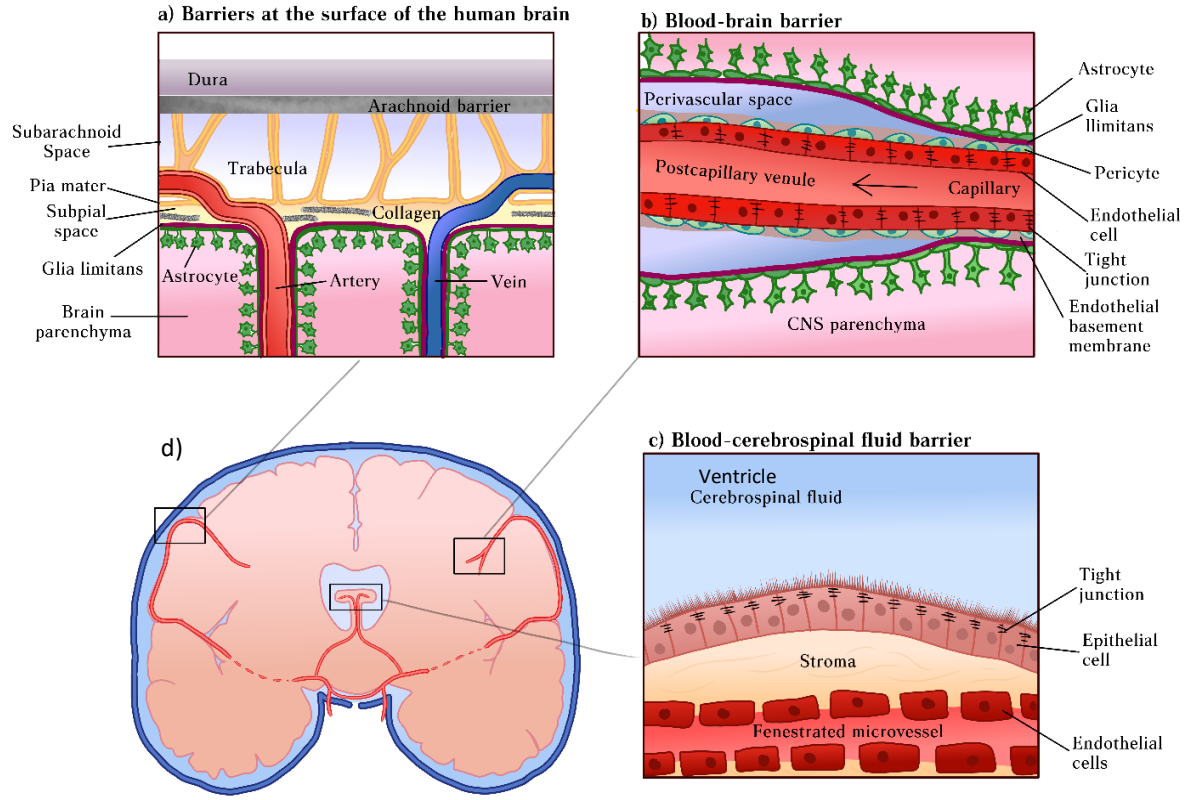

Figure 1.5. Schematic representation of the brain barriers.

(a) In humans, the brain is covered by three membrane layers. The dura mater is the outer layer, adjacent to the arachnoid mater, which forms a barrier between CSF and blood. The subarachnoid space is filled with CSF and it is crossed by sheet-like trabeculae connecting the arachnoid matter to the pia mater and leptomeningeal arteries and veins. The pia mater separates the subarachnoid spacefrom the subpial space and surrounds arteries entering the brain. (b) The endothelial cells from the blood brain barrier are the main site of controlled transport into the CNS. Highly restricted diffusion is achieved by an increased expression of tight junction proteins. (c) The blood-CSF barrier is mainly formed by the epithelial cells located at the choroid plexus. The blood vessels in the choroid plexus do not have a BBB; instead, choroid plexus epithelial cells actively control diffusion of molecules and ions, which drive a passive movement of water from blood to CSF and is the main mechanism of CSF secretion. (d) the location of the three brain barriers within the structure of the brain (Diagram by Ester Pascual Baixauli).

I. Barriers at the surface of the brain

The CNS is surrounded by three membranous layers called meninges which, together with the CSF, protect the system from mechanical damage. In the head, the meninges can be found between the brain and the skull.

The outer layer is the dura mater, a thick and dense collagenous membrane that is tightly fixed to the inner surface of the skull. It contains numerous blood vessels, the dural venous sinuses, where the venous blood from the brain gets drained, and lymphatic vessels where the CSF gets drained (Brunori, Vagnozzi and Giuffrè, 1993; Dasgupta and Jeong, 2019). The middle meninge is the arachnoid mater, a thin membrane containing a few layers of flattened epithelium cells. This layer is one of the three interfaces between blood and brain that can be found in mammal brains. However, its contribution to the molecular exchange between blood and CNS is insignificant due to its avascular nature and relatively small surface area (Abbott *et al.*, 2010). The subarachnoid space (SAS), an area of connective tissue located underneath the arachnoid membrane, also provides openings through which blood vessels interconnect and CSF flows (Da Mesquita, Fu and Kipnis, 2018; Weller *et al.*, 2018). Strands of connective tissue called arachnoid trabeculae can be found in the subarachnoid space connecting the arachnoid mater with the inner meninge, the pia mater. This membrane is formed by a single cell layer that closely adheres to the surface of the brain. It is separated from the brain parenchyma by a subpial space containing blood vessels and collagen and by the glial limitans, a thin barrier formed by astrocyte foot processes (Weller *et al.*, 2018; Dasgupta and Jeong, 2019). Blood vessels branching out from subarachnoid space through pia mater and into the brain are also considered a continuation of this meninge (Lopes, 2009; Decimo *et al.*, 2012).

The meninges not only perform a protective function; recent evidence suggests that they also have complex functions including controlling and facilitating movement of solutes at the surface and within the parenchyma of the CNS (Weller *et al.*, 2018). Furthermore, the outer barriers of the brain also play important roles in mechanisms such as the regulation of the immune cell entry into the CNS or the stem cell niche (Brøchner, Holst and Møllgård, 2015; Da Mesquita, Fu and Kipnis, 2018; Brioschi and Colonna, 2019).

II. Blood-brain barrier

The blood-brain barrier (BBB) separates peripheral blood from the CNS and is formed by a tight monolayer of brain endothelial cells (BEC) which constitute the walls of capillaries. BECs, together with surrounding pericytes, astrocytes, microglia and neurons

form the neurovascular unit (Abbott *et al.*, 2010; Obermeier, Verma and Ransohoff, 2016). Inter-endothelial junctions restrict paracellular diffusion of water-soluble substances which grants the BBB its characteristic restricted permeability. Furthermore, the BBB also shows restricted transport of most polar solutes and reduced vesicular transport across the barrier (Abbott *et al.*, 2010; Hladky and Barrand, 2016; Ueno *et al.*, 2016). Both characteristics are highly controlled by several different mechanisms including cytokines and vascular endothelial growth factor, and their disruption is linked to neuroinflammatory diseases such as Alzheimer´s and Multiple Sclerosis (Hawkins and Davis, 2005; Abbott, Rönnbäck and Hansson, 2006; Armulik *et al.*, 2010; Ueno *et al.*, 2016; Thomas and Eichmann, 2018) However, the BBB allows the diffusion of gasses such as O_2 and CO_2, and facilitates the passage of essential nutrients for brain metabolism such as glucose (Hladky and Barrand, 2016). Furthermore, recent research has shown that BBB also contributes to ISF secretion and CNS waste removal, although the movement rates are smaller than those at the CP level (Abbott, 2004; Zhao *et al.*, 2015; Marchi, Banjara and Janigro, 2016).

III. Blood-cerebrospinal fluid barrier

The blood-cerebrospinal fluid barrier (BCSFB) is formed by choroid plexus epithelial cells (CPEC). The CP is a villous structure of vascularized layers protruding from the walls of the ventricles thought to be the main site of CSF secretion (Tumani, Huss and Bachhuber, 2017; Ghersi-Egea *et al.*, 2018). The microvessels found in the CP are fenestrated, however, the apical ends of CPEC express TJs, which prevents blood and CSF to diffuse freely (Kratzer *et al.*, 2012; Liddelow *et al.*, 2012). CPEC actively control molecular transport across the barrier. CSF secretion is mainly driven by active ion net transport from the blood side to the CSF side, which drives water movement in the same direction via alterations in osmotic pressures (Speake *et al.*, 2001).

The BCSFB interface is key for many processes, including CSF secretion and brain waste removal (Emerich *et al.*, 2004; Wolburg and Paulus, 2010). The present study will focus on CSF and BCSFB, therefore these processes will be explained with more detail below.

1.2.3 Choroid Plexus

I. Choroid Plexus Morphology

The CP is formed by a tight epithelium enclosing a highly vascularized stroma. More specifically, this tissue is composed of a single layer of cuboidal CPECs surrounding a network of capillaries embedded in connective tissue. The capillaries in the CP are fenestrated, providing little resistance to the free movement of ions, small molecules and water from and to the blood (Keep and Jones, 1990; Tumani, Huss and Bachhuber, 2017). CPECs are polarized, with apical TJs and microvilli on the apical membrane facing the CSF (**Figure 1.6**). The apical microvilli on CPEC greatly increase its apical surface area (Keep, Jones and Cawkwell, 1986). In fact, Keep and Jones estimated that the apical surface area–to-epithelium volume ratio in rat CPEC was ~ 30 fold bigger than expected from a 10 µm cuboidal cell with no microvilli (Keep and Jones, 1990). Furthermore, the CP structures also form elongated villi, further increasing the surface for molecular exchange (Ghersi-Egea *et al.*, 2018; Fleischman and Berdahl, 2019).

Intercellular junctions between CPEC comprise adherens junctions (AJs) and TJs (**Figure 1.7**). AJs are essential during development and their existence is required for TJs formation. AJs initiate cell-to-cell contacts and promote their maturation, plasticity and maintenance while also regulating tensile forces. AJs in the CP are usually formed by homophilic interactions of E-cadherin molecules between two cells. E-cadherin cytoplasmic tail binds to p120 and β catenin, which then binds to α catenin, connecting it to the actin cytoskeleton. AJs formed by the nectin-afadin complex are also thought to exist in the CP, although its presence is not well defined yet (Ikeda *et al.*, 1999; Lagaraine *et al.*, 2011).

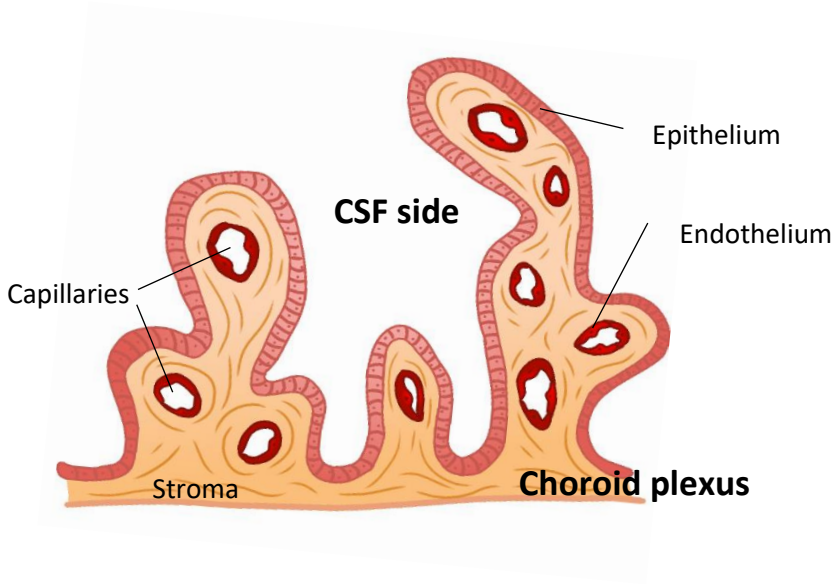

Figure 1.6. Schematic cross section of choroid plexus.

The choroid plexus is formed by fenestrated capillaries, stroma and epithelium. The ventricle side of the epithelium is bathed in CSF (Diagram by Ester Pascual Baixauli).

TJs are the most apical components of junctional complexes. TJs are essential for CSF secretion because they restrict the paracellular permeability and are the most apical components of junctional complexes (Szmydynger-Chodobska *et al.*, 2007; Ghersi-Egea *et al.*, 2018). TJs are comprised of a combination of transmembrane proteins, either claudins, occludin or JAM-3, interacting with the cytoskeleton through scaffold cytoplasmic proteins such as the zonula occludens (ZO) family (Kratzer *et al.*, 2012; Ghersi-Egea *et al.*, 2018). They are present at the most apical part of the lateral space between neighbouring cells and control paracellular movement of molecules between CSF and blood, and guarantee cell polarity by restricting diffusion of transmembrane proteins (Zihni *et al.*, 2016; Ghersi-Egea *et al.*, 2018). In this capacity, the apical TJs form the BCSFB.

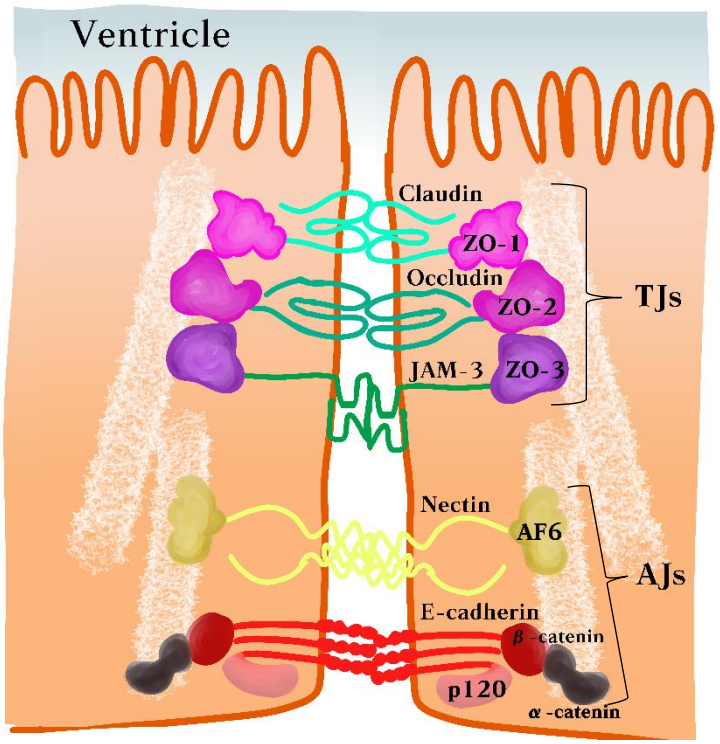

Figure 1.7. Intercellular junctions between choroid plexus epithelial cells.

TJs in the CP are formed by a combination of transmembrane proteins interacting with scaffold proteins which, in turn, are bound to the cytoskeleton. TJs are essential for control of paracellular permeability and they form the BCSFB. CPEC also present AJs. AJs in the CP are normally formed by E-cadherin binding to p120 or β catenin, which in turn binds to α catenin, which interacts with the cytoskeleton. AJs formed by the nectin-afadin complex are also thought to happen in the CP. AF6 = afadin, TJs = tight junctions, AJs= adherens junctions. (Diagram by Ester Pascual Baixauli)

CPECs have a large mitochondrial content, particularly in areas close to the apical "brush" border (Cornford *et al.*, 1997; Bouzinova *et al.*, 2005). This is an indicative that the BCSFB is an active interface rather than just a simple barrier. Controlling the molecular interchange between CSF and blood is very energy demanding as it is mediated by specific transmembrane transporters and reabsorptive transporters. (McComb, 1983; Ghersi-Egea *et al.*, 2018).

The local blood flow in CP is amongst the highest found in the brain as a result of the extensive network of wide capillaries throughout the choroidal stroma, around 4ml·g^{-1} ·min^{-1} in a healthy adult human. The blood arrives by the anterior and posterior choroidal arteries and is drained by the choroidal vein (Szmydynger-Chodobska, Chodobski and Johanson, 1994; Fleischman and Berdahl, 2019).

II. Choroid Plexus Physiology

The CP performs essential functions for CNS homeostasis. As indicated above, it provides a neuroprotective barrier controlling and restricting diffusion of substances between the blood and the CSF and secretes CSF, both of which are interrelated. Specific transporters expressed in apical and basolateral membranes control the molecular exchange between the blood and CSF (Figure 1.8). These transporters allow movement of ions against their concentration gradient, which drives water movement and CSF formation. For example, the activity of carbonic anhydrase and the sodium-potassium adenosine triphosphatase (Na^+-K^+ ATPase) enzymes drive a unidirectional active transcellular flux of Na^+, Cl^- and HCO_3^- from blood to CSF, which creates an osmotic gradient that results in water movement in the same direction. To complement this specific molecular transport, the CP also expresses metabolizing enzymes specialised in transforming endogenous molecules and toxicants into inactive metabolites. These enzymes, coupled with the basolateral specific transporters, form a highly efficient metabolic barrier which protects the CNS from unwanted substances, constituting the major site of xenobiotic metabolism in the brain (Ghersi-Egea *et al.*, 2006; Strazielle and Ghersi-Egea, 2013).

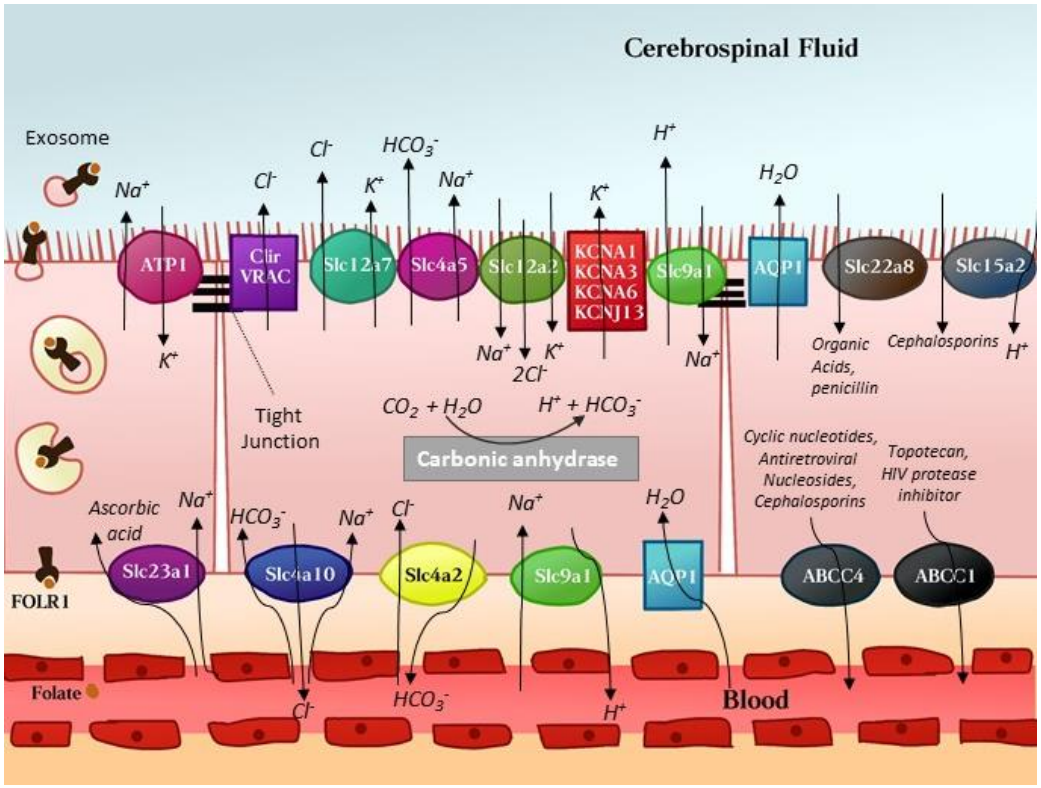

Figure 1.8. Schematic representation of transporters in choroid plexus epithelial cells.

The CP consists of a monolayer of cuboidal epithelial cells surrounding a highly vascularised stroma. CPEC form the BCSFB because of the TJs joining adjacent cells, which restrict passage of solutes, ions and water. CPEC regulates production and composition of CSF and, because of that, it presents polarised expression of molecular transporters. The secretion of CSF by CPEC depends on the transport of sodium (Na^+), potassium (K^+), cloride (Cl^-), bicarbonate (HCO_3^-) and water (H_2O). The active movement of ions into the CSF creates an osmotic gradient which then drives the secretion of H_2O mainly by aquaporin 1 (AQP1). CSF secretion requires the cell production of HCO_3^- by the carbonic anhydrase. HCO_3^- is involved in the transport of Cl^- by the Cl^--HCO_3^- exchange (Slc4a2) in the basolateral membrane. Cl^- is transported into the CSF by Cl^- channels (Clir and VRAC) and also by the K^+- Cl^- cotransporter 4 (Slc12a7). CSF secretion is highly dependent on the active secretion of Na^+ into the CSF by the sodium-potassium adenosine triphosphatase (Na^+-K^+-ATPase). Na^+ is also transported by the Na^+- HCO_3^- cotransporters (Slc4a5 in the apical membrane, Slc4a10 in the basolateral membrane) and by the Na^+-H^+ exchanger (Slc9a1). K^+ is actively taken up from the CSF by the Na^+-K^+-ATPase, and also by the Na^+-K^+-$2Cl^-$ cotransporter-1 (Slc12a2). The majority of K^+ is taken back to the CSF by the inward rectifying channels (KCNA 1, KCNA 3, KCNA 6 and KCNJ 13). CPEC also facilitate the transcellular passage into CSF of molecules essential for brain functioning, such as vitamin C, through the Na^+- dependent vitamin C transporter (Slc23a1), and folate, through the folate receptor alpha (FOLR1), which transports the active metabolite of folic acid, 5-methyltetrahydrofolate. CPEC basolateral membrane expresses the multidrug resistance related proteins 1 and 4 (ABCC1 and ABCC4), and the apical membrane has the peptide transporter

2 (Slc15a2) and the organic acid transporter 3 (Slc22a8). These transporters are thought to be involved in the reduced availability of therapeutic drugs in the CSF (Diagram by Ester Pascual Baixauli).

In addition to the role in CSF formation, the CP is a key component of metabolic and neuroendocrine regulations. The CP synthesizes diverse signalling factors essential for CNS functioning, such as regulating factors of adult neural stem cell niches (Lun, Monuki and Lehtinen, 2015; Silva-Vargas *et al.*, 2016). CPECs express a range of growth factor and hormone receptors, which respond to signals from the circulation, CNS and immune system by changing its secretome dynamically (Sawamoto *et al.*, 2006; Grapp *et al.*, 2013). Moreover, the CP is an important source of other CSF proteins, such as transthyterin (TTR), a thyroxine and retinol transport protein that is the most abundantly synthetized and secreted protein in the CP (Aldred, Brack and Schreiber, 1995). Evidence also suggests that the CP is one of the main regulators of CNS immunity by controlling immune cell entry into the ventricles of the brain (Nathanson and Chun, 1989; Reboldi *et al.*, 2009; Netsky and Shuangshoti, 2013).

1.2.4 Cerebrospinal Fluid Dynamics

I. Composition.

As indicated above, the CSF is derived from plasma and thus the composition of CSF is similar to that of plasma, but contains distinct concentrations of specific components. For example, CSF, contains less than 0.45mg ml^{-1} protein, the biggest fraction of which is albumin, which is around 300 times lower than protein concentrations in the blood (H Uhmer *et al.*, 2006; Tumani, Huss and Bachhuber, 2017). Peptides and proteins found in the CSF can be either actively transported from the blood, such as leptin, or synthesized and secreted by CPEC, such as transthyretin (TTR) or insulin-like growth factor (Strazielle and Ghersi-Egea, 2013; Spector, Snodgrass and Johanson, 2015). In order to compensate for the lack of negative charges amongst CSF solutes due to reduced plasma proteins and lower concentrations of HCO_3^- and K^+, the CSF has altered concentrations of some specific ions, such as increased concentrations of Mg^{++}, ascorbic acid and folate and a Cl^- concentration around 12mM higher than the blood. In addition, within the CSF, the glucose

concentration is 60% higher than in the serum, and fewer than 5000 mononuclear cells ml^{-1} are to be found in healthy CSF (Sakka, Coll and Chazal, 2011; Spector, Snodgrass and Johanson, 2015; Adigun and Al-Dhahir, 2019). The active molecular transport through the CP allows for concentrations of some ions in the CSF to be carefully regulated independently of variations in the plasma concentrations of these ions (Husted and Reed, 1976; Murphy, Smith and Rapoport, 1986; Praetorius and Damkier, 2017).

The next sections will discuss current hypotheses regarding CSF secretion, circulation and drainage. However, it should be noted that knowledge of CSF dynamics is still a matter of debate and an area of active research which continues to generate additional experiments and interpretation.

II. Secretion.

The CSF is mainly produced by CPEC, although the brain interstitium and meninges are thought to contribute in a smaller scale (Sakka, Coll and Chazal, 2011; Damkier, Brown and Praetorius, 2013; Orešković and Klarica, 2014). In a healthy adult human, the volume of CSF is around 150 ml, with a rate of secretion from CP of approximately 0.4ml $min^{-1}g^{-1}$ of tissue, suggesting that CSF is replaced between 3 and 4 times in a day (Speake *et al.*, 2001; Benarroch, 2016). . It is thought that CSF secretion rate varies during a 24 hour period in a cyclic manner and coupled with circadian rhythms (Nilsson *et al.*, 1992; Myung *et al.*, 2018; Yamaguchi *et al.*, 2020).

The initial step that allows CSF secretion is passive filtration of plasma through the fenestrated capillary network into the connective tissue in the CP. The second step is dependent on the active unidirectional transport of ions by the CPEC, which creates the osmotic gradient that drives the movement of water into the ventricle. This task is carried out by transport proteins that are located on the apical and basolateral membranes of the cells (Speake *et al.*, 2001; Alimajstorovic, Pascual-Baixauli, *et al.*, 2020) (Figure 1.9).

There are net fluxes of many ions, organic anions and organic cations across the CP, important for the normal function of the CNS. CPECs also mediate the net absorption of K^+ into blood, necessary for maintaining K^+ concentration in CSF, which is closely linked to CSF

secretion (Ames, Higashi and Nesbett, 1965; Roepke *et al.*, 2011). However, the ions that most contribute to the osmotic gradient that drives CSF secretion are Na^+, Cl^- and HCO_3^- (Saito and Wright, 1983; Brown *et al.*, 2004). More specifically, it primarily depends on the active transport of Na^+ by the Na^+-K^+ ATPase (ATP1) and the production of HCO_3^- by the carbonic anhydrase in CPEC, which catalyses the conversion of H_2O and CO_2 into HCO_3^- and H^+ (Speake *et al.*, 2001; Millar, Bruce and Brown, 2007). The Cl^- transport from the blood side is driven by the anion exchange 2 (SLC4A2) which mediates HCO_3^- and Cl^- interchange. The secretion of Cl^- into CSF is mediated by the K^+-Cl^- cotransporter 4 (KCC4) and an inward rectifying channel, while the secretion of HCO_3^- happens through the electrogenic Na^+-HCO_3^- cotransporter (NBCe2). Water moves into the ventricles through either aquaporin channels in the cell membrane or the paracellular pathway once the osmotic gradient is created (Speake *et al.*, 2001; Brown *et al.*, 2004; Benarroch, 2016; Bothwell, Janigro and Patabendige, 2019).

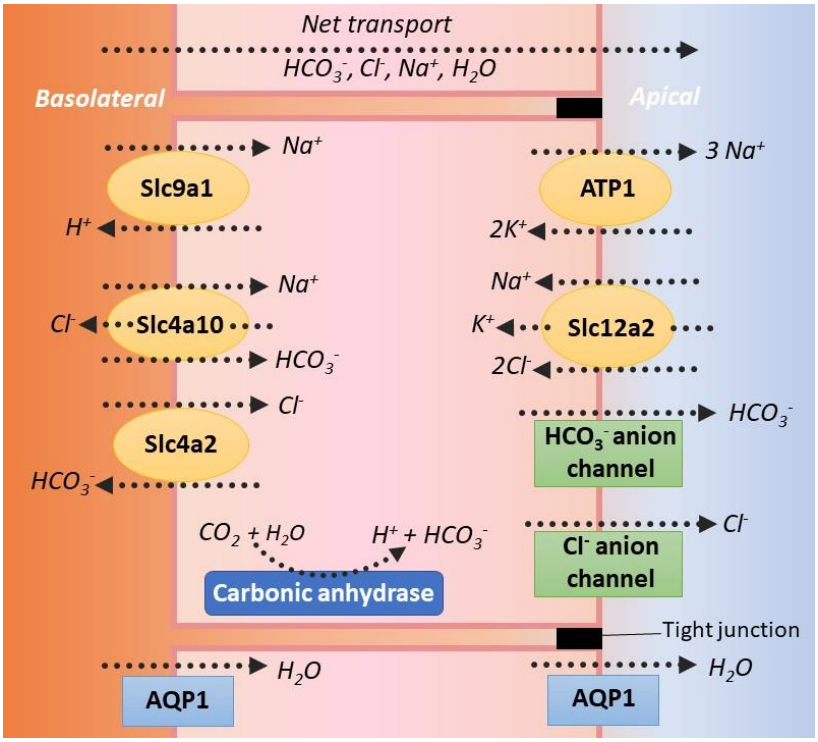

Figure 1.9. Model of cerebrospinal fluid secretion by the choroid plexus epithelial cell.

Summary of ion transporter expression in CPEC and how they facilitate CSF secretion. CPEC form the BCSF because of the TJs joining adjacent cells, which restrict passage of solutes, ions and water. The secretion of CSF creates a net transport from blood into CSF of Na^+, HCO_3^-, Cl^- and H_2O. This model of CSF secretion schematically represents locations of transporters. Briefly, the ion transporters the Na^+-H^+ exchanger (Slc9a1), the Na^+- HCO_3^- cotransporter (Slc4a10) and the Cl^--HCO_3^- exchanger (Slc4a2) are located basolaterally while the sodium-potassium adenosine triphosphatase (ATP1) and the Na^+-K^+-$2Cl^-$ cotransporter-1 (SLC12A2) are located in the apical membrane. Transport of HCO_3^- and Cl^- into the CSF is mediated by HCO_3^-/ Cl^- anion channels. Aquaporin 1 (AQP1) is expressed both basolateral and apically and it mediates passage of H_2O. (Diagram by Ester Pascual Baixauli).

A small percentage of CSF is also derived from extrachoroidal components. This extrachoroidal component usually results from exchanges between ISF in the CNS parenchyma, and CSF in the ventricles through the ependyma lining. However, this pathway appears to play a minimal role under physiological conditions (Sakka, Coll and Chazal, 2011; Benarroch, 2016).

III. Circulation

As previously mentioned, CSF fills the ventricular system and the cranial and spinal subarachnoid spaces. The constant production of new CSF by CPEC displaces fluid and drives its drainage, ensuring a stable environment for the brain and removing waste products (Orešković and Klarica, 2014; Bothwell, Janigro and Patabendige, 2019). Once thought to be unidirectional, CSF generally flows from secretion sites towards drainage points (Figure **1.10**); however, growing evidence suggests that CSF circulation is an extremely complex process with changing rates, directions and paths depending not only on the circadian clock but also on behavioural states, such as stress response (Mokri, 2001; Sakka, Coll and Chazal, 2011; Tumani, Huss and Bachhuber, 2017). There seems to be a very strong cardiorespiratory pulsatile modulation of CSF movement, especially in adults (O'Connell, 1943; Greitz *et al.*, 1992; Wagshul, Eide and Madsen, 2011; Dreha-Kulaczewski *et al.*, 2018; Mestre *et al.*, 2018). In large ventricles, CSF bulk flow is mostly driven by secretion and drainage rates, while in smaller spaces, such as the third ventricle, multi-ciliated ependymal cells appear to have a big role on circulation dynamics (Orešković and Klarica, 2014; Linninger *et al.*, 2016; Abdelhamed *et al.*, 2018; Eichele *et al.*, 2020).

Generally, the CSF produced in the lateral ventricles flows through the intraventricular foramina into the third ventricle, then flows through the cerebral aqueduct to the fourth ventricle, where more fluid is secreted (Gideon *et al.*, 1994; Falcão *et al.*, 2012; Akay *et al.*, 2015; Reiber, 2016). From there, the CSF can either reach the subarachnoid space near the pontine cistern via the lateral apertures and the median aperture or continue within the ventricular system flowing down the central canal of the spinal cord. The lateral apertures, also called foramina of Luschka, are located in each lateral recess of the fourth ventricle, while the median aperture, also called foramen of Magendie, is located medially to the ventricle (Falcão *et al.*, 2012; Ray and Heys, 2019).

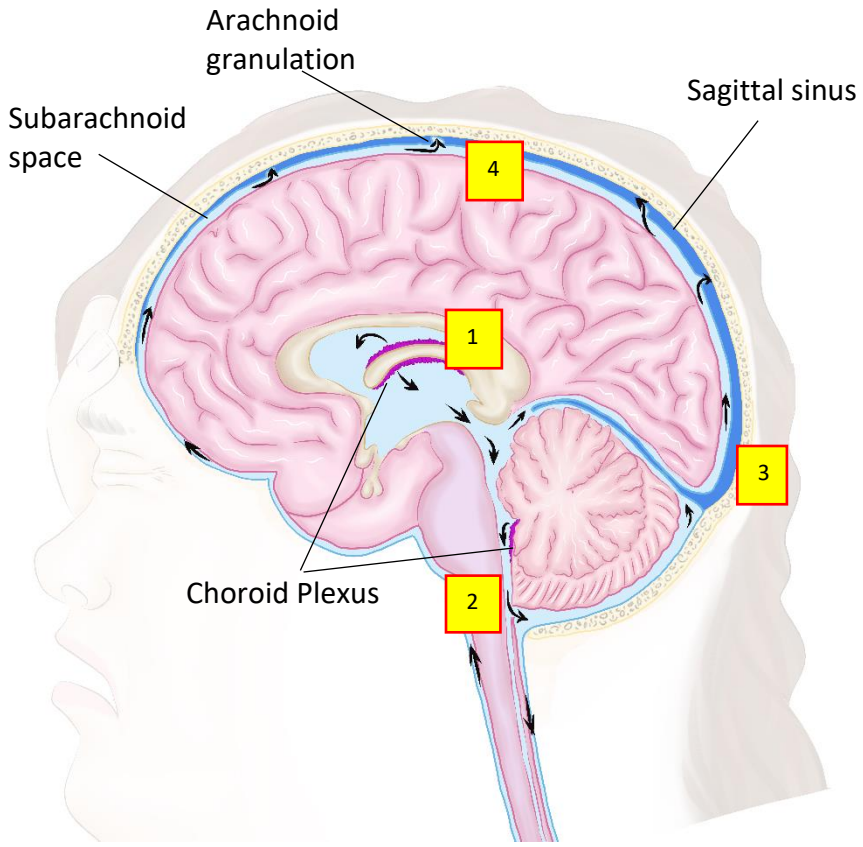

Figure 1.10. Cerebrospinal fluid dynamics in the human.

Simplified representation of CSF dynamics in the human brain. 1. CSF is produced in the CP of each ventricle. 2. CSF flows through the ventricles and into the subarachnoid space via the median and lateral apertures, or through the central canal of the spinal cord. 3. CSF flows through the subarachnoid space and 4. CSF can get drained in different sites, such as through arachnoid granulationsinto the sagittal sinus. (Illustration by Ester Pascual Baixauli).

IV. Drainage

CSF drainage is a complicated process that can occur at different sites, which fall into three functionally distinct categories: the arachnoid granulations, the perineural sheaths surrounding cranial and spinal nerves and the dural lymphatic vessels.

The first described CSF drainage pathway was via the arachnoid villi granulations into the dural venous sinuses to reach the venous circulation. Each arachnoid villus acts as a one-way valve and allows the unidirectional flow of CSF from the subarachnoid space into the systemic circulation while preventing retrograde blood flow into the subarachnoid

space (Ueno *et al.*, 2016). Originally this was believed to be the only CSF drainage pathway. However, further evidence suggests that CSF drainage can also occur in other locations, such as via the spinal arachnoid villi, by diffusion into the ISF through the ependymal layer and then into the blood through the BBB, or via the nasal lymphatics (Pollay, 2012; Chen *et al.*, 2015). Spinal arachnoid villi granulations are anatomically similar to the brain arachnoid villi granulations, and some research supports the idea that they also allow drainage of CSF into the venous blood system (Seyfert, Koch and Kunzmann, 2003).

The importance of the lymphatic system on CSF drainage has been accepted relatively recently after several studies have provided strong support for the existence and relevance of this physiological pathway (Johnston and Papaiconomou, 2002; Iliff *et al.*, 2012; Raper, Louveau and Kipnis, 2016; Gillooly *et al.*, 2017). The most commonly observed drainage routes by the lymphatic system involves CSF flowing along the perineural space of the olfactory nerve into nasal mucosa of the nasal cavity (Pollay, 2012; Chen *et al.*, 2015) Here, it gets absorbed through the submucosal lymphatic system and gets ultimately drained to the nasopharynx regional lymph nodes (Raper, Louveau and Kipnis, 2016).

The glymphatic pathway was firstly observed in the 1980s, although it was not until 2012 when the pathway was properly identified and it has been gaining importance ever since (Figure 1.11) (Cserr *et al.*, 1981; Fossan *et al.*, 1985; Iliff *et al.*, 2012). In this hypothesis, CSF flowing through the subarachnoid space enters the glymphatic flow by the perivascular space of major cerebral arteries on the brain surface. From there, the CSF flows towards the brain parenchyma along the arteries as it branches into penetrating arteries. The glymphatic system is characterized by an influx of CSF into ISF in extracellular spaces facilitated by a polarised expression of aquaporin 4 (AQP4) at the astrocytic end-feet lining the perivascular space (Rasmussen, Mestre and Nedergaard, 2018; Nakada and Kwee, 2019). Bulk clearance of fluid from brain parenchyma moves towards the venous perivascular space; once this space is reached, the fluid is drained by convection into meningeal and cervical lymphatic drainage vessels (Xie *et al.*, 2013; Marchi, Banjara and Janigro, 2016; Iliff, Thrane and Nedergaard, 2017; Da Mesquita, Fu and Kipnis, 2018; Sokołowski *et al.*, 2018).

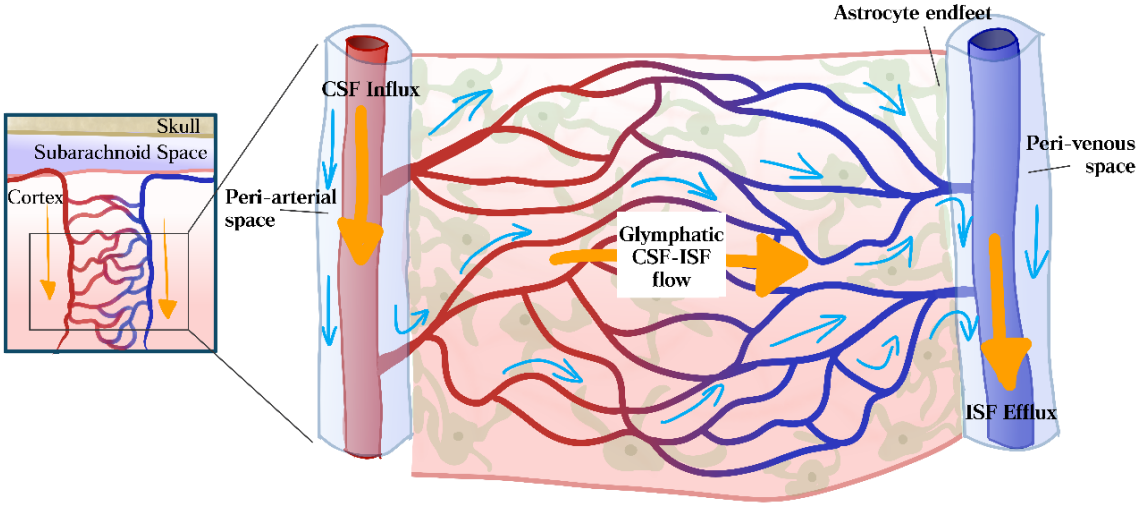

Figure 1.11. Glymphatic fluid drainage pathway in the brain.

CSF enters the glymphatic flow by the perivascular space of major cerebral arteries on the brain surface. From there, the CSF flows towards the brain parenchyma along the arteries as it branches into penetrating arteries. The glymphatic system is characterized by an influx of CSF into ISF in extracellular spaces. Bulk clearance of fluid from brain parenchyma moves towards the venous perivascular space; once this space is reached, the fluid is drained by convection into meningeal and cervical lymphatic drainage vessels. (Diagram by Ester Pascual Baixauli).

The proportion of CSF that efflux through each pathway is not yet known in humans. However, some animal studies suggest that CSF drainage through the lymphatic pathways might account for up to 50% of total CSF outflow (Pollay, 2012; Sokołowski *et al.*, 2018). It is important to remark that these studies were performed in rodents; while they are accepted as a good model for disease research, there are important anatomical and physiological differences between species therefore the lymphatic pathway of CSF drainage in humans might be less important than in rodents. All main drainage pathways have shown to be pressure gradient dependent in healthy individuals (Boulton *et al.*, 1998).

1.2.5 Preclinical Research on Cerebrospinal Fluid Secretion Dynamics

I. In vivo Assessment of Cerebrospinal Fluid Secretion

In vivo CSF secretion measurements are challenging and many techniques have been developed in order to measure *in vivo* CSF secretion. The most common ones are summarized below.

a) Cerebrospinal fluid drainage

CSF drainage is the simplest and oldest technique to measure CSF formation *in vivo* (Flexner and Winters, 1932; Greenberg *et al.*, 1943; Orešković and Klarica, 2010). In brief, this method consists on introducing a needle into the CSF space and collecting the CSF outflow. At the beginning of the experiment, a large amount of CSF will escape, therefore it is necessary to wait until the CSF outflow rate stabilizes. Once the CSF flows out of the needle in a steadily manner, the CSF formation rate can be directly visualised and calculating by measuring the CSF volume in time (Flexner and Winters, 1932; Orešković and Klarica, 2010). Another variant of this technique involves measuring the *in vivo* CSF pressure before removing a known volume of CSF from the CSF space. The time elapsed between this removal until the initial pressure is reached again is measured and the secretion rate is calculated from this (Orešković and Klarica, 2010). However, this is not a very popular method for CSF secretion studies due to the possibility of this abrupt decrease on CSF volume affecting CSF secretion rates, which would make the measurement of physiologically normal secretion rates difficult to assess.

b) Magnetic resonance imaging

MRI is a non-invasive imaging technique that can be performed in living animals. This method allows for evaluation of direction and velocity of liquid flow through an internal vessel, in this case the Sylvius aqueduct (Figure 1.12) (Mark and Feinberg, 1986; Mascalchi *et al.*, 1988). General CSF flow happens from secretion sites towards drainage points, therefore the flow measured in the Sylvius aqueduct can be assumed to be newly

secreted CSF and therefore CSF secretion rate can be calculated from it using the equations specified in **Figure 1.12** (Brinkmann *et al.*, 2000). This method has been effectively used in humans (Brodsky and Vaphiades, 1998; Brinkmann *et al.*, 2000; Akay *et al.*, 2015). However, very specialised and expensive machinery is needed, making it a difficult technique for animal studies.

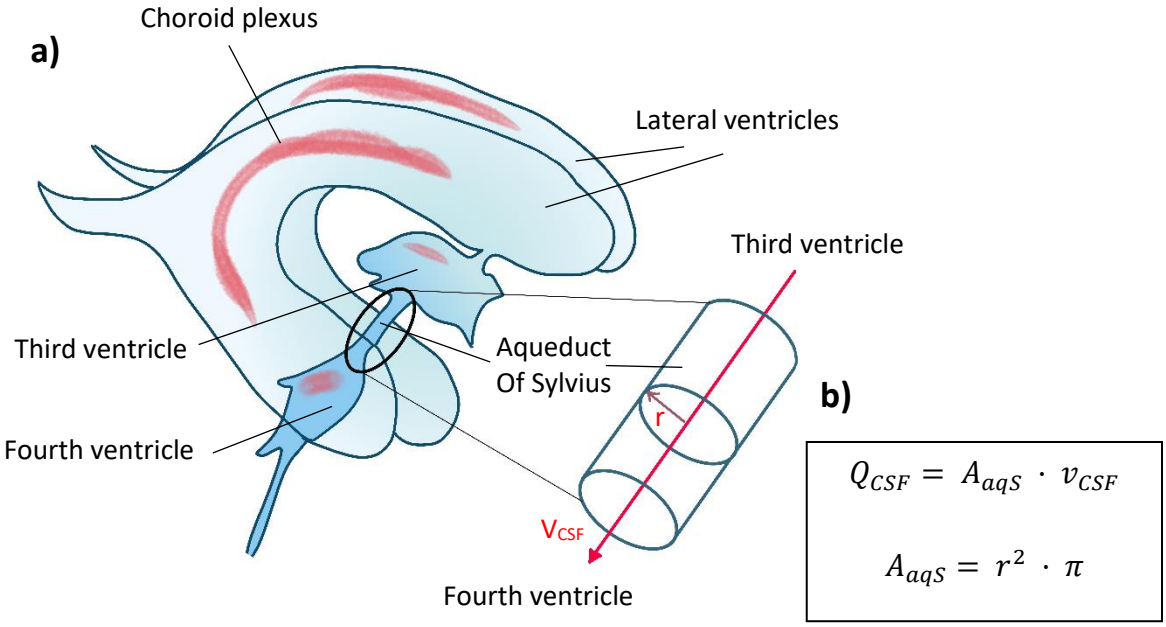

Figure 1.12. Scheme of measurements of cerebrospinal flow rate in the human brain using MRI.
(a) Schematic of the human brain ventricles, with emphasis in the choroid plexi and the Aqueduct of Sylvius. (b) The equation that allows calculation of CSF secretion by calculation on CSF velocity using the MRI method, where Q_{CSF}= CSF flow (m^3/s), A_{aqS}= cross section area of Aqueduct of Sylvius (m^2), v_{CSF}=difference between integrated CSF velocity in cranial and caudal directions (m/s). r =radius. (Diagram by Ester Pascual Baixauli)

c) The ventriculo-cisternal perfusion technique.

The main method used to measure CSF secretion in animals is the ventriculo-cisternal perfusion technique, which has been used extensively for the study of CSF dynamics since it was first established (Heisey, Held and Pappenheimer, 1962; Pappenheimer *et al.*, 1962) (Figure 1.13) . In this technique, artificial CSF (aCSF) is infused

into the ventricles of a living anaesthetised animal and CSF samples are collected from cisterna magna. The aCSF contains a tracer molecule which allows calculation of dilution factors from the samples collected. Endogenous CSF secretion rates can be calculated based on dilution rates of the tracer. While this procedure has been widely used for CSF dynamic studies, it presumes that endogenous CSF secretion is the only factor that contributes to the dilution of aCSF. As such, other processes that could affect the dilution rate, such as diffusion of aCSF into ISF, are not considered (Martins, Newby and Doyle, 1977). However, this technique presents advantages when compared to other CSF secretion measurement techniques. First of all, there is no need for highly specialised machinery and expertise on the procedure can be relatively easily acquired. Furthermore, the CSF at the cisterna magna flows freely, which balances the pressure increase due to aCSF insertion (Fenstermacher, 1972; Davson *et al.*, 1982; Oreskovic *et al.*, 2003).

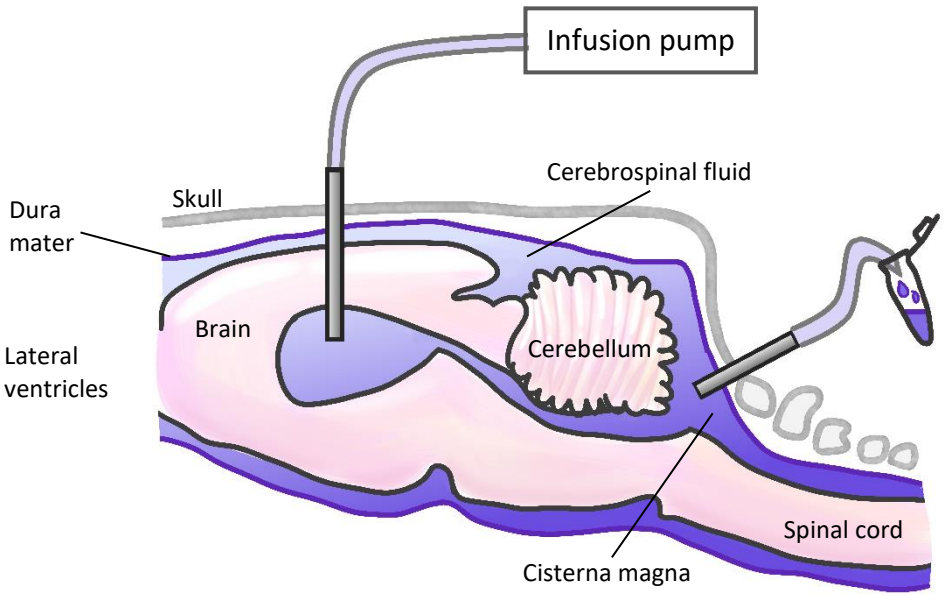

Figure 1.13. Schematic representation of the ventriculo-cisternal perfusion technique.

Dextran blue is used as a marker and is infused in artificial CSF in both ventricles in the rat. The marker gets distributed equally inside the brain CSF and gets collected from the cisterna magna. (Diagram by Ester Pascual Baixauli).

II. In vitro Assessment of Cerebrospinal Fluid Secretion

In vitro models are very important because they allow a controlled study of a specific process avoiding external factors that could affect an organism, such as water or food intake of the animal. They are also more financially viable as *in vitro* materials are usually cheaper than many *in vivo* studies. Furthermore, the ethical considerations of performing experiments *in vivo* are generally not applicable in an *in vitro* experiment.

In vitro modelling of CSF secretion typically involves the use of CPECs, which can be obtained from *ex vivo* CP or from an immortalised cell line, or the use of whole CP, and are used to assess CSF secretion directly or by the use of surrogates of CSF secretion (Vates, Bonting and Oppelt, 1964; Pollay *et al.*, 1972; Klarr *et al.*, 1997; Petersen *et al.*, 2020).

Porcine primary cultures have been used to assess CSF secretion and study the effect of certain molecules on this process (Hakvoort, Haselbach and Galla, 1998). However, lack of availability of primary pig cells and differences between the pig and human CNS limit the usefulness of this model. Human immortalized CPECs have also been used in an attempt to more closely model human physiology. However, because human CPECs are obtained from a CP carcinoma, whether they accurately replicate healthy CP tissue is questionable (Redzic, 2013; Bernd *et al.*, 2015; Dinner *et al.*, 2016). Rodent CPEC lines are the most commonly used in this kind of research because of their easy care and research versatility (Kitazawa *et al.*, 2001; Zheng and Zhao, 2002; Kläs *et al.*, 2010; Strazielle and Ghersi-Egea, 2011).

Direct measurement of CSF secretion can be done by assessing the production of fluid or dilution of marker in the apical side or transport through the cell layer of specific molecules such as thyroxine, thymidine or leptin (Kitazawa *et al.*, 2001; Strazielle and Preston, 2003; Shi *et al.*, 2008)

Indirectly, CSF secretion can be estimated by measuring the activity of enzymes or transporters that are involved in CSF production (e.g. Na^+K^+ATPase activity) (Vates, Bonting and Oppelt, 1964). Assessing ionic movements and ATPase activity can therefore allow for estimation of CSF secretion *in vitro* (Klarr *et al.*, 1997; O'Reilly *et al.*, 2019).

a) Extracorporeal perfusion of the choroid plexus

This technique is performed by the rapid dissection of CP from freshly sacrificed animals followed by a perfusion of the *ex vivo* CP with a saline infusion (Pollay *et al.*, 1972; Deane and Segal, 1985). It is important to preserve the vessels at the base of the CP when extracting it from the brain, as they will be used for the perfusion. The carotid artery above the anterior choroidal artery is ligated and the internal cerebral vein is cannulated and perfused (Pollay, 1975). The CSF secretion is then calculated from the change in haematocrit between the inflow and outflow fluids (Orešković and Klarica, 2010). Although this method is no longer in use by the scientific community due to the intrinsic difficulty of the technique and the development of easier reliable methods, it is important to note that it played an essential role in the acceptance of the hypothesis of CSF secretion by the CP.

b) Functional studies on human choroid plexus samples.

Human CP samples may be obtained as spare material from neurosurgery, usually following the procedure of removal of a large CP papilloma. If this is the case, it is important to separate pathologically-unaltered tissue and use it for uptake studies, immunocytochemistry or molecular biology (Nyland and Matre, 1978; Redzic, 2013).

Uptake studies usually involve use of test and reference molecule, which also serves as a marker of the extracellular space (Fagan and Cowan, 1971; Kaplan *et al.*, 1973). Both molecules are incubated in aCSF after which the sample is analysed to determine the quantity of each molecule in the CP cells. The total amount of test molecule found in the sample after incubation is composed of two groups: molecules diffused from aCSF into the extracellular fluid of the CP; and molecules that entered the CPECs during the experiment via membrane transporters. In order to estimate the molecules that were taken up by the cells, the reference molecule is used. An ideal reference molecule extracellularly behaves as the test molecule but is unable to enter CPEC due to the lack of specific transporters. Therefore, the amount of test molecule in the extracellular fluid can be calculated by determining the quantity of reference molecule, which is then extracted to the total quantity of test molecule in the sample (Redzic *et al.*, 2010; Redzic, 2013). The main

difficulty in using this technique is the lack of human samples and the ethical concerns associated with working with human tissues.

c) *In vitro* cell cultures of choroid plexus epithelial cells

CPEC cell lines, either primary or immortalised, can be used to study vectorial transport of solutes as a model for CSF secretion. However, it is important to take into account the possible phenotypic differences between immortalised cell lines and *in vivo* CPECs, due to their origin, which is usually a carcinoma for human cells, but also due to the process used to confer cell immortality. It is also important to consider the innate differences due to the species from which they are derived. Nevertheless, they are a good *in vitro* model of blood-CSF barrier and they can be used for uptake and secretion studies (Kitazawa *et al.*, 2001; Wollack *et al.*, 2008; Alimajstorovic, Westgate, *et al.*, 2020). CPEC used for BCSFB studies are usually grown on a permeable membrane which separates two compartments; the upper chamber representing the CSF side and the bottom one as the stromal blood side (Figure 1.14).

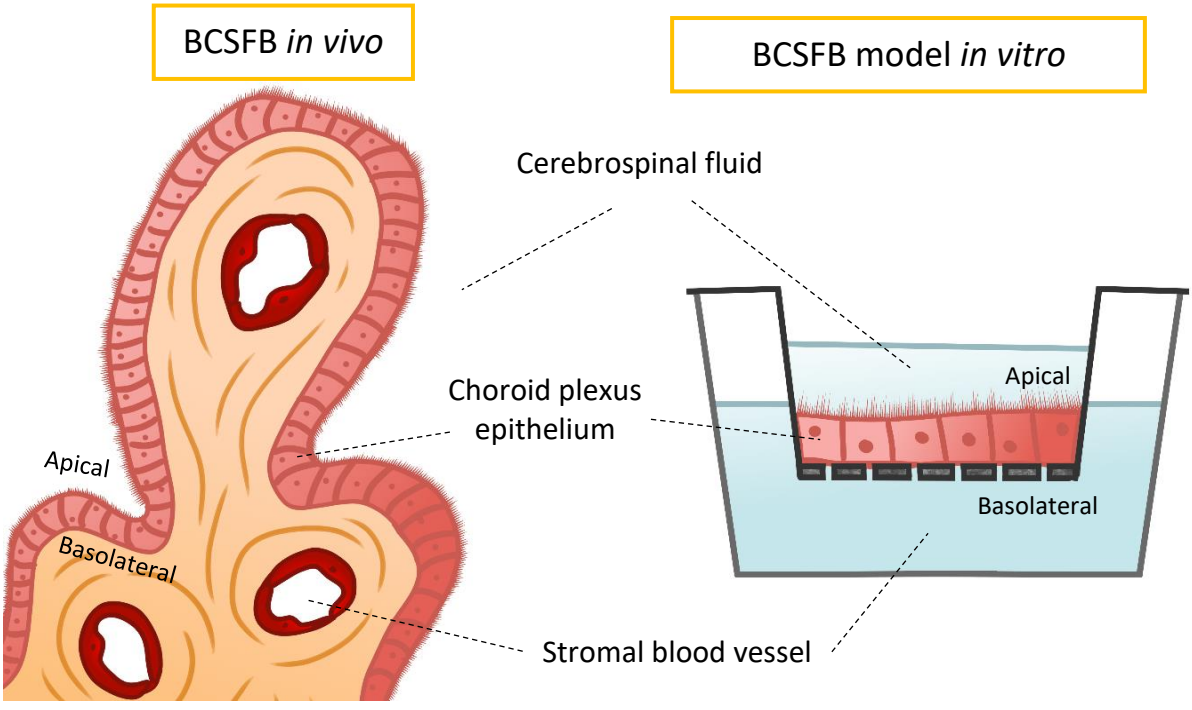

Figure 1.14. Blood-cerebrospinal fluid barrier *in vivo* and *in vitro*.

Comparison of blood-cerebrospinal fluid-barrier (BCSFB) *in vivo* (left) and an *in vitro* model composed of choroidal epithelium cells grown on a permeable membrane. In the model, the basolateral area which is directly underneath the membrane represents the stromal blood vessel, while the apical area which is usually

composed by cell medium on top of the cells represent the cerebrospinal fluid. (Diagram by Ester Pascual Baixauli)

In order to stimulate CSF secretion *in vitro,* ion gradients across the cell monolayer are needed (Strazielle and Ghersi-Egea, 2005). Inhibition of the Na^+K^+ATPase has shown to decrease the fluid secretion in *in vitro* cultures of CPEC (Haselbach *et al.*, 2001), showing that the mechanism by which the cultured CPEC secrete CSF can be related to the *in vivo* pathway.

1.1 Idiopathic Intracranial Hypertension

Idiopathic Intracranial Hypertension (IIH), previously called Pseudotumor Cerebri or Benign Intracranial Hypertension, is a rare disorder in which the patient shows elevated intracranial pressure (ICP) for no obvious reasons (Farb *et al.*, 2003; Binder *et al.*, 2004; Julayanont *et al.*, 2016). The first cases of IIH were reported in the 1890s by the German physician Heinrich Quincke under the name “meningitis serosa” (Quincke, 1893). The term Pseudotumor Cerebri was coined by Max Nonne in 1904 due to symptomatic similarities with a brain tumour but without the existence of such. Many cases appeared in the literature afterwards. However, several of them were actually due to underlying conditions, making them secondary intracranial hypertensions. In order to be able to distinguish between these and IIH, the neurosurgeon Walter Dandy developed in 1937 several diagnosis criteria (Dandy, 1937). In 1955, this disease was renamed “Benign Intracranial Hypertension” to distinguish it from increased ICP due to life-threatening conditions, such as cancer (Foley, 1955). Nevertheless, because of the association with severe symptoms which are not considered to be benign, the name was further changed in 1989 to Idiopathic (of unknown causes) Intracranial Hypertension (Baker, Baumann and Buncic, 1989). Nowadays, this denomination is still considered the most appropriate as it best represents the condition.

1.2.6 What is Idiopathic Intracranial Hypertension?

A patient suffering from IIH shows normal neurodiagnostic tests, including an absence of disruption or damage to the ventricular system including brain tumours. However, individuals with IIH will have an increased ICP that is greater than 200 mm of water measured in a lumbar puncture (Wall, 1991; Friedman and Jacobson, 2002; Binder *et al.*, 2004; Bidot and Bruce, 2015).

The symptoms of IIH usually include debilitating headaches, hearing problems such as pulsatile tinnitus or hearing loss, back, shoulder and/or neck pain, and visual problems such as visual loss, diplopia, reduced acuity or transient visual obscuration (Radhakrishnan *et al.*, 1993; Binder *et al.*, 2004; Fraser *et al.*, 2010).

Nowadays, treatments for IIH do not ensure an improvement in the symptoms experienced by the patient or the condition itself. As the underlying reasons for the increase in ICP during IIH are unknown, current therapies are focused on tackling the patient's symptoms (Bagga *et al.*, 2005; Dykhuizen and Hall, 2011; Karmaniolou, Petropoulos and Theodoraki, 2011). The only available cure is weight loss, which can take weeks or months until the patient shows any improvement (Kupersmith *et al.*, 1998; Rowe and Sarkies, 1999; Manfield *et al.*, 2017). Furthermore, if visual problems are experienced by the patient, these might become chronic if not solved on time (Moreau, Lao and Farris, 2014; Wagner *et al.*, 2016; Agarwal *et al.*, 2017).

1.2.7 Epidemiology

IIH is considered a rare disease and not much information about its incidence and prevalence is available. In Iowa and Louisiana, USA, an epidemiological study on IIH was performed to try to get a wider view about this condition. In this study, IIH incidence was estimated to be around 0.9 in 100,000 in the general population. However, in women that are 20% or more above their ideal weight, the incidence rose up to 19 cases in every 100,000. Furthermore, 90% of IIH patients were female (Durcan, Corbett and Wall, 1988). The incidence of this disease is slowly increasing in the world population, probably due to both a higher awareness of the condition and the current global epidemic of obesity.

Recently, a new study was performed in Scotland, a nation with a 29% prevalence of obesity on its adult population. In this study, the incidence of IIH was found to be 38 in 100,000 in obese females of childbearing age. Nevertheless, the true incidence is probably higher as numerous patients suffering from IIH do not present with papilledema, which can make their condition potentially misdiagnosed as this is still considered to be one of the main IIH characteristics.

1.2.8 Diagnosis

In order to diagnose IIH, three characteristics should be met: no signs of abnormalities on brain imaging, raised ICP with normal CSF constituents, and exclusion of any other possible causes for raised ICP. Modified Dandy criteria are usually used to assure an accurate diagnosis (**Table 1.1**). These criteria were established in 1955 and further updated in 2002 (Friedman and Jacobson, 2002) to distinguish individuals with IIH from patients with increased ICP due to another underlying condition.

Table 1.1. Modified Dandy criteria for IIH diagnosis. Adapted from Friedman and Jacobson, 2002.

1. **Symptoms** (if present) may only reflect those of generalized intracranial hypertension or papilledema.
2. **Signs** (if present) may only reflect those of generalized intracranial hypertension or papilledema.
3. **Elevated ICP** measured in the lateral decubitus position.
4. **Normal CSF composition** regarding CSF levels of protein and main ions.
5. **No evidence of brain lesion or venous sinus thrombosis** on imaging.
6. **No other identifiable cause** of raised ICP.

Fundus exam is an initial investigation that the practitioner might use to quickly assess the possibility of increased ICP (Figure **1.15**). In this exam, the optic disc, situated at the back of the eye, is observed. A normal disc is small in size and has very defined borders. However, if the disc is swollen and present blurry borders, an excess of ICP will be suspected (Karmaniolou, Petropoulos and Theodoraki, 2011). This optic disc increased in

size is named papilledema; while papilledema is always related to increased pressure in the optic nerve, an increased ICP does not always result in an occurrence of papilledema (Binder *et al.*, 2004; Chen and Wall, 2014; Markey *et al.*, 2016).

Brain imaging, preferably magnetic resonance imaging (MRI), is used to exclude brain anomalies. However, it is important to take into account that patients who suffer from high CSF pressure for a long time might present small changes in ventricular compression, partial empty sella and perioptic CSF distension (Brodsky and Vaphiades, 1998; Agarwal *et al.*, 2017).

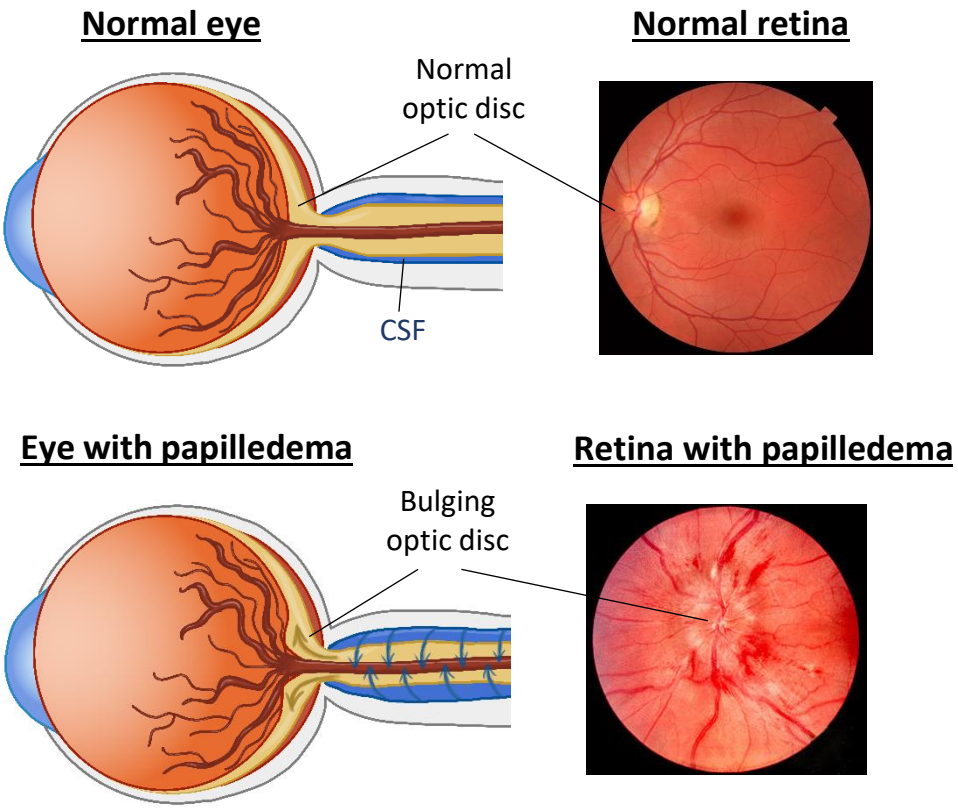

Figure 1.15. Comparation between an eye with a normal optic disc and an eye with papilledema.
In papilledema, cerebrospinal fluid (CSF) increases pressure around the optic nerve, which creates a bilging optic disc classified as papilledema, which can be seen in an eye fundus exam. (Normal retina photography obtained from Häggström, 2014. Retina with papilledema photography obtained from Trobe, 2011. Eye diagrams by Ester Pascual Baixauli).

A lumbar puncture is used to measure CSF pressure. In adult humans, CSF has a normal opening pressure between 100 and 200 mm of water in a lumbar puncture (Adigun

and Al-Dhahir, 2019). A pressure of > 250 mm of water is indicative of IIH (Figure **1.16**). Using this technique, CSF samples can also be obtained for further analysis to determine cell count, glucose, ions and protein concentrations, and cell count, all of which should be within the normal range. Further investigations to exclude underlying pathologies might include thrombophilia screens, serum vitamin A and iron levels and renal and thyroid function tests. (Brodsky and Vaphiades, 1998; Wolburg and Paulus, 2010)

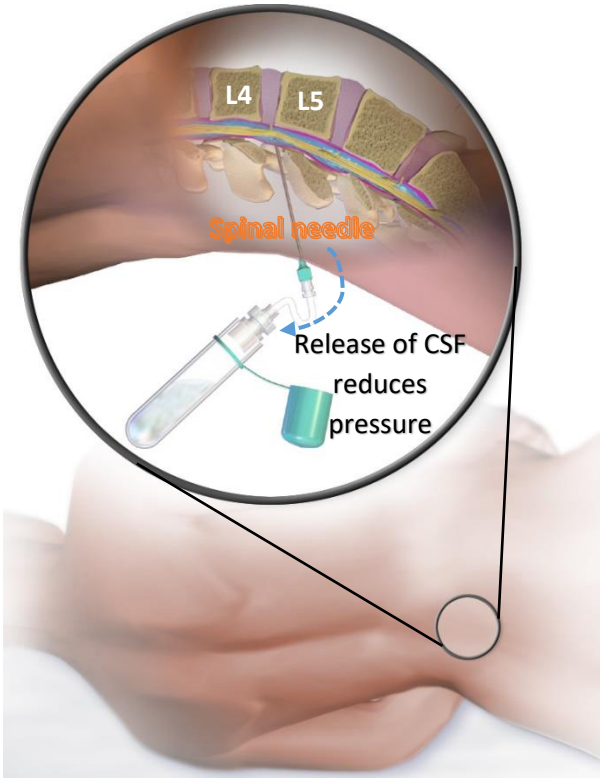

Figure 1.16. Measurement of intracranial pressure by lumbar puncture.

A pressure higher than 250 mm of water will be considered high. Furthermore, a CSF sample can be released to relieve pressure and/or to analyse CSF components and dismiss other possible reasons for elevated ICP. (Modified from Blaus, 2014).

1.2.9 Risk Factors

Although the pathogenesis of IIH remains unknown, there are several characteristics that many IIH patients share, therefore they can be classified as risk factors for developing this condition.

I. Obesity

IIH is indisputably linked to obesity. This association has been confirmed by many studies (Radhakrishnan *et al.*, 1993; Rowe and Sarkies, 1999; Glueck *et al.*, 2005; Sinclair *et al.*, 2008, 2010; Schwartz *et al.*, 2013; Chen and Wall, 2014; Goudie *et al.*, 2019). The incidence of IIH is higher in countries where rates of obesity are high (McCluskey *et al.*, 2018). For instance, a study performed in Spain determined an incidence of 5.1 IIH cases every 100 000 in the general population (Asensio-Sanchez et al, 2007), but another study in the UK measured a prevalence of 10.9 per 100 000 (Raoof et al, 2011). In Spain the incidence of obesity in the adult population is 13.3%, which is significantly lower than the 22.7% obesity incidence in the UK. Furthermore, it has been frequently observed that losing weight reduces ICP and lowers headache symptoms in female IIH patients (Kupersmith *et al.*, 1998; Manfield *et al.*, 2017). Recent weight gain is also a common characteristic in newly diagnosed patients (Giuseffi *et al.*, 1991; Friedman and Jacobson, 2002)

The importance of obesity in IIH pathogenesis is also highlighted by the effectiveness of weight loss in improving the disease. Weight loss has been shown to be the most reliable treatment for reducing ICP and improving symptoms and even a small weight loss can yield better results than the most common drug treatment, the carbonic anhydrase inhibitor acetazolamide, alone (Johnson *et al.*, 1998; Kupersmith *et al.*, 1998; Binder *et al.*, 2004; Subramaniam and Fletcher, 2017) In addition, reduction in body weight is the most effective mechanism to eliminate IIH symptoms (Wong *et al.*, 2007; Manfield *et al.*, 2017)

Although there is a strong association between obesity and IIH, it is likely that IIH is caused by a mix of factors, in which obesity would play an important but not exclusive role. Indeed, even if obesity nowadays is a common condition in Europe and North America, IIH

remains a rare disease. Recently, chronic inflammation associated with obesity has been proposed as one of the possible factors for IIH development. However, no definitive association between inflammation and IIH has yet been established (Sinclair *et al.*, 2008; Dhungana, Sharrack and Woodroofe, 2009a).

II. Sex Hormones

Several studies have suggested that sex hormones may also play an important role in IIH development. This is supported by the higher incidence of IIH in adult females, whereas a sex difference is almost non-existent in paediatric patients (Glueck *et al.*, 2005; Fraser *et al.*, 2010; Besch *et al.*, 2012; Sheldon *et al.*, 2016). Many patients have a history of menstrual irregularities and a link has been established between IIH and polycystic ovary syndrome (PCOS), which is a condition characterized by a dysregulation of sex hormones (Glueck *et al.*, 2003, 2005; Hornby *et al.*, 2016; O'Reilly *et al.*, 2019). Numerous cases have been reported of IIH linked to the use of oral hormonal contraception, emergency oral contraception and pregnancy (Giuseffi *et al.*, 1991; Radhakrishnan *et al.*, 1993; Bagga *et al.*, 2005; Zotz, 2015). In addition, at least three cases of secondary intracranial hypertension have been reported in association with testosterone treatment in transgender patients (Park *et al.*, 2014; Bedolla, Buchanan and Hansen, 2017; Hornby *et al.*, 2017).

The study of hormone levels in IIH patients has been a long quest in IIH research. The main impediment for this kind of study is the usual protocol followed for collecting samples from female patients. As IIH is a rare disease, these kind of studies tend to be performed retrospectively using data that was collected when the patient was admitted for treatment, a time at which some practitioners collect blood and CSF samples for analysis. However, with this method, the menstrual cycle of the patient will not be taken into account and samples will be obtained at random days. Reproductive hormone levels of any woman of child-bearing age will greatly vary over the month (Sherman and Korenman, 1975). Therefore, the comparison of hormonal levels in blood and CSF samples of women at different stages of their menstrual cycle will not yield reliable results, as usually concluded by the authors themselves. Nevertheless, the most important conclusions will be reviewed below.

Several studies have demonstrated increased levels of oestrogens in IIH patients compared to a control group (Donaldson and Horakt, 1982; Toscano *et al.*, 1991). However, the stage of the cycle was not taken into account when comparing samples and these studies had a very low number of samples. Recent studies reported that IIH patients had increased concentrations of testosterone in the serum and increased CSF testosterone and androstenedione compared to age-matched controls with either simple obesity or PCOS, a condition which is usually related to obesity and androgen excess (Hornby *et al.*, 2016; O'Reilly *et al.*, 2019).

Following these results, it would be easy to deduce that men should suffer IIH more often due to their higher levels of testosterone, which is not the case. However, it is important to note that androgens exert sexually dimorphic effects in human metabolism, and men with hypogonadism develop similar metabolic phenotypes to women with an excess of androgens (Kautzky-Willer, Harreiter and Pacini, 2016; Schiffer *et al.*, 2017). A possible explanation for the involvement of androgens in IIH is that the IIH symptoms would be triggered by a certain concentration of testosterone rather than simply a very high level; this hypothetic IIH triggering androgen concentration would be higher than the normal levels in females and lower than the normal male concentrations, but closer to the former. Therefore it would be "easier" for females experiencing an increase of androgen concentration to reach that level (O'Reilly *et al.*, 2019). It is important to note that men suffering with IIH tend to be morbidly obese and have larger waist circumference and waist-to-hip ratio than female patients (Schwartz *et al.*, 2013); those characteristics have been linked to decreased androgen levels in men, which supports this hypothesis (Giagulli, Kaufman and Vermeulen, 1994; Allan and McLachlan, 2010). Furthermore, androgen deprivation therapy can increase the chance of developing IIH in men (Valcamonico *et al.*, 2014).

III. Growth Hormone alteration

Growth Hormone (GH) and its primary mediator insulin-like growth factor 1 (IGF-1) are thought to play a role in IIH development because some cases have been reported in individuals following treatment with either of them, especially in children and adolescents

(Darendeliler, Karagiannis and Wilton, 2007; Obinata *et al.*, 2010; Besch *et al.*, 2012). Moreover, Octreotide, a drug that mimics the GH inhibiting hormone, has been effectively used to treat IIH in several patients (House and Stodieck, 2016), including improvement in both symptoms and CSF pressure (Panagopoulos *et al.*, 2007).

IV. Other associated conditions

In addition to obesity and variations in sex hormone concentrations, other conditions and medications have also been associated with increased risk of developing IIH. Some of the diseases most frequently reported are hypothyroidism and lupus erythematosus (Markey *et al.*, 2016; Mollan *et al.*, 2016). Tetracyclines, vitamin A medications and steroid withdrawal have also been associated with increased ICP leading to symptoms similar to those experienced in IIH (Markey *et al.*, 2016). However, cases such as the ones where the ICP can be linked to a specific underlying disease or medication are better described as secondary intracranial hypertension, especially if the symptoms remit after the disease is treated or the medication is withdrawn. These cases can provide an insight into possible mechanisms driving the increase of ICP and can thus be incredibly helpful for IIH research.

1.2.10 Treatment

Current treatments for IIH are palliative and focused on ameliorating symptoms. The main goal after IIH is diagnosed is to preserve the patient's visual function (Wall, 1991; Karmaniolou, Petropoulos and Theodoraki, 2011; Wagner *et al.*, 2016). Overweight patients will be encouraged to lose weight, as it has been shown to be able to improve mild symptoms. However, patients who show intractable headaches and/or optic nerve involvement should be further treated. Treatment options include weight loss, drug therapies, lumbar punctures and surgery.

I. Weight loss

Weight loss improving symptoms on IIH patients was firstly described in 1974 (Newborg, 1974). In most patients, a loss of 6-10% is enough to show papilledema

remission and a decrease in ICP (Rowe and Sarkies, 1999; Daniels *et al.*, 2007). Moreover, some studies have shown that patients that lose weight have a more rapid recovery of visual problems than those who do not (Johnson *et al.*, 1998; Kupersmith *et al.*, 1998; Glueck *et al.*, 2006).

However, not all cases show improvement after weight loss (Panagopoulos *et al.*, 2007; House and Stodieck, 2016). Those cases typically need more aggressive therapies to achieve recovery.

II. Drug therapies

Pharmaceutical treatment of IIH usually involves administration of drugs that reduce CSF production. Among these, acetazolamide, a carbonic anhydrase inhibitor that acts by decreasing Na^+ transport across the CPEC and therefore decreases CSF production, is the most frequently prescribed (Johnson *et al.*, 1998; Wall *et al.*, 2014; Bidot and Bruce, 2015; Supuran, 2015). For individuals who cannot tolerate acetazolamide, other diuretic drugs may be used, such as topiramate, an anti-epileptic drug which possibly reduces CSF production by carbonic anhydrase inhibition and also helps with weight loss (Çelebisoy *et al.*, 2007; Noda *et al.*, 2017; Meibodi *et al.*, 2018).

Patients who develop rapid visual deterioration and do not respond to other types of medication may be administered corticosteroids (Binder *et al.*, 2004; Thambisetty *et al.*, 2007). However, these drugs will not be the first therapy choice due to their side effects, which include weight gain, and also because steroid withdrawal is thought to be related to the development of IIH in some cases (Zadik *et al.*, 1985; Liu *et al.*, 1994).

III. Lumbar puncture

Lumbar puncture is an emergency procedure to relieve ICP acutely (Thambisetty *et al.*, 2007; Obinata *et al.*, 2010; Biousse, Bruce and Newman, 2011). This technique is not desirable to use as a long-term therapy because of their painful nature and difficulties to perform on obese patients (House and Stodieck, 2016). Furthermore, there is little evidence of its efficacy long-term (Yri *et al.*, 2014; Hoffmann, 2019).

IV. Surgery

Surgical treatment is usually contemplated if the patient does not respond to medication or if visual loss is progressing irremediably and the probability of chronic visual problems is increasing. Nowadays the surgery of choice is usually either optic nerve decompression or CSF diversion (Bidot and Bruce, 2015; Wagner *et al.*, 2016).

Optic nerve decompression is usually achieved by performing an optic nerve sheath fenestration (Figure 1.17, left). In this procedure, the surgeon will make an incision in the meninges surrounding the optic nerve, which will relieve the ICP exerted against the nerve. This technique is very effective in reducing papilledema and the patient will usually experience an improvement in their sight. However, the probabilities of experiencing post-operative complications, such as ocular motility disturbance or retinal vascular problems, can be as high as 40% (Moreau, Lao and Farris, 2014; Julayanont *et al.*, 2016).

The most widely performed CSF diversion surgery is lumboperitoneal shunt due to its relative simplicity when compared to other shunt surgeries (Figure 1.17, right) (Tarnaris *et al.*, 2011; Julayanont *et al.*, 2016). In this procedure, a valved tube is implanted to connect lumbar CSF to the abdomen to allow unidirectional flow of CSF into the abdomen (Abubaker *et al.*, 2011; El-Saadany, Farhoud and Zidan, 2012). The patient will show a rapid resolution of ICP soon after shunt surgery. However, there is a high chance of experiencing complications such as problems with the catheter, valve obstruction, shunt infection or overdrainage (Jusué-Torres, Hoffberger and Rigamonti, 2015). Furthermore, this type of shunt is less durable than ventriculoperitoneal ones (a catheter connecting brain lateral ventricles with abdomen) although the insertion surgery is easier to perform (Tarnaris *et al.*, 2011).

In summary, surgery options for IIH patients can be useful in extreme cases but they are not widely used to treat the disease due to increased risk of post-operative complications.

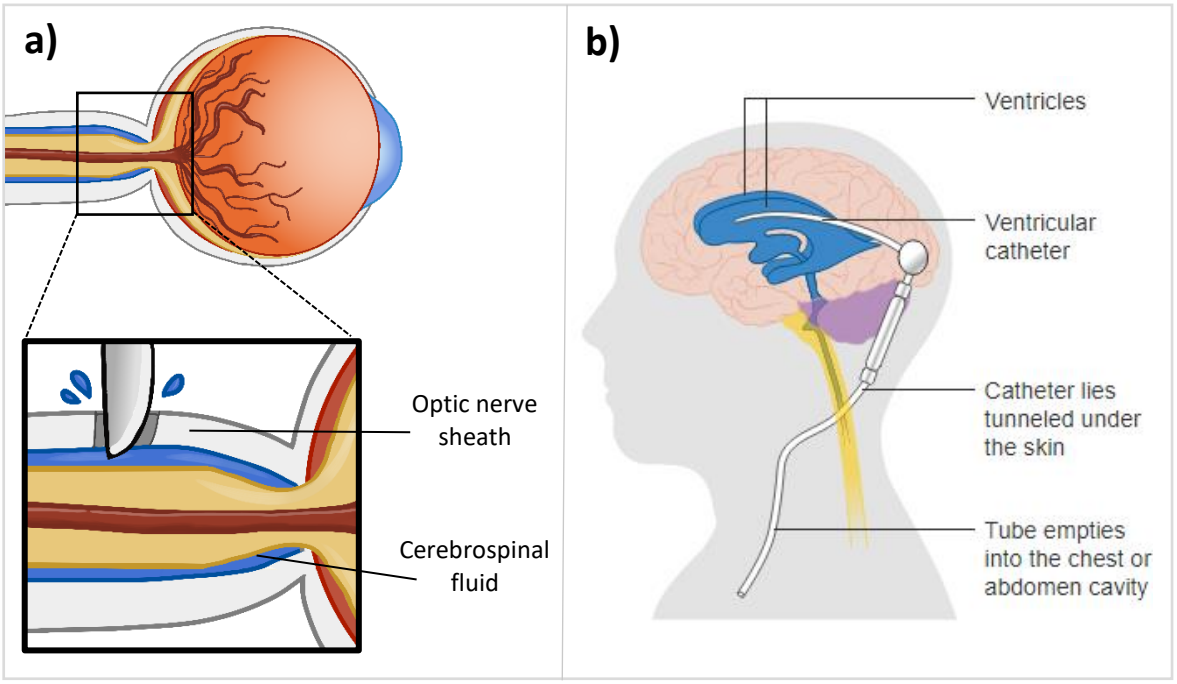

Figure 1.17. Some of the surgery options available for IIH patients.

(a) In the optic nerve fenestration surgery, an incision is made in order to release some CSF and decrease ICP. (b) In shunt surgery, a catheter is inserted into the lateral ventricles which then empties the excess of CSF into the chest cavity or, more commonly, in the abdomen cavity (a by Ester Pascual Baixauli, b) by Cancer Research UK, 2014).

1.2 Cerebrospinal Fluid in Idiopathic Intracranial Hypertension.

1.2.11 Cerebrospinal Fluid Composition in Idiopathic Intracranial Hypertension.

One of the characteristics of IIH is the normal composition of CSF in terms of protein and ion content (Friedman and Jacobson, 2002; Friedman, Liu and Digre, 2013). Ion concentrations in the CSF of 150 mM Na^+, 2.86 mM K^+, 113 mM Cl^- and 23.3 mM HCO_3^- are considered to be within the normal range. Some IIH patients present protein concentrations lower than normal CSF, although this is not considered to be the usual case (Chandra, Bellur and Anderson, 1986; Berezovsky *et al.*, 2017). There have been reported

cases of IIH where the concentration of other components, such as cytokines or hormones, was different from those measured in healthy individuals (Edwards *et al.*, 2013; Samancı *et al.*, 2017; O'Reilly *et al.*, 2019). However, there is no consensus on the concentration of these molecules in the CSF of IIH patients. For example, one study assessing the different levels in serum and CSF of a range of cytokines such as TNF-α, found no significant differences between IIH patients and a group of unmatched controls (Ball *et al.*, 2009). By contrast, another study found that TNF-α concentrations in IIH patients were elevated compared to healthy unmatched controls (Altokika-Uzun *et al.*, 2015). Regarding hormonal concentration, studies are scarce and contradicting. However, two studies have found increased levels of androgens in IIH patients (Hornby *et al.*, 2016; O'Reilly *et al.*, 2019). While the mechanisms by which sex hormones could alter CSF dynamics are unknown, *in vitro* studies have demonstrated that oestrogen and progesterone are able to reduce CSF secretion by the CP while testosterone can increase it (Lindvall-Axelsson and Owman, 1989; O'Reilly *et al.*, 2019).

In summary, there is not a profile yet on CSF composition regarding smaller components, thus further work is needed in this topic.

1.2.12 Cerebrospinal Fluid Dynamics in Idiopathic Intracranial Hypertension

The mechanisms underlying the pathogenesis of IIH remain unknown, however it is probable that the condition is a disorder of CSF dynamics regulation, including CSF secretion and drainage impairments.

I. Cerebrospinal fluid hypersecretion

A significant and sustained increase in CSF secretion has been hypothesised to contribute to the formation of IIH. Some initial perfusion studies suggested CSF hypersecretion as one of the mechanisms in IIH (Donaldson, 1979). However, long-term infusion investigation into CSF hydrodynamics of IIH patients did not find an increase in CSF secretion (Malm *et al.*, 1992). Modern MRI studies have not provided conclusive results either regarding CSF secretion. While some studies noted an increase in aqueductal CSF

flow dynamics which can be directly linked to increased secretion (Akay *et al.*, 2015; Agarwal *et al.*, 2018), others pointed to abnormalities within the CSF fluid cavities rather than increased flow rate as the main differences between patients and controls (Yılmaz *et al.*, 2019). A study by Gideon *et al,* reported the analysis of CSF secretion, flow and of blood flow using velocity mapping MRI in a small number of IIH patients and healthy controls. The authors found a correlation between CSF volume flow amplitude and resistance to CSF outflow (Gideon *et al.*, 1994). While there was no statistically significant difference between mean CSF secretion rates in patients and controls, three of the patients were found to have hypersecretion, and increased CSF transependymal flow in another two (Gideon *et al.*, 1994). While it is not fully understood yet whether CSF hypersecretion occurs, the fact that the most effective drug treatments for IIH, such as acetazolamide and topiramate, act by reducing CSF production, points out to the strong possibility of this mechanism being deregulated and contributing to IIH.

II. Cerebrospinal flow obstructions and malabsorption

MRI imaging studies have found that a considerable number of IIH patients share several characteristics: empty sella, slit-like ventricles, subarachnoid space volume alterations or venous sinus stenosis. While some authors defend that these anatomical alterations are caused by the increase in ICP or that their effects on CSF flow are negligible, others hypothesise that they could be contributing directly to IIH (Higgins *et al.*, 2004; Dykhuizen and Hall, 2011; Zotz, 2015; Morris *et al.*, 2017). Empty sella is a flattening of the pituitary gland caused by an increased in ICP. Empty sella can lead to altered endocrine functions, although in most cases the pituitary gland will continue to work normally despite its appearance (Ranganathan *et al.*, 2013; Saindane *et al.*, 2013). Lateral ventricles are considered slit-like when their walls are collapsed, which decreases their volume. This phenomenon is probably caused by increased ICP or brain edema, although it could contribute to the former (Binder *et al.*, 2004; Degnan and Levy, 2011). In IIH, the subarachnoid cisterns appear tighter while the subarachnoid space surrounding the optic nerve appears distended. The former could be caused by brain edema and contribute to raised ICP, while the latter could be explained by increased ICP (Killer *et al.*, 2007; Bäuerle

and Nedelmann, 2011). Venous sinus stenosis is the narrowing of venous sinus, which could be caused and consequence of higher ICP values, and is hypothesised to strongly contribute to IIH (Bussiere *et al.*, 2010; Dykhuizen and Hall, 2011). According to this hypothesis, the narrowing of dural venous sinuses would increase the pressure inside these vessels. As CSF drainage is thought to be driven by a pressure gradient from the CSF ventricles outwards, this increase in venous pressure would lead to a decrease in CSF drainage, causing a further increase in ICP (Nedelmann, Kaps and Mueller-Forell, 2009; De Simone, Ranieri and Bonavita, 2010). The reason why sinus stenosis would happen is not clear yet; however, some authors claim that this narrowing would be caused by an increase of ICP, therefore hypothesising that venous sinus stenosis is not the original cause of IIH although it can contribute to it (Friedman, 2010; Giridharan *et al.*, 2018). One long-term study of 16 patients with IIH for up to 15 years after onset reported persistent disturbances in CSF hydrodynamics. These disturbances were classified into two categories depending on the identified mechanism: rise of sagittal sinus pressure, whose cause was speculated to be due to extracellular edema causing partial compression of the major venous sinus; or a low conductance of CSF flow coupled with a compensatory increase in CSF pressure in order to sustain the bulk flow (Malm *et al.*, 1992). Venous sinus stenting, which involves surgically widening narrowed venous sinus by introducing a stent, has been suggested as a surgical option for IIH patients whose symptoms are not alleviated by medical therapy, weight-loss regimens or classical surgery options. However, while this procedure has been shown to relieve increased ICP, the patients experienced many post-surgical complications (Bussiere *et al.*, 2010), emphasizing the need for further studies into possible pathogenic mechanisms of IIH.

Other authors point to increased arachnoid resistance to CSF efflux and reduced drainage by arachnoid villi as characteristic phenomenon in IIH patients, which would reduce CSF secretion and contribute to an increased ICP (Malm *et al.*, 1992; Orefice *et al.*, 1992). An impairment in the glymphatic drainage has also been postulated as an influence for increased ICP in IIH (Lenck *et al.*, 2018; Mondejar and Patsalides, 2020). According to this hypothesis, the decrease in drainage through other mechanisms would overflow and congest the glymphatic pathway, causing a diffuse stagnation of flow and solutes in the

interstitium and/or paravascular spaces and contributing to the ICP increase characteristic of IIH. Nevertheless, the glymphatic dysfunction as cause of IIH hypothesis is relatively recent and further investigations are needed in order to further characterise its mechanisms and its influence in the development of IIH.

III. Other factors

It has been hypothesised that IIH is influenced by an increase in intra-abdominal pressure caused by obesity which would then increase venous pressure and alter drainage, as mentioned above (Bloomfield *et al.*, 1997; Sugerman *et al.*, 1997; Sugerman, 2001). Other studies postulate adipokines and other inflammatory mediators typically associated with overweightness as factors for IIH development (Sinclair *et al.*, 2008; Samancı *et al.*, 2017). However, despite the rise in obesity worldwide, IIH remains a rare disease (Mollan *et al.*, 2016; Goudie *et al.*, 2019). Furthermore, its preference for women indicates that IIH pathophysiology might be related not just to the overweightness state but also to the female sex. As a matter of fact, previous studies from our group examining the role of diet and cytokines on CSF secretion rate and resistance to drainage in male and female Wistar rats found increased baseline CSF secretion and reduced CSF drainage rates in female animals fed a high fat diet (Alimajstorovic, Pascual-Baixauli, *et al.*, 2020). These results support a role for obesity and female sex as important contributors to regulation of CSF dynamics. Furthermore, a recent study that found increased levels of androgens in serum and CSF of IIH patients also reported an increase of CSF secretion *in vitro* when CPECs were exposed to testosterone (O'Reilly *et al.*, 2019).

In summary, the exact pathophysiologies underlying IIH are unknown. IIH is likely to be a disorder of CSF dynamic regulation in which CSF secretion and drainage are impaired, and which might be related to obesity and female sex.

1.3 Hypothesis and Objectives

We hypothesise that CSF secretion can be altered by diet-induced obesity and increased inflammatory mediators in the CSF or sex hormones.

The present research was aimed at studying the molecular mechanisms that mediate CSF secretion in the obese rat. In order to do so, four objectives were set:

1. To determine if there is an additive effect of pro-inflammatory and diet-induced obesity on CSF secretion in male rats.

Previous work from our group has shown that CSF secretion is significantly increased in male and female rats fed a diet high in fat (Alimajstorovic, Pascual-Baixauli, *et al.*, 2020). Obesity is associated with chronic low-grade pro-inflammation and increased levels of cytokines have been identified in IIH patients (Dhungana, Sharrack and Woodroofe, 2009a; Edwards *et al.*, 2013; Samancı *et al.*, 2017). Therefore, the first objective of this thesis was to study the effect of hydrocortisone (HC, synthetic cortisol), Tumour Necrosis Factor Alpha (TNFα), Chemokine Ligand 2 (CCL2), Interleukin 6 (IL-6) and Interleukin 17 (IL-17) on CSF secretion in lean and overweight male rats in order to study their effect without interferences from female hormones.

2. To characterise CSF secretion in overweight and obese female rats

It has been shown that administration of a high fat diet to female rats significantly increases CSF secretion in after 7 weeks of feeding (Alimajstorovic, Pascual-Baixauli, *et al.*, 2020). However, more longitudinal studies and analysis of hormone levels have not been conducted. This aim was to assess CSF secretion in female rats fed calorically dense foods to induce obesity.

3. To identify changes in the gene expression profile of the choroid plexus in diet-induced female rats, especially expression of genes associated with CSF secretion

Dietary fat is a known gene expression regulator (Jump and Clarke, 1999; Jump, 2004; Siersbaek *et al.*, 2017). Altered CSF secretion rates could be caused by a change in

gene expression levels of the CP (Janssen *et al.*, 2013; Kant *et al.*, 2018). CP samples of female rats fed a control and calorically dense foods were assessed by RNAseq to determine the molecular changes associated with obesity-induced increase in CSF secretion and validation of protein expression.

4. To investigate the effects of testosterone in an *in vitro* model of CP

Testosterone has been shown to be increased in IIH patients. Furthermore, this hormone increases CSF secretion *in vitro* (O'Reilly *et al.*, 2019). This aim investigated the effects of testosterone on permeability and gene expression in an *in vitro* model of the CP.

Chapter 2. Effect of Diet and Cytokines on Cerebrospinal Fluid Secretion in Male Rats

2.1 Introduction

As mentioned previously, the development of IIH is strongly correlated with being overweight or obese. Obesity is a chronic condition in which there is an excess of accumulated white adipose tissue that may affect health negatively (Kopelman, 2000). This condition is often associated with other problems such as hypertension or glucose intolerance. Obesity has also been linked to predisposition of developing chronic inflammation mainly due to the endocrine properties of adipose tissue. Several studies have demonstrated a connection between obesity and increased levels of pro-inflammatory cytokines such as TNFα, CCL2 and IL6 (Lyon, Law and Hsueh, 2003; Stępień *et al.*, 2014; Ellulu *et al.*, 2017). Therefore, given the association between IIH and obesity, it has been suggested that IIH might be related to a specific inflammatory profile (Sinclair *et al.*, 2008).

Since this association was proposed, many experts in the field have been trying to unravel the possible connection between cytokines and IIH. The current set of experiments focus on the impact of HC (synthetic cortisol), TNFα, CCL2, IL-6 and IL-17 on CSF secretion. It has been reported there is an increase in cortisol levels within CPEC in IIH obese patients (Sinclair *et al.*, 2010). **Table 2.1** shows a summary of the results of concentrations of IL6, IL-17, CCL2 and TNFα in plasma of IIH patients obtained from different studies. Some studies have shown cytokine profiles or inflammation levels in serum and/or CSF specific to IIH, such as increased levels of CCL2 and IL17 in CSF or altered levels of TNF-α in plasma (Edwards *et al.*, 2013; Altıokka-Uzun *et al.*, 2015; Samancı *et al.*, 2017). Others have found no difference in cytokine CSF or plasma levels between IIH patients and control individuals including individuals with headaches, multiple sclerosis and cerebrovascular diseases (Dhungana, Sharrack and Woodroofe, 2009b).

Table 2.1. Cytokine concentration in plasma and CSF of IIH patients.

*Concentrations in IIH patients compared to controls.

--- the cytokine was not measured.

Reference	Methods used	Cytokines in Blood*				Cytokines in CSF*			
		TNFα	CCL2	IL-6	IL-17	TNFα	CCL2	IL-6	IL-17
(ReihaniKer-mani et al., 2008)	ELISA	---	---	---	---	---	---	↑	---
(Ball et al., 2009)	Multiplex bead immunoassay	=	=	=	---	=	=	=	---
(Dhungana, Sharrack and Woodroofe, 2009a)	Semi-quantitative assay, ELISA	---	↑	---	---	---	=	---	---
(Dhungana, Sharrack and Woodroofe, 2009b)	Custom 10-plex assay	=	---	=	↑	=	---	=	=
(Edwards *et al.*, 2013)	Custom 10-plex assay	=	---	=	↑	=	---	=	=
(Altıokka-Uzun *et al.*, 2015)	ELISA	↑	---	---	↑	---	---	---	↑
(Samancı *et al.*, 2017)	ELISA, Multiplex bead immunoassay	=	---	=	---	↓	---	=	---

It has been speculated that cytokines might contribute to the aetiology of IIH by ultimately altering CSF dynamics (Sinclair *et al.*, 2008). However, the physiological impact of cytokines on CSF secretion *in vivo* is not clear. Furthermore, the impact that increased cytokine levels in the CSF can have on CSF secretion itself has not yet been determined.

IIH is highly related to obesity (Friesner *et al.*, 2011; Markey *et al.*, 2016). Previous work by our group investigated the effect of obesity on CSF dynamics in male and female rats, followed by an investigation into the effect of cytokines on CSF dynamics in the context of obesity in female rats (Alimajstorovic, Pascual-Baixauli, *et al.*, 2020). This work led to the finding that female rats fed a HFD had the biggest changes in CSF dynamics when compared to their control group (**Figure 2.1**). It is possible that the effect of cytokines on CSF secretion was masked by female hormones, therefore a study focusing on the effect of diet and cytokines on CSF secretion in the male was necessary in order to determine if those results were specific to females. The present study was a contribution to a larger study that was performed by Dr Alimajstorović (Alimajstorovic, Pascual-Baixauli, *et al.*, 2020) the present research was carried out on male rats.

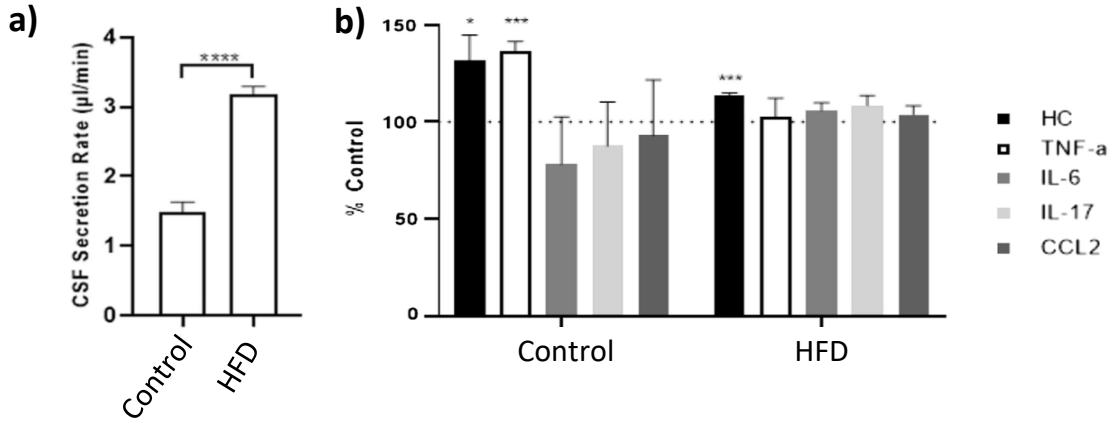

Figure 2.1. Effect of diet and cytokine administration on CSF secretion of female rats.

Female rats were kept under either ND or HFD for seven weeks. CSF secretion was measured by ventriculo-cisternal perfusion of blue dextran. A) CSF secretion rates of rats depending on diet. B) results after treatment with cytokinecalculated as a percentage change from each respective control. Data is shown as average ±SD, n=3. A t-test (a) or two-way ANOVA (b) were used to analyse the statistical significance. *=*P value* ≤ 0.05, ***=*P value*≤ 0.001, ****=*P value* ≤ 0.0001. (Alimajstorovic *et al*., 2020)

The experiments carried out in this chapter were aimed at exploring the effects that HFD and cytokines added to CSF can have on CSF secretion. In order to do that, CSF secretion rates were measured in rats under dietary manipulation. Furthermore, the CSF secretion rates of males with added cytokines into their CSF was also measured.

2.2 Materials and Methods

2.2.1 Materials

All materials used were obtained from Sigma-Aldrich (Poole, Dorset, UK) unless otherwise specified.

2.2.2 Animals

Male Wistar rats were ordered at 4 weeks of age from Envigo (UK) and maintained in the Biological Research Unit at the Open University for 7 weeks on either ND or HFD.

The animals were housed in standard polypropylene cages (three animals per cage) and maintained under controlled humidity (55 ± 5%) and temperature (22 ± 2 ^{o}C) on a 12:12h light and dark cycle. Rats were fed *ad-libitum* and weighed every week. Fresh water was always available for them to drink. Rats were killed by Schedule 1 procedures. All animal work was performed in accordance with Home Office project licence ("Cerebrovascular changes in the aged and diseased brain", PPL number: 70/8507) and with approval from the Open University Animal Welfare and Ethical Review Body.

2.2.3 Dietary manipulation

The ND was the commercially available “Rat and Mouse No. 1 Maintenance Diet”, containing 2.7% fat, 45% carbohydrates and 14.3% protein, purchased from Special Diet Services (SDS, Essex, UK). The HFD diet was the “Rodent Maintenance Atwater Fuel Energy High Fat Diet”, containing 22.6% fat, 39.8% carbohydrates and 23% protein, purchased from SDS, (Essex, UK).

Further information about diet composition can be found in Appendix A(**Table 0.1**, **Table 0.2**).

2.2.4 Preparation of artificial cerebrospinal fluid

Artificial CSF (aCSF) containing 0.5% (w/v) blue dextran was used for the *in vivo* ventriculo-cisternal perfusion (Table 2.2). The final ion concentrations were based on those previously described in the rat CSF (Davson, 1967).

Table 2.2. Composition of aCSF, including the molecular weight (MW) for every compound and their concentration in the aCSF solution.

Compound	Provider	Molecular Weight (g/mol)	Concentration (mM)
Sodium chloride (NaCl)	Sigma-Aldrich, Dorset, UK	58	122
Potassium chloride (KCl)	Sigma-Aldrich, Dorset, UK	74	4
Calcium chloride ($CaCl_2$)	BDH Laboratory Supplies, Dorset, UK	111	1
Magnesium chloride ($MgCl_2$)	Sigma-Aldrich, Dorset, UK	95	1
Sodium bicarbonate ($NaHCO_3$)	BDH Laboratory Supplies, Dorset, UK	84	15
HEPES	Sigma-Aldrich, Dorset, UK	238	15
Disodium phosphate (Na_2HPO_4)	Sigma-Aldrich, Dorset, UK	142	0.5
Glucose	Sigma-Aldrich, Dorset, UK	180	17.5
Blue dextran	Sigma-Aldrich, Dorset, UK	2,000,000	0.0025

To study the effect of cytokines on CSF secretion, aCSF was supplemented with one specific cytokine for each experiment at the concentration indicated in Table 2.3 as based on literature reports.

Table 2.3 Concentration of treatment of interest in aCSF for ventriculo-cisternal perfusion.

Treatment	Dose	Reference
Hydrocortisone (HC)	500 ng/ml	Sinclair et al., 2010
Tumour Necrosis Factor Alpha (TNFα)	0.1 ng/ml	Hayakata et al., 2004
Chemokine Ligand 2 (CCL2)	50 ng/ml	Dhungana, Sharrack, & Woodroofe, 2010
Interleukin 6 (IL-6)	0.1 ng/ml	ReihaniKermani, Faramarzi, Ansari, & Ghafarinejad, 2008
Interleukin 17 (IL-17)	0.1 ng/ml	Li, Yu, Li, Zhang, & Jiang, 2012

2.2.5 Ventriculo-cisternal perfusion

CSF secretion rate was measured by performing the ventriculo-cisternal perfusion technique in the brain of anaesthetised living rats (Davson *et al.*, 1982; Oreskovic *et al.*, 2003). Before starting the procedure, the rat was introduced to an inhalation chamber where 4% isofluorane inhalation vapour (Merial Animals Health, Essex, UK) mixed with oxygen at 3.5l min^{-1} was administered for 5 minutes. A dose of 20µl/100g weight of Domitor (medetonidine hydrochloride) and 50µl/100 g weight of Vetalar (ketamine) (both supplied by the Home Office Named Veterinary Surgeon, Red Kite Veterinary Consultants Centaur Services, Castle Cary, UK) were administered by intraperitoneal injections on both sides of the animal. The rat was again put in the inhalation chamber with 2% isofluorane inhalation vapour mixed with oxygen at 2.5 l min^{-1} for 5 further minutes to potentiate the action of the injectable anaesthetic. After that, the animal was removed from the chamber and laid on a warm pad to maintain constant body temperature throughout the procedure. Once an anaesthetized rat did not respond to reflex-inducing external stimuli (i.e. toe pinch) for more than 2 minutes, it was mounted into a stereotaxic frame (Kopf Instruments, Los Angeles, USA). Using a scalpel, a midline incision was made in order to expose the top of the skull. A 0.65 mm hand-chuck drill (Farnell Element, Leeds, UK) was used to drill bilateral holes above the lateral ventricles, followed by insertion of two metal cannulae with a

diameter of 0.6 mm (0.8 mm posterior, 1.5mm laterally either side, 4mm depth, relative to Bregma). Both cannulae were attached to a water manometer. A drop in pressure when the cannulae were in place confirmed correct positioning within the ventricle. Simultaneous perfusion of both lateral ventricles with aCSF containing Blue Dextran using a Harvard slow-drive syringe pump (Harvard Apparatus UK, Cambridge, UK) was started immediately and taken as time zero of the experiment.

The experiments were carried out using aCSF with or without cytokine of interest (Figure 2.2). The perfusion was performed for a period of 90 minutes per animal. Two 10 ml syringes, one for each ventricle, with a diameter of 14.5 mm, were used. Perfusion inflow rate of aCSF was 20 µl min^{-1} for each ventricle for the first 20 minutes and 10 µl min^{-1} for the remaining 70 minutes. The experiment started with a period of 20 minutes when the aCSF was perfused at a higher rate in order to remove possible blood clots resulting from cannulae insertion and to rapidly flush out endogenous CSF.

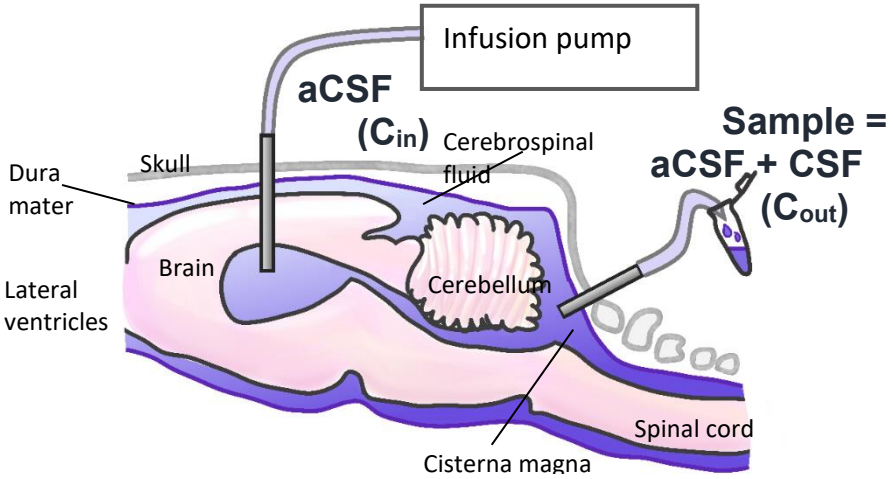

Figure 2.2 *In vivo* experiment of ventriculo-cisternal perfusion in male adult Wistar rats.

aCSF (containing blue dextran) was perfused into each lateral ventricle of the rat brain. Samples were collected every 10 min for a period of 90 min from the cisterna magna. Each sample was analysed by reading the absorbance at a 625 nm wavelength on a spectrophotometer (C_{in} for initial aCSF, C_{out} for Sample). The dilution of the blue dextran within the aCSF in each sample indicates CSF secretion over the course of the experiment (Diagram by Ester Pascual-Baixauli)

A 1 mm diameter blunt needle was inserted into the cisterna magna for collection of CSF. The needle was attached to a 5 cm piece of tubing with a 1 mm bore (Altec Products Ltd, St Austell, UK). The insertion point was determined by locating the base of the occipital bone, at the back of the exposed rat skull. The subarachnoid membrane was pierced below the bone and the needle was inserted into the subarachnoid space in the cisterna magna. Correct positioning was confirmed by immediate visualisation of flowing CSF through the needle into the tubing. CSF samples from the cisterna magna were collected over 10-minute periods during the whole experiment and then stored in ice for further analysis. The amount of dextran in each sample was measured using a spectrophotometer (Fluostar Optima, BMG labtech, Aylesbury, UK) at 625nm wavelength.

The CSF secretion rate was calculated from the samples collected once the initial endogenous CSF had been removed. This was determined by establishing the steady state. In order to do so, the absorbance value of each sample was divided by the absorbance value of the initial aCSF (Equation 2.1), and the results were plotted. The steady state was determined when a plateau was reached.

Equation 2.1. Steady state calculation.

$$\boldsymbol{aCSF\ Sample\ Steady\ State} = \frac{\boldsymbol{C_{out}}}{\boldsymbol{C_{in}}}$$

Where:

- C_{out}= Absorbance value of sample (composed of aCSF and CSF)
- C_{in} = Absorbance value of aCSF.

The CSF secretion rate was calculated using Equation 2.2. The final calculation of secretion rate of the individual was an average of secretion rates measured from samples in the steady state.

Equation 2.2. CSF Secretion rate calculation.

$$\boldsymbol{SR} = \frac{\boldsymbol{C_{in}} - \boldsymbol{C_{out}}}{\boldsymbol{C_{out}}} \cdot \boldsymbol{PR}$$

Where:

- SR = CSF secretion rate (µl min^{-1})
- C_{in} = Absorbance value of aCSF.
- C_{out} = Absorbance value of sample (composed of aCSF and CSF)
- PR = Perfusion rate (µl min^{-1}); Sum of the inflow rate of both syringes used.

The initial volume of endogenous CSF was calculated by multiplying the CSF secretion rate from each sample by the period the animal was perfused in order to obtain that sample, adding up the results from all the samples, and then subtracting the CSF secreted during the time the experiment was running (Equation 2.3).

Equation 2.3.Calculations of initial CSF volume.

$$\boldsymbol{Initial\ CSF\ Volume\ (\mu l) = \quad V_T - \quad V_S}$$

$$\boldsymbol{V_T = \sum_{10}^{1} (SR_n \cdot T_n)}$$

$$\boldsymbol{V_S = SR_{Av} \cdot T}$$

Where:

- V_T = Total volume (µl) of endogenous CSF measured during the whole experiment.
- V_s= Volume (µl) of CSF secreted while the experiment was running.
- SR_n= CSF secretion rate (µl min^{-1}) calculated from a specific sample
- T_n= Duration of a specific sample collection (min)
- SR_{Av}= Average CSF secretion rate (µl min^{-1}) at the steady state.
- T= Duration of the experiment (min).

2.2.6 Statistical analysis

Each group had three individuals (n=3) and all results are presented as average ± SEM unless otherwise specified. Normal distribution of data was confirmed by Q-Q plot.

Differences in weight gain and CSF between ND and HFD at individual time points were analysed using a one way repeated measures ANOVA with Tukey post hoc to control for repeated sampling of the same animal across multiple time points. The final weight and differences in CSF secretion were analysed by two-tailed t test while the changes due to cytokine administration were analysed by a one way ANOVA with Tukey post hoc. The relationship between two parameters was measured using the Pearson correlation coefficient (r), where a coefficient higher than 0.6 and a significant *P* value was considered a strong correlation. A *P* value < 0.05 was considered significant. Statistical analysis was performed using IBM SPSS Statistics (IBM Corporation, 2017), JASP (JASP Team, 2019) and GraphPad (Graphpad Software, 2019).

2.3 Results

2.3.1 Animal model: diet and weight

To study the effects of obesity on CSF secretion, rats were fed either ND or HFD *ad libitum* for 7 weeks starting at 4 weeks of age. The mean weights for ND and HFD rats over time are shown in Figure 2.3. Weight increased with time in both groups ($F(1.682, 35.322) = 623.662$, $P < 0.001$) although the increase was significantly greater in the HFD group compared to ND-fed rats ($F(1.682, 35.322) = 14.925$, *P value* < 0.01).

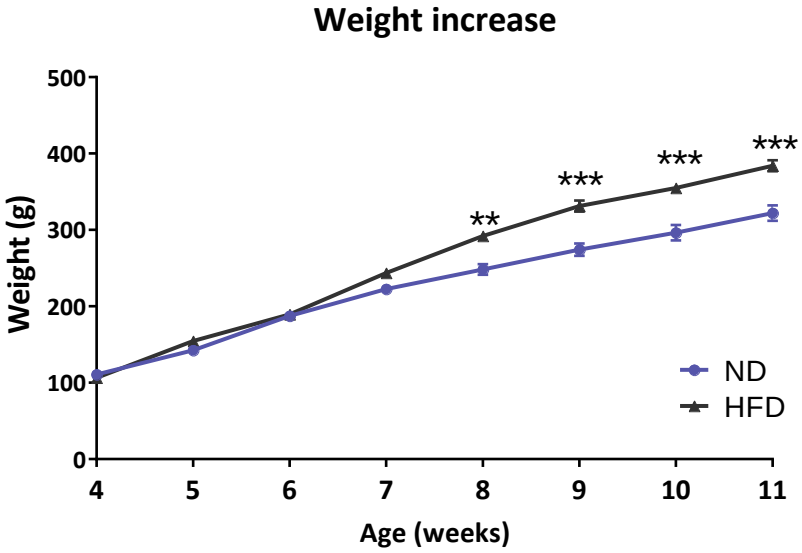

Figure 2.3 Weight of male rats on ND or HFD over a seven-week period.

Rats were obtained at 4 weeks of age and kept under either ND or HFD for 7 weeks. Weights were recorded weekly. Data is presented as average±SEM ND n=5, HFD n=18. A one-way repeated measures ANOVA was used to test the statistical significance of the change over time. Statistical differences between groups at each time point were tested using Tukey Post Hoc test. n=3, **= *P value* <0.01, *** = *P value*<0.001

Although both groups had similar weights when they started the respective diets, the final weight of rats under ND was 290.36 ± 1.74% of their initial weight, while rats under HFD weighed 361.94 ± 8.06% of their initial weight after 7 weeks under the diet (**Figure 2.4**).

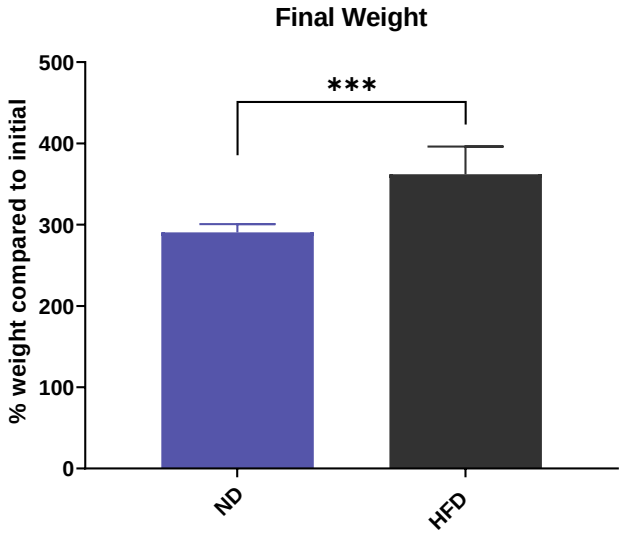

Figure 2.4 Final weight comparison between ND and HFD rats.

Rats were obtained at 4 weeks of age and kept under either ND or HFD for 7 weeks. Data is calculated as percentage of final weight compared to initial weight and it is presented as average±SEM ND n=5, HFD n=18. A t-test was used to test statistical difference between groups. n=3, *** = *P value*<0.001

2.3.2 Effect of Diet on Cerebrospinal Fluid Secretion Rates

I. Steady state determination

To determine whether diet-induced obesity affects the dynamics of CSF secretion and volume, ND and HFD rats underwent ventriculo-cisternal perfusion as adapted from Oreskovic et al. 2003. Endogenous CSF was flushed and a steady state of CSF secretion was determined. The steady state was typically reached within 20 minutes of the start of the experiment (Figure 2.5) and, while C_{out}/C_{in} values obtained for the whole experiment changed over time, ($F(9, 36)=508.638$, *P value* < 0.001), values obtained during the steady state were not altered across the perfusion time ($F(6, 24)=0.711$, *P value* > 0.05). Diet did not affect C_{out}/C_{in} values ($F(9, 36)=1.993$, *P value* > 0.05).

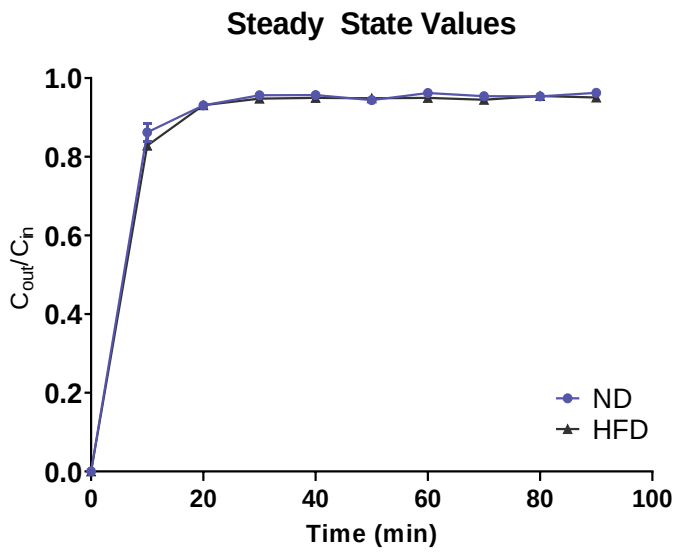

Figure 2.5 Steady state determination using C_{out}/C_{in} values.

C_{out}/C_{in} values were calculated using Equation 2.1. Steady state determined from C_{out}/C_{in} values was used to select which samples could be used for CSF secretion rate calculations. Data represented as average ±SEM, n=3. A one-way repeated measures ANOVA was used to test the statistical significance of the change over. Statistical differences between groups at each time point were tested using Tukey Post Hoc test. n=3

II. Cerebrospinal fluid secretion rate

The absorbance values of the perfusate samples collected from the cisterna magna at steady state were then used to calculate CSF secretion rates for each diet. As shown in **Figure 2.6**, the secretion rate in rats fed with ND was significantly lower than those fed the HFD.

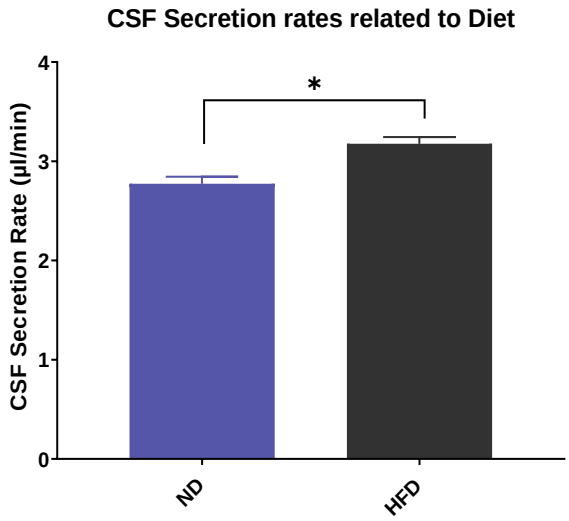

Figure 2.6 CSF Secretion rates in male Wistar rats.

CSF secretion rates were calculated by averaging secretion rates once the steady state was reached. Data shown as average ±SEM, n=3. A t-test was used to test statistical difference between groups. * = *P value*<0.05

CSF secretion rates were plotted against final weight in order to evaluate a possible relationship between the two values (**Figure 2.7**). Although there was a trend towards a positive correlation between rat weight and rate of CSF secretion, it did not reach statistical significance (r=0.78, *P value*>0.05).

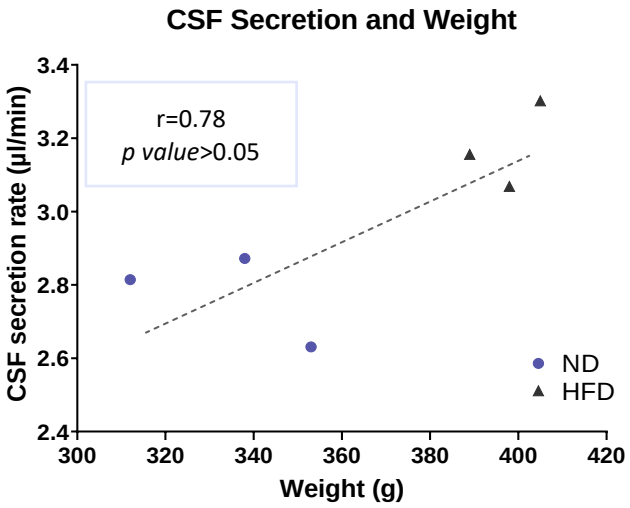

Figure 2.7. Correlation between CSF secretion rate and weight in male rats.

CSF secretion rate was measured using the ventriculo-cisternal perfusion technique. Weight measurement was taken on the day of the surgery. Data was analysed with Pearson correlation. n=3

III. Initial Cerebrospinal Fluid Volume

Because higher CSF volume is one of the main characteristics of IIH (Friedman and Jacobson, 2002), the initial volume of endogenous CSF was also calculated. The initial volume of CSF was calculated using **Equation 2.3** and is represented in **Figure 2.8**. Initial CSF volume in ND rats was significantly lower than in HFD rats.

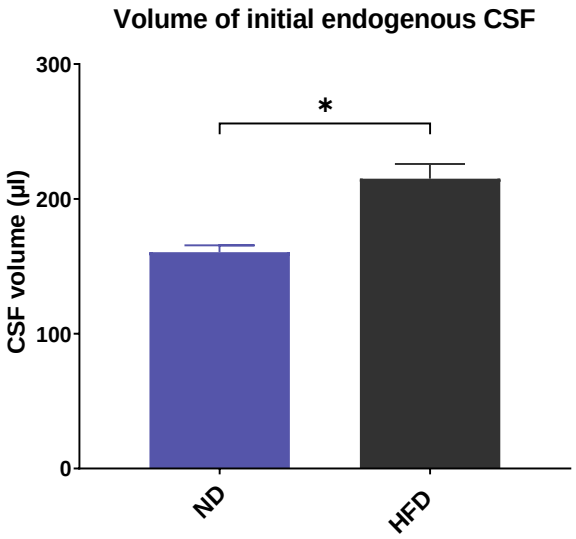

Figure 2.8 Initial CSF volume in male Wistar rats.

Initial endogenous CSF volume was measured using the ventriculo-cisternal perfusion technique. Data shown as average ±SEM, n=3. A t-test was used to test statistical difference between groups. * = *P value*<0.05.

Endogenous CSF volume was plotted against weight to evaluate a possible relationship (**Figure 2.9**). There was a significant correlation between these two values (r=0.85, *P value* <0.05).

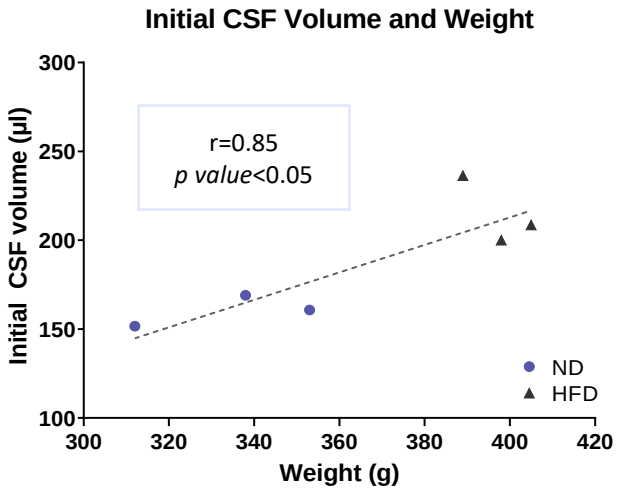

Figure 2.9. Initial endogenous CSF volume versus weight.

Initial endogenous CSF volume was measured using the ventriculo-cisternal perfusion technique. Weight measurement was taken on the day of the surgery. Data was analysed with Pearson correlation. n=3

2.3.3 Effect of diet and cytokine administration on CSF secretion.

To investigate the effects of cytokines on CSF secretion in the presence of obesity, the ventriculo-cisternal technique was repeated but in this case the perfused aCSF was supplemented with various cytokines as stated in Table 2.3.

I. Steady state determination

The steady state determination calculations were performed for all rats in order to be able to select the appropriate samples for CSF secretion calculations. As in the previous experiment, the steady state was typically reached after 20 minutes (**Figure 2.10**).

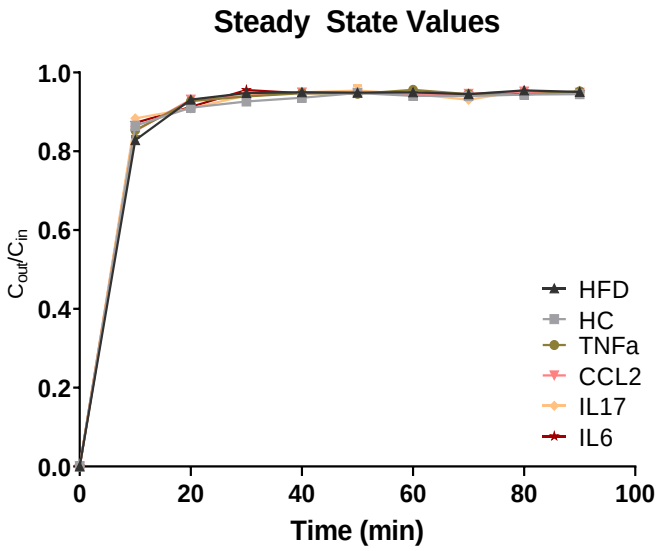

Figure 2.10. Mean steady state values for each cytokine treatment.

C_{out}/C_{in} values were calculated using Equation 2.1. Steady state determined from C_{out}/C_{in} values was used to select which samples could be used for CSF secretion rate calculations. Data represented as average ±SEM, n=3. A one-way repeated measures ANOVA was used to test the statistical significance of the change over time. Statistical differences between groups at each time point were tested using Tukey Post Hoc test.

There was a variation related to time on C_{out}/C_{in} values for all treatments ($F(2.559, 30.712)=1764.026$, *P value* < 0.001). However, treatment did not specifically alter these values ($F(12.797, 30.712)=1.205$, *P value* > 0.05). Cytokine treatment did not alter CSF secretion rates at any time point during the steady state period ($F(3.822, 45.867)=1.146$, *P value* > 0.05).

II. Cerebrospinal fluid secretion rate

The CSF secretion rates of rats fed HFD in the presence of different cytokines were measured and are shown in **Figure 2.11**.

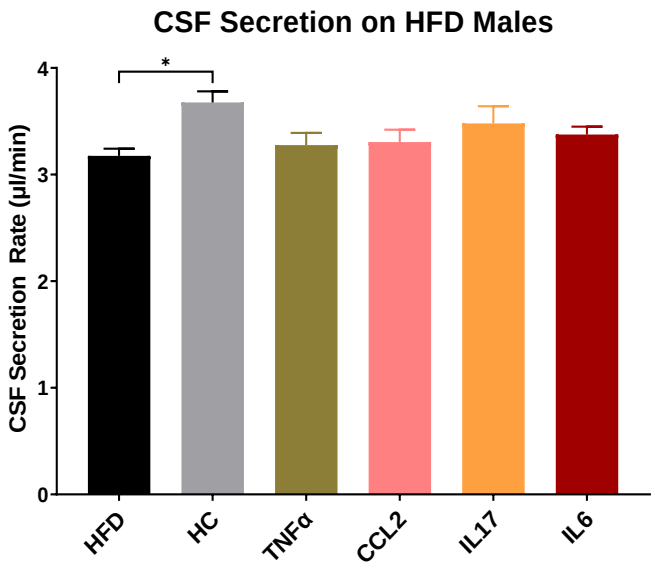

Figure 2.11. CSF Secretion rates in male Wistar rats under HFD and different treatments using ventriculo-cisternal perfusion.

Data shown as average ±SEM, n=3. A one-way ANOVA was used to test statistical difference HFD and each treatment. n=3, * = *P value*<0.05

Rats perfused with HC showed higher rates of CSF secretion compared to untreated HFD-fed rats. Although administration of other cytokines caused a small fluctuation in CSF secretion rates, none were statistically significant compared to untreated HFD-fed rats.

III. Initial Cerebrospinal Fluid Volume

As explained previously, cytokines were administered with the aCSF during the ventriculo-cisternal perfusion, therefore it could not affect initial endogenous CSF volume. However, it is important to calculate the initial volume of the CSF in the rats in order to assess inter-individual variability and confirm the absence of underlying disturbances in CSF dynamics that could affect the results; a significantly higher initial CSF volume could indicate an underlying impairment between CSF secretion and drainage which would affect the results of the experiment.

The initial CSF volume was calculated and compared between the rats prior to treatments to determine if CSF was building up inside the skull. The initial volume for each group was calculated following **Equation 2.3** and is represented in **Figure 2.12**.

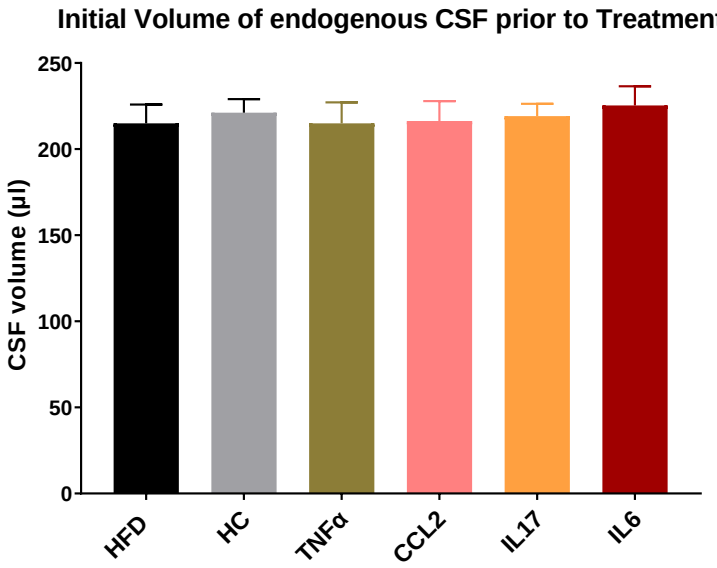

Figure 2.12 Initial CSF volume in male Wistar rats using ventriculo-cisternal perfusion before treatment. Rats were obtained at 4 weeks of age and kept under either ND or HFD for 7 weeks. Initial endogenous CSF volume was calculated using the ventriculo-cisternal perfusion technique. Data shown as average ±SEM, n=3. A one-way ANOVA was used to test statistical difference HFD and each group.

There was no significant difference in initial volume of CSF among any of the groups when compared to the control.

2.4 Discussion

IIH is a neurological condition which typically affects overweight or obese adults and its main characteristic is an excess of intracranial pressure (ICP) for unknown reasons. ICP can be raised by different mechanisms, such as impaired CSF dynamics and increased CSF secretion. Some studies have found that IIH patients have altered cytokine levels in CSF (Dhungana, Sharrack and Woodroofe, 2009a; Edwards *et al.*, 2013; Samancı *et al.*, 2017). The present study hypothesised that overweightness is associated with increased CSF secretion rates, and increased levels of some specific cytokines in CSF could potentiate this

difference. The results of the present study suggest that overweightness can increase CSF secretion rates; only the addition of HC into CSF in HFD-fed rats increased these rates further.

In order to study IIH, it was essential to use an overweightness animal model and compare it to a lean control group. IIH patients have also typically gained a high percentage of body weight over the year prior to diagnosis, which is why it is important to compare weight gain with respect to the individual initial weight between overweight and lean groups when studying this condition (Daniels et al., 2007).The statistically significant difference between the final weight as a percentage of starting weight for animals fed ND and HFD allows the consideration of HFD rats as overweight for the purposes of this experiment.

In order to perform an accurate calculation of CSF secretion using the ventriculo-cisternal perfusion technique, it is essential to properly determine when the steady state is reached and only use the values obtained during that state (Davson *et al.*, 1982; Oreskovic *et al.*, 2003). The steady state is characterised by a stability on C_{out}/C_{in} values. While these values increase directionally at the beginning of the experiment due to the presence of endogenous CSF, they must remain invariable during the rest of the experiment to allow for accurate calculations. During these experiments, C_{out}/C_{in} values increased greatly at the beginning, as expected. They also presented a steady state, thus allowing for proper measurements. There was no statistical difference on C_{out}/C_{in} values related to diet.

An increased CSF secretion rate and initial CSF volume related to HFD was observed. Since HFD also increased weight gain and final body weight as expected, it was necessary to explore a possible relationship between these parameters and CSF secretion and initial volume. There was no significant correlation between CSF secretion and body weight. There was however a strong positive correlation between initial CSF volume and weight. In humans, CSF pressure has been shown to have a positive correlation with overweightness (Berdahl *et al.*, 2012; Ren *et al.*, 2012). While CSF volume was not measured in these clinical studies, increased CSF volume can cause increased CSF pressure; therefore, these patients might also have had increased CSF volume.

It is known that obesity increases the concentration of some cytokines but, according to some studies, IIH patients show a specific cytokine concentration pattern both in blood and CSF (Dhungana, Sharrack and Woodroofe, 2009b; Edwards *et al.*, 2013; Shaw *et al.*, 2014; Samancı *et al.*, 2017). However, authors have yet to agree on a specific pattern. Some authors have reported different cytokine patterns on CSF or blood of IIH patients (Edwards *et al.*, 2013; Altıokka-Uzun *et al.*, 2015; Samancı *et al.*, 2017), while others found no differences between patients and controls (Dhungana, Sharrack and Woodroofe, 2009b). Such discrepant and sometimes conflicting results point to the probable heterogeneity of the condition. It is possible that what is nowadays considered to be IIH will, in the future, be categorised into several different conditions depending on their pathophysiology or other differentiated characteristics of which we are not yet aware. Furthermore, the use of various different techniques with distinct detection limits may account for discrepancies in results. Furthermore, different patterns of deregulated cytokines could have similar causes and/or end up causing the same consequences. While this might also indicate that a similar treatment could have positive effects for patients with different etiologies of IIH, this is just a speculation and no evidence has been obtained yet pointing to this direction. On the other hand, if IIH patients can eventually be classified into several distinct conditions in need of different treatments, the rarity of these diseases would increase exponentially, increasing also the difficulties to overcome when studying them, including lack of funding and shortage of patients to study. At the moment however there is no research in this specific direction.

While obesity also increases cytokine concentration (Shaw *et al.*, 2014), the specific patterns mentioned in the previous paragraph could be related to IIH pathophysiology either causally or consequentially. The present study was designed to investigate the effect of increased cytokine levels in CSF in combination with overweightness on CSF secretion, which is thought to be one of the mechanisms by which ICP is increased in IIH (Sinclair *et al.*, 2008). Several cytokine treatments, as well as a HC treatment, were selected on the basis of published studies of cytokine and cortisol levels in IIH patients, and were added individually at clinically relevant concentrations to the artificial CSF that was perfused during the ventriculo-cisternal technique.

HC was the only cytokine that caused a significant change in CSF secretion when compared to control rats. HC has been previously reported to increase CSF secretion in females (Alimajstorovic, Pascual-Baixauli, *et al.*, 2020). In the literature, there have been several cases of IIH related to acute steroid withdrawal (Zada *et al.*, 2010; Wagner *et al.*, 2016), while other studies report increased cortisol in IIH patients and decreased cortisol levels in patients under weight management treatments (Tomlinson *et al.*, 2004; Pollak *et al.*, 2015). While HC has not been reported as an altered cytokine in CSF of IIH patients, the fact that it was able to increase CSF secretion matches a case report recently published (Mohammad *et al.*, 2019). A 19-year-old man presented headaches and pulsating tinnitus for 2 months. He also presented normal brain venography and optic disc swelling; CSF pressure was not measured but a case of IIH was suspected. However, there was an underlying treated condition that might have been causing the symptoms: the patient had been previously diagnosed with psoriasis for which he had been applying topical HC three to four times a day. IIH symptoms started showing after the patient had started this treatment, and they improved after treatment with acetazolamide for increased ICP and cessation of topical hydrocortisone. This case, although rare, is very interesting because it is the first reported case that links overuse of topical steroids with IIH symptoms, and also matches the results of the present research: in both cases, HC lead to altered CSF dynamics.

The approach of studying the effect of one cytokine at a time was selected in order to simplify experiments and be able to distinguish the effect a certain cytokine will have on CSF secretion; thus the interaction between the effects of different cytokines was not explored. The fact that IIH could show a specific pattern of cytokine levels might indicate that the final effect is produced by a combination of these mediators, thus an additional study investigating this possibility further would be beneficial.

In conclusion, HFD was related to higher weight, higher initial volume of endogenous CSF and also higher rates of CSF secretion, which match with the typical IIH patient and one of the possible causes for such increased ICP. In HFD rats, only HC increased CSF secretion rates, which could be relevant for understanding how topical HC could alter CSF dynamics in a case study (Mohammad *et al.*, 2019) . In the future, performing a study

including more biological replicates or different diets would be appropriate in order to further investigate the relationships between weight, CSF volume and CSF secretion. Nonetheless, and also taking into account the results obtained by Dr Alimajstorović (Alimajstorovic, Pascual-Baixauli, *et al.*, 2020), the focus of our project was switched to a more promising animal model. The subsequent research activities were designed to explore the molecular and physiological mechanisms by which female sex coupled with a HFD was able to alter CSF secretion so extremely *in vivo*.

Chapter 3. Characterisation of the Effect of High-Fat Diet on Physiological Functions and Cerebrospinal Fluid Secretion in Female Rats

3.1 Introduction

In preclinical biomedical research, the preference of using male animals over females is, unfortunately, a reality. Moreover, many papers fail to report the sex of the subjects or cells used, making it impossible to assess whether their results were influenced by sex (Mogil and Chanda, 2005; Zucker and Beery, 2010; Beery and Zucker, 2011; Itoh and Arnold, 2015). These issues raise the concern that previous scientific findings might actually just apply to male individuals. The bias over the use of male animal models is usually a product of the common assumption that female individuals are more variable due to the oestrous cycle. However, recent research has shown that hormone levels in female rodents are not more variable than males and, under some conditions, males are more variable than females (Prendergast, Onishi and Zucker, 2014; Becker, Prendergast and Liang, 2016; Smarr, Rowland and Zucker, 2019). It is thought that male variability is mainly caused by the dominance hierarchy established in group-housed male rodents, while female variability is due to the oestrous cycle (Selmanoff, Goldman and Ginsburg, 1977; Machida, Yonezawa and Noumura, 1981; Henry, Meehan and Stephens, 1982). Our research was carried out in female rodents because of the female sex being an important risk factor for IIH development, as mentioned in Chapter 1, but also to explore further the effect of a high fat diet on different body parameters in the female.

The oestrous cycle in the rat has been shown to affect many aspects of the individual ranging from effects of opioids to the stress response in critical situations, therefore, cycle monitoring is essential in order to reduce bias of research results (Pfaff, 1970; Eliasson and Meyerson, 1975; Roberts, Bennett and Vickers, 1989; Marcondes *et al.*, 2001; Terner, Lomas and Picker, 2005; Friesner *et al.*, 2011). The typical young adult female Wistar rat has a weight ranging between 250 and 300g and an oestrous cycle lasting between 4 and 5 days (Rivest, 1991; McCutcheon and Marinelli, 2009; Sengupta, 2013).

The rat oestrous cycle can be divided into four clearly identified stages. The cycle starts with proestrus, lasting around 12 hours, which corresponds to the onset of mating behaviour. This behaviour includes increased running activity, hopping, and the oestrus dance, which features freezing and ear quivering when handled (Stramek, Johnson and Taylor, 2019). In proestrus there is an increase in levels of prolactin, luteinizing hormone (LH) and follicle-stimulating hormone (FSH) coupled with the beginning of ovulation. Elevated levels of these hormones persist until the end of the next stage, oestrus, which lasts 26 hours. Metoestrus, the next stage, takes around 8 hours and it is followed by dioestrus which can last up to 50 hours and is the stage at which the sex hormones are at their lowest levels (Feder, 1981; Westwood, 2008; Stramek, Johnson and Taylor, 2019). The gold standard for cycle monitoring is by cytologic analysis of vaginal lavage samples. Each stage of the cycle is characterised by different proportions of nucleated cells, cornified cells and leucocytes evident in the lavage (Westwood, 2008). Furthermore, the oestrus dance has been shown to be very effective for cycle monitoring due to its specificity: this behaviour only appears at the beginning of the proestrus, which usually starts with the dark period of the day. The simultaneous use of both vaginal cytology and detection of the oestrus dance increases the reliability of the cycle monitoring (Westwood, 2008; Stramek, Johnson and Taylor, 2019).

Diet has been proven one of the most important environmental factors in health and disease, and it can also impact health state of offspring (Ng *et al.*, 2010; Jakobsdottir *et al.*, 2013; Nizari, Carare and Hawkes, 2016; Contu and Hawkes, 2017). A diet high in fat can affect many metabolic and physiological processes such as reproduction, energy storing, feeding behaviours and cholesterol level (Corbit and Stellar, 1964; Akiyama *et al.*, 1996; Buettner *et al.*, 2006; Aubin *et al.*, 2008; Aslani *et al.*, 2015; Bazzano *et al.*, 2015). Diet can directly impact adiposity and obesity, which is a risk factor for IIH. Increased adiposity is linked to cholesterol problems, specifically an excess of low-density lipoproteins (LDL) and a reduction of high-density lipoproteins (HDL) (Tchernof and Després, 2013). While cholesterol is a necessary molecule for many biological processes, an imbalance of LDL/VLDL and HDL can have a negative impact on cardiovascular health

(Kannel, 1983; Jakobsdottir *et al.*, 2013; Martins *et al.*, 2015). However, the impact of cholesterol on CSF dynamics is unknown. Adiposity can also alter sex hormone levels, which in their turn might be linked to other altered parameters, such as CSF secretion.

The aims of this chapter were to determine the effect of a diet high in fat on female rats, specifically on: feeding and drinking behaviour; physiological effects including weight, plasma cholesterol concentrations and sex hormones; and rates of CSF secretion. In order to study this, rats were divided into two groups depending on the length of dietary manipulation, and further divided into smaller subgroups depending on the type of diet used.

3.2 Materials and Methods

3.2.1 Materials

All materials used were obtained from Sigma-Aldrich (Poole, Dorset, UK) unless otherwise specified.

3.2.2 Animals

Female Wistar rats were obtained from Envigo (Bicester, UK) at 4 weeks of age and maintained in the biological research unit of the Open University for either 7 or 11 weeks.

The animals were housed in standard wiretop ventilated polypropylene cages in groups of three to four within larger cabinets (Scantainer, Scanbur, Denmark). Four males housed in groups of two were also present in the Scantainer to keep female rats cycling normally. Rats were maintained under controlled humidity (55 ± 5%) and temperature (22 ± 2°C) on a 12:12h light and dark cycle. Fresh water was always available for them to drink. All animal work was performed in accordance with Home Office project licence ("Cerebrovascular changes in the aged and disease brain", PPL number: 70/8507) and with approval from the Open University Animal Welfare and Ethical Review Body.

3.2.3 Dietary manipulation

The study was separated into two different groups depending on age: a first group was kept until they were 11 weeks of age (11w) and they were fed either ND or HFD for 7 weeks; and a second group that was kept until they were 15 weeks of age (15w) that was fed either ND or HFD for 11 weeks, with an additional HFD group supplemented with peanut butter (HFD+PB) from weeks 7-11.

ND was the commercially available "Rat and Mouse No. 1 Maintenance" in pellets, containing 2.7% fat, 45% carbohydrates and 14.3% protein, purchased from SDS (Essex, UK). The HFD used was the commercially available "Western Rodent Diet", containing 21.4% fat, 50% carbohydrates and 17.5% protein, purchased from SDS (Essex, UK). The HFD+PB diet was the "Western Rodent Diet" supplemented with approximately 8g of peanut butter (PB) per cage each day. The PB was the commercially available "Grandessa Peanut Butter Crunchy", containing 50% fat, 13% carbohydrates and 26% protein, purchased from Aldi, UK.

Further details about dietary components and ingredients can be found on Appendix A (**Table 0.1**, **Table 0.3**, **Table 0.4**)

Rats were fed *ad-libitum* and weighed every week. Water intake was recorded daily and food consumption was recorded weekly except for the peanut butter supplement, which was refreshed and recorded daily. All consumption was recorded per cage and further calculations are described in section 3.2.4.

3.2.4 Food, water and caloric intake calculations

Absolute food intake (FI) and absolute caloric intake (CI) were calculated using **Equation 3.1**. Values were corrected to represent daily intake. Caloric intake of rats on a HFD+PB diet was calculated by adding the caloric value of the amount of PB added.

Equation 3.1. Calculation of food and caloric intake per rat

$$\boldsymbol{FI(g) = \frac{FI_c}{n}}$$

$$\boldsymbol{CI(kcal) = FI \cdot CV}$$

Where:

FI= absolute food intake per animal (g)

FI_C= Food Intake of the cage (g)

n= number of rats in the cage

CI = absolute caloric intake per animal (kcal)

CV= Caloric value of diet ($kcal \cdot g^{-1}$)

Adjusted daily food intake (AdFI), calculated as food intake per g of body weight, and the adjusted daily caloric intake (AdCI) calculated as the caloric intake per g of body weight were calculated using **Equation 3.2**.

Equation 3.2. Calculation of adjusted food intake and adjusted water intake.

$$\boldsymbol{AdFI = \frac{FI}{AvW}}$$

$$\boldsymbol{AdCI\ (kcal\ g^{-1}) = \frac{CI}{AvW}}$$

Where:

AvW= Average weight of the animals in the cage (g)

Absolute water intake (WI) and adjusted water intake (AdWI) were calculated using **Equation 3.3**.

Equation 3.3. Calculation of absolute and adjusted water intake.

$$\boldsymbol{WI\ (ml) = \frac{WI_C}{n}}$$

$$\boldsymbol{AdWI\ (ml \cdot g^{-1}) = \frac{WI}{AvW}}$$

Where;

WI_C = Water intake of the animals in the cage (ml)

Food, water and caloric intakes of 11w rats were taken from one cohort while the ones of 15w rats were recorded from two different cohorts: the rats which CSF secretion was measured in this chapter and those used for gene and protein expression analysis in Chapter 4.

3.2.5 Measurement of body parameters

I. Weight calculations

Final weight was measured just prior to the ventriculo-cisternal perfusion experiments, while the other body parameters were measured and calculated afterwards. The body mass index (BMI) was calculated using Equation **3.4** (Gargiulo et al., 2014), and body fat content was estimated using **Equation 3.5** (Rogers and Webb, 1980). Nasoanal length was measured on supine position. The gonadal fat pad was located surrounding the ovaries.

Equation 3.4. BMI calculation.

$$\boldsymbol{Body\ surface\ (m^2) = \left(\frac{weight\ (g)}{1000}\right)^{0.425} \cdot \left(Nasoanal\ length\ (cm)^{\,0.725}\right) \cdot 0.007184}$$

$$\boldsymbol{BMI\ (g\ m^{-2}) = \frac{Weight(g)}{Body\ surface\ (m^2)}}$$

Equation 3.5. Body fat content calculation.

$$\boldsymbol{Body\ Fat\ Content} = \frac{\boldsymbol{Weight\ of\ gonadal\ fat\ pad\ (g)}}{\boldsymbol{Body\ weight\ (g)}} \cdot \mathbf{100}$$

II. Oestrous cycle recordings

On the two weeks prior to the ventriculo-cisternal experiment, oestrous cycle of each female rat was recorded daily by vaginal cytology. Vaginal lavages were obtained every day, approximately one hour after the dark period started. The cellular composition of these lavages was used to determine the stage of the cycle (**Figure 3.1**). Most times, vaginal lavages were easily classified in one of the four stages of the oestrous cycle. However, in the odd occasions when the observed cell types of a lavage appeared to belong to two different but consecutive stages, the rat was classified as being between those stages. For example, a lavage showing a big proportion of leucocytes and also some nucleated cells would be classified as between dioestrus and proestrus. The presence of the oestrus dance was also used to confirm the cycle stage (Stramek, Johnson and Taylor, 2019).Length of oestrous cycle was calculated as the average time in days between a rat being in proestrus and getting into proestrus again in the time period of two weeks. (normally 3-4 cycles).

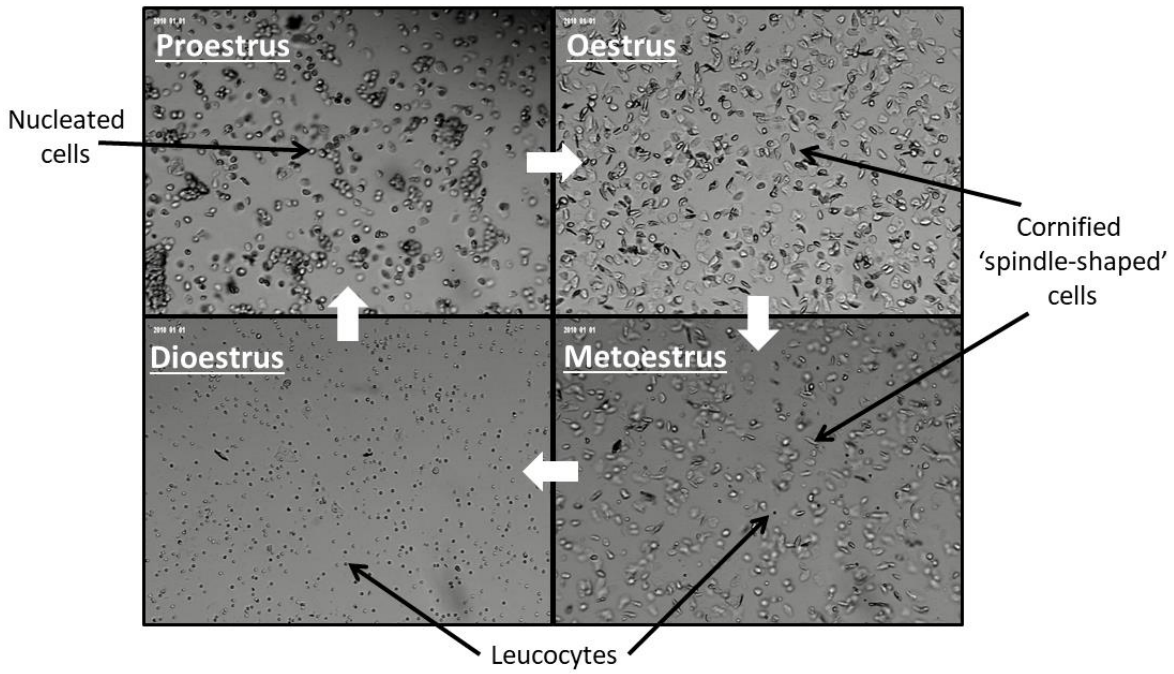

Figure 3.1. Typical cell composition of vaginal lavage samples in each stage of the oestrous cycle of the female rat.

X100 magnification

III. Hormone and cholesterol analysis

Blood samples were collected by cardiac puncture under terminal anaesthesia when the rats were in dioestrus. Plasma samples were separated using tubes with heparin (Sarstedt, Nümbrecht, Germany) and stored at -80 ^{o}C until further processing. Plasma was then used to measure hormone and cholesterol levels.

Hormone levels were measured using commercially available ELISA kits following the manufacturer's instructions: Oestradiol and Testosterone kits were purchased from Calbiotech, El Cajon, CA, USA, while Cortisol kit was obtained from BT-Lab, Birmingham, UK and Progesterone kit was acquired from Crystal Chem, Netherlands. Testosterone to Oestradiol ratio (T/E2) and oestradiol to progesterone (E2/P) ratio were also calculated. LDL/VLDL, HDL and Total Cholesterol levels were measured using a commercially available ELISA kit purchased from Abcam, Cambridge, UK, following the manufacturer's protocols.

3.2.6 Ventriculo-cisternal perfusion

The preparation of aCSF is described in Section 2.2.2. The ventriculo-cisternal perfusion technique was performed following the protocol described in section 2.2.3, with some small changes. In brief, the rat was introduced to an inhalation chamber where 4% isofluorane inhalation vapour (Merial Animals Health, Essex, UK) mixed with oxygen at 3.5 $l \cdot min^{-1}$ was administered for 10 min in order to induce anaesthesia. After that, the animal was transferred to the stereotaxic frame fitted with an anaesthesia facemask. During the experiment, anaesthesia was maintained with 2.5% v/v isofluorane inhalation vapour mixed with oxygen at 2 $l \cdot min^{-1}$. The animal was placed on a warm pad with an output maintained at approximately 37°C and was covered with insulation material to prevent the body temperature dropping. Body temperature was always monitored using a rectal thermometer and kept between 37ºC and 38ºC (Rufiange *et al.*, 2020). Once anaesthetized rats did not respond to reflex-inducing external stimuli (i.e. pinching) for longer than 2 min, the skull was exposed, and two holes were drilled using a 0.65 mm hand-chuck drill on 0.8 mm posterior to bregma and 1.5 mm laterally either side. Two 21-gauge metal cannulae (Bilaney Consultants Ltd, Sevenoaks, UK) were inserted into the skull to a depth of 4mm, where lateral ventricles are located. The perfusion was started immediately and taken as time zero of the experiment, which kept running for 120 min per animal. Perfusion inflow rate was 10 $\mu l \cdot min^{-1}$ for each ventricle for the first 20 min and 5 $\mu l \cdot min^{-1}$ for the remaining time. A 1 mm blunt needle was inserted into the cisterna magna for collection of CSF. Samples were collected over 20 minutes. Further analysis and calculations were performed following the procedure explained on section 2.2.3. All CSF secretion rate measurements were performed when the rats were in dioestrus.

I. ICP monitoring

In 15w rats, ICP was monitored for the length of the ventriculo-cisternal perfusion. Pressure readings were obtained using the LifeSens single channel signal conditioner system and the Opp-M250 fibre optic pressure sensor (OpSens Solutions, Québec, Canada) following a protocol described previously (Murtha, Mcleod and Spratt, 2012). In summary, once the holes for ventriculo-cisternal perfusion were drilled, a third hole was drilled using a 2 mm hand-chuck drill on 3 mm posterior to bregma and 2 mm laterally on the right side, ensuring the dura was not damaged. A polyetheretherketone screw (Misumi, Frankfurt am Main, Germany) was screwed into the hole and secured using PermaCem Smartmix (DMG Dental, Porthcawl, UK). The screw had been previously perforated with a 0.7 mm drill. The hole in the screw was filled with 0.9% w/v NaCl solution in water. An ICP probe was inserted into the screw and was lowered to the end of the screw, avoiding piercing the dura. The depth of insertion was then carefully adjusted until ventilation and blood pressure pulse waves were detected by the pressure transducer. The probe was sealed in place using Silagum-Light Fast (DMG Dental, Porthcawl, UK) and pressures were recorded for the length of the ventriculo-cisternal perfusion. A schematic representation of the setup can be found in **Figure 3.2.**

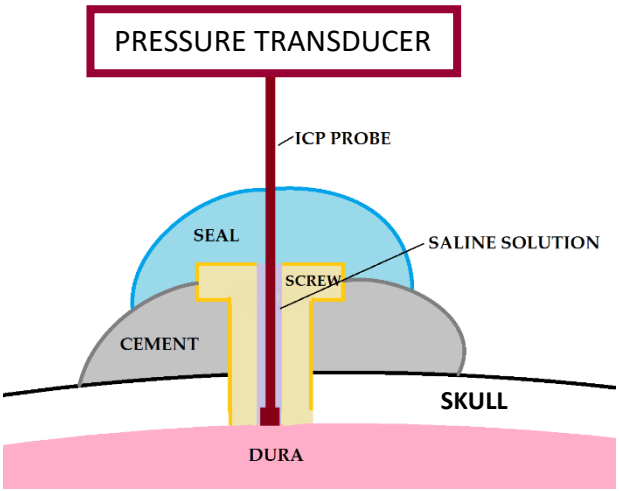

Figure 3.2. Schematic representation of setup for intracranial pressure monitoring.

3.2.7 Statistical analysis

Each 11w diet group had n=3 rats and each 15w diet group had n=5 unless otherwise specified. All results are presented as average ± SEM. Normal distribution of data was confirmed by Q-Q plot. Differences in weight gain, food intake and water intake over time were analysed using a two-way repeated measures ANOVA and differences between groups at each time point were tested using Tukey Post Hoc test. The differences on final measured parameters, such as final weight and CSF secretion rates between the HFD and ND at 11w were carried out using a two-tailed t-test, while differences between 15w ND, HFD and HFD+PB were analysed using a one-way ANOVA with Tukey Post Hoc test. The coefficient of variation was calculated in order to evaluate irregularities of oestrous cycle length. A data set was considered highly variable when their coefficient of variation >20%. The relationship between two parameters was measured using the Pearson correlation coefficient (r), where a coefficient higher than 0.6 was considered a strong correlation. A *P* value smaller than 0.05 was considered to indicate a significant difference.

Statistical analysis was performed using IBM SPSS Statistics (IBM Corporation, 2017) for statistical analysis of weight increase over time, JASP (JASP Team, 2019), and for the remaining experiments, one-way repeated measures ANOVA and their post-hoc tests. GraphPad (Graphpad Software, 2019) was used for graph plotting and all other statistical analyses.

3.3 Results

3.3.1 Animal model: diet and weight

Due to the strong relationship between IIH and obesity and female sex, this study was focused on exploring the effect of HFD-induced obesity on CSF secretion in females. An experiment was designed in which five groups of rats would be exposed to either ND, HFD or HFD+PB with their CSF secretion being measured at 11 weeks of age (ND 11w and HFD 11w) or 15 weeks of age (ND 15w, HFD 15w and HFD+PB 15w). The weight was recorded during the experiment and is represented on **Figure 3.3** and **Figure 3.4**.

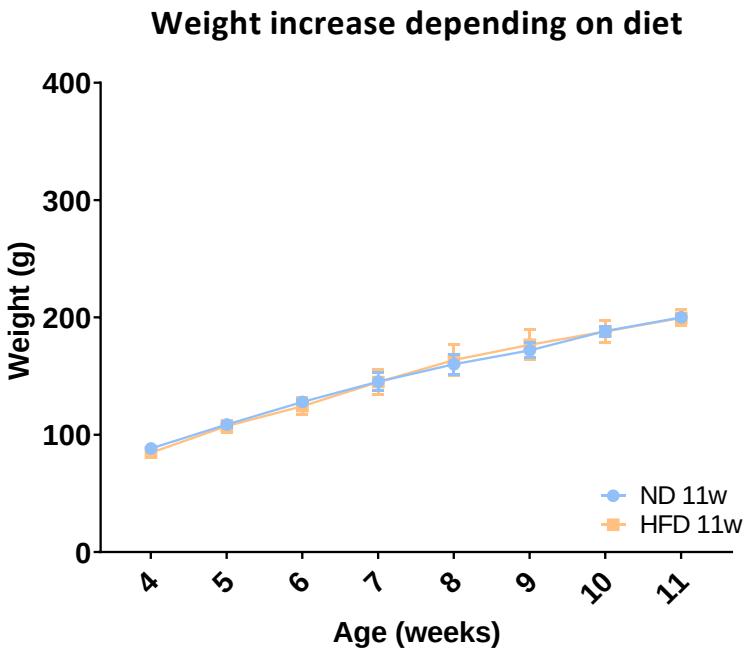

Figure 3.3. Weight of female rats on ND or HFD over a seven-week period.

Weights were recorded weekly and averaged per diet group. Data is presented as average ± SEM, n=3. A one-way repeated measures ANOVA was used to test the statistical significance of the change over time. Statistical differences between groups at each time point were tested using Tukey Post Hoc test.

In the first cohort of rats, weight increased over time in both the ND and HFD groups ($F(7,28)=918$, *P* value <0.001), but there was no difference in weight gain between diets ($F(7,28)=0.262$, *P* value>0.05). As HFD did not induce overweightness in these rats, we decided to add a third group to the second cohort of rats, to be studied at 15w, which would be fed HFD until week 11 and then their HFD would be supplemented with a small amount of PB daily in order to increase weight gain.

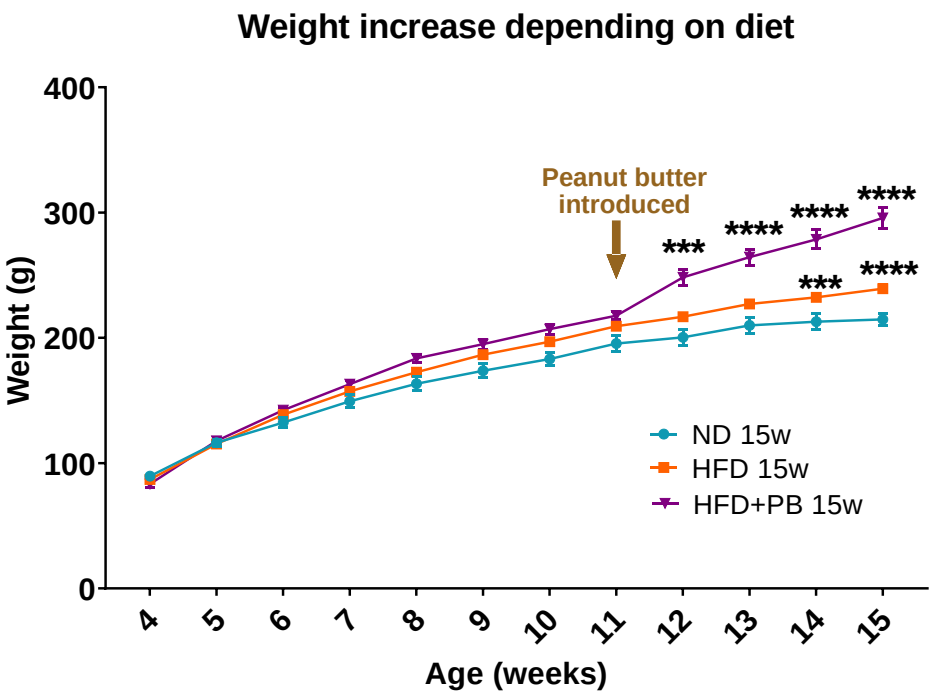

Figure 3.4. Weight of female rats on ND or HFD over an eleven-week period.

Weights were recorded weekly and averaged per diet group. Data is presented as average ± SEM, n=11. A two-way repeated measures ANOVA was used to test the statistical significance of the change over time. Statistical differences between groups at each time point were tested using Tukey Post Hoc test. ***= *P* value < 0.001, **** = *P* value < 0.0001.

In the second cohort of rats, weight also increased with time in all groups ($F(2.284, 352)=1464.332$, *P* value<0.001). The addition of PB to HFD in HFD+PB group from week 11 led to a weight gain higher than that in the other two groups (Figure 3.4). This difference was observed as early as week 12, within a week of introduction of the PB supplement, and the increase in body weight of HFD+PB group was maintained until the end of the experiment. Rats fed the HFD also weighed significantly more than those fed the ND at weeks 14 and 15.

Assessment of the effect of dietary manipulation at 11w and 15w of age is shown in Figure 3.5. The percent weight gain of HFD 11w rats was not different to that of ND 11w rats (ND 11w 227.77 ± 11.12%, HFD 11w 245.34 ± 33.12%, *P* value>0.05). However, in 15w rats, there was a significant increase on final weight as percentage of initial weight in both

HFD groups when compared to ND, especially in the HFD+PB (ND 15w 244.26 ± 13.55%, HFD 15w 284.43 ± 24.28%, HFD+PB 15w 388.14 ± 26.98%, *P* value<0.01)

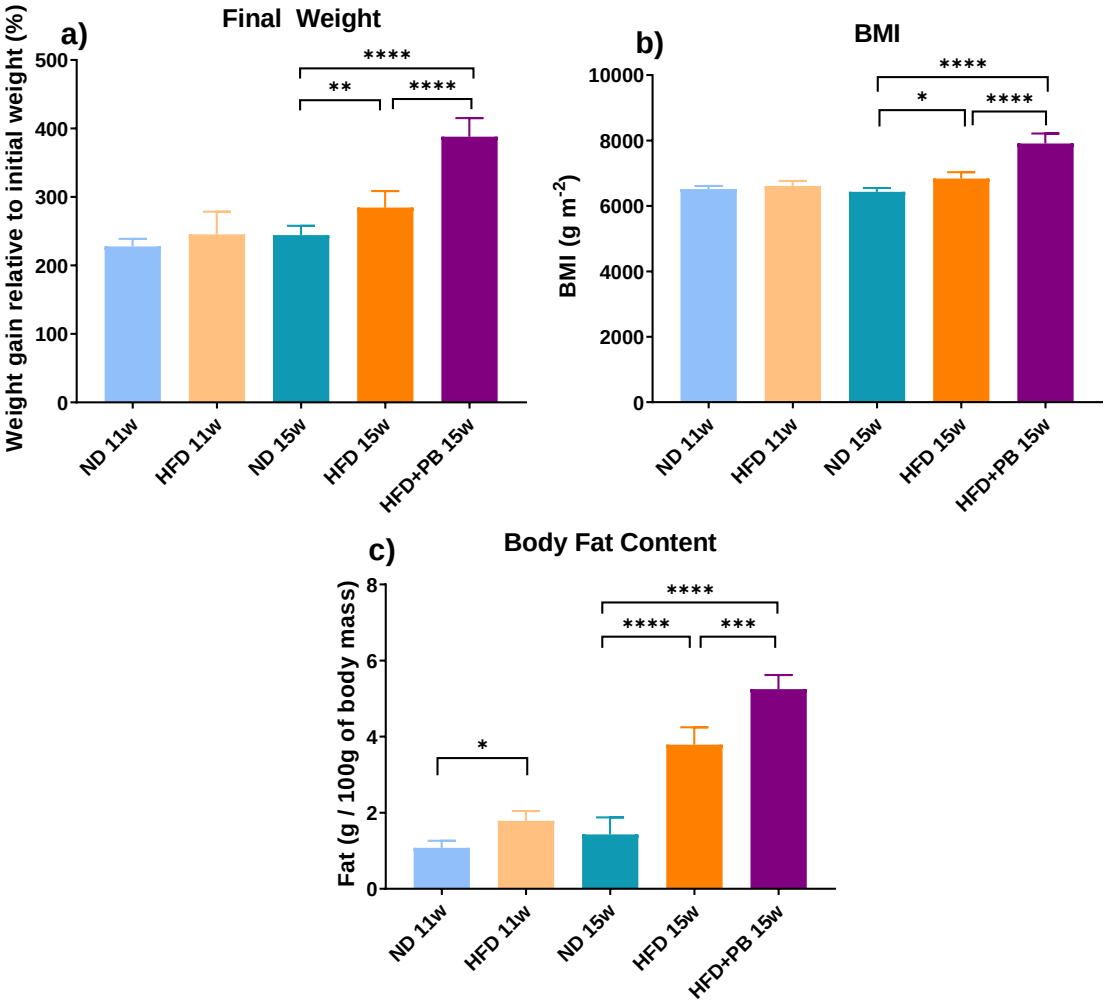

Figure 3.5. Evaluation of overweightness level of rat model depending on diet and age.

(a) Data is calculated as percentage of final weight measured on the day of the surgery relative to weight at 4 weeks of age. (b) Data is calculated using **Equation 3.4**. (c) Data is calculated using **Equation 3.5**. All data is presented as average ± SEM, 11w n=3, 15w n=5. Groups were compared amongst each other on the same age group using a t-test for 11w and one-way ANOVA for 15w. * = *P* value <0.05, **= *P* value <0.01, *** = *P* value<0.001, **** = *P* value <0.0001.

BMI was calculated using **Equation 3.4** as a way of assessing overweightness. There was no significant difference between ND 11w and HFD 11w, but at 15w the HFD groups had a significantly higher BMI when compared to ND, specially the HFD+PB.

Body fat content of rats was calculated using **Equation 3.5** as a way of assessing adiposity level. All HFD groups had a higher body fat content than their respective controls at both 11 and 15w. The largest difference observed was that between ND and HFD+PB, the latter being also significantly higher than at HFD 15w.

3.3.2 Food and water intake

Data on food and caloric intake from 11w rats is shown in **Figure 3.6**.

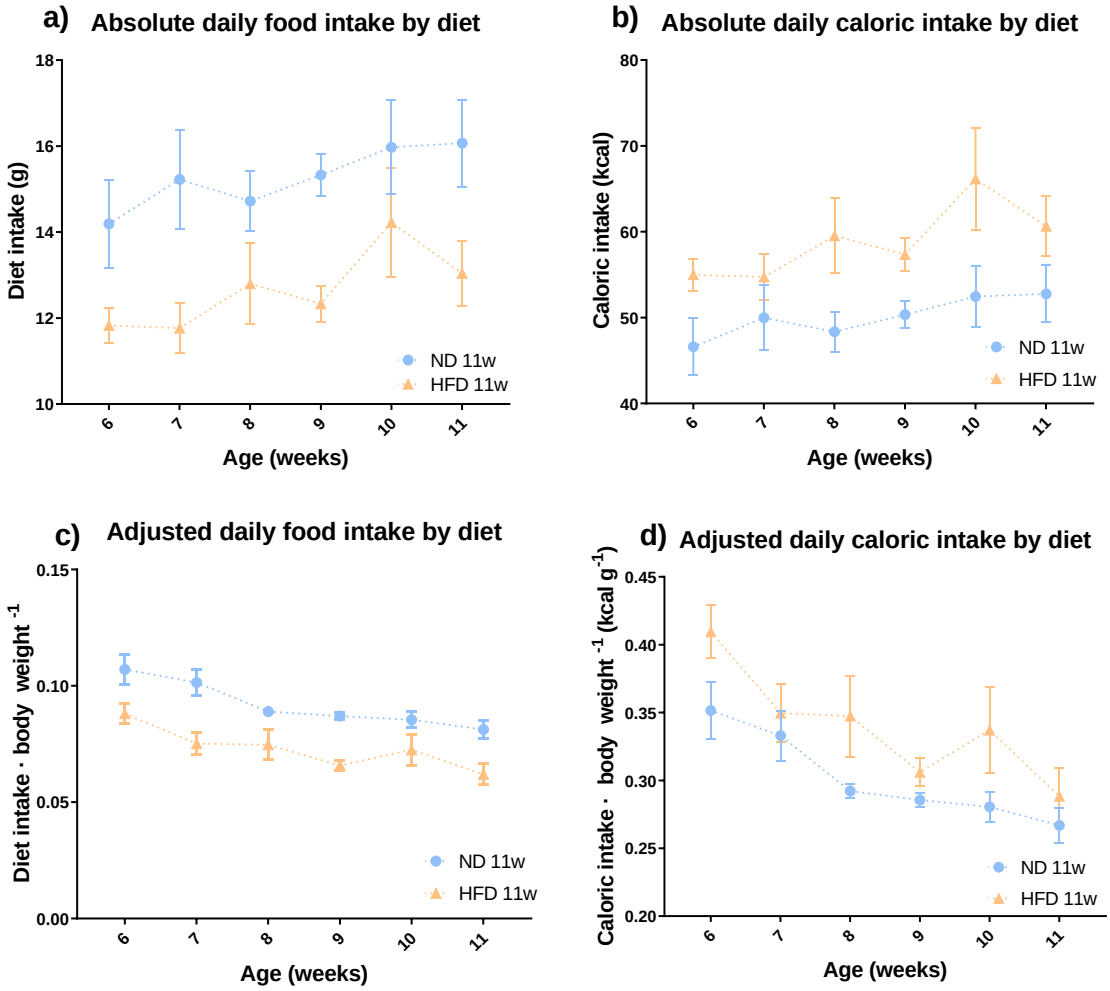

Figure 3.6. Daily food (a, c) and caloric (b, d) intake in 11w rats.

Data is calculated as average of cage. (a) FI and (b) CI data is calculated per rat per day. (c) AdFI and (d) AdCI data is calculated per weight of rat per day. A two-way repeated measures ANOVA was used to test the statistical significance of the change over time. Statistical differences between groups at each time point were tested using Tukey Post Hoc test. n=3

There was an increase in absolute food intake (FI) with time ($F(5, 20)=4.226$, P value<0.05), however adjusted food intake (AdFI) decreased with time for both diets ($F(5, 20)=17.9$, P value<0.001). Absolute caloric intake (CI) increased with time for both diets

(F(5, 20)=3.717 *P* value<0.05), but adjusted caloric intake (AdCI) decreased with time (F(5, 20)= 16.418, *P* value<0.001). There was no difference in food or caloric intakes between diets (FI: F(1, 4)=6.32, *P* value>0.05; AdFI: F(1,4)=13.399, *P* value>0.05; CI: F(1, 4)=5.355, *P* value>0.05; AdCI: F(1, 4)= 3.141, *P* value>0.05). There was no significant difference in either food or caloric intake between both diet groups at any given week.

Data on water intake values are represented in **Figure 3.7**.

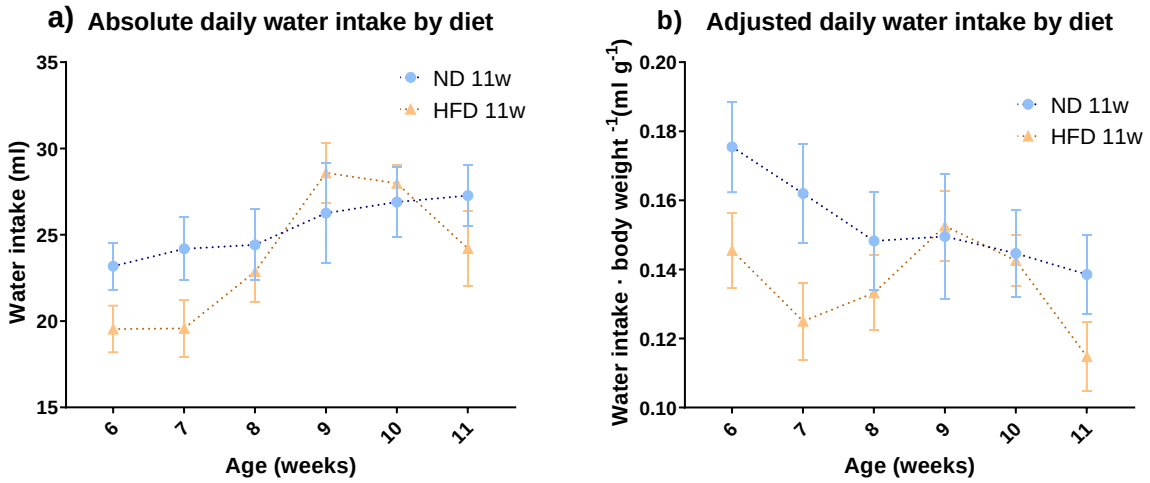

Figure 3.7. Daily water intake for 11w rats.

Data is calculated as average of cage. (a) WI data is calculated per rat per day. (b) AdWI data is calculated per weight of rat per day. A one-way repeated measures ANOVA was used to test the statistical significance of the change over time. Statistical differences between groups at each time point were tested using Tukey Post Hoc test. n=3

Absolute water intake (WI) increased with time (F(5, 20)=11.586, *P* value<0.05) while adjusted water intake (AdWI) decreased with time (F(5, 20)=7.618, *P* value<0.05), but they showed no difference between diet groups (WI: F(1,4)=0.509, *P* value>0.05; AdWI: F(1, 4)=1.23, *P* value>0.05). There was no significant difference in water intake between both diet groups at any given week.

A separate group of rats (15w) was studied for 4 further weeks, including an additional group of HFD animals that received a supplementation with PB starting at week 11 to increase the calorific value of the diet and enhance weight gain. The diet intake data for these older rats is represented in **Figure 3.8**. Note that the FI values represented on **Figure 3.8** were calculated based on the intake of the HFD and does not include PB weight; however, caloric calculations do take PB into account.

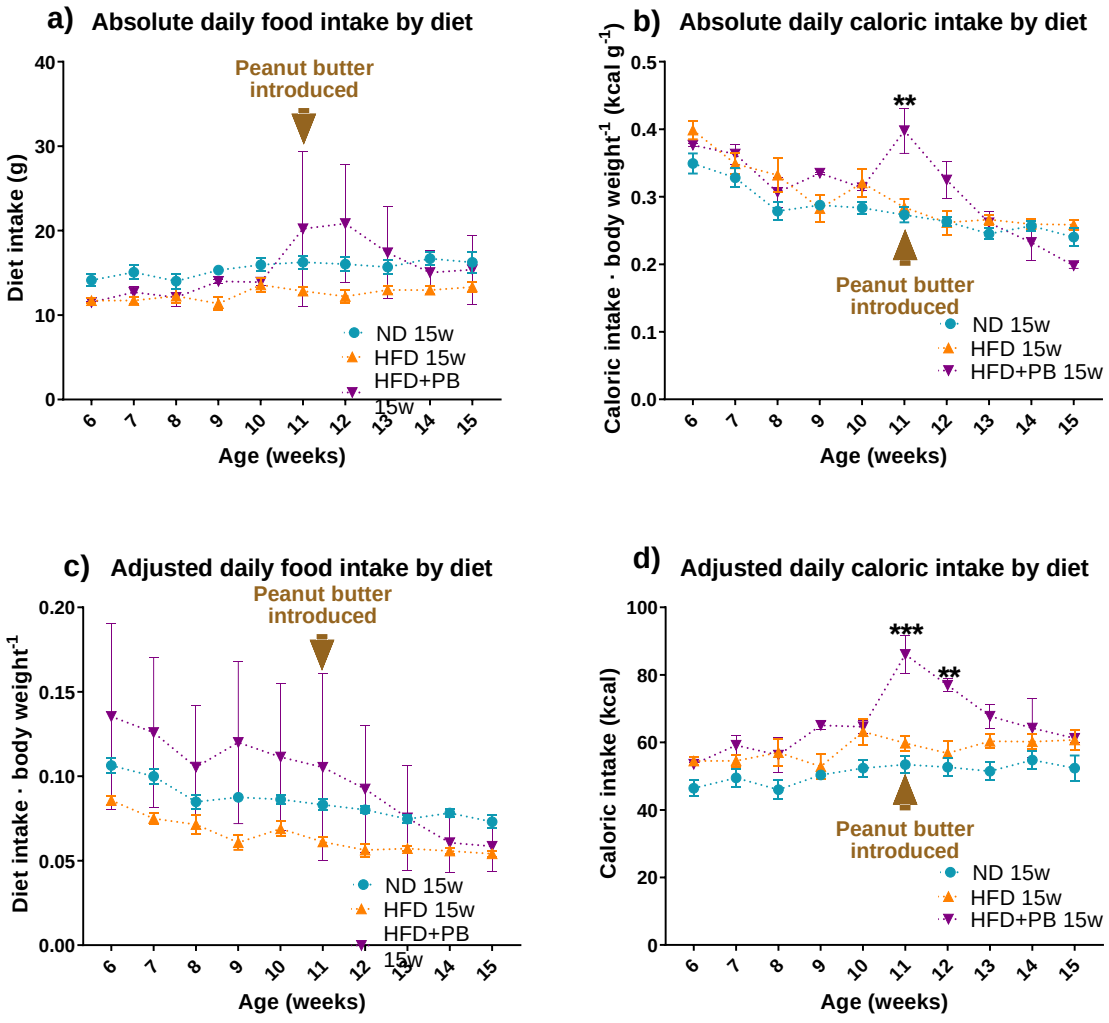

Figure 3.8. Daily food (a, c) and caloric intake (b, d) on 15w rats.

Data is calculated as average of cage. (a) FI and (b) CI Data is calculated per rat per day. (c) AdFI and (d) AdCI data is calculated per weight of rat per day. All data is presented as average ± SEM, n=11. A one-way repeated measures ANOVA was used to test the statistical significance of the change over time. Statistical differences

between groups at each time point were tested using Tukey Post Hoc test. **= *P* value <0.01, *** = *P* value<0.001.

FI did not change significantly with time (F(1.133, 10.196)=2.459, *P* value>0.05) or diet (F(1.133, 10.196)=2.459, *P* value<0.05) (**Figure 3.8**.a), however, AdFI decreased with time (F(1.544, 13.895)=18.610, *P* value<0.001) although there was no difference related to diet (F(3.088, 13.895)=2.642, *P* value>0.05) (**Figure 3.8**.c). CI and AdCI had a sudden increase in week 11 and 12 and they varied with time (**Figure 3.8**.b, d) (CI F(3.265, 29.386) = 10.889, *P* value<0.001; AdCI F(8,72)=24.989, *P* value<0.001) and also differed between diet groups (CI F(6.53, 29.386) = 4.094, *P* value<0.01; AdCI F(16,72)=3.697, *P* value<0.001).

Water intake was recorded daily and is represented on **Figure 3.9**.

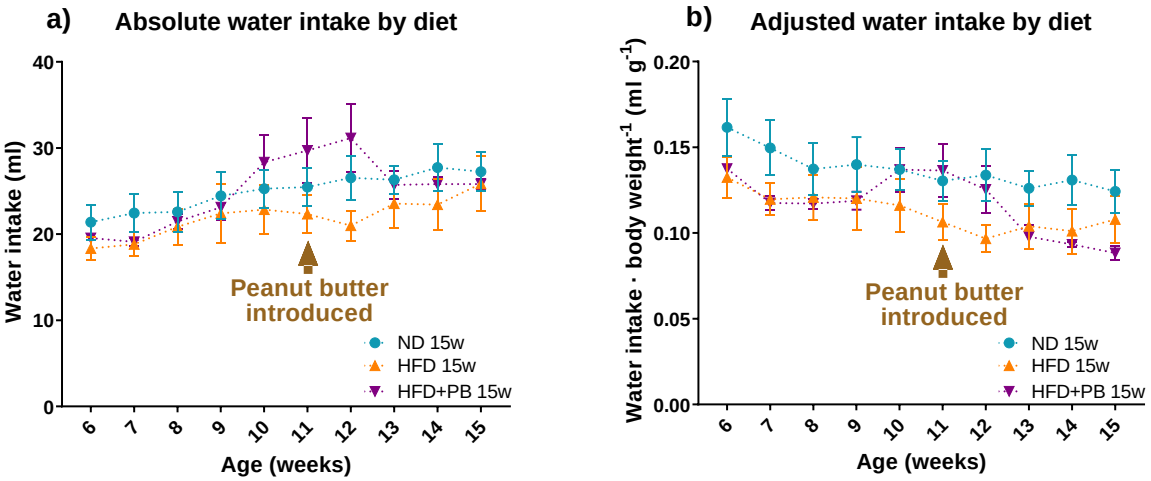

Figure 3.9. Daily water intake during the experiment.

Water intake was recorded daily and data is calculated as average of cage. (a) WI data is calculated per rat per day. (b) AdWI data is calculated per weight of rat per day. All data is presented as average ± SEM, n=11. A one-way repeated measures ANOVA was used to test the statistical significance of the change over time . Statistical differences between groups at each time point were tested using Tukey Post Hoc test.

WI increased with time (Figure 3.9.a) (F(3.478, 31.298)=12.836, *P* value<0.001) whereas AdWI decreased with time (Figure 3.9.b) (F(3.051, 27.46)=8.907, *P* value<0.01). Moreover, WI was affected by diet (F(6.955, 31.298)=2.367, *P* value<0.05) (Figure 3.9.a),

being higher in average in the HFD+PB group and lower in the HFD; while AdWI was not altered by diet (Figure 3.9.b) ($F(6.102, 27.46)=1.941$, *P* value>0.05).

3.3.3 Cholesterol levels

Increased adiposity has been shown to be linked to an excess of LDL/VLDL and a reduction of HDL (Tchernof and Després, 2013). Plasma concentrations of LDL, HDL and total cholesterol are shown in **Figure 3.10.**

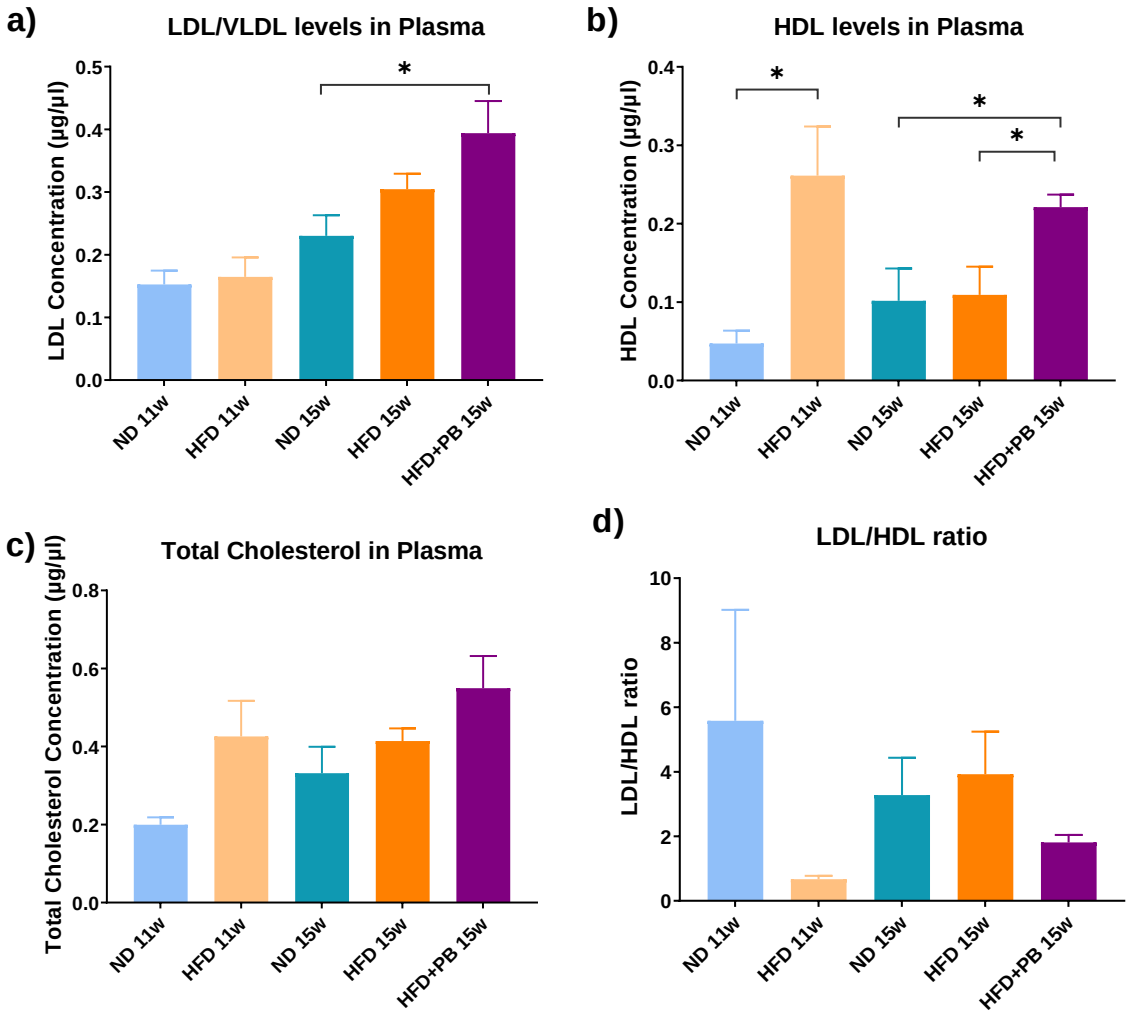

Figure 3.10. Cholesterol concentration in plasma of rats under different diets and at different ages.

(a) LDL/VLDL, (b) HDL and (c) total cholesterol were measured from plasma samples. (d) LDL/HDL ratio was calculated using the individual values of each rat. All data is presented as average ± SEM, ND and HFD 11w

n=3, ND 15w n=4, HFD 15w n=4, HFD+PB 15w n=5. Groups were compared within the same age group using a t-test for 11w and one-way ANOVA for 15w. * = *P* value <0.05

There was no difference in LDL/VLDL concentrations between ND and HFD rats at 11w. In the 15w groups, there was a significant increase in HFD+PB when compared to ND (**Figure 3.10**.a).

There was an increase in HDL concentrations in the HFD 11w compared to its control. At 15w, ND and HFD had similar levels of HDL while it was significantly increased in the HFD+PB group (**Figure 3.10**.b).

There was no significant difference in total cholesterol between any of the groups (**Figure 3.10**.c). A similar finding was also observed for the LDL/HDL ratio (**Figure 3.10**.d).

In order to investigate the relationship between adiposity and cholesterol, both parameters were compared to each other. There was a strong positive correlation between body fat and both LDL/VLDL concentration and total cholesterol concentration, but there was no correlation between body fat and HDL concentration nor with LDL/HDL ratio (**Figure 3.11**).

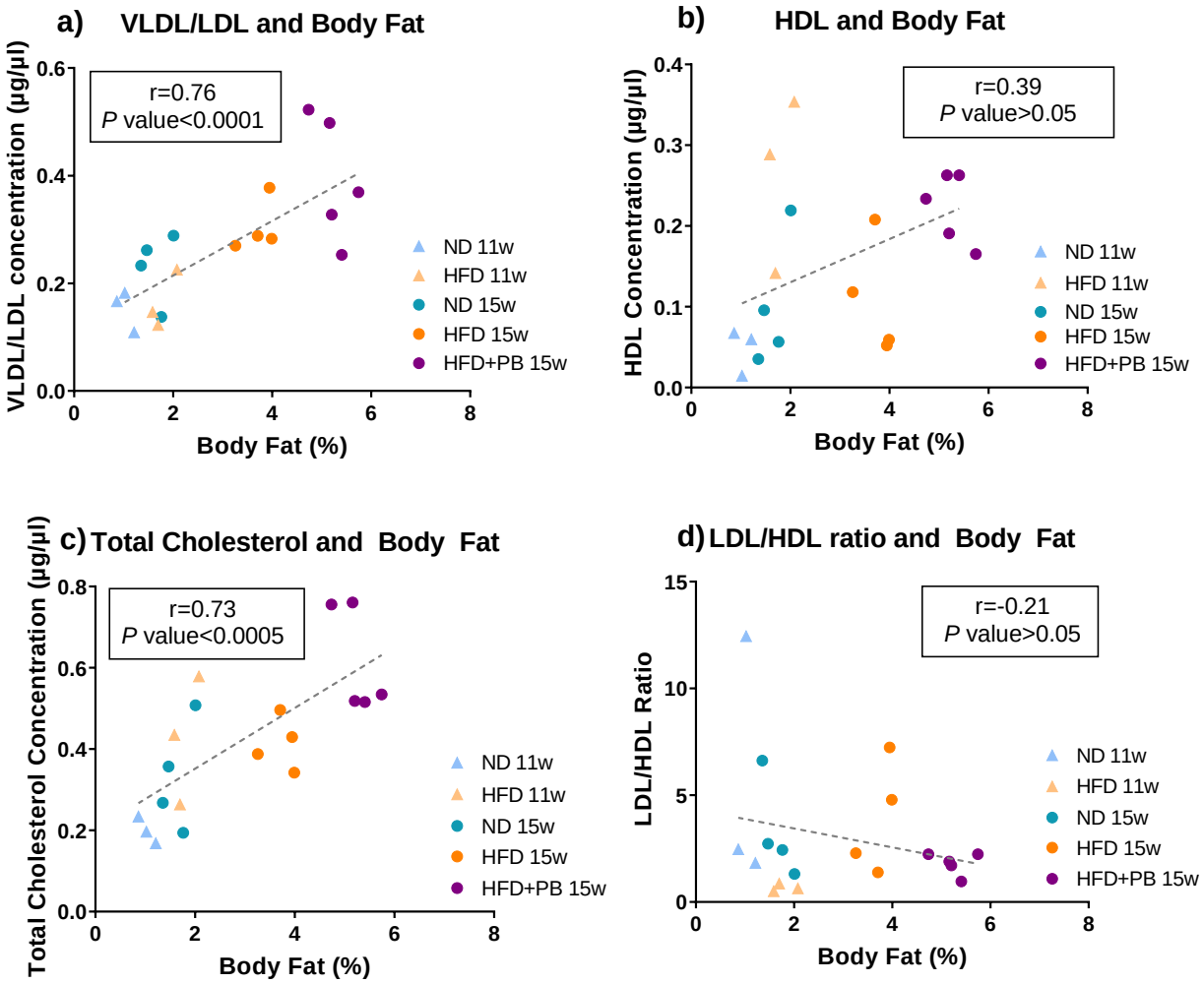

Figure 3.11. Correlation between body fat composition and plasma cholesterol levels depending on diet and age.

Rats were obtained at 4 weeks of age and kept for either 7 or 11 weeks. Rats were fed either ND or HFD. HFD+PB rats were fed HFD until week 7, after which their food was supplemented with a small quantity of PB daily. (a) LDL/VLDL, (b) HDL and (c) total cholesterol were measured from plasma samples. (d) LDL/HDL ratio was calculated with the individual values of each rat. Data was analysed with Pearson correlation. 11w n=3, ND 15w n=4, HFD 15w n=5, HFD+PB 15w n=5

3.3.4 Oestrous cycle

To evaluate the impact of diet on the oestrous cycle, vaginal lavage was taken daily during the last 12 days of diet feeding. Four examples of each group are represented in **Figure 3.12** and **Figure 3.14**.

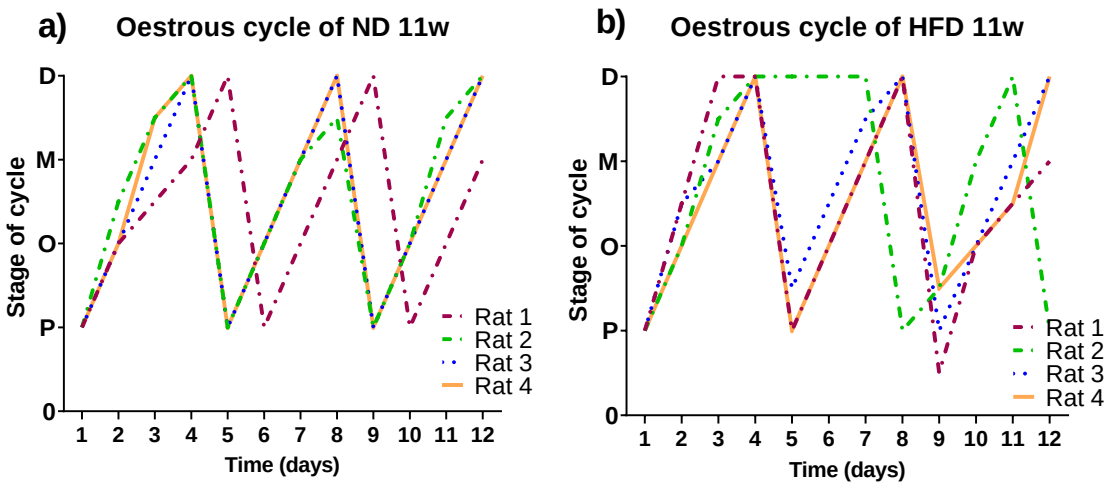

Figure 3.12. Oestrous cycle of 11w rats.

Rats were obtained at 4 weeks of age and were fed either ND or HFD for 7 weeks. The stage of the cycle was assessed daily for the last 2 weeks. Four examples for (a) ND and (b) HFD were plotted in order to visually estimate regularity. Day 1 is adjusted to be the first day of proestrus for each individual.

Cycle lengths were compared between groups (**Figure 3.14**). There was no significant difference in cycle length between 11w rats nor was there was any significant difference between the 15w groups. However, the coefficient of variation was higher in HFD groups than their respective ND, and the HFD 15w and HFD+PB 15w were highly variable.

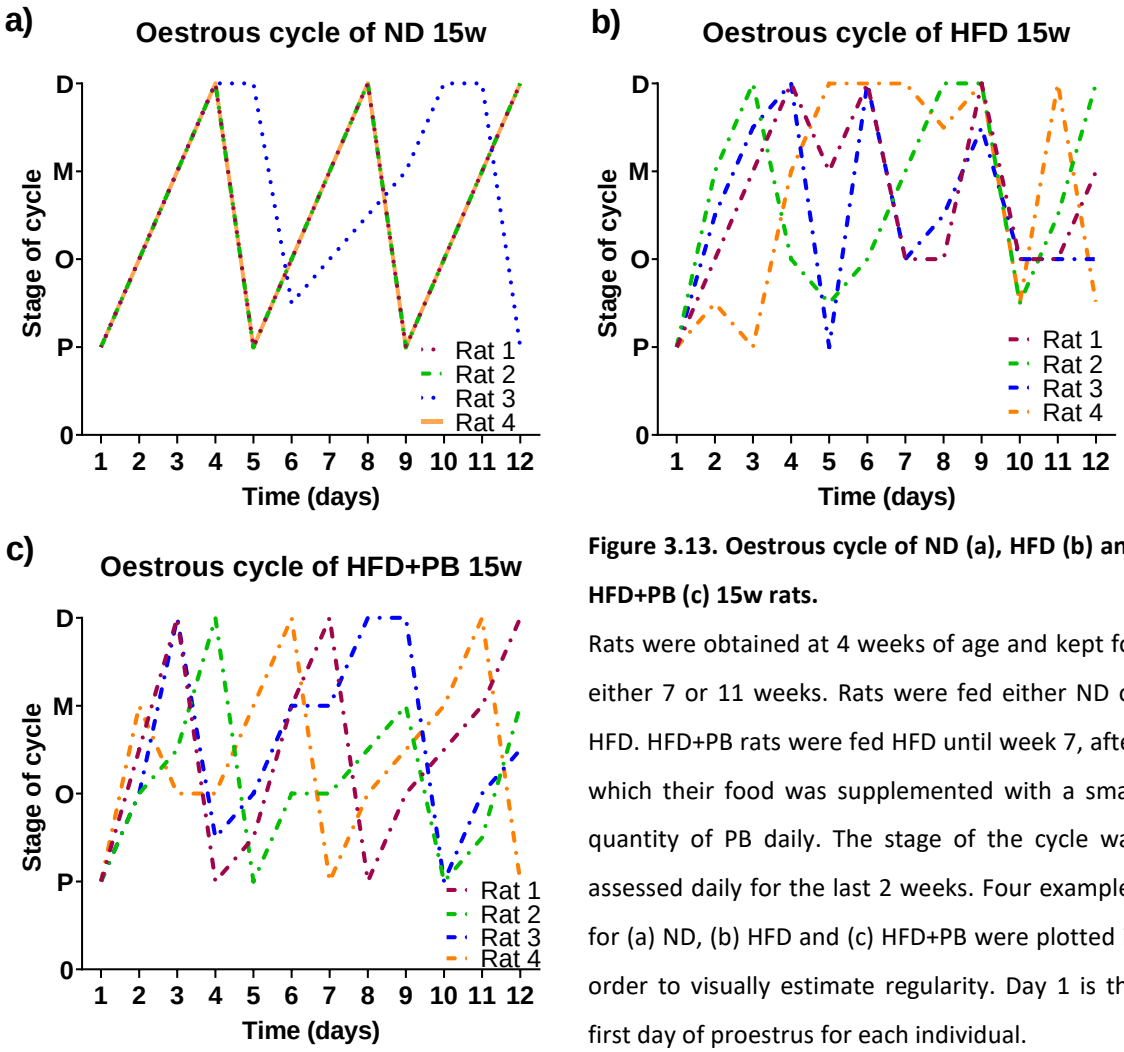

Figure 3.13. Oestrous cycle of ND (a), HFD (b) and HFD+PB (c) 15w rats.

Rats were obtained at 4 weeks of age and kept for either 7 or 11 weeks. Rats were fed either ND or HFD. HFD+PB rats were fed HFD until week 7, after which their food was supplemented with a small quantity of PB daily. The stage of the cycle was assessed daily for the last 2 weeks. Four examples for (a) ND, (b) HFD and (c) HFD+PB were plotted in order to visually estimate regularity. Day 1 is the first day of proestrus for each individual.

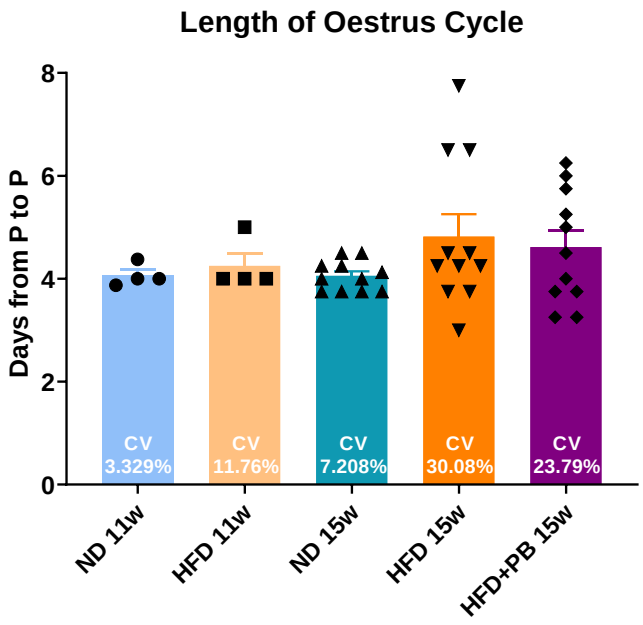

Figure 3.14. Length of oestrous cycle of rats under different diets and ages.

The stage of the cycle was assessed daily for the last 2 weeks. All data is presented as average ± SEM, 11w n=4, 15w n=11. Groups were compared amongst each other on the same age group using a t-test for 11w and one-way ANOVA for 15w. Cv = coefficient of variation

3.3.5 Hormone levels

All experiments were run on rats that were in dioestrus, therefore all sex hormone levels should be similarly low (Smith, Freeman and Neill, 1975; Marcondes *et al.*, 2001). The plasma concentrations of progesterone, oestradiol, testosterone and cortisol in all groups were measured and compared amongst rats of the same age (**Figure 3.15**).

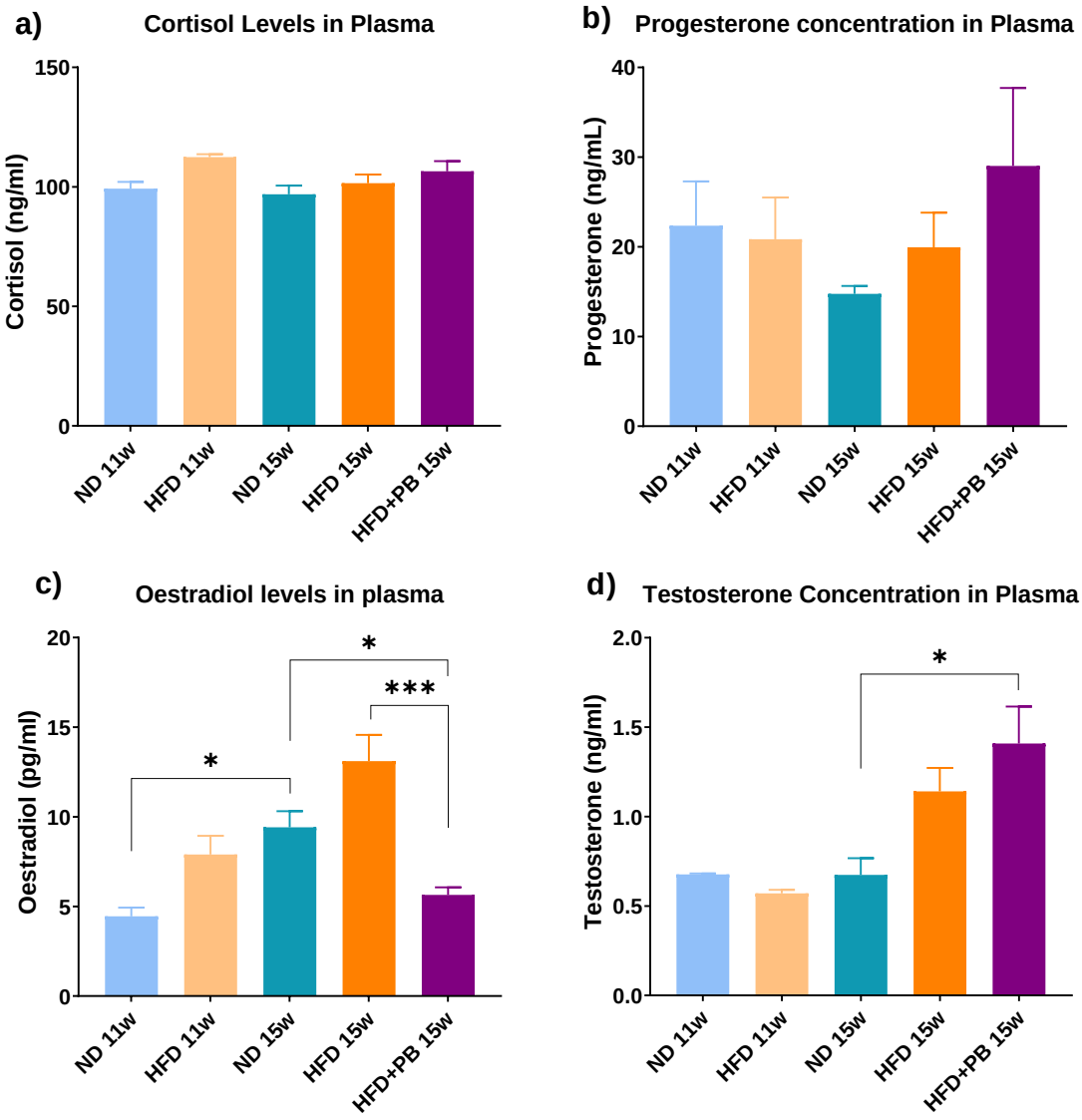

Figure 3.15. Hormone concentrations on plasma of rats under different diets and ages.

(a) Cortisol, (b) progesterone, (c) oestradiol and (d) testosterone were measured from plasma samples. All data is presented as average ± SEM, ND 11w and HFD 11w n=3, ND 15w n=4, HFD 15w n=4, HFD+PB 15w n=5, except for progesterone at 15w where n=3. * = *P* value <0.05, **= *P* value <0.01, *** = *P* value<0.001

No differences were observed between ND 11w and HFD 11w groups for any of the measured hormones. In 15w rats, there was a significant increase of testosterone concentration in the animals fed HFD+PB when compared to ND, coupled with a significant decrease in plasma oestradiol when compared to those in the ND and HFD groups. As a result, there was an increase in T/E2 ratio for HFD+PB when compared to any of the other

15w diet groups (**Figure 3.16**). Animals in the ND 15w group showed a significant increase in oestradiol compared to ND 11w. No other differences were observed between the diet groups for any of the other hormones.

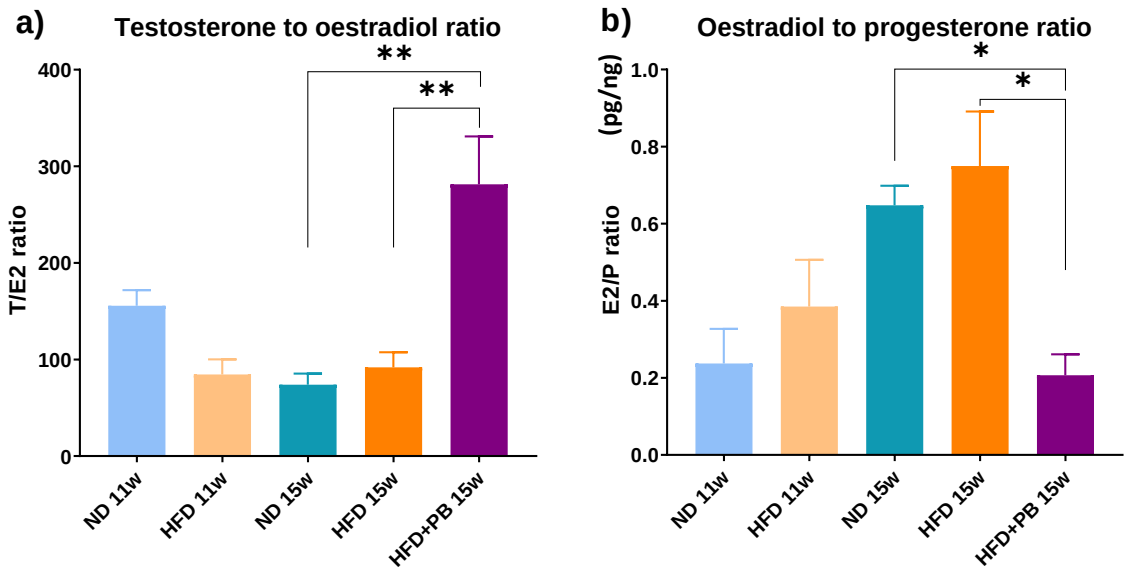

Figure 3.16. Hormone ratios of rats under different diets and ages.

(a) Testosterone to oestradiol ratio and (b) oestradiol to progesterone ratio were calculated for each individual. All data is presented as average ± SEM, ND 11w and HFD 11w n=3, ND 15w n=4, HFD 15w n=4, HFD+PB 15w n=5, except for E2/P ratio where 15w n=3. Groups were compared amongst each other on the same age group using a t-test for 11w and one-way ANOVA for 15w. * = *P* value <0.05, **= *P* value <0.01

3.3.6 Effect of Diet on Cerebrospinal Fluid Secretion Rates

I. Steady state determination

To determine whether age and diet-induced obesity affected the dynamics of CSF secretion, 11w and 15w rats underwent ventriculo-cisternal perfusion (Pappenheimer *et al.*, 1962; Oreskovic *et al.*, 2003; Alimajstorovic, Pascual-Baixauli, *et al.*, 2020). Endogenous CSF was flushed, and a steady state of CSF secretion was confirmed. The steady state was typically reached within 40 min of the start of the experiment (**Figure 3.17**). C_{out}/C_{in} values obtained changed over the perfusion period for both 11w and 15w rats, (11w: F(6, 24)=1407.021, *P* value < 0.001; 15w: F(2.505, 30.058)=8746.083, *P* value < 0.001). However, values obtained during the steady state were not altered across the perfusion time (11w:

F(3, 12)= 0.468, *P* value > 0.05; 15w F(3, 6)=0.681, *P* value>0.05). Diet did not affect C_{out}/C_{in} values (11w: F(6,24)=0.156, *P* value > 0.05; 15w F(5.01, 30.058)=4.08, *P* value > 0.05).

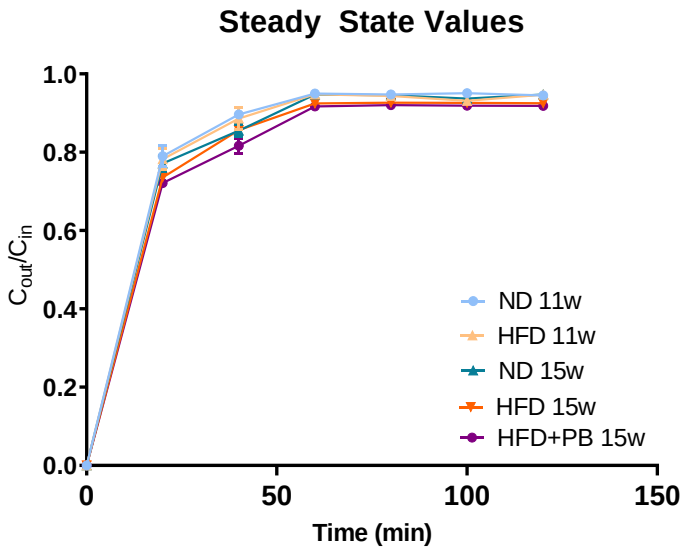

Figure 3.17. Steady state determination using C_{out}/C_{in} values.

C_{out}/C_{in} values were calculated using the Equation 2.1 . Data represented as average ±SEM, 11w n=3, 15w n=5. A two-way repeated measures ANOVA was used to test the statistical significance of the change over time amongst the same-age group (Greenhouse-Geisser correction). Statistical differences between same-age groups at each time point were tested using Tukey Post Hoc test.

II. Cerebrospinal fluid secretion rates

The rates of CSF secretion of each group are plotted in **Figure 3.18**.

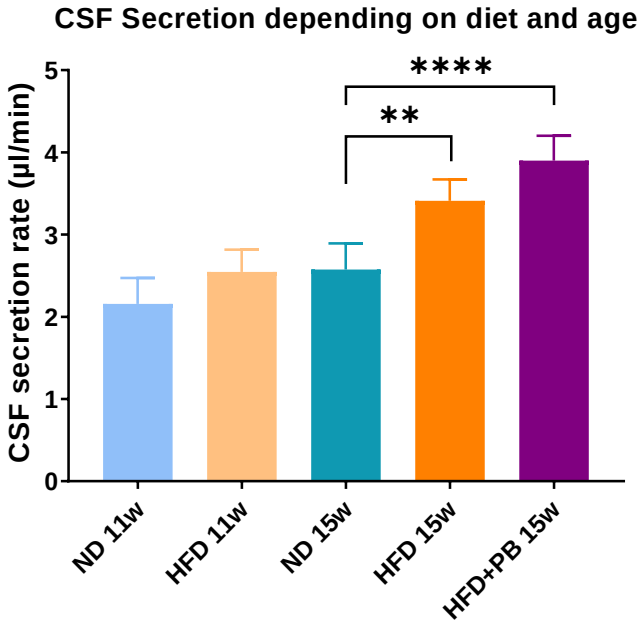

Figure 3.18. Cerebrospinal fluid secretion rates of rats under different diets and ages.

CSF secretion rate was measured using the ventriculo-cisternal perfusion technique. CSF secretion rates were calculated by averaging secretion rates once the steady state was reached using Equation 2.2 (see Chapter 2). 11w n=3, 15w n=5, ** = *P* value<0.01, ****= *P* value<0.0001

There was no significant difference between groups at 11w. However, at 15w the CSF secretion rates of both HFD groups were significantly higher than their ND controls. While secretion rates of animals fed HFD+PB were the highest, they were not significantly different to HFD rats.

Intracranial pressure was also measured at the beginning, middle and the end of the ventricular perfusion procedure in order to compare this measure between diets but also to monitor the CSF perfusion surgery, as a drastic change in pressure during the procedure would mean that the ventricular system might be disrupted (**Figure 3.19**). Baseline intracranial pressures are represented relative to those recorded for animals on ND, while pressures during the perfusion procedure are represented as a percentage of each individual's starting pressure.

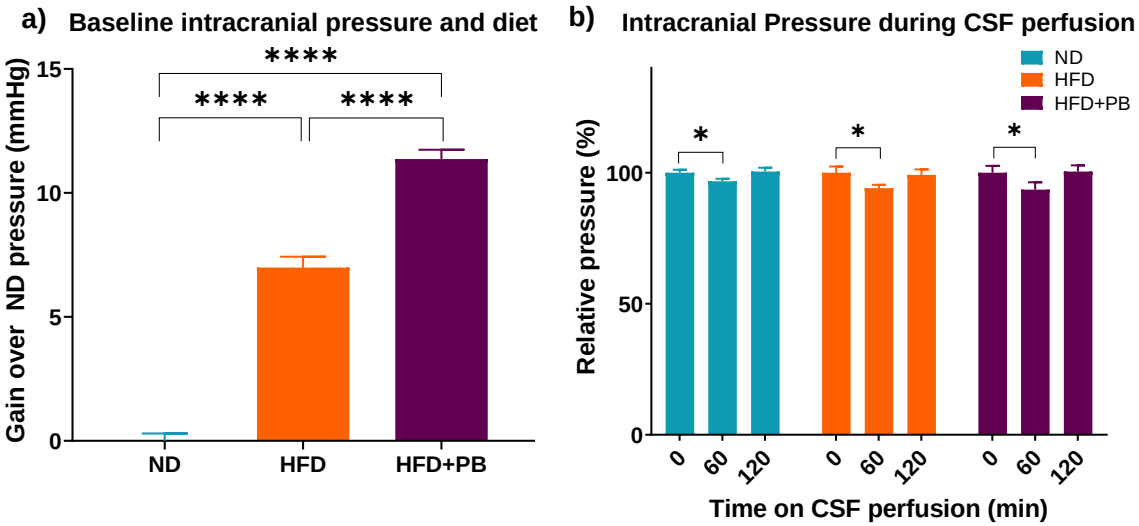

Figure 3.19. Intracranial pressures depending on diet.

In figure a) data is represented as pressure relative to ND. In figure b) data is represented as percentage of baseline pressure for each individual. n=5 * = *P* value<0.05

Both high fat diet groups had significantly higher initial pressures than ND 15w, and HFD+PB pressures were significantly higher than those recorded for HFD animals. There was a decrease in pressure after 60 min of perfusion in all three diet groups, but the pressure had returned to initial values by the end of the perfusion.

III. Cerebrospinal fluid secretion and obesity

The correlation between CSF secretion rate and obesity was analysed (**Figure 3.20**). There was a strong positive correlation between CSF secretion rate and BMI, body fat and final body weight.

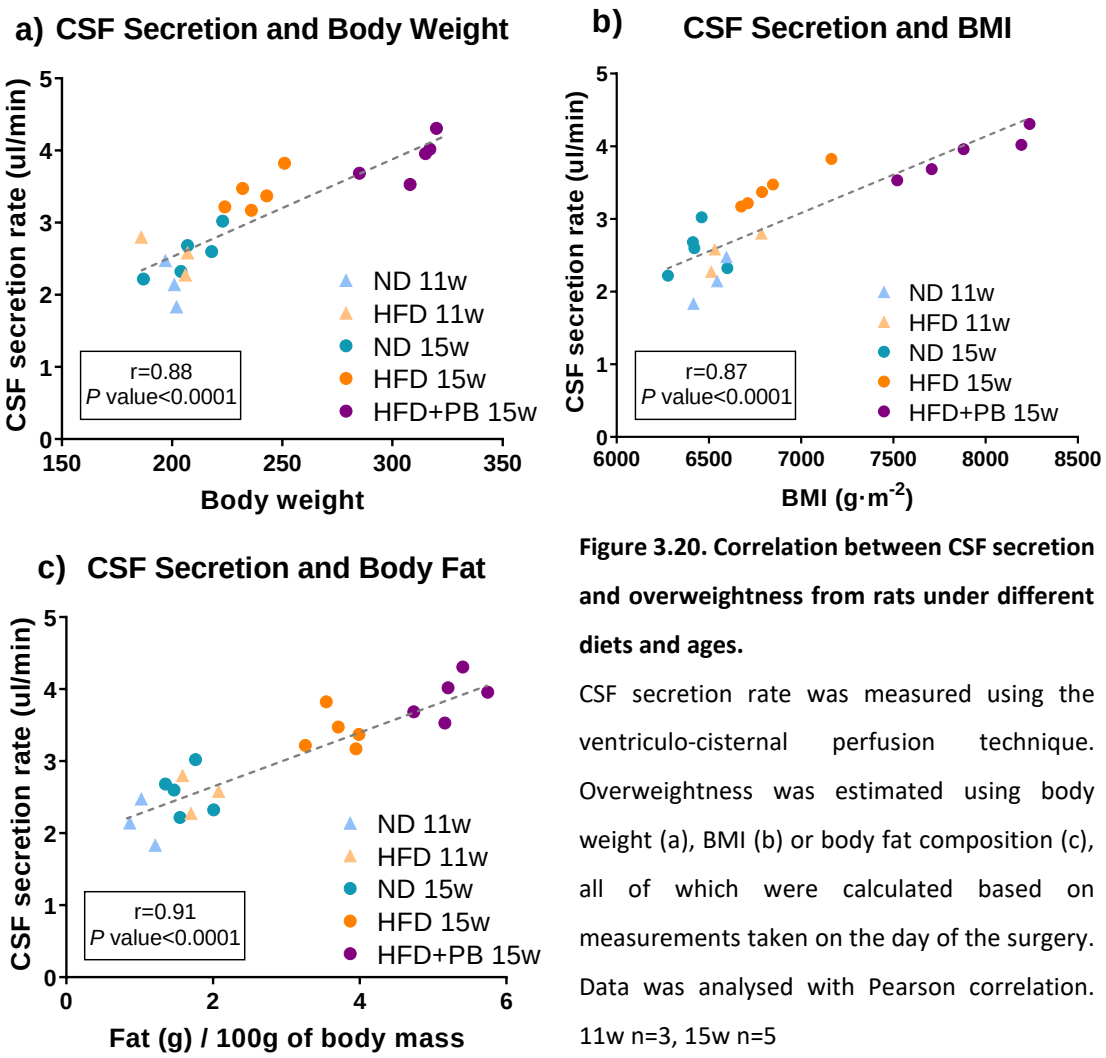

Figure 3.20. Correlation between CSF secretion and overweightness from rats under different diets and ages.

CSF secretion rate was measured using the ventriculo-cisternal perfusion technique. Overweightness was estimated using body weight (a), BMI (b) or body fat composition (c), all of which were calculated based on measurements taken on the day of the surgery. Data was analysed with Pearson correlation. 11w n=3, 15w n=5

IV. Cerebrospinal fluid secretion and cholesterol

A similar analysis was carried out to determine the relationship between plasma cholesterol levels and CSF secretion rates (**Figure 3.21**).

There was no correlation between CSF secretion and HDL concentrations or LDL/HDL ratio. A moderate positive correlation between LDL/VLDL levels and CSF secretion rates was observed. Total cholesterol also had a moderate positive correlation with CSF secretion rates.

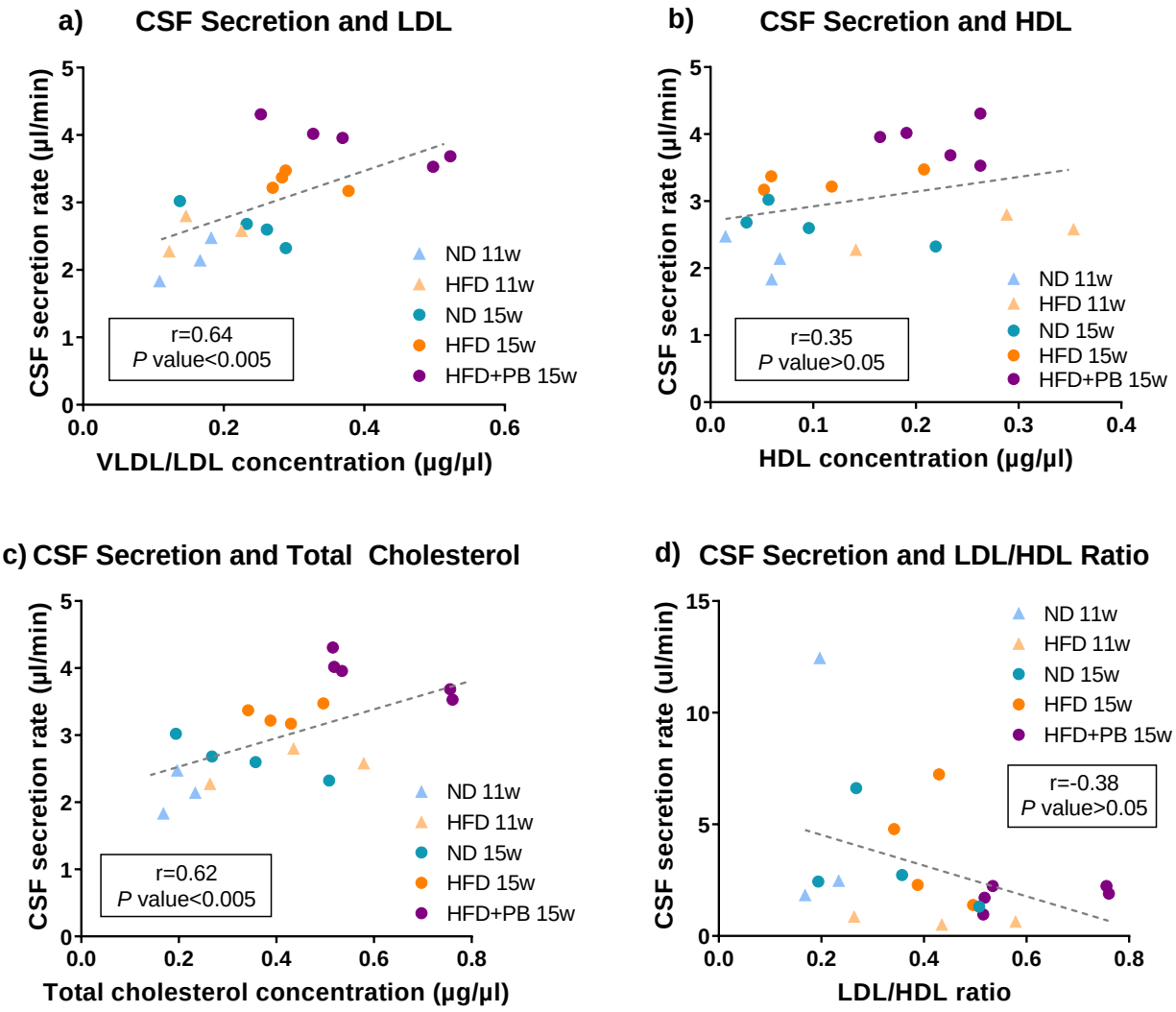

Figure 3.21. Correlation between CSF secretion and cholesterol on plasma of rats under different diets and ages.

LDL/VLDL (a), HDL (b) and total cholesterol (c) were measured from plasma samples. LDL/HDL ratio (d) was calculated with the individual values of each rat. Data was analysed with Pearson correlation. ND 11w and HFD 11w n=3, ND 15w n=4, HFD 15w n=4, HFD+ PB 15w n=5

V. Cerebrospinal fluid secretion and hormones

The correlation coefficients between cortisol, progesterone, oestradiol and testosterone and rate of CSF secretion were calculated and are represented on **Figure 3.22**.

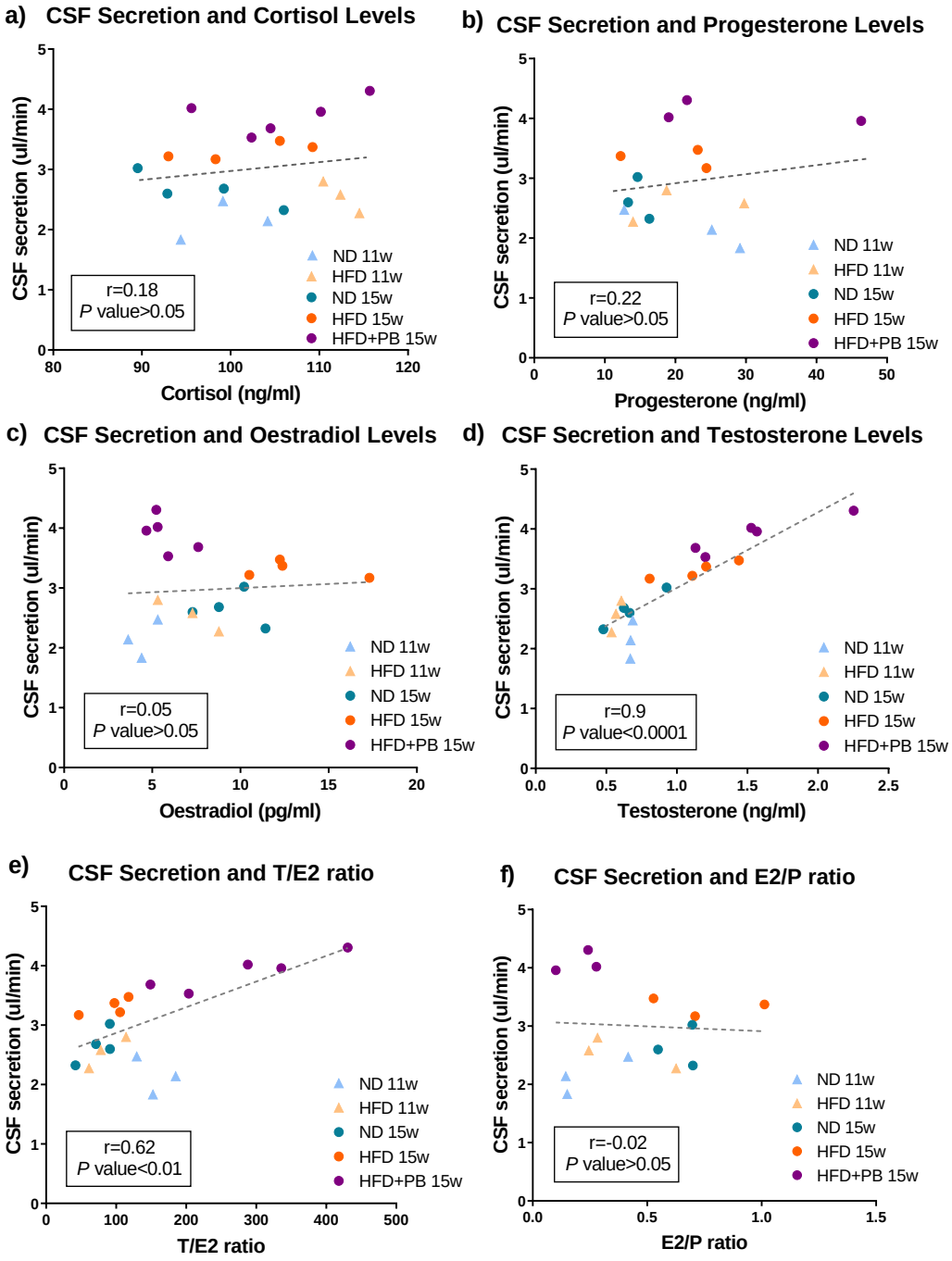

Figure 3.22. Correlation between hormone concentrations and CSF secretion.

Cortisol (a), progesterone (b), oestradiol (c) and testosterone (d) were measured from plasma samples. Testosterone to oestradiol ratio (e) and oestradiol to progesterone ratio (f) were calculated for each individual. CSF secretion rate was measured using the ventriculo-cisternal perfusion technique. Data was

analysed with Pearson correlation. ND 11w and HFD 11w n=3, ND 15w n=4, HFD 15w n=4, HFD+PB 15w n=5, except for progesterone 15w n=3.

Neither cortisol, progesterone, oestradiol nor E2/P ratio showed any correlation with CSF secretion. However, testosterone and CSF secretion did show a strong correlation. Furthermore, T/E2 ratio and CSF secretion also showed positive correlation.

3.4 Discussion

The increased prevalence of IIH in overweight women of childbearing age points to the likelihood of age, weight and sex being directly related to the disease. In this chapter, the relationship between diet and CSF secretion was studied. No difference in final weight, BMI, total cholesterol, sex hormone levels or CSF secretion rates was found between ND and HFD-fed rats at 11w, while body fat content and HDL concentration were increased in rats fed a HFD when compared to ND. The 4 weeks of further feeding and the addition of PB also resulted in an increased fat content and elevated cholesterol, while also significantly increasing body weight, LDL, testosterone and oestradiol concentrations, CSF secretion and CSF baseline pressure, compared to ND-fed rats. CSF secretion was found to show a strong and positive correlation with overweightness and testosterone concentrations.

The rapid, significant increase in weight after the introduction of PB was caused by a sudden increase in caloric intake. This increase in caloric intake was related to both higher calories per gram of diet but also to a change in flavour or texture of the diet, increasing its palatability. It is known that rats fed a HFD tend to eat smaller quantities of food to compensate for the higher caloric values (Oscai, Brown and Miller, 1984; Buettner, Schölmerich and Bollheimer, 2007; Aslani *et al.*, 2015). On the other hand, rats enjoy highly palatable foods such as chocolate and PB, and will indulge in them if given the chance (Cabanac and Johnson, 1983; Anderson, 1990; Zeeni *et al.*, 2013). All 15w rats fed HFD, regardless of PB addition, had significantly higher BMI, greater body weight and body fat

content compared to ND of the same age, which supports the appropriateness of this model to induce obesity in rats.

Rats studied at 11w did not show any diet-induced differences in CSF secretion rates in this study. At 15w, however, the CSF secretion rate was significantly increased in the two HFD groups, especially in the HFD+PB, which matches the results described in Chapter 2. Similarly, baseline intracranial pressure was increased in both HFD groups at 15w, especially in the HFD+PB group. These results indicate that our model of diet-induced obesity resulted in increased CSF secretion, making it a suitable model for the study of the effects of diet on CSF dynamics and, ultimately, IIH.

In our study, CSF secretion showed a significant positive relationship with body weight, BMI and body fat content. Severe obesity can affect CSF pressure directly by increasing abdominal pressure, which can concurrently alter CSF drainage or cause CSF leaks (Hogan *et al.*, 1996; Bloomfield *et al.*, 1997; Sugerman, 2001; Stucken, Selesnick and Brown, 2012; Rabbani *et al.*, 2018). However, the effect of obesity on CSF secretion is not well known yet (Bono *et al.*, 2002; Whiteley *et al.*, 2006). Our results supported the hypothesis that CSF dynamics, specifically CSF secretion, can be altered by obesity.

While hypercholesterolemia is present in approximately half of IIH patients, the relationship between cholesterol levels and CSF dynamics are still unknown and, it has been suggested that the increase in cholesterol is directly related to obesity status rather than IIH itself (Pollak *et al.*, 2015). In the present study, HDL levels were elevated in HFD rats, which is in keeping with previous reports that dietary fat increases HDL in rodents (Hayek *et al.*, 1993; Stephens *et al.*, 2010). HDL did not appear to alter CSF secretion, while LDL and total cholesterol did show a small positive correlation with CSF secretion. While cholesterol itself is not able to cross the BBB or the BCSFB, the side-chain oxidized metabolites 24S-hydrocholesterol and 27-hydroxycholesterol can cross the barrier (Meaney *et al.*, 2002; Björkhem, Leoni and Svenningsson, 2019). The possibility and extent at which an excess of these molecules caused by elevated cholesterol levels in plasma could affect CSF secretion are unknown. However, it is important to keep in mind that excess weight and obesity are known drivers for increased levels of cholesterol (Akiyama *et al.*, 1996; Dobrian *et al.*, 2000;

Tchernof and Després, 2013), thus we hypothesised that the weak correlation between higher CSF secretion rates and higher cholesterol levels are actually related to the obesity of the individuals, as discussed above, rather than the cholesterol increase itself.

Sex hormones have significant effects on the brain and they also vary greatly during the oestrous cycle (Marcondes *et al.*, 2001; Terner, Lomas and Picker, 2005). In women, obesity caused by diets high in fat has been linked to altered sex hormones and reproductive function (Bennett and Ingram, 1990; Varlamov, 2017). In rats, a HFD increases the chance of irregular cycles even in rats genetically resistant to diet-induced obesity (Whitaker, Shaw and Hervey, 1983; Balasubramanian *et al.*, 2012; Lie, Overgaard and Mikkelsen, 2013; Bazzano *et al.*, 2015; Markey *et al.*, 2016; Broughton and Moley, 2017). In the present study, a difference in cycle regularities between HFD and ND rats was detected, especially in 15w rats. No difference was found in plasma oestradiol levels between 11w diet groups, but there was an increase between 11w and 15w in animals fed a ND. This difference could be related to ongoing growth of the rats, as oestradiol concentration has shown a positive correlation with body weight in lean female rats (Banu *et al.*, 2001). Oestradiol levels were further increased in HFD 15w compared to animals of the same age in the ND group, but in the HFD+PB group at this age, plasma levels of this hormone were significantly lower than that observed in both the ND and the HFD groups. This may relate to the higher body fat content, as diet-induced obesity is associated with lower levels of oestradiol in the rat (Balasubramanian *et al.*, 2012). The effects of low oestrogen levels in females include increase of overeating behaviours and adipose tissue formation, which can increase obesity in the individual further (Leeners *et al.*, 2017).

Plasma testosterone levels in 11w and ND 15w were similar to those reported in the literature for rats (Zeng *et al.*, 2003). However, testosterone concentration was increased in HFD+PB 15w when compared to ND 15w. This result is consistent with reports in the literature of increased plasma testosterone levels in dioestrus as a result of diet-induced obesity in rats (Volk *et al.*, 2017). This phenomenon has also been described in obese women and it is linked to lower fertility rates in both species (Kopelman *et al.*, 1980; Wajchenberg *et al.*, 1989; Nestler, 2000; Tchernof and Després, 2013). Testosterone was

the parameter measured in the present study which showed the strongest positive correlation with CSF secretion rates. Raised levels of androgens have been found in IIH when compared to healthy overweight women (Hornby *et al.*, 2016; O'Reilly *et al.*, 2019). These results suggest that ours was a reliable model to study the mechanisms behind the possible increase in CSF secretion that result in IIH.

The testosterone to oestradiol ratio is an important steroid hormone ratio to evaluate the steroidogenesis pathway. This pathway occurs mainly in the ovary, and it starts with androgen synthesis occurring in theca cells, followed by testosterone transformation into oestrogens in the granulosa cells (Fauser and Van Heusden, 1997). A decrease of oestradiol and an imbalance between testosterone and oestradiol concentrations could be due to two different reasons. Firstly, it could be caused by a decrease in the conversion rate of testosterone to oestradiol, but it could also be due to an increase in testosterone production which is not coupled with an increase in the conversion enzyme. In the present research, the decrease in oestradiol and increase in testosterone levels which resulted in an altered T/E2 ratio in the animals in the HFD+PB group when compared to ND at 15w suggests that both mechanisms could be contributing to this observation. While it has been shown that testosterone concentration was increased, the concentrations and effectivity of the conversion enzyme were not evaluated. In the future, studying these parameters could help in discovering whether T/E2 ratio discrepancy is caused by an alteration in conversion rate or if its origins are more complicated.

Although no correlation was found between CSF secretion rate and cortisol, progesterone or oestradiol levels, there was strong positive correlation with testosterone levels and also with the T/E2 ratio. These results fit with the previous findings that testosterone can alter CSF dynamics and, especially, increase CSF secretion in IIH female patients (Klein *et al.*, 2013; Hornby *et al.*, 2017; O'Reilly *et al.*, 2019). Additionally, testosterone has been shown to increase hyperphagia and fat storage in females, whereas, on the other hand, obesity in females has been linked to altered androgen secretions (Evans *et al.*, 1983; Bray, 1997; Tchernof and Després, 2000; Watson, Mayes and Watson, 2004; Pasquali, 2006). Whether increased testosterone levels drive obesity or if obesity

increases testosterone concentration in females is not yet known; nevertheless, we hypothesised that an increase in testosterone concentration in the plasma of our rats affected CSF secretion rates by altering protein expression patterns of the CP in the lateral ventricles. In order to test this, the gene and protein expression of CP from 15w rats was studied and data from these investigations are presented in the following chapter.

Chapter 4. Diet-related Changes to the mRNA and Protein Expression Profile in the Choroid Plexus of Female Rats

4.1 Introduction

The CP is essential to CSF dynamics as it is considered to be the main site for CSF secretion (Speake *et al.*, 2001; Emerich *et al.*, 2004; Tumani, Huss and Bachhuber, 2017). As previously described in Chapter 1, the CP is a secretory epithelium which actively controls the passage of molecules and water in and out of the CSF in order to keep its composition stable and adequate for CNS homeostasis. Although the specific mechanisms by which this equilibrium is maintained are not well known, three main types of proteins are involved in the functioning of the CP: transport proteins, water channels and tight junctional proteins. (Emerich *et al.*, 2004; Quintela *et al.*, 2013; Orešković and Klarica, 2014; Praetorius and Damkier, 2017).

Transport proteins and channels, such as the solute carrier family (Slc) and KCNA6, mediate transcellular movement of molecules between blood and CSF, facilitating the movement of specific ions between the apical and basolateral areas of the CP and thus inducing an osmosis gradient which drives water movement from the blood into the CSF. Active transport of molecules requires cellular energy in the form of ATP, produced by Na^+/K^+ ATPase 1 (ATP1) and an available transporter protein (Kyte, 1981; Praetorius & Damkier, 2017; Speake, Whitwell, Kajita, Majid, & Brown, 2001). ATP1 found in the CP is an heterodimer formed by two units, ATP1A1 and either ATP1B1 or ATP1B2, the first of them being the dominant catalytic subunit (Zlokovic *et al.*, 1993; Kant *et al.*, 2018).

Water channels expressed in the membrane of CPEC facilitate water transport between apical and basolateral areas of the CP following the ion gradient. Aquaporin-1 (AQP1) is thought to be the main water channel expressed in CP, although expression of AQP7 and 9 has also been observed (Speake, Freeman and Brown, 2003; Yaba *et al.*, 2017). While Aqp4 has been reported to appear diffusely expressed in the cytosol of CP epithelial

cells (CPEC), it is mainly expressed by ependymal cells lining the ventricles and therefore its contribution to CSF dynamics would be independent of CP activity (Frigeri *et al.*, 1995; Venero *et al.*, 1999; Speake, Freeman and Brown, 2003). Deregulation of aquaporin expression in the CP has been shown to affect brain fluid dynamics (Oshio *et al.*, 2004; Trillo-Contreras *et al.*, 2019).

The barrier properties of the BCSFB are dependent on the presence of organised tight junctional complexes between CPECs, which are mediated by intracellular proteins like ZO1, and transcellular proteins such as JAM3 or CLDN1. These junctions act as a barrier to paracellular molecular movement, restricting it to the more controlled transcellular transport mentioned above (Damkier, Brown and Praetorius, 2010; Kratzer *et al.*, 2012; Ghersi-Egea *et al.*, 2018). Nevertheless, an underexpression of tight junction proteins could lead to an increase of barrier leakiness, which might alter CSF dynamics (Redzic, 2011; Naessens *et al.*, 2018).

It is known that diet can affect many different biological aspects of an individual, ranging from changes in physiological processes to epigenetic alterations. As a matter of fact, it has been shown that dietary fat can alter gene expression by mechanisms such as regulation of transcription factors at the cellular level or alteration of hormonal levels at the organismal level (Beato, 1993; Jump and Clarke, 1999). In the CP, HFD and diet-induced obesity can alter not only the expression of functional genes such as prolactin and lactin receptors but also those involved in the formation of TJs such as claudin 5 (Lin, Storlien and Huang, 2000; Kanoski *et al.*, 2010; Kalyani *et al.*, 2016). In addition, there appear to be sex-based differences in the gene expression profile of the CP. Indeed, the CP expresses both oestrogen and androgen receptors (ER and AR), and sex hormones have been shown to regulate the expression of choroid plexus genes, such as transthyretin and circadian clock genes (Alves *et al.*, 2009; Quintela *et al.*, 2009, 2015; Santos *et al.*, 2017).

The current study was designed to investigate whether the change in CSF secretion observed between diet groups in female rats in Chapter 3 was related to alterations in gene expression in the CP. The gene expression profile of CP isolated from female rats fed HFD, HFD+PB or ND for 11w and 15w was first characterised using RNAseq techniques. Then,

differences in the expression of selected water channels, ion transporters and TJ proteins between diet groups at 15w were further investigated at the protein level using immunohistochemistry.

4.2 Materials and Methods

All materials used were obtained from Sigma-Aldrich (Poole, Dorset, UK) unless otherwise specified.

4.2.1 Animals

Animals were housed and cared for as specified in Chapter 3.

Choroid plexus of rats used for the preliminary gene expression study were obtained from rats used for CSF secretion measurement (Chapter 3) after the surgery was performed.

Animals used for the further gene expression experiments, including Massive Analysis of cDNA Ends (RNAseq-MACE) and qPCR, belonged to a separate cohort that did not undergo surgery.

4.2.2 Choroid plexus extraction

Rats were terminally anaesthetised with 140 mg/kg pentobarbital. Once anaesthetized rats did not respond to reflex-inducing external stimuli (i.e. pinching) for more than 2 min, blood samples were obtained by cardiac puncture and, immediately after, perfusion with PBS was started and run for 10 min or until waste liquid ran clear. Rats were then perfused with 0.5% toluine blue for 3 min to help visualise the CP. Brains were dissected and cut sagittally to reveal the lateral ventricles. The lateral ventricle CP was dissected on ice using forceps and its RNA was extracted using RNeasy Micro Kit (Qiagen, Manchester, UK) and stored at -80C.

4.2.3 Gene expression analysis

Three samples of each group (ND 15w, HFD 15w, HFD+PB 15w) were sent to GenXPro (Frankfurt am Main, Germany) for analysis using RNAseq-MACE. RNA samples were processed and analysed using a modified protocol previously described in the literature using the MACE kit (Nold-Petry *et al.*, 2015). In brief, 100ng of DNase-treated RNA were used for library preparation. cDNA was produced by oligo dT priming, sheared to an average size of 200bps and ligated to "TrueQuant" unique molecular identifiers included in the MACE kit. Tags were amplified with 13 PCR cycles. Libraries were sequenced using an Illumina NextSeq 500 sequencer.

For qPCR analysis, reverse transcription was performed using the High Capacity cDNA Reverse Transcription Kit (Thermofisher Scientific, UK) and qPCR was carried out using the QuantiTect SYBR® Green PCR Kit (Qiagen, Manchester, UK) and KiCqStart® SyBR® Green predesigned primers for rat (Table 4.1). Relative expression was calculated using the $2^{-\Delta\Delta Ct}$ method as previously described in the literature (Livak and Schmittgen, 2001; Schmittgen and Livak, 2008). ND was taken as a control for the respective ages, and actin-β was used as reference gene to measure relative expression. For the preliminary study, genes were selected from literature to scan for changes in expression of water channels, ATP1, molecular transporters and sex hormone receptors.

Table 4.1. Sequences of primers used in qPCR analysis.

Gene	Symbol	Sequence
Actin Beta	Actin β	Forward 5'-AAGACCTCTATGCCAACAC Reverse 5'-TGATCTTCATGGTGCTAGG
Aquaporin 1	AQP1	Forward 5'-CAAACCACTGGATTTTCTGG Reverse 5'-ATATCATCAGCATCCAGGTC
Aquaporin 4	AQP4	Forward 5'-GAAAACCACTGGATATATTGGG Reverse 5'-CAGAAGACATACTCGTAAAGTG
Aquaporin 7	AQP7	Forward 5'-CTTCGTGGATGAGGTATTTG Reverse 5'-TGATTGCATATCCTGTGTTC

Gene	Symbol	Sequence
Aquaporin 9	AQP9	Forward 5'-CATGTTTGACTCCAGAAACC Reverse 5'-CAACTGTGAAGACCTCAAAC
Electrogenic Sodium Bicarbonate Cotransporter 4	SLC4A5	Forward 5'-AGAAAAGGTAGAGGAAGGAG Reverse 5'-CATCATCTATGATCTGTGGTAG
Sodium-Driven Chloride Bicarbonate Exchanger	SLC4A10	Forward 5'-GGAGAGAGAGGTTGATCTTC Reverse 5'-ACAGTTCTGTCTAGAAACTCC
Basolateral Na-K-Cl Symporter	SLC12A2	Forward 5'-AGTGTCTGTAGGTTCTTGTG Reverse 5'-GCAGAAGTACAGTTAGTTAGC
Androgen Receptor	AR	Forward 5'-CCTTGTTCCCTTTTCAGATG Reverse 5'-GTAAAAGAGGCAGAGAAGAAG
ATPase Na+/K+ Transporting Subunit Alpha 1	ATP1A1	Forward 5'-GAGTAGAAGAAGGTCGTCTG Reverse 5'-CCGGAATGTTACTTGTTAGG
ATPase Na+/K+ Transporting Subunit Beta 1	ATP1B1	Forward 5'-CAAGAATGAATCCTTGGAGAC Reverse 5'-GTAGGGATAGTACTGCAGAG
ATPase Na+/K+ Transporting Subunit Beta 2	ATP1B2	Forward 5'-GTGTTGGGAAGAAAGATGAAG Reverse 5'-AATACATCAGGTCGATGTTG
Oestrogen Receptor Alpha	ERa	Forward 5'-GGCTGCGCAAGTGTTACGAA Reverse 5'-CATTTCGGCCTTCCAAGTCAT
Oestrogen Receptor Beta	ERb	Forward 5'-GAGGCAGAAAGTAGCCGGAA Reverse 5'-CGTGAGAAAGAAGCATCAGGA
Claudin 1	CLDN1	Forward 5'-AGAATTCTATGACCCCATGAC Reverse 5'-GTAGTCTTTCCCAGTAGAAGG
Claudin 2	CLDN2	Forward 5'-GAAATCCCTTATCATCACAG Reverse 5'-CAAGAAGGCATCTAGAAAACG
Potassium Voltage-Gated Channel Subfamily A Member 6	KCNA6	Forward 5'-AAATGAGAGGAGACGATTTG Reverse 5'-TCTTGCTTTCTCACATTCAC
Zona Occludens 1	ZO-1	Forward 5'-CACTCTTCCAGAACCAAAAC Reverse 5'-ACCCACACTATCTCCTTTTC
Zona Occludens 3	ZO-3	Forward 5'-AAGAAACAGCGAAGAGTTTG Reverse 5'-TCACTCAGGGATAGATTAGC
Junctional Adhesion Molecule 3	JAM3	Forward 5'-GGACATGGAAGTCTATGATTTG Reverse 5'-CCTGGGCTTTTATAACTTTCTC

4.2.4 Bioinformatic analysis of RNAseq-MACE results

An initial bioinformatic analysis of the RNAseq-MACE data was performed by GenXpro. Raw data sets were quality trimmed, including deletion of PCR duplicated reads. Filtered reads were aligned to the Rattus norvegicus reference genome (Rnor_6.0) using the Bowtie 2 mapping tool (Langmead and Salzberg, 2012). The Rnor_6.0 Ensembl annotation file was imported into the Htseq-count annotation tool to annotate bam files. Normalization of gene count data and differential gene expression analysis between the samples were performed using the DEGseq R/Bioconductor package (Wang *et al.*, 2010).

A *P* value smaller than 0.05 determined that the difference in gene expression levels between two groups was significantly altered. Relevantly up- and downregulated genes were selected following two criteria: log2fold change greater than 1 or less than -1, and a *P* value smaller than 0.05.

The first step to further analyse deregulated genes was to determine the functional classification of their related protein using Panther Classification System (Mi *et al.*, 2019). Upregulated and downregulated genes from each comparison were studied as two different groups, and in each, their molecular and biological function, cell compartment and protein classification were determined. PANTHER did not hold enough information on some of the selected genes, which were then excluded from the analysis, thus the number of genes in each analysis differ from the total number of deregulated genes found in each comparison. For each group, the total number of genes included in the analysis is shown next to the title, while each parameter also shows the number of hits that were found. These two numbers can differ for two reasons: either the parameter is not known for all the genes selected, or they fulfil two or more different categories, such as performing several functions.

Each comparison was then analysed to find expression trends or deregulated pathways that could affect CSF secretion or increase leakage of the BCSFB using DAVID Bioinformatics Resources 6.8 (Huang, Brad T Sherman and Lempicki, 2009; Huang, Brad T. Sherman and Lempicki, 2009).

4.2.5 Immunohistochemistry

Three rats per dietary condition were anaesthetised and perfused intracardially with 0.01M PBS. Brains were extracted, snap frozen and stored at -80^{o}C. Brains were sliced on a cryostat to a thickness of 20µm and collected on glass slides, which were then desiccated under vacuum in a desiccator for 24h and kept at -80C until the experiments started.

Sections were fixed with either acetone (ZO1 and CLDN1 staining) or ethanol (AQP4 staining) for 10 min, washed with 0.01M PBS (5 min, 3 times) and blocked with 15% goat

serum in PBS for 15 min. Sections were incubated overnight at 4°C with either anti-ZO1, anti-CLDN1 or anti-AQP4 (1:100; Thermofisher Scientific, UK), washed with 0.01M PBS at RT (5 min, 3 times) and incubated with Alexa Fluor 488 anti-rabbit (1:500; Thermofisher Scientific, UK) protected from light for 2h at RT. The mounting media used was ProLong™ Gold Antifade Mountant with DAPI (Thermofisher Scientific, UK). After mounting, slides were left to dry for at least 48h at 4°C and then were imaged using confocal microscopy (Leica confocal, Leica Microsystems Ltd, UK). Five sections per animal were analysed for each protein of interest.

Images were processed using ImageJ software (Rasband and U. S. National Institutes of Health, 2018). Area of interest was the area where the protein was expected to be expressed, e.g. the CP was selected for CLDN1 analysis while the ependyma was the area of interest for AQP4 expression. The area of interest was manually traced and selected for further analysis. Cellular fluorescence intensity and area of staining were used to compare protein expression levels between samples for each protein studied. Corrected total cellular fluorescence (CTCF) was calculated using **Equation 4.1**. Relative area of staining was calculated using **Equation 4.2**.

Equation 4.1. Calculation of corrected total cellular fluorescence.

$$\boldsymbol{CTCF = Integrated\ Density - (Area\ of\ Interest \cdot\ Mean\ Fluorescence\ of\ Background)}$$

Equation 4.2. Calculation of relative area of staining

$$\boldsymbol{Relative\ Area\ of\ Staining = \frac{Area\ of\ Staining\ of\ Protein\ of\ Interest\ (\%)}{Area\ of\ Staining\ of\ DAPI\ (\%)}}$$

4.2.6 Statistical analysis

Each diet group had 3 animals (n=3). All data is presented as average ± SEM unless otherwise specified. Differences in gene expression measured by RNAseq were analysed statistically using the DESeq2 analysis (Love, Huber and Anders, 2014). Shapiro-Wilk normality test and Q-Q plots were used to assess normal distribution of qPCR and

immunostaining data. Statistical analysis was performed using one-way ANOVA with Tukey post hoc test. Pathway analysis was assessed using Fisher's Exact Test. A *P* value smaller than 0.05 was considered significantly different. Statistical analysis was performed using Graphpad 8 (Graphpad Software, 2019).

4.3 Results

4.3.1 Preliminary study of gene expression profile of choroid plexus related to age and diet

A preliminary study was performed in which the CP gene expression profile of some key genes for CSF secretion or CP function, were studied as a function of duration of dietary manipulation. Comparative expression of genes associated with water channels, ATP1, tight junction proteins and sex hormones was carried out in HFD and ND rats of the same age, and the results are shown in **Figure 4.1**.

In 11-week rats fed diets for 7 weeks, mRNA levels of Slc4a5 were significantly higher and levels of AQP7 and AQP9 were significantly lower in HFD-groups compared to ND-fed rats (Figure 4.1.a). In 15-week rats, HFD-fed rats showed significantly higher mRNA levels of ATP1B1, Slc4a5 and ERb compared to ND 15w (Figure 4.1.b). HFD 15w rats also expressed significantly lower levels of AQP7 and AQP9. The expression of other genes were not significantly changed.

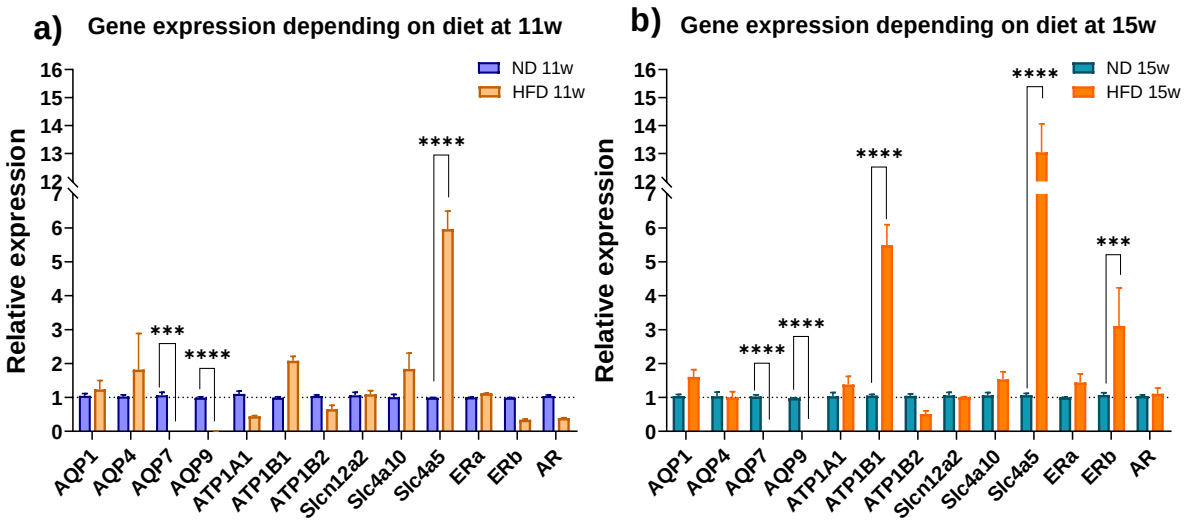

Figure 4.1. RT-qPCR showing relative gene expression on CP of female rats depending on diet.

Gene expression in HFD groups were compared to ND group for a) 11w and b) 15w rats. *=*P* value < 0.05, ***=*P* value < 0.001, **** *P* value < 0.0001. ER=Oestrogen Receptor, AR=Androgen receptor. n=3

Based on these results, the focus of further gene expression studies focused on 15w rats due to the bigger changes in gene expression and also the highest differences in CSF secretion and other body parameters described in Chapter 3.

4.3.2 Gene expression profile of choroid plexus related to diet in 15w rats.

MACE-RNAseq identified 15705 genes in our samples. Analysis of gene expression in HFD vs ND, HFD+PB vs ND and HFD+PB vs HFD was then carried out.

I. HFD vs ND

Gene expression in HFD samples compared to ND as a function of log2fold change and *P* value were used to plot **Figure 4.2**.

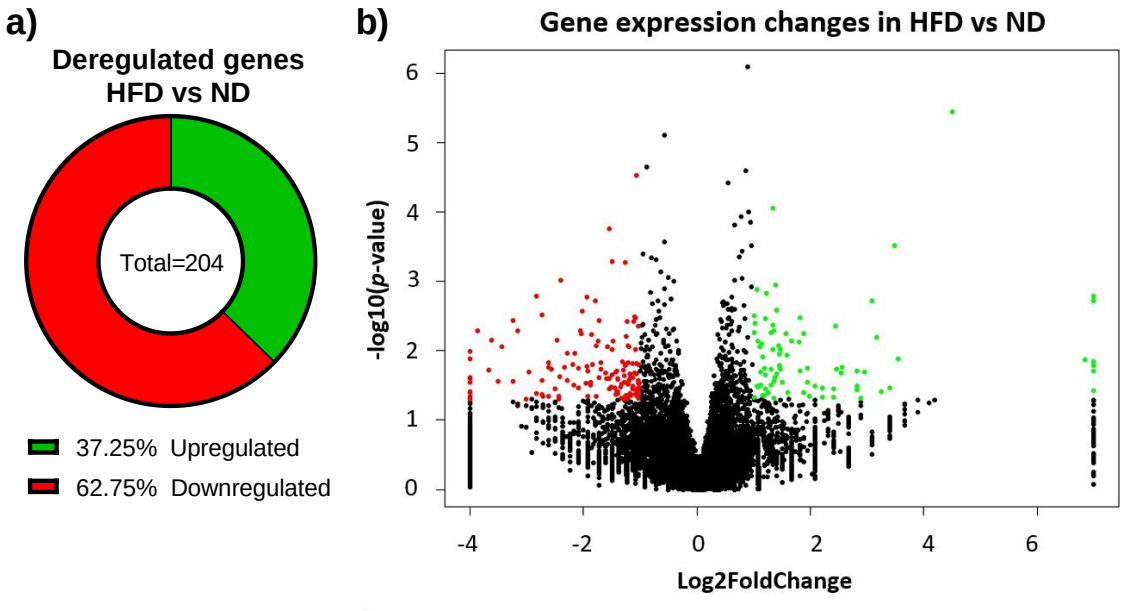

Figure 4.2. Distribution of differently expressed genes in HFD vs ND comparison.

In (a) the proportion of each gene group compared to the total number of deregulated genes, in (b) volcano plot of relative expression and *P* value for each gene. n=3

13757 genes were detected in the HFD vs ND comparison. From those, 128 were upregulated and 75 were downregulated. The functional classification of deregulated genes in HFD vs ND is shown in **Figure 4.3**.

58 of the upregulated genes were selected by PANTHER in the HFD vs ND. The most common molecular function for upregulated genes appeared to be related to binding, including binding to nucleic acids and protein receptors. Analysis of the genes according to 'cellular process' produced a higher number of hits and included proteins related to cytoskeleton organisation and nucleic acids such as the ATP-dependent DNA helicase Q5. Most of the proteins resulting from the upregulated genes in the HFD vs ND comparison were intracellular, and they belonged to a wide range of protein types. The most common ones were cytoskeletal proteins and hydrolases.

102 of the downregulated genes were selected by PANTHER. The most common molecular function in this group was related to catalytic activities, performed by proteins

such as kinases and proteases. The most common biological function was related to cellular processes, including transcription factors and carrier proteins. The majority of downregulated genes resulted in intracellular proteins and the most common protein types were nucleic acid binding proteins and transcription factors.

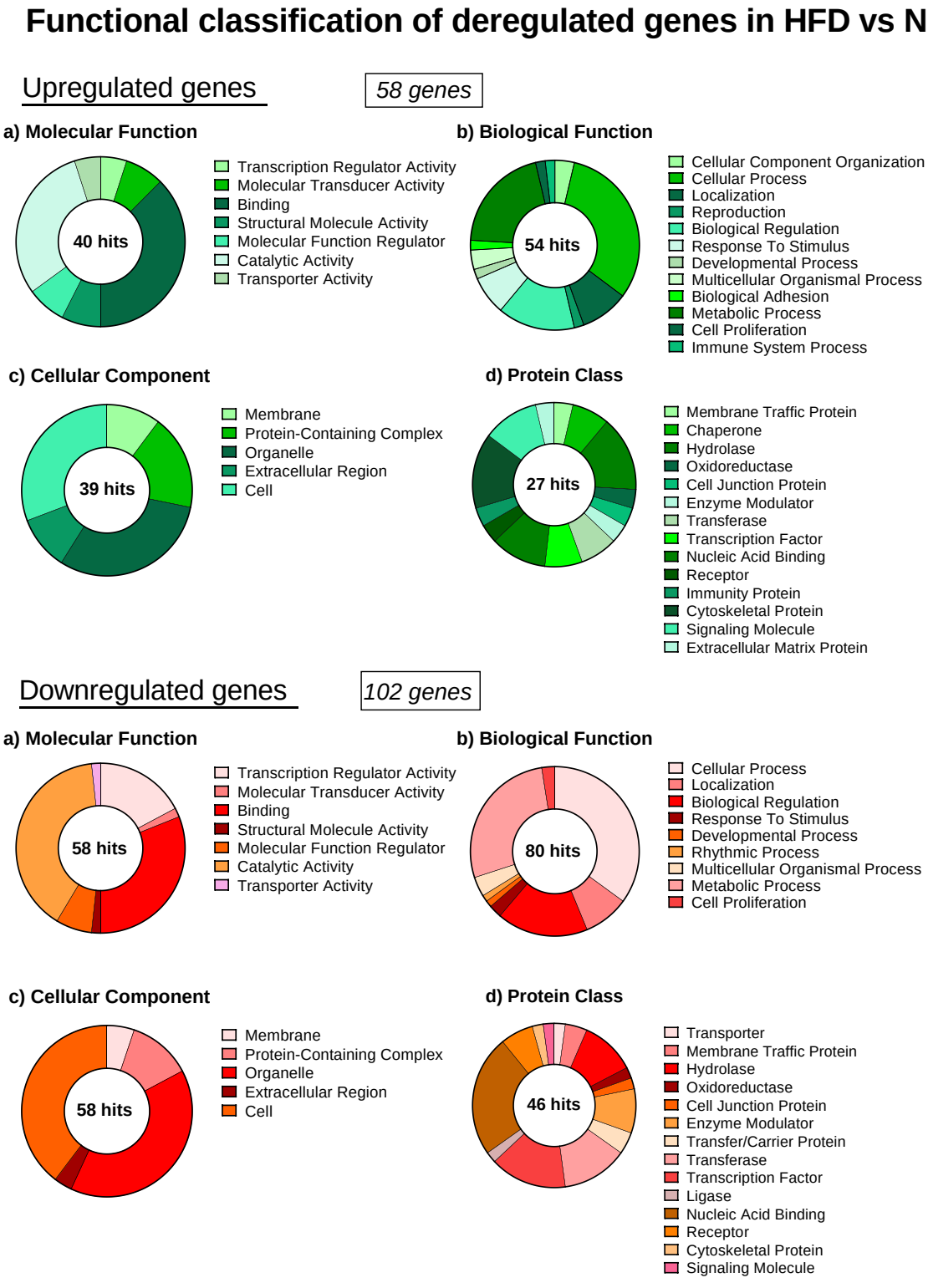

Figure 4.3. Functional classification of highly deregulated genes in the HFD vs ND comparison.

Both up and downregulated genes were analysed using PANTHER to determine the (a) molecular function, (b) biological function, (c) cellular component and (d) protein class of their related proteins. n=3

A full list of deregulated genes in the HFD vs ND comparison and their functional classifications can be found in Appendix B, **Table 0.5** and **Table 0.6**.

Upregulated and downregulated pathways in the HFD vs ND comparison were obtained using DAVID Bioinformatics and are shown in **Table 4.2**.

Table 4.2. Deregulated pathways in the HFD vs ND comparison.

Highly deregulated genes were selected using the parameters explained above and, using two tools from DAVID Bioinformatics (GO Analysis: Biological Process and KEGG Pathway), up to ten relevant deregulated pathways were selected for each tool used. "Total" is the number of total affected pathways highlighted by DAVID on that specific database.

UPREGULATED PATHWAYS				
	Term	**Pathway**	**No. transcripts**	**P value**
GO Analysis: Biological Process	GO:0001504	Neurotransmitter Uptake	2	0.016
	GO:0045110	Intermediate Filament Bundle Assembly	2	0.019
	GO:0045104	Intermediate Filament Cytoskeleton Organization	2	0.048
Total	3			
KEGG Pathway	rno04913	Ovarian steroidogenesis	3	0.012
	rno04918	Thyroid hormone synthesis	3	0.017
Total	2			

DOWNREGULATED PATHWAYS				
	Term	**Pathway**	**No. transcripts**	**P value**
GO Analysis: Biological Process	GO:0045944	Positive Regulation of Transcription from RNA Polymerase II Promoter	15	0.003
	GO:0006355	Regulation of Transcription, DNA-Templated	12	0.048
	GO:0006974	Cellular Response to DNA Damage Stimulus	6	0.012
	GO:0045665	Negative Regulation of Neuron Differentiation	4	0.009
	GO:0008104	Protein Localization	4	0.012
	GO:0000209	Protein Polyubiquitination	4	0.026
	GO:0043434	Response to Peptide Hormone	4	0.041
	GO:0048469	Cell Maturation	3	0.027

	GO:0045907	Positive Regulation of Vasoconstriction	3	0.029
	GO:0032570	Response to Progesterone	3	0.049
Total	20			
KEGG Pathway	----	----	----	----
Total	0			

A total of 5 differentially upregulated and 20 downregulated pathways were identified. The upregulated pathways picked up by DAVID bioinformatics from the HFD vs ND comparison were mostly related to hormones and to the cytoskeleton, while downregulated pathways were more varied. The pathways involving the greatest number of downregulated genes were related to nucleic acids. There were also pathways related to hormone response and cellular regulation.

II. HFD+PB vs ND

Gene expression in HFD+PB samples compared to ND as a function of log2fold change and *P* value are shown in **Figure 4.4**.

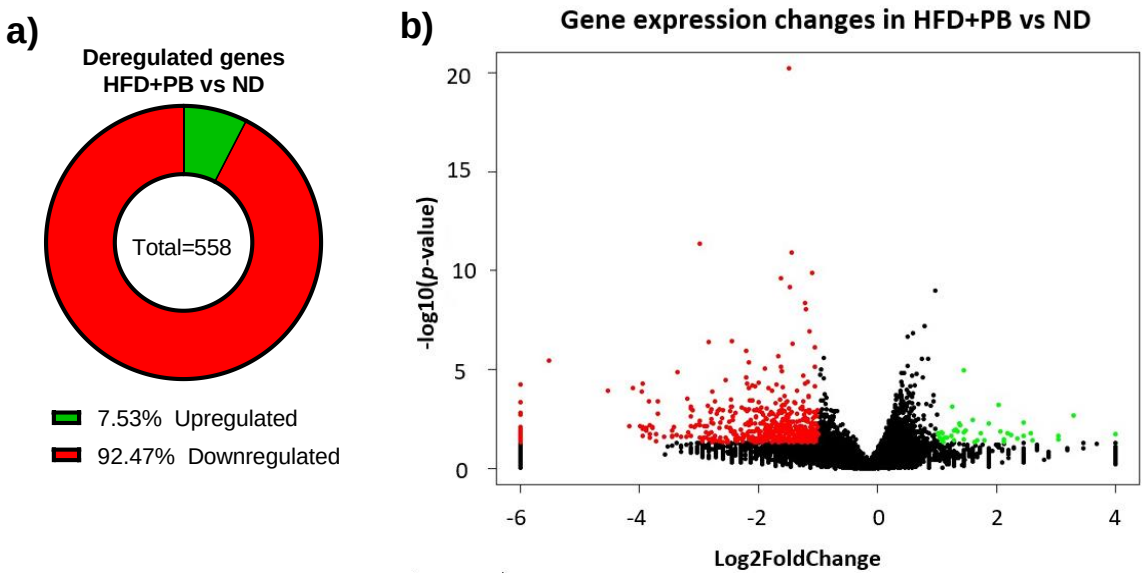

Figure 4.4. Distribution of differently expressed genes in the HFD+PB vs ND comparison.
In (a) the proportion of each gene group compared to the total number of deregulated genes, in (b) volcano plot of relative expression and *P* value for each gene. n=3

In HFD+PB vs ND comparison, 13588 genes were identified. From those, 514 were found to be downregulated and 43 upregulated. The functional classification of deregulated genes in HFD+PB vs ND can be found in **Figure 4.5**.

PANTHER selected 34 of the highly upregulated genes and 419 of the highly downregulated genes. Amongst the upregulated genes, the most common molecular function was binding, including binding to proteins and binding to nucleic acids. The most common biological function in this group was related to cellular processes, such as cytoskeleton organisation and DNA repairing. The proteins in this group were mostly intracellular, and they belonged to a wide range of protein types, the most common of which were enzyme modulators and hydrolases.

Highly downregulated genes produced proteins with a wider range of molecular functions, the most common being binding, especially protein binding and nucleic acid

binding. Most of these genes encoded proteins with biological functions regarding cellular processes, such as transcription and translation factors, and most of them were intracellular. The proteins from this group belonging to a wide range of protein classes, but the most common ones were hydrolases and enzyme modulators.

A full list of deregulated genes in the HFD+PB vs ND comparison and their functional classifications can be found in Appendix B, **Table 0.7** and **Table 0.8.**

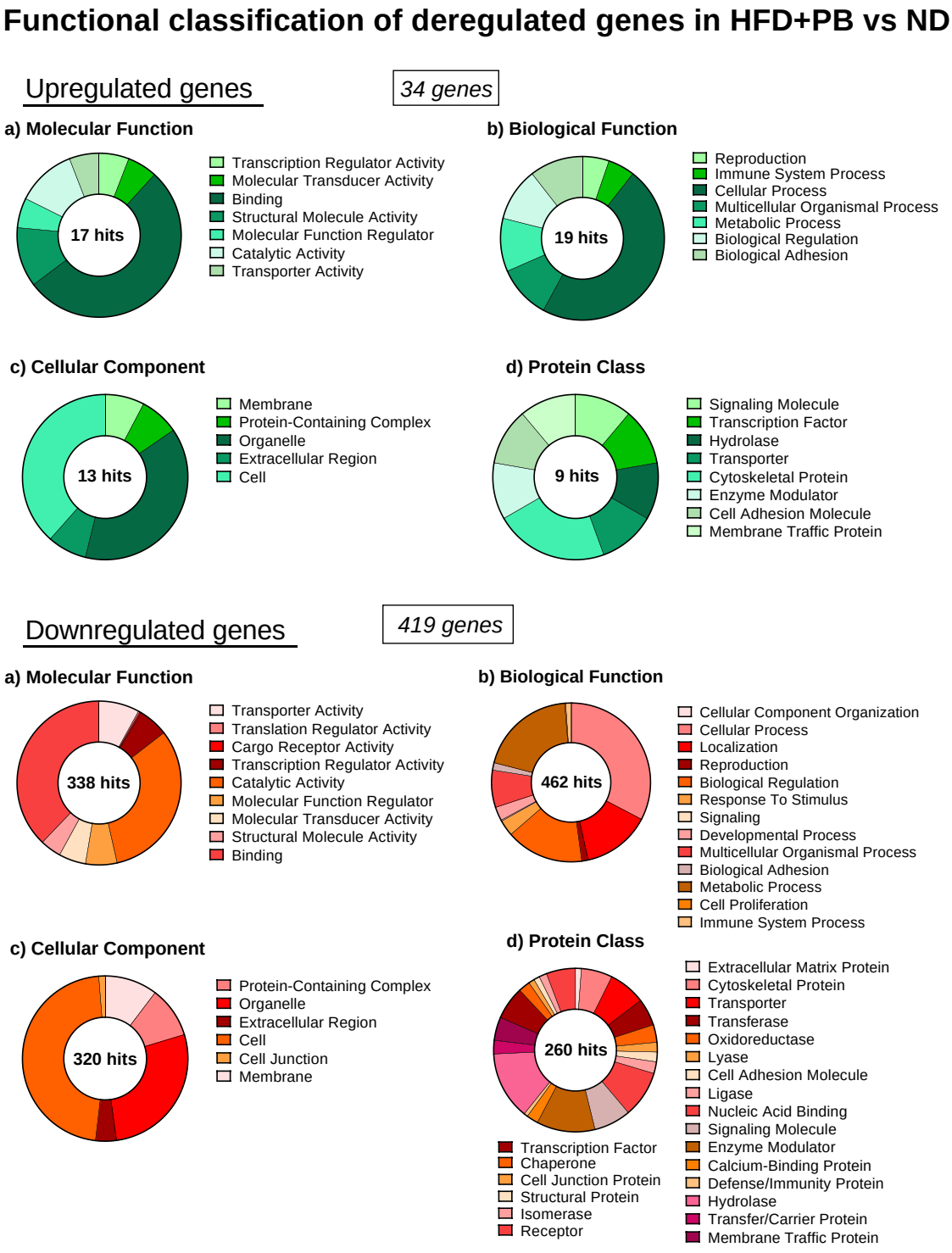

Figure 4.5. Functional classification of deregulated genes in the comparison HFD+PB vs ND.

Both up and downregulated genes were analysed using PANTHER to determine the (a) molecular function, (b) biological function, (c) cellular component and (d) protein class of their related proteins. n=3

Bioinformatic tools were used to select up and downregulated pathways in the HFD+PB vs ND comparison, and the results are shown in **Table 4.3**.

A total of 6 differentially upregulated and 33 downregulated pathways were selected by DAVID bioinformatics for the HFD+PB vs ND comparison. The overexpressed pathways were related to DNA repairing, while downregulated pathways had varied functions. The pathways involving the highest number of downregulated proteins were related to transport and cell adhesion. Furthermore, pathways related to hormone response and various signalling pathways were also selected.

Table 4.3. Deregulated pathways in the HFD+PB vs ND comparison.

Highly deregulated genes were selected using the parameters explained above and, using two tools from DAVID Bioinformatics (GO Analysis: Biological Process and KEGG Pathway), up to ten relevant deregulated pathways were selected for each tool used. "Total" is the number of total affected pathways highlighted by DAVID on that specific database.

UPREGULATED PATHWAYS

	Term	Pathway	No. transcripts	P value
GO Analysis: Biological Process	GO:0006303	Double-Strand Break Repair Via Nonhomologous End Joining	3	0.001
	GO:0010212	Response to Ionizing Radiation	3	0.011
	GO:0033151	V(D)J Recombination	2	0.028
	GO:0033591	Response To L-Ascorbic Acid	2	0.032
Total	4			
KEGG Pathway	rno03450	Non-homologous end-joining	2	0.025
Total	2			

DOWNREGULATED PATHWAYS

	Term	Pathway	No. transcripts	P value
GO Analysis: Biological Process	GO:0006886	Intracellular Protein Transport	14	0.003
	GO:0007155	Cell Adhesion	14	0.019
	GO:0007264	Small GTPase Mediated Signal Transduction	12	0.041
	GO:0034220	Ion Transmembrane Transport	10	7.80E-04

DOWNREGULATED PATHWAYS				
	Term	**Pathway**	**No. transcripts**	**P value**
	GO:0006979	Response to Oxidative Stress	9	0.036
	GO:0009725	Response to Hormone	7	0.043
	GO:0030100	Regulation of Endocytosis	5	0.007
	GO:0030521	Androgen Receptor Signalling Pathway	4	0.018
	GO:0002092	Positive Regulation of Receptor Internalization	4	0.035
	GO:0016338	Calcium-Independent Cell-Cell Adhesion Via Plasma Membrane Cell-Adhesion Molecules	3	0.026
Total	20			
KEGG Pathway	rno04014	RAS Signalling Pathway	12	2.23E-04
	rno04713	Circadian Entrainment	11	1.03E-04
	rno04728	Dopaminergic Synapse	11	0.001
	rno04727	GABAergic Synapse	10	0.001
	rno04724	Glutamatergic Synapse	10	0.002
	rno04024	cAMP signalling pathway	10	0.041
	rno04540	Gap junction	9	0.001
	rno00190	Oxidative phosphorylation	9	0.021
	rno04725	Cholinergic synapse	7	0.049
	rno03022	Basal transcription factors	5	0.021
Total	13			

III. HFD+PB vs HFD

Gene expression in HFD+PB samples compared to HFD as a function of log2fold change and *P* value are shown in **Figure 4.6**.

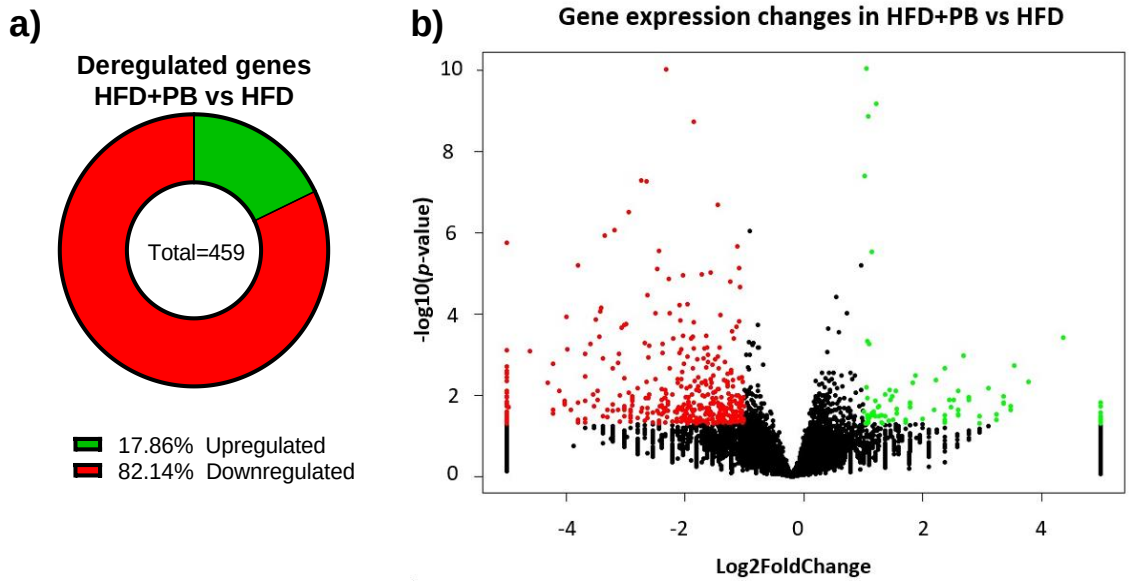

Figure 4.6. Distribution of differently expressed genes in HFD+PB vs HFD comparison.
In (a) the proportion of each gene group compared to the total number of deregulated genes, in (b) volcano plot of relative expression and *P* value for each gene. n=3

In the HFD+PB vs HFD comparison, 13120 genes were identified. From those, 377 were found to be downregulated and 82 upregulated. The functional classification of deregulated genes in the HFD+PB vs HFD comparison can be found on **Figure 4.7**.

PANTHER selected 65 genes from the group of highly upregulated genes of the HFD+PB vs HFD comparison. Most of these genes had molecular functions related to binding, including protein and nucleic acids, and catalytic activities. The most common biological functions were cellular processes, and most of them were components of the cell or the organelle. Enzyme modulators and hydrolases were the most common protein classes.

PANTHER found information about proteins related to 302 of the highly deregulated genes of the HFD+PB vs HFD comparison. As with the other comparisons, most of the

proteins related to these genes performed binding functions, especially binding to proteins and binding to nucleic acids, and performed cellular processes with proteins such as transcription factors and traffic proteins. Most of these proteins were intracellular, and the most common protein classes were hydrolases and enzyme modulators.

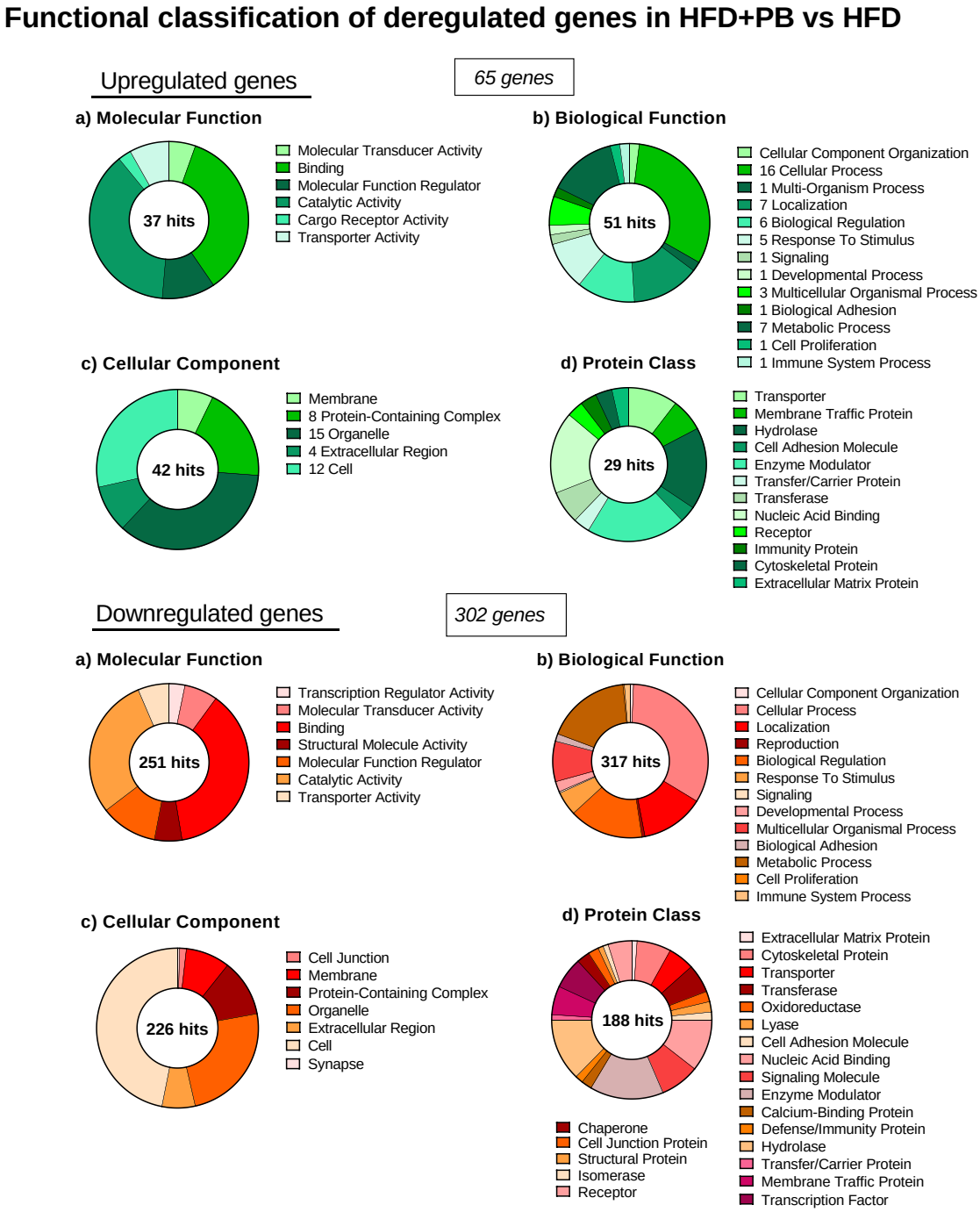

Figure 4.7. Functional classification of highly deregulated genes in the HFD+PB vs HFD comparison.
Both highly up and downregulated genes were analysed using PANTHER to determine the (a) molecular function, (b) biological function, (c) cellular component and (d) protein class of their related proteins. n=3

A full list of deregulated genes in the HFD+PB vs HFD comparison and their functional classifications can be found in Appendix B, **Table 0.9** and **Table 0.10.**

Using DAVID bioinformatic tools, up and downregulated pathways were selected and are shown in **Table 4.4**.

Table 4.4. Deregulated pathways in the HFD+PB vs HFD comparison.

Highly deregulated genes were selected using the parameters explained above and, using two tools from DAVID Bioinformatics (GO Analysis: Biological Process and KEGG Pathway), up to ten relevant deregulated pathways were selected for each tool used. "Total" is the number of total affected pathways highlighted by DAVID on that specific database.

UPREGULATED PATHWAYS				
	Term	**Pathway**	**No. transcripts**	**P value**
GO Analysis: Biological Process	GO:0030154	Cell Differentiation	5	0.044
	GO:0019886	Antigen Processing and Presentation of Exogenous Peptide Antigen Via MHC Class II	3	0.001
	GO:0045600	Positive Regulation of Fat Cell Differentiation	3	0.013
	GO:0034220	Ion Transmembrane Transport	3	0.046
	GO:0002506	Polysaccharide Assembly with MHC Class II Protein Complex	2	0.007
	GO:0031547	Brain-Derived Neurotrophic Factor Receptor Signalling Pathway	2	0.014
	GO:0002503	Peptide Antigen Assembly with MHC Class II Protein Complex	2	0.014
	GO:0002862	Negative Regulation of Inflammatory Response to Antigenic Stimulus	2	0.035
	GO:0002504	Antigen Processing and Presentation of Peptide Or Polysaccharide Antigen Via MHC Class II	2	0.039
	GO:0051085	Chaperone Mediated Protein Folding Requiring Cofactor	2	0.046
Total	11			
KEGG Pathway	rno05152	Tuberculosis	6	0.001
	rno05164	Influenza A	4	0.035
	rno05150	Staphylococcus aureus infection	3	0.022
Total	3			

DOWNREGULATED PATHWAYS				
	Term	**Pathway**	**No. transcripts**	**P value**
GO Analysis: Biological Process	GO:0008285	Negative Regulation of Cell Proliferation	15	0.011
	GO:0007399	Nervous System Development	12	0.001
	GO:0007264	Small GTPase Mediated Signal Transduction	10	0.032
	GO:0007166	Cell Surface Receptor Signalling Pathway	9	0.028
	GO:0034220	Ion Transmembrane Transport	7	0.009
	GO:0051592	Response to Calcium Ion	6	0.022
	GO:0017158	Regulation of Calcium Ion-Dependent Exocytosis	4	0.023
	GO:0048791	Calcium Ion-Regulated Exocytosis of Neurotransmitter	4	0.034
	GO:0043507	Positive Regulation of JUN Kinase Activity	4	0.044
	GO:2001275	Positive Regulation of Glucose Import In Response To Insulin Stimulus	4	0.002
Total	72			
KEGG Pathway	rno04014	Ras signalling pathway	10	0.020
	rno04024	cAMP signalling pathway	9	0.021
	rno04713	Circadian entrainment	8	0.002
	rno04728	Dopaminergic synapse	8	0.007
	rno04724	Glutamatergic synapse	7	0.015
	rno04727	GABAergic synapse	6	0.018
	rno04540	Gap junction	6	0.019
	rno05030	Cocaine addiction	5	0.008
	rno04721	Synaptic vesicle cycle	5	0.023
Total	11			

A total of 14 differentially upregulated and 83 downregulated pathways were selected by DAVID bioinformatics for the HFD+PB vs HFD comparison. Upregulated pathways included cell differentiation and ion transport. Downregulated pathways included ion transport and various signalling pathways.

IV. Differences in expression of genes related to CSF secretion

Ion transporters and channels and tight junction proteins expressed in human CP were selected from literature to analyse their gene expression changes in our study related to diet (Brown *et al.*, 2004; Emerich *et al.*, 2004; Kratzer *et al.*, 2012; Praetorius and Damkier, 2017). Relative expression of genes related to these three categories is shown in **Table 4.5**.

The largest differences in expression were found in the HFD+PB vs ND comparison, specifically amongst tight junction proteins.

Out of 11 transporters analysed, only AQP1 and Slc4a5 were slightly overexpressed. Three transporters were highly downregulated, KCNA6, Slc4a10 and Aqp4. Three out of ten tight junctions proteins were upregulated, ZO-3, CLDN2 and CLDN22, although the difference in mRNA levels for all were < 1 therefore they were not considered highly deregulated. Four TJ genes were highly downregulated, ZO-1, Cadm1, CLDN11 and JAM3.

Table 4.5. Relative gene expression in all three comparisons measured by MACE RNAseq of genes relevant to choroid plexus function related to CSF.

Highlighted in red and bold lettering the downregulated genes for each specific comparison as determined by a significant *P* value; highlighted in green and bold lettering the upregulated genes for each specific comparison as determined by a significant *P* value. Underlined values mark deregulated genes with a log2fold change >1 or <-1.

TRANSPORTERS

Gene	HFD vs ND	*P* value	HFD+PB vs ND	*P* value	HFD+PB vs HFD	*P* value
Slc9a1	-0.239	0.705	0.195	0.579	0.434	0.354
Kcna1	-0.472	0.686	-0.689	0.625	-0.217	0.932
KCNA6	0.413	0.433	**-1.457**	**0.004**	**-1.867**	**>0.001**
Slc12a2	-0.001	0.753	-0.491	0.224	-0.491	0.129
Slc12a7	0.251	0.638	0.305	0.198	0.054	0.431
AQP1	0.078	0.471	**0.073**	**0.039**	0.008	0.186
Aqp4	-0.133	0.477	**-3.373**	**0.021**	-3.24	0.121
Na^+/K^+ATPase1	0.134	0.598	0.022	0.852	-0.111	0.734
Slc12a6	0.688	0.124	-0.330	0.925	-1.018	0.108

Slc4a10	-0.721	0.110	**-1.331**	**0.031**	-0.610	0.577
Slc4a2	0.078	0.926	0.151	0.076	0.073	0.095
Slc4a5	**0.619**	**0.017**	**0.494**	**0.009**	0.125	0.823
Slc4a7	0.670	0.817	-1.131	0.639	-1.801	0.464

TIGHT JUNCTION PROTEINS

Gene	HFD vs ND	*P* value	HFD+PB vs ND	*P* value	HFD+PB vs HFD	*P* value
ZO-1	**-1.039**	**0.027**	**-1.437**	**0.014**	-0.398	0.813
ZO-2	-0.051	0.793	0.181	0.501	-0.232	0.357
ZO-3	-0.239	0.510	**0.285**	**0.045**	**0.524**	**0.010**
Cadm1	-0.743	0.246	**-2.098**	**0.026**	-1.355	0.286
CLDN1	-0.074	0.496	-0.321	0.380	-0.246	0.846
CLDN2	**0.347**	**0.013**	**0.194**	**0.006**	-0.154	0.777
Cldn9	0.195	0.411	-0.014	0.446	-0.209	0.953
CLDN11	0.079	0.853	**-1.352**	**0.027**	**-1.431**	**0.043**
CLDN19	-0.024	0.930	-0.133	0.660	-0.109	0.729
CLDN22	0.163	0.572	**0.604**	**0.001**	**0.441**	**0.008**
Ocln	-0.527	0.068	-0.438	0.181	0.089	0.625
JAM3	-0.408	0.095	**-1.068**	**0.001**	-0.661	0.130

V. Validation by qPCR

The alteration of CP gene expression of key genes detected by MACE-RNASeq was validated by qPCR analysis using the same CP samples (**Figure 4.8**).

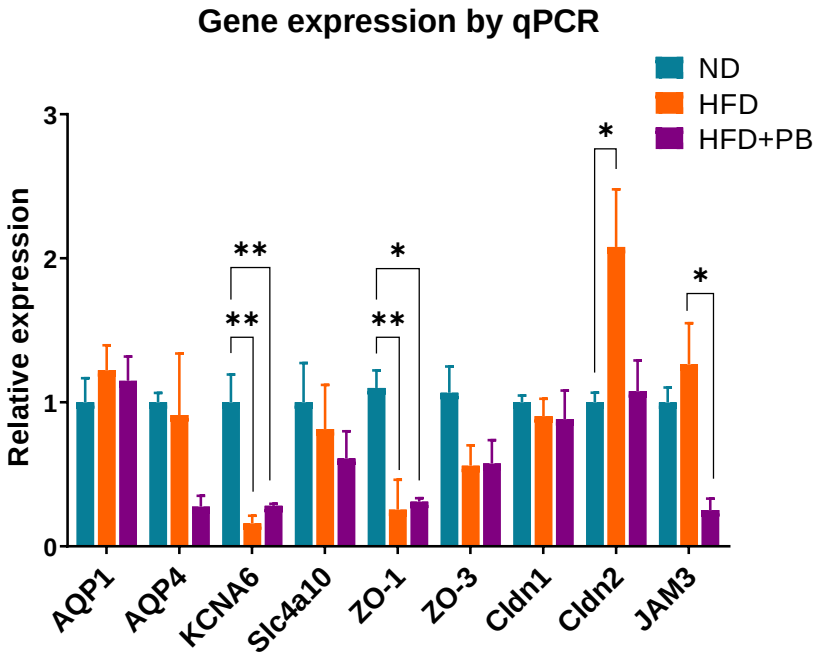

Figure 4.8. Gene expression levels on a selection of genes of the CP of rats under three different diets.

*= *P* value<0.05, **= *P* value<0.01. n=3

Gene expression levels of KCNA6 and ZO-1 appeared downregulated in both HFD and HFD+PB rats when compared to their ND control. CLDN2 expression levels were significantly higher in the HFD rats than in the ND rats, while JAM3 expression was significantly lower in HFD+PB when compared to HFD.

Gene expression changes between HFD or HFD+PB and ND as measured by both MACE-RNAseq and qPCR were compared in **Table 4.6**. In the HFD vs ND comparison, the results of both techniques were similar: both detected a downregulation of ZO-1 and an upregulation of CLDN2 while the rest of the genes remained unchanged, except for KCNA6 which was downregulated according to the qPCR. In the HFD+PB vs ND comparison, both techniques identified a decrease in expression levels of KCNA6 and ZO-1. However, the results of the qPCR suggested that the remaining tested genes were unchanged, while according to the results from the MACE-RNAseq most of them were up or downregulated.

Table 4.6. Gene expression level changes depending on diet on a selection of genes as measured by MACE-RNAseq and qPCR.

Due to the differences between techniques, results are indicated as level of gene expression change in either HFD or HFD+PB rats when compared to ND, and they are expressed as : unchanged (=), overexpressed (↑) or downregulated (↓).

Gene	MACE-RNAseq		qPCR	
	HFD vs ND	HFD+PB vs ND	HFD vs ND	HFD+PB vs ND
AQP1	=	↑	=	=
AQP4	=	↓	=	=
KCNA6	=	↓	↓	↓
Slc4a10	=	↓	=	=
ZO-1	↓	↓	↓	↓
ZO-3	=	↑	=	=
CLDN1	=	=	=	=
CLDN2	↑	↑	↑	=
JAM3	=	↓	=	=

4.3.3 Protein expression of choroid plexus by immunohistochemistry on female rats related to diet

The protein expression of ZO-1 and CLDN1 was studied further because they are essential TJ-forming proteins. AQP4 was not expected to be found in the CP samples taken from our rats because this gene is expressed in ependymal cells (Verkman *et al.*, 2017; Trillo-Contreras *et al.*, 2019). However, AQP4 expression was detected in our samples and it was decreased in HFD+PB vs ND, therefore its protein expression needed to be studied further. Photomicrograms of AQP4 staining in lateral ventricles of rats in brains from ND, HFD or HFD+PB rats can be found in **Figure 4.9**.a. No difference in intensity (**Figure 4.9**.b) or area of positive AQP4 staining relative to DAPI staining (**Figure 4.9**.c) was found between the different diets.

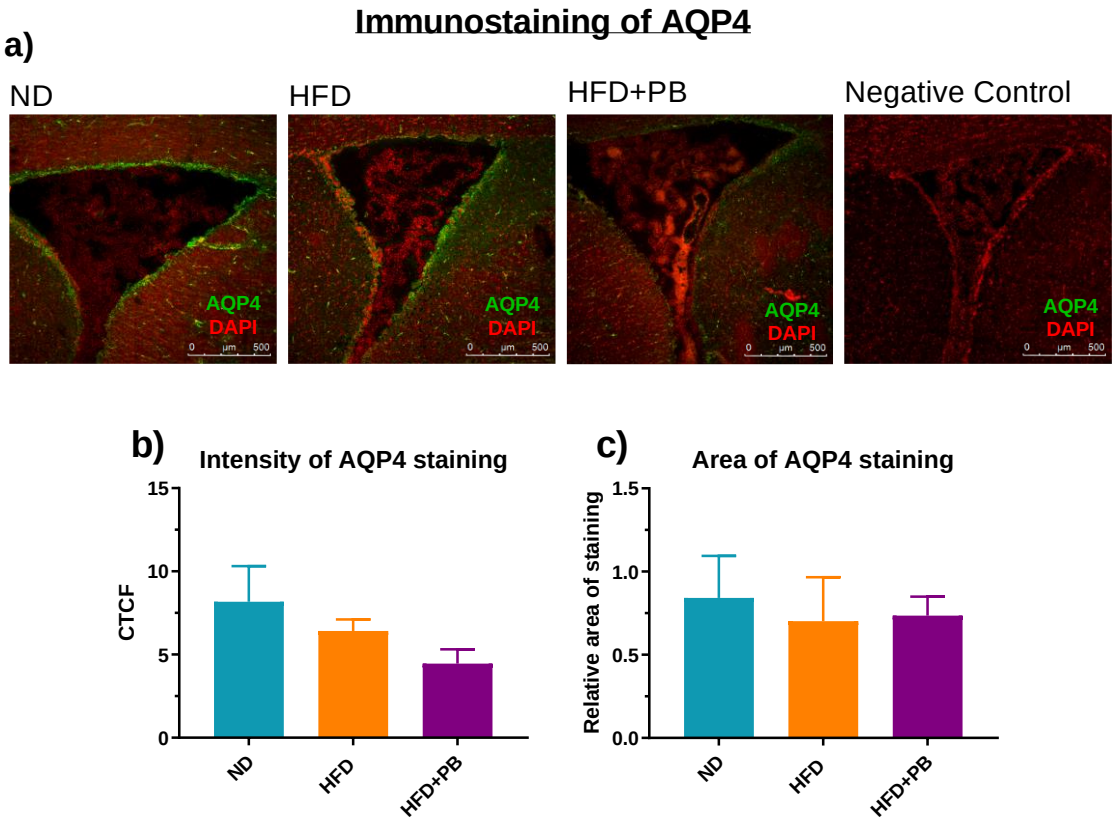

Figure 4.9. Immunostaining of AQP4 in choroid plexus of female rats under different diets.

(a) photomicrograms of images of AQP4 (green) and DAPI (red) staining in the lateral ventricle of ND, HFD and HFD+PB rats. (b) analysis of staining intensity and (c) area of AQP4 staining relative to DAPI. CTCF = corrected total cellular fluorescence, n = 3

Images of ZO-1 staining in lateral ventricles of rats under the different diets are shown in **Figure 4.10**.a. No differences in staining intensity (**Figure 4.10**.b) or relative area of ZO-1 staining (**Figure 4.10**.c) were observed related to diet.

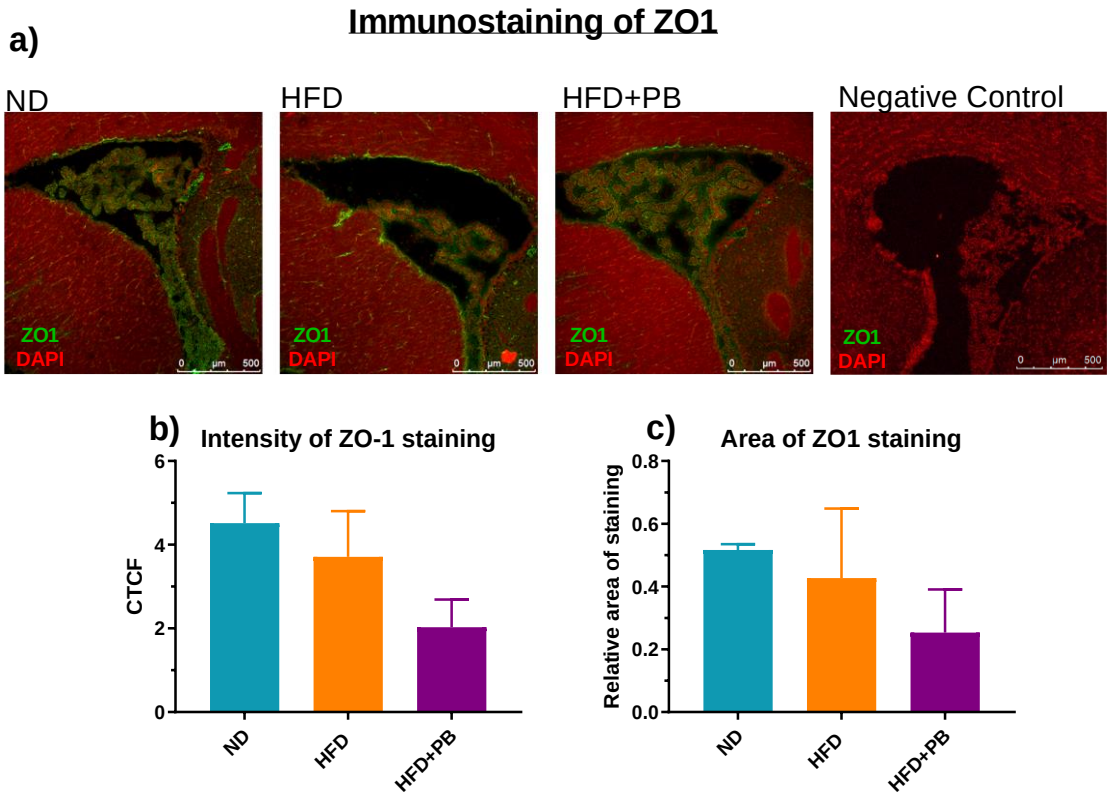

Figure 4.10. Immunostaining of ZO-1 in choroid plexus of female rats under different diets.
(a) photomicrograms of images of ZO-1 (green) and DAPI (red) staining in the lateral ventricle of ND, HFD and HFD+PB rats. (b) analysis of staining intensity and (c) area of ZO-1 staining relative to DAPI. CTCF = corrected total cellular fluorescence, n=3

The typical staining of CLDN1 observed in the lateral ventricles of the rats under ND, HFD or HFD+PB can be seen in **Figure 4.11**.a. There was a significant difference between intensity of staining between HFD and HFD+PB samples (**Figure 4.11**.b), but there was no difference in relative area of CLDN1 staining depending on diet (**Figure 4.11**.c).

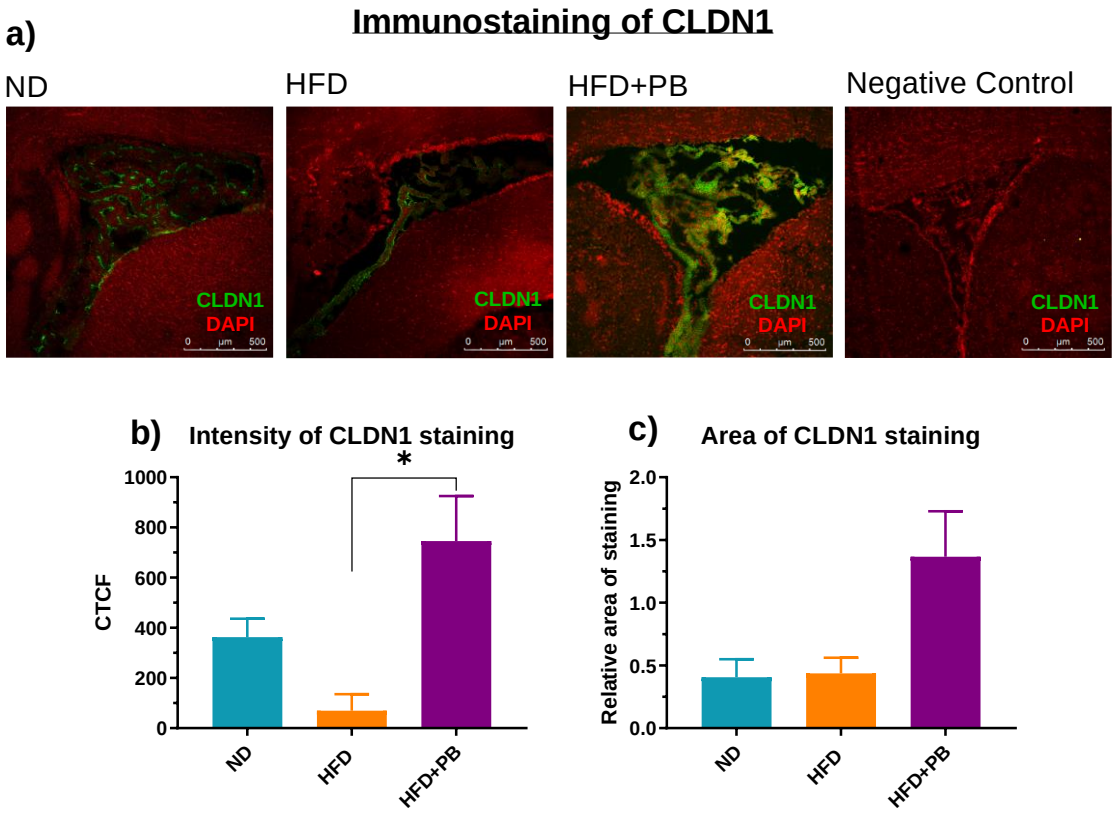

Figure 4.11. Immunostaining of CLDN1 in choroid plexus of female rats under different diets.

(a) photomicrograms of images of CLDN1 (green) and DAPI (red) staining in the lateral ventricle of ND, HFD and HFD+PB rats. (b) analysis of staining intensity and (c) area of CLDN1 staining relative to DAPI. CTCF = corrected total cellular fluorescence, n=3, * = *p* value < 0.05

4.4 Discussion

Results shown in Chapter 3 demonstrated that diet and obesity influence CSF secretion in the female rat. The current study tested the hypothesis that this functional change was related to a diet-induced deregulation of gene and/or protein expression in the CP. A preliminary study was performed in which gene expression of select genes were compared between ND and HFD at 11w and 15w. The biggest difference was found to be between the 15w rats, therefore the following experiments were focused on studying possible changes between ND, HFD and HFD+PB at 15w. MACE-RNAseq analysis found that the HFD+PB group showed the largest changes in gene expression compared to the ND group, although those genes thought to be key for CSF dynamics were not altered.

However, some tight junction proteins appeared downregulated. Furthermore, CLDN1 immunostaining showed an increase of staining in HFD+PB when compared to HFD.

HFD+PB had a decrease in expression levels of AQP7 and AQP9 compared to rats fed the ND. AQP7 is located on the apical membrane, which suggests a possible collaboration with AQP1 in CSF secretion, while the exact location of AQP9 within the CPEC is not known yet (Nazari *et al.*, 2014; Patyal and Alvarez-Leefmans, 2016). Neither of these genes are thought to be essential for CSF secretion though, therefore the implication of their deregulation in CSF secretion is unknown. However, decreased levels of AQP7 and AQP9 could be a balance mechanism to decrease an already increased secretion of CSF. Nevertheless, more research is needed in order to investigate the extent at which these proteins collaborate on CSF secretion.

HFD 15w rats showed an overexpression increase in mRNA levels of ATP1B1 while ATP1A1 and ATP1B2 remained unaltered. ATP1B1 function within the ATP1 family is thought to be related to stability and separation of this subunit from the heterodimer has been shown to irreversibly inactivate both transport and enzymatic activities of ATP1 (McDonough, Geering and Farley, 1990). Consequently, an increased of expression of ATP1B1 would not affect ATP1 activity directly.

The increase in Slc4a5 expression in HFD rats could be directly related to the differences in diet rather than the increase in body weight. In the renal epithelium, Slc4a5 expression has been found to be increased following an intracellular sodium increase (Gildea *et al.*, 2015). In the CP, Slc4a5 is essential for maintaining a stable pH in the CSF. While a lower expression of Slc4a5 has been shown to lead to altered CPEC, an overexpression of this gene has not been reported to significantly affect CPEC or CSF secretion on its own (Kao *et al.*, 2011; Christensen *et al.*, 2018)

ERb was overexpressed in HFD15w when compared to ND of the same age. This protein can directly regulate transcription of specific target genes such as transthyretin, but it also requires a number of coregulatory proteins to function properly (Heldring *et al.*, 2007; Quintela *et al.*, 2009; Wilson, Westberry and Trout, 2011; Paterni *et al.*, 2014). In an

ex vivo model of rabbit CP, oestrogen and progesterone were able to reduce CSF secretion on their own and in combination (Lindvall-Axelsson and Owman, 1989). A study of CP gene expression in ovariectomised female rodents reported upregulated levels of CSF secretion-related genes, giving a further glimpse into the regulating role of sex hormones on CSF secretion (Santos *et al.*, 2017). None of the genes analysed in our preliminary study appeared altered in their study, however. The total implication of sex hormones in CSF secretion is not well known yet, but the evidence points out to them being an important regulator.

Due to the fact that the biggest difference in gene expression depending on diet was found on the 15w rats, the extensive gene expression analysis was performed on this group and the three available diets were tested.

Gene expression from 15w ND, HFD and HFD+PB was analysed using the MACE-RNAseq technique and compared between diet groups. HFD+PB vs ND was the comparison with the highest quantity of deregulated genes, which suggests that diet-induced obesity can alter gene expression levels in the CP. Dietary fat is a known gene expression regulator (Jump and Clarke, 1999; Jump, 2004; Siersbaek *et al.*, 2017). Furthermore, CP is thought to be involved in lipid-related activities such as supplying brain tissue with polyunsaturated fatty acids and regulation of the sleep-inducing lipid oleamide, which could be affected by an increase in dietary fat (Bourrea *et al.*, 1997; Egertová, Cravatt and Elphick, 2000; Raatz *et al.*, 2001; Egertová *et al.*, 2004).

The most common biological functions amongst deregulated genes between diet groups were related to cell processes. The most common cell process in upregulated genes in all three comparisons was related to the cytoskeleton. Alterations in cytoskeletal-related proteins in the brain of rodents under a HFD have been previously reported, and it is thought to be a consequence of cell stress (Smine *et al.*, 2017; McLean, Campbell, Langston, *et al.*, 2019; McLean, Campbell, Sergi, *et al.*, 2019). Amongst downregulated genes, the most common cell processes were related to gene transcription and carrier proteins.

Using DAVID bioinformatics, deregulated pathways were analysed. Deregulated pathways in all comparisons were also characterised by increased pathways related to cellular structure and decreased pathways related to gene transcription and transport. However, other interesting pathways were also detected.

HFD+PB group showed a deregulation in circadian pathways when compared to either HFD or ND. HFD has previously been reported as an alterator of the circadian clock, including changes on patterns of circulating levels of sex hormones (Kohsaka *et al.*, 2007; Cano *et al.*, 2008). The CP is highly influenced by circadian rhythms and sex hormone levels (Myung *et al.*, 2018; Quintela *et al.*, 2018; Yamaguchi *et al.*, 2020). The extent at which an alteration of circadian rhythms would affect CSF secretion is not well explored yet. However, these alterations would certainly have an effect on CSF secretion rate, and further investigation into this topic is needed in order to understand this relationship better.

Both HFD vs ND and HFD+PB vs ND showed a decrease in pathways related to hormonal response including the androgen receptor signalling pathway, which could be a compensatory mechanism to highly altered hormonal levels related to increased adiposity (Sidhu, Parikh and Burman, 2017; Varlamov, 2017; Volk *et al.*, 2017). Cell adhesion pathways were also decreased, which could lead to an increase in permeability of the CP which could ultimately affect CSF dynamics (Wolburg and Paulus, 2010; Kant *et al.*, 2018). Interestingly, HFD+PB vs ND showed a decrease in ion transmembrane transport. CSF secretion directly depends on ion transport across the BCSFB, therefore a decrease of this type of transport would cause a decrease in CSF secretion. However, HFD+PB rats had an increased secretion rate of CSF in Chapter 3. It is possible that the decrease in ion transport seen in this analysis is a compensatory mechanism caused by an increase of CSF secretion caused by other mechanisms, such as by an increase in paracellular permeability.

Furthermore, several signalling pathways appeared downregulated in HFD+PB when compared to either ND or HFD. Whether they are directly related to the changes in CSF dynamics observed in HFD+PB rats in Chapter 3 is not known yet. However, it is a possibility. The cyclic adenosine 3’,5’-monophosphate (cAMP) signalling pathway, for

example, has an essential role in cellular response to different neurotransmitters and hormones (Watson, Mayes and Watson, 2004; Sassone-Corsi, 2012). It is important to keep in mind that HFD+PB rats were found to have the highest rates of CSF secretion and also the highest concentration of testosterone in plasma, and that those two parameters correlated positively. Testosterone has been seen to increase fluid secretion and solute transport by increasing cAMP generation in kidney epithelial cells *in vitro* (Sandhu *et al.*, 1997). In CP, CSF secretion is increased by agents increasing intracellular cAMP (Saito and Wright, 1983). It is possible that testosterone could increase cAMP generation in CP epithelium, increasing CSF secretion, and the downregulation of the cAMP pathway observed in HFD+PB rats could be a compensatory mechanism to compensate for the big alteration caused by testosterone. Another downregulated signalling pathway was the renin angiotensin system (RAS). Sex hormones and especially testosterone have been shown to alter RAS activity in kidney epithelium (Fortepiani *et al.*, 2003; Komukai, Mochizuki and Yoshimura, 2010). RAS controls fluid homeostasis, therefore an alteration in activity could alter fluid secretion (Kapsha and Severs, 1983; Savaskan, 2005). However, these are only speculations, and further research is needed in order to study the possible effect of testosterone on signalling pathways in the CP and, ultimately, in CSF secretion.

As mentioned in the introduction, the roles that CP carries out regarding CSF secretion and integrity are dependent on proper functioning of molecular transporters and integrity of tight junction proteins. In the current experiment, it was found that HFD+PB highly decreased gene expression of two molecular transporters, KCNA6 and Slc4a10. The effect of decreased expression levels of KCNA6 in the CP functionality are not known. In animal models, deletion of the Slc4a10 gene in the CP results in a redistribution and altered polarisation of important proteins such as ATP1, AQP1 and Slc9a1 within the CPEC (Jacobs *et al.*, 2008; Damkier and Praetorius, 2012; Christensen *et al.*, 2020). This deletion can also lead to decreased total ion transport and thus a decrease in CSF secretion due to the lack of Na^+ transport into the CSF (Jacobs *et al.*, 2008; Christensen *et al.*, 2013, 2020). However, it is important to note that these effects are seen in gene deletion *in vivo* models which are unable to express the Slc4a10 gene altogether, which is not the case of our animals. While the exact effect that decreased levels of Slc4a10 can have in CP function is unknown, this

gene is still expressed therefore the effect might not be as dramatic as what was observed in Slc4a10 knock out animals.

AQP1 expression was slightly increased in the HFD+PB vs ND comparison. However, as log2fold change<1, the difference in expression was not enough to be considered highly overexpressed. The same was also observed with three tight junction proteins, ZO-3, CLDN2 and CLDN22. By contrast, ZO-1, JAM3, Cadm1 and CLDN11 appeared highly downregulated in the HFD+PB group when compared to ND. ZO-1 is thought to be essential for epithelial barrier functionality, and its decrease has been linked with increased paracellular permeability in different epitheliums, including the CP (Scudamore *et al.*, 1998; Guo *et al.*, 2011; Kaur, Rathnasamy and Ling, 2016; Kim and Kim, 2017). JAM3 is thought to be important for CP integrity of TJs, and its deficiency has been linked with severe hydrocephalus in a mouse model as well as enlarged ventricles in a rare human condition caused by a mutated JAM3 leading to a non-functional protein (Mochida *et al.*, 2010; Wyss *et al.*, 2012). In animal models and human cases of neuroinflammation and Alzheimer's disease, decreased tight junction protein expression in the CP is linked to increased leakage of the BCSFB and disruption of the barrier functions (Coisne and Engelhardt, 2011; Kooij *et al.*, 2014; Brkic *et al.*, 2015). Inflammation is thought to alter CP gene expression and functionality, including changes protein expression, barrier tightness and CSF secretion (Marques *et al.*, 2007; Shrestha, Paul and Pachter, 2014; Kant *et al.*, 2018). As mentioned in Chapter 1, diet-related obesity can be accompanied by general inflammation (Shaw *et al.*, 2014; Ellulu *et al.*, 2017; Stolarczyk, 2017). Furthermore, increased proinflammatory cytokines have been shown to increase CSF secretion in the rat using the ventriculo-cisternal perfusion technique (Alimajstorovic, Pascual-Baixauli, *et al.*, 2020). In the present study, the biggest alteration in tight junction protein expression was seen in our HFD+PB rats, which are also the group with highest BMI. It is possible that these rats were experiencing general inflammation, which might be promoting downregulation of these proteins. Another important characteristic of our HFD+PB rats is that they had increased levels of testosterone. Androgens have the ability to alter tight junction protein expression in some epithelia, such as prostate and seminiferous, and in the blood-testis barrier (Meng *et al.*, 2005, 2011; Chakraborty *et al.*, 2014). While the effect of androgens in tight junction

proteins of the CP is not well studied yet, the fact that CPEC express AR indicates that androgen signalling might play a role in CP regulation, including being able to alter tight junction protein expression. Furthermore, IIH is characterised by female sex, obesity and higher levels of androgen levels (O'Reilly *et al.*, 2019). According to our results, inflammation and androgen excess could both contribute to altering CSF dynamics by changing the expression of tight junction proteins. This possible increase in barrier leakage could lead to a higher paracellular passage of water, which could contribute to higher rates of CSF secretion.

The samples analysed by MACE-RNAseq were also measured using qPCR in order to doublecheck the results obtained by the former technique. Both techniques are fundamentally different as their approach for gene expression measurement differs. MACE RNAseq appeared to be able to point out differences in gene expression that qPCR considered unchanged. However, neither of the results were contradictory – neither gene appeared as upregulated in one analysis and downregulated in the other. RNAseq is indeed considered to be more sensitive and precise than qPCR because it does not rely on the expression of housekeeping genes (Fassbinder-Orth, 2014; Nonis, De Nardi and Nonis, 2014; Su *et al.*, 2014; Pombo *et al.*, 2017). However, it was important to also measure gene expression by qPCR in order to facilitate reproducibility by other researchers. qPCR is still the technique of choice nowadays for medium-throughput gene expression analysis in most laboratories, due to its relative low cost, time frame and difficulties to perform and analyse while maintaining analysis reliability.

AQP4 is mainly found in the ependymal cells rather than CPEC, therefore its presence in our samples was not expected and it might mean that the extraction technique used yielded some contamination from the ventricle lining (Verkman *et al.*, 2017; Trillo-Contreras *et al.*, 2019). However, MACE-RNAseq results showed that AQP4 was highly deregulated in HFD+PB when compared to ND, thus immunostaining of AQP4 protein was performed in order to analyse the difference of protein expression related to diet. AQP4 is thought to be important for CSF flow and water homeostasis in the brain ventricles, therefore a decrease in expression caused by diet could alter CSF dynamics (Speake,

Freeman and Brown, 2003; Iliff *et al.*, 2012). After performing immunostaining experiments, we can safely conclude that AQP4 is mainly expressed in the ventricle lining and its expression was not significantly changed by diet in our experiment.

Immunostaining of CLDN1 showed an increase in intensity of staining in HFD+PB when compared to HFD. In the literature, ovariectomised rodents have been shown to have downregulated CLDN1 expression when compared to controls (Santos *et al.*, 2017). However, the exact mechanism by which sex hormones could alter CLDN1 expression in CP has not been studied yet. Interestingly, oestradiol levels measured in Chapter 3 were increased in HFD rats and decreased in HFD+PB when compared to ND, following an opposite pattern to the intensity of CLDN1 staining detected in this chapter. However, whether oestradiol levels can alter CLDN1 expression in the CP cannot be concluded from these results. Furthermore, the increase in CLDN1 seen in HFD+PB could be due to other parameters not measured in this experiment, such as alteration in expression levels of other claudins as seen in intestinal epithelium (Sakaguchi *et al.*, 2002; Yang *et al.*, 2014).

In summary, diet-induced obesity was able to alter gene expression in the CP of female rats. The most remarkable changes included a decrease in TJs gene expression. The biggest changes were seen in the rat group with highest testosterone plasma concentrations in Chapter 3. Due to this, the effect of testosterone in in a model of CP *in vitro* was investigated in Chapter 5.

Chapter 5. Investigation into the Effects of Testosterone on Barrier Functionality of an *In vitro* Model of Choroid Plexus

5.1 Introduction

Sex hormones were firstly thought to mainly influence processes related to sex differentiation and reproduction (Moore, 1941, 1947; Jost, 1970). However, it has been shown that sex hormones can also affect a wide number of different physiological processes which are not directly related to sex or reproduction, such as the immune response, the circadian clock or food intake (Verthelyi, 2001; Pasquali, 2006; Quintela *et al.*, 2015). Furthermore, sex hormone levels can be altered by several different mechanisms, including body fat composition. Specifically, obesity in women is known to increase testosterone levels, while in men, the opposite effect is observed (Evans *et al.*, 1983; Bray, 1997; Pasquali, 2006).

Sex hormones have long been suspected to be potential key effectors for development of IIH, due to the demographics of this condition in the general population (see Section 1.3.4). The great majority of patients fall inside a very specific demographic group: overweight women of childbearing age (Radhakrishnan *et al.*, 1993; Bidot and Bruce, 2015). Furthermore, conditions characterised by altered sex hormones such as PCOS and pregnancy or the use of hormonal oral contraceptives are linked to higher risk of developing IIH (Bagga *et al.*, 2005; Glueck *et al.*, 2005; Karmaniolou, Petropoulos and Theodoraki, 2011; Chen and Wall, 2014). Additionally, secondary intracranial hypertension in transgender individuals associated with testosterone treatment has been reported in the literature (Park *et al.*, 2014; Bedolla, Buchanan and Hansen, 2017; Hornby *et al.*, 2017).

Little research has been developed in this area, however. While the possible role of sex hormones in IIH has long been speculated, most of the studies into this topic lack accuracy due to the very low numbers of studied patients and a failure to take menstrual cycle into account when obtaining and analysing the samples (Donaldson and Horak, 1982; Toscano *et al.*, 1991). More recent research has shown a link between increased

testosterone levels and IIH, especially in young onset (<25 years of age) patients (Klein *et al.*, 2013; O'Reilly *et al.*, 2019). An *in vitro* investigation into the effect of sex hormones on CSF secretion by the CP suggests that testosterone can increase secretion of CSF by increasing ATPase activity while progesterone and oestrogen are able to decrease secretion by a different but unknown mechanism (Lindvall-Axelsson and Owman, 1989; O'Reilly *et al.*, 2019). In addition, the results from the previous Chapter show that the expression of some TJ proteins in the CP may be altered in diet-caused obesity, thereby suggesting alterations in the permeability of the CP. The effects of testosterone on permeability and gene expression of the CP have not yet been described.

The research described in this chapter was aimed at exploring the effect of testosterone in an *in vitro* model of CP based on the immortalised rat choroid plexus epithelial cell line Z310. The morphology and gene expression of this cell line was first characterised, then, to establish the CP in vitro model, the culture conditions for growth of Z310 on a permeable membrane were optimised to identify those that would yield the tightest monolayer. Lastly, the effects of testosterone on cell morphology, gene expression and barrier functionality were studied in the optimised culture system.

5.2 Materials and Methods

All materials used were obtained from Sigma-Aldrich (Poole, Dorset, UK) unless otherwise specified.

5.2.1 Cell culture

The rat choroid plexus epithelium immortalised cell line Z310 was kindly provided by Dr Wei Zheng (Purdue University, West Lafayette, IN, USA) and was cultured following a protocol previously described in the literature (Zheng and Zhao, 2002). Briefly, cells were cultured in flasks in Dulbecco's Modified Eagle Medium (DMEM, ThermoFisher Scientific, UK) with phenol red and supplemented with foetal calf serum (FBS, 10% v/v, ThermoFisher Scientific, UK), streptomycin (100µg/ml, ThermoFisher Scientific, UK), penicillin (100 U/ml, ThermoFisher Scientific, UK), gentamycin (40µg/ml) and epidermal growth factor (5µg/ml, ThermoFisher Scientific, UK) and maintained in a humidified incubator with 5% CO_2/95%

air v/v at 37°C. The culture medium was changed every two days and cells were passaged when 80% confluence was reached, typically twice a week. Cells were discarded after 8th passage, and all experiments were performed on cells between passage 5 and 7.

The effect of testosterone in Z310 cells was studied. Testosterone-treated cells were incubated with either 0 (Control), 1, 3 or 10 ng/ml testosterone for 12h prior to the assay. For treatment with the androgen receptor antagonist flutamide, cells were incubated with 10µM of for 1h before testosterone was added in order to test whether the changes in gene expression and barrier functionality detected were due to testosterone.

5.2.2 Gene expression analysis

For gene expression analysis, cells were seeded at $2x10^5$, grown until confluence and then washed with PBS three times. Cells were trypsinized for 10 min at 37° and, once they appeared round, birefringent and detached under the microscope, digestion was stopped by the addition of culture medium containing serum. Cells were then centrifuged at 200 xg for 10 min at 4°C to obtain a pellet, which was placed on ice. RNA was extracted immediately using the RNeasy Micro Kit (Qiagen, Manchester, UK) following manufacturer's instructions. Reverse transcription was then performed using the High capacity cDNA Reverse Transcription Kit (Thermofisher Scientific, UK) and qPCR was carried out using the QuantiTect SYBR® Green PCR Kit (Qiagen, Manchester, UK) and KiCqStart® SyBR® Green predesigned primers for rat (**Table 5.1, Table 4.1**).

Table 5.1. Sequences of primers used in qPCR analysis.

Gene	Symbol	Sequence
Organic Anion Transporter 2	SLC22A7	Forward 5'-TGGTATCCTTGGAGACTAAG Reverse 5'-CGTAGTAAAAGCAGCTTCAG
Organic Anion Transporter 3	SLC22A8	Forward 5'-GGTAGAAGAATTTGGAGTCAAC Reverse 5'-TTTCTGAAGGCACAAAGATG
solute carrier organic anion transporter family, member 1a4	OATP1A4	Forward 5'-TGAGCCTTTAAAGAAACAGG Reverse 5'-GGGGAAGACTTTAATAAACTGG
Organic Anion Transporter B	OATP2B1	Forward 5'-TGGGTCTTTATATGTTACCTCC Reverse 5'-CATAAGAGGTTGTTAAGCCTG
Transthyretin	TTR	Forward 5'-ACTGATATTTGCGTCTGAAG Reverse 5'-TCTGCAGTCTTTTTGAACAC
ATP-Dependent Phospholipid Transporter a	ABCB1A	Forward 5'-GCATTCTGGTATGGGACTT Reverse 5'-GTCTTTTCGAGACGGGTA
ATP-Dependent Phospholipid Transporter b	ABCB1B	Forward 5'-CATTCTGCCGAGCGTTAC Reverse 5'-CCCGTGTAATAGTAGGCGTA
Multi-Specific Organic Anion Transporter B	ABCC4	Forward 5'-CCATTCT GGTTATTCTGCTG Reverse 5'-TCAGATTGGTTATGAGGTCG

For cell characterisation, gene expression relative to actin- β was normalised to GAPDH expression using **Equation 5.1** (Kläs *et al.*, 2010). Genes were selected based on either the results from Chapter 4 or from genes typically expressed in the choroid plexus (Szmydynger-Chodobska *et al.*, 2007; Kläs *et al.*, 2010).

Equation 5.1. Calculation of relative expression levels of gene of interest.

$$\Delta Ct_{GOI} = Ct_{GOI} - Ct_{Actin\ \beta}$$

$$Relative\ expression\ of\ GOI = 2^{-(\Delta Ct_{GAPDH} - \Delta Ct_{GOI})}$$

Where:

Ct= Quantification cycle threshold

GOI = Gene of Interest

For analysis of the effect of testosterone on gene expression, expression relative to control was calculated using the $2^{-\Delta\Delta Ct}$ method as previously described in the literature

(Livak and Schmittgen, 2001; Schmittgen and Livak, 2008). Cells with no testosterone nor flutamide treatment were used as control, and actin-β was used as reference gene. Genes were selected from the results of Section 4.3.2.IV.

5.2.3 Study of Z310 monolayer barrier functionality

In order to study the barrier characteristics of the cell monolayer, cells were cultured in a two-chamber system following a protocol previously described in the literature (Zheng and Zhao, 2002; Shi *et al.*, 2008).

Briefly, Corning™ Transwell™ inserts with either polyester or polytetrafluoroethylene (PTFE) 12 mm in diameter 0.4μm pore size permeable membrane were used (ThermoFisherScientific, UK).

For optimisation of the rat CP model, different extracellular matrices and seeding numbers were first tested in order to find the culture conditions which yielded the tightest monolayer as measured by transepithelial electrical resistance (TEER). For collagen I coating, the insert was incubated with collagen I (100μg/ml, ThermoFisher Scientific, UK) at RT for 4 hours. For laminin coating, membranes were incubated with laminin (14μg/ml) for 15 min. For fibronectin coating, collagen I-pretreated membranes were incubated with fibronectin (5 μg/ml, ThermoFisher Scientific, UK) at RT for 1 hour. In all cases, excess liquid was removed after the incubation period and the membrane was left to air dry overnight at RT.

In order to determine optimum cell seeding concentration, cells were seeded on collagen I pre-treated membranes at either $5x10^4$, $2x10^5$ or $4x10^5$ cells per insert (1.13 cm^2 growing surface).

The cell monolayer was typically formed 4-5 days after seeding, and it was determined by three criteria: cells forming a confluent monolayer without visible spaces when observed under an inverted light microscope; culture medium in the inner chamber being at least 2mm higher than that in the outer chamber and a constant TEER value across the insert (Zheng and Zhao, 2002; Shi *et al.*, 2008). Cells were kept in confluency for a day before experiments were performed.

I. Electrical resistance

Electrical resistance of the barrier was estimated by TEER values. TEER was measured using an EVOM™ device coupled with an EndOhm chamber (World Precision Instruments, Hitchin, UK). The chamber was sterilised with 70% Ethanol for 10min at RT and then washed three times with autoclaved highly-purified water. The chamber was then filled with 1.5ml of pre-warmed culture medium. The insert was gently placed inside the chamber and filled with 500µl of pre-warmed medium. It was essential to avoid the formation of bubbles as they can affect TEER readings. The lid was placed over the insert and TEER was recorded three times per insert and averaged to increase measurement accuracy.

II. Paracellular permeability

Basolateral-to-apical paracellular permeability of the monolayer was calculated using 70kDa fluorescein isothiocyanate–Dextran (FITC-Dextran). Briefly, culture media was substituted by phenol red-free culture media 12h prior to the experiment. On the day of the experiment, the lower chamber was filled with phenol red-free media containing 1mg/ml FITC-Dextran while the upper chamber did not contain any FITC-Dextran. Samples were collected from the upper chamber every 5 min for a total time of 30 min and measured using a spectrophotometer (Fluostar Optima, BMG labtech, Aylesbury, UK) with a 485nm excitation and 525nm emission wavelengths. Extracted samples were immediately replaced with fresh phenol red-free media and the dilution was calculated accordingly. The permeability coefficient (Pe) was calculated using **Equation 5.2** (Dehouck *et al.*, 1992; Tai *et al.*, 2009).

Equation 5.2. Permeability coefficient calculations

$$P_e = \frac{PS}{s_f}$$

$$\frac{1}{PS} = \frac{1}{m_e} - \frac{1}{m_f}$$

Where:

PS = Permeability surface area of epithelial monolayer

s_f = Surface area of filter

m_e = slope of the curve corresponding to epithelial cells on filter

m_f = slope of the curve corresponding to empty filter

5.2.4 Statistical analysis

Each experiment consisted of 3 technical replicates averaged per biological replicate for a total of 3 biological replicates unless otherwise specified. All results are presented as average of biological replicates ± SEM. Normal distribution of data was confirmed by Q-Q plot. One-way ANOVA with Tukey Post Hoc test were used to analyse differences between groups for model optimisation and two-way ANOVA with Tukey Post Hoc tests to determine the effect of testosterone on Z310 cells. Statistical analysis was performed using GraphPad (Graphpad Software, 2019).

5.3 Results

5.3.1 Z310 characterisation

Z310 were firstly characterised by morphological observation using phase-contrast microscopy. When the cells formed a confluent layer, they had a predominantly polygonal morphology (**Figure 5.1**).

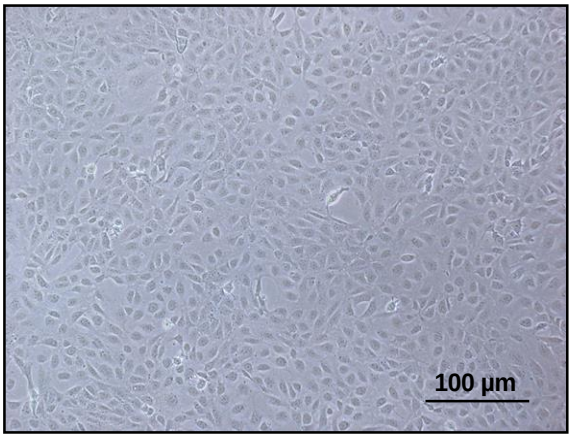

Figure 5.1. Morphology of Z310

Cell morphology of Z310 monolayer was observed using phase-contrast microscopy. Cells were imaged 12h after confluence was reached. This is a representative image of a Z310 confluent monolayer.

Z310 cells were further characterised by gene expression analysis. Genes typically expressed in the CP epithelium were selected and are shown in

Figure 5.2. Analysed genes included: TJs, such as CLDN1 and ZO-1; transporters, such as ABCC4 and Slc4a10; water channels such as AQP1 and AQP4; and other genes expected to be expressed in the CP, such as TTR and AR. Z310 expressed all the analysed genes with the exception of OATP1a4, KCNA6 and AQP4.

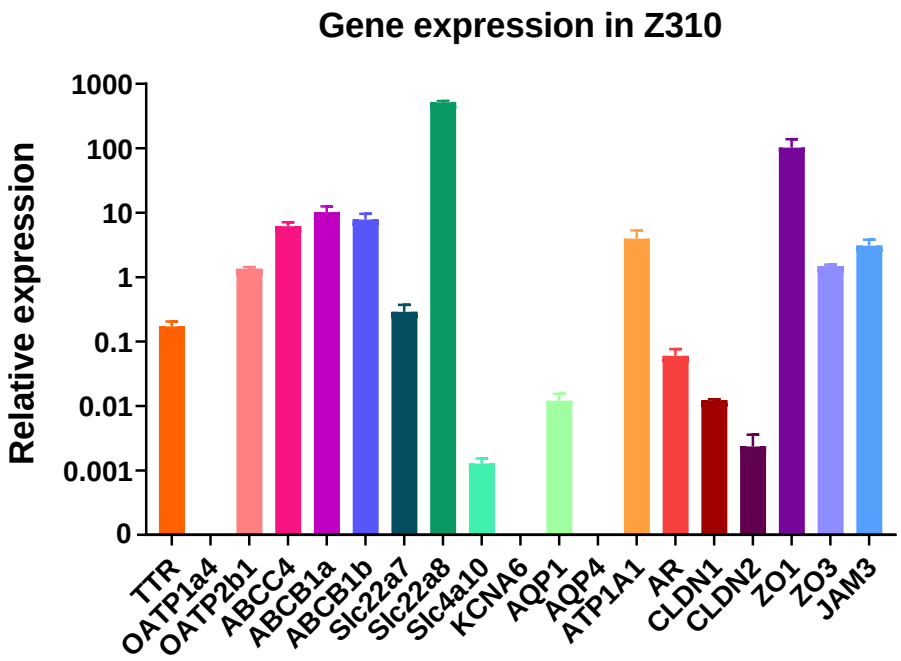

Figure 5.2. Gene expression in Z310 of genes typically expressed in CP.

Cells were grown to confluence before RNA was extracted. Gene expression relative to actin-β was normalised to GAPDH expression for each gene studied. n=3

A comparison of the expression of selected genes in Z310 and those from *in vivo* in the choroid plexus of female rats on a normal diet (ND 15w, determined using the MACE-RNAseq technique and as reported in Chapter 4) is summarised in Table 5.2. Due to the differing techniques, results are only reported qualitatively, as expressed (+) or not expressed (-) (**Table 5.2**).

Table 5.2. Gene expression in Z310 cells and female rats.

Summary of gene expression in Z310 cells (determined by qPCR) and in rat choroid plexus (Rat CP; 15w ND, determined by MACE-RNAseq). Genes were selected from (a) results of Chapter 4 or (b) genes typically expressed in the CP. + denotes gene detection, - denotes no detection.

a)

Gene	Z310	Rat CP
ATP1A1	+	+
CLDN1	+	+
CLDN2	+	+
ZO1	+	+
ZO3	+	+
JAM3	+	+
AQP1	+	+
AQP4	-	+
Slc4a10	+	+
KCNA6	-	+

b)

Gene	Z310	Rat CP
AR	+	+
Slc22a7	+	+
Slc22a8	+	+
OATP2b1	+	+
OATP1a4	-	+
ABCC4	+	+
ABCB1a	+	-
ABCB1b	+	-
TTR	+	+

There were several differences between the expression profiles of the rat CP cell line and rat choroid plexus. Expression of AQP4, KCNA6 and OATP1a4, which were detected in rat CP, were not detected in Z310 cells, whilst ABCB1a and ABCB1b, which were not expressed in rat CP were in fact expressed by Z310 cells.

5.3.2 CP Model optimisation

In order to determine which surface and coating resulted in the optimal barrier properties for the model system, Z310 cells were cultured on two different membranes (PTFA and polyester) with four different pre-treatments (none, laminin, collagen I or collagen I with fibronectin). Once confluence was reached, TEER was recorded for the different parameters (**Figure 5.3**).

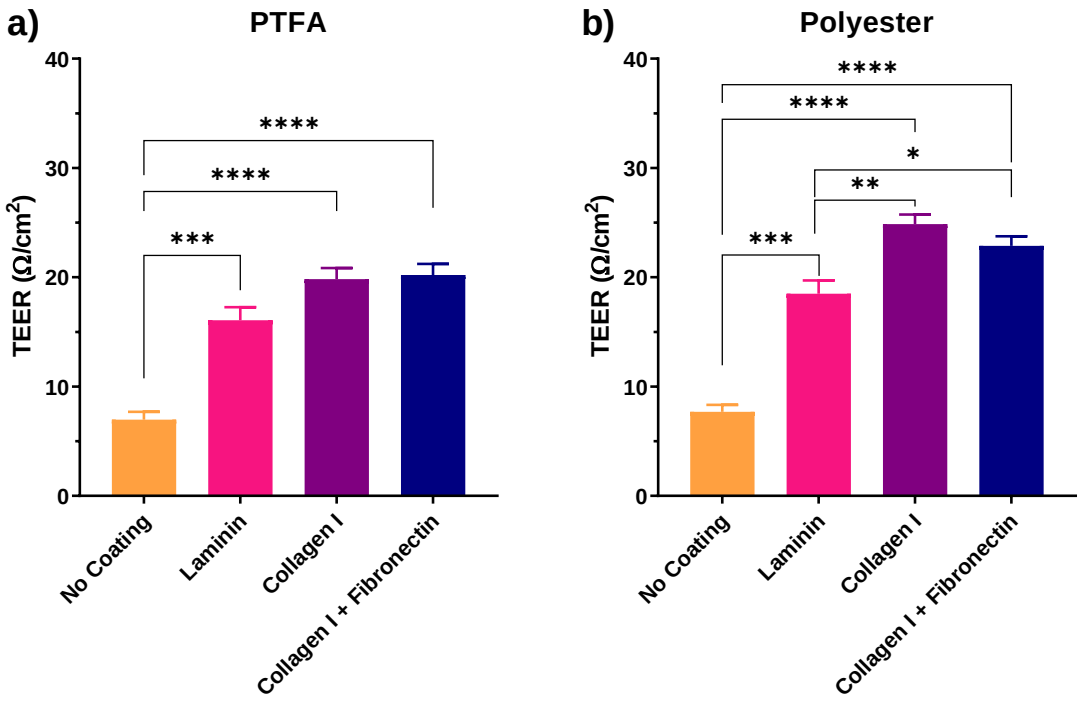

Figure 5.3. Dependency of monolayer resistance on membrane material and coating.

TEER was recorded for Z310 cultures grown to confluence on (a) PTFA or (b) polyester membranes in Transwells with one of four different matrices. n=3, *=*P* value < 0.05, **=*P* value < 0.01, ***=*P* value < 0.001, **** *P* value < 0.0001.

Lack of coating yielded the lowest TEER values for both types of membranes. In PTFA inserts, laminin, collagen I and collagen I with fibronectin had significantly higher TEER values when compared to no coating, although there was no significant difference between these three coatings. While in polyester membranes lack of coating also showed significantly lower TEER values when compared to all the other treatments, there was also a difference between resistance recorded for cells grown on the other three matrices. Specifically, the monolayers cultured on both collagen I and collagen I with fibronectin showed significantly higher TEER than those cultured with a laminin coating. Polyester membranes with a collagen I coating gave the highest TEER values and hence were selected as the most suitable option for further *in vitro* CP model investigations.

Three different initial cell seeding numbers were tested in order to assess which resulted in the tightest monolayer. Three seeding numbers were tested, and their TEER values once confluency was reached are shown in **Figure 5.4**. Seeding of $5x10^4$ cells / Transwell gave significantly lower TEER values once confluency was reached when compared to the other two cell seeding numbers. As a result, $2x10^5$ cells / Transwell was selected for the model system in our barrier testing experiments.

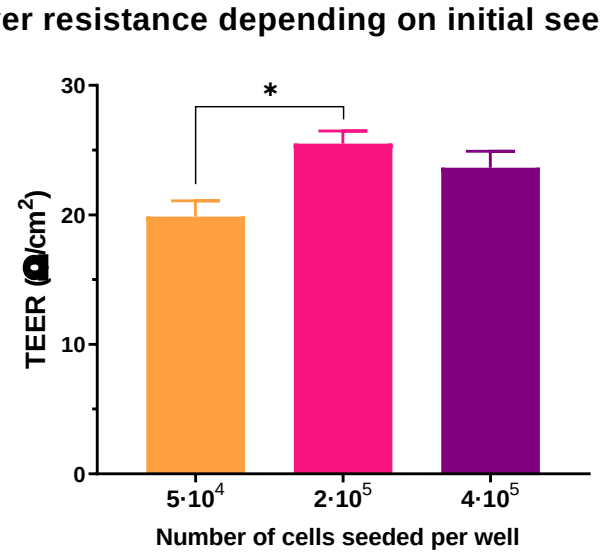

Figure 5.4 Dependency of cell layer resistance on initial seeding number.

Cells were seeded on collagen I pre-coated polyester membranes and grown to confluency. n=3, *=*P* value < 0.05, **=*P* value < 0.01

5.3.3 Effect of testosterone on morphology of Z310

Three different testosterone concentrations were tested to investigate the possible effect of this hormone on morphology (**Figure 5.5**). No apparent differences in morphology were observed between different testosterone treatments and control.

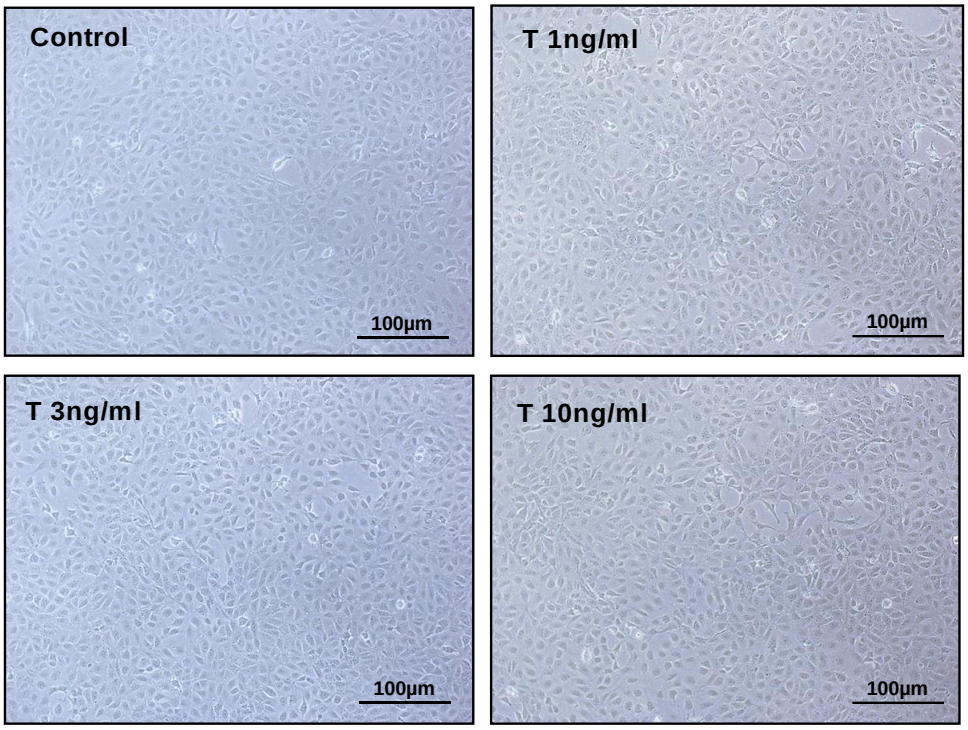

Figure 5.5. Effect of testosterone on morphology of Z310 cells.

Cells were cultured until confluence was reached. Then, cells were incubated with the concentrations of testosterone indicated for 12 h before images were taken.

5.3.4 Effect of testosterone on gene expression of Z310

The effect of testosterone was tested on Z310 cells using three different concentrations. The androgen receptor antagonist flutamide was used in order to assess which observed changes were due to testosterone action. Gene expression was measured in these cells and it is shown in **Figure 5.6**.

Expression of ATP1A1, AQP1, Slc4a10, JAM3, CLDN1, CLDN2, ZO-1 and ZO-3 was analysed in this experiment. There was a significant dose-dependent increase in ATP1A1 expression caused by all three concentrations of testosterone tested while just the highest concentration of testosterone was able to significantly increase AQP1 expression when compared to control. On the other hand, all three concentrations of testosterone greatly decreased Slc4a10 levels in Z310 cells. Furthermore, 3 and 10ng/ml of testosterone were both able to decrease ZO1 levels when compared to control while just the highest concentration decreased ZO3 expression levels significantly. None of the cells treated with

flutamide showed any differences in gene expression, suggesting that testosterone induced gene expression changes detected.

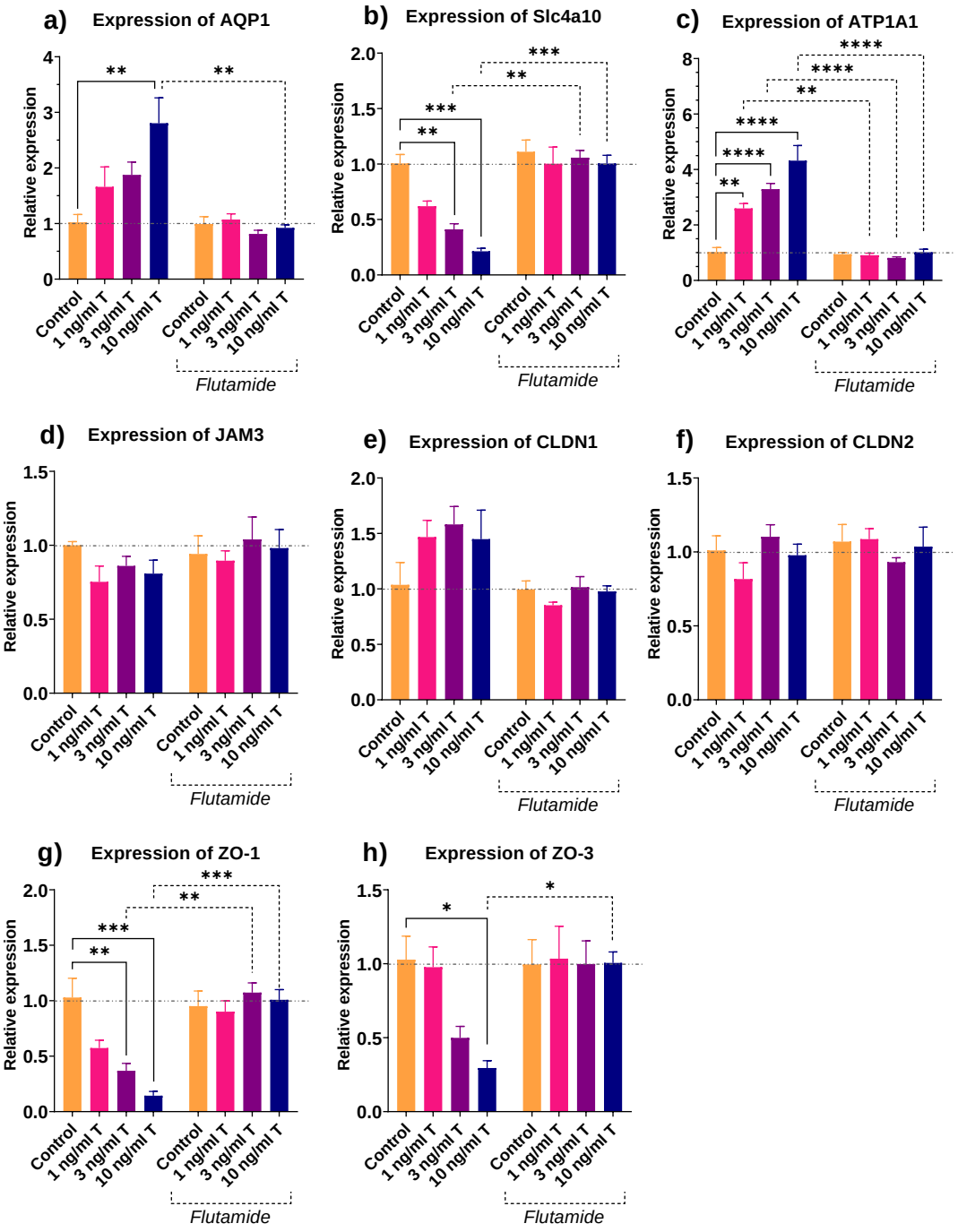

Figure 5.6. Gene expression levels of Z310 cells under different treatments with testosterone (T), with and without flutamide, relative to control.

Cells were cultured until confluence was reached. Then, cells were incubated with a variable concentration of testosterone for 12 h before RNA was extracted. Groups labelled with an F were treated with flutamide

before testosterone treatment. n=3, *=*P* value < 0.05, **=*P* value < 0.01, ***=*P* value < 0.001, **** *p* value < 0.0001.

Testosterone-induced changes in gene expression relative to control in Z310 cells are summarised in **Table 5.3**, alongside a summary on gene expression changes *in vivo* in the choroid plexus of the female rat group showing the highest levels of testosterone, the HFD+PB 15w. Changes in expression of Z310 cells was measured by qPCR while changes in rats were measured using MACE-RNAseq and compared to female rats of the same age under ND. Due to the differing techniques, results are only reported qualitatively, as overexpressed (↑), unaltered (=) or downregulated (↓).

Table 5.3. Gene expression in testosterone-treated Z310 cells and female rats.

Summary of expression of selected genes in testosterone-treated Z310 cells (determined by qPCR) and in rat choroid plexus (Rat CP; HFD+PB 15w vs ND 15w, determined by MACE-RNAseq, as reported in Chapter 4). T stands for testosterone treatment. ↑ denotes increase in gene expression relative to their control, ↓ denotes decrease in gene expression relative to their control, = denotes no alteration. "Slightly" denotes that the *p* value was < 0.05, but log2fold change was between -1 and 1.

Gene	Z310 1ng/ml T	Z310 10ng/ml T	Rat CP
AQP1	=	↑	Slightly ↑
Slc4a10	=	↓	↓
ATP1A1	↑	↑	=
JAM3	=	=	↓
CLDN1	=	=	=
CLDN2	=	=	Slightly ↑
ZO-1	=	↓	↓
ZO-3	=	↓	Slightly ↑

There were a number of differences between alterations by testosterone treatment on *in vitro* cells and changes in expression measured in rats. In cells treated with 1 ng/ml of testosterone, all analysed genes remained unchanged except for ATP1A1, which was upregulated. Cells treated with 10 ng/ml of testosterone showed an increase in expression of AQP1 and ATP1A1, while having a decrease in expression of Slc4a10, ZO-1 and ZO-3. The CP of rats belonging to the group with highest testosterone concentrations had a slight

increase in expression levels of AQP1, CLDN2 and ZO-3. They also had a decrease in expression of Slc4a10, JAM3 and ZO-1.

5.3.5 Effect of testosterone on Z310 barrier functionality

Three different testosterone concentrations were tested to investigate the possible effect of this hormone the barrier functionality, specifically electrical resistance and permeability coefficient of the Z310 monolayer (**Figure 5.7**).

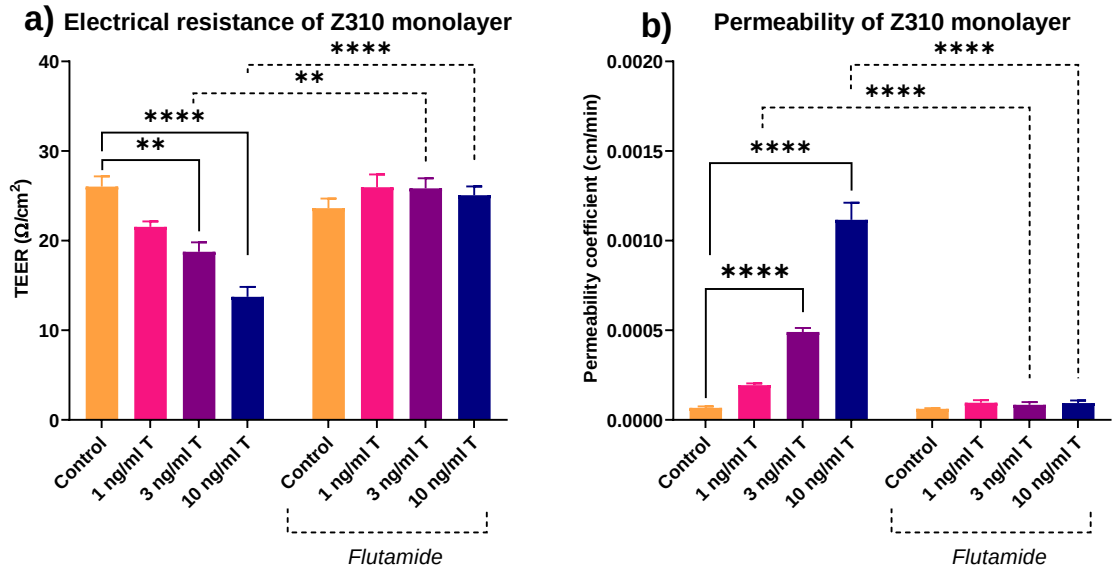

Figure 5.7. Changes on barrier functionality depending on testosterone treatment.

Barrier functionality was estimated by measuring (a) electrical resistance and (b) paracellular permeability of the monolayer. Cells were cultured on polyester membranes coated with collagen I until confluence was reached. Then, cells were incubated with the indicated concentrations of testosterone for 12 h before analysis was performed. Flutamide treatment was performed before testosterone treatment. After this, electrical resistance and permeability of the cell monolayer were measured. n=3, *=*P* value < 0.05, **=*P* value < 0.01, ***=*P* value < 0.001, **** *P* value < 0.0001.

The highest concentrations of testosterone (3 and 10 ng/ml respectively) caused a significant decrease in TEER values, suggesting that monolayer electrical resistance was decreased. Permeability was also increased in the samples treated with both 3 and 10 ng/ml of testosterone. Neither electrical resistance nor permeability were altered in cells pre-treated with flutamide no matter the testosterone concentration tested.

5.4 Discussion

In order to investigate changes in CP caused by testosterone, an *in vitro* CP model was set up using Z310 cells. Firstly, cell characterisation was performed. Z310 presented a predominantly polygonal morphology and they expressed most of the genes typically expressed in CP, including transporters, water channels, and TJs, with the exception of OATP1a4, KCNA6 and AQP4. When compared to rat CP expression, the latter did express AQP4 and KCNA6. However, rat CP did not express ABCB1a and ABCB1b while Z310 did. The optimised CP model consisted of Z310 cells growing on a collagen I pre-coated polyester insert at a seeding concentration of $2 \cdot 10^5$ cells per insert (1.13 cm^2 growing area). After confluence, cells were incubated with different concentrations of testosterone and gene expression, electrical resistance and paracellular permeability were measured. Testosterone treatment had the effect of increasing expression of AQP1 and ATP1A1, but reduced expression of Slc4a10, ZO-1 and ZO-3. Furthermore, testosterone treatment was also able to decrease monolayer electrical resistance and increase paracellular permeability. Pre-treatment with the AR antagonist Flutamide was able to prevent those changes from happening with testosterone treatment, which pointed out to testosterone being responsible for those changes.

Characterisation of Z310 was performed by morphological observation and gene expression analysis. The observed morphology was very similar to that described in literature for this cell line (Zheng and Zhao, 2002; Monnot and Zheng, 2012). All genes reported in the literature as being expressed in Z310 were also detected in this study. However, Z310 has been reported to be deficient in Slc22a7, Slc22a8, CLDN2 and OATP2b1 (Szmydynger-Chodobska *et al.*, 2007; Shi *et al.*, 2008; Kläs *et al.*, 2010), while these genes were detected in our experiment. It is important to note that both primers and PCR systems were different in each report, which could explain the discrepancies in detected gene expressions between the current research and those reported in the literature. This was not researched further though, therefore no conclusions can be currently drawn. It is interesting to note that all four genes mentioned above that were detected in our experiment but not reported in the literature were also detected in the rat CP by RNAseq-MACE, which points to the possibility that in our hands Z310 gene expression reflects more

accurately the profile of expression in the choroid plexus *in vivo* than those mentioned above. The lack of AQP4 in Z310 when compared to rat CP was expected, as AQP4 is mainly expressed in the ependyma, and it is consistent with the reasoning that the CP samples analysed in Chapter 4 were contaminated with some ependymal cells.

Z310 cells have already been used as a model of CP for several *in vitro* studies (Shi *et al.*, 2008; Monnot and Zheng, 2013; Costa *et al.*, 2016; Tomás *et al.*, 2019), but it is important to keep in mind that this is an immortalised cell line. Due to the immortalisation process, which includes genetic manipulation, immortalised cell lines can present alterations in characteristics such as genotype and phenotype when compared to *in vivo* CPEC. Furthermore, serial passage can increase phenotypic and genotypic variation even more. These possible changes are the reason why characterisation of immortalised cells is essential before starting a new experiment. Thanks to this process, the degree of similarity between a prospective *in vitro* model and the *in vivo* cells / tissues can be studied and the suitability of the cells can be judged. Z310 not expressing KCNA6 or OATP1a4 while rat CP did, falls inside the expected differences between immortalised and *in vivo* cells. However, the fact that Z310 expressed ABCB1a and ABCB1b whereas rat CP did not, was unusual, especially so because ABCB1 has previously been detected in the CP of rats (Mercier *et al.*, 2004; Niehof and Borlak, 2009; Gazzin *et al.*, 2011). As mentioned before, gene expression in Z310 and in rat CP were measured using different techniques therefore this discrepancy could be an artefact and no conclusions can be drawn with the present results. It is important to remember that qPCR and MACE-RNAseq use different approaches for gene expression measurements, therefore, when a discrepancy is found, further analysis using the same technique for both samples is needed in order to draw conclusions. In summary, Z310 cells and rat CP expressed most of the selected genes, therefore Z310 was determined to be a suitable *in vitro* model.

The different materials, coatings and initial seeding numbers used in our research were selected based on published reports and compared to identify the conditions that yielded the tightest monolayer (Gath *et al.*, 1997; Shi *et al.*, 2008; Kläs *et al.*, 2010). *In vivo* reported TEER values for CP epithelium range between 19 and 200 $\Omega \cdot cm^{-2}$, while Z310 TEER reported values ranging between 25 and 100 $\Omega \cdot cm^{-2}$ (Wright, 1972; Welch, 1975; Saito and

Wright, 1983; Shi *et al.*, 2008; Kläs *et al.*, 2010). The TEER values obtained in our experiment were on the lower end of those reported, however they were stable and similar amongst replicates, therefore they were considered appropriate for our experiments. The differences in TEER values between reports could be related to the use of different equipment or even differences in temperature during TEER measurement (Srinivasan *et al.*, 2015).

Testosterone was able to increase gene expression of ATP1A1. In vas deferens epithelium of orchiectomised rats, testosterone has been shown to cause increased fluid secretion by upregulating ATPase expression (Khadijah Ramli *et al.*, 2018; Khadijah Ramli, Giribabu and Salleh, 2018). In the brain, testosterone has been shown to alter ATPase activity, including ATP1 in the CP (García, Cabezas and Pérez-González, 1985; Guerra *et al.*, 1987; O'Reilly *et al.*, 2019). ATP1 activity was not measured in our experiment, however an increase of gene expression is consistent with an increase in activity. On the other hand, it has been observed that hypo and hyperkalaemia can alter ATP1 expression in the CP without altering CSF secretion, suggesting the presence of compensatory mechanisms to further regulate CSF secretion (Keep *et al.*, 1997). Therefore, no specific conclusions can be drawn from our study about the effect that increased expression of ATP1 in the presence of testosterone might have on CSF secretion.

Testosterone also increased AQP1 expression in Z310 cells. While the extent to which testosterone can alter gene and protein expression in CP has not been explored yet, it has been seen that testosterone can alter AQP1 expression in epithelium of uterus and proximal convoluted tubules of the kidney in female rats (Salleh *et al.*, 2015; Loh, Giribabu and Salleh, 2017). In the present study, AQP1 appeared slightly increased in the CP of the group of rats having the highest levels of testosterone when compared to their control. In the CP, increased AQP1 has been linked to hydrocephalus and formation of hydrocephalic oedema in animal and *in vitro* models (Moon *et al.*, 2006; Stępień *et al.*, 2014; Sveinsdottir *et al.*, 2014; Verkman *et al.*, 2017), as well as to BCSFB disruption and increased intracranial pressure in hyponatremia in murine models (Kim and Jung, 2011, 2012). Our experiments showed that barrier functionality was altered by testosterone, however whether these

parameters are directly altered by AQP1 expression or both are a result of a third effector, remains unknown.

Testosterone was able to decrease Slc4a10 expression in Z310 cells. This decrease was also seen in the CP of female rats with the highest testosterone levels. Slc4a10 is important for CSF secretion and its deletion leads to an alteration of polarisation of the CPEC including alteration of expression patterns of other transporters, decreased CSF secretion and a decrease in brain ventricle size (Jacobs *et al.*, 2008; Christensen *et al.*, 2013, 2020). While the decreased Slc4a10 expression seen in our cells after treatment with testosterone could lead one to hypothesise that CSF secretion would be decreased by testosterone, this parameter was not measured in our experiment; therefore the link between testosterone, Slc4a10 and CSF secretion in our CP model remains unexplored. It is possible that the decrease in Slc4a10 expression might be a compensatory mechanism to counteract increased CSF secretion driven by other gene or protein expression changes, however not enough data was obtained to draw any conclusions in this matter.

Paracellular permeation in epithelial barriers is regulated by the protein composition of the barrier, especially tight junction location and expression, thus a decrease in expression of those can increase permeability and negatively affect barrier integrity (Gardner, 1995; Youakim and Ahdieh, 1999; Ahdieh, Vandenbos and Youakim, 2001; Musch, Walsh-Reitz and Chang, 2006). In the CP, decreased or damaged tight junctions negatively impact barrier functionality, increasing paracellular permeability and thus allowing greater molecular leakage into CSF (Murphy and Johanson, 1985; Engelhardt and Sorokin, 2009; Johanson, Stopa and Mcmillan, 2011). Additionally, testosterone is known to regulate tight junctions in the epithelium of male reproductive organs (Meng *et al.*, 2005, 2011; Chakraborty *et al.*, 2014; Boivin and Schmidt-Ott, 2017). Testosterone has also been shown to perturb epidermal permeability in foetal murine skin (Kao *et al.*, 2001). In our experiment, testosterone treatment was able to decrease ZO-1 and ZO-3 expression while also altering electrical resistance and permeability of the barrier, two effects that are most likely causally related. Testosterone also decreased gene expression of JAM3 and ZO-1 *in vivo* in the group of female rats showing the highest concentrations of testosterone in plasma. Increased permeability of solutes into the CSF has been shown to have an effect

on osmotic pressure, increasing CSF secretion by increasing water movement from blood to CSF (Palm *et al.*, 1995; Damkier, Brown and Praetorius, 2013). Taking this into account, we theorised that the increase in CSF secretion observed in the rat group which also had higher levels of testosterone (HFD+PB 15w rats, see Chapter 4) could be caused by an alteration in TJs expression caused by increased levels of testosterone, amongst other things.

In conclusion, in our in vitro model of CP, testosterone treatment altered gene expression and barrier functionality while maintaining cell morphology. The extent at which alteration of expression of certain genes such as AQP1 or Slc4a10 can have on barrier integrity is not well known yet. However, tight junctions are essential for maintaining barrier functions, therefore the decrease in ZO-1 and ZO-3 gene expression and decrease in barrier functionality are indeed related. It is theorized that the alteration in gene expression seen in HFD+PB 15w rats was affected, although not exclusively, by increased testosterone levels, which affected barrier permeability, allowing the passage of an increased amount of water, therefore contributing to the elevated CSF secretion rates seen in those animals. More work is needed in order to explore the relationship between testosterone levels and CSF dynamics *in vivo.* However, if testosterone is shown to increase CSF secretion in IIH patients, this alteration could most likely be treated with antiandrogens, a therapy which is already in use for the treatment of other hormonal-related problems.

Chapter 6. General Discussion

The present study was designed to explore the effects of diet on CSF secretion in the rat with the aim to unravel possible pathogenic mechanisms underlying IIH. Other parameters, such as sex and elevated proinflammatory mediators in CSF, were also studied. In summary, it was found that a HFD was able to increase both body weight and CSF secretion in males and female rats, although the differences related to diet appeared earlier in males than in females. However, the females fed a HFD showed a higher increase in CSF secretion than males. Furthermore, the addition of HC into the CSF of HFD male rats was able to potentiate HF-diet induced increase in CSF secretion. In females, intracranial pressure was increased by HFD, and weight was positively correlated with CSF secretion. Additionally, testosterone concentration in plasma also correlated positively with CSF secretion in females. The group showing the highest levels of CSF secretion rate, body weight and testosterone levels also had the highest deregulation in gene expression at the mRNA level. In that group, most of the genes related to CSF secretion remained unaltered; however, two transporters, Slc4a10 and Kcna6, and several TJs, including ZO-1, were downregulated. *In vitro* tests using a CP cell model showed that testosterone treatment altered gene expression of CPEC including decreased expression of TJs including ZO-1, Slc4a10, and overexpression of AQP1 and ATP1A1. Additionally, testosterone was also able to decrease barrier functionality in the *in vitro* CP model.

IIH is a rare disease but its prevalence is increased in overweight women of childbearing age (Rowe and Sarkies, 1999; McCluskey *et al.*, 2018). While the pathophysiology is not well known, it is thought that IIH is caused by an impairment of CSF dynamics influenced by the female sex and by either obesity or a factor causing obesity (Daniels *et al.*, 2007; Markey *et al.*, 2016; Zanello *et al.*, 2018). In view of the results from the present study and previous studies reported in the literature, possible mechanisms underlying IIH have been summarised in **Figure 6.1** and will be discussed below.

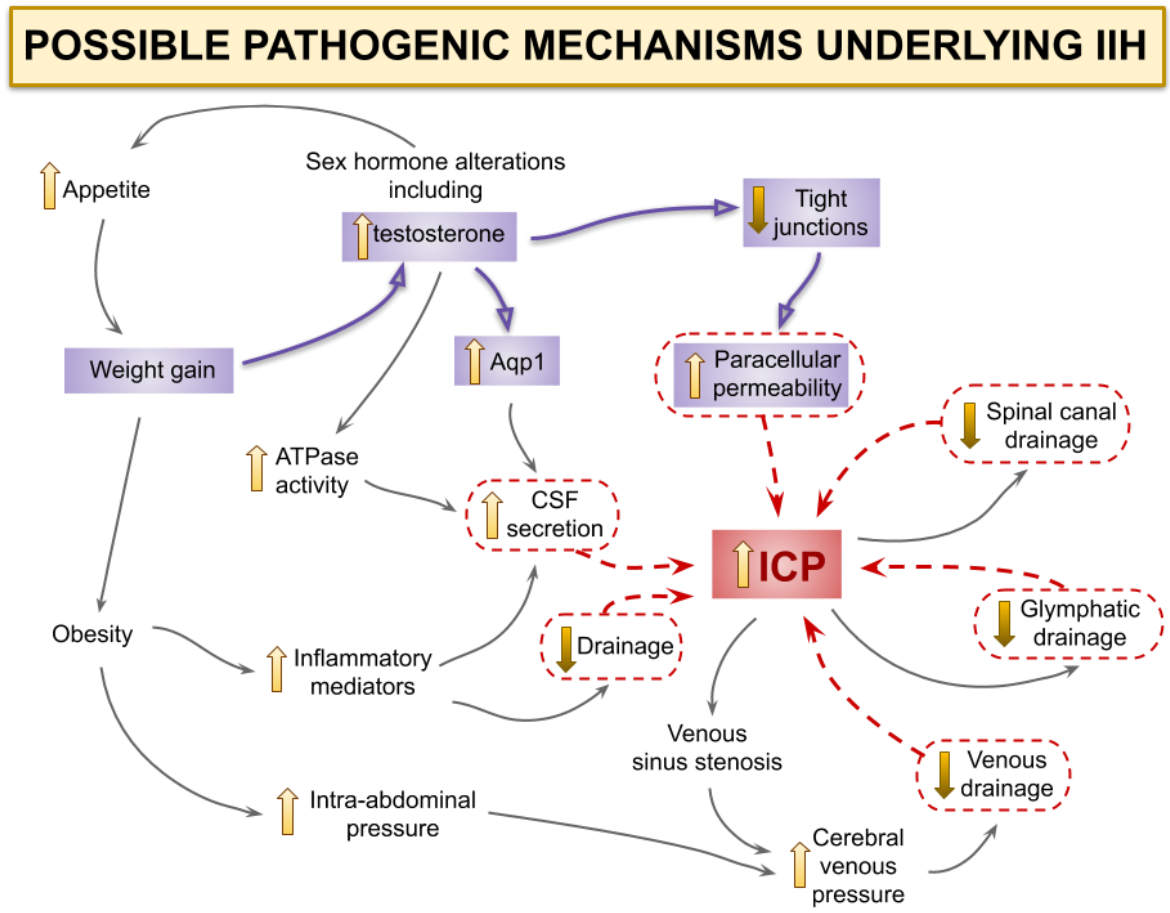

Figure 6.1. Possible pathogenic mechanisms underlying Idiopathic Intracranial Hypertension.

Upward arrows denote an increase while downward arrows denote a decrease. Red dashed lines and arrows mark direct contributors to raising ICP. Highlighted in purple are the findings of the present study and how they fit amongst the hypothesised mechanisms that contribute to the increased ICP characteristic of IIH. CSF = cerebrospinal fluid, ICP = Intracranial pressure (Sugerman *et al.*, 1995; Biousse, Bruce and Newman, 2012; Kalani, Filippidis and Rekate, 2012; Lam, Alperin and Ranganathan, 2012; Paganini *et al.*, 2017; Verkman *et al.*, 2017; Bezerra, Ferreira and de Oliveira-Souza, 2018; Dokras *et al.*, 2018; O'Reilly *et al.*, 2019; Alimajstorovic, Pascual-Baixauli, *et al.*, 2020)

The CSF is mainly produced by CPEC, although the brain interstitium and meninges are thought to contribute on a smaller scale (Sakka, Coll and Chazal, 2011; Damkier, Brown and Praetorius, 2013; Orešković and Klarica, 2014). CSF fills the ventricular system and the cranial and spinal subarachnoid spaces. CSF generally flows from secretion sites towards drainage points. In large ventricles, CSF bulk flow is mostly driven by secretion and drainage rates, while in smaller spaces, such as the third ventricle, multi-ciliated ependymal cells appear to have a big role in circulation dynamics (Orešković and Klarica, 2014; Linninger *et*

al., 2016; Abdelhamed *et al.*, 2018; Eichele *et al.*, 2020). CSF drainage is a complicated process that can occur through different sites, which fall into three functionally distinct categories: the arachnoid granulations, the perineural sheaths surrounding cranial and spinal nerves and the dural lymphatic vessels.

Ninety per cent of IIH patients are overweight postpubescent premenopausal women. Additionally, IIH has been previously linked to use of hormonal oral contraceptives, PCOS and pregnancy. While IIH paediatric patients are a minority, it is important to note that, in children, sex does not appear to be a risk factor for developing IIH whereas obesity mainly increases the risk of recurrence (Stiebel-Kalish *et al.*, 2014; Sheldon *et al.*, 2016). This fits the hypothesis of sex hormones playing an important role in IIH pathophysiology, as the differences in sex hormone levels between men and women start being noticeable at puberty. While the influence of sex hormones on CSF dynamics and its contribution to IIH is not fully understood yet, it has been shown that IIH patients have higher androgen levels than healthy overweight women (Hornby *et al.*, 2016; O'Reilly *et al.*, 2019). Furthermore, sex hormones have been shown to alter CSF secretion in *in vitro* models of CP (Lindvall-Axelsson and Owman, 1989; O'Reilly *et al.*, 2019).

Plasma testosterone concentration positively correlated with CSF secretion rate of female rats in our research. It has previously been reported that testosterone can increase CSF secretion by increasing ATP1 activity (O'Reilly *et al.*, 2019). In the current study, the rat group with highest CSF secretion rates and highest testosterone levels also had the highest difference in gene expression levels when compared to their controls, including a decrease in expression levels of two ion transporters and a small increase in AQP1. CSF secretion directly depends on ion transport across the BCSFB, therefore a decrease of expression this type of transport would cause a decrease in CSF secretion, but that was not the case. *In vivo* studies showed that these rats had the highest increase in CSF secretion when compared to their controls. It is possible that the decrease in ion transport seen in their CPEC is a compensatory mechanism caused by an increase of CSF secretion driven by other mechanisms, such as by an increase in paracellular permeability or increased water movement into CSF. Testosterone-treated cells also showed an increase in AQP1 expression. AQP1 is essential for CSF secretion and its overexpression has been linked to

increased CSF secretion in hydrocephalus models and to increased ICP in obese rats (Kalani, Filippidis and Rekate, 2012; Uldall *et al.*, 2017; Castañeyra-Ruiz *et al.*, 2019).

The animal group with larger rats and higher testosterone levels also showed gene expression alteration of different signalling pathways which could have an effect on CSF secretion. For example, cAMP pathways appeared downregulated. Testosterone has been seen to increase fluid secretion and solute transport by increasing cAMP generation in kidney epithelial cells *in vitro* (Sandhu *et al.*, 1997). It is possible that testosterone could increase cAMP generation in CP epithelium. In CP, CSF secretion is increased by agents increasing intracellular cAMP (Saito and Wright, 1983). This increase of CSF secretion by cAMP signalling pathway could be mediated by ATP1 and cAMP-activated anion channels, which would fit the results reported by O'Reilly *et al* about testosterone increasing ATP1 activity (Jentsch *et al.*, 2002; O'Reilly *et al.*, 2019). Furthermore, the RAS pathway appeared altered in the CP of the rat group with highest CSF secretion rates in our study. RAS deregulation has been hypothesised as a contributor to altered CSF production levels in IIH (Brettschneider *et al.*, 2011). However, it is possible that testosterone affects the CP and alters CSF dynamics in more than just one way. We found that testosterone was able to decrease barrier functionality of the CP *in vitro*. Furthermore, testosterone was also able to replicate gene expression alterations observed in the female rats with highest weight and testosterone levels. Both rats and testosterone treated Z310 cell line had a decreased expression of ZO-1 and Slc4a10. The CP of the rat group with the highest secretion rates had decreased expression of TJ and downregulated cell adhesion pathways. Barrier functionality is highly dependant on tight junction complexes, and decreased expression of these proteins are known to increase paracellular permeability (Ward, Tippin and Thakker, 2000; Kratzer *et al.*, 2012; Shen, 2012). The BCSFB is a highly regulated barrier, and a change in its permeability could have big effects for CSF dynamics, therefore it is possible that the differences in CSF secretion rates measured in the female rats and the changes in permeability observed in Z310 after testosterone treatment are the same mechanism. Increased CSF secretion has been previously linked to BCSF hyperpermeability in animal models of traumatic brain injury and hydrocephalus (Özevren, Deveci and Tuncer, 2018; Yang *et al.*, 2019). If this was the case in our model, however, the CSF secretion observed

in vivo would not strictly be such but rather an increase in permeability that would result in increased water flow across the CP epithelium into the ventricles, increasing CSF volume and ICP if drainage pathways are unable to compensate for the increase in flow. However it could also be considered increased CSF secretion because it would result in an increased flow of liquid through the BCSFB, which would lead to a higher passive rate of CSF production.

Overweightness in humans is usually accompanied by elevated concentrations of proinflammatory mediators (Björntorp and Rosmond, 2000; Tchernof and Després, 2013; Shaw *et al.*, 2014). It is speculated that an excess of these mediators might be behind the pathophysiology of IIH (Sinclair *et al.*, 2008; Dhungana, Sharrack and Woodroofe, 2009a; Samancı *et al.*, 2017). In our experiments, we found that the addition of HC into the CSF of overweight male rats increased CSF secretion. In females, HC and TNFα have been reported to increase CSF secretion in lean individuals, the former also being able to increase CSF secretion in diet-induced overweight females (Alimajstorovic, Pascual-Baixauli, *et al.*, 2020). The exact mechanisms by which obesity-related cytokines and adipokines can influence CSF secretion is not known yet. Proinflammatory mediators have been shown to be able to alter barrier permeability of the BCSFB. However, whether this alteration is due to a decrease in TJs, an increase in cell senescence or another mechanism is not well known yet (Coisne and Engelhardt, 2011; Ghersi-Egea *et al.*, 2018; Johanson and Johanson, 2018). Furthermore, CCL2 was able to decrease CSF drainage in female rats, although the exact mechanism by which this happens has not been explored yet (Alimajstorovic, Pascual-Baixauli, *et al.*, 2020).

IIH is most likely caused by a combination of factors, including an inadequate rate of CSF drainage (Julayanont *et al.*, 2016; Mollan *et al.*, 2016). As mentioned in Chapter 1, CSF gets absorbed by several different pathways, and it is currently unknown which, if any, is affected in IIH. Nevertheless, it is possible that the deregulation of more than one drainage pathway of CSF is involved in the development of IIH (Baykan, Ekizoğlu and Altiokka, 2015).

Obesity can affect physiological processes due to the endocrine nature of adipose tissue but also because of physical effects caused by the increase in body mass (Lyon, Law and Hsueh, 2003; Watson and Pride, 2005; Coelho, Oliveira and Fernandes, 2013). It has been postulated that IIH is influenced by an increase in intra-abdominal pressure caused by obesity which would then increase venous pressure (Sugerman *et al.*, 1995, 1997; Bloomfield *et al.*, 1997). This change in venous pressure would decrease CSF drainage into the venous flow as this process is mainly driven by a pressure gradient from the ventricles outwards (Bono *et al.*, 2008; Friedman, 2010). Impaired drainage would contribute to the increase of ICP with a further related increase in cerebral venous pressure by narrowing the sinuses to the point of stenosis (Jones and Gratton, 1989; Nedelmann, Kaps and Mueller-Forell, 2009; De Simone, Ranieri and Bonavita, 2010). It is thought that this positive feedback loop is self-limiting though: once the maximum stretching of the venous wall is reached, no additional narrowing could increase CSF pressure further. This would lead to a new balance at higher intracranial and venous pressures, which would remain stable for a longer period, even if the original cause of increased ICP disappeared (Mokri, 2001; Giridharan *et al.*, 2018). However, according to this hypothesis, it would be possible to return to the original pressure balance by increasing CSF drainage. Indeed, it has been observed in IIH patients that surgical drainage of CSF, sometimes even after only one treatment, can resolve venous stenosis and improve the condition (De Simone *et al.*, 2005; Horev *et al.*, 2013; Shields *et al.*, 2019).

Venous sinus stenosis and impaired venous CSF drainage does not always result in increased ICP (Fargen, 2020). In these cases however, the glymphatic pathway could be acting as a compensatory mechanism to drain CSF at a rate high enough to prevent development of significant increase in ICP (Lenck *et al.*, 2018). Nevertheless, in other circumstances the glymphatic pathway might become congested by an impaired flow of ISF. This could lead to diffuse stagnation of flow and solutes in the interstitium and/or paravascular spaces, congesting the glymphatic system and increasing ICP (Bezerra, Ferreira and de Oliveira-Souza, 2018; Mondejar and Patsalides, 2020). Authors defending this hypothesis base it on several observations, such as the smaller ventricular size observed in some IIH patients, the fact that obesity is associated with paravascular

inflammation and lymphatic disturbance and also on the observation that, in Alzheimer's disease, glymphatic dysfunction has been related to the deposition of β-amyloid molecules (Reid, Matheson and Teasdale, 1980; Bezerra, Ferreira and de Oliveira-Souza, 2018; Lenck *et al.*, 2018). Nevertheless, the glymphatic dysfunction as cause of IIH hypothesis is relatively recent and further investigations are needed in order to further characterise its mechanisms and its influence in the development of IIH.

Other drainage mechanisms thought to be impaired in IIH include reduced CSF drainage by the arachnoid villi, which would be decreased by the increased venous pressure mentioned above, and from the spinal canal, which CSF volume would appear reduced in IIH (Glueck *et al.*, 2005; Alperin *et al.*, 2012; Lam, Alperin and Ranganathan, 2012; Mondejar and Patsalides, 2020). However, the reason why the spinal canal compliance appears reduced in this condition has not been explored yet.

According to the results obtained in the present study, we hypothesise that an obesity-related increase in testosterone plasma concentration contributes to the development of IIH by increasing CSF production and paracellular permeability of the BCSFB.

6.1 Future Work

Future work on this subject should include a bigger study on the effects of factors such as diet and altered hormonal levels on ICP. Future *in vivo* experiments could test different diets to induce overweightness, such as high-carbohydrate low-fat or cafeteria diet. It would be interesting to observe whether there is a difference in CSF dynamics or hormonal levels depending on the ingredients of the diet. Additionally, the use of different formulations of HFD could also result in different levels of overweightness, providing an easy tool to study the relationship between body weight or weight gain and CSF dynamics. Furthermore, it would be very interesting to study the relationship between increased permeability of BCSF and CSF dynamics, including ICP.

Following our results, it would be extremely interesting to explore the effects of increased testosterone levels in the female rat. Experiments to test barrier permeability,

ICP, CSF secretion rates and gene expression, especially that of TJs and AQP1, should be included. It would also be interesting to note if increased testosterone levels affect food intake, body weight and body fat composition. These experiments should include animals treated with anti-androgens such as flutamide. Furthermore, it would be interesting to observe the effect of anti-androgens on the animal model established in our project in order to see if parameters such as weight gain, CSF secretion rate or ICP are altered; if that was the case, it would be an indicator that testosterone directly affects these factors.

Additionally, testing how testosterone can alter barrier functionality and gene expression of other *in vitro* models of CP, including human cells, would be beneficial. By using different cell lines, the validity of our results could be tested. If our results could be replicated in other cells lines, it would be more likely that they are reproducing molecular mechanisms happening *in vivo.* In the future, if testosterone is found to be a direct contributor to IIH, anti-androgens would be an ideal treatment due to their specificity and also because antiandrogens have long been used to treat other health issues in women, therefore not much work would be needed in order to develop this possible new therapy.

References

Abbott, N. J. (2004) 'Evidence for bulk flow of brain interstitial fluid: significance for physiology and pathology', *Neurochemistry International*, 45(4), pp. 545–552. doi: 10.1016/j.neuint.2003.11.006.

Abbott, N. J., Patabendige, A. A. K., Dolman, D. E. M., Yusof, S. R. and Begley, D. J. (2010) 'Structure and function of the blood?brain barrier', *Neurobiology of Disease*, 37(1), pp. 13–25. doi: 10.1016/j.nbd.2009.07.030.

Abbott, N. J., Rönnbäck, L. and Hansson, E. (2006) 'Astrocyte-endothelial interactions at the blood-brain barrier', *Nature Reviews Neuroscience*, pp. 41–53. doi: 10.1038/nrn1824.

Abdelhamed, Z., Vuong, S. M., Hill, L., Shula, C., Timms, A., Beier, D., Campbell, K., Mangano, F. T., Stottmann, R. W. and Goto, J. (2018) 'A mutation in Ccdc39 causes neonatal hydrocephalus with abnormal motile cilia development in mice', *Development (Cambridge)*. Company of Biologists Ltd, 145(1). doi: 10.1242/dev.154500.

Abubaker, K., Ali, Z., Raza, K., Bolger, C., Rawluk, D. and O'Brien, D. (2011) 'Idiopathic intracranial hypertension: Lumboperitoneal shunts versus ventriculoperitoneal shunts - Case series and literature review', *British Journal of Neurosurgery*. Taylor & Francis, 25(1), pp. 94–99. doi: 10.3109/02688697.2010.544781.

Adigun, O. O. and Al-Dhahir, M. A. (2019) *Anatomy, Head and Neck, Cerebrospinal Fluid*, *StatPearls*. Available at: http://www.ncbi.nlm.nih.gov/pubmed/29083815 (Accessed: 9 January 2020).

Agarwal, A., Vibha, D., Prasad, K., Bhatia, R., Singh, M. B., Garg, A. and Saxena, R. (2017) 'Predictors of poor visual outcome in patients with Idiopathic Intracranial Hypertension (IIH): An ambispective cohort study', *Clinical Neurology and Neurosurgery*. Elsevier B.V., 159, pp. 13–18. doi: 10.1016/j.clineuro.2017.05.009.

Agarwal, N., Contarino, C., Limbucci, N., Bertazzi, L. and Toro, E. (2018) 'Intracranial

Fluid Dynamics Changes in Idiopathic Intracranial Hypertension: Pre and Post Therapy', *Current Neurovascular Research*. Bentham Science Publishers Ltd., 15(2), pp. 164–172. doi: 10.2174/1567202615666180528113616.

Ahdieh, M., Vandenbos, T. and Youakim, A. (2001) 'Lung epithelial barrier function and wound healing are decreased by IL-4 and IL-13 and enhanced by IFN-γ', *American Journal of Physiology - Cell Physiology*. American Physiological Society, 281(6 50-6). doi: 10.1152/ajpcell.2001.281.6.c2029.

Akay, R., Kamisli, O., Kahraman, A., Oner, S. and Tecellioglu, M. (2015) 'Evaluation of aqueductal CSF flow dynamics with phase contrast cine MR imaging in idiopathic intracranial hypertension patients: preliminary results.', *European review for medical and pharmacological sciences*, 19(18), pp. 3475–9. Available at: http://www.ncbi.nlm.nih.gov/pubmed/26439045 (Accessed: 31 January 2020).

Akiyama, T., Tachibana, I., Shirohara, H., Watanabe, N. and Otsuki, M. (1996) 'High-fat hypercaloric diet induces obesity, glucose intolerance and hyperlipidemia in normal adult male Wistar rat', *Diabetes Research and Clinical Practice*. Elsevier, 31(1–3), pp. 27–35. doi: 10.1016/0168-8227(96)01205-3.

Aldred, A. R., Brack, C. M. and Schreiber, G. (1995) 'The cerebral expression of plasma protein genes in different species.', *Comparative biochemistry and physiology. Part B, Biochemistry & molecular biology*, 111(1), pp. 1–15. Available at: http://www.ncbi.nlm.nih.gov/pubmed/7749630 (Accessed: 3 July 2017).

Alimajstorovic, Z., Pascual-Baixauli, E., Hawkes, C. A., Sharrack, B., Loughlin, A. J., Romero, I. A. and Preston, J. E. (2020) 'Cerebrospinal fluid dynamics modulation by diet and cytokines in rats', *Fluids and Barriers of the CNS*. BioMed Central, 17(1), p. 10. doi: 10.1186/s12987-020-0168-z.

Alimajstorovic, Z., Westgate, C. S. J., Jensen, R. H., Eftekhari, S., Mitchell, J., Vijay, V., Seneviratne, S. Y., Mollan, S. P. and Sinclair, A. J. (2020) 'Guide to preclinical models used to study the pathophysiology of idiopathic intracranial hypertension', *Eye*. Springer

Nature, 34(8), pp. 1321–1333. doi: 10.1038/s41433-019-0751-1.

Allan, C. A. and McLachlan, R. I. (2010) 'Androgens and obesity', *Current Opinion in Endocrinology, Diabetes and Obesity*, 17(3), pp. 224–232. doi: 10.1097/MED.0b013e3283398ee2.

Alperin, N., Lam, B. L., Tain, R. W., Ranganathan, S., Letzing, M., Bloom, M., Alexander, B., Aroucha, P. R. and Sklar, E. (2012) 'Evidence for altered spinal canal compliance and cerebral venous drainage in untreated idiopathic intracranial hypertension', in *Acta Neurochirurgica, Supplementum*. Springer-Verlag Wien, pp. 201–205. doi: 10.1007/978-3-7091-0956-4_39.

Alpers, B. J. (1959) 'Anatomical Studies of the Circle of Willis in Normal Brain', *A.M.A. Arch. Neurol.*, 81(April), p. 409.

Altıokka-Uzun, G., Tüzün, E., Ekizoğlu, E., Ulusoy, C., Yentür, S., Kürtüncü, M., Saruhan-Direskeneli, G. and Baykan, B. (2015) 'Oligoclonal bands and increased cytokine levels in idiopathic intracranial hypertension', *Cephalalgia*, 35(13), pp. 1153–1161. doi: 10.1177/0333102415570762.

Altokika-Uzun, G., Tuzun, E., Ekizolu, E., Ulusoy, C., Yentr, S., K?rt?nc?, M., Saruhan-Direskeneli, G. and Baykan, B. (2015) 'Oligoclonal bands and increased cytokine levels in idiopathic intracranial hypertension', *Cephalalgia*. SAGE PublicationsSage UK: London, England, 35(13), pp. 1153–1161. doi: 10.1177/0333102415570762.

Alves, C. H., Gonçalves, I., Socorro, S., Baltazar, G., Quintela, T. and Santos, C. R. A. (2009) 'Androgen Receptor is Expressed in Murine Choroid Plexus and Downregulated by 5α-Dihydrotestosterone in Male and Female Mice', *Journal of Molecular Neuroscience*. Humana Press Inc, 38(1), pp. 41–49. doi: 10.1007/s12031-008-9157-4.

Ames, A., Higashi, K. and Nesbett, F. B. (1965) 'Relation of potassium concentration in choroidplexus fluid to that in plasma.', *The Journal of Physiology*. J Physiol, 181(3), pp. 506–515. doi: 10.1113/jphysiol.1965.sp007779.

Anderson, J. J. B. (1990) 'Relationship of dietary fat content to food preferences in young rats Zoe S. Warwick Susan S. Schiffman', *Physiology and Behavior*. Elsevier Inc., 48(5), pp. 581–586. doi: 10.1016/0031-9384(90)90195-A.

Armulik, A., Genové, G., Mäe, M., Nisancioglu, M. H., Wallgard, E., Niaudet, C., He, L., Norlin, J., Lindblom, P., Strittmatter, K., Johansson, B. R. and Betsholtz, C. (2010) 'Pericytes regulate the blood-brain barrier', *Nature*, 468(7323), pp. 557–561. doi: 10.1038/nature09522.

Aslani, S., Vieira, N., Marques, F., Costa, P. S., Sousa, N. and Palha, J. A. (2015) 'The effect of high-fat diet on rat's mood, feeding behavior and response to stress', *Translational Psychiatry*. Nature Publishing Group, 5(11), pp. e684–e684. doi: 10.1038/tp.2015.178.

Aubin, M. C., Lajoie, C., Clément, R., Gosselin, H., Calderone, A. and Perrault, L. P. (2008) 'Female rats fed a high-fat diet were associated with vascular dysfunction and cardiac fibrosis in the absence of overt obesity and hyperlipidemia: Therapeutic potential of resveratrol', *Journal of Pharmacology and Experimental Therapeutics*. American Society for Pharmacology and Experimental Therapeutics, 325(3), pp. 961–968. doi: 10.1124/jpet.107.135061.

Bagga, R., Jain, V., Das, C. P., Gupta, K. R., Gopalan, S. and Malhotra, S. (2005) 'Choice of therapy and mode of delivery in idiopathic intracranial hypertension during pregnancy.', *MedGenMed : Medscape general medicine*. WebMD/Medscape Health Network, 7(4), p. 42.

Baker, R. S., Baumann, R. J. and Buncic, J. R. (1989) 'Idiopathic intracranial hypertension (pseudotumor cerebri) in pediatric patients.', *Pediatric neurology*, 5(1), pp. 5–11. Available at: http://www.ncbi.nlm.nih.gov/pubmed/2653341 (Accessed: 10 July 2017).

Balasubramanian, P., Jagannathan, L., Mahaley, R. E., Subramanian, M., Gilbreath, E. T., MohanKumar, P. S. and MohanKumar, S. M. J. (2012) 'High Fat Diet Affects Reproductive Functions in Female Diet-Induced Obese and Dietary Resistant Rats', *Journal*

of Neuroendocrinology. John Wiley & Sons, Ltd (10.1111), 24(5), pp. 748–755. doi: 10.1111/j.1365-2826.2011.02276.x.

Ball, A. K., Sinclair, A. J., Curnow, S. J., Tomlinson, J. W., Burdon, M. A., Walker, E. A., Stewart, P. M., Nightingale, P. G., Clarke, C. E. and Rauz, S. (2009) 'Elevated cerebrospinal fluid (CSF) leptin in idiopathic intracranial hypertension (IIH): evidence for hypothalamic leptin resistance?', *Clinical Endocrinology*, 70(6), pp. 863–869. doi: 10.1111/j.1365-2265.2008.03401.x.

Banu, S. K., Arosh, J. A., Govindarajulu, P. and Aruldhas, M. M. (2001) 'Testosterone and estradiol differentially regulate thyroid growth in wistar rats from immature to adult age', *Endocrine Research*, 27(4), pp. 447–463. doi: 10.1081/ERC-100107868.

Bäuerle, J. and Nedelmann, M. (2011) 'Sonographic assessment of the optic nerve sheath in idiopathic intracranial hypertension', *Journal of Neurology*. Springer, 258(11), pp. 2014–2019. doi: 10.1007/s00415-011-6059-0.

Baykan, B., Ekizoğlu, E. and Altiokka, G. (2015) 'An update on the pathophysiology of idiopathic intracranial hypertension alias pseudotumor cerebri İdiyopatik intrakraniyal hipertansiyonun-diğer adıyla psödotümör serebrinin-patofizyolojisi üzerine bir güncelleme Özet', *AĞRI*, 27(2), pp. 63–72. doi: 10.5505/agri.2015.22599.

Bazzano, M. V., Torelli, C., Pustovrh, M. C., Paz, D. A. and Elia, E. M. (2015) 'Obesity induced by cafeteria diet disrupts fertility in the rat by affecting multiple ovarian targets', *Reproductive BioMedicine Online*, 31(5), pp. 655–667. doi: 10.1016/j.rbmo.2015.08.004.

Beato, M. (1993) 'Gene Regulation by Steroid Hormones', in *Gene Expression*. Boston, MA: Birkhäuser Boston, pp. 43–75. doi: 10.1007/978-1-4684-6811-3_3.

Becker, J. B., Prendergast, B. J. and Liang, J. W. (2016) 'Female rats are not more variable than male rats: A meta-analysis of neuroscience studies', *Biology of Sex Differences*. BioMed Central Ltd., 7(1). doi: 10.1186/s13293-016-0087-5.

Bedolla, J., Buchanan, I. and Hansen, K. (2017) 'Idiopathic Intracranial Hypertension

in a Transgender Male on Hormone Therapy', *Arch Emerg Med Crit Care*, 2(1). Available at: https://www.jscimedcentral.com/EmergencyMedicine/emergencymedicine-2-1019.pdf (Accessed: 26 July 2017).

Bedussi, B., Naessens, D. M. P., De Vos, J., Olde Engberink, R., Wilhelmus, M. M. M., Richard, E., Ten Hove, M., Vanbavel, E. and Bakker, E. N. T. P. (2017) 'Enhanced interstitial fluid drainage in the hippocampus of spontaneously hypertensive rats', *Scientific Reports*. Nature Publishing Group, 7(1). doi: 10.1038/s41598-017-00861-x.

Beery, A. K. and Zucker, I. (2011) 'Sex bias in neuroscience and biomedical research', *Neuroscience and Biobehavioral Reviews*, pp. 565–572. doi: 10.1016/j.neubiorev.2010.07.002.

Benarroch, E. E. (2016) 'Choroid plexus–CSF system', *Neurology*. Lippincott Williams and Wilkins, 86(3), pp. 286–296. doi: 10.1212/WNL.0000000000002298.

Bennett, F. C. and Ingram, D. M. (1990) *Diet and female sex hormone concentrations: an intervention study for the type of fat consumed*, *The American Journal of Clinical Nutrition*. doi: https://doi.org/10.1093/ajcn/52.5.808.

Berdahl, J. P., Fleischman, D., Zaydlarova, J., Stinnett, S., Rand Allingham, R. and Fautsch, M. P. (2012) 'Body mass index has a linear relationship with cerebrospinal fluid pressure', *Investigative Ophthalmology and Visual Science*, pp. 1422–1427. doi: 10.1167/iovs.11-8220.

Berezovsky, D. E., Bruce, B. B., Vasseneix, C., Peragallo, J. H., Newman, N. J. and Biousse, V. (2017) 'Cerebrospinal fluid total protein in idiopathic intracranial hypertension', *Journal of the Neurological Sciences*. Elsevier B.V., 381, pp. 226–229. doi: 10.1016/j.jns.2017.08.3264.

Bernd, A., Ott, M., Ishikawa, H., Schroten, H., Schwerk, C. and Fricker, G. (2015) 'Characterization of efflux transport proteins of the human choroid plexus papilloma cell line HIBCPP, a functional in vitro model of the blood-cerebrospinal fluid barrier',

Pharmaceutical Research, 32(9), pp. 2973–2982. doi: 10.1007/s11095-015-1679-1.

Besch, D., Makowski, C., Steinborn, M.-M., Bonfig, W. and Sadowski, B. (2012) 'Visual Loss without Headache in Children with Pseudotumor Cerebri and Growth Hormone Treatment', *Neuropediatrics*, 44(04), pp. 203–207. doi: 10.1055/s-0032-1330855.

Bezerra, M. L. de S., Ferreira, A. C. A. de F. and de Oliveira-Souza, R. (2018) 'Pseudotumor Cerebri and Glymphatic Dysfunction', *Frontiers in Neurology*. Frontiers Media S.A., 8(JAN), p. 16. doi: 10.3389/fneur.2017.00734.

Bidot, S. and Bruce, B. (2015) 'Update on the Diagnosis and Treatment of Idiopathic Intracranial Hypertension', *Seminars in Neurology*, 35(05), pp. 527–538. doi: 10.1055/s-0035-1563569.

Binder, D. K., Horton, J. C., Lawton, M. T., McDermott, M. W., Dempsey, R. J., Bergsneider, M., Kelly, D. F., Chandler, W. F., Selman, W. R. and Grossman, R. G. (2004) 'Idiopathic intracranial hypertension.', *Neurosurgery*, 54(3), pp. 538–51; discussion 551-2. doi: 10.1227/01.NEU.0000109042.87246.3C.

Biousse, V., Bruce, B. B. and Newman, N. J. (2011) 'Update on the pathophysiology and management of idiopathic intracranial hypertension', *American Journal of Ophthalmology*, 152(2), pp. 163–169. doi: 10.1136/jnnp-2011-302029.

Biousse, V., Bruce, B. B. and Newman, N. J. (2012) 'Update on the pathophysiology and management of idiopathic intracranial hypertension', *Journal of Neurology, Neurosurgery and Psychiatry*. BMJ Publishing Group, pp. 488–494. doi: 10.1136/jnnp-2011-302029.

Björkhem, I., Leoni, V. and Svenningsson, P. (2019) 'On the fluxes of side-chain oxidized oxysterols across blood-brain and blood-CSF barriers and origin of these steroids in CSF (Review)', *Journal of Steroid Biochemistry and Molecular Biology*. Elsevier Ltd, pp. 86–89. doi: 10.1016/j.jsbmb.2018.12.009.

Björntorp, P. and Rosmond, R. (2000) 'Obesity and cortisol', *Nutrition*, 16(10), pp.

924–936. doi: 10.1016/S0899-9007(00)00422-6.

Blaus, B. (2013) *Ventricles of the Brain*, *WikiJournal of Medicine*. doi: 10.15347/wjm/2014.010.

Blaus, B. (2014) 'Medical gallery of Blausen Medical 2014', *WikiJournal of Medicine*. Wikiversity Journal of Medicine, 1(2), p. 10. doi: 10.15347/wjm/2014.010.

Bloomfield, G. L., Ridings, P. C., Blocher, C. R., Marmarou, A. and Sugerman, H. J. (1997) 'A proposed relationship between increased intra-abdominal, intrathoracic, and intracranial pressure', *Critical Care Medicine*, 25(3), pp. 496–503. doi: 10.1097/00003246-199703000-00020.

Boespflug, E. L. and Iliff, J. J. (2018) 'The Emerging Relationship Between Interstitial Fluid–Cerebrospinal Fluid Exchange, Amyloid-β and Sleep', *Biological Psychiatry*. Elsevier USA, pp. 328–336. doi: 10.1016/j.biopsych.2017.11.031.

Boivin, F. J. and Schmidt-Ott, K. M. (2017) 'Transcriptional mechanisms coordinating tight junction assembly during epithelial differentiation', *Annals of the New York Academy of Sciences*. Blackwell Publishing Inc., 1397(1), pp. 80–99. doi: 10.1111/nyas.13367.

Bono, F., Lupo, M. R., Serra, P., Cantafio, C., Lucisano, A., Lavano, A., Fera, F., Pardatscher, K. and Quattrone, A. (2002) 'Obesity does not induce abnormal CSF pressure in subjects with normal cerebral MR venography', *Neurology*. Lippincott Williams and Wilkins, 59(10), pp. 1641–1643. doi: 10.1212/01.WNL.0000035628.81384.5F.

Bono, F., Messina, D., Giliberto, C., Cristiano, D., Broussard, G., D'Asero, S., Condino, F., Mangone, L., Mastrandrea, C., Fera, F. and Quattrone, A. (2008) 'Bilateral transverse sinus stenosis and idiopathic intracranial hypertension without papilledema in chronic tension-type headache', *Journal of Neurology*. Springer, 255(6), pp. 807–812. doi: 10.1007/s00415-008-0676-2.

Bothwell, S. W., Janigro, D. and Patabendige, A. (2019) 'Cerebrospinal fluid dynamics and intracranial pressure elevation in neurological diseases', *Fluids and Barriers*

of the CNS. BioMed Central Ltd. doi: 10.1186/s12987-019-0129-6.

Boulton, M., Armstrong, D., Flessner, M., Hay, J., Szalai, J. P. and Johnston, M. (1998) 'Raised intracranial pressure increases CSF drainage through arachnoid villi and extracranial lymphatics.', *The American journal of physiology*, 275(3 Pt 2), pp. R889-96. Available at: http://www.ncbi.nlm.nih.gov/pubmed/9728088 (Accessed: 3 July 2017).

Bourrea, J. M., Dinh, L., Boithias, C., Dumont, O., Piciotti, M. and Cunnane, S. (1997) 'Possible role of the choroid plexus in the supply of brain tissue with polyunsaturated fatty acids', *Neuroscience Letters*. Elsevier Ireland Ltd, 224(1), pp. 1–4. doi: 10.1016/S0304-3940(97)13440-1.

Bouzinova, E. V., Praetorius, J., Virkki, L. V., Nielsen, S., Boron, W. F. and Aalkjaer, C. (2005) 'Na+-dependent HCO3- uptake into the rat choroid plexus epithelium is partially DIDS sensitive', *American Journal of Physiology - Cell Physiology*, 289(6 58-6). doi: 10.1152/ajpcell.00313.2005.

Bray, G. A. (1997) 'Obesity and reproduction', *Human Reproduction*. Narnia, 12(suppl 1), pp. 26–32. doi: 10.1093/humrep/12.suppl_1.26.

Brettschneider, J., Hartmann, N., Lehmensiek, V., Mogel, H., Ludolph, A. C. and Tumani, H. (2011) 'Cerebrospinal fluid markers of idiopathic intracranial hypertension: Is the renin-angiotensinogen system involved?', *Cephalalgia*. SAGE PublicationsSage UK: London, England, 31(1), pp. 116–121. doi: 10.1177/0333102410375726.

Brinkmann, G., Harlandt, O., Muhle, C., Brossmann, J. and Heller, M. (2000) 'Quantification of fluid flow in magnetic resonance tomography: an experimental study of a flow model and liquid flow measurements in the cerebral aqueduct in volunteers.', *RoFo : Fortschritte auf dem Gebiete der Rontgenstrahlen und der Nuklearmedizin*, 172(12), pp. 1043–51. doi: 10.1055/s-2000-9217.

Brioschi, S. and Colonna, M. (2019) 'The CNS Immune-Privilege Goes Down the Drain(age)', *Trends in Pharmacological Sciences*. Elsevier Ltd, pp. 1–3. doi:

10.1016/j.tips.2018.11.006.

Brkic, M., Balusu, S., Van Wonterghem, E., Gorlé, N., Benilova, I., Kremer, A., Van Hove, I., Moons, L., De Strooper, B., Kanazir, S., Libert, C. and Vandenbroucke, R. E. (2015) 'Amyloid β oligomers disrupt blood–CSF barrier integrity by activating matrix metalloproteinases', *Journal of Neuroscience*. Society for Neuroscience, 35(37), pp. 12766–12778. doi: 10.1523/JNEUROSCI.0006-15.2015.

Brøchner, C. B., Holst, C. B. and Møllgård, K. (2015) 'Outer brain barriers in rat and human development', *Frontiers in Neuroscience*. Frontiers Research Foundation, 9(FEB). doi: 10.3389/fnins.2015.00075.

Brodsky, M. and Vaphiades, M. (1998) 'Magnetic resonance imaging in pseudotumor cerebri', *Ophthalmology*, 105(9), pp. 1686–1693. doi: 10.1016/S0161-6420(98)99039-X.

Brody, H. (2017) 'Nature outlook: BLOOD', *Nature*. Nature Publishing Group, p. S11. doi: 10.1038/549S11a.

Broughton, D. E. and Moley, K. H. (2017) 'Obesity and female infertility: potential mediators of obesity's impact', *Fertility and Sterility*, 107(4), pp. 840–847. doi: 10.1016/j.fertnstert.2017.01.017.

Brown, P. D., Davies, S. L., Speake, T. and Millar, I. D. (2004) 'Molecular mechanisms of cerebrospinal fluid production', *Neuroscience*, 129(4), pp. 955–968. doi: 10.1016/j.neuroscience.2004.07.003.

Brunori, A., Vagnozzi, R. and Giuffrè, R. (1993) 'Antonio Pacchioni (1665–1726): early studies of the dura mater', *Journal of Neurosurgery*, 78(3), pp. 515–518. doi: 10.3171/jns.1993.78.3.0515.

Buettner, R., Parhofer, K. G., Woenckhaus, M., Wrede, C. E., Kunz-Schughart, L. A., Schölmerich, J. and Bollheimer, L. C. (2006) 'Defining high-fat-diet rat models: Metabolic and molecular effects of different fat types', *Journal of Molecular Endocrinology*, 36(3), pp.

485–501. doi: 10.1677/jme.1.01909.

Buettner, R., Schölmerich, J. and Bollheimer, L. C. (2007) 'High-fat Diets: Modeling the Metabolic Disorders of Human Obesity in Rodents*', *Obesity*, 15(4), pp. 798–808. doi: 10.1038/oby.2007.608.

Bussiere, M., Falero, R., Nicolle, D., Proulx, A., Patel, V. and Pelz, D. (2010) 'Unilateral Transverse Sinus Stenting of Patients with Idiopathic Intracranial Hypertension', *American Journal of Neuroradiology*, 31(4), pp. 645–650. doi: 10.3174/ajnr.A1890.

Cabanac, M. and Johnson, K. G. (1983) 'Analysis of a conflict between Palatability and cold exposure in rats', *Physiology & Behavior*. Elsevier, 31(2), pp. 249–253. doi: 10.1016/0031-9384(83)90128-2.

Cancer Research UK (2014) *Diagram showing a brain shunt CRUK* , *Wikimedia Commons*. Available at: https://commons.wikimedia.org/wiki/File:Diagram_showing_a_brain_shunt_CRUK_052.svg (Accessed: 13 September 2020).

Cano, P., Jiménez-Ortega, V., Larrad, Á., Toso, C. F. R., Cardinali, D. P. and Esquifino, A. I. (2008) 'Effect of a high-fat diet on 24-h pattern of circulating levels of prolactin, luteinizing hormone, testosterone, corticosterone, thyroid-stimulating hormone and glucose, and pineal melatonin content, in rats', *Endocrine*. Springer, 33(2), pp. 118–125. doi: 10.1007/s12020-008-9066-x.

Castañeyra-Ruiz, L., Hernández-Abad, L., Carmona-Calero, E., Castañeyra-Perdomo, A. and González-Marrero, I. (2019) 'AQP1 Overexpression in the CSF of Obstructive Hydrocephalus and Inversion of Its Polarity in the Choroid Plexus of a Chiari Malformation Type II Case', *Journal of neuropathology and experimental neurology*. J Neuropathol Exp Neurol, 78(7). doi: 10.1093/JNEN/NLZ033.

Çelebisoy, N., Gökçay, F., Şirin, H. and Akyürekli, Ö. (2007) 'Treatment of idiopathic intracranial hypertension: Topiramate vs acetazolamide, an open-label study', *Acta*

Neurologica Scandinavica. John Wiley & Sons, Ltd, 116(5), pp. 322–327. doi: 10.1111/j.1600-0404.2007.00905.x.

Chakraborty, P., William Buaas, F., Sharma, M., Smith, B. E., Greenlee, A. R., Eacker, S. M. and Braun, R. E. (2014) 'Androgen-Dependent Sertoli Cell Tight Junction Remodeling Is Mediated by Multiple Tight Junction Components', *Molecular Endocrinology*. Endocrine Society, 28(7), pp. 1055–1072. doi: 10.1210/me.2013-1134.

Chandra, V., Bellur, S. N. and Anderson, R. J. (1986) 'Low CSF protein concentration in idiopathic pseudotumor cerebri', *Annals of Neurology*, 19(1), pp. 80–82. doi: 10.1002/ana.410190116.

Chen, J. and Wall, M. (2014) 'Epidemiology and Risk Factors for Idiopathic Intracranial Hypertension', *Int Ophthalmol Clin*, 54(1). doi: 10.1097/IIO.0b013e3182aabf11.

Chen, L., Elias, G., Yostos, M. P., Stimec, B., Fasel, J. and Murphy, K. (2015) 'Pathways of cerebrospinal fluid outflow: a deeper understanding of resorption', *Neuroradiology*, 57(2), pp. 139–147. doi: 10.1007/s00234-014-1461-9.

Christensen, H. L., Barbuskaite, D., Rojek, A., Malte, H., Christensen, I. B., Füchtbauer, A. C., Füchtbauer, E. M., Wang, T., Praetorius, J. and Damkier, H. H. (2018) 'The choroid plexus sodium-bicarbonate cotransporter NBCe2 regulates mouse cerebrospinal fluid pH', *Journal of Physiology*. Blackwell Publishing Ltd, 596(19), pp. 4709–4728. doi: 10.1113/JP275489.

Christensen, I. B., Gyldenholm, T., Damkier, H. H. and Praetorius, J. (2013) 'Polarization of membrane associated proteins in the choroid plexus epithelium from normal and slc4a10 knockout mice', *Frontiers in Physiology*. Frontiers, 4, p. 344. doi: 10.3389/fphys.2013.00344.

Christensen, I. B., Wu, Q., Bohlbro, A. S., Skals, M. G., Damkier, H. H., Hübner, C. A., Fenton, R. A. and Praetorius, J. (2020) 'Genetic disruption of slc4a10 alters the capacity for

cellular metabolism and vectorial ion transport in the choroid plexus epithelium', *Fluids and Barriers of the CNS*. BioMed Central Ltd., 17(1), p. 2. doi: 10.1186/s12987-019-0162-5.

Cipolla, M. (2009) 'Anatomy and Ultrastructure', in Sciences, M. & C. L. (ed.) *The Cerebral Circulation*. Available at: https://www.ncbi.nlm.nih.gov/books/NBK53086/ (Accessed: 24 February 2020).

Coelho, M., Oliveira, T. and Fernandes, R. (2013) 'Biochemistry of adipose tissue: An endocrine organ', *Archives of Medical Science*. Termedia Publishing, pp. 191–200. doi: 10.5114/aoms.2013.33181.

Coisne, C. and Engelhardt, B. (2011) 'Tight junctions in brain barriers during central nervous system inflammation', *Antioxidants and Redox Signaling*. Mary Ann Liebert, Inc. 140 Huguenot Street, 3rd Floor New Rochelle, NY 10801 USA , pp. 1285–1303. doi: 10.1089/ars.2011.3929.

Contu, L. and Hawkes, C. A. (2017) 'A Review of the Impact of Maternal Obesity on the Cognitive Function and Mental Health of the Offspring', *International Journal of Molecular Sciences*. MDPI AG, 18(5), p. 1093. doi: 10.3390/ijms18051093.

Corbit, J. D. and Stellar, E. (1964) 'Palatability, food intake, and obesity in normal and hyperphagic rats', *Journal of Comparative and Physiological Psychology*, 58(1), pp. 63–67. doi: 10.1037/h0039787.

Cornford, E. M., Varesi, J. B., Hyman, S., Damian, R. T. and Raleigh, M. J. (1997) 'Mitochondrial content of choroid plexus epithelium', *Experimental Brain Research*. Springer, 116(3), pp. 399–405. doi: 10.1007/PL00005768.

Costa, A. R., Marcelino, H., Gonçalves, I., Quintela, T., Tomás, J., Duarte, A. C., Fonseca, A. M. and Santos, C. R. A. (2016) 'Sex Hormones Protect Against Amyloid-β Induced Oxidative Stress in the Choroid Plexus Cell Line Z310', *Journal of Neuroendocrinology*, 28(9). doi: 10.1111/jne.12404.

Crispino, M. and Crispino, E. (2015) *Atlas of Imaging Anatomy*. Springer. Available

at: https://books.google.co.uk/books?hl=en&lr=&id=eRPmBQAAQBAJ&oi=fnd&pg=PR7&dq=brain+anatomy+vascularised&ots=znejD10Mer&sig=Xhzxm-l4wqlX4nOx6kIcooVjnyY&redir_esc=y#v=onepage&q&f=false (Accessed: 24 February 2020).

Cserr, H. F. (1983) 'Flow of Brain Interstitial Fluid and Drainage into Cerebrospinal Fluid and Lymph', in *Intracranial Pressure V*. Springer Berlin Heidelberg, pp. 618–621. doi: 10.1007/978-3-642-69204-8_105.

Cserr, H. F., Cooper, D. N., Suri, P. K. and Patlak, C. S. (1981) 'Efflux of radiolabeled polyethylene glycols and albumin from rat brain', *American Journal of Physiology - Renal Fluid and Electrolyte Physiology*. American Physiological Society Bethesda, MD , 9(4), pp. 319–328. doi: 10.1152/ajprenal.1981.240.4.f319.

Damkier, H. H., Brown, P. D. and Praetorius, J. (2010) 'Epithelial Pathways in Choroid Plexus Electrolyte Transport'. doi: 10.1152/physiol.00011.2010.

Damkier, H. H., Brown, P. D. and Praetorius, J. (2013) 'Cerebrospinal fluid secretion by the choroid plexus', *Physiological Reviews*, pp. 1847–1892. doi: 10.1152/physrev.00004.2013.

Damkier, H. H. and Praetorius, J. (2012) 'Genetic ablation of *Slc4a10* alters the expression pattern of transporters involved in solute movement in the mouse choroid plexus', *American Journal of Physiology-Cell Physiology*. American Physiological Society Bethesda, MD, 302(10), pp. C1452–C1459. doi: 10.1152/ajpcell.00285.2011.

Dandy, W. E. (1937) 'INTRACRANIAL PRESSURE WITHOUT BRAIN TUMOR DIAGNOSIS AND TREATMENT', *Annals of Surgery*, 106(4). Available at: https://www.ncbi.nlm.nih.gov/pmc/articles/PMC1390605/pdf/annsurg00527-0013.pdf (Accessed: 29 June 2017).

Daniels, A. B., Liu, G. T., Volpe, N. J., Galetta, S. L., Moster, M. L., Newman, N. J.,

Biousse, V., Lee, A. G., Wall, M., Kardon, R., Acierno, M. D., Corbett, J. J., Maguire, M. G. and Balcer, L. J. (2007) 'Profiles of Obesity, Weight Gain, and Quality of Life in Idiopathic Intracranial Hypertension (Pseudotumor Cerebri)', *American Journal of Ophthalmology*. Elsevier, 143(4), pp. 635-641.e1. doi: 10.1016/J.AJO.2006.12.040.

Darendeliler, F., Karagiannis, G. and Wilton, P. (2007) 'Headache, Idiopathic Intracranial Hypertension and Slipped Capital Femoral Epiphysis during Growth Hormone Treatment: A Safety Update from the KIGS Database', *Hormone Research in Paediatrics*, 68(5), pp. 41–47. doi: 10.1159/000110474.

Dasgupta, K. and Jeong, J. (2019) 'Developmental biology of the meninges', *Genesis*. John Wiley and Sons Inc. doi: 10.1002/dvg.23288.

Davson, H. (1967) 'Chemical composition and secretory nature of the fluids', *Physiology of the Cerebrospinal Fluid*. J&A Churchill Ltd., pp. 33–54. Available at: https://ci.nii.ac.jp/naid/10026566555 (Accessed: 10 September 2020).

Davson, H., Hollingsworth, J. G., Carey, M. B. and Fenstermacher, J. D. (1982) 'Ventriculo–cisternal perfusion of twelve amino acids in the rabbit', *Journal of Neurobiology*. J Neurobiol, 13(4), pp. 293–318. doi: 10.1002/neu.480130402.

Deane, R. and Segal, M. B. (1985) 'The transport of sugars across the perfused choroid plexus of the sheep.', *The Journal of Physiology*. John Wiley & Sons, Ltd, 362(1), pp. 245–260. doi: 10.1113/jphysiol.1985.sp015674.

Decimo, I., Fumagalli, G., Berton, V., Krampera, M. and Bifari, F. (2012) 'Meninges: From protective membrane to stem cell niche', *American Journal of Stem Cells*. E-Century Publishing Corporation, pp. 92–105.

Degnan, A. J. and Levy, L. M. (2011) 'Pseudotumor cerebri: Brief review of clinical syndrome and imaging findings', *American Journal of Neuroradiology*. American Journal of Neuroradiology, pp. 1986–1993. doi: 10.3174/ajnr.A2404.

Dehouck, M. -P, Jolliet-Riant, P., Brée, F., Fruchart, J. -C, Cecchelli, R. and Tillement,

J. -P (1992) 'Drug Transfer Across the Blood-Brain Barrier: Correlation Between In Vitro and In Vivo Models', *Journal of Neurochemistry*, 58(5), pp. 1790–1797. doi: 10.1111/j.1471-4159.1992.tb10055.x.

Dhungana, S., Sharrack, B. and Woodroofe, N. (2009a) 'Cytokines and Chemokines in Idiopathic Intracranial Hypertension', *Headache: The Journal of Head and Face Pain*. John Wiley & Sons, Ltd (10.1111), 49(2), pp. 282–285. doi: 10.1111/j.1526-4610.2008.001329.x.

Dhungana, S., Sharrack, B. and Woodroofe, N. (2009b) *IL-1β, TNF and IP-10 in the cerebrospinal fluid and serum are not altered in patients with idiopathic intracranial hypertension compared to controls*, *Clinical Endocrinology*. John Wiley & Sons, Ltd (10.1111). doi: 10.1111/j.1365-2265.2009.03593.x.

Dhungana, S., Sharrack, B. and Woodroofe, N. (2010) 'Idiopathic intracranial hypertension', *Acta Neurologica Scandinavica*. Blackwell Publishing Ltd, 121(2), pp. 71–82. doi: 10.1111/j.1600-0404.2009.01172.x.

Dinner, S., Borkowski, J., Stump-Guthier, C., Ishikawa, H., Tenenbaum, T., Schroten, H. and Schwerk, C. (2016) 'A Choroid Plexus Epithelial Cell-based Model of the Human Blood-Cerebrospinal Fluid Barrier to Study Bacterial Infection from the Basolateral Side', *Journal of Visualized Experiments*, (111). doi: 10.3791/54061.

Dobrian, A. D., Davies, M. J., Prewitt, R. L. and Lauterio, T. J. (2000) 'Development of Hypertension in a Rat Model of Diet-Induced Obesity', *Hypertension*. Lippincott Williams and Wilkins, 35(4), pp. 1009–1015. doi: 10.1161/01.HYP.35.4.1009.

Dóczi, T. (1993) 'Volume regulation of the brain tissue-a survey', *Acta Neurochirurgica*. Springer-Verlag, 121(1–2), pp. 1–8. doi: 10.1007/BF01405174.

Dohrmann, G. J. (1970) 'The choroid plexus: A historical review', *Brain Research*, 18(2), pp. 197–218. doi: 10.1016/0006-8993(70)90324-0.

Dokras, A., Stener-Victorin, E., Yildiz, B. O., Li, R., Ottey, S., Shah, D., Epperson, N. and Teede, H. (2018) 'Androgen Excess- Polycystic Ovary Syndrome Society: position

statement on depression, anxiety, quality of life, and eating disorders in polycystic ovary syndrome', *Fertility and Sterility*. Elsevier Inc., 109(5), pp. 888–899. doi: 10.1016/j.fertnstert.2018.01.038.

Donaldson, J. 0 and Horakt, E. (1982) 'Cerebrospinal fluid oestrone in pseudotumour cerebri', *Journal of Neurology Neurosurgery, and Psychiatry*, 45(8), pp. 734–736. Available at: http://jnnp.bmj.com/content/jnnp/45/8/734.full.pdf (Accessed: 5 July 2017).

Donaldson, J. O. (1979) 'Cerebrospinal fluid hypersecretion in pseudotumor cerebri.', *Transactions of the American Neurological Association*, 104, pp. 196–8. Available at: http://www.ncbi.nlm.nih.gov/pubmed/553408 (Accessed: 31 January 2020).

Donaldson, J. O. and Horak, E. (1982) 'Cerebrospinal fluid oestrone in pseudotumour cerebri.', *Journal of neurology, neurosurgery, and psychiatry*, 45(8), pp. 734–6.

Dreha-Kulaczewski, S., Konopka, M., Joseph, A. A., Kollmeier, J., Merboldt, K. D., Ludwig, H. C., Gärtner, J. and Frahm, J. (2018) 'Respiration and the watershed of spinal CSF flow in humans', *Scientific Reports*. Nature Publishing Group, 8(1), pp. 1–7. doi: 10.1038/s41598-018-23908-z.

Durcan, F. J., Corbett, J. J. and Wall, M. (1988) 'The incidence of pseudotumor cerebri. Population studies in Iowa and Louisiana.', *Archives of neurology*, 45(8), pp. 875–7. Available at: http://www.ncbi.nlm.nih.gov/pubmed/3395261 (Accessed: 29 June 2017).

Dykhuizen, M. J. and Hall, J. (2011) 'Cerebral venous sinus system and stenting in pseudotumor cerebri', *Current Opinion in Ophthalmology*, 22(6), pp. 458–462. doi: 10.1097/ICU.0b013e32834bbf9f.

Edwards, L. J., Sharrack, B., Ismail, A., Tench, C. R., Gran, B., Dhungana, S., Brettschneider, J., Tumani, H. and Constantinescu, C. S. (2013) 'Increased levels of interleukins 2 and 17 in the cerebrospinal fluid of patients with idiopathic intracranial

hypertension.', *American journal of clinical and experimental immunology*. e-Century Publishing Corporation, 2(3), pp. 234–44. Available at: http://www.ncbi.nlm.nih.gov/pubmed/24179731 (Accessed: 24 January 2019).

Egemen, E. and Solaroglu, I. (2017) 'Anatomy of Cerebral Veins and Dural Sinuses', in *Primer on Cerebrovascular Diseases: Second Edition*. Elsevier Inc., pp. 32–36. doi: 10.1016/B978-0-12-803058-5.00005-9.

Egertová, M., Cravatt, B. F. and Elphick, M. R. (2000) 'Fatty acid amide hydrolase expression in rat choroid plexus: Possible role in regulation of the sleep-inducing action of oleamide', *Neuroscience Letters*. Elsevier, 282(1–2), pp. 13–16. doi: 10.1016/S0304-3940(00)00841-7.

Egertová, M., Michael, G. J., Cravatt, B. F. and Elphick, M. R. (2004) 'Fatty acid amide hydrolase in brain ventricular epithelium: Mutually exclusive patterns of expression in mouse and rat', *Journal of Chemical Neuroanatomy*. Elsevier, 28(3), pp. 171–181. doi: 10.1016/j.jchemneu.2004.07.001.

Eichele, G., Bodenschatz, E., Ditte, Z., Günther, A.-K., Kapoor, S., Wang, Y. and Westendorf, C. (2020) 'Cilia-driven flows in the brain third ventricle', *Philosophical Transactions of the Royal Society B: Biological Sciences*. Royal Society Publishing, 375(1792), p. 20190154. doi: 10.1098/rstb.2019.0154.

El-Saadany, W. F., Farhoud, A. and Zidan, I. (2012) 'Lumboperitoneal shunt for idiopathic intracranial hypertension: patients' selection and outcome', *Neurosurgical Reviews*, 35, pp. 239–244. doi: 10.1007/s10143-011-0350-5.

Eliasson, M. and Meyerson, B. J. (1975) 'Sexual preference in female rats during estrous cycle, pregnancy and lactation', *Physiology and Behavior*, 14(6), pp. 705–710. doi: 10.1016/0031-9384(75)90061-X.

Ellulu, M. S., Patimah, I., Khaza'ai, H., Rahmat, A. and Abed, Y. (2017) 'Obesity and inflammation: the linking mechanism and the complications.', *Archives of medical science :*

AMS. Termedia Publishing, 13(4), pp. 851–863. doi: 10.5114/aoms.2016.58928.

Emerich, D. F., Vasconcellos, A. V, Elliott, R. B., Skinner, S. J. and Borlongan, C. V (2004) 'The choroid plexus: function, pathology and therapeutic potential of its transplantation', *Expert Opinion on Biological Therapy*, 4(8), pp. 1191–1201. doi: 10.1517/14712598.4.8.1191.

Engelhardt, B. and Sorokin, L. (2009) 'The blood-brain and the blood-cerebrospinal fluid barriers: Function and dysfunction', *Seminars in Immunopathology*. Springer, pp. 497–511. doi: 10.1007/s00281-009-0177-0.

Engelhardt, B., Vajkoczy, P. and Weller, R. O. (2017) 'The movers and shapers in immune privilege of the CNS', *Nature Immunology*. Nature Publishing Group, pp. 123–131. doi: 10.1038/ni.3666.

Evans, D. J., Hoffmann, R. G., Kalkhoff, R. K. and Kissebah, A. H. (1983) 'Relationship of androgenic activity to body fat topography, fat cell morphology, and metabolic aberrations in premenopausal women', *Journal of Clinical Endocrinology and Metabolism*, 57(2), pp. 304–310. doi: 10.1210/jcem-57-2-304.

Fagan, J. A. and Cowan, R. J. (1971) 'The effect of potassium perchlorate on the uptake of 99mTc-pertechnetate in choroid plexus papillomas: a report of two cases.', *Journal of Nuclear Medicine*. J Nucl Med, 12(6), pp. 312–314. Available at: https://pubmed.ncbi.nlm.nih.gov/4325621/ (Accessed: 11 September 2020).

Falcão, A. M., Marques, F., Novais, A., Sousa, N., Palha, J. a and Sousa, J. C. (2012) 'The path from the choroid plexus to the subventricular zone: go with the flow!', *Frontiers in cellular neuroscience*. doi: 10.3389/fncel.2012.00034.

Farb, R. I., Vanek, I., Scott, J. N., Mikulis, D. J., Willinsky, R. A., Tomlinson, G. and terBrugge, K. G. (2003) 'Idiopathic intracranial hypertension: the prevalence and morphology of sinovenous stenosis.', *Neurology*, 60(9), pp. 1418–24.

Fargen, K. M. (2020) 'Idiopathic intracranial hypertension is not idiopathic: Proposal

for a new nomenclature and patient classification', *Journal of NeuroInterventional Surgery*. BMJ Publishing Group, pp. 110–114. doi: 10.1136/neurintsurg-2019-015498.

Fassbinder-Orth, C. A. (2014) 'Methods for quantifying gene expression in ecoimmunology: From qPCR to RNA-Seq', in *Integrative and Comparative Biology*. Oxford University Press, pp. 396–406. doi: 10.1093/icb/icu023.

Fauser, B. C. J. M. and Van Heusden, A. M. (1997) *Manipulation of Human Ovarian Function: Physiological Concepts and Clinical Consequences**.

Feder, H. H. (1981) 'Estrous Cyclicity in Mammals', in *Neuroendocrinology of Reproduction*. Springer US, pp. 279–348. doi: 10.1007/978-1-4684-3881-9_10.

Fenstermacher, J. D. (1972) 'Ventriculocisternal Perfusion as a Technique for Studying Transport and Metabolism Within the Brain', in *Research Methods in Neurochemistry*. Springer US, pp. 165–178. doi: 10.1007/978-1-4615-7748-5_7.

Fleischman, D. and Berdahl, J. (2019) *Anatomy and Physiology of the Cerebrospinal Fluid*. Edited by G. Guidoboni, A. Harris, and R. Sacco. Cham: Springer International Publishing (Modeling and Simulation in Science, Engineering and Technology). doi: 10.1007/978-3-030-25886-3.

Flexner, L. B. and Winters, H. (1932) 'The Rate Of Formation Of Cerebrospinal Fluid In Etherized Cats', *American Journal of Physiology-Legacy Content*. American Physiological Society, 101(4), pp. 697–710. doi: 10.1152/ajplegacy.1932.101.4.697.

Foley, J. (1955) 'Benign forms of intracranial hypertension; toxic and otitic hydrocephalus.', *Brain : a journal of neurology*, 78(1), pp. 1–41. Available at: http://www.ncbi.nlm.nih.gov/pubmed/14378448 (Accessed: 10 July 2017).

Fortepiani, L. A., Yanes, L., Zhang, H., Racusen, L. C. and Reckelhoff, J. F. (2003) 'Role of Androgens in Mediating Renal Injury in Aging SHR', *Hypertension*. Lippincott Williams & Wilkins, 42(5), pp. 952–955. doi: 10.1161/01.HYP.0000099241.53121.7F.

Fossan, G., Cavanagh, M. E., Evans, C. A. N., Malinowska, D. H., Møllgård, K., Reynolds, M. L. and Saunders, N. R. (1985) 'CSF-Brain permeability in the immature sheep fetus: A CSF-brain barrier', *Developmental Brain Research*. Elsevier, 18(1–2), pp. 113–124. doi: 10.1016/0165-3806(85)90255-X.

Fraser, J. A., Bruce, B. B., Rucker, J., Fraser, L.-A., Atkins, E. J., Newman, N. J. and Biousse, V. (2010) 'Risk factors for idiopathic intracranial hypertension in men: A case–control study', *Journal of the Neurological Sciences*, 290(1–2), pp. 86–89. doi: 10.1016/j.jns.2009.11.001.

Friedman, D. I. and Jacobson, D. M. (2002) 'Diagnostic criteria for idiopathic intracranial hypertension.', *Neurology*, 59(10), pp. 1492–5. Available at: http://www.ncbi.nlm.nih.gov/pubmed/12455560 (Accessed: 30 June 2017).

Friedman, D. I., Liu, G. T. and Digre, K. B. (2013) 'Revised diagnostic criteria for the pseudotumor cerebri syndrome in adults and children', *Neurology*. Neurology, pp. 1159–1165. doi: 10.1212/WNL.0b013e3182a55f17.

Friedman, D. L. (2010) 'Intracranial hypertension, headache and obesity: Insights from magnetic resonance venography', *Cephalalgia*. SAGE PublicationsUK, pp. 1415–1416. doi: 10.1177/0333102410370872.

Friesner, D., Rosenman, R., Lobb, B. M. and Tanne, E. (2011) 'Idiopathic intracranial hypertension in the USA: the role of obesity in establishing prevalence and healthcare costs', *Obesity Reviews*, 12(5), pp. e372–e380. doi: 10.1111/j.1467-789X.2010.00799.x.

Frigeri, A., Gropper, M. A., Umenishi, F., Kawashima, M., Brown, D. and Verkman, A. S. (1995) 'Localization of MIWC and GLIP water channel homologs in neuromuscular, epithelial and glandular tissues', *Journal of Cell Science*, 108(9), pp. 2993–3002.

García, M. V., Cabezas, J. A. and Pérez-González, M. N. (1985) 'Effects of oestradiol, testosterone and medroxyprogesterone on subcellular fraction marker enzyme activities from rat liver and brain', *Comparative Biochemistry and Physiology -- Part B: Biochemistry*

and, 80(2), pp. 347–354. doi: 10.1016/0305-0491(85)90217-2.

Gardner, T. W. (1995) 'Histamine, ZO-1 and increased blood-retinal barrier permeability in diabetic retinopathy', in *Transactions of the American Ophthalmological Society*. American Ophthalmological Society, pp. 583–621. Available at: /pmc/articles/PMC1312073/?report=abstract (Accessed: 5 August 2020).

Gargiulo, S., Gramanzini, M., Megna, R., Greco, A., Albanese, S., Manfredi, C. and Brunetti, A. (2014) 'Evaluation of Growth Patterns and Body Composition in C57Bl/6J Mice Using Dual Energy X-Ray Absorptiometry', *BioMed Research International*, 2014, pp. 1–11. doi: 10.1155/2014/253067.

Gath, U., Hakvoort, A., Wegener, J., Decker, S. and Galla, H. J. (1997) 'Porcine choroid plexus cells in culture: expression of polarized phenotype, maintenance of barrier properties and apical secretion of CSF-components.', *European journal of cell biology*, 74(1), pp. 68–78. Available at: http://www.ncbi.nlm.nih.gov/pubmed/9309392 (Accessed: 3 August 2020).

Gazzin, S., Berengeno, A. L., Strazielle, N., Fazzari, F., Raseni, A., Ostrow, J. D., Wennberg, R., Ghersi-Egea, J.-F. and Tiribelli, C. (2011) 'Modulation of Mrp1 (ABCc1) and Pgp (ABCb1) by Bilirubin at the Blood-CSF and Blood-Brain Barriers in the Gunn Rat', *PLoS ONE*. Edited by R. Linden. Public Library of Science, 6(1), p. e16165. doi: 10.1371/journal.pone.0016165.

Ghersi-Egea, J.-F., Strazielle, N., Murat, A., Jouvet, A., Buénerd, A. and Belin, M.-F. (2006) 'Brain protection at the blood-cerebrospinal fluid interface involves a glutathione-dependent metabolic barrier mechanism.', *Journal of cerebral blood flow and metabolism : official journal of the International Society of Cerebral Blood Flow and Metabolism*, 26(9), pp. 1165–75. doi: 10.1038/sj.jcbfm.9600267.

Ghersi-Egea, J. F., Strazielle, N., Catala, M., Silva-Vargas, V., Doetsch, F. and Engelhardt, B. (2018) 'Molecular anatomy and functions of the choroidal blood-cerebrospinal fluid barrier in health and disease', *Acta Neuropathologica*. Springer Verlag,

pp. 337–361. doi: 10.1007/s00401-018-1807-1.

Giagulli, V. A., Kaufman, J. M. and Vermeulen, A. (1994) 'Pathogenesis of the decreased androgen levels in obese men.', *The Journal of Clinical Endocrinology & Metabolism*, 79(4), pp. 997–1000. doi: 10.1210/jcem.79.4.7962311.

Gideon, P., Sørensen, P. S., Thomsen, C., Ståhlberg, F., Gjerris, F. and Henriksen, O. (1994) 'Assessment of CSF dynamics and venous flow in the superior sagittal sinus by MRI in idiopathic intracranial hypertension: a preliminary study.', *Neuroradiology*, 36(5), pp. 350–4. Available at: http://www.ncbi.nlm.nih.gov/pubmed/7936173 (Accessed: 5 July 2017).

Gildea, J. J., Xu, P., Carlson, J. M., Gaglione, R. T., Wang, D. B., Kemp, B. A., Reyes, C. M., McGrath, H. E., Carey, R. M., Jose, P. A. and Felder, R. A. (2015) 'The sodium-bicarbonate cotransporter NBCE2 (slc4a5) expressed in human renal proximal tubules shows increased apical expression under high-salt conditions', *American Journal of Physiology - Regulatory Integrative and Comparative Physiology*. American Physiological Society, 309(11), pp. R1447–R1459. doi: 10.1152/ajpregu.00150.2015.

Gillooly, C., Belov, V., Belova, E., Levine, D., Appleton, J. and Papisov, M. (2017) 'Cerebrospinal fluid drainage to the lymphatic system in rats and nonhuman primates', *Journal of Nuclear Nuclear Medicine*, 58. Available at: http://jnm.snmjournals.org/content/58/supplement_1/656.short (Accessed: 17 August 2020).

Giridharan, N., Patel, S. K., Ojugbeli, A., Nouri, A., Shirani, P., Grossman, A. W., Cheng, J., Zuccarello, M. and Prestigiacomo, C. J. (2018) 'Understanding the complex pathophysiology of idiopathic intracranial hypertension and the evolving role of venous sinus stenting: A comprehensive review of the literature', *Neurosurgical Focus*. American Association of Neurological Surgeons, 45(1), pp. 1–13. doi: 10.3171/2018.4.FOCUS18100.

Giuseffi, V., Wall, M., Siegel, P. Z. and Rojas, P. B. (1991) 'Symptoms and disease associations in idiopathic intracranial hypertension (pseudotumor cerebri): A case-control

study', *Neurology*. Wolters Kluwer Health, Inc. on behalf of the American Academy of Neurology, 41(2), pp. 239–244. doi: 10.1212/wnl.41.2_part_1.239.

Glueck, C. J., Aregawi, D., Goldenberg, N., Golnik, K. C., Sieve, L. and Wang, P. (2005) 'Idiopathic intracranial hypertension, polycystic-ovary syndrome, and thrombophilia', *Journal of Laboratory and Clinical Medicine*, 145(2), pp. 72–82. doi: 10.1016/j.lab.2004.09.011.

Glueck, C. J., Golnik, K. C., Aregawi, D., Goldenberg, N., Sieve, L. and Wang, P. (2006) 'Changes in weight, papilledema, headache, visual field, and life status in response to diet and metformin in women with idiopathic intracranial hypertension with and without concurrent polycystic ovary syndrome or hyperinsulinemia', *Translational Research*. Mosby Inc., 148(5), pp. 215–222. doi: 10.1016/j.trsl.2006.05.003.

Glueck, C. J., Iyengar, S., Goldenberg, N., Smith, L.-S. and Wang, P. (2003) 'Idiopathic intracranial hypertension: associations with coagulation disorders and polycystic-ovary syndrome', *Journal of Laboratory and Clinical Medicine*, 142(1), pp. 35–45. doi: 10.1016/S0022-2143(03)00069-6.

Goudie, C., Shah, P., McKee, J., Foot, B., Kousha, O. and Blaikie, A. (2019) 'The incidence of idiopathic intracranial hypertension in Scotland: a SOSU study', *Eye (Basingstoke)*. Nature Publishing Group, 33(10), pp. 1570–1576. doi: 10.1038/s41433-019-0450-y.

Graphpad Software (2019) 'GraphPad Prism'. La Jolla, California, USA.

Grapp, M., Wrede, A., Schweizer, M., Hüwel, S., Galla, H. J., Snaidero, N., Simons, M., Bückers, J., Low, P. S., Urlaub, H., Gärtner, J. and Steinfeld, R. (2013) 'Choroid plexus transcytosis and exosome shuttling deliver folate into brain parenchyma', *Nature Communications*, 4. doi: 10.1038/ncomms3123.

Greenberg, D. M., Aird, R. B., Boelter, M. D. D., Campbell, W. W., Cohn, W. E. and Murayama, M. M. (1943) 'A Study With Radioactive Isotopes Of The Permeability Of The

Blood-Cerebrospinal Fluid Barrier To Ions', *American Journal of Physiology-Legacy Content*. American Physiological Society, 140(1), pp. 47–64. doi: 10.1152/ajplegacy.1943.140.1.47.

Greitz, D., Wirestam, R., Franck, A., Nordell, B., Thomsen, C. and Ståhlberg, F. (1992) 'Pulsatile brain movement and associated hydrodynamics studied by magnetic resonance phase imaging - The Monro-Kellie doctrine revisited', *Neuroradiology*. Springer-Verlag, 34(5), pp. 370–380. doi: 10.1007/BF00596493.

Guerra, M., Rodriguez Del Castillo, A., Battaner, E. and Mas, M. (1987) 'Androgens stimulate preoptic area Na+,K+-ATPase activity in male rats', *Neuroscience Letters*. Elsevier, 78(1), pp. 97–100. doi: 10.1016/0304-3940(87)90568-4.

Guo, X., Yan, Hanying, Zhu, L., Zeng, L., Xiong, F. and Yan, Hong (2011) 'Effects of acrylamide on rat neurobehavior, the contents of dopamine and its metabolites in nigrostriatal dopaminergic pathways.', *Wei sheng yan jiu = Journal of hygiene research*, 40(4), pp. 441–444.

H Uhmer, A. F., Biringer, R. G., Amato, H., Fonteh, A. N. and Harrington, M. G. (2006) *Protein analysis in human cerebrospinal fluid: Physiological aspects, current progress and future challenges*.

Häggström, M. (2014) 'Medical gallery of Mikael Häggström 2014', *WikiJournal of Medicine*. Wikiversity Journal of Medicine, 1(2). doi: 10.15347/wjm/2014.008.

Haines, D. E. (2018) 'A Survey of the Cerebrovascular System', in *Fundamental Neuroscience for Basic and Clinical Applications*. Elsevier, pp. 122-137.e1. doi: 10.1016/B978-0-323-39632-5.00008-6.

Hakvoort, A., Haselbach, M. and Galla, H. J. (1998) 'Active transport properties of porcine choroid plexus cells in culture', *Brain Research*, 795(1–2), pp. 247–256. doi: 10.1016/S0006-8993(98)00284-4.

Hart, G. D. (2001) 'Descriptions of blood and blood disorders before the advent of laboratory studies', *British Journal of Haematology*, pp. 719–728. doi: 10.1046/j.1365-

2141.2001.03130.x.

Haselbach, M., Wegener, J., Decker, S., Engelbertz, C. and Galla, H.-J. (2001) 'Porcine choroid plexus epithelial cells in culture: Regulation of barrier properties and transport processes', *Microscopy Research and Technique*, 52(1), pp. 137–152. doi: 10.1002/1097-0029(20010101)52:1<137::AID-JEMT15>3.0.CO;2-J.

Hawkins, B. T. and Davis, T. P. (2005) 'The blood-brain barrier/neurovascular unit in health and disease', *Pharmacological Reviews*, pp. 173–185. doi: 10.1124/pr.57.2.4.

Hayakata, T., Shiozaki, T., Tasaki, O., Ikegawa, H., Inoue, Y., Toshiyuki, F., Hosotubo, H., Kieko, F., Yamashita, T., Tanaka, H., Shimazu, T. and Sugimoto, H. (2004) 'CHANGES IN CSF S100B AND CYTOKINE CONCENTRATIONS IN EARLY-PHASE SEVERE TRAUMATIC BRAIN INJURY', *Shock*, 22(2), pp. 102–107. doi: 10.1097/01.shk.0000131193.80038.f1.

Hayek, T., Ito, Y., Azrolan, N., Verdery, R. B., Aalto-Setala, K., Walsh, A. and Breslow, J. L. (1993) 'Dietary fat increases high density lipoprotein (HDL) levels both by increasing the transport rates and decreasing the fractional catabolic rates of HDL cholesterol ester and apolipoprotein (apo) A-I. Presentation of a new animal model and mechanistic studies in human apo A-I transgenic and control mice', *Journal of Clinical Investigation*. American Society for Clinical Investigation, 91(4), pp. 1665–1671. doi: 10.1172/JCI116375.

Healy, A. and Vogelbaum, M. (2015) 'Convection-enhanced drug delivery for gliomas', *Surgical Neurology International*. Medknow Publications, 6(2), pp. S59–S67. doi: 10.4103/2152-7806.151337.

Heisey, S. R., Held, D. and Pappenheimer, J. R. (1962) 'Bulk flow and diffusion in the cerebrospinal fluid system of the goat', *The American journal of physiology*. Am J Physiol, 203, pp. 775–781. doi: 10.1152/ajplegacy.1962.203.5.775.

Heldring, N., Pike, A., Andersson, S., Matthews, J., Cheng, G., Hartman, J., Tujague, M., Ström, A., Treuter, E., Warner, M. and Gustafsson, J. Å. (2007) 'Estrogen receptors: How do they signal and what are their targets', *Physiological Reviews*. Physiol Rev, pp. 905–931.

doi: 10.1152/physrev.00026.2006.

Henry, J. P., Meehan, W. P. and Stephens, P. M. (1982) 'Role of subordination in nephritis of socially stressed mice.', *Contributions to nephrology*, 30, pp. 38–42. doi: 10.1159/000406416.

Higgins, J. N. P., Gillard, J. H., Owler, B. K., Harkness, K. and Pickard, J. D. (2004) 'MR venography in idiopathic intracranial hypertension: unappreciated and misunderstood.', *Journal of neurology, neurosurgery, and psychiatry*. BMJ Publishing Group Ltd, 75(4), pp. 621–5. doi: 10.1136/JNNP.2003.021006.

Hladky, S. B. and Barrand, M. A. (2016) 'Fluid and ion transfer across the blood–brain and blood–cerebrospinal fluid barriers; a comparative account of mechanisms and roles', *Fluids and Barriers of the CNS*. BioMed Central, 13(1), p. 19. doi: 10.1186/s12987-016-0040-3.

Hoffmann, J. (2019) 'The utility of the lumbar puncture in idiopathic intracranial hypertension.', *Cephalalgia : an international journal of headache*. SAGE Publications Ltd, 39(2), pp. 171–172. doi: 10.1177/0333102418787301.

Hogan, Q. H., Prost, R., Kulier, A., Taylor, M. Lou and Liu, S. (1996) 'Magnetic Resonance Imaging of Cerebrospinal Fluid and the Influence of Body Habitus and Abdominal Pressure', *Anesthesiology*. The American Society of Anesthesiologists, 84(6), p. 1341. doi: 0000542-199606000-00010.

Horev, A., Hallevy, H., Plakht, Y., Shorer, Z., Wirguin, I. and Shelef, I. (2013) 'Changes in cerebral venous sinuses diameter after lumbar puncture in idiopathic intracranial hypertension: A prospective MRI study', *Journal of Neuroimaging*, 23(3), pp. 375–378. doi: 10.1111/j.1552-6569.2012.00732.x.

Hornby, C., Mollan, S. P., Mitchell, J., Markey, K. A., Yangou, A., Wright, B. L. C., O'Reilly, M. W. and Sinclair, A. J. (2017) 'What Do Transgender Patients Teach Us About Idiopathic Intracranial Hypertension?', *Neuro-Ophthalmology*. Taylor & Francis, 41(6), pp.

326–329. doi: 10.1080/01658107.2017.1316744.

Hornby, C., O'Reilly, M., Botfield, H., Markey, K., Kempegowda, P., Taylor, A., Hughes, B., Tomlinson, J., Arlt, W. and Sinclair, A. (2016) 'The Andro-Metabolic Signature Of Iih Compared With Pcos And Simple Obesity', *Journal of Neurology, Neurosurgery & Psychiatry*. BMJ, 87(12), p. e1.46-e1. doi: 10.1136/jnnp-2016-315106.14.

House, P. M. and Stodieck, S. R. G. (2016) 'Octreotide: The IIH therapy beyond weight loss, carbonic anhydrase inhibitors, lumbar punctures and surgical/interventional treatments', *Clinical Neurology and Neurosurgery*. doi: 10.1016/j.clineuro.2016.09.016.

Huang, D. W., Sherman, Brad T. and Lempicki, R. A. (2009) 'Bioinformatics enrichment tools: paths toward the comprehensive functional analysis of large gene lists', *Nucleic Acids Research*, 37(1), pp. 1–13. doi: 10.1093/nar/gkn923.

Huang, D. W., Sherman, Brad T and Lempicki, R. A. (2009) 'Systematic and integrative analysis of large gene lists using DAVID bioinformatics resources', *Nature Protocols*, 4(1), pp. 44–57. doi: 10.1038/nprot.2008.211.

Husted, R. F. and Reed, D. J. (1976) 'Regulation of cerebrospinal fluid potassium by the cat choroid plexus.', *The Journal of physiology*, 259(1), pp. 213–21. Available at: http://www.ncbi.nlm.nih.gov/pubmed/957213 (Accessed: 3 July 2017).

IBM Corporation (2017) 'IBM SPSS Statistics for Windows'. Armonk, NY.

Ikeda, T., Xia, X. Y., Xia, Y. X., Ikenoue, T. and Choi, B. H. (1999) 'Expression of glial cell line-derived neurotrophic factor in the brain and cerebrospinal fluid of the developing rat', *International Journal of Developmental Neuroscience*. No longer published by Elsevier, 17(7), pp. 681–691. doi: 10.1016/S0736-5748(99)00057-X.

Iliff, J. J., Thrane, A. S. and Nedergaard, M. (2017) 'The Glymphatic System and Brain Interstitial Fluid Homeostasis', in *Primer on Cerebrovascular Diseases: Second Edition*. Elsevier Inc., pp. 17–25. doi: 10.1016/B978-0-12-803058-5.00003-5.

Iliff, J. J., Wang, M., Liao, Y., Plogg, B. A., Peng, W., Gundersen, G. A., Benveniste, H., Vates, G. E., Deane, R., Goldman, S. A., Nagelhus, E. A. and Nedergaard, M. (2012) 'A paravascular pathway facilitates CSF flow through the brain parenchyma and the clearance of interstitial solutes, including amyloid β', *Science Translational Medicine*, 4(147). doi: 10.1126/scitranslmed.3003748.

Itoh, Y. and Arnold, A. P. (2015) 'Are females more variable than males in gene expression? Meta-analysis of microarray datasets', *Biology of Sex Differences*. BioMed Central Ltd., 6(1), p. 18. doi: 10.1186/s13293-015-0036-8.

Jacobs, S., Ruusuvuori, E., Sipilä, S. T., Haapanen, A., Damkier, H. H., Kurth, I., Hentschke, M., Schweizer, M., Rudhard, Y., Laatikainen, L. M., Tyynelä, J., Praetorius, J., Voipio, J. and Hübner, C. A. (2008) 'Mice with targeted Slc4a10 gene disruption have small brain ventricles and show reduced neuronal excitability', *Proceedings of the National Academy of Sciences of the United States of America*. National Academy of Sciences, 105(1), pp. 311–316. doi: 10.1073/pnas.0705487105.

Jakobsdottir, G., Xu, J., Molin, G., Ahrné, S. and Nyman, M. (2013) 'High-fat diet reduces the formation of butyrate, but increases succinate, inflammation, liver fat and cholesterol in rats, while dietary fibre counteracts these effects', *PLoS ONE*. Public Library of Science, 8(11). doi: 10.1371/journal.pone.0080476.

Janssen, S. F., Van Der Spek, S. J. F., Ten Brink, J. B., Essing, A. H. W., Gorgels, T. G. M. F., Van Der Spek, P. J., Jansonius, N. M. and Bergen, A. A. B. (2013) 'Gene expression and functional annotation of the human and mouse choroid plexus epithelium', *PLoS ONE*. PLoS One, 8(12). doi: 10.1371/journal.pone.0083345.

JASP Team (2019) 'JASP'.

Jentsch, T. J., Stein, V., Weinreich, F. and Zdebik, A. A. (2002) 'Molecular structure and physiological function of chloride channels', *Physiological Reviews*. American Physiological Society, pp. 503–568. doi: 10.1152/physrev.00029.2001.

Johanson, C. E. and Johanson, N. L. (2018) *Choroid Plexus Blood-CSF Barrier: Major Player in Brain Disease Modeling and Neuromedicine*, *J Neurol Neuromedicine*. Available at: www.jneurology.comNeuromedicine (Accessed: 8 September 2020).

Johanson, C. E., Stopa, E. G. and Mcmillan, P. N. (2011) 'The Blood-Brain and Other Neural Barriers: Reviews and Protocols', *Methods in Molecular Biology*, 686(101–131). doi: 10.1007/978-1-60761-938-3_4.

Johnson, L. N., Krohel, G. B., Madsen, R. W. and March, G. A. (1998) 'The role of weight loss and acetazolamide in the treatment of idiopathic intracranial hypertension (pseudotumor cerebri)', *Ophthalmology*. Elsevier Inc., 105(12), pp. 2313–2317. doi: 10.1016/S0161-6420(98)91234-9.

Johnston, M. and Papaiconomou, C. (2002) 'Cerebrospinal fluid transport: a lymphatic perspective.', *News in physiological sciences : an international journal of physiology produced jointly by the International Union of Physiological Sciences and the American Physiological Society*, 17, pp. 227–30. Available at: http://www.ncbi.nlm.nih.gov/pubmed/12433975 (Accessed: 3 July 2017).

Jones, H. C. and Gratton, J. A. (1989) 'The effect of cerebrospinal fluid pressure on dural venous pressure in young rats', *Journal of Neurosurgery*. Journal of Neurosurgery Publishing Group, 71(1), pp. 119–123. doi: 10.3171/jns.1989.71.1.0119.

Jost, A. (1970) 'Hormonal factors in the sex differentiation of the mammalian foetus', *Philosophical Transactions of the Royal Society of London. B, Biological Sciences*. The Royal SocietyLondon, 259(828), pp. 119–131. doi: 10.1098/rstb.1970.0052.

Julayanont, P., Karukote, A., Ruthirago, D., Panikkath, D. and Panikkath, R. (2016) 'Idiopathic intracranial hypertension: Ongoing clinical challenges and future prospects', *Journal of Pain Research*. Dove Medical Press Ltd., pp. 87–99. doi: 10.2147/JPR.S60633.

Jump, D. B. (2004) 'Fatty Acid Regulation of Gene Transcription', *Critical Reviews in Clinical Laboratory Sciences*. Taylor & Francis, pp. 41–78. doi:

10.1080/10408360490278341.

Jump, D. B. and Clarke, S. D. (1999) ‘regulation of gene expression by dietary fat’, *Annual Review of Nutrition*. Annual Reviews, 19(1), pp. 63–90. doi: 10.1146/annurev.nutr.19.1.63.

Jusué-Torres, I., Hoffberger, J. B. and Rigamonti, D. (2015) ‘Complications specific to lumboperitoneal shunt’, in *Complications of CSF Shunting in Hydrocephalus: Prevention, Identification, and Management*. Springer International Publishing, pp. 203–211. doi: 10.1007/978-3-319-09961-3_14.

Kalani, M. Y. S., Filippidis, A. S. and Rekate, H. L. (2012) ‘Hydrocephalus and aquaporins: The role of aquaporin-1’, *Acta Neurochirurgica, Supplementum*. Springer-Verlag Wien, 113(113), pp. 51–54. doi: 10.1007/978-3-7091-0923-6_11.

Kalyani, M., Hasselfeld, K., Janik, J. M., Callahan, P. and Shi, H. (2016) ‘Effects of high-fat diet on stress response in male and female wildtype and prolactin knockout mice’, *PLoS ONE*. Public Library of Science, 11(11). doi: 10.1371/journal.pone.0166416.

Kannel, W. B. (1983) ‘High-density lipoproteins: Epidemiologic profile and risks of coronary artery disease’, *The American Journal of Cardiology*. Excerpta Medica, 52(4), pp. B9–B12. doi: 10.1016/0002-9149(83)90649-5.

Kanoski, S. E., Zhang, Y., Zheng, W. and Davidson, T. L. (2010) ‘The effects of a high-energy diet on hippocampal function and blood-brain barrier integrity in the rat’, *Journal of Alzheimer’s Disease*. IOS Press, 21(1), pp. 207–219. doi: 10.3233/JAD-2010-091414.

Kant, S., Stopa, E. G., Johanson, C. E., Baird, A. and Silverberg, G. D. (2018) ‘Choroid plexus genes for CSF production and brain homeostasis are altered in Alzheimer’s disease’, *Fluids and Barriers of the CNS*. BioMed Central Ltd., 15(1), p. 34. doi: 10.1186/s12987-018-0120-7.

Kao, J. S., Garg, A., Mao-Qiang, M., Crumrine, D., Ghadially, R., Feingold, K. R. and Elias, P. M. (2001) ‘Testosterone perturbs epidermal permeability barrier homeostasis’,

Journal of Investigative Dermatology. Blackwell Publishing Inc., 116(3), pp. 443–451. doi: 10.1046/j.1523-1747.2001.01281.x.

Kao, L., Kurtz, L. M., Shao, X., Papadopoulos, M. C., Liu, L., Bok, D., Nusinowitz, S., Chen, B., Stella, S. L., Andre, M., Weinreb, J., Luong, S. S., Piri, N., Kwong, J. M. K., Newman, D. and Kurtz, I. (2011) 'Severe neurologic impairment in mice with targeted disruption of the electrogenic sodium bicarbonate cotransporter NBCe2 (Slc4a5 gene).', *The Journal of biological chemistry*. American Society for Biochemistry and Molecular Biology, 286(37), pp. 32563–74. doi: 10.1074/jbc.M111.249961.

Kaplan, W. D., McComb, J. G., Strand, R. D. and Treves, S. (1973) 'Suppression of 99mTc pertechnetate uptake in a choroid plexus papilloma', *Radiology*. Radiology, 109(2), pp. 395–396. doi: 10.1148/109.2.395.

Kapsha, J. M. and Severs, W. B. (1983) 'Renin activity in rat choroid plexi: effects of water-deprivation and hypovolemia', *Experientia*. Birkhäuser-Verlag, 39(4), pp. 429–430. doi: 10.1007/BF01963164.

Karmaniolou, I., Petropoulos, G. and Theodoraki, K. (2011) 'Management of idiopathic intracranial hypertension in parturients: anesthetic considerations', *Canadian Journal of Anesthesia/Journal canadien d'anesth?sie*, 58(7), pp. 650–657. doi: 10.1007/s12630-011-9508-4.

Kaur, C., Rathnasamy, G. and Ling, E. A. (2016) 'The choroid plexus in healthy and diseased brain', *Journal of Neuropathology and Experimental Neurology*. Lippincott Williams and Wilkins, pp. 198–213. doi: 10.1093/jnen/nlv030.

Kautzky-Willer, A., Harreiter, J. and Pacini, G. (2016) 'Sex and gender differences in risk, pathophysiology and complications of type 2 diabetes mellitus', *Endocrine Reviews*. Endocrine Society, pp. 278–316. doi: 10.1210/er.2015-1137.

Keep, R. F. and Jones, H. C. (1990) 'A morphometric study on the development of the lateral ventricle choroid plexus, choroid plexus capillaries and ventricular ependyma in

the rat', *Developmental Brain Research*, 56(1), pp. 47–53. doi: 10.1016/0165-3806(90)90163-S.

Keep, R. F., Jones, H. C. and Cawkwell, R. D. (1986) 'A morphometric analysis of the development of the fourth ventricle choroid plexus in the rat', *Developmental Brain Research*. Elsevier, 27(1), pp. 77–85. doi: 10.1016/0165-3806(86)90234-8.

Keep, R. F., Xiang, J., Ulanski, L. J., Brosius, F. C. and Betz, A. L. (1997) 'Choroid Plexus Ion Transporter Expression and Cerebrospinal Fluid Secretion', *Acta Neurochirurgica, Supplement*. Springer Wien, 1997(70), pp. 279–281. doi: 10.1007/978-3-7091-6837-0_86.

Khadijah Ramli, N. S., Giribabu, N., Muniandy, S. and Salleh, N. (2018) 'Testosterone up-regulates vacuolar ATPase expression and functional activities in vas deferens of orchidectomized rats', *Theriogenology*. Elsevier Inc., 108, pp. 354–361. doi: 10.1016/j.theriogenology.2017.12.035.

Khadijah Ramli, N. S., Giribabu, N. and Salleh, N. (2018) 'Testosterone enhances expression and functional activity of epithelial sodium channel (ENaC), cystic fibrosis transmembrane regulator (CFTR) and sodium hydrogen exchanger (NHE) in vas deferens of sex-steroid deficient male rats', *Steroids*. Elsevier Inc., 138, pp. 117–133. doi: 10.1016/j.steroids.2018.06.012.

Killer, H. E., Jaggi, G. P., Flammer, J., Miller, N. R., Huber, A. R. and Mironov, A. (2007) 'Cerebrospinal fluid dynamics between the intracranial and the subarachnoid space of the optic nerve. Is it always bidirectional?', *Brain*. Oxford University Press, 130(2), pp. 514–520. doi: 10.1093/brain/awl324.

Kim, J. and Jung, Y. (2011) 'Different expressions of AQP1, AQP4, eNOS, and VEGF proteins in ischemic versus non-ischemic cerebropathy in rats: potential roles of AQP1 and eNOS in hydrocephalic and vasogenic edema formation', *Anatomy & Cell Biology*. Korean Association of Anatomists (KAMJE), 44(4), p. 295. doi: 10.5115/acb.2011.44.4.295.

Kim, J. and Jung, Y. (2012) 'Increased aquaporin-1 and Na+-K+-2Cl- cotransporter 1

expression in choroid plexus leads to blood-cerebrospinal fluid barrier disruption and necrosis of hippocampal CA1 cells in acute rat models of hyponatremia', *Journal of Neuroscience Research*. John Wiley & Sons, Ltd, 90(7), pp. 1437–1444. doi: 10.1002/jnr.23017.

Kim, S. and Kim, G. H. (2017) 'Roles of claudin-2, ZO-1 and occludin in leaky HK-2 cells', *PLoS ONE*. Public Library of Science, 12(12). doi: 10.1371/journal.pone.0189221.

Kitazawa, T., Hosoya, K., Watanabe, M., Takashima, T., Ohtsuki, S., Takanaga, H., Ueda, M., Yanai, N., Obinata, M. and Terasaki, T. (2001) 'Characterization of the amino acid transport of new immortalized choroid plexus epithelial cell lines: a novel in vitro system for investigating transport functions at the blood-cerebrospinal fluid barrier.', *Pharmaceutical research*, 18(1), pp. 16–22. doi: 10.1023/a:1011014424212.

Klarr, S. A., Ulanski, L. J., Stummer, W., Xiang, J., Betz, A. L. and Keep, R. F. (1997) 'The effects of hypo- and hyperkalemia on choroid plexus potassium transport', *Brain Research*. Elsevier, 758(1–2), pp. 39–44. doi: 10.1016/S0006-8993(96)01440-0.

Kläs, J., Wolburg, H., Terasaki, T., Fricker, G. and Reichel, V. (2010) 'Characterization of immortalized choroid plexus epithelial cell lines for studies of transport processes across the blood-cerebrospinal fluid barrier', *Cerebrospinal Fluid Research*. BioMed Central, 7(1), p. 11. doi: 10.1186/1743-8454-7-11.

Klein, A., Stern, N., Osher, E., Kliper, E. and Kesler, A. (2013) 'Hyperandrogenism is Associated with Earlier Age of Onset of Idiopathic Intracranial Hypertension in Women', *Current Eye Research*. Taylor & Francis, 38(9), pp. 972–976. doi: 10.3109/02713683.2013.799214.

Kohsaka, A., Laposky, A. D., Ramsey, K. M., Estrada, C., Joshu, C., Kobayashi, Y., Turek, F. W. and Bass, J. (2007) 'High-Fat Diet Disrupts Behavioral and Molecular Circadian Rhythms in Mice', *Cell Metabolism*. Cell Press, 6(5), pp. 414–421. doi: 10.1016/j.cmet.2007.09.006.

Komukai, K., Mochizuki, S. and Yoshimura, M. (2010) 'Gender and the renin-angiotensin-aldosterone system', *Fundamental and Clinical Pharmacology*. John Wiley & Sons, Ltd, pp. 687–698. doi: 10.1111/j.1472-8206.2010.00854.x.

Kooij, G., Kopplin, K., Blasig, R., Stuiver, M., Koning, N., Goverse, G., Van Der Pol, S. M. A., Van Het Hof, B., Gollasch, M., Drexhage, J. A. R., Reijerkerk, A., Meij, I. C., Mebius, R., Willnow, T. E., Müller, D., Ingolf, ·, Blasig, E. and De Vries, H. E. (2014) 'Disturbed function of the blood-cerebrospinal fluid barrier aggravates neuro-inflammation', *Acta Neuropathol*, 3, pp. 267–277. doi: 10.1007/s00401-013-1227-1.

Kopelman, P. G. (2000) 'Obesity as a medical problem', *Nature*, 404(6778), pp. 635–643. doi: 10.1038/35007508.

Kopelman, P. G., Pilkington, T. R. E., White, N. and Jeffcoate, S. L. (1980) 'ABNORMAL SEX STEROID SECRETION AND BINDING IN MASSIVELY OBESE WOMEN', *Clinical Endocrinology*, 12(4), pp. 363–369. doi: 10.1111/j.1365-2265.1980.tb02721.x.

Kratzer, I., Vasiljevic, A., Rey, C., Fevre-Montange, M., Saunders, N., Strazielle, N. and Ghersi-Egea, J.-F. (2012) 'Complexity and developmental changes in the expression pattern of claudins at the blood–CSF barrier', *Histochemistry and Cell Biology*, 138(6), pp. 861–879. doi: 10.1007/s00418-012-1001-9.

Kupersmith, M. J., Gamell, L., Turbin, R., Peck, V., Spiegel, P. and Wall, M. (1998) 'Effects of weight loss on the course of idiopathic intracranial hypertension in women.', *Neurology*, 50(4), pp. 1094–8. Available at: http://www.ncbi.nlm.nih.gov/pubmed/9566400 (Accessed: 10 July 2017).

Kyte, J. (1981) 'Molecular considerations relevant to the mechanism of active transport', *Nature*, 292(5820), pp. 201–204. doi: 10.1038/292201a0.

Lagaraine, C., Skipor, J., Szczepkowska, A., Dufourny, L. and Thiery, J. C. (2011) 'Tight junction proteins vary in the choroid plexus of ewes according to photoperiod', *Brain Research*. Elsevier, 1393, pp. 44–51. doi: 10.1016/j.brainres.2011.04.009.

Lam, B., Alperin, N. and Ranganathan, S. (2012) 'Evidence for Larger Extra Ventricular Cranial CSF Volume in Idiopathic Intracranial Hypertension (IIH)', *Investigative Ophthalmology & Visual Science*, 53. Available at: https://iovs.arvojournals.org/article.aspx?articleid=2350672 (Accessed: 4 September 2020).

Langmead, B. and Salzberg, S. L. (2012) 'Fast gapped-read alignment with Bowtie 2', *Nature Methods*. Nature Publishing Group, 9(4), pp. 357–359. doi: 10.1038/nmeth.1923.

Leeners, B., Geary, N., Tobler, P. N. and Asarian, L. (2017) 'Ovarian hormones and obesity', *Human Reproduction Update*, 23(3), pp. 300–321. doi: 10.1093/humupd/dmw045.

Lei, Y., Han, H., Yuan, F., Javeed, A. and Zhao, Y. (2017) 'The brain interstitial system: Anatomy, modeling, in vivo measurement, and applications', *Progress in Neurobiology*. Elsevier Ltd, pp. 230–246. doi: 10.1016/j.pneurobio.2015.12.007.

Lenck, S., Radovanovic, I., Nicholson, P., Hodaie, M., Krings, T. and Mendes-Pereira, V. (2018) 'Idiopathic intracranial hypertension The veno glymphatic connections', *Neurology*. Lippincott Williams and Wilkins, 91(11), pp. 515–522. doi: 10.1212/WNL.0000000000006166.

Li, S., Yu, M., Li, H., Zhang, H. and Jiang, Y. (2012) 'IL-17 and IL-22 in Cerebrospinal Fluid and Plasma Are Elevated in Guillain-Barré Syndrome', *Mediators of Inflammation*. Hindawi, 2012, pp. 1–7. doi: 10.1155/2012/260473.

Liddelow, S. A., Temple, S., Møllgård, K., Gehwolf, R., Wagner, A., Bauer, H., Bauer, H.-C., Phoenix, T. N., Dziegielewska, K. M. and Saunders, N. R. (2012) 'Molecular characterisation of transport mechanisms at the developing mouse blood-CSF interface: a transcriptome approach.', *PloS one*. Public Library of Science, 7(3), p. e33554. doi: 10.1371/journal.pone.0033554.

Lie, M. E. K., Overgaard, A. and Mikkelsen, J. D. (2013) 'Effect of a postnatal high-fat

diet exposure on puberty onset, estrous cycle regularity, and kisspeptin expression in female rats', *Reproductive Biology*. Elsevier B.V., 13(4), pp. 298–308. doi: 10.1016/j.repbio.2013.08.001.

Lin, S., Storlien, L. H. and Huang, X. F. (2000) 'Leptin receptor, NPY, POMC mRNA expression in the diet-induced obese mouse brain', *Brain Research*. Brain Res, 875(1–2), pp. 89–95. doi: 10.1016/S0006-8993(00)02580-4.

Lindvall-Axelsson, M. and Owman, C. (1989) 'Changes in transport functions of isolated rabbit choroid plexus under the influence of oestrogen and progesterone.', *Acta physiologica Scandinavica*, 136(1), pp. 107–11. doi: 10.1111/j.1748-1716.1989.tb08635.x.

Linninger, A. A., Tangen, K., Hsu, C.-Y. and Frim, D. (2016) 'Cerebrospinal Fluid Mechanics and Its Coupling to Cerebrovascular Dynamics', *Annual Review of Fluid Mechanics*. Annual Reviews Inc., 48(1), pp. 219–257. doi: 10.1146/annurev-fluid-122414-034321.

Liu, G. T., Kay, M. D., Bienfang, D. C. and Schatz, N. J. (1994) 'Pseudotumor cerebri associated with corticosteroid withdrawal in inflammatory bowel disease.', *American journal of ophthalmology*, 117(3), pp. 352–7. Available at: http://www.ncbi.nlm.nih.gov/pubmed/8129010 (Accessed: 10 July 2017).

Livak, K. J. and Schmittgen, T. D. (2001) 'Analysis of relative gene expression data using real-time quantitative PCR and the 2-ΔΔCT method', *Methods*. Academic Press Inc., 25(4), pp. 402–408. doi: 10.1006/meth.2001.1262.

Loh, S. Y., Giribabu, N. and Salleh, N. (2017) 'Effects of gonadectomy and testosterone treatment on aquaporin expression in the kidney of normotensive and hypertensive rats.', *Experimental biology and medicine (Maywood, N.J.)*. SAGE Publications Inc., 242(13), pp. 1376–1386. doi: 10.1177/1535370217703360.

Lopes, M. B. S. (2009) 'Meninges: Embryology', in *Meningiomas*. Springer London, pp. 25–29. doi: 10.1007/978-1-84628-784-8_4.

Love, M. I., Huber, W. and Anders, S. (2014) 'Moderated estimation of fold change and dispersion for RNA-seq data with DESeq2', *Genome Biology*. BioMed Central Ltd., 15(12), p. 550. doi: 10.1186/s13059-014-0550-8.

Lun, M. P., Monuki, E. S. and Lehtinen, M. K. (2015) 'Development and functions of the choroid plexus-cerebrospinal fluid system', *Nature Reviews Neuroscience*. Nature Publishing Group, pp. 445–457. doi: 10.1038/nrn3921.

Lyon, C. J., Law, R. E. and Hsueh, W. a. (2003) 'Minireview: Adiposity, inflammation, and atherogenesis', *Endocrinology*, 144(6), pp. 2195–2200. doi: 10.1210/en.2003-0285.

Machida, T., Yonezawa, Y. and Noumura, T. (1981) 'Age-associated changes in plasma testosterone levels in male mice and their relation to social dominance or subordinance', *Hormones and Behavior*. Horm Behav, 15(3), pp. 238–245. doi: 10.1016/0018-506X(81)90013-1.

Malm, J., Kristensen, B., Markgren, P. and Ekstedt, J. (1992) 'CSF hydrodynamics in idiopathic intracranial hypertension: A long-term study', *Neurology*. Neurology, 42(4), pp. 851–858. doi: 10.1212/wnl.42.4.851.

Manfield, J. H., Yu, K. K. H., Efthimiou, E., Darzi, A., Athanasiou, T. and Ashrafian, H. (2017) 'Bariatric Surgery or Non-surgical Weight Loss for Idiopathic Intracranial Hypertension? A Systematic Review and Comparison of Meta-analyses', *Obesity Surgery*. Springer New York LLC, pp. 513–521. doi: 10.1007/s11695-016-2467-7.

Marchi, N., Banjara, M. and Janigro, D. (2016) 'Blood-brain barrier, bulk flow, and interstitial clearance in epilepsy', *Journal of Neuroscience Methods*. Elsevier B.V., 260, pp. 118–124. doi: 10.1016/j.jneumeth.2015.06.011.

Marcondes, F. K., Miguel, K. J., Melo, L. L. and Spadari-Bratfisch, R. C. (2001) 'Estrous cycle influences the response of female rats in the elevated plus-maze test', *Physiology and Behavior*. Elsevier Inc., 74(4–5), pp. 435–440. doi: 10.1016/S0031-9384(01)00593-5.

Mark, A. S. and Feinberg, D. A. (1986) 'CSF flow: Correlation between signal void

and CSF velocity measured by gated velocity phase-encoded MR imaging'. Available at: https://inis.iaea.org/search/search.aspx?orig_q=RN:19036082 (Accessed: 10 September 2020).

Markey, K. A., Uldall, M., Botfield, H., Cato, L. D., Miah, M. A. L., Hassan-Smith, G., Jensen, R. H., Gonzalez, A. M. and Sinclair, A. J. (2016) 'Idiopathic intracranial hypertension, hormones, and 11β-hydroxysteroid dehydrogenases.', *Journal of pain research*. Dove Press, 9, pp. 223–32. doi: 10.2147/JPR.S80824.

Marques, F., Sousa, J. C., Correia-Neves, M., Oliveira, P., Sousa, N. and Palha, J. A. (2007) 'The choroid plexus response to peripheral inflammatory stimulus', *Neuroscience*. Pergamon, 144(2), pp. 424–430. doi: 10.1016/j.neuroscience.2006.09.029.

Martins, A. N., Newby, N. and Doyle, T. F. (1977) 'Sources of error in measuring cerebrospinal fluid formation by ventriculocisternal perfusion', *Journal of Neurology, Neurosurgery and Psychiatry*. BMJ Publishing Group, 40(7), pp. 645–650. doi: 10.1136/jnnp.40.7.645.

Martins, F., Campos, D. H. S., Pagan, L. U., Martinez, P. F., Okoshi, K., Okoshi, M. P., Padovani, C. R., Souza, A. S. de, Cicogna, A. C. and Oliveira, S. A. de (2015) 'High-fat Diet Promotes Cardiac Remodeling in an Experimental Model of Obesity', *Arquivos Brasileiros de Cardiologia*, 105(5), pp. 479–86. doi: 10.5935/abc.20150095.

Mascalchi, M., Ciraolo, L., Tanfani, G., Taverni, N., Inzitari, D., Siracusa, G. F. and Dal Pozzo, G. C. (1988) 'Cardiac-Gated Phase MR Imaging of Aqueductal CSF Flow', *Journal of Computer Assisted Tomography*, 12(6), pp. 923–926. doi: 10.1097/00004728-198811000-00003.

Mathew, J. and Bhimji, S. S. (2018) *Physiology, Blood Plasma*, *StatPearls*. Available at: http://www.ncbi.nlm.nih.gov/pubmed/30285399 (Accessed: 28 January 2020).

McCluskey, G., Doherty-Allan, R., McCarron, P., Loftus, A. M., McCarron, L. V., Mulholland, D., McVerry, F. and McCarron, M. O. (2018) 'Meta-analysis and systematic

review of population-based epidemiological studies in idiopathic intracranial hypertension', *European Journal of Neurology*. Blackwell Publishing Ltd, 25(10), pp. 1218–1227. doi: 10.1111/ene.13739.

McComb, J. G. (1983) 'Recent research into the nature of cerebrospinal fluid formation and absorption', *Journal of Neurosurgery*, 59(3), pp. 369–383. doi: 10.3171/jns.1983.59.3.0369.

McCutcheon, J. E. and Marinelli, M. (2009) 'Age matters', *European Journal of Neuroscience*, 29(5), pp. 997–1014. doi: 10.1111/j.1460-9568.2009.06648.x.

McDonough, A. A., Geering, K. and Farley, R. A. (1990) 'The sodium pump needs its β subunit', *The FASEB Journal*. Wiley, 4(6), pp. 1598–1605. doi: 10.1096/fasebj.4.6.2156741.

McLean, F. H., Campbell, F. M., Langston, R. F., Sergi, D., Resch, C., Grant, C., Morris, A. C., Mayer, C. D. and Williams, L. M. (2019) 'A high-fat diet induces rapid changes in the mouse hypothalamic proteome', *Nutrition and Metabolism*. BioMed Central Ltd., 16(1), p. 26. doi: 10.1186/s12986-019-0352-9.

McLean, F. H., Campbell, F. M., Sergi, D., Grant, C., Morris, A. C., Hay, E. A., MacKenzie, A., Mayer, C. D., Langston, R. F. and Williams, L. M. (2019) 'Early and reversible changes to the hippocampal proteome in mice on a high-fat diet', *Nutrition and Metabolism*. BioMed Central Ltd., 16(1), pp. 1–12. doi: 10.1186/s12986-019-0387-y.

Meaney, S., Bodin, K., Diczfalusy, U. and Björkhem, I. (2002) 'On the rate of translocation in vitro and kinetics in vivo of the major oxysterols in human circulation: critical importance of the position of the oxygen function', *2130 Journal of Lipid Research*, 44. doi: 10.1194/jlr.M200293-JLR200.

Meibodi, R., Ali, M. A., Mohammad, S., Mehrdad, M. and Abolfazl, A. (2018) 'The effect of topiramate as an adjunct therapy to acetazolamide in Idiopathic intracranial hypertension patients.', *Bali Medical Journal*. DiscoverSys, Inc., 7(1), p. 201. doi:

10.15562/bmj.v7i1.894.

Meng, J., Holdcraft, R. W., Shima, J. E., Griswold, M. D. and Braun, R. E. (2005) 'Androgens regulate the permeability of the blood-testis barrier', *Proceedings of the National Academy of Sciences of the United States of America*. National Academy of Sciences, 102(46), pp. 16696–16700. doi: 10.1073/pnas.0506084102.

Meng, J., Mostaghel, E. A., Vakar-Lopez, F., Montgomery, B., True, L. and Nelson, P. S. (2011) 'Testosterone Regulates Tight Junction Proteins and Influences Prostatic Autoimmune Responses', *Hormones and Cancer*. NIH Public Access, 2(3), pp. 145–156. doi: 10.1007/s12672-010-0063-1.

Mercier, C., Masseguin, C., Roux, F., Gabrion, J. and Scherrmann, J. M. (2004) 'Expression of P-glycoprotein (ABCB1) and Mrp1 (ABCC1) in adult rat brain: Focus on astrocytes', *Brain Research*. Elsevier, 1021(1), pp. 32–40. doi: 10.1016/j.brainres.2004.06.034.

Da Mesquita, S., Fu, Z. and Kipnis, J. (2018) 'The Meningeal Lymphatic System: A New Player in Neurophysiology', *Neuron*. Cell Press, pp. 375–388. doi: 10.1016/j.neuron.2018.09.022.

Mestre, H., Tithof, J., Du, T., Song, W., Peng, W., Sweeney, A. M., Olveda, G., Thomas, J. H., Nedergaard, M. and Kelley, D. H. (2018) 'Flow of cerebrospinal fluid is driven by arterial pulsations and is reduced in hypertension', *Nature Communications*. Nature Publishing Group, 9(1), pp. 1–9. doi: 10.1038/s41467-018-07318-3.

Mi, H., Muruganujan, A., Ebert, D., Huang, X. and Thomas, P. D. (2019) 'PANTHER version 14: more genomes, a new PANTHER GO-slim and improvements in enrichment analysis tools', *Nucleic Acids Research*. Narnia, 47(D1), pp. D419–D426. doi: 10.1093/nar/gky1038.

Millar, I. D., Bruce, J. I. E. and Brown, P. D. (2007) 'Ion channel diversity, channel expression and function in the choroid plexuses', *Cerebrospinal Fluid Research*. BioMed

Central, pp. 1–16. doi: 10.1186/1743-8454-4-8.

Mochida, G. H., Ganesh, V. S., Felie, J. M., Gleason, D., Hill, R. S., Clapham, K. R., Rakiec, D., Tan, W. H., Akawi, N., Al-Saffar, M., Partlow, J. N., Tinschert, S., Barkovich, A. J., Ali, B., Al-Gazali, L. and Walsh, C. A. (2010) 'A homozygous mutation in the tight-junction protein JAM3 causes hemorrhagic destruction of the brain, subependymal calcification, and congenital cataracts', *American Journal of Human Genetics*. Elsevier, 87(6), pp. 882–889. doi: 10.1016/j.ajhg.2010.10.026.

Mogil, J. S. and Chanda, M. L. (2005) 'The case for the inclusion of female subjects in basic science studies of pain', *Pain*, pp. 1–5. doi: 10.1016/j.pain.2005.06.020.

Mohammad, Y., Aljafen, B. N., Alnafisah, M. S. and Al-Hussain, F. A. (2019) 'Pseudotumor cerebri induced by topical application of steroid: a case report.', *The Journal of international medical research*, 47(7), pp. 3435–3437. doi: 10.1177/0300060519857852.

Mokri, B. (2001) 'The Monro–Kellie hypothesis: applications in CSF volume depletion', *AAN Enterprises*, 56(12). doi: doi.org/10.1212/WNL.56.12.1746.

Moll, S. and Waldron, B. (2014) 'Cerebral and sinus vein thrombosis.', *Circulation*, 130(8), pp. e68-70. doi: 10.1161/CIRCULATIONAHA.113.008018.

Mollan, S. P., Ali, F., Hassan-Smith, G., Botfield, H., Friedman, D. I. and Sinclair, A. J. (2016) 'Evolving evidence in adult idiopathic intracranial hypertension: pathophysiology and management.', *Journal of neurology, neurosurgery, and psychiatry*. BMJ Publishing Group, 87(9), pp. 982–92. doi: 10.1136/jnnp-2015-311302.

Mondejar, V. and Patsalides, A. (2020) 'The Role of Arachnoid Granulations and the Glymphatic System in the Pathophysiology of Idiopathic Intracranial Hypertension', *Current Neurology and Neuroscience Reports*. doi: 10.1007/s11910-020-01044-4.

Monnot, A. D. and Zheng, W. (2012) 'Culture of Choroid Plexus Epithelial Cells and In Vitro Model of Blood–CSF Barrier', in. Humana Press, Totowa, NJ, pp. 13–29. doi: 10.1007/978-1-62703-125-7_2.

Monnot, A. D. and Zheng, W. (2013) 'Culture of choroid plexus epithelial cells and in vitro model of blood-CSF barrier.', *Methods in molecular biology (Clifton, N.J.)*. NIH Public Access, 945, pp. 13–29. doi: 10.1007/978-1-62703-125-7_2.

Moon, Y., Hong, S. J., Shin, D. and Jung, Y. (2006) 'Increased aquaporin-1 expression in choroid plexus epithelium after systemic hyponatremia', *Neuroscience Letters*. Elsevier, 395(1), pp. 1–6. doi: 10.1016/j.neulet.2005.10.060.

Moore, C. (1947) 'Embryonic sex hormones and sexual differentiation.', *cabdirect.org*. Available at: https://www.cabdirect.org/cabdirect/abstract/19480101695 (Accessed: 3 August 2020).

Moore, C. R. (1941) 'On the Role of Sex Hormones in Sex Differentiation in the Opossum (Didelphys virginiana)', *Physiological Zoology*. University of Chicago Press, 14(1), pp. 1–47. doi: 10.1086/physzool.14.1.30151596.

Moreau, A., Lao, K. C. and Farris, B. K. (2014) 'Optic Nerve Sheath Decompression', *Journal of Neuro-Ophthalmology*, 34(1), pp. 34–38. doi: 10.1097/WNO.0000000000000065.

Morris, P. P., Black, D. F., Port, J. and Campeau, N. (2017) 'Transverse sinus stenosis is the most sensitive MR imaging correlate of idiopathic intracranial hypertension', *American Journal of Neuroradiology*. American Society of Neuroradiology, 38(3), pp. 471–477. doi: 10.3174/ajnr.A5055.

Murphy, V. A. and Johanson, C. E. (1985) 'Adrenergic-induced enhancement of brain barrier system permeability to small nonelectrolytes: Choroid plexus versus cerebral capillaries', *Journal of Cerebral Blood Flow and Metabolism*. SAGE PublicationsSage UK: London, England, 5(3), pp. 401–412. doi: 10.1038/jcbfm.1985.55.

Murphy, V. A., Smith, Q. R. and Rapoport, S. I. (1986) 'Homeostasis of brain and cerebrospinal fluid calcium concentrations during chronic hypo- and hypercalcemia.', *Journal of neurochemistry*, 47(6), pp. 1735–41. Available at:

http://www.ncbi.nlm.nih.gov/pubmed/3772375 (Accessed: 3 July 2017).

Murtha, L., Mcleod, D. and Spratt, N. (2012) 'Epidural Intracranial Pressure Measurement in Rats Using a Fiber-optic Pressure Transducer', *J. Vis. Exp*, (62). doi: 10.3791/3689.

Musch, M. W., Walsh-Reitz, M. M. and Chang, E. B. (2006) 'Roles of ZO-1, occludin, and actin in oxidant-induced barrier disruption', *American Journal of Physiology - Gastrointestinal and Liver Physiology*. American Physiological Society, 290(2), pp. 222–231. doi: 10.1152/ajpgi.00301.2005.

Myung, J., Schmal, C., Hong, S., Tsukizawa, Y., Rose, P., Zhang, Y., Holtzman, M. J., De Schutter, E., Herzel, H., Bordyugov, G. and Takumi, T. (2018) 'The choroid plexus is an important circadian clock component', *Nature Communications*. Nature Publishing Group, 9(1). doi: 10.1038/s41467-018-03507-2.

Naessens, D. M. P., de Vos, J., VanBavel, E. and Bakker, E. N. T. P. (2018) 'Blood–brain and blood–cerebrospinal fluid barrier permeability in spontaneously hypertensive rats', *Fluids and Barriers of the CNS*. BioMed Central Ltd., 15(1), p. 26. doi: 10.1186/s12987-018-0112-7.

Nakada, T. and Kwee, I. L. (2019) 'Fluid Dynamics Inside the Brain Barrier: Current Concept of Interstitial Flow, Glymphatic Flow, and Cerebrospinal Fluid Circulation in the Brain', *Neuroscientist*. SAGE Publications Inc., pp. 155–166. doi: 10.1177/1073858418775027.

Nathanson, J. A. and Chun, L. L. Y. (1989) *Immunological function of the blood-cerebrospinal fluid barrier (choroid plexus/antigen presentation/lymphocytes/epithelial cells/nervous system immunology)*, *Neurobiology*.

Nazari, Z., Nabiuni, M., Safaei Nejad, Z., Delfan, B. and Irian, S. (2014) 'Expression of Aquaporins in the Rat Choroid Plexus', *Archives of Neuroscience*. Kowsar Medical Institute, 2(2). doi: 10.5812/archneurosci.17312.

Nedelmann, M., Kaps, M. and Mueller-Forell, W. (2009) 'Venous obstruction and jugular valve insufficiency in idiopathic intracranial hypertension', *Journal of Neurology*. Springer, 256(6), pp. 964–969. doi: 10.1007/s00415-009-5056-z.

Nestler, J. E. (2000) 'Obesity, insulin, sex steroids and ovulation', in *International Journal of Obesity*. doi: 10.1038/sj.ijo.0801282.

Netsky, M. and Shuangshoti, S. (2013) *The choroid plexus in health and disease*. Available at: https://books.google.com/books?hl=en&lr=&id=-r3YBAAAQBAJ&oi=fnd&pg=PP1&ots=s69HMPbSRG&sig=xxdN_lXqF_gjlUXeKKTt500WLjg (Accessed: 30 January 2020).

Newborg, B. (1974) 'Pseudotumor Cerebri Treated: By Rice-Reduction Diet', *Archives of Internal Medicine*. American Medical Association, 133(5), pp. 802–807. doi: 10.1001/archinte.1974.00320170084007.

Ng, S. F., Lin, R. C. Y., Laybutt, D. R., Barres, R., Owens, J. A. and Morris, M. J. (2010) 'Chronic high-fat diet in fathers programs β 2-cell dysfunction in female rat offspring', *Nature*. Nature Publishing Group, 467(7318), pp. 963–966. doi: 10.1038/nature09491.

Niehof, M. and Borlak, J. (2009) 'Expression of HNF4alpha in the human and rat choroid plexus - Implications for drug transport across the blood-cerebrospinal-fluid (CSF) barrier', *BMC Molecular Biology*. BioMed Central, 10(1), pp. 1–14. doi: 10.1186/1471-2199-10-68.

Nilsson, C., Stahlberg, F., Thomsen, C., Henriksen, O., Herning, M. and Owman, C. (1992) 'Circadian variation in human cerebrospinal fluid production measured by magnetic resonance imaging', *American Journal of Physiology - Regulatory Integrative and Comparative Physiology*, 262(1 31-1). doi: 10.1152/ajpregu.1992.262.1.r20.

Nizari, S., Carare, R. O. and Hawkes, C. A. (2016) 'Increased Aβ pathology in aged Tg2576 mice born to mothers fed a high fat diet', *Scientific Reports*. Nature Publishing Group, 6(1), pp. 1–10. doi: 10.1038/srep21981.

Noda, M., Sonoda, Y., Takemoto, M. and Kira, R. (2017) 'Successful treatment with topiramate in a case of idiopathic intracranial hypertension refractory to acetazolamide', *No To Hattatsu .*, 49(3), pp. 207–210. Available at: https://pubmed.ncbi.nlm.nih.gov/30113799/ (Accessed: 13 August 2020).

Nold-Petry, C. A., Lo, C. Y., Rudloff, I., Elgass, K. D., Li, S., Gantier, M. P., Lotz-Havla, A. S., Gersting, S. W., Cho, S. X., Lao, J. C., Ellisdon, A. M., Rotter, B., Azam, T., Mangan, N. E., Rossello, F. J., Whisstock, J. C., Bufler, P., Garlanda, C., Mantovani, A., Dinarello, C. A. and Nold, M. F. (2015) 'IL-37 requires the receptors IL-18Rα and IL-1R8 (SIGIRR) to carry out its multifaceted anti-inflammatory program upon innate signal transduction', *Nature Immunology*. Nature Publishing Group, 16(4), pp. 354–365. doi: 10.1038/ni.3103.

Nonis, Alberto, De Nardi, B. and Nonis, Alessandro (2014) 'Choosing between RT-qPCR and RNA-seq: A back-of-the-envelope estimate towards the definition of the break-even-point', *Analytical and Bioanalytical Chemistry*. Springer Verlag, 406(15), pp. 3533–3536. doi: 10.1007/s00216-014-7687-x.

Nyland, H. and Matre, R. (1978) 'Feσ Receptors In Human Choroid Plexus', *Acta Pathologica Microbiologica Scandinavica Section C Immunology*. John Wiley & Sons, Ltd, 86C(1–6), pp. 141–143. doi: 10.1111/j.1699-0463.1978.tb02571.x.

O'Connell, J. E. A. (1943) 'The Vascular factor in intracranial pressure and the maintenance of the cerebrospinal fluid circulation', 66(3), pp. 204–228. doi: 10.1093/brain/66.3.204.

O'Reilly, M. W., Westgate, C. S. J., Hornby, C., Botfield, H., Taylor, A. E., Markey, K., Mitchell, J. L., Scotton, W. J., Mollan, S. P., Yiangou, A., Jenkinson, C., Gilligan, L. C., Sherlock, M., Gibney, J., Tomlinson, J. W., Lavery, G. G., Hodson, D. J., Arlt, W. and Sinclair, A. J. (2019) 'A unique androgen excess signature in idiopathic intracranial hypertension is linked to cerebrospinal fluid dynamics', *JCI Insight*. American Society for Clinical Investigation, 4(6). doi: 10.1172/jci.insight.125348.

Obermeier, B., Verma, A. and Ransohoff, R. M. (2016) 'The blood-brain barrier', in

Handbook of Clinical Neurology. Elsevier, pp. 39–59. doi: 10.1016/B978-0-444-63432-0.00003-7.

Obinata, K., Kamata, A., Kinoshita, K., Nakazawa, T., Haruna, H., Hosaka, A. and Shimizu, T. (2010) 'Prolonged Intracranial Hypertension after Recombinant Growth Hormone Therapy due to Impaired CSF Absorption', *Clinical Pediatric Endocrinology*, 19(2), pp. 39–44. doi: 10.1297/cpe.19.39.

Ono, M., Rhoton, A. L., Peace, D. and Rodriguez, R. J. (1984) 'Microsurgical Anatomy of the Deep Venous System of the Brain', *Neurosurgery*. Oxford Academic, 15(5), pp. 621–657. doi: 10.1227/00006123-198411000-00002.

OpenStax (2016) *Brain Sinuses - OpenStax Anatomy and Physiology*. Version 8.25. Available at: https://commons.wikimedia.org/wiki/File:1315_Brain_Sinuses.jpg?uselang=fr (Accessed: 26 September 2020).

Orefice, G., Celentano, L., Scaglione, M., Davoli, M. and Striano, S. (1992) 'Radioisotopic cisternography in benign intracranial hypertension of young obese women. A seven-case study and pathogenetic suggestions.', *Acta neurologica*, 14(1), pp. 39–50. Available at: http://www.ncbi.nlm.nih.gov/pubmed/1580203 (Accessed: 31 January 2020).

Orešković, D. and Klarica, M. (2010) 'The formation of cerebrospinal fluid: Nearly a hundred years of interpretations and misinterpretations', *Brain Research Reviews*, pp. 241–262. doi: 10.1016/j.brainresrev.2010.04.006.

Orešković, D. and Klarica, M. (2014) 'A new look at cerebrospinal fluid movement', *Fluids and barriers of the CNS*, 11(16). doi: 10.1186/2045-8118-11-16.

Oreskovic, D., Klarica, M., Vukic, M. and Marakovic, J. (2003) 'Evaluation of ventriculo-cisternal perfusion model as a method to study cerebrospinal fluid formation', *Croatian Medical Journal*, 44(2), pp. 161–164.

Oscai, L. B., Brown, M. M. and Miller, W. C. (1984) 'Effect of dietary fat on food

intake, growth and body composition in rats.', *Growth*, 48(4), pp. 415–24. Available at: http://www.ncbi.nlm.nih.gov/pubmed/6532899 (Accessed: 13 February 2020).

Oshio, K., Watanabe, H., Song, Y., Verkman, A. S. and Manley, G. T. (2004) 'Reduced cerebrospinal fluid production and intracranial pressure in mice lacking choroid plexus water channel Aquaporin-1', *The FASEB Journal*. Wiley, 19(1), pp. 76–78. doi: 10.1096/fj.04-1711fje.

Özevren, H., Deveci, E. and Tuncer, M. C. (2018) 'Histopathological changes in the choroid plexus after traumatic brain injury in the rats: A histologic and immunohistochemical study', *Folia Morphologica (Poland)*. Via Medica, 77(4), pp. 642–648. doi: 10.5603/FM.a2018.0029.

Paganini, C., Peterson, G., Stavropoulos, V. and Krug, I. (2017) 'The overlap between Binge Eating Behaviors and Polycystic Ovarian Syndrome: An etiological integrative model', *Current Pharmaceutical Design*. Bentham Science Publishers Ltd., 24. doi: 10.2174/1381612824666171204151209.

Palm, D., Knuckey, N., Guglielmo, M., Watson, P., Primiano, M. and Johanson, C. (1995) 'Choroid plexus electrolytes and ultrastructure following transient forebrain ischemia', *American Journal of Physiology - Regulatory Integrative and Comparative Physiology*. American Physiological Society, 269(1 38-1/II). doi: 10.1152/ajpregu.1995.269.1.r73.

Panagopoulos, G. N., Deftereos, S. N., Tagaris, G. A., Gryllia, M., Kounadi, T., Karamani, O., Panagiotidis, D., Koutiola-Pappa, E., Karageorgiou, C. E. and Piadites, G. (2007) 'Octreotide: a therapeutic option for idiopathic intracranial hypertension.', *Neurology, neurophysiology, and neuroscience*, p. 1. Available at: http://www.ncbi.nlm.nih.gov/pubmed/17700925 (Accessed: 27 July 2017).

Pappenheimer, J. R., Heisey, S. R., Jordan, E. F. and Downer, J. deC. (1962) 'Perfusion of the cerebral ventricular system in unanesthetized goats', *American Journal of Physiology-Legacy Content*. American Physiological Society, 203(5), pp. 763–774. doi:

10.1152/ajplegacy.1962.203.5.763.

Park, S., Cheng, C. P., Lim, L. T. and Gerber, D. (2014) 'Secondary intracranial hypertension from testosterone therapy in a transgender patient', *Seminars in Ophthalmology*. Informa Healthcare, 29(3), pp. 156–158. doi: 10.3109/08820538.2013.788678.

Pasquali, R. (2006) 'Obesity and androgens: facts and perspectives', *Fertility and Sterility*. Elsevier, 85(5), pp. 1319–1340. doi: 10.1016/j.fertnstert.2005.10.054.

Paterni, I., Granchi, C., Katzenellenbogen, J. A. and Minutolo, F. (2014) 'Estrogen receptors alpha (ERα) and beta (ERβ): Subtype-selective ligands and clinical potential', *Steroids*. Elsevier Inc., pp. 13–29. doi: 10.1016/j.steroids.2014.06.012.

Patyal, P. and Alvarez-Leefmans, F. (2016) 'Expression of NKCC1 and aquaporins 4, 7 and 9 in mouse choroid plexus and ependymal cells', *Federation of American Societies for Experimental Biology Journal*.

Petersen, N., Torz, L., Jensen, K. H. R., Hjortø, G. M., Spiess, K. and Rosenkilde, M. M. (2020) 'Three-Dimensional Explant Platform for Studies on Choroid Plexus Epithelium', *Frontiers in Cellular Neuroscience*. Frontiers Media S.A., 14, p. 108. doi: 10.3389/fncel.2020.00108.

Pfaff, D. (1970) 'Nature of sex hormone effects on rat sex behavior: Specificity of effects and individual patterns of response', *Journal of Comparative and Physiological Psychology*, 73(3), pp. 349–358. doi: 10.1037/h0030242.

Pollak, L., Zohar, E., Glovinsky, Y. and Huna-Baron, R. (2015) 'The laboratory profile in idiopathic intracranial hypertension', *Neurological Sciences*. Springer Milan, 36(7), pp. 1189–1195. doi: 10.1007/s10072-015-2071-y.

Pollay, M. (1975) 'Formation of cerebrospinal fluid. Relation of studies of isolated choroid plexus to the standing gradient hypothesis', *Journal of Neurosurgery*, 42(6), pp. 665–673. doi: 10.3171/jns.1975.42.6.0665.

Pollay, M. (2012) 'Overview of the CSF Dual Outflow System', in *Acta neurochirurgica. Supplement*, pp. 47–50. doi: 10.1007/978-3-7091-0923-6_10.

Pollay, M., Stevens, A., Estrada, E. and Kaplan, R. (1972) 'Extracorporeal perfusion of choroid plexus.', *Journal of applied physiology*, 32(5), pp. 612–617. doi: 10.1152/jappl.1972.32.5.612.

Pombo, M. A., Zheng, Y., Fei, Z., Martin, G. B. and Rosli, H. G. (2017) 'Use of RNA-seq data to identify and validate RT-qPCR reference genes for studying the tomato-Pseudomonas pathosystem', *Scientific Reports*. Nature Publishing Group, 7(1), pp. 1–11. doi: 10.1038/srep44905.

Praetorius, J. and Damkier, H. H. (2017) *Transport across the choroid plexus epithelium*, *American Journal of Physiology - Cell Physiology*. American Physiological Society. doi: 10.1152/ajpcell.00041.2017.

Prendergast, B. J., Onishi, K. G. and Zucker, I. (2014) 'Female mice liberated for inclusion in neuroscience and biomedical research', *Neuroscience and Biobehavioral Reviews*. Neurosci Biobehav Rev, pp. 1–5. doi: 10.1016/j.neubiorev.2014.01.001.

Prince, E. A. and Ahn, S. H. (2013) 'Basic vascular neuroanatomy of the brain and spine: What the general interventional radiologist needs to know', *Seminars in Interventional Radiology*. Thieme Medical Publishers, Inc., 30(3), pp. 234–239. doi: 10.1055/s-0033-1353475.

Purves, D., Augustine, G. J., Fitzpatrick, D., Hall, W. C. and LaMantia, A.-S. (2018) *Neuroscience*. 6th edn. Available at: https://www.booktopia.com.au/neuroscience-dale-purves/book/9781605353807.html (Accessed: 24 February 2020).

Quincke, H. (1893) 'Meningitis serosa', *Sammlung Klinischer Vorträge*, 67(655).

Quintela, T., Albuquerque, T., Lundkvist, G., Carmine Belin, A., Talhada, D., Gonçalves, I., Carro, E. and Santos, C. R. A. (2018) 'The choroid plexus harbors a circadian oscillator modulated by estrogens', *Chronobiology International*. Taylor and Francis Ltd,

35(2), pp. 270–279. doi: 10.1080/07420528.2017.1400978.

Quintela, T., Gonçalves, A. I., Baltazar, A. G., Alves, A. C. H., Saraiva, A. M. J. and Santos, A. C. R. A. (2009) '7b-Estradiol Induces Transthyretin Expression in Murine Choroid Plexus via an Oestrogen Receptor Dependent Pathway', *Cellular and Molecular Neurobiology*, 29, pp. 475–483. doi: 10.1007/s10571-008-9339-1.

Quintela, T., Gonçalves, I., Carreto, L. C., Santos, M. A. S., Marcelino, H., Patriarca, F. M. and Santos, C. R. A. (2013) 'Analysis of the Effects of Sex Hormone Background on the Rat Choroid Plexus Transcriptome by cDNA Microarrays', *PLoS ONE*, 8(4).

Quintela, T., Sousa, • C, Patriarca, F. M., Gonçalves, • I and Santos, • C R A (2015) 'Gender associated circadian oscillations of the clock genes in rat choroid plexus', *Brain Structure and Function*, 220, pp. 1251–1262. doi: 10.1007/s00429-014-0720-1.

Raatz, S. K., Bibus, D., Thomas, W. and Kris-Etherton, P. (2001) 'Human Nutrition and Metabolism: Total fat intake modifies plasma fatty acid composition in humans', *Journal of Nutrition*. American Institute of Nutrition, 131(2), pp. 231–234. doi: 10.1093/jn/131.2.231.

Rabbani, C. C., Saltagi, M. Z., Manchanda, S. K., Yates, C. W. and Nelson, R. F. (2018) 'Prevalence of Obstructive Sleep Apnea (OSA) in Spontaneous Cerebrospinal Fluid (CSF) Leaks: A Prospective Cohort Study', *Otology and Neurotology*. Lippincott Williams and Wilkins, 39(6), pp. e475–e480. doi: 10.1097/MAO.0000000000001805.

Radhakrishnan, K., Thacker, A. K., Bohlaga, N. H., Maloo, J. C., Gerryo, S. E., Blétry, O. and Godeau, P. (1993) 'Epidemiology of idiopathic intracranial hypertension: a prospective and case-control study.', *Journal of the neurological sciences*. SAS Institute, Inc, Cary, North Carolina, 116(1), pp. 18–28. doi: 10.1016/0022-510X(93)90084-C.

Ranganathan, S., Lee, S. H., Checkver, A., Sklar, E., Lam, B. L., Danton, G. H. and Alperin, N. (2013) 'Magnetic resonance imaging finding of empty sella in obesity related idiopathic intracranial hypertension is associated with enlarged sella turcica',

Neuroradiology, 55, pp. 955–961. doi: 10.1007/s00234-013-1207-0.

Raper, D., Louveau, A. and Kipnis, J. (2016) 'How Do Meningeal Lymphatic Vessels Drain the CNS?', *Trends in Neurosciences*. Elsevier Ltd, pp. 581–586. doi: 10.1016/j.tins.2016.07.001.

Rasband, W. S. and U. S. National Institutes of Health (2018) 'ImageJ'. Bethesda, Maryland, USA. Available at: https://imagej.nih.gov/ij/ (Accessed: 1 July 2020).

Rasmussen, M. K., Mestre, H. and Nedergaard, M. (2018) 'The glymphatic pathway in neurological disorders', *The Lancet Neurology*. Lancet Publishing Group, pp. 1016–1024. doi: 10.1016/S1474-4422(18)30318-1.

Ray, L. A. and Heys, J. J. (2019) 'Fluid Flow and Mass Transport in Brain Tissue', *Fluids*, 4(4), p. 196. doi: 10.3390/fluids4040196.

Reboldi, A., Coisne, C., Baumjohann, D., Benvenuto, F., Bottinelli, D., Lira, S., Uccelli, A., Lanzavecchia, A., Engelhardt, B. and Sallusto, F. (2009) 'C-C chemokine receptor 6-regulated entry of TH-17 cells into the CNS through the choroid plexus is required for the initiation of EAE', *Nature Immunology*, 10(5), pp. 514–523. doi: 10.1038/ni.1716.

Redzic, Z. (2011) 'Molecular biology of the blood-brain and the blood-cerebrospinal fluid barriers: Similarities and differences', *Fluids and Barriers of the CNS*. BioMed Central, p. 3. doi: 10.1186/2045-8118-8-3.

Redzic, Z. B. (2013) 'Studies on the human choroid plexus in vitro.', *Fluids and barriers of the CNS*. BioMed Central, 10(1), p. 10. doi: 10.1186/2045-8118-10-10.

Redzic, Z. B., Malatiali, S. A., Grujicic, D. and Isakovic, A. J. (2010) 'Expression and functional activity of nucleoside transporters in human choroid plexus', *Cerebrospinal Fluid Research*, 7(1), p. 2. doi: 10.1186/1743-8454-7-2.

Reiber, H. (2016) 'Knowledge-base for interpretation of cerebrospinal fluid data patterns. Essentials in neurology and psychiatry.', *Arquivos de neuro-psiquiatria*, 74(6), pp.

501–12. doi: 10.1590/0004-282X20160066.

Reid, A. C., Matheson, M. S. and Teasdale, G. (1980) 'Volume Of The Ventricles In Benign Intracranial Hypertension', *The Lancet*. Elsevier, 316(8184), pp. 7–8. doi: 10.1016/S0140-6736(80)92889-5.

ReihaniKermani, H., Faramarzi, M. S. G., Ansari, M. and Ghafarinejad, A. (2008) 'Cerebrospinal fluid concentration of interleukin-6 and interleukin-10 in idiopathic intracranial hypertension', *Journal of Medical Sciences*, 8(2), pp. 205–208.

Ren, R., Wang, N., Zhang, X., Tian, G. and Jonas, J. B. (2012) 'Cerebrospinal fluid pressure correlated with body mass index', *Graefe's Archive for Clinical and Experimental Ophthalmology*, 250(3), pp. 445–446. doi: 10.1007/s00417-011-1746-1.

Rivest, R. W. (1991) 'Sexual maturation in female rats: Hereditary, developmental and environmental aspects', *Experientia*. Birkhäuser-Verlag, pp. 1026–1038. doi: 10.1007/BF01923338.

Roberts, D. C. S., Bennett, S. A. L. and Vickers, G. J. (1989) 'The estrous cycle affects cocaine self-administration on a progressive ratio schedule in rats', *Psychopharmacology*. Springer-Verlag, 98(3), pp. 408–411. doi: 10.1007/BF00451696.

Roepke, T. K., Kanda, V. A., Purtell, K., King, E. C., Lerner, D. J. and Abbott, G. W. (2011) 'KCNE2 forms potassium channels with KCNA3 and KCNQ1 in the choroid plexus epithelium.', *FASEB journal : official publication of the Federation of American Societies for Experimental Biology*, 25(12), pp. 4264–73. doi: 10.1096/fj.11-187609.

Rogers, P. and Webb, G. P. (1980) 'Estimation of body fat in normal and obese mice', *British Journal of Nutrition*. Cambridge University Press, 43(1), pp. 83–86. doi: 10.1079/BJN19800066.

Rowe, F. J. and Sarkies, N. J. (1999) 'The relationship between obesity and idiopathic intracranial hypertension.', *International journal of obesity and related metabolic disorders : journal of the International Association for the Study of Obesity*, 23(1), pp. 54–

9.

Rufiange, M., Leung, V. S. Y., Simpson, K. and Pang, D. S. J. (2020) 'Pre-warming before general anesthesia with isoflurane delays the onset of hypothermia in rats', *PLOS ONE*. Edited by M. Parker. Public Library of Science, 15(3), p. e0219722. doi: 10.1371/journal.pone.0219722.

Saindane, A. M., Lim, P. P., Aiken, A., Chen, Z. and Hudgins, P. A. (2013) 'Factors Determining the Clinical Significance of an "Empty" Sella Turcica', *American Journal of Roentgenology*. American Roentgen Ray Society , 200(5), pp. 1125–1131. doi: 10.2214/AJR.12.9013.

Saito, Y. and Wright, E. M. (1983) 'Bicarbonate transport across the frog choroid plexus and its control by cyclic nucleotides.', *The Journal of Physiology*, 336(1). doi: 10.1113/jphysiol.1983.sp014602.

Sakaguchi, T., Köhler, H., Gu, X., McCormick, B. A. and Reinecker, H. C. (2002) 'Shigella flexneri regulates tight junction-associated proteins in human intestinal epithelial cells', *Cellular Microbiology*. Cell Microbiol, 4(6), pp. 367–381. doi: 10.1046/j.1462-5822.2002.00197.x.

Sakka, L., Coll, G. and Chazal, J. (2011) 'Anatomy and physiology of cerebrospinal fluid', *European Annals of Otorhinolaryngology, Head and Neck Diseases*, 128(6), pp. 309–316. doi: 10.1016/j.anorl.2011.03.002.

Saladin, K. (2014) *Anatomy & Physiology: The Unity of Form and Function*, *Anatomy & Physiology: The Unity of Form and Function*. Available at: https://books.google.com/books?id=lmr8nQEACAAJ&pgis=1 (Accessed: 3 July 2017).

Salleh, N., Mokhtar, H. M., Kassim, N. M. and Giribabu, N. (2015) 'Testosterone Induces Increase in Aquaporin (AQP)-1, 5, and 7 Expressions in the Uteri of Ovariectomized Rats', *Journal of Membrane Biology*. Springer New York LLC, 248(6), pp. 1097–1105. doi: 10.1007/s00232-015-9823-8.

Samancı, B., Samancı, Y., Tüzün, E., Altıokka-Uzun, G., Ekizoğlu, E., İçöz, S., Şahin, E., Küçükali, C. İ. and Baykan, B. (2017) 'Evidence for potential involvement of pro-inflammatory adipokines in the pathogenesis of idiopathic intracranial hypertension', *Cephalalgia*, 37(6), pp. 525–531. doi: 10.1177/0333102416650705.

Sandhu, S., Silbiger, S. R., Lei, J. and Neugarten, J. (1997) *Effects of sex hormones on fluid and solute transport in Madin-Darby canine kidney cells*, *Kidney international*. doi: 10.1038/ki.1997.211.

Santos, C. R. A., Duarte, A. C., Quintela, T., Tomás, J., Albuquerque, T., Marques, F., Palha, J. A. and Gonçalves, I. (2017) 'The choroid plexus as a sex hormone target: Functional implications', *Frontiers in Neuroendocrinology*. Academic Press Inc., pp. 103–121. doi: 10.1016/j.yfrne.2016.12.002.

Sassone-Corsi, P. (2012) 'The Cyclic AMP pathway', *Cold Spring Harbor Perspectives in Biology*. Cold Spring Harbor Laboratory Press, 4(12). doi: 10.1101/cshperspect.a011148.

Savaskan, E. (2005) 'The Role of the Brain Renin-Angiotensin System in Neurodegenerative Disorders', *Current Alzheimer Research*. Bentham Science Publishers Ltd., 2(1), pp. 29–35. doi: 10.2174/1567205052772740.

Sawamoto, K., Wichterle, H., Gonzalez-Perez, O., Cholfin, J. A., Yamada, M., Spassky, N., Murcia, N. S., Garcia-Verdugo, J. M., Marin, O., Rubenstein, J. L. R., Tessier-Lavigne, M., Okano, H. and Alvarez-Buylla, A. (2006) 'New neurons follow the flow of cerebrospinal fluid in the adult brain', *Science*, 311(5761), pp. 629–632. doi: 10.1126/science.1119133.

Schiffer, L., Kempegowda, P., Arlt, W. and O'Reilly, M. W. (2017) 'Mechanisms in endocrinology: The sexually dimorphic role of androgens in human metabolic disease', *European Journal of Endocrinology*. BioScientifica Ltd., pp. R125–R143. doi: 10.1530/EJE-17-0124.

Schmittgen, T. D. and Livak, K. J. (2008) 'Analyzing real-time PCR data by the comparative CT method', *Nature Protocols*. Nat Protoc, 3(6), pp. 1101–1108. doi:

10.1038/nprot.2008.73.

Schwartz, R., Kliper, E., Stern, N., Dotan, G., Berliner, S. and Kesler, A. (2013) 'The obesity pattern of idiopathic intracranial hypertension in men', *Graefe's Archive for Clinical and Experimental Ophthalmology*, 251(11), pp. 2643–2646. doi: 10.1007/s00417-013-2420-6.

Scudamore, C. L., Jepson, M. A., Hirst, B. H. and Miller, H. R. P. (1998) 'The rat mucosal mast cell chymase, RMCP-II, alters epithelial cell monolayer permeability in association with altered distribution of the tight junction proteins ZO-1 and occludin', *European Journal of Cell Biology*. Elsevier GmbH, 75(4), pp. 321–330. doi: 10.1016/S0171-9335(98)80065-4.

Selmanoff, M. K., Goldman, B. D. and Ginsburg, B. E. (1977) 'Serum testosterone, agonistic behavior, and dominance in inbred strains of mice', *Hormones and Behavior*, 8(1), pp. 107–119. doi: 10.1016/0018-506X(77)90026-5.

Sengupta, P. (2013) 'The laboratory rat: Relating its age with human's', *International Journal of Preventive Medicine*, pp. 624–630.

Seyfert, S., Koch, H. C. and Kunzmann, V. (2003) 'Conditions of iodine contrast transfer from lumbosacral CSF to blood.', *Journal of the neurological sciences*, 206(1), pp. 85–90. Available at: http://www.ncbi.nlm.nih.gov/pubmed/12480090 (Accessed: 3 July 2017).

Sharma, R. and Sharma, S. (2018) *Physiology, Blood Volume*, *StatPearls*. Available at: http://www.ncbi.nlm.nih.gov/pubmed/30252333 (Accessed: 28 January 2020).

Shaw, O. M., Pool, B., Dalbeth, N. and Harper, J. L. (2014) 'The effect of diet-induced obesity on the inflammatory phenotype of non-adipose-resident macrophages in an in vivo model of gout', *Rheumatology*, 53(10), pp. 1901–1905. doi: 10.1093/rheumatology/keu174.

Sheldon, C. A., Paley, G. L., Xiao, R., Kesler, A., Eyal, O., Ko, M. W., Boisvert, C. J.,

Avery, R. A., Salpietro, V., Phillips, P. H., Heidary, G., McCormack, S. E. and Liu, G. T. (2016) 'Pediatric Idiopathic Intracranial Hypertension: Age, Gender, and Anthropometric Features at Diagnosis in a Large, Retrospective, Multisite Cohort', in *Ophthalmology*. Elsevier Inc., pp. 2424–2431. doi: 10.1016/j.ophtha.2016.08.004.

Shen, L. (2012) 'Tight junctions on the move: Molecular mechanisms for epithelial barrier regulation', *Annals of the New York Academy of Sciences*. Blackwell Publishing Inc., 1258(1), pp. 9–18. doi: 10.1111/j.1749-6632.2012.06613.x.

Sherman, B. M. and Korenman, S. G. (1975) 'Hormonal characteristics of the human menstrual cycle throughout reproductive life.', *The Journal of clinical investigation*. American Society for Clinical Investigation, 55(4), pp. 699–706. doi: 10.1172/JCI107979.

Shi, C., Lei, Y., Han, H., Zuo, L., Yan, J., He, Q., Yuan, L., Liu, H., Xu, G. and Xu, W. (2015) 'Transportation in the Interstitial Space of the Brain Can Be Regulated by Neuronal Excitation', *Scientific Reports*. Nature Publishing Group, 5. doi: 10.1038/srep17673.

Shi, L. Z., Li, G. J., Wang, S. and Zheng, W. (2008) 'Use of Z310 cells as an in vitro blood–cerebrospinal fluid barrier model: Tight junction proteins and transport properties', *Toxicology in Vitro*. NIH Public Access, 22(1), pp. 190–199. doi: 10.1016/j.tiv.2007.07.007.

Shields, L. B. E., Shields, C. B., Yao, T. L., Plato, B. M., Zhang, Y. P. and Dashti, S. R. (2019) 'Endovascular Treatment for Venous Sinus Stenosis in Idiopathic Intracranial Hypertension: An Observational Study of Clinical Indications, Surgical Technique, and Long-Term Outcomes', *World Neurosurgery*. Elsevier Inc., 121, pp. e165–e171. doi: 10.1016/j.wneu.2018.09.070.

Shrestha, B., Paul, D. and Pachter, J. S. (2014) 'Alterations in Tight Junction Protein and IgG Permeability Accompany Leukocyte Extravasation Across the Choroid Plexus During Neuroinflammation', *Journal of Neuropathology & Experimental Neurology*. Lippincott Williams and Wilkins, 73(11), pp. 1047–1061. doi: 10.1097/NEN.0000000000000127.

Sidhu, S., Parikh, T. and Burman, K. D. (2017) 'Endocrine Changes in Obesity', in *Perioperative Anesthetic Care of the Obese Patient*. CRC Press, pp. 41–49. doi: 10.3109/9781420095319-6.

Siersbaek, M., Varticovski, L., Yang, S., Baek, S., Nielsen, R., Mandrup, S., Hager, G. L., Chung, J. H. and GrØntved, L. (2017) 'High fat diet-induced changes of mouse hepatic transcription and enhancer activity can be reversed by subsequent weight loss', *Scientific Reports*. Nature Publishing Group, 7(1), pp. 1–13. doi: 10.1038/srep40220.

Silva-Vargas, V., Maldonado-Soto, A. R., Mizrak, D., Codega, P. and Doetsch, F. (2016) 'Age-Dependent Niche Signals from the Choroid Plexus Regulate Adult Neural Stem Cells', *Cell Stem Cell*. Cell Press, 19(5), pp. 643–652. doi: 10.1016/j.stem.2016.06.013.

De Simone, R., Marano, E., Fiorillo, C., Briganti, F., Di Salle, F., Volpe, A. and Bonavita, V. (2005) 'Sudden re-opening of collapsed transverse sinuses and longstanding clinical remission after a single lumbar puncture in a case of idiopathic intracranial hypertension. Pathogenetic implications', *Neurological Sciences*. Neurol Sci, 25(6), pp. 342–344. doi: 10.1007/s10072-004-0368-3.

De Simone, R., Ranieri, A. and Bonavita, V. (2010) 'Advancement in idiopathic intracranial hypertension pathogenesis: Focus on sinus venous stenosis', *Neurological Sciences*. Springer, 31(SUPPL.1), pp. 33–39. doi: 10.1007/s10072-010-0271-z.

Sinclair, A. J., Ball, A. K., Burdon, M. A., Clarke, C. E., Stewart, P. M., Curnow, S. J. and Rauz, S. (2008) 'Exploring the pathogenesis of IIH: An inflammatory perspective', *Journal of Neuroimmunology*. Elsevier, 201–202(C), pp. 212–220. Available at: https://www-sciencedirect-com.libezproxy.open.ac.uk/science/article/pii/S0165572808002208 (Accessed: 24 January 2019).

Sinclair, A. J., Walker, E. A., Burdon, M. A., van Beek, A. P., Kema, I. P., Hughes, B. A., Murray, P. I., Nightingale, P. G., Stewart, P. M., Rauz, S. and Tomlinson, J. W. (2010) 'Cerebrospinal fluid corticosteroid levels and cortisol metabolism in patients with

idiopathic intracranial hypertension: a link between 11beta-HSD1 and intracranial pressure regulation?', *The Journal of clinical endocrinology and metabolism*, 95(12), pp. 5348–5356. doi: 10.1210/jc.2010-0729.

Smarr, B., Rowland, N. E. and Zucker, I. (2019) 'Male and female mice show equal variability in food intake across 4-day spans that encompass estrous cycles', *PLoS ONE*. Public Library of Science, 14(7). doi: 10.1371/journal.pone.0218935.

Smine, S., Obry, A., Kadri, S., Hardouin, J., Fréret, M., Amri, M., Jouenne, T., Limam, F., Cosette, P. and Aouani, E. (2017) 'Brain proteomic modifications associated to protective effect of grape extract in a murine model of obesity', *Biochimica et Biophysica Acta - Proteins and Proteomics*. Elsevier B.V., 1865(5), pp. 578–588. doi: 10.1016/j.bbapap.2017.03.001.

Smith, M. S., Freeman, M. E. and Neill, J. D. (1975) 'The control of progesterone secretion during the estrous cycle and early pseudopregnancy in the rat: Prolactin, gonadotropin and steroid levels associated with rescue of the corpus luteum of pseudopregnancy', *Endocrinology*. Endocrinology, 96(1), pp. 219–226. doi: 10.1210/endo-96-1-219.

Sokołowski, W., Barszcz, K., Kupczyńska, M., Czubaj, N., Skibniewski, M. and Purzyc, H. (2018) 'Lymphatic drainage of cerebrospinal fluid in mammals – are arachnoid granulations the main route of cerebrospinal fluid outflow?', *Biologia (Poland)*. Springer, pp. 563–568. doi: 10.2478/s11756-018-0074-x.

Speake, T., Freeman, L. J. and Brown, P. D. (2003) 'Expression of aquaporin 1 and aquaporin 4 water channels in rat choroid plexus', *Biochimica et Biophysica Acta - Biomembranes*. Elsevier, 1609(1), pp. 80–86. doi: 10.1016/S0005-2736(02)00658-2.

Speake, T., Whitwell, C., Kajita, H., Majid, A. and Brown, P. D. (2001) 'Mechanisms of CSF secretion by the choroid plexus', 52(1), pp. 49–59. doi: 10.1002/1097-0029(20010101)52:1<49::AID-JEMT7>3.0.CO;2-C.

Spector, R. (2009) 'Nutrient transport systems in brain: 40 years of progress', *Journal of Neurochemistry*. J Neurochem, pp. 315–320. doi: 10.1111/j.1471-4159.2009.06326.x.

Spector, R. and Johanson, C. E. (2007) 'Vitamin transport and homeostasis in mammalian brain: Focus on vitamins B and E', *Journal of Neurochemistry*, pp. 425–438. doi: 10.1111/j.1471-4159.2007.04773.x.

Spector, R., Snodgrass, R. S. and Johanson, C. E. (2015) *A balanced view of the cerebrospinal fluid composition and functions: Focus on adult humans*, *Experimental Neurology*. Academic Press Inc. doi: 10.1016/j.expneurol.2015.07.027.

Srinivasan, B., Kolli, A. R., Esch, M. B., Abaci, H. E., Shuler, M. L. and Hickman, J. J. (2015) 'TEER measurement techniques for in vitro barrier model systems.', *Journal of laboratory automation*. SAGE Publications Inc., 20(2), pp. 107–26. doi: 10.1177/2211068214561025.

Stephens, A. M., Dean, L. L., Davis, J. P., Osborne, J. A. and Sanders, T. H. (2010) 'Peanuts, Peanut Oil, and Fat Free Peanut Flour Reduced Cardiovascular Disease Risk Factors and the Development of Atherosclerosis in Syrian Golden Hamsters', *Journal of Food Science*. John Wiley & Sons, Ltd, 75(4), pp. H116–H122. doi: 10.1111/j.1750-3841.2010.01569.x.

Stępień, M., Stępień, A., Wlazeł, R. N., Paradowski, M., Banach, M. and Rysz, J. (2014) 'Obesity indices and inflammatory markers in obese non-diabetic normo- and hypertensive patients: a comparative pilot study.', *Lipids in health and disease*. BioMed Central, 13, p. 29. doi: 10.1186/1476-511X-13-29.

Stiebel-Kalish, H., Serov, I., Sella, R., Chodick, G. and Snir, M. (2014) 'Childhood overweight or obesity increases the risk of IIH recurrence fivefold', *International Journal of Obesity*. Nature Publishing Group, 38(11), pp. 1475–1477. doi: 10.1038/ijo.2014.44.

Stolarczyk, E. (2017) 'Adipose tissue inflammation in obesity: a metabolic or

immune response?', *Current Opinion in Pharmacology*, 37, pp. 35–40. doi: 10.1016/j.coph.2017.08.006.

Stramek, A. K., Johnson, M. L. and Taylor, V. J. (2019) 'Improved timed-mating, non-invasive method using fewer unproven female rats with pregnancy validation via early body mass increases', *Laboratory Animals*. SAGE Publications Ltd, 53(2), pp. 148–159. doi: 10.1177/0023677218774076.

Strazielle, N. and Ghersi-Egea, J.-F. (2005) 'In Vitro Investigation of the Blood-Cerebrospinal Fluid Barrier Properties', *The Blood-Cerebrospinal Fluid Barrier*, pp. 553–593. doi: 10.1201/9781420023404.ch23.

Strazielle, N. and Ghersi-Egea, J. F. (2011) 'In vitro models of the blood-cerebrospinal fluid barrier and their use in neurotoxicological research', *Neuromethods*, 56, pp. 161–184. doi: 10.1007/978-1-61779-077-5_8.

Strazielle, N. and Ghersi-Egea, J. F. (2013) 'Physiology of blood-brain interfaces in relation to brain disposition of small compounds and macromolecules', *Molecular Pharmaceutics*, pp. 1473–1491. doi: 10.1021/mp300518e.

Strazielle, N. and Preston, J. E. (2003) 'Transport across the choroid plexuses in vivo and in vitro.', *Methods in molecular medicine*, 89, pp. 291–304. doi: 10.1385/1-59259-419-0:291.

Stucken, E. Z., Selesnick, S. H. and Brown, K. D. (2012) 'The Role of Obesity in Spontaneous Temporal Bone Encephaloceles and CSF Leak', *Otology & Neurotology*, 33(8), pp. 1412–1417. doi: 10.1097/MAO.0b013e318268d350.

Su, Z., Łabaj, P. P., Li, Sheng, Thierry-Mieg, J., Thierry-Mieg, D., Shi, W., Wang, C., Schroth, G. P., Setterquist, R. A., Thompson, J. F., Jones, W. D., Xiao, W., Xu, W., Jensen, R. V., Kelly, R., Xu, J., Conesa, A., Furlanello, C., Gao, Hanlin, Hong, H., Jafari, N., Letovsky, S., Liao, Y., Lu, F., Oakeley, E. J., Peng, Z., Praul, C. A., Santoyo-Lopez, J., Scherer, A., Shi, T., Smyth, G. K., Staedtler, F., Sykacek, P., Tan, X. X., Thompson, E. A., Vandesompele, J., Wang,

M. D., Wang, Jian, Wolfinger, R. D., Zavadil, J., Auerbach, S. S., Bao, W., Binder, H., Blomquist, T., Brilliant, M. H., Bushel, P. R., Cai, W., Catalano, J. G., Chang, C. W., Chen, T., Chen, G., Chen, R., Chierici, M., Chu, T. M., Clevert, D. A., Deng, Y., Derti, A., Devanarayan, V., Dong, Z., Dopazo, J., Du, T., Fang, H., Fang, Y., Fasold, M., Fernandez, A., Fischer, M., Furió-Tari, P., Fuscoe, J. C., Caimet, F., Gaj, S., Gandara, J., Gao, Huan, Ge, W., Gondo, Y., Gong, B., Gong, M., Gong, Z., Green, B., Guo, C., Guo, L., Guo, L. W., Hadfield, J., Hellemans, J., Hochreiter, S., Jia, M., Jian, M., Johnson, C. D., Kay, S., Kleinjans, J., Lababidi, S., Levy, S., Li, Q. Z., Li, L., Li, L., Li, P., Li, Y., Li, H., Li, J., Li, Shiyong, Lin, S. M., López, F. J., Lu, X., Luo, H., Ma, X., Meehan, J., Megherbi, D. B., Mei, N., Mu, B., Ning, B., Pandey, A., Pérez-Florido, J., Perkins, R. G., Peters, R., Phan, J. H., Pirooznia, M., Qian, F., Qing, T., Rainbow, L., Rocca-Serra, P., Sambourg, L., Sansone, S. A., Schwartz, S., Shah, R., Shen, J., Smith, T. M., Stegle, O., Stralis-Pavese, N., Stupka, E., Suzuki, Y., Szkotnicki, L. T., Tinning, M., Tu, B., Van Delft, J., Vela-Boza, A., Venturini, E., Walker, S. J., Wan, L., Wang, W., Wang, Jinhui, Wang, Jun, Wieben, E. D., Willey, J. C., Wu, P. Y., Xuan, J., Yang, Y., Ye, Z., Yin, Y., Yu, Y., Yuan, Y. C., Zhang, J., Zhang, K. K., Zhang, Wenqian, Zhang, Wenwei, Zhang, Y., Zhao, C., Zheng, Y., Zhou, Y., Zumbo, P., Tong, W., Kreil, D. P., Mason, C. E. and Shi, L. (2014) 'A comprehensive assessment of RNA-seq accuracy, reproducibility and information content by the Sequencing Quality Control Consortium', *Nature Biotechnology*. Nature Publishing Group, 32(9), pp. 903–914. doi: 10.1038/nbt.2957.

Subramaniam, S. and Fletcher, W. A. (2017) 'Obesity and Weight Loss in Idiopathic Intracranial Hypertension', *Journal of Neuro-Ophthalmology*, 37(2), pp. 197–205. doi: 10.1097/WNO.0000000000000448.

Sugerman, H. J. (2001) 'Effects of increased intra-abdominal pressure in severe obesity', *Surgical Clinics of North America*. W.B. Saunders, 81(5), pp. 1063–1075. doi: 10.1016/S0039-6109(05)70184-5.

Sugerman, H. J., Felton, W. L., Salvant, J. B., Sismanis, A. and Kellum, J. M. (1995) 'Effects of surgically induced weight loss on idiopathic intracranial hypertension in morbid obesity', *Neurology*. Neurology, 45(9), pp. 1655–1659. doi: 10.1212/WNL.45.9.1655.

Sugerman, H., Windsor, A., Bessos, M. and Wolfe, L. (1997) 'Intra-abdominal pressure, sagittal abdominal diameter and obesity comorbidity', *Journal of Internal Medicine*. Blackwell Publishing Ltd, 241(1), pp. 71–79. doi: 10.1046/j.1365-2796.1997.89104000.x.

Supuran, C. T. (2015) 'Acetazolamide for the treatment of idiopathic intracranial hypertension', *Expert Review of Neurotherapeutics*. Taylor and Francis Ltd, pp. 851–856. doi: 10.1586/14737175.2015.1066675.

Sveinsdottir, S., Gram, M., Cinthio, M., Sveinsdottir, K., Mörgelin, M. and Ley, D. (2014) 'Altered expression of aquaporin 1 and 5 in the choroid plexus following preterm intraventricular hemorrhage', *Developmental Neuroscience*. S. Karger AG, 36(6), pp. 542–551. doi: 10.1159/000366058.

Szentistvanyi, I., Patlak, C. S., Ellis, R. A. and Cserr, H. F. (1984) 'Drainage of interstitial fluid from different regions of rat brain', *American Journal of Physiology - Renal Fluid and Electrolyte Physiology*, 15(6). doi: 10.1152/ajprenal.1984.246.6.f835.

Szmydynger-Chodobska, J., Chodobski, A. and Johanson, C. E. (1994) 'Postnatal developmental changes in blood flow to choroid plexuses and cerebral cortex of the rat', *American Journal of Physiology - Regulatory Integrative and Comparative Physiology*, 266(5 35-5). doi: 10.1152/ajpregu.1994.266.5.r1488.

Szmydynger-Chodobska, J., Pascale, C. L., Pfeffer, A. N., Coulter, C. and Chodobski, A. (2007) 'Expression of junctional proteins in choroid plexus epithelial cell lines: A comparative study', *Cerebrospinal Fluid Research*. BioMed Central, 4, p. 11. doi: 10.1186/1743-8454-4-11.

Tai, L. M., Holloway, K. A., Male, D. K., Loughlin, A. J. and Romero, I. A. (2009) 'Amyloid-β-induced occludin down-regulation and increased permeability in human brain endothelial cells is mediated by MAPK activation', *Journal of Cellular and Molecular Medicine*. John Wiley & Sons, Ltd, 14(5), pp. 1101–1112. doi: 10.1111/j.1582-4934.2009.00717.x.

Tanaka, M. (2017) 'Functional vascular anatomy of the brain', *Neurologia Medico-Chirurgica*. Japan Neurosurgical Society, 57(11), pp. 584–589. doi: 10.2176/nmc.ra.2017-0030.

Tarnaris, A., Toma, A. K., Watkins, L. D. and Kitchen, N. D. (2011) 'Is there a difference in outcomes of patients with idiopathic intracranial hypertension with the choice of cerebrospinal fluid diversion site: A single centre experience', *Clinical Neurology and Neurosurgery*, 113(6), pp. 477–479. doi: 10.1016/j.clineuro.2011.02.008.

Tchernof, A. and Després, J.-P. (2013) 'Pathophysiology of Human Visceral Obesity: An Update', *Physiological Reviews*, 93(1), pp. 359–404. doi: 10.1152/physrev.00033.2011.

Tchernof, A. and Després, J. P. (2000) 'Sex steroid hormones, sex hormone-binding globulin, and obesity in men and women', *Hormone and Metabolic Research*, pp. 526–536. doi: 10.1055/s-2007-978681.

Terner, J. M., Lomas, L. M. and Picker, M. J. (2005) 'Influence of estrous cycle and gonadal hormone depletion on nociception and opioid antinociception in female rats of four strains', *Journal of Pain*, 6(6), pp. 372–383. doi: 10.1016/j.jpain.2005.01.354.

Thambisetty, M., Lavin, P. J., Newman, N. J. and Biousse, V. (2007) 'Fulminant idiopathic intracranial hypertension', *Neurology*. Wolters Kluwer Health, Inc. on behalf of the American Academy of Neurology, 68(3), pp. 229–232. doi: 10.1212/01.wnl.0000251312.19452.ec.

Thomas, J. L. and Eichmann, A. (2018) 'To BBB or Not to BBB?', *Developmental Cell*. Cell Press, pp. 689–691. doi: 10.1016/j.devcel.2018.11.039.

Tomás, J., Santos, C. R. A., Duarte, A. C., Maltez, M., Quintela, T., Lemos, M. C. and Gonçalves, I. (2019) 'Bitter taste signaling mediated by Tas2r144 is down-regulated by 17β-estradiol and progesterone in the rat choroid plexus', *Molecular and Cellular Endocrinology*. Elsevier Ireland Ltd, 495. doi: 10.1016/j.mce.2019.110521.

Tomlinson, J. W., Walker, E. a., Bujalska, I. J., Draper, N., Lavery, G. G., Cooper, M.

S., Hewison, M. and Stewart, P. M. (2004) '11β-Hydroxysteroid dehydrogenase type 1: A tissue-specific regulator of glucocorticoid response', *Endocrine Reviews*, 25, pp. 831–866. doi: 10.1210/er.2003-0031.

Toscano, V., Sancesario, G., Bianchi, P., Cicardi, C., Casilli, D. and Giacomini, P. (1991) 'Cerebrospinal fluid estrone in pseudotumor cerebri: A change in cerebral steroid hormone metabolism?', *Journal of Endocrinological Investigation*, 14(2), pp. 81–6. doi: 10.1007/BF03350271.

Trillo-Contreras, J., Toledo-Aral, J., Echevarría, M. and Villadiego, J. (2019) 'AQP1 and AQP4 Contribution to Cerebrospinal Fluid Homeostasis', *Cells*. MDPI AG, 8(2), p. 197. doi: 10.3390/cells8020197.

Trobe, J. (2011) *Papilledema*, *Wikimedia Commons*. Available at: https://commons.wikimedia.org/wiki/File:Papilledema.jpg (Accessed: 13 September 2020).

Tumani, H., Huss, A. and Bachhuber, F. (2017) 'The cerebrospinal fluid and barriers – anatomic and physiologic considerations', in *Handbook of Clinical Neurology*. Elsevier B.V., pp. 3–20. doi: 10.1016/B978-0-12-804279-3.00002-2.

Uddin, M., Haq, T. and Rafique, M. (2006) 'Cerebral venous system anatomy', *Journal of Pakistan Medical Association*, 56(11). Available at: https://ecommons.aku.edu/pakistan_fhs_mc_radiol/160 (Accessed: 16 August 2020).

Ueno, M., Chiba, Y., Murakami, R., Matsumoto, K., Kawauchi, M. and Fujihara, R. (2016) 'Blood–brain barrier and blood–cerebrospinal fluid barrier in normal and pathological conditions', *Brain Tumor Pathology*, 33(2), pp. 89–96. doi: 10.1007/s10014-016-0255-7.

Uldall, M., Bhatt, D. K., Kruuse, C., Juhler, M., Jansen-Olesen, I. and Jensen, R. H. (2017) 'Choroid plexus aquaporin 1 and intracranial pressure are increased in obese rats: Towards an idiopathic intracranial hypertension model?', *International Journal of Obesity*.

Nature Publishing Group, 41(7), pp. 1141–1147. doi: 10.1038/ijo.2017.83.

Valcamonico, F., Arcangeli, G., Consoli, F., Nonnis, D., Grisanti, S., Gatti, E., Berruti, A. and Ferrari, V. (2014) 'Idiopathic intracranial hypertension: A possible complication in the natural history of advanced prostate cancer', *International Journal of Urology*, 21(3), pp. 335–337. doi: 10.1111/iju.12273.

Varlamov, O. (2017) 'Western-style diet, sex steroids and metabolism', *Biochimica et Biophysica Acta - Molecular Basis of Disease*. Elsevier B.V., 1863(5), pp. 1147–1155. doi: 10.1016/j.bbadis.2016.05.025.

Vates, T. S., Bonting, S. L. and Oppelt, W. W. (1964) 'Na-K Activated Adenosine Triphosphatase Formation Of Cerebrospinal Fluid In The Cat.', *The American journal of physiology*. American Physiological Society, 206, pp. 1165–1172. doi: 10.1152/ajplegacy.1964.206.5.1165.

Venero, J. L., Vizuete, M. L., Ilundáin, A. A., Machado, A., Echevarria, M. and Cano, J. (1999) 'Detailed localization of aquaporin-4 messenger RNA in the CNS: Preferential expression in periventricular organs', *Neuroscience*. Pergamon, 94(1), pp. 239–250. doi: 10.1016/S0306-4522(99)00182-7.

Verkman, A. S., Tradtrantip, L., Smith, A. J. and Yao, X. (2017) 'Aquaporin Water Channels and Hydrocephalus.', *Pediatric neurosurgery*. S. Karger AG, 52(6), pp. 409–416. doi: 10.1159/000452168.

Verthelyi, D. (2001) 'Sex hormones as immunomodulators in health and disease', *International Immunopharmacology*. Elsevier, pp. 983–993. doi: 10.1016/S1567-5769(01)00044-3.

De Villota, E. D., Carmona, M. T. G., Rubio, J. J. and De Andrés, S. R. (1981) 'Equality of the In vivo and In vitro oxygen-binding capacity of haemoglobin in patients with severe respiratory disease', *British Journal of Anaesthesia*. Oxford University Press, 53(12), pp. 1325–1328. doi: 10.1093/bja/53.12.1325.

Volk, K. M., Pogrebna, V. V, Roberts, J. A., Zachry, J. E., Blythe, S. N. and Toporikova, N. (2017) 'High-Fat, High-Sugar Diet Disrupts the Preovulatory Hormone Surge and Induces Cystic Ovaries in Cycling Female Rats', *Journal of the Endocrine Society*. The Endocrine Society, 1(12), pp. 1488–1505. doi: 10.1210/js.2017-00305.

Wagner, J., Fleseriu, C. M., Ibrahim, A. and Cetas, J. S. (2016) 'Idiopathic Intracranial Hypertension After Surgical Treatment of Cushing Disease: Case Report and Review of Management Strategies', *World Neurosurgery*. Elsevier Inc., 96, pp. 611.e15-611.e18. doi: 10.1016/j.wneu.2016.09.008.

Wagshul, M. E., Eide, P. K. and Madsen, J. R. (2011) 'The pulsating brain: A review of experimental and clinical studies of intracranial pulsatility', *Fluids and Barriers of the CNS*. BioMed Central, pp. 1–23. doi: 10.1186/2045-8118-8-5.

Wajchenberg, B. L., Marcondes, J. A. M., Mathor, M. B., Achando, S. S., Germak, O. A. and Kirschner, M. A. (1989) 'Free testosterone levels during the menstrual cycle in obese versus normal women', *Fertility and Sterility*, 51(3), pp. 535–537. doi: 10.1016/S0015-0282(16)60571-X.

Wall, M. (1991) 'Idiopathic intracranial hypertension', *Neurologic Clinics*. Elsevier, pp. 73–95. doi: 10.1016/s0733-8619(18)30304-9.

Wall, M., McDermott, M. P., Kieburtz, K. D., Corbett, J. J., Feldon, S. E., Friedman, D. I., Katz, D. M., Keltner, J. L., Schron, E. B. and Kupersmith, M. J. (2014) 'Effect of acetazolamide on visual function in patients with idiopathic intracranial hypertension and mild visual loss: The idiopathic intracranial hypertension treatment trial', *JAMA - Journal of the American Medical Association*. American Medical Association, 311(16), pp. 1641–1651. doi: 10.1001/jama.2014.3312.

Wang, L., Feng, Z., Wang, Xi, Wang, Xiaowo and Zhang, X. (2010) 'DEGseq: an R package for identifying differentially expressed genes from RNA-seq data', *BIOINFORMATICS APPLICATIONS NOTE*, 26(1), pp. 136–138. doi: 10.1093/bioinformatics/btp612.

Ward, P. D., Tippin, T. K. and Thakker, D. R. (2000) 'Enhancing paracellular permeability by modulating epithelial tight junctions', *Pharmaceutical Science and Technology Today*. Elsevier Current Trends, pp. 346–358. doi: 10.1016/S1461-5347(00)00302-3.

Watson, G., Mayes, J. S. and Watson, G. H. (2004) 'Direct effects of sex steroid hormones on adipose tissues and obesity', *obesity reviews Blackwell*.

Watson, R. A. and Pride, N. B. (2005) 'Postural changes in lung volumes and respiratory resistance in subjects with obesity', *Journal of Applied Physiology*. American Physiological Society, 98(2), pp. 512–517. doi: 10.1152/japplphysiol.00430.2004.

Welch, K. (1975) 'The principles of physiology of the cerebrospinal fluid in relation to hydrocephalus including normal pressure hydrocephalus - PubMed', *Advances in Neurology*, pp. 247–332. Available at: https://pubmed.ncbi.nlm.nih.gov/766597/ (Accessed: 4 August 2020).

Weller, R. O., Sharp, M. M., Christodoulides, M., Carare, R. O. and Møllgård, K. (2018) 'The meninges as barriers and facilitators for the movement of fluid, cells and pathogens related to the rodent and human CNS', *Acta Neuropathologica*. Springer Verlag, pp. 363–385. doi: 10.1007/s00401-018-1809-z.

Westwood, F. R. (2008) 'The Female Rat Reproductive Cycle: A Practical Histological Guide to Staging', *Toxicologic Pathology*, pp. 375–384. doi: 10.1177/0192623308315665.

Whitaker, E. M., Shaw, M. A. and Hervey, G. R. (1983) 'Plasma oestradiol-17β and testosterone concentrations as possible causes of the infertility of congenitally obese Zucker rats', *Journal of Endocrinology*, 99(3), pp. 485–490. doi: 10.1677/joe.0.0990485.

Whiteley, W., Al-Shahi, R., Warlow, C. P., Zeidler, M. and Lueck, C. J. (2006) 'CSF opening pressure: Reference interval and the effect of body mass index', *Neurology*. Wolters Kluwer Health, Inc. on behalf of the American Academy of Neurology, 67(9), pp. 1690–1691. doi: 10.1212/01.wnl.0000242704.60275.e9.

Wilson, M. E., Westberry, J. M. and Trout, A. L. (2011) 'Estrogen receptor-alpha gene expression in the cortex: Sex differences during development and in adulthood', *Hormones and Behavior*, pp. 353–357. doi: 10.1016/j.yhbeh.2010.08.004.

Wolburg, H. and Paulus, W. (2010) 'Choroid plexus: Biology and pathology', *Acta Neuropathologica*, pp. 75–88.

Wollack, J. B., Makori, B., Ahlawat, S., Koneru, R., Picinich, S. C., Smith, A., Goldman, I. D., Qiu, A., Cole, P. D., Glod, J. and Kamen, B. (2008) 'Characterization of folate uptake by choroid plexus epithelial cells in a rat primary culture model', *Journal of Neurochemistry*. John Wiley & Sons, Ltd, 104(6), pp. 1494–1503. doi: 10.1111/j.1471-4159.2007.05095.x.

Wong, R., Madill, S. A., Pandey, P. and Riordan-Eva, P. (2007) 'Idiopathic intracranial hypertension: The association between weight loss and the requirement for systemic treatment', *BMC Ophthalmology*, 7. doi: 10.1186/1471-2415-7-15.

Wright, E. M. (1972) 'Mechanisms of ion transport across the choroid plexus', *The Journal of Physiology*. Wiley-Blackwell, 226(2), pp. 545–571. doi: 10.1113/jphysiol.1972.sp009997.

Wyss, L., Schäfer, J., Liebner, S., Mittelbronn, M., Deutsch, U., Enzmann, G., Adams, R. H., Aurrand-Lions, M., Plate, K. H., Imhof, B. A. and Engelhardt, B. (2012) 'Junctional Adhesion Molecule (JAM)-C Deficient C57BL/6 Mice Develop a Severe Hydrocephalus', *PLoS ONE*. Edited by R. Mohanraj. Public Library of Science, 7(9), p. e45619. doi: 10.1371/journal.pone.0045619.

Xie, L., Kang, H., Xu, Q., Chen, M. J., Liao, Y., Thiyagarajan, M., O'Donnell, J., Christensen, D. J., Nicholson, C., Iliff, J. J., Takano, T., Deane, R. and Nedergaard, M. (2013) 'Sleep drives metabolite clearance from the adult brain', *Science*. American Association for the Advancement of Science, 342(6156), pp. 373–377. doi: 10.1126/science.1241224.

Yaba, A., Sozen, B., Suzen, B. and Demir, N. (2017) 'Expression de l'aquaporine-7 et de l'aquaporine-9 dans les tanycytes et les plexus choroides au cours du cycle œstral chez

la souris', *Morphologie*. Elsevier Masson SAS, 101(332), pp. 39–46. doi: 10.1016/j.morpho.2016.09.001.

Yamaguchi, T., Hamada, T., Matsuzaki, T. and Iijima, N. (2020) 'Characterization of the circadian oscillator in the choroid plexus of rats', *Biochemical and Biophysical Research Communications*. Elsevier B.V. doi: 10.1016/j.bbrc.2020.01.125.

Yang, G., Wang, H., Kang, Y. and Zhu, M. J. (2014) 'Grape seed extract improves epithelial structure and suppresses inflammation in ileum of IL-10-deficient mice', *Food and Function*. Royal Society of Chemistry, 5(10), pp. 2558–2563. doi: 10.1039/c4fo00451e.

Yang, J., Simonneau, C., Kilker, R., Oakley, L., Byrne, M. D., Nichtova, Z., Stefanescu, I., Pardeep-Kumar, F., Tripathi, S., Londin, E., Saugier-Veber, P., Willard, B., Thakur, M., Pickup, S., Ishikawa, H., Schroten, H., Smeyne, R. and Horowitz, A. (2019) ' Murine MPDZ -linked hydrocephalus is caused by hyperpermeability of the choroid plexus ', *EMBO Molecular Medicine*. EMBO, 11(1). doi: 10.15252/emmm.201809540.

Yılmaz, T. F., Aralasmak, A., Toprak, H., Mehdi, E., Kocaman, G., Kurtcan, S., Kaya, M. O. and Alkan, A. (2019) 'Evaluation of CSF flow metrics in patients with communicating hydrocephalus and idiopathic intracranial hypertension', *Radiologia Medica*. Springer-Verlag Italia s.r.l., 124(5), pp. 382–391. doi: 10.1007/s11547-018-0979-z.

Youakim, A. and Ahdieh, M. (1999) 'Interferon-γ decreases barrier function in T84 cells by reducing ZO-1 levels and disrupting apical actin', *American Journal of Physiology - Gastrointestinal and Liver Physiology*. American Physiological SocietyBethesda, MD , 276(5 39-5). doi: 10.1152/ajpgi.1999.276.5.g1279.

Yri, H. M., Rönnbäck, C., Wegener, M., Hamann, S. and Jensen, R. H. (2014) 'The course of headache in idiopathic intracranial hypertension: a 12-month prospective follow-up study', *European Journal of Neurology*. Blackwell Publishing Ltd, 21(12), pp. 1458–1464. doi: 10.1111/ene.12512.

Zada, G., Tirosh, A., Kaiser, U. B., Laws, E. R. and Woodmansee, W. W. (2010)

'Cushing's disease and idiopathic intracranial hypertension: case report and review of underlying pathophysiological mechanisms.', *The Journal of clinical endocrinology and metabolism*, 95(11), pp. 4850–4. doi: 10.1210/jc.2010-0896.

Zadik, Z., Barak, Y., Stager, D., Kaufman, H., Levin, S. and Gadoth, N. (1985) 'Pseudotumor cerebri in a boy with 11-beta-hydroxylase deficiency--a possible relation to rapid steroid withdrawal.', *Child's nervous system : ChNS : official journal of the International Society for Pediatric Neurosurgery*, 1(3), pp. 179–81. Available at: http://www.ncbi.nlm.nih.gov/pubmed/3876152 (Accessed: 10 July 2017).

Zanello, S. B., Tadigotla, V., Hurley, J., Skog, J., Stevens, B., Calvillo, E. and Bershad, E. (2018) 'Inflammatory gene expression signatures in idiopathic intracranial hypertension: possible implications in microgravity-induced ICP elevation', *npj Microgravity*, 4(1), p. 1. doi: 10.1038/s41526-017-0036-6.

Zeeni, N., Daher, C., Fromentin, G., Tome, D., Darcel, N. and Chaumontet, C. (2013) 'A cafeteria diet modifies the response to chronic variable stress in rats', *Stress*. Taylor & Francis, 16(2), pp. 211–219. doi: 10.3109/10253890.2012.708952.

Zeng, X., Jin, T., Zhou, Y. and Nordberg, G. F. (2003) 'Changes of serum sex hormone levels and MT mRNA expression in rats orally exposed to cadmium', *Toxicology*. Elsevier Ireland Ltd, 186(1–2), pp. 109–118. doi: 10.1016/S0300-483X(02)00725-4.

Zhao, Z., Nelson, A. R., Betsholtz, C. and Zlokovic, B. V. (2015) 'Establishment and Dysfunction of the Blood-Brain Barrier', *Cell*. Cell Press, pp. 1064–1078. doi: 10.1016/j.cell.2015.10.067.

Zheng, W. and Zhao, Q. (2002) 'Establishment and characterization of an immortalized Z310 choroidal epithelial cell line from murine choroid plexus.', *Brain research*, 958(2), pp. 371–80. Available at: http://www.ncbi.nlm.nih.gov/pubmed/12470873 (Accessed: 20 July 2017).

Zihni, C., Mills, C., Matter, K. and Balda, M. S. (2016) 'Tight junctions: From simple

barriers to multifunctional molecular gates', *Nature Reviews Molecular Cell Biology*. Nature Publishing Group, pp. 564–580. doi: 10.1038/nrm.2016.80.

Zlokovic, B. V, Mackic, J. B., Wang, L., Mccomb, J. G. and Mcdonough, A. (1993) *Differential Expression of Na,K-ATPase alpha and beta subunit Isoforms at the Blood-Brain Barrier and the Choroid Plexus*, *THE JOURNAL OF BIOLOGICAL CHEMISTRY*.

Zotz, R. B. (2015) 'Sinus thrombosis and idiopathic intracerebral hypertension: Thrombophilia and hormonal influence as potentially relevant causal connections.', *Der Ophthalmologe : Zeitschrift der Deutschen Ophthalmologischen Gesellschaft*, 112(10), pp. 828–33. doi: 10.1007/s00347-015-0061-3.

Zucker, I. and Beery, A. K. (2010) 'Males still dominate animal studies', *Nature*, p. 690. doi: 10.1038/465690a.

Appendix A

Table 0.1. Further information about Rat and Mouse No.1 Maintenance Diet.

Calculated Analysis

INGREDIENTS

Wheat, Barley, Wheatfeed, De-hulled Extracted Toasted Soya, Soya Protein Concentrate, Macro Minerals, Soya Oil, Whey Powder, Amino Acids, Vitamins, Micro Minerals.

NUTRIENTS		Total	Supp (9)
Proximate Analysis			
Moisture (1)	%	10.00	
Crude Oil	%	2.71	
Crude Protein	%	14.38	
Crude Fibre	%	4.65	
Ash	%	6.00	
Nitrogen Free Extract	%	61.73	
Digestibility Co-Efficients (7)			
Digestible Crude Oil	%	2.47	
Digestible Crude Protein	%	12.92	
Carbohydrates, Fibre and Non Starch Polysaccharides (NSP)			
Total Dietary Fibre	%	17.05	
Pectin	%	1.52	
Hemicellulose	%	10.17	
Cellulose	%	4.32	
Lignin	%	1.68	
Starch	%	44.97	
Sugar	%	4.05	
Energy (5)			
Gross Energy	MJ/kg	14.74	
Digestible Energy (15)	MJ/kg	11.90	
Metabolisable Energy (15)	MJ/kg	10.74	
Atwater Fuel Energy (AFE)(8)	MJ/kg	13.75	
AFE from Oil	%	7.42	
AFE from Protein	%	17.49	
AFE from Carbohydrate	%	75.09	
Fatty Acids			
Saturated Fatty Acids			
C12:0 Lauric	%	0.02	
C14:0 Myristic	%	0.14	
C16:0 Palmitic	%	0.31	
C18:0 Stearic	%	0.04	
Monounsaturated Fatty Acids			
C14:1 Myristoleic	%	0.02	
C16:1 Palmitoleic	%	0.09	
C18:1 Oleic	%	0.77	
Polyunsaturated Fatty Acids			
C18:2(ω6) Linoleic	%	0.69	
C18:3(ω3) Linolenic	%	0.06	
C20:4(ω6) Arachidonic	%	0.13	
C22:5(ω3) Clupanodonic	%		
Amino Acids			
Arginine	%	0.91	
Lysine (6)	%	0.66	0.07
Methionine	%	0.22	0.04
Cystine	%	0.24	
Tryptophan	%	0.18	
Histidine	%	0.35	
Threonine	%	0.49	
Isoleucine	%	0.54	
Leucine	%	0.98	
Phenylalanine	%	0.66	
Valine	%	0.69	
Tyrosine	%	0.49	
Taurine	%		
Glycine	%	1.11	
Aspartic Acid	%	0.67	
Glutamic Acid	%	3.17	
Proline	%	1.20	
Serine	%	0.56	
Hydroxyproline	%		
Hydroxylysine	%		
Alanine	%	0.16	
Macro Minerals			
Calcium	%	0.73	0.63
Total Phosphorus	%	0.52	0.04
Phytate Phosphorus	%	0.24	
Available Phosphorus	%	0.28	0.04
Sodium	%	0.25	0.19
Chloride	%	0.38	0.32
Potassium	%	0.67	
Magnesium	%	0.23	
Micro Minerals			
Iron	mg/kg	159.30	82.50
Copper	mg/kg	11.50	1.94
Manganese	mg/kg	72.44	19.22
Zinc	mg/kg	35.75	
Cobalt	µg/kg	634.10	550.00
Iodine	µg/kg	1202.69	1085.00
Selenium	µg/kg	298.99	100.00
Fluorine	mg/kg	10.49	
Vitamins			
β-Carotene (2)	mg/kg	0.16	
Retinol (2)	µg/kg	2566.38	2400.00
Vitamin A (2)	iu/kg	8554.27	8000.00
Cholecalciferol (3)	µg/kg	15.54	15.00
Vitamin D (3)	iu/kg	621.70	600.00
α-Tocopherol (4)	mg/kg	76.45	56.82
Vitamin E (4)	iu/kg	84.10	62.50
Vitamin B_1 (Thiamine)	mg/kg	8.58	1.96
Vitamin B_2 (Riboflavin)	mg/kg	4.33	2.94
Vitamin B_6 (Pyridoxine)	mg/kg	4.81	0.98
Vitamin B_{12} (Cyanocobalamine)	µg/kg	7.49	6.00
Vitamin C (Ascorbic Acid)	mg/kg	2.59	
Vitamin K (Menadione)	mg/kg	10.17	9.36
Folic Acid (Vitamin B_9)	mg/kg	0.79	
Nicotinic Acid (Vitamin PP) (6)	mg/kg	61.32	2.45
Pantothenic Acid (Vitamin $B_{3/5}$)	mg/kg	20.17	5.80
Choline (Vitamin $B_{4/7}$)	mg/kg	1080.14	366.60
Inositol	mg/kg	2369.59	
Biotin (Vitamin H) (6)	µg/kg	277.13	

Notes

1. All values are calculated using a moisture basis of 10%. Typical moisture levels will range between 9.5 - 11.5%.
2. a. Vitamin A includes Retinol and the Retinol equivalents of β-carotene
   b. Retinol includes the Retinol equivalents of β-Carotene.
   c. 0.48 µg Retinol = 1 µg β-carotene = 1.6 iu Vitamin A activity
   d. 1 µg Retinol = 3.33* iu Vitamin A activity
   e. 1 iu Vitamin A = 0.3 µg Retinol = 0.6 µg β-carotene
   f. The standard analysis for Vitamin A does not detect β-carotene
3. 1µg Cholecalciferol (D_3) = 40.0 iu Vitamin D
4. 1 mg all-*rac*-α-tocopherol = 1.1 iu Vitamin E activity
   1 mg all-*rac*-α-tocopherol acetate = 1.0 iu Vitamin E activity
5. 1 MJ = 239.23 Kcalories = 239.23 Calories = 239,230 calories
6. These nutrients coming from natural raw materials such as cereals may have low availabilities due to the interactions with other compounds.
7. Based on in-vitro digestibility analysis.
8. AF Energy = Atwater Fuel Energy = ((CO%/100)*9000)+ ((CP%/100)*4000)+((NFE%/100)*4000)/239.23
9. Supplemented nutrients from manufactured and mined sources.
15. Calculated.

Table 0.2. Further information about Rodent Maintenance Atwater Fuel Energy High Fat Diet.

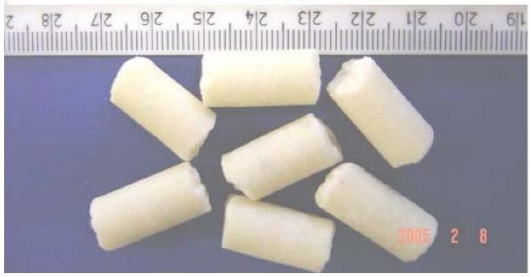

Diet Code: **824018**

Diet Name:

RM AFE45%FAT 20%CP 35%CHO (P)

Description:

Purified laboratory rodent diet.

'High Fat' diet for use with 829050 or other 'Rodent AFE' diets in this series.

Useful for studying obesity, diabetes and other fat/energy induced diseases.

BASIC INFORMATION

DIET	824018 - '45% AFE Fat'
INGREDIENT	g% (w/w)
Casein	26.507
Choline Bitartrate	0.296
L-Cystine	0.398
Lard	18.000
Rice Starch	18.428
Cellulose	6.164
Soya Oil	4.315
Sucrose	20.343
Mineral Mix	4.315
Vitamin Mix	1.233
Total	100.000

SPECIFICATION	% (w/w)	kcal/g	% kcal
Crude Fat	22.6	2.03	45
Crude Protein	23.0	0.92	20
Crude Fibre	4.5	/	/
Ash	4.4	/	/
Carbohydrate	40.2	1.61	35
Total AFE		4.56	100

OTHER INFORMATION

Storage:
This is a perishable material. Please store in a cool dry place. If possible store refrigerated or even freeze to reduce nutrient oxidation.

Shelf Life:
3 months from date of manufacture.
6 months if stored refrigerated.
9 months if stored frozen.

Feeding Directions:
Feed ad-libitum. Clean drinking water should be available at all times.

Product Form, Packaging & Net Weight:
Standard: 10 mm diameter pellets. Packed in sealed plastic buckets. **3 kg net weight.**

Nutrient Information:
AFE = ATWATER FUEL ENERGY = Decimal fractions of Fat, Protein, Carbohydrate multiplied by 9, 4 & 4 respectively to give kcal AFE / g of diet.
1 MJ = 239.23 Kcal
Nutrient figures on a fresh weight basis unless otherwise stated

Table 0.3. Further information about Western Rodent Diet.

CALCULATED ANALYSIS:

		FRESH	10% H2O
TOTAL	%	100.00	100.00
MOISTURE	%	2.35	10.00
CRUDE OIL	%	21.43	19.75
CRUDE PROTEIN	%	17.54	16.17
CRUDE FIBRE	%	3.50	3.23
ASH	%	3.99	3.68
NFE	%	50.52	46.56
PECTIN	%	0.00	0.00
HEMICELLULOSE	%	0.10	0.09
CELLULOSE	%	4.80	4.42
LIGNIN	%	0.00	0.00
STARCH	%	4.75	4.38
SUGAR	%	44.27	40.80
GROSS ENERGY	MJ/kg	20.39	18.79
DIGESTIBLE ENERGY	MJ/kg	18.77	17.30
METABOLISABLE ENERGY	MJ/kg	17.08	15.74
AF ENERGY	kcal/kg	4650.55	4286.22
C14 1 MYRISTOLEIC	%	0.17	0.16
C16 1 PALMITOLEIC	%	0.38	0.35
C18 1 W9 OLEIC	%	5.64	5.20
C18 2 W6 LINOLEIC	%	0.83	0.76
C18 3 W3 LINOLENIC	%	0.13	0.12
C20 4 W6 ARICHIDONIC	%	0.01	0.01
C22 5 W3 CLUPANODONIC	%	0.00	0.00
C12:0 LAURIC	%	0.62	0.57
C14:0 MYRISTIC	%	2.00	1.84
C16:0 PALMITIC	%	6.07	5.59
C18:0 STEARIC	%	2.66	2.45
ARGININE	%	0.44	0.41
LYSINE	%	1.07	0.99
S LYS	%	0.00	0.00
METHIONINE	%	0.42	0.39
S METH	%	0.00	0.00
CYSTINE	%	0.34	0.31
S CYST	%	0.30	0.28

		FRESH	10% H2O
CL	%	0.22	0.20
S CL	%	0.16	0.15
K	%	0.36	0.33
S K	%	0.36	0.33
MG	%	0.06	0.06
S MG	%	0.05	0.05
FE	mg/kg	47.75	44.01
S FE	mg/kg	40.91	37.71
CU	mg/kg	7.50	6.91
S CU	mg/kg	6.03	5.56
MN	mg/kg	54.15	49.91
S MN	mg/kg	52.68	48.55
ZN	mg/kg	53.08	48.92
S ZN	mg/kg	29.18	26.89
CO	µg/kg	0.00	0.00
S CO	µg/kg	0.00	0.00
I	µg/kg	206.50	190.32
S I	µg/kg	206.50	190.32
SE	µg/kg	159.95	147.42
S SE	µg/kg	159.95	147.42
F	mg/kg	0.00	0.00
VIT A	iu/kg	10055.00	9267.28
S VIT A	iu/kg	4000.00	3686.64
VIT D3	iu/kg	2322.00	2140.09
S VIT D3	iu/kg	1000.00	921.66
VIT E	iu/kg	62.39	57.50
S VIT E	iu/kg	50.00	46.08
VIT B1 THI	mg/kg	5.75	5.30
S VIT B1	mg/kg	5.67	5.23
VIT B2 RIB	mg/kg	6.73	6.20
S VIT B2	mg/kg	6.40	5.90
VIT B6 PYR	mg/kg	5.78	5.33
S VIT B6	mg/kg	5.71	5.26
VIT B12 CY	µg/kg	10.00	9.22
S VIT B12	µg/kg	10.00	9.22
VIT C ASCO	mg/kg	0.00	0.00
S VIT C	mg/kg	0.00	0.00

TRYPTOPHAN	%	0.15	0.14
S TRYPT	%	0.00	0.00
HISTIDINE	%	0.39	0.36
THREONINE	%	0.59	0.54
S THREO	%	0.00	0.00
ISOLEUCINE	%	0.86	0.79
LEUCINE	%	1.29	1.19
PHENYLALAN	%	0.70	0.65
VALINE	%	1.02	0.94
TYROSINE	%	0.70	0.65
TAURINE	%	0.00	0.00
GLYCINE	%	0.67	0.62
ASPARTIC A	%	0.96	0.88
GLUTAMIC A	%	2.77	2.55
PROLINE	%	1.16	1.07
SERINE	%	0.64	0.59
HYD PROLIN	%	0.00	0.00
HYD LYSINE	%	0.00	0.00
ALANINE	%	0.54	0.50
CA	%	0.68	0.63
S CA	%	0.67	0.62
TOTAL P	%	0.46	0.42
S PHOS	%	0.40	0.37
PHYTATE P	%	0.00	0.00
AVAIL P	%	0.46	0.42
NA	%	0.13	0.12
S NA	%	0.10	0.09

VIT K MENE	mg/kg	0.52	0.48
S VIT K	mg/kg	0.52	0.48
FOLIC ACID	mg/kg	1.91	1.76
S FOLIC	mg/kg	1.90	1.75
NICOTINIC	mg/kg	29.67	27.35
S NICOTIN	mg/kg	29.40	27.10
PANTOTHENI	mg/kg	15.81	14.57
S PANTOTH	mg/kg	15.25	14.06
CHOLINE	mg/kg	822.06	757.66
S CHOLINE	mg/kg	822.00	757.60
INOSITOL	mg/kg	0.00	0.00
S INOSITOL	mg/kg	0.00	0.00
BIOTIN	µg/kg	200.00	184.33
S BIOTIN	µg/kg	200.00	184.33

INGREDIENTS:

NAME	% INCLUSION
SUCROSE	33.94
MILK FAT ANHYDROUS	20.00
CASEIN ACID 88.5%CP	19.50
MALTODEXTRIN	10.00
CORN STARCH	5.00
CELLULOSE	5.00
AIN-76A-MX	3.50
CORN OIL	1.00
AIN-76A-VX	1.00
CALCIUM CARBONATE	0.40
L-CYSTINE	0.30
CHOLINE BITARTRATE	0.20
CHOLESTEROL	0.15
ANTIOXIDANT	0.01

Table 0.4. Further information about "Grandessa Peanut Butter Crunchy".

Ingredients: Peanuts (95%), Palm Oil, Sugar, Peanut Oil, Sea Salt.

Nutrient	Typical Values per 100g
Energy	2552kJ / 616 kcal
Fat	50g
of which saturates	9.5g
Carbohydrate	12g
of which sugars	6.4g
Fibre	8.3g
Protein	25g
Salt	0.9g

Appendix B

I. Deregulated genes in HFD vs ND comparison

Table 0.5. Highly upregulated genes in HFD rats when compared to ND and their functional classification as determined by PANTHER bioinformatics.

Genes were determined to be highly deregulated if they had a log2 fold change (log2FC) > 1 and a *P* value < 0.05. "Hit" refers to whether the gene was found by PANTHER.

HFD vs ND – UPREGULATED GENES							
Gene Symbol	**log2FC**	**P value**	**Hit?**	**Molecular Function**	**Biological Function**	**Cellular Component**	**Protein Class**
Cga	6.839	0.014	Yes	hormone activity (GO:0005179).	cellular aromatic compound metabolic process (GO:0006725). regulation of lipid biosynthetic process (GO:0046890). positive regulation of biosynthetic process (GO:0009891). cellular modified amino acid metabolic process (GO:0006575). steroid biosynthetic process (GO:0006694). hormone metabolic process (GO:0042445). organic hydroxy compound metabolic process (GO:1901615).	extracellular space (GO:0005615). protein-containing complex (GO:0032991).	————

HFD vs ND – UPREGULATED GENES							
Gene Symbol	**log2FC**	**P value**	**Hit?**	**Molecular Function**	**Biological Function**	**Cellular Component**	**Protein Class**
Slc17a6	4.499	0.000	No	————	————	————	————
Dclre1c	3.544	0.013	Yes	5'-3' exonuclease activity (GO:0008409). damaged DNA binding (GO:0003684). exodeoxyribonuclease activity, producing 5'-phosphomonoesters (GO:0016895).	interstrand cross-link repair (GO:0036297). telomere capping (GO:0016233). double-strand break repair via nonhomologous end joining (GO:0006303).	nuclear chromosome, telomeric region (GO:0000784).	————
Pomc	3.479	0.000	No	————	————	————	————
RGD1561730	3.406	0.035	Yes	signaling receptor binding (GO:0005102).	————	————	————
LOC100909657	3.254	0.039	Yes	————	————	————	C2H2 zinc finger transcription factor (PC00248).
LOC108348122	3.254	0.039	Yes	————	————	————	chaperone (PC00072).

HFD vs ND – UPREGULATED GENES							
Gene Symbol	**log2FC**	**P value**	**Hit?**	**Molecular Function**	**Biological Function**	**Cellular Component**	**Protein Class**
Fam83h	3.172	0.006	Yes	————	————	————	————
Pinlyp	3.084	0.002	Yes	————	————	————	scaffold/adaptor protein (PC00226).
Adra1b	2.959	0.020	No	————	————	————	————
Adra1b	2.959	0.020	No	————	————	————	————
Asb13	2.892	0.048	Yes	————	————	————	————
Ctla2a	2.892	0.048	Yes	cysteine-type endopeptidase activity (GO:0004197).	proteolysis involved in cellular protein catabolic process (GO:0051603).	extracellular space (GO:0005615). lysosome (GO:0005764).	cysteine protease (PC00081).
Vapb	2.821	0.036	Yes	protein binding (GO:0005515).	membrane organization (GO:0061024). organelle localization (GO:0051640). endoplasmic reticulum organization (GO:0007029).	endoplasmic reticulum membrane (GO:0005789). vacuole (GO:0005773). plasma membrane (GO:0005886).	membrane trafficking regulatory protein (PC00151).

Ccl9	2.821	0.032	Yes	G protein-coupled receptor binding (GO:0001664). cytokine activity (GO:0005125). cytokine receptor binding (GO:0005126).	ERK1 and ERK2 cascade (GO:0070371). inflammatory response (GO:0006954). G protein-coupled receptor signaling pathway (GO:0007186). chemokine-mediated signaling pathway (GO:0070098). innate immune response (GO:0045087). positive regulation of ERK1 and ERK2 cascade (GO:0070374). response to interleukin-1 (GO:0070555).	extracellular space (GO:0005615).	cytokine (PC00083).

HFD vs ND – UPREGULATED GENES							
Gene Symbol	**log2FC**	**P value**	**Hit?**	**Molecular Function**	**Biological Function**	**Cellular Component**	**Protein Class**
					cellular response to tumor necrosis factor (GO:0071356). granulocyte chemotaxis (GO:0071621). lymphocyte migration (GO:0072676). positive regulation of GTPase activity (GO:0043547).		
Mkrn2os	2.821	0.020	Yes	————	————	————	————
Krt14	2.567	0.018	Yes	————	————	————	————

HFD vs ND – UPREGULATED GENES							
Gene Symbol	**log2FC**	**P value**	**Hit?**	**Molecular Function**	**Biological Function**	**Cellular Component**	**Protein Class**
Hnf1b	2.544	0.021	Yes	DNA-binding transcription factor activity (GO:0003700). RNA polymerase II regulatory region sequence-specific DNA binding (GO:0000977).	positive regulation of transcription, DNA-templated (GO:0045893). transcription by RNA polymerase II (GO:0006366). regulation of transcription by RNA polymerase II (GO:0006357).	nucleus (GO:0005634).	DNA-binding transcription factor (PC00218).
Golm1	2.460	0.019	Yes	————	————	————	————
Mical1	2.445	0.004	Yes	————	————	————	————

LOC680875	2.406	0.036	Yes	————	cell-matrix adhesion (GO:0007160). wound healing (GO:0042060). adherens junction organization (GO:0034332). cytoskeleton organization (GO:0007010). regulation of cellular component biogenesis (GO:0044087). cellular component assembly (GO:0022607). regulation of cell adhesion (GO:0030155). microtubule-based process (GO:0007017).	cytoplasm (GO:0005737). actin cytoskeleton (GO:0015629). intermediate filament (GO:0005882). microtubule (GO:0005874).	intermediate filament binding protein (PC00130).

HFD vs ND – UPREGULATED GENES							
Gene Symbol	**log2FC**	**P value**	**Hit?**	**Molecular Function**	**Biological Function**	**Cellular Component**	**Protein Class**
					regulation of cellular component organization (GO:0051128). regulation of microtubule-based process (GO:0032886).		
Cyp1b1	2.406	0.047	No	————	————	————	————
Slc4a1ap	2.219	0.035	Yes	mRNA binding (GO:0003729).	————	————	RNA splicing factor (PC00148).
Tubg2	2.219	0.048	Yes	GTP binding (GO:0005525). structural molecule activity (GO:0005198).	mitotic spindle organization (GO:0007052). mitotic sister chromatid segregation (GO:0000070). microtubule polymerization (GO:0046785). meiotic nuclear division (GO:0140013).	nucleus (GO:0005634). centrosome (GO:0005813). centriole (GO:0005814). spindle (GO:0005819). gamma-tubulin complex (GO:0000930). microtubule (GO:0005874).	tubulin (PC00228).

HFD vs ND – UPREGULATED GENES							
Gene Symbol	**log2FC**	**P value**	**Hit?**	**Molecular Function**	**Biological Function**	**Cellular Component**	**Protein Class**
Etnk2	2.082	0.032	Yes	————	————	————	kinase (PC00137).
Tcea3	1.976	0.045	Yes	————	————	————	general transcription factor (PC00259).
Oas1a	1.945	0.018	No	————	————	————	————
Nefh	1.945	0.028	No	————	————	————	————
Wdr5b	1.890	0.040	Yes	histone binding (GO:0042393).	histone H3-K4 methylation (GO:0051568).	histone methyltransferase complex (GO:0035097).	————
Akap1	1.890	0.006	No	————	————	————	————
Hpdl	1.820	0.019	Yes	————	————	————	oxygenase (PC00177).
Larp7	1.820	0.003	No	————	————	————	————

Vegfb	1.805	0.007	Yes	growth factor activity (GO:0008083). growth factor receptor binding (GO:0070851). cytokine receptor binding (GO:0005126).	positive chemotaxis (GO:0050918). sprouting angiogenesis (GO:0002040). positive regulation of leukocyte chemotaxis (GO:0002690). transmembrane receptor protein tyrosine kinase signaling pathway (GO:0007169). protein phosphorylation (GO:0006468). positive regulation of angiogenesis (GO:0045766). response to hypoxia (GO:0001666).	extracellular space (GO:0005615).	growth factor (PC00112).

HFD vs ND – UPREGULATED GENES							
Gene Symbol	**log2FC**	**P value**	**Hit?**	**Molecular Function**	**Biological Function**	**Cellular Component**	**Protein Class**
					cellular response to growth factor stimulus (GO:0071363). positive regulation of protein phosphorylation (GO:0001934). endothelial cell proliferation (GO:0001935). leukocyte chemotaxis (GO:0030595). myeloid leukocyte migration (GO:0097529). positive regulation of epithelial cell proliferation (GO:0050679).		

HFD vs ND – UPREGULATED GENES							
Gene Symbol	**log2FC**	**P value**	**Hit?**	**Molecular Function**	**Biological Function**	**Cellular Component**	**Protein Class**
Dpysl5	1.668	0.007	Yes	dihydropyrimidinase activity (GO:0004157).	pyrimidine nucleobase catabolic process (GO:0006208).	————	hydrolase (PC00121).
LOC691083	1.598	0.040	Yes	hydrolase activity, acting on ester bonds (GO:0016788).	————	————	————
Susd2	1.590	0.011	Yes	————	————	————	————
Crmp1	1.568	0.006	Yes	dihydropyrimidinase activity (GO:0004157).	pyrimidine nucleobase catabolic process (GO:0006208).	————	hydrolase (PC00121).
LOC103690116	1.472	0.010	No	————	————	————	————
Adcy5	1.466	0.019	No	————	————	————	————

HFD vs ND – UPREGULATED GENES							
Gene Symbol	**log2FC**	**P value**	**Hit?**	**Molecular Function**	**Biological Function**	**Cellular Component**	**Protein Class**
Tril	1.457	0.011	Yes	lipopolysaccharide binding (GO:0001530).	toll-like receptor signaling pathway (GO:0002224). innate immune response (GO:0045087). cytokine production (GO:0001816). immune effector process (GO:0002252). regulation of cytokine production (GO:0001817).	membrane protein complex (GO:0098796). extracellular space (GO:0005615). integral component of membrane (GO:0016021). receptor complex (GO:0043235). extracellular matrix (GO:0031012).	transmembrane signal receptor (PC00197).

HFD vs ND – UPREGULATED GENES							
Gene Symbol	**log2FC**	**P value**	**Hit?**	**Molecular Function**	**Biological Function**	**Cellular Component**	**Protein Class**
Chgb	1.449	0.016	Yes	————	————	extracellular space (GO:0005615). secretory granule (GO:0030141). vacuole (GO:0005773). plasma membrane (GO:0005886).	————
Recql5	1.431	0.008	Yes	3'-5' DNA helicase activity (GO:0043138).	DNA biosynthetic process (GO:0071897). double-strand break repair via homologous recombination (GO:0000724). DNA unwinding involved in DNA replication (GO:0006268).	cytoplasm (GO:0005737). chromosome (GO:0005694).	DNA helicase (PC00011).
Cxcl17	1.412	0.003	Yes	————	————	————	————

HFD vs ND – UPREGULATED GENES							
Gene Symbol	**log2FC**	**P value**	**Hit?**	**Molecular Function**	**Biological Function**	**Cellular Component**	**Protein Class**
Crlf1	1.410	0.022	Yes	cytokine binding (GO:0019955). cytokine receptor activity (GO:0004896).	————	leaflet of membrane bilayer (GO:0097478). external side of plasma membrane (GO:0009897). receptor complex (GO:0043235).	cytokine (PC00083).
Fam198b	1.389	0.001	Yes	————	————	————	————
Ccdc136	1.380	0.025	Yes	————	————	————	scaffold/adaptor protein (PC00226).
Tsen54	1.358	0.049	Yes	catalytic activity, acting on a tRNA (GO:0140101). endoribonuclease activity (GO:0004521).	tRNA splicing, via endonucleolytic cleavage and ligation (GO:0006388).	catalytic complex (GO:1902494). nuclear part (GO:0044428).	endoribonuclease (PC00094).
Acap3	1.354	0.027	Yes	————	————	————	————

HFD vs ND – UPREGULATED GENES							
Gene Symbol	**log2FC**	**P value**	**Hit?**	**Molecular Function**	**Biological Function**	**Cellular Component**	**Protein Class**
Fbxw9	1.352	0.005	Yes	————	maturation of 5.8S rRNA (GO:0000460). maturation of LSU-rRNA (GO:0000470).	t-UTP complex (GO:0034455). 90S preribosome (GO:0030686). preribosome, large subunit precursor (GO:0030687).	————
Slc44a3	1.346	0.010	No	————	————	————	————
Resp18	1.338	0.004	Yes	————	————	endoplasmic reticulum (GO:0005783). vacuole (GO:0005773). plasma membrane (GO:0005886).	————
Sncg	1.337	0.000	No	————	————	————	————
Ppp1r42	1.314	0.032	Yes	————	————	————	————
Zfp688	1.312	0.019	Yes	————	————	————	————
Htatip2	1.305	0.005	Yes	————	————	————	————

HFD vs ND – UPREGULATED GENES							
Gene Symbol	**log2FC**	**P value**	**Hit?**	**Molecular Function**	**Biological Function**	**Cellular Component**	**Protein Class**
Prune1	1.263	0.040	Yes	pyrophosphatase activity (GO:0016462).	organic substance catabolic process (GO:1901575). phosphorus metabolic process (GO:0006793). cellular catabolic process (GO:0044248). oxoacid metabolic process (GO:0043436).	cytoplasm (GO:0005737).	————
Zscan10	1.227	0.001	Yes	————	————	————	————
Gjb6	1.209	0.035	Yes	————	————	————	gap junction (PC00105).
Mob3b	1.201	0.022	Yes	————	————	————	kinase activator (PC00138).
Gprasp2	1.201	0.003	Yes	————	————	————	————
Nat8f1	1.190	0.018	No	————	————	————	————
RGD1306502	1.188	0.045	Yes	————	————	————	————

HFD vs ND – UPREGULATED GENES							
Gene Symbol	**log2FC**	**P value**	**Hit?**	**Molecular Function**	**Biological Function**	**Cellular Component**	**Protein Class**
LOC367117	1.165	0.013	Yes	————	————	mitochondrial large ribosomal subunit (GO:0005762).	ribosomal protein (PC00202).
Tubb6	1.163	0.045	Yes	GTP binding (GO:0005525). structural molecule activity (GO:0005198).	mitotic nuclear division (GO:0140014). microtubule cytoskeleton organization (GO:0000226).	cytoplasm (GO:0005737). microtubule (GO:0005874).	tubulin (PC00228).
Prorsd1	1.148	0.008	Yes	————	————	————	————
Ptprn	1.122	0.020	Yes	————	————	————	————
Ftsj3	1.121	0.031	Yes	RNA methyltransferase activity (GO:0008173).	RNA methylation (GO:0001510).	————	————
Tpp1	1.115	0.009	No	————	————	————	————
St6galnac2	1.083	0.007	Yes	————	————	————	————
Blvra	1.083	0.033	No	————	————	————	————
Patj	1.063	0.001	Yes	————	————	————	————

HFD vs ND – UPREGULATED GENES							
Gene Symbol	**log2FC**	**P value**	**Hit?**	**Molecular Function**	**Biological Function**	**Cellular Component**	**Protein Class**
LOC103689949	1.052	0.032	Yes	————	————	cytoplasmic vesicle (GO:0031410).	————
Sv2a	1.027	0.004	Yes	————	————	integral component of membrane (GO:0016021). plasma membrane region (GO:0098590). synaptic vesicle membrane (GO:0030672). neuron projection (GO:0043005). vacuole (GO:0005773).	————
Gpx3	1.012	0.003	No	————	————	————	————

HFD vs ND – UPREGULATED GENES							
Gene Symbol	**log2FC**	**P value**	**Hit?**	**Molecular Function**	**Biological Function**	**Cellular Component**	**Protein Class**
Agl	1.007	0.005	Yes	transferase activity, transferring hexosyl groups (GO:0016758). glucosidase activity (GO:0015926).	glycogen metabolic process (GO:0005977). macromolecule catabolic process (GO:0009057). cellular catabolic process (GO:0044248).	————	glycosyltransferase (PC00111). glycosidase (PC00110).
LOC102551435	1.007	0.047	Yes	————	————	————	————

Table 0.6. Highly downregulated genes in HFD rats when compared to ND and their functional classification as determined by PANTHER bioinformatics.

Genes were determined to be highly deregulated if they had a log2 fold change (log2FC) < -1 and a *P* value < 0.05. "Hit" refers to whether the gene was found by PANTHER.

HFD VS ND – DOWNREGULATED GENES							
Gene Symbol	**log2FC**	***P* value**	**Hit?**	**Molecular Function**	**Biological Function**	**Cellular Component**	**Protein Class**
Junb	-3.869	0.005	No	————	————	————	————
RGD1560608	-3.669	0.019	Yes	————	————	————	————
Dtwd1	-3.615	0.007	No	————	————	————	————
Chek2	-3.499	0.028	Yes	————	nucleus (GO:0005634). cytoplasm (GO:0005737).	————	mitotic DNA damage checkpoint (GO:0044773). mitotic nuclear division (GO:0140014). signal transduction in response to DNA damage (GO:0042770).

HFD VS ND – DOWNREGULATED GENES							
Gene Symbol	**log2FC**	***P* value**	**Hit?**	**Molecular Function**	**Biological Function**	**Cellular Component**	**Protein Class**
Dgkd	-3.438	0.009	Yes	kinase (PC00137).	————	————	acylglycerol metabolic process (GO:0006639). phosphorylation (GO:0016310). intracellular signal transduction (GO:0035556).
Slc35f5	-3.239	0.004	Yes	secondary carrier transporter (PC00258).	————	————	————
Tmem178a	-3.236	0.028	Yes	————	————	————	————
Pxdc1	-3.165	0.005	Yes	————	————	————	————
Bex4	-3.002	0.049	Yes	————	nucleus (GO:0005634). cytoplasm (GO:0005737).	————	————

HFD VS ND – DOWNREGULATED GENES							
Gene Symbol	**log2FC**	***P* value**	**Hit?**	**Molecular Function**	**Biological Function**	**Cellular Component**	**Protein Class**
Prkdc	-2.962	0.020	Yes	non-receptor serine/threonine protein kinase (PC00167).	nucleus (GO:0005634).	————	telomere maintenance (GO:0000723). double-strand break repair (GO:0006302).
Fam167b	-2.823	0.002	Yes	————	————	————	————
Grip1	-2.822	0.042	Yes	————	————	————	————
Rc3h2	-2.725	0.043	Yes	————	————	————	————
LOC688553	-2.725	0.003	Yes	————	————	————	————
B3galt4	-2.725	0.027	Yes	————	————	————	————
Gramd4	-2.721	0.045	Yes	————	————	————	————
Meis2	-2.618	0.018	Yes	homeodomain transcription factor (PC00119).	————	————	————
Gria3	-2.618	0.015	Yes	————	————	————	————

HFD VS ND – DOWNREGULATED GENES							
Gene Symbol	**log2FC**	***P* value**	**Hit?**	**Molecular Function**	**Biological Function**	**Cellular Component**	**Protein Class**
Exo5	-2.615	0.045	Yes	————	nucleus (GO:0005634).	————	interstrand cross-link repair (GO:0036297).
Galnt18	-2.561	0.019	Yes	glycosyltransferase (PC00111).	Golgi apparatus (GO:0005794). vacuole (GO:0005773). plasma membrane (GO:0005886).	————	————
Shprh	-2.502	0.035	Yes	————	————	————	————
Negr1	-2.461	0.007	No	————	————	————	————
Tcaim	-2.441	0.049	Yes	————	mitochondrion (GO:0005739).	————	————
Cttnbp2	-2.441	0.045	Yes	————	————	————	————

HFD VS ND – DOWNREGULATED GENES							
Gene Symbol	**log2FC**	***P* value**	**Hit?**	**Molecular Function**	**Biological Function**	**Cellular Component**	**Protein Class**
H2afx	-2.409	0.023	Yes	histone (PC00118).	nuclear chromatin (GO:0000790).	————	transcription, DNA-templated (GO:0006351). chromatin silencing (GO:0006342). cellular response to DNA damage stimulus (GO:0006974).
Ube2d1	-2.402	0.001	Yes	ubiquitin-protein ligase (PC00234).	ubiquitin ligase complex (GO:0000151).	————	ubiquitin-dependent protein catabolic process (GO:0006511).

HFD VS ND – DOWNREGULATED GENES							
Gene Symbol	**log2FC**	***P* value**	**Hit?**	**Molecular Function**	**Biological Function**	**Cellular Component**	**Protein Class**
Ttc8	-2.331	0.017	Yes	————	BBSome (GO:0034464). ciliary basal body (GO:0036064). non-motile cilium (GO:0097730). intraciliary transport particle (GO:0030990). plasma membrane region (GO:0098590).	————	intraciliary transport involved in cilium assembly (GO:0035735). non-motile cilium assembly (GO:1905515). vesicle targeting, trans-Golgi to periciliary membrane compartment (GO:0097712). axoneme assembly (GO:0035082). ciliary transition zone assembly (GO:1905349). protein localization to cilium (GO:0061512).
Fam193a	-2.285	0.027	Yes	————	————	————	————
Ptgs1	-2.285	0.011	Yes	————	————	————	————

HFD VS ND – DOWNREGULATED GENES							
Gene Symbol	**log2FC**	***P* value**	**Hit?**	**Molecular Function**	**Biological Function**	**Cellular Component**	**Protein Class**
Acap2	-2.189	0.016	Yes	————	————	————	————
Efemp1	-2.165	0.031	Yes	————	————	————	————
Med1	-2.149	0.011	Yes	general transcription factor (PC00259).	————	————	————
LOC499643	-2.087	0.018	Yes	————	————	————	————
RGD1359508	-2.086	0.035	Yes	————	————	————	————
Nampt	-2.054	0.005	Yes	transferase (PC00220).	————	————	————
Tradd	-2.032	0.006	Yes	————	————	————	————

HFD VS ND – DOWNREGULATED GENES							
Gene Symbol	**log2FC**	***P* value**	**Hit?**	**Molecular Function**	**Biological Function**	**Cellular Component**	**Protein Class**
Nr2f1	-2.021	0.003	Yes	C4 zinc finger nuclear receptor (PC00169).	nucleus (GO:0005634).	————	negative regulation of transcription by RNA polymerase II (GO:0000122). anatomical structure development (GO:0048856). cell differentiation (GO:0030154). transcription by RNA polymerase II (GO:0006366). positive regulation of transcription by RNA polymerase II (GO:0045944).
Arntl	-1.962	0.029	No	————	————	————	————

HFD VS ND – DOWNREGULATED GENES							
Gene Symbol	**log2FC**	***P* value**	**Hit?**	**Molecular Function**	**Biological Function**	**Cellular Component**	**Protein Class**
Gar1	-1.947	0.017	Yes	RNA binding protein (PC00031).	catalytic complex (GO:1902494). nucleolar part (GO:0044452). small nucleolar ribonucleoprotein complex (GO:0005732).	————	rRNA modification (GO:0000154). pseudouridine synthesis (GO:0001522).
Rpgr	-1.935	0.002	Yes	————	————	————	————
RGD1565323	-1.918	0.046	No	————	————	————	————
Cnot6l	-1.917	0.020	Yes	mRNA polyadenylation factor (PC00146).	nucleus (GO:0005634). cytoplasm (GO:0005737). CCR4-NOT complex (GO:0030014).	————	gene expression (GO:0010467). nuclear-transcribed mRNA poly (A). tail shortening (GO:0000289).
Zfp189	-1.871	0.029	Yes	————	————	————	————

HFD VS ND – DOWNREGULATED GENES							
Gene Symbol	**log2FC**	***P* value**	**Hit?**	**Molecular Function**	**Biological Function**	**Cellular Component**	**Protein Class**
LOC680227	-1.871	0.032	No	————	————	————	————
LOC108348326	-1.856	0.006	Yes	transfer/carrier protein (PC00219).	integral component of peroxisomal membrane (GO:0005779). transporter complex (GO:1990351).	————	protein import into peroxisome matrix (GO:0016558). protein monoubiquitination (GO:0006513).
Cav1	-1.843	0.016	No	————	————	————	————
Cbfb	-1.797	0.002	Yes	DNA-binding transcription factor (PC00218).	RNA polymerase II transcription factor complex (GO:0090575).	————	transcription by RNA polymerase II (GO:0006366). regulation of transcription by RNA polymerase II (GO:0006357).

HFD VS ND – DOWNREGULATED GENES							
Gene Symbol	**log2FC**	***P* value**	**Hit?**	**Molecular Function**	**Biological Function**	**Cellular Component**	**Protein Class**
Klf15	-1.775	0.009	Yes	C2H2 zinc finger transcription factor (PC00248).	nucleus (GO:0005634).	————	transcription by RNA polymerase II (GO:0006366). regulation of transcription by RNA polymerase II (GO:0006357).
Ube2ql1	-1.775	0.046	Yes	ubiquitin-protein ligase (PC00234).	————	————	————

HFD VS ND – DOWNREGULATED GENES							
Gene Symbol	**log2FC**	***P* value**	**Hit?**	**Molecular Function**	**Biological Function**	**Cellular Component**	**Protein Class**
Brwd1	-1.743	0.007	Yes	————	nucleus (GO:0005634).	————	regulation of cell shape (GO:0008360). cytoskeleton organization (GO:0007010). cell morphogenesis (GO:0000902). transcription by RNA polymerase II (GO:0006366). regulation of transcription by RNA polymerase II (GO:0006357).
Mknk1	-1.725	0.024	Yes	non-receptor serine/threonine protein kinase (PC00167).	nucleus (GO:0005634). cytoplasm (GO:0005737).	————	peptidyl-serine phosphorylation (GO:0018105). intracellular signal transduction (GO:0035556).

HFD VS ND – DOWNREGULATED GENES							
Gene Symbol	**log2FC**	***P* value**	**Hit?**	**Molecular Function**	**Biological Function**	**Cellular Component**	**Protein Class**
Dgkb	-1.725	0.004	No	————	————	————	————
Rapgef2	-1.699	0.019	Yes	guanyl-nucleotide exchange factor (PC00113).	————	————	————
Camkk2	-1.694	0.015	Yes	————	————	————	————
Mlh3	-1.601	0.021	Yes	DNA binding protein (PC00009).	mismatch repair complex (GO:0032300).	————	mismatch repair (GO:0006298).
Fam135a	-1.590	0.025	Yes	————	————	————	cellular lipid metabolic process (GO:0044255).
Herc3	-1.580	0.009	Yes	————	————	————	————
Dusp6	-1.548	0.000	Yes	————	cytosol (GO:0005829).	————	inactivation of MAPK activity (GO:0000188). MAPK cascade (GO:0000165).
Gnl3	-1.542	0.036	Yes	————	nucleolus (GO:0005730).	————	————

HFD VS ND – DOWNREGULATED GENES							
Gene Symbol	**log2FC**	***P* value**	**Hit?**	**Molecular Function**	**Biological Function**	**Cellular Component**	**Protein Class**
Tmem117	-1.536	0.025	Yes	————	————	————	intrinsic apoptotic signaling pathway in response to endoplasmic reticulum stress (GO:0070059).
Ints8	-1.502	0.022	Yes	————	integrator complex (GO:0032039).	————	snRNA 3'-end processing (GO:0034472).
RGD1563354	-1.502	0.010	Yes	————	————	————	————
Zfp280d	-1.502	0.034	Yes	C2H2 zinc finger transcription factor (PC00248).	nucleus (GO:0005634).	————	transcription, DNA-templated (GO:0006351). regulation of transcription, DNA-templated (GO:0006355).
Arpp21	-1.492	0.001	Yes	————	————	————	————
Mpdz	-1.475	0.007	Yes	————	————	————	————
Jag1	-1.441	0.034	Yes	————	————	————	————

HFD VS ND – DOWNREGULATED GENES							
Gene Symbol	**log2FC**	***P* value**	**Hit?**	**Molecular Function**	**Biological Function**	**Cellular Component**	**Protein Class**
Galns	-1.435	0.043	Yes	hydrolase (PC00121).	————	————	————
Btg2	-1.428	0.020	Yes	————	nucleus (GO:0005634). cytoplasm (GO:0005737).	————	cell population proliferation (GO:0008283). negative regulation of cell population proliferation (GO:0008285). mitotic nuclear division (GO:0140014). negative regulation of mitotic cell cycle (GO:0045930).
Ehmt1	-1.420	0.039	Yes	————	————	————	————
Sclt1	-1.419	0.020	Yes	————	————	————	————
Usp38	-1.402	0.039	Yes	cysteine protease (PC00081).	————	————	protein deubiquitination (GO:0016579).

HFD VS ND – DOWNREGULATED GENES							
Gene Symbol	**log2FC**	***P* value**	**Hit?**	**Molecular Function**	**Biological Function**	**Cellular Component**	**Protein Class**
Enah	-1.402	0.026	Yes	scaffold/adaptor protein (PC00226).	————	————	cell motility (GO:0048870). actin polymerization or depolymerization (GO:0008154). axon guidance (GO:0007411).

Htr2a	-1.401	0.042	Yes	G-protein coupled receptor (PC00021).	dendrite (GO:0030425). integral component of plasma membrane (GO:0005887). plasma membrane region (GO:0098590).	————	cyclic-nucleotide-mediated signaling (GO:0019935). inositol phosphate-mediated signaling (GO:0048016). G protein-coupled receptor signaling pathway, coupled to cyclic nucleotide second messenger (GO:0007187). response to drug (GO:0042493). activation of phospholipase C activity (GO:0007202). chemical synaptic transmission (GO:0007268). sequestering of calcium ion (GO:0051208). phospholipase C-activating G protein-coupled receptor

HFD VS ND – DOWNREGULATED GENES							
Gene Symbol	**log2FC**	***P* value**	**Hit?**	**Molecular Function**	**Biological Function**	**Cellular Component**	**Protein Class**
							signaling pathway (GO:0007200). release of sequestered calcium ion into cytosol (GO:0051209).
Nup58	-1.388	0.026	Yes	————	vacuole (GO:0005773). plasma membrane (GO:0005886). nuclear pore (GO:0005643).	————	————
Eed	-1.346	0.034	Yes	chromatin/chromatin-binding, or -regulatory protein (PC00077).	histone methyltransferase complex (GO:0035097). PcG protein complex (GO:0031519).	————	negative regulation of transcription by RNA polymerase II (GO:0000122). transcription by RNA polymerase II (GO:0006366). chromatin silencing (GO:0006342).

HFD VS ND – DOWNREGULATED GENES							
Gene Symbol	**log2FC**	***P* value**	**Hit?**	**Molecular Function**	**Biological Function**	**Cellular Component**	**Protein Class**
Dnajc21	-1.332	0.030	Yes	————	————	————	————
Fat3	-1.332	0.049	No	————	————	————	————
Ptprz1	-1.310	0.015	Yes	————	————	————	————
Rcor1	-1.296	0.019	Yes	DNA-binding transcription factor activity (GO:0003700). transcription corepressor activity (GO:0003714). transcription regulatory region DNA binding (GO:0044212). transcription factor binding (GO:0008134).	————	nucleus (GO:0005634). transcriptional repressor complex (GO:0017053).	————

HFD VS ND – DOWNREGULATED GENES							
Gene Symbol	**log2FC**	***P* value**	**Hit?**	**Molecular Function**	**Biological Function**	**Cellular Component**	**Protein Class**
Heatr5a	-1.283	0.023	Yes	————	endocytic vesicle (GO:0030139). Golgi apparatus (GO:0005794). vacuole (GO:0005773). plasma membrane (GO:0005886).	————	vesicle budding from membrane (GO:0006900). protein localization (GO:0008104). membrane invagination (GO:0010324). endocytosis (GO:0006897). retrograde transport, endosome to Golgi (GO:0042147).
Gin1	-1.275	0.029	Yes	————	————	————	————
LOC100910506	-1.275	0.050	No	————	————	————	————
Epsti1	-1.268	0.045	Yes	————	————	————	————
Rdh5	-1.268	0.001	Yes	dehydrogenase (PC00092).	————	————	————

Timp1	-1.261	0.016	Yes	protease inhibitor (PC00191).	extracellular space (GO:0005615). extracellular matrix (GO:0031012).	————	response to cytokine (GO:0034097). protein catabolic process (GO:0030163). membrane protein proteolysis (GO:0033619). cellular protein metabolic process (GO:0044267). negative regulation of endopeptidase activity (GO:0010951). negative regulation of protein catabolic process (GO:0042177). negative regulation of cellular catabolic process (GO:0031330).

HFD VS ND – DOWNREGULATED GENES							
Gene Symbol	**log2FC**	***P* value**	**Hit?**	**Molecular Function**	**Biological Function**	**Cellular Component**	**Protein Class**
							response to hormone (GO:0009725). cellular catabolic process (GO:0044248).
Nkapd1	-1.258	0.016	Yes	————	————	————	————
Tmem38b	-1.253	0.046	Yes	————	————	————	————
Lrrc20	-1.239	0.006	Yes	————	————	————	————
Ddx42	-1.239	0.044	Yes	————	nucleus (GO:0005634).	————	————
Azin1	-1.224	0.004	Yes	————	————	————	————
Slc25a51	-1.222	0.030	Yes	————	————	————	————

HFD VS ND – DOWNREGULATED GENES							
Gene Symbol	**log2FC**	***P* value**	**Hit?**	**Molecular Function**	**Biological Function**	**Cellular Component**	**Protein Class**
Qrich1	-1.218	0.015	Yes	zinc finger transcription factor (PC00244).	nucleus (GO:0005634).	————	regulation of cell morphogenesis (GO:0022604). cell morphogenesis (GO:0000902). transcription by RNA polymerase II (GO:0006366). regulation of transcription by RNA polymerase II (GO:0006357).

HFD VS ND – DOWNREGULATED GENES							
Gene Symbol	**log2FC**	***P* value**	**Hit?**	**Molecular Function**	**Biological Function**	**Cellular Component**	**Protein Class**
Id2	-1.214	0.048	Yes	DNA-binding transcription factor (PC00218).	nucleus (GO:0005634). cytoplasm (GO:0005737).	————	neuron differentiation (GO:0030182). negative regulation of neuron differentiation (GO:0045665). cell development (GO:0048468). regulation of cell cycle (GO:0051726). circadian rhythm (GO:0007623). cell cycle (GO:0007049). negative regulation of molecular function (GO:0044092).
Ddn	-1.206	0.008	No	————	————	————	————

HFD VS ND – DOWNREGULATED GENES							
Gene Symbol	**log2FC**	***P* value**	**Hit?**	**Molecular Function**	**Biological Function**	**Cellular Component**	**Protein Class**
Hdac9	-1.205	0.009	Yes	histone modifying enzyme (PC00261).	————	————	————
Qser1	-1.200	0.027	Yes	————	————	————	————
Gcc2	-1.184	0.021	Yes	————	————	————	————
Vps33b	-1.176	0.025	Yes	membrane trafficking regulatory protein (PC00151).	————	————	————
Setd2	-1.176	0.041	Yes	————	————	————	————
Capn7	-1.165	0.044	Yes	————	————	————	————
Plppr4	-1.165	0.042	No	————	————	————	————
Pter	-1.139	0.016	Yes	hydrolase (PC00121).	————	————	————

HFD VS ND – DOWNREGULATED GENES							
Gene Symbol	**log2FC**	***P* value**	**Hit?**	**Molecular Function**	**Biological Function**	**Cellular Component**	**Protein Class**
Btg1	-1.133	0.025	Yes	————	nucleus (GO:0005634). cytoplasm (GO:0005737).	————	cell population proliferation (GO:0008283). negative regulation of cell population proliferation (GO:0008285). mitotic nuclear division (GO:0140014). negative regulation of mitotic cell cycle (GO:0045930).
Lrif1	-1.130	0.032	No	————	————	————	————
Zbtb11	-1.123	0.035	Yes	————	————	————	————
Vegfa	-1.114	0.004	No	————	————	————	————
Fam91a1	-1.105	0.003	Yes	————	————	————	————
Esrrg	-1.094	0.021	Yes	————	————	————	————

HFD VS ND – DOWNREGULATED GENES							
Gene Symbol	**log2FC**	***P* value**	**Hit?**	**Molecular Function**	**Biological Function**	**Cellular Component**	**Protein Class**
Fam149a	-1.087	0.042	Yes	————	————	————	————
Pole4	-1.080	0.003	Yes	DNA binding protein (PC00009).	transferase complex, transferring phosphorus-containing groups (GO:0061695). ATPase complex (GO:1904949). nuclear chromatin (GO:0000790).	————	transcription, DNA-templated (GO:0006351). regulation of transcription, DNA-templated (GO:0006355).

HFD VS ND – DOWNREGULATED GENES							
Gene Symbol	**log2FC**	***P* value**	**Hit?**	**Molecular Function**	**Biological Function**	**Cellular Component**	**Protein Class**
Arid1a	-1.080	0.009	Yes	————	ATPase complex (GO:1904949). nuclear chromatin (GO:0000790). neuron part (GO:0097458). nucleoplasm (GO:0005654).	————	positive regulation of transcription, DNA-templated (GO:0045893). ATP-dependent chromatin remodeling (GO:0043044). transcription by RNA polymerase II (GO:0006366). regulation of transcription by RNA polymerase II (GO:0006357).
Fam3c	-1.075	0.037	Yes	antimicrobial response protein (PC00051).	extracellular space (GO:0005615).	————	————

HFD VS ND – DOWNREGULATED GENES							
Gene Symbol	**log2FC**	***P* value**	**Hit?**	**Molecular Function**	**Biological Function**	**Cellular Component**	**Protein Class**
Ift80	-1.073	0.022	Yes	————	centrosome (GO:0005813). centriole (GO:0005814). cilium (GO:0005929). plasma membrane region (GO:0098590). intraciliary transport particle B (GO:0030992).	————	intraciliary transport involved in cilium assembly (GO:0035735). vesicle targeting, trans-Golgi to periciliary membrane compartment (GO:0097712). axoneme assembly (GO:0035082). ciliary transition zone assembly (GO:1905349). protein localization to cilium (GO:0061512).
RT1-Ba	-1.061	0.000	Yes	————	————	————	————

HFD VS ND – DOWNREGULATED GENES							
Gene Symbol	**log2FC**	***P* value**	**Hit?**	**Molecular Function**	**Biological Function**	**Cellular Component**	**Protein Class**
Arcn1	-1.059	0.044	Yes	vesicle coat protein (PC00235).	cytosol (GO:0005829). vacuole (GO:0005773). plasma membrane (GO:0005886). COPI vesicle coat (GO:0030126).	————	endoplasmic reticulum to Golgi vesicle-mediated transport (GO:0006888). organelle localization (GO:0051640). retrograde vesicle-mediated transport, Golgi to endoplasmic reticulum (GO:0006890).
Plpp4	-1.058	0.015	Yes	phosphatase (PC00181).	————	————	————
Jade1	-1.055	0.041	Yes	zinc finger transcription factor (PC00244).	————	————	————

HFD VS ND – DOWNREGULATED GENES							
Gene Symbol	**log2FC**	***P* value**	**Hit?**	**Molecular Function**	**Biological Function**	**Cellular Component**	**Protein Class**
Lyar	-1.051	0.046	Yes	RNA processing factor (PC00147).	nucleolus (GO:0005730).	————	negative regulation of transcription by RNA polymerase II (GO:0000122). transcription by RNA polymerase II (GO:0006366). rRNA processing (GO:0006364).
Grp	-1.047	0.036	Yes	————	————	————	————
Phf2	-1.041	0.048	Yes	————	————	————	————
Ptcra	-1.040	0.004	Yes	————	————	————	————
Tjp1	-1.039	0.027	Yes	tight junction (PC00214).	————	————	————
LOC100174910	-1.038	0.016	Yes	————	————	————	————

HFD VS ND – DOWNREGULATED GENES							
Gene Symbol	**log2FC**	***P* value**	**Hit?**	**Molecular Function**	**Biological Function**	**Cellular Component**	**Protein Class**
Dyrk2	-1.033	0.040	Yes	non-receptor tyrosine protein kinase (PC00168). non-receptor serine/threonine protein kinase (PC00167).	nucleus (GO:0005634). cytoskeleton (GO:0005856). cytoplasm (GO:0005737).	————	peptidyl-serine phosphorylation (GO:0018105). peptidyl-threonine phosphorylation (GO:0018107).
Dcdc2	-1.033	0.040	Yes	————	microtubule organizing center (GO:0005815). cortical actin cytoskeleton (GO:0030864). microtubule (GO:0005874).	————	————
Crls1	-1.028	0.030	Yes	transferase (PC00220).	————	————	glycerophospholipid biosynthetic process (GO:0046474).
Omg	-1.012	0.033	Yes	————	————	————	————

HFD VS ND – DOWNREGULATED GENES							
Gene Symbol	**log2FC**	***P* value**	**Hit?**	**Molecular Function**	**Biological Function**	**Cellular Component**	**Protein Class**
Tbc1d15	-1.010	0.029	Yes	GTPase-activating protein (PC00257).	————	————	intracellular protein transport (GO:0006886). positive regulation of GTPase activity (GO:0043547).

II. Deregulated genes in HFD+PB vs ND comparison

Table 0.6. Highly upregulated genes in HFD+PB rats when compared to ND and their functional classification as determined by PANTHER bioinformatics.

Genes were determined to be highly deregulated if they had a log2 fold change (log2FC) > 1 and a *P* value < 0.05. "Hit" refers to whether the gene was found by PANTHER.

HFD+PB vs ND – UPREGULATED GENES							
Gene Symbol	**log2FC**	***P* value**	**Hit?**	**Molecular Function**	**Biological Function**	**Cellular Component**	**Protein Class**
Npb	3.282	0.002	Yes	G protein-coupled receptor binding (GO:0001664).	G protein-coupled receptor signaling pathway (GO:0007186). behavior (GO:0007610).	————	————
Dclre1c	3.036	0.036	Yes	5'-3' exonuclease activity (GO:0008409). damaged DNA binding (GO:0003684). exodeoxyribonuclease activity, producing 5'-phosphomonoesters (GO:0016895).	interstrand cross-link repair (GO:0036297). telomere capping (GO:0016233). double-strand break repair via nonhomologous end joining (GO:0006303).	nuclear chromosome, telomeric region (GO:0000784).	————
Zmynd15	3.036	0.037	Yes	————	————	————	————

HFD+PB vs ND – UPREGULATED GENES							
Gene Symbol	**log2FC**	***P* value**	**Hit?**	**Molecular Function**	**Biological Function**	**Cellular Component**	**Protein Class**
Zfp267	3.036	0.024	Yes	————	————	————	C2H2 zinc finger transcription factor (PC00248).
Itga2	2.603	0.040	Yes	————	————	————	————
Pla2g1b	2.567	0.017	Yes	————	————	————	phospholipase (PC00186).
Sypl1	2.451	0.024	Yes	syntaxin binding (GO:0019905).	————	synaptic vesicle membrane (GO:0030672). vacuole (GO:0005773). plasma membrane (GO:0005886).	membrane trafficking regulatory protein (PC00151).
Pth1r	2.449	0.005	Yes	G protein-coupled peptide receptor activity (GO:0008528). peptide hormone binding (GO:0017046).	————	————	————
Ints13	2.349	0.031	Yes	————	————	————	————

HFD+PB vs ND – UPREGULATED GENES							
Gene Symbol	**log2FC**	***P* value**	**Hit?**	**Molecular Function**	**Biological Function**	**Cellular Component**	**Protein Class**
Golm1	2.243	0.020	Yes	————	————	————	————
Neto2	2.186	0.017	No	————	————	————	————
Adgra3	2.127	0.046	Yes	————	————	————	————
Tiam1	2.127	0.034	Yes	Rac GTPase binding (GO:0048365). Rho guanyl-nucleotide exchange factor activity (GO:0005089).	positive regulation of axonogenesis (GO:0050772). small GTPase mediated signal transduction (GO:0007264). axonogenesis (GO:0007409). positive regulation of GTPase activity (GO:0043547).	cytosol (GO:0005829). plasma membrane (GO:0005886).	————
Slc36a1	2.058	0.013	Yes	amino acid transmembrane transporter activity (GO:0015171).	amino acid transmembrane transport (GO:0003333).	————	amino acid transporter (PC00046).

HFD+PB vs ND – UPREGULATED GENES							
Gene Symbol	**log2FC**	***P* value**	**Hit?**	**Molecular Function**	**Biological Function**	**Cellular Component**	**Protein Class**
Fcgr2b	2.035	0.001	Yes	————	————	————	immunoglobulin receptor superfamily (PC00124).
Sipa1	1.865	0.006	Yes	————	————	————	GTPase-activating protein (PC00257).
Crip3	1.791	0.037	Yes	————	————	————	actin or actin-binding cytoskeletal protein (PC00041).
Doc2a	1.728	0.017	Yes	————	————	————	————
Ccdc187	1.672	0.037	Yes	————	————	————	non-motor microtubule binding protein (PC00166).

HFD+PB vs ND – UPREGULATED GENES							
Gene Symbol	**log2FC**	***P* value**	**Hit?**	**Molecular Function**	**Biological Function**	**Cellular Component**	**Protein Class**
Xrcc4	1.631	0.047	Yes	————	positive regulation of catalytic activity (GO:0043085). double-strand break repair via nonhomologous end joining (GO:0006303). response to ionizing radiation (GO:0010212).	nuclear part (GO:0044428). DNA repair complex (GO:1990391).	————
Larp7	1.602	0.004	No	————	————	————	————
Eloa	1.478	0.013	No	————	————	————	————
Insig2	1.451	0.036	Yes	————	————	————	————
St6galnac2	1.450	0.000	Yes	————	————	————	————
Rhbdl2	1.450	0.016	Yes	————	————	————	————
Sez6l	1.385	0.007	Yes	————	————	————	————
RGD1305347	1.374	0.006	Yes	————	————	————	————
Zfp426	1.342	0.014	Yes	————	————	————	————

HFD+PB vs ND – UPREGULATED GENES							
Gene Symbol	**log2FC**	***P* value**	**Hit?**	**Molecular Function**	**Biological Function**	**Cellular Component**	**Protein Class**
Xbp1	1.309	0.011	No	————	————	————	————
Nrg4	1.280	0.012	No	————	————	————	————
Sntb2	1.280	0.039	Yes	————	————	plasma membrane protein complex (GO:0098797). intracellular (GO:0005622).	————
Tpp1	1.259	0.001	No	————	————	————	————
Capn1	1.244	0.024	No	————	————	————	————
Cyren	1.155	0.029	Yes	————	————	————	————
Lexm	1.128	0.030	Yes	————	————	————	————
Gli4	1.106	0.049	Yes	————	————	————	C2H2 zinc finger transcription factor (PC00248).
Cys1	1.088	0.017	No	————	————	————	————

HFD+PB vs ND – UPREGULATED GENES							
Gene Symbol	**log2FC**	***P* value**	**Hit?**	**Molecular Function**	**Biological Function**	**Cellular Component**	**Protein Class**
Cenpv	1.077	0.015	Yes	————	chromatin remodeling (GO:0006338). membrane fission (GO:0090148). protein-DNA complex assembly (GO:0065004). regulation of chromosome organization (GO:0033044). chromatin assembly or disassembly (GO:0006333). cytokinesis (GO:0000910). DNA packaging (GO:0006323). positive regulation of cytokinesis (GO:0032467).	nucleus (GO:0005634). spindle midzone (GO:0051233). kinetochore (GO:0000776).	————
Cyp11a1	1.072	0.038	No	————	————	————	————

HFD+PB vs ND – UPREGULATED GENES							
Gene Symbol	**log2FC**	***P* value**	**Hit?**	**Molecular Function**	**Biological Function**	**Cellular Component**	**Protein Class**
Tubb6	1.058	0.030	Yes	GTP binding (GO:0005525). structural molecule activity (GO:0005198).	mitotic nuclear division (GO:0140014). microtubule cytoskeleton organization (GO:0000226).	cytoplasm (GO:0005737). microtubule (GO:0005874).	tubulin (PC00228).
Ppih	1.035	0.029	Yes	catalytic activity, acting on a protein (GO:0140096). drug binding (GO:0008144). peptide binding (GO:0042277). unfolded protein binding (GO:0051082). isomerase activity (GO:0016853).	protein folding (GO:0006457).	————	————
Frem3	1.015	0.017	Yes	————	————	————	————

HFD+PB vs ND – UPREGULATED GENES							
Gene Symbol	**log2FC**	***P* value**	**Hit?**	**Molecular Function**	**Biological Function**	**Cellular Component**	**Protein Class**
Zfat	1.005	0.018	Yes	DNA binding (GO:0003677). DNA-binding transcription factor activity (GO:0003700).	transcription, DNA-templated (GO:0006351). regulation of transcription, DNA-templated (GO:0006355).	nucleus (GO:0005634).	C2H2 zinc finger transcription factor (PC00248).

Table 0.7. Highly downregulated genes in HFD+PB rats when compared to ND and their functional classification as determined by PANTHER bioinformatics.

Genes were determined to be highly deregulated if they had a log2 fold change (log2FC) < -1 and a *P* value < 0.05. "Hit" refers to whether the gene was found by PANTHER.

HFD+PB vs ND - DOWNREGULATED							
Gene Symbol	**log2FC**	***P* value**	**Hit?**	**Molecular Function**	**Biological Function**	**Cellular Component**	**Protein Class**
Ptprz1	-5.524	0.000	No	————	————	————	————
Pter	-4.524	0.000	Yes	————	————	————	hydrolase (PC00121).
Fam84a	-4.176	0.007	Yes	————	————	————	————
Lpar1	-4.113	0.000	Yes	————	————	————	G-protein coupled receptor (PC00021).
Scai	-3.990	0.007	Yes	transcription corepressor activity (GO:0003714).	————	nucleus (GO:0005634).	————

HFD+PB vs ND - DOWNREGULATED							
Gene Symbol	**log2FC**	***P* value**	**Hit?**	**Molecular Function**	**Biological Function**	**Cellular Component**	**Protein Class**
Gpr88	-3.968	0.000	Yes	G protein-coupled receptor activity (GO:0004930).	cellular response to light stimulus (GO:0071482). response to external stimulus (GO:0009605). G protein-coupled receptor signaling pathway (GO:0007186). detection of stimulus (GO:0051606).	integral component of plasma membrane (GO:0005887).	G-protein coupled receptor (PC00021).
Wasf1	-3.943	0.000	Yes	————	————	————	non-motor actin binding protein (PC00165).
Vwa1	-3.940	0.024	No	————	————	————	————

HFD+PB vs ND - DOWNREGULATED							
Gene Symbol	**log2FC**	***P* value**	**Hit?**	**Molecular Function**	**Biological Function**	**Cellular Component**	**Protein Class**
Ldb2	-3.940	0.010	Yes	RNA polymerase II-specific DNA-binding transcription factor binding (GO:0061629). activating transcription factor binding (GO:0033613).	negative regulation of transcription by RNA polymerase II (GO:0000122). multicellular organism development (GO:0007275). transcription by RNA polymerase II (GO:0006366). positive regulation of transcription by RNA polymerase II (GO:0045944).	nucleus (GO:0005634). transcription factor complex (GO:0005667).	transcription cofactor (PC00217).

HFD+PB vs ND - DOWNREGULATED							
Gene Symbol	**log2FC**	***P* value**	**Hit?**	**Molecular Function**	**Biological Function**	**Cellular Component**	**Protein Class**
Grm3	-3.940	0.009	Yes	G protein-coupled receptor activity (GO:0004930). glutamate receptor activity (GO:0008066). amino acid binding (GO:0016597). adenylate cyclase activity (GO:0004016).	G protein-coupled receptor signaling pathway (GO:0007186). regulation of synaptic transmission, glutamatergic (GO:0051966). glutamate receptor signaling pathway (GO:0007215). synaptic transmission, glutamatergic (GO:0035249).	integral component of plasma membrane (GO:0005887).	G-protein coupled receptor (PC00021).
RT1-N3	-3.887	0.012	Yes	peptide binding (GO:0042277). signaling receptor binding (GO:0005102).	T cell mediated immunity (GO:0002456). positive regulation of adaptive immune response (GO:0002821).	————	————

HFD+PB vs ND - DOWNREGULATED							
Gene Symbol	**log2FC**	***P* value**	**Hit?**	**Molecular Function**	**Biological Function**	**Cellular Component**	**Protein Class**
Fgf12	-3.887	0.009	Yes	————	————	————	growth factor (PC00112).
Slc32a1	-3.836	0.000	Yes	neurotransmitter transmembrane transporter activity (GO:0005326). solute:proton symporter activity (GO:0015295). amino acid transmembrane transporter activity (GO:0015171). monocarboxylic acid transmembrane transporter activity (GO:0008028).	neurotransmitter transport (GO:0006836). synaptic vesicle cycle (GO:0099504).	dendrite (GO:0030425). plasma membrane region (GO:0098590). synaptic vesicle membrane (GO:0030672). vacuole (GO:0005773). integral component of organelle membrane (GO:0031301). neuron projection terminus (GO:0044306).	————
B3gat2	-3.833	0.027	No	————	————	————	————
Chia	-3.833	0.020	No	————	————	————	————
Dtwd1	-3.833	0.007	No	————	————	————	————

HFD+PB vs ND - DOWNREGULATED							
Gene Symbol	**log2FC**	***P* value**	**Hit?**	**Molecular Function**	**Biological Function**	**Cellular Component**	**Protein Class**
Scn4b	-3.776	0.009	Yes	————	————	————	scaffold/adaptor protein (PC00226).
Galnt18	-3.776	0.009	Yes	————	————	Golgi apparatus (GO:0005794). vacuole (GO:0005773). plasma membrane (GO:0005886).	glycosyltransferase (PC00111).
Tbc1d8b	-3.717	0.045	Yes	GTPase activity (GO:0003924). GTPase activator activity (GO:0005096). Rab GTPase binding (GO:0017137).	intracellular protein transport (GO:0006886). positive regulation of GTPase activity (GO:0043547).	————	GTPase-activating protein (PC00257).

HFD+PB vs ND - DOWNREGULATED							
Gene Symbol	**log2FC**	***P* value**	**Hit?**	**Molecular Function**	**Biological Function**	**Cellular Component**	**Protein Class**
Dennd1b	-3.717	0.018	Yes	phosphatidylinositol phosphate binding (GO:1901981). Rab guanyl-nucleotide exchange factor activity (GO:0017112).	vesicle budding from membrane (GO:0006900). membrane invagination (GO:0010324). endocytosis (GO:0006897). endocytic recycling (GO:0032456).	intracellular membrane-bounded organelle (GO:0043231). cytosol (GO:0005829).	————
Btbd17	-3.690	0.002	Yes	————	————	————	————
Snca	-3.690	0.000	Yes	————	————	————	membrane trafficking regulatory protein (PC00151).

HFD+PB vs ND - DOWNREGULATED							
Gene Symbol	**log2FC**	***P* value**	**Hit?**	**Molecular Function**	**Biological Function**	**Cellular Component**	**Protein Class**
Kif6	-3.591	0.025	Yes	ATPase activity (GO:0016887). microtubule binding (GO:0008017). motor activity (GO:0003774).	microtubule-based movement (GO:0007018).	microtubule associated complex (GO:0005875). microtubule (GO:0005874).	microtubule binding motor protein (PC00156).
Tmem178a	-3.454	0.027	No	————	————	————	————
Wdr89	-3.454	0.022	Yes	————	————	————	————
Adhfe1	-3.454	0.013	Yes	oxidoreductase activity, acting on the CH-OH group of donors, NAD or NADP as acceptor (GO:0016616).	————	————	————

HFD+PB vs ND - DOWNREGULATED							
Gene Symbol	**log2FC**	***P* value**	**Hit?**	**Molecular Function**	**Biological Function**	**Cellular Component**	**Protein Class**
Rab40b	-3.421	0.008	Yes	————	vesicle fusion to plasma membrane (GO:0099500). organelle localization (GO:0051640). regulation of exocytosis (GO:0017157). protein secretion (GO:0009306). protein localization to plasma membrane (GO:0072659).	endosome (GO:0005768). synaptic vesicle (GO:0008021). vacuole (GO:0005773). plasma membrane (GO:0005886).	————
Aqp4	-3.373	0.021	Yes	————	————	basolateral plasma membrane (GO:0016323).	transporter (PC00227).
Omg	-3.367	0.000	Yes	————	————	————	————

HFD+PB vs ND - DOWNREGULATED							
Gene Symbol	**log2FC**	***P* value**	**Hit?**	**Molecular Function**	**Biological Function**	**Cellular Component**	**Protein Class**
Pex11a	-3.302	0.026	Yes	————	organelle fission (GO:0048285). peroxisome organization (GO:0007031). regulation of cellular component size (GO:0032535).	peroxisomal membrane (GO:0005778).	————
Ercc5	-3.220	0.026	Yes	endodeoxyribonuclease activity (GO:0004520). single-stranded DNA binding (GO:0003697).	nucleotide-excision repair, DNA incision (GO:0033683).	nucleus (GO:0005634).	————
Ncam1	-3.202	0.000	No	————	————	————	————
Tmem229a	-3.180	0.015	Yes	————	————	————	————
Ifrd1	-3.135	0.007	No	————	————	————	————

HFD+PB vs ND - DOWNREGULATED							
Gene Symbol	**log2FC**	***P* value**	**Hit?**	**Molecular Function**	**Biological Function**	**Cellular Component**	**Protein Class**
Gap43	-3.135	0.001	Yes	calmodulin binding (GO:0005516). carbohydrate derivative binding (GO:0097367). phosphatidylinositol phosphate binding (GO:1901981).	wound healing (GO:0042060). axon guidance (GO:0007411). cellular response to stress (GO:0033554). developmental growth (GO:0048589). tissue development (GO:0009888).	postsynaptic density (GO:0014069). cytoplasm (GO:0005737). plasma membrane (GO:0005886).	————
Icam5	-3.134	0.003	Yes	integrin binding (GO:0005178).	cell adhesion (GO:0007155).	integral component of plasma membrane (GO:0005887).	————
Gad2	-3.134	0.001	Yes	————	————	————	decarboxylase (PC00089).
RGD1565323	-3.132	0.024	No	————	————	————	————

HFD+PB vs ND - DOWNREGULATED							
Gene Symbol	**log2FC**	***P* value**	**Hit?**	**Molecular Function**	**Biological Function**	**Cellular Component**	**Protein Class**
Gpr37	-3.113	0.001	Yes	G protein-coupled peptide receptor activity (GO:0008528). peptide binding (GO:0042277).	adenylate cyclase-inhibiting G protein-coupled receptor signaling pathway (GO:0007193). MAPK cascade (GO:0000165). negative regulation of adenylate cyclase activity (GO:0007194). positive regulation of MAPK cascade (GO:0043410). negative regulation of cAMP-mediated signaling (GO:0043951). cAMP-mediated signaling (GO:0019933).	receptor complex (GO:0043235). plasma membrane (GO:0005886).	————

HFD+PB vs ND - DOWNREGULATED							
Gene Symbol	**log2FC**	***P* value**	**Hit?**	**Molecular Function**	**Biological Function**	**Cellular Component**	**Protein Class**
Nap1l5	-3.073	0.008	Yes	————	————	————	chromatin/chromatin-binding, or -regulatory protein (PC00077).
Nov	-3.042	0.007	Yes	heparin binding (GO:0008201). integrin binding (GO:0005178).	cell death (GO:0008219). signal transduction (GO:0007165). negative regulation of cell death (GO:0060548). cell adhesion (GO:0007155).	extracellular matrix (GO:0031012).	growth factor (PC00112).
Dpf1	-3.009	0.006	No	————	————	————	————
Vsnl1	-2.995	0.000	Yes	————	————	————	————
Ntm	-2.993	0.029	No	————	————	————	————

HFD+PB vs ND - DOWNREGULATED							
Gene Symbol	**log2FC**	***P* value**	**Hit?**	**Molecular Function**	**Biological Function**	**Cellular Component**	**Protein Class**
Gclc	-2.993	0.007	Yes	ligase activity (GO:0016874).	cofactor biosynthetic process (GO:0051188). glutathione metabolic process (GO:0006749). peptide biosynthetic process (GO:0043043).	————	ligase (PC00142).
Grin2b	-2.983	0.004	No	————	————	————	————
Arhgef16	-2.943	0.042	Yes	————	————	————	————
Edil3	-2.924	0.028	Yes	————	————	————	oxidoreductase (PC00176).
Abca8a	-2.907	0.007	Yes	ATPase activity (GO:0016887). ATPase-coupled transmembrane transporter activity (GO:0042626). lipid transporter activity (GO:0005319).	lipid transport (GO:0006869).	mitochondrial inner membrane (GO:0005743).	ATP-binding cassette (ABC). transporter (PC00003).

HFD+PB vs ND - DOWNREGULATED							
Gene Symbol	**log2FC**	***P* value**	**Hit?**	**Molecular Function**	**Biological Function**	**Cellular Component**	**Protein Class**
Rasa2	-2.890	0.027	Yes	————	————	————	GTPase-activating protein (PC00257).
Aurkb	-2.890	0.016	Yes	protein serine/threonine kinase activity (GO:0004674).	membrane fission (GO:0090148). mitotic spindle organization (GO:0007052). mitotic nuclear division (GO:0140014). regulation of cytokinesis (GO:0032465). cytokinesis (GO:0000910).	spindle microtubule (GO:0005876). centrosome (GO:0005813). condensed nuclear chromosome, centromeric region (GO:0000780). spindle midzone (GO:0051233). centriole (GO:0005814). spindle pole (GO:0000922). microtubule associated complex (GO:0005875).	non-receptor serine/threonine protein kinase (PC00167).

HFD+PB vs ND - DOWNREGULATED							
Gene Symbol	**log2FC**	***P* value**	**Hit?**	**Molecular Function**	**Biological Function**	**Cellular Component**	**Protein Class**
Gng8	-2.871	0.008	Yes	protein binding (GO:0005515).	G protein-coupled receptor signaling pathway (GO:0007186).	catalytic complex (GO:1902494). leaflet of membrane bilayer (GO:0097478). plasma membrane protein complex (GO:0098797). extrinsic component of cytoplasmic side of plasma membrane (GO:0031234). cytoplasmic part (GO:0044444).	heterotrimeric G-protein (PC00117).
Dtna	-2.851	0.001	Yes	————	————	————	————
Prkar2b	-2.836	0.034	Yes	————	————	————	————
S100a3	-2.836	0.019	Yes	————	————	————	calmodulin-related (PC00061).

HFD+PB vs ND - DOWNREGULATED							
Gene Symbol	**log2FC**	***P* value**	**Hit?**	**Molecular Function**	**Biological Function**	**Cellular Component**	**Protein Class**
Meis2	-2.836	0.018	Yes	————	————	————	homeodomain transcription factor (PC00119).
Arpp21	-2.835	0.000	Yes	————	————	————	————
Gng13	-2.811	0.001	Yes	————	————	————	heterotrimeric G-protein (PC00117).
Frrs1l	-2.797	0.016	Yes	————	————	————	————
Cav1	-2.797	0.005	No	————	————	————	————
Ugt8	-2.797	0.003	Yes	UDP-glycosyltransferase activity (GO:0008194).	————	intracellular membrane-bounded organelle (GO:0043231).	————
Fam131b	-2.790	0.001	No	————	————	————	————

HFD+PB vs ND - DOWNREGULATED							
Gene Symbol	**log2FC**	***P* value**	**Hit?**	**Molecular Function**	**Biological Function**	**Cellular Component**	**Protein Class**
Usp18	-2.780	0.033	Yes	thiol-dependent ubiquitin-specific protease activity (GO:0004843). cysteine-type endopeptidase activity (GO:0004197).	protein deubiquitination (GO:0016579).	————	cysteine protease (PC00081).
Ctrb1	-2.779	0.047	No	————	————	————	————
Gatm	-2.779	0.040	No	————	————	————	————
Enpp4	-2.778	0.000	Yes	————	————	————	nucleotide phosphatase (PC00173).
Gltpd2	-2.759	0.005	Yes	phospholipid transporter activity (GO:0005548). amide binding (GO:0033218). phospholipid binding (GO:0005543).	lipid transport (GO:0006869). membrane organization (GO:0061024). amide transport (GO:0042886).	cytosol (GO:0005829).	transfer/carrier protein (PC00219).

HFD+PB vs ND - DOWNREGULATED							
Gene Symbol	**log2FC**	***P* value**	**Hit?**	**Molecular Function**	**Biological Function**	**Cellular Component**	**Protein Class**
Rbfox1	-2.739	0.000	Yes	————	nervous system development (GO:0007399).	————	RNA splicing factor (PC00148).
Agt	-2.728	0.022	Yes	endopeptidase inhibitor activity (GO:0004866). serine-type endopeptidase activity (GO:0004252). protease binding (GO:0002020).	proteolysis (GO:0006508). cellular protein metabolic process (GO:0044267). negative regulation of endopeptidase activity (GO:0010951).	extracellular space (GO:0005615).	protease inhibitor (PC00191).
Dclk3	-2.720	0.037	Yes	————	————	————	non-receptor serine/threonine protein kinase (PC00167).
Tspan2	-2.699	0.002	Yes	————	————	integral component of plasma membrane (GO:0005887).	————

HFD+PB vs ND - DOWNREGULATED							
Gene Symbol	**log2FC**	***P* value**	**Hit?**	**Molecular Function**	**Biological Function**	**Cellular Component**	**Protein Class**
Mal	-2.689	0.001	Yes	structural molecule activity (GO:0005198).	myelination (GO:0042552).	integral component of membrane (GO:0016021).	membrane traffic protein (PC00150).
Arhgap21	-2.659	0.009	Yes	————	————	————	————
Cttnbp2	-2.659	0.043	Yes	————	————	————	————

HFD+PB vs ND - DOWNREGULATED							
Gene Symbol	**log2FC**	***P* value**	**Hit?**	**Molecular Function**	**Biological Function**	**Cellular Component**	**Protein Class**
Bbs5	-2.658	0.001	Yes	phosphatidylinositol-3-phosphate binding (GO:0032266).	intraciliary transport involved in cilium assembly (GO:0035735). vesicle targeting, trans-Golgi to periciliary membrane compartment (GO:0097712). axoneme assembly (GO:0035082). ciliary transition zone assembly (GO:1905349). protein localization to cilium (GO:0061512).	BBSome (GO:0034464). ciliary basal body (GO:0036064). intraciliary transport particle (GO:0030990). plasma membrane region (GO:0098590).	————
Thrsp	-2.637	0.044	No	————	————	————	————

HFD+PB vs ND - DOWNREGULATED							
Gene Symbol	**log2FC**	***P* value**	**Hit?**	**Molecular Function**	**Biological Function**	**Cellular Component**	**Protein Class**
Pik3c2b	-2.637	0.029	Yes	phosphotransferase activity, alcohol group as acceptor (GO:0016773). kinase activity (GO:0016301).	phosphatidylinositol 3-kinase signaling (GO:0014065). phosphatidylinositol-3-phosphate biosynthetic process (GO:0036092). phosphatidylinositol phosphorylation (GO:0046854). cell migration (GO:0016477).	phosphatidylinositol 3-kinase complex (GO:0005942). cytoplasm (GO:0005737). plasma membrane (GO:0005886).	kinase (PC00137).
Pcdha6	-2.637	0.005	No	————	————	————	————
Ptprd	-2.620	0.003	Yes	phosphoprotein phosphatase activity (GO:0004721).	protein dephosphorylation (GO:0006470). synaptic membrane adhesion (GO:0099560).	————	protein phosphatase (PC00195).

HFD+PB vs ND - DOWNREGULATED							
Gene Symbol	**log2FC**	***P* value**	**Hit?**	**Molecular Function**	**Biological Function**	**Cellular Component**	**Protein Class**
Diaph3	-2.595	0.047	No	————	————	————	————
LOC103694870	-2.594	0.001	Yes	solute:sodium symporter activity (GO:0015370). sugar transmembrane transporter activity (GO:0051119).	sodium ion transport (GO:0006814).	integral component of membrane (GO:0016021). plasma membrane (GO:0005886).	secondary carrier transporter (PC00258).
Ak5	-2.549	0.029	Yes	————	————	————	nucleotide kinase (PC00172).
Kif5a	-2.547	0.000	No	————	————	————	————
Taf5	-2.542	0.008	Yes	————	————	————	————
Pdik1l	-2.528	0.049	Yes	protein serine/threonine kinase activity (GO:0004674).	————	nucleus (GO:0005634).	non-receptor serine/threonine protein kinase (PC00167).

HFD+PB vs ND - DOWNREGULATED							
Gene Symbol	**log2FC**	***P* value**	**Hit?**	**Molecular Function**	**Biological Function**	**Cellular Component**	**Protein Class**
Tph2	-2.528	0.040	Yes	oxidoreductase activity, acting on paired donors, with incorporation or reduction of molecular oxygen (GO:0016705). monooxygenase activity (GO:0004497).	————	plasma membrane region (GO:0098590). neuron projection (GO:0043005).	————
Phlda1	-2.504	0.046	No	————	————	————	————
Lrp12	-2.493	0.004	Yes	————	————	————	————
RGD1308544	-2.485	0.011	Yes	————	————	————	————
Matk	-2.480	0.009	Yes	————	————	————	————
Gpm6b	-2.480	0.001	No	————	————	————	————
Plp1	-2.468	0.014	Yes	————	neuron projection development (GO:0031175).	plasma membrane (GO:0005886).	myelin protein (PC00161).

HFD+PB vs ND - DOWNREGULATED							
Gene Symbol	**log2FC**	***P* value**	**Hit?**	**Molecular Function**	**Biological Function**	**Cellular Component**	**Protein Class**
Mt-nd4l	-2.457	0.000	Yes	NADH dehydrogenase activity (GO:0003954).	————	NADH dehydrogenase complex (GO:0030964).	oxidoreductase (PC00176).
Esm1	-2.456	0.012	Yes	————	————	————	————
Smyd4	-2.456	0.001	Yes	————	————	————	————
Ptn	-2.444	0.000	Yes	growth factor activity (GO:0008083).	————	————	growth factor (PC00112).
Sst	-2.442	0.001	Yes	————	regulation of cell migration (GO:0030334). cell migration (GO:0016477).	extracellular space (GO:0005615).	peptide hormone (PC00179).
Nfyb	-2.432	0.002	Yes	————	————	————	————

HFD+PB vs ND - DOWNREGULATED							
Gene Symbol	**log2FC**	***P* value**	**Hit?**	**Molecular Function**	**Biological Function**	**Cellular Component**	**Protein Class**
Rit2	-2.428	0.004	Yes	GTP binding (GO:0005525). calmodulin binding (GO:0005516). GTPase activity (GO:0003924).	neuron projection development (GO:0031175). Ras protein signal transduction (GO:0007265). positive regulation of neuron projection development (GO:0010976).	plasma membrane (GO:0005886).	small GTPase (PC00208).
Efnb3	-2.421	0.019	Yes	signaling receptor binding (GO:0005102).	axon guidance (GO:0007411). transmembrane receptor protein tyrosine kinase signaling pathway (GO:0007169).	plasma membrane (GO:0005886).	membrane-bound signaling molecule (PC00152).
Carmil2	-2.398	0.014	Yes	————	————	————	————

HFD+PB vs ND - DOWNREGULATED							
Gene Symbol	**log2FC**	***P* value**	**Hit?**	**Molecular Function**	**Biological Function**	**Cellular Component**	**Protein Class**
Ttc9b	-2.391	0.002	Yes	————	————	————	————
Snapc1	-2.383	0.038	Yes	sequence-specific DNA binding (GO:0043565).	transcription by RNA polymerase III (GO:0006383). transcription by RNA polymerase II (GO:0006366).	nuclear transcription factor complex (GO:0044798).	————
Efemp1	-2.383	0.031	No	————	————	————	————

HFD+PB vs ND - DOWNREGULATED							
Gene Symbol	**log2FC**	***P* value**	**Hit?**	**Molecular Function**	**Biological Function**	**Cellular Component**	**Protein Class**
Rxfp2	-2.368	0.022	Yes	G protein-coupled peptide receptor activity (GO:0008528). peptide binding (GO:0042277).	regulation of cAMP-mediated signaling (GO:0043949). regulation of adenylate cyclase activity (GO:0045761). adenylate cyclase-activating G protein-coupled receptor signaling pathway (GO:0007189). activation of adenylate cyclase activity (GO:0007190). hormone-mediated signaling pathway (GO:0009755).	integral component of plasma membrane (GO:0005887).	G-protein coupled receptor (PC00021).
Ercc6	-2.357	0.044	Yes	————	————	————	————

HFD+PB vs ND - DOWNREGULATED							
Gene Symbol	**log2FC**	***P* value**	**Hit?**	**Molecular Function**	**Biological Function**	**Cellular Component**	**Protein Class**
Magohb	-2.345	0.027	Yes	————	RNA splicing (GO:0008380).	exon-exon junction complex (GO:0035145). catalytic step 2 spliceosome (GO:0071013). U5 snRNP (GO:0005682). Prp19 complex (GO:0000974).	————

HFD+PB vs ND - DOWNREGULATED							
Gene Symbol	**log2FC**	***P* value**	**Hit?**	**Molecular Function**	**Biological Function**	**Cellular Component**	**Protein Class**
Efhc2	-2.305	0.033	Yes	alpha-tubulin binding (GO:0043014).	membrane fission (GO:0090148). mitotic cytokinesis (GO:0000281). mitotic spindle organization (GO:0007052). cilium-dependent cell motility (GO:0060285). mitotic nuclear division (GO:0140014). cilium movement (GO:0003341).	mitotic spindle (GO:0072686). intraciliary transport particle (GO:0030990). plasma membrane region (GO:0098590). axoneme (GO:0005930). microtubule (GO:0005874).	————

HFD+PB vs ND - DOWNREGULATED							
Gene Symbol	**log2FC**	***P* value**	**Hit?**	**Molecular Function**	**Biological Function**	**Cellular Component**	**Protein Class**
Zfp280d	-2.305	0.012	Yes	DNA binding (GO:0003677). DNA-binding transcription factor activity (GO:0003700).	transcription, DNA-templated (GO:0006351). regulation of transcription, DNA-templated (GO:0006355).	nucleus (GO:0005634).	C2H2 zinc finger transcription factor (PC00248).
Gdap1l1	-2.304	0.033	Yes	————	protein targeting to mitochondrion (GO:0006626). mitochondrial fusion (GO:0008053). mitochondrial fission (GO:0000266).	integral component of mitochondrial outer membrane (GO:0031307).	————
Tubb3	-2.284	0.001	Yes	GTP binding (GO:0005525). structural molecule activity (GO:0005198).	mitotic nuclear division (GO:0140014). microtubule cytoskeleton organization (GO:0000226).	cytoplasm (GO:0005737). microtubule (GO:0005874).	tubulin (PC00228).

HFD+PB vs ND - DOWNREGULATED							
Gene Symbol	**log2FC**	***P* value**	**Hit?**	**Molecular Function**	**Biological Function**	**Cellular Component**	**Protein Class**
Kpna2	-2.265	0.041	Yes	signal sequence binding (GO:0005048).	NLS-bearing protein import into nucleus (GO:0006607).	cytosol (GO:0005829). vacuole (GO:0005773). plasma membrane (GO:0005886). nuclear pore (GO:0005643). nucleoplasm (GO:0005654).	transporter (PC00227).
Klhl5	-2.265	0.019	Yes	————	————	————	scaffold/adaptor protein (PC00226).
Gria3	-2.250	0.028	No	————	————	————	————
Zfx	-2.250	0.022	Yes	————	multicellular organism development (GO:0007275).	————	C2H2 zinc finger transcription factor (PC00248).
Gad1	-2.222	0.001	Yes	————	————	————	decarboxylase (PC00089).
Ptpn5	-2.222	0.006	No	————	————	————	————
Ptcra	-2.211	0.000	Yes	————	————	————	————

HFD+PB vs ND - DOWNREGULATED							
Gene Symbol	**log2FC**	***P* value**	**Hit?**	**Molecular Function**	**Biological Function**	**Cellular Component**	**Protein Class**
Stoml3	-2.210	0.021	Yes	————	————	plasma membrane (GO:0005886).	cytoskeletal protein (PC00085).
Agap2	-2.203	0.000	Yes	————	————	nucleus (GO:0005634).	————
LOC361016	-2.199	0.001	No	————	————	————	————
Nrsn1	-2.197	0.000	Yes	————	nervous system development (GO:0007399).	plasma membrane region (GO:0098590). neuronal cell body (GO:0043025). transport vesicle (GO:0030133). neuron projection (GO:0043005). vacuole (GO:0005773).	————

Lats1	-2.186	0.005	Yes	protein serine/threonine kinase activity (GO:0004674).	regulation of developmental process (GO:0050793). G1/S transition of mitotic cell cycle (GO:0000082). apoptotic process (GO:0006915). positive regulation of apoptotic process (GO:0043065). mitotic nuclear division (GO:0140014). developmental growth (GO:0048589). peptidyl-serine phosphorylation (GO:0018105).	————	non-receptor serine/threonine protein kinase (PC00167).

HFD+PB vs ND - DOWNREGULATED							
Gene Symbol	**log2FC**	***P* value**	**Hit?**	**Molecular Function**	**Biological Function**	**Cellular Component**	**Protein Class**
					regulation of multicellular organismal process (GO:0051239). regulation of growth (GO:0040008). intracellular signal transduction (GO:0035556). multicellular organismal process (GO:0032501).		
Tsc22d2	-2.180	0.022	Yes	————	————	————	————
Ncoa6	-2.180	0.016	Yes	nuclear receptor transcription coactivator activity (GO:0030374).	transcription by RNA polymerase II (GO:0006366). positive regulation of transcription by RNA polymerase II (GO:0045944).	transcription factor complex (GO:0005667). histone methyltransferase complex (GO:0035097).	chromatin/chromatin-binding, or -regulatory protein (PC00077).

HFD+PB vs ND - DOWNREGULATED							
Gene Symbol	**log2FC**	***P* value**	**Hit?**	**Molecular Function**	**Biological Function**	**Cellular Component**	**Protein Class**
Fastkd3	-2.170	0.035	Yes	————	————	————	————
Grin1	-2.165	0.001	Yes	ligand-gated ion channel activity (GO:0015276). signaling receptor activity (GO:0038023).	————	plasma membrane (GO:0005886).	————
Penk	-2.162	0.000	Yes	G protein-coupled receptor binding (GO:0001664).	neuropeptide signaling pathway (GO:0007218). chemical synaptic transmission (GO:0007268). sensory perception (GO:0007600).	dendrite (GO:0030425). plasma membrane region (GO:0098590). neuronal cell body (GO:0043025). axon terminus (GO:0043679).	neuropeptide (PC00162).
Cep290	-2.161	0.007	Yes	————	————	————	————
Ddn	-2.160	0.000	No	————	————	————	————
Lgi4	-2.157	0.014	Yes	————	————	————	————

HFD+PB vs ND - DOWNREGULATED							
Gene Symbol	**log2FC**	***P* value**	**Hit?**	**Molecular Function**	**Biological Function**	**Cellular Component**	**Protein Class**
Stxbp3	-2.150	0.000	Yes	————	————	————	membrane trafficking regulatory protein (PC00151).
Vps37a	-2.135	0.014	Yes	————	ubiquitin-dependent protein catabolic process via the multivesicular body sorting pathway (GO:0043162). multivesicular body sorting pathway (GO:0071985). protein targeting to membrane (GO:0006612). protein targeting to vacuole (GO:0006623). protein catabolic process in the vacuole (GO:0007039).	ESCRT I complex (GO:0000813). vacuole (GO:0005773). plasma membrane (GO:0005886).	————

HFD+PB vs ND - DOWNREGULATED							
Gene Symbol	**log2FC**	***P* value**	**Hit?**	**Molecular Function**	**Biological Function**	**Cellular Component**	**Protein Class**
Tubb2b	-2.135	0.003	Yes	GTP binding (GO:0005525). structural molecule activity (GO:0005198).	neuron migration (GO:0001764). mitotic nuclear division (GO:0140014). microtubule cytoskeleton organization (GO:0000226).	cytoplasm (GO:0005737). microtubule (GO:0005874).	tubulin (PC00228).

Akr1c14	-2.134	0.037	Yes	carboxylic acid binding (GO:0031406). oxidoreductase activity, acting on the CH-OH group of donors, NAD or NADP as acceptor (GO:0016616). oxidoreductase activity, acting on paired donors, with incorporation or reduction of molecular oxygen, NAD (P).H as one donor, and incorporation of one atom of oxygen (GO:0016709).	cellular aromatic compound metabolic process (GO:0006725). secondary metabolic process (GO:0019748). cofactor metabolic process (GO:0051186). carbohydrate derivative metabolic process (GO:1901135). drug metabolic process (GO:0017144). steroid metabolic process (GO:0008202). alcohol metabolic process (GO:0006066). prostaglandin metabolic process (GO:0006693).	cytosol (GO:0005829).	reductase (PC00198).

HFD+PB vs ND - DOWNREGULATED							
Gene Symbol	**log2FC**	***P* value**	**Hit?**	**Molecular Function**	**Biological Function**	**Cellular Component**	**Protein Class**
					hormone metabolic process (GO:0042445). ammonium ion metabolic process (GO:0097164).		
Calb1	-2.112	0.005	Yes	calcium ion binding (GO:0005509).	positive regulation of synaptic transmission (GO:0050806). regulation of synaptic plasticity (GO:0048167). regulation of cytosolic calcium ion concentration (GO:0051480). chemical synaptic transmission (GO:0007268). anatomical structure homeostasis (GO:0060249).	dendrite (GO:0030425). nucleus (GO:0005634). terminal bouton (GO:0043195). cytosol (GO:0005829). plasma membrane region (GO:0098590).	calmodulin-related (PC00061).

HFD+PB vs ND - DOWNREGULATED							
Gene Symbol	**log2FC**	***P* value**	**Hit?**	**Molecular Function**	**Biological Function**	**Cellular Component**	**Protein Class**
Olig1	-2.108	0.000	No	————	————	————	————
Rnf139	-2.104	0.000	Yes	ubiquitin protein ligase activity (GO:0061630).	————	endoplasmic reticulum (GO:0005783). vacuole (GO:0005773). plasma membrane (GO:0005886).	————
Cadm1	-2.098	0.026	No	————	————	————	————
Elovl2	-2.098	0.013	Yes	transferase activity, transferring acyl groups other than amino-acyl groups (GO:0016747).	fatty acid biosynthetic process (GO:0006633). very long-chain fatty acid metabolic process (GO:0000038). sphingolipid biosynthetic process (GO:0030148).	integral component of endoplasmic reticulum membrane (GO:0030176). vacuole (GO:0005773). plasma membrane (GO:0005886).	acyltransferase (PC00042).
Tmem59l	-2.078	0.001	No	————	————	————	————

HFD+PB vs ND - DOWNREGULATED							
Gene Symbol	**log2FC**	***P* value**	**Hit?**	**Molecular Function**	**Biological Function**	**Cellular Component**	**Protein Class**
Mlc1	-2.077	0.046	Yes	————	regulation of response to stress (GO:0080134). response to osmotic stress (GO:0006970).	cytoplasmic vesicle (GO:0031410). endoplasmic reticulum (GO:0005783). vacuole (GO:0005773). plasma membrane (GO:0005886).	————

HFD+PB vs ND - DOWNREGULATED							
Gene Symbol	**log2FC**	***P* value**	**Hit?**	**Molecular Function**	**Biological Function**	**Cellular Component**	**Protein Class**
Gabrd	-2.073	0.036	Yes	transmembrane signaling receptor activity (GO:0004888). chloride channel activity (GO:0005254).	regulation of membrane potential (GO:0042391). chloride transmembrane transport (GO:1902476). signal transduction (GO:0007165). chemical synaptic transmission (GO:0007268). nervous system process (GO:0050877).	integral component of plasma membrane (GO:0005887). plasma membrane region (GO:0098590). neuron projection (GO:0043005).	ligand-gated ion channel (PC00141).
Dennd4a	-2.073	0.014	Yes	————	————	————	————

HFD+PB vs ND - DOWNREGULATED							
Gene Symbol	**log2FC**	***P* value**	**Hit?**	**Molecular Function**	**Biological Function**	**Cellular Component**	**Protein Class**
Dgkd	-2.073	0.033	Yes	phosphotransferase activity, alcohol group as acceptor (GO:0016773). kinase activity (GO:0016301).	acylglycerol metabolic process (GO:0006639). phosphorylation (GO:0016310). intracellular signal transduction (GO:0035556).	————	kinase (PC00137).
Apba2	-2.065	0.031	Yes	amyloid-beta binding (GO:0001540).	chemical synaptic transmission (GO:0007268).	cytoplasm (GO:0005737). dendritic spine (GO:0043197). plasma membrane region (GO:0098590).	membrane trafficking regulatory protein (PC00151).
Rnf146	-2.061	0.000	No	————	————	————	————

HFD+PB vs ND - DOWNREGULATED							
Gene Symbol	**log2FC**	***P* value**	**Hit?**	**Molecular Function**	**Biological Function**	**Cellular Component**	**Protein Class**
Ufl1	-2.055	0.006	Yes	ubiquitin-like protein transferase activity (GO:0019787).	proteasome-mediated ubiquitin-dependent protein catabolic process (GO:0043161). regulation of proteasomal ubiquitin-dependent protein catabolic process (GO:0032434). response to endoplasmic reticulum stress (GO:0034976). protein modification by small protein conjugation (GO:0032446).	endoplasmic reticulum membrane (GO:0005789). vacuole (GO:0005773). plasma membrane (GO:0005886).	————

Fbxl12	-2.042	0.032	Yes	ubiquitin protein ligase activity (GO:0061630).	G2/M transition of mitotic cell cycle (GO:0000086). response to external stimulus (GO:0009605). mitotic nuclear division (GO:0140014). SCF-dependent proteasomal ubiquitin-dependent protein catabolic process (GO:0031146). regulation of cell cycle (GO:0051726). circadian rhythm (GO:0007623). regulation of circadian rhythm (GO:0042752).	nucleus (GO:0005634). cytosol (GO:0005829). SCF ubiquitin ligase complex (GO:0019005).	————

HFD+PB vs ND - DOWNREGULATED							
Gene Symbol	**log2FC**	***P* value**	**Hit?**	**Molecular Function**	**Biological Function**	**Cellular Component**	**Protein Class**
					response to light stimulus (GO:0009416).		
Map7d2	-2.042	0.003	Yes	————	microtubule cytoskeleton organization (GO:0000226).	microtubule cytoskeleton (GO:0015630).	non-motor microtubule binding protein (PC00166).
Rab3b	-2.042	0.002	Yes	————	vesicle fusion to plasma membrane (GO:0099500). organelle localization (GO:0051640). regulation of exocytosis (GO:0017157). protein secretion (GO:0009306). protein localization to plasma membrane (GO:0072659).	endosome (GO:0005768). synaptic vesicle (GO:0008021). vacuole (GO:0005773). plasma membrane (GO:0005886).	————

HFD+PB vs ND - DOWNREGULATED							
Gene Symbol	**log2FC**	***P* value**	**Hit?**	**Molecular Function**	**Biological Function**	**Cellular Component**	**Protein Class**
Cbs	-2.041	0.046	Yes	drug binding (GO:0008144). small molecule binding (GO:0036094). anion binding (GO:0043168). heme binding (GO:0020037).	secondary metabolic process (GO:0019748). alpha-amino acid metabolic process (GO:1901605). sulfur compound metabolic process (GO:0006790). drug metabolic process (GO:0017144). cellular biosynthetic process (GO:0044249).	cytoplasm (GO:0005737).	lyase (PC00144).
Sparcl1	-2.037	0.001	No	————	————	————	————

HFD+PB vs ND - DOWNREGULATED							
Gene Symbol	**log2FC**	***P* value**	**Hit?**	**Molecular Function**	**Biological Function**	**Cellular Component**	**Protein Class**
Stx1b	-2.029	0.001	Yes	SNARE binding (GO:0000149).	vesicle fusion to plasma membrane (GO:0099500). organelle localization (GO:0051640). synaptic vesicle exocytosis (GO:0016079). intracellular protein transport (GO:0006886).	presynaptic membrane (GO:0042734). presynaptic active zone (GO:0048786). synaptic vesicle (GO:0008021). integral component of membrane (GO:0016021). SNARE complex (GO:0031201). vacuole (GO:0005773).	SNARE protein (PC00034).

HFD+PB vs ND - DOWNREGULATED							
Gene Symbol	**log2FC**	***P* value**	**Hit?**	**Molecular Function**	**Biological Function**	**Cellular Component**	**Protein Class**
Hsd11b1	-2.028	0.010	Yes	oxidoreductase activity, acting on the CH-OH group of donors, NAD or NADP as acceptor (GO:0016616). steroid binding (GO:0005496).	organic cyclic compound catabolic process (GO:1901361). lipid catabolic process (GO:0016042). steroid metabolic process (GO:0008202).	————	————
Ampd3	-2.022	0.039	No	————	————	————	————
Gria2	-2.017	0.011	No	————	————	————	————
Lamp5	-2.009	0.049	Yes	————	establishment of protein localization to organelle (GO:0072594).	late endosome membrane (GO:0031902). lysosomal membrane (GO:0005765). plasma membrane (GO:0005886).	membrane trafficking regulatory protein (PC00151).

HFD+PB vs ND - DOWNREGULATED							
Gene Symbol	**log2FC**	***P* value**	**Hit?**	**Molecular Function**	**Biological Function**	**Cellular Component**	**Protein Class**
Mt1m	-2.000	0.014	Yes	metal ion binding (GO:0046872).	cellular zinc ion homeostasis (GO:0006882). response to cadmium ion (GO:0046686). response to toxic substance (GO:0009636). cellular response to chemical stimulus (GO:0070887). response to stress (GO:0006950).	nucleus (GO:0005634). cytoplasm (GO:0005737).	————
Amn1	-1.995	0.000	Yes	ubiquitin-protein transferase activity (GO:0004842).	SCF-dependent proteasomal ubiquitin-dependent protein catabolic process (GO:0031146).	SCF ubiquitin ligase complex (GO:0019005).	————
Gjc1	-1.995	0.000	Yes	————	————	————	gap junction (PC00105).

HFD+PB vs ND - DOWNREGULATED							
Gene Symbol	**log2FC**	***P* value**	**Hit?**	**Molecular Function**	**Biological Function**	**Cellular Component**	**Protein Class**
Acap2	-1.993	0.029	Yes	————	————	————	————
Fam212b	-1.983	0.035	Yes	protein kinase binding (GO:0019901). protein serine/threonine kinase activity (GO:0004674). protein kinase inhibitor activity (GO:0004860).	————	nucleus (GO:0005634).	————

HFD+PB vs ND - DOWNREGULATED							
Gene Symbol	**log2FC**	***P* value**	**Hit?**	**Molecular Function**	**Biological Function**	**Cellular Component**	**Protein Class**
Rnf144b	-1.983	0.019	Yes	ubiquitin-like protein conjugating enzyme binding (GO:0044390). ubiquitin protein ligase activity (GO:0061630).	proteasome-mediated ubiquitin-dependent protein catabolic process (GO:0043161). protein polyubiquitination (GO:0000209). positive regulation of proteasomal ubiquitin-dependent protein catabolic process (GO:0032436).	ubiquitin ligase complex (GO:0000151). cytoplasm (GO:0005737).	ubiquitin-protein ligase (PC00234).
Togaram1	-1.983	0.001	Yes	————	————	————	non-motor microtubule binding protein (PC00166).
Opalin	-1.976	0.027	Yes	————	————	cell-cell contact zone (GO:0044291). plasma membrane (GO:0005886).	————

HFD+PB vs ND - DOWNREGULATED							
Gene Symbol	**log2FC**	***P* value**	**Hit?**	**Molecular Function**	**Biological Function**	**Cellular Component**	**Protein Class**
Camk2g	-1.976	0.013	Yes	calmodulin binding (GO:0005516). protein serine/threonine kinase activity (GO:0004674).	————	cytoplasm (GO:0005737). plasma membrane region (GO:0098590). neuron projection (GO:0043005).	non-receptor serine/threonine protein kinase (PC00167).
Ina	-1.971	0.038	No	————	————	————	————
Herc3	-1.968	0.006	Yes	————	————	————	————
Rundc3a	-1.952	0.001	Yes	————	cGMP-mediated signaling (GO:0019934). positive regulation of intracellular signal transduction (GO:1902533).	cytosol (GO:0005829).	————
Mbtps2	-1.942	0.006	Yes	————	————	————	metalloprotease (PC00153).
Mettl25	-1.942	0.034	Yes	————	————	————	RNA methyltransferase (PC00033).

HFD+PB vs ND - DOWNREGULATED							
Gene Symbol	**log2FC**	***P* value**	**Hit?**	**Molecular Function**	**Biological Function**	**Cellular Component**	**Protein Class**
Nacad	-1.942	0.049	Yes	————	————	————	basic helix-loop-helix transcription factor (PC00055).
Rttn	-1.942	0.036	Yes	————	centriole replication (GO:0007099). cilium organization (GO:0044782).	centriole (GO:0005814). ciliary basal body (GO:0036064). intraciliary transport particle (GO:0030990). plasma membrane region (GO:0098590).	————
Grp	-1.942	0.002	Yes	————	————	————	————

HFD+PB vs ND - DOWNREGULATED							
Gene Symbol	**log2FC**	***P* value**	**Hit?**	**Molecular Function**	**Biological Function**	**Cellular Component**	**Protein Class**
Dagla	-1.942	0.040	Yes	————	G protein-coupled receptor signaling pathway (GO:0007186). trans-synaptic signaling (GO:0099537). regulation of neurotransmitter levels (GO:0001505). neurogenesis (GO:0022008). cellular biosynthetic process (GO:0044249). glutamate receptor signaling pathway (GO:0007215).	postsynaptic membrane (GO:0045211).	————

HFD+PB vs ND - DOWNREGULATED							
Gene Symbol	**log2FC**	***P* value**	**Hit?**	**Molecular Function**	**Biological Function**	**Cellular Component**	**Protein Class**
Ttbk1	-1.942	0.026	Yes	protein serine/threonine kinase activity (GO:0004674).	peptidyl-serine phosphorylation (GO:0018105).	nucleus (GO:0005634). cytoplasm (GO:0005737).	non-receptor serine/threonine protein kinase (PC00167).
Fem1c	-1.921	0.002	Yes	————	————	————	————
RGD1307100	-1.919	0.005	Yes	————	————	————	————
Dhx36	-1.907	0.006	Yes	RNA binding (GO:0003723).	————	nucleus (GO:0005634).	RNA helicase (PC00032).
Rbp4	-1.907	0.033	Yes	————	————	————	transfer/carrier protein (PC00219).
Bcat1	-1.898	0.000	Yes	transferase activity (GO:0016740).	alpha-amino acid metabolic process (GO:1901605). oxidation-reduction process (GO:0055114). branched-chain amino acid biosynthetic process (GO:0009082).	mitochondrion (GO:0005739).	transaminase (PC00216).

HFD+PB vs ND - DOWNREGULATED							
Gene Symbol	**log2FC**	***P* value**	**Hit?**	**Molecular Function**	**Biological Function**	**Cellular Component**	**Protein Class**
Tril	-1.889	0.017	Yes	lipopolysaccharide binding (GO:0001530).	toll-like receptor signaling pathway (GO:0002224). innate immune response (GO:0045087). cytokine production (GO:0001816). immune effector process (GO:0002252). regulation of cytokine production (GO:0001817).	membrane protein complex (GO:0098796). extracellular space (GO:0005615). integral component of membrane (GO:0016021). receptor complex (GO:0043235). extracellular matrix (GO:0031012).	transmembrane signal receptor (PC00197).
Ngdn	-1.889	0.012	Yes	————	maturation of SSU-rRNA from tricistronic rRNA transcript (SSU-rRNA, 5.8S rRNA, LSU-rRNA). (GO:0000462).	small-subunit processome (GO:0032040). t-UTP complex (GO:0034455).	RNA binding protein (PC00031).
Synm	-1.889	0.011	Yes	————	————	————	————

HFD+PB vs ND - DOWNREGULATED							
Gene Symbol	**log2FC**	***P* value**	**Hit?**	**Molecular Function**	**Biological Function**	**Cellular Component**	**Protein Class**
Adgrb2	-1.884	0.008	Yes	G protein-coupled receptor activity (GO:0004930).	regulation of cAMP-mediated signaling (GO:0043949). regulation of adenylate cyclase activity (GO:0045761). adenylate cyclase-activating G protein-coupled receptor signaling pathway (GO:0007189). activation of adenylate cyclase activity (GO:0007190).	integral component of plasma membrane (GO:0005887).	G-protein coupled receptor (PC00021).
Mbp	-1.883	0.035	Yes	————	————	————	————
Ppat	-1.882	0.039	Yes	————	————	————	transferase (PC00220).
Evi2a	-1.876	0.003	No	————	————	————	————

HFD+PB vs ND - DOWNREGULATED							
Gene Symbol	**log2FC**	***P* value**	**Hit?**	**Molecular Function**	**Biological Function**	**Cellular Component**	**Protein Class**
Sfxn1	-1.862	0.026	No	————	————	————	————
Ddx50	-1.861	0.003	Yes	————	————	nucleolus (GO:0005730).	————
Nefl	-1.857	0.001	Yes	————	————	————	————
Nfrkb	-1.857	0.038	Yes	————	————	————	chromatin/chromatin-binding, or -regulatory protein (PC00077).
LOC100125362	-1.857	0.033	Yes	————	————	————	————
Apod	-1.855	0.027	No	————	————	————	————

HFD+PB vs ND - DOWNREGULATED							
Gene Symbol	**log2FC**	***P* value**	**Hit?**	**Molecular Function**	**Biological Function**	**Cellular Component**	**Protein Class**
Cacnb4	-1.851	0.025	Yes	voltage-gated calcium channel activity (GO:0005245).	synapse organization (GO:0050808). calcium ion transmembrane transport (GO:0070588). chemical synaptic transmission (GO:0007268). regulation of calcium ion transport (GO:0051924). regulation of cation transmembrane transport (GO:1904062). regulation of ion transmembrane transporter activity (GO:0032412).	voltage-gated calcium channel complex (GO:0005891).	————
Nap1l3	-1.851	0.013	Yes	————	————	————	chromatin/chromatin-binding, or -regulatory protein (PC00077).

HFD+PB vs ND - DOWNREGULATED							
Gene Symbol	**log2FC**	***P* value**	**Hit?**	**Molecular Function**	**Biological Function**	**Cellular Component**	**Protein Class**
Sash1	-1.851	0.013	Yes	————	————	————	————
Stk26	-1.848	0.025	Yes	————	————	————	————
Tbc1d23	-1.848	0.007	Yes	————	————	————	————
Chrm4	-1.836	0.030	No	————	————	————	————
Tmem87b	-1.835	0.011	Yes	————	————	————	G-protein coupled receptor (PC00021).
Bbs10	-1.835	0.012	Yes	————	————	————	————

Htr2a	-1.829	0.024	Yes	G protein-coupled receptor activity (GO:0004930). heterocyclic compound binding (GO:1901363). organic cyclic compound binding (GO:0097159). neurotransmitter binding (GO:0042165). neurotransmitter receptor activity (GO:0030594). ammonium ion binding (GO:0070405).	cyclic-nucleotide-mediated signaling (GO:0019935). inositol phosphate-mediated signaling (GO:0048016). G protein-coupled receptor signaling pathway, coupled to cyclic nucleotide second messenger (GO:0007187). response to drug (GO:0042493). activation of phospholipase C activity (GO:0007202). chemical synaptic transmission (GO:0007268). sequestering of calcium ion (GO:0051208). phospholipase C-activating G protein-coupled receptor	dendrite (GO:0030425). integral component of plasma membrane (GO:0005887). plasma membrane region (GO:0098590).	G-protein coupled receptor (PC00021).

HFD+PB vs ND - DOWNREGULATED							
Gene Symbol	**log2FC**	***P* value**	**Hit?**	**Molecular Function**	**Biological Function**	**Cellular Component**	**Protein Class**
					signaling pathway (GO:0007200). release of sequestered calcium ion into cytosol (GO:0051209).		
Cd24	-1.828	0.000	Yes	————	————	————	————
Plat	-1.826	0.008	Yes	serine-type endopeptidase activity (GO:0004252).	proteolysis (GO:0006508).	extracellular space (GO:0005615).	serine protease (PC00203).
S100b	-1.816	0.002	Yes	————	————	————	calmodulin-related (PC00061).
Lrif1	-1.807	0.010	No	————	————	————	————
Spata18	-1.798	0.015	No	————	————	————	————

HFD+PB vs ND - DOWNREGULATED							
Gene Symbol	**log2FC**	***P* value**	**Hit?**	**Molecular Function**	**Biological Function**	**Cellular Component**	**Protein Class**
Dhx9	-1.790	0.009	Yes	RNA binding (GO:0003723). 3'-5' DNA helicase activity (GO:0043138).	regulation of mRNA processing (GO:0050684). transcription by RNA polymerase II (GO:0006366). mRNA processing (GO:0006397). positive regulation of transcription by RNA polymerase II (GO:0045944).	cytoplasm (GO:0005737). nucleolus (GO:0005730). ribonucleoprotein complex (GO:1990904).	RNA helicase (PC00032).
Nudt21	-1.787	0.023	Yes	mRNA binding (GO:0003729).	mRNA processing (GO:0006397).	mRNA cleavage factor complex (GO:0005849).	RNA splicing factor (PC00148).
Mag	-1.783	0.008	Yes	carboxylic acid binding (GO:0031406). carbohydrate derivative binding (GO:0097367).	cell adhesion (GO:0007155).	plasma membrane (GO:0005886).	immunoglobulin superfamily cell adhesion molecule (PC00125).

HFD+PB vs ND - DOWNREGULATED							
Gene Symbol	**log2FC**	***P* value**	**Hit?**	**Molecular Function**	**Biological Function**	**Cellular Component**	**Protein Class**
Gja1	-1.783	0.001	Yes	————	————	————	gap junction (PC00105).
Mobp	-1.781	0.000	Yes	actin binding (GO:0003779). myosin binding (GO:0017022). Rab GTPase binding (GO:0017137).	————	cortical actin cytoskeleton (GO:0030864).	myelin protein (PC00161).
Sptbn2	-1.769	0.006	No	————	————	————	————
Ebag9	-1.769	0.045	Yes	————	————	secretory granule (GO:0030141). vacuole (GO:0005773). plasma membrane (GO:0005886).	————
Cpped1	-1.767	0.004	Yes	————	————	————	————

HFD+PB vs ND - DOWNREGULATED							
Gene Symbol	**log2FC**	***P* value**	**Hit?**	**Molecular Function**	**Biological Function**	**Cellular Component**	**Protein Class**
Cck	-1.764	0.002	Yes	neuropeptide hormone activity (GO:0005184).	digestion (GO:0007586).	extracellular space (GO:0005615). plasma membrane region (GO:0098590). axon (GO:0030424).	————
Cav2	-1.754	0.035	No	————	————	————	————
Ugcg	-1.749	0.021	Yes	UDP-glucosyltransferase activity (GO:0035251).	ceramide biosynthetic process (GO:0046513). glycolipid biosynthetic process (GO:0009247).	————	glycosyltransferase (PC00111).
Abhd17b	-1.749	0.004	Yes	————	————	————	serine protease (PC00203).
Cenpe	-1.744	0.014	Yes	————	mitotic metaphase plate congression (GO:0007080).	————	————

HFD+PB vs ND - DOWNREGULATED							
Gene Symbol	**log2FC**	***P* value**	**Hit?**	**Molecular Function**	**Biological Function**	**Cellular Component**	**Protein Class**
Btg1	-1.738	0.006	Yes	————	cell population proliferation (GO:0008283). negative regulation of cell population proliferation (GO:0008285). mitotic nuclear division (GO:0140014). negative regulation of mitotic cell cycle (GO:0045930).	nucleus (GO:0005634). cytoplasm (GO:0005737).	————
Usp53	-1.720	0.015	Yes	————	sensory perception of sound (GO:0007605). response to mechanical stimulus (GO:0009612).	cell-cell junction (GO:0005911).	cysteine protease (PC00081).
RGD1563354	-1.720	0.010	Yes	————	————	————	————

HFD+PB vs ND - DOWNREGULATED							
Gene Symbol	**log2FC**	***P* value**	**Hit?**	**Molecular Function**	**Biological Function**	**Cellular Component**	**Protein Class**
Rasgrp3	-1.720	0.024	Yes	————	————	————	guanyl-nucleotide exchange factor (PC00113).
Rab30	-1.719	0.040	Yes	————	————	————	————

Pard3b	-1.719	0.029	Yes	phosphatidylinositol binding (GO:0035091).	centrosome localization (GO:0051642). establishment or maintenance of epithelial cell apical/basal polarity (GO:0045197). protein localization (GO:0008104). establishment of cell polarity (GO:0030010). cell adhesion (GO:0007155). establishment of localization in cell (GO:0051649). microtubule cytoskeleton organization (GO:0000226).	cell-cell adherens junction (GO:0005913). cell cortex (GO:0005938). apical junction complex (GO:0043296). apical plasma membrane (GO:0016324).	————

HFD+PB vs ND - DOWNREGULATED							
Gene Symbol	**log2FC**	***P* value**	**Hit?**	**Molecular Function**	**Biological Function**	**Cellular Component**	**Protein Class**
					establishment of organelle localization (GO:0051656).		

HFD+PB vs ND - DOWNREGULATED							
Gene Symbol	**log2FC**	***P* value**	**Hit?**	**Molecular Function**	**Biological Function**	**Cellular Component**	**Protein Class**
Atp1a3	-1.712	0.005	Yes	ATPase activity (GO:0016887). ATPase-coupled transmembrane transporter activity (GO:0042626). potassium ion transmembrane transporter activity (GO:0015079). active ion transmembrane transporter activity (GO:0022853). sodium ion transmembrane transporter activity (GO:0015081).	potassium ion transmembrane transport (GO:0071805). import into cell (GO:0098657). proton transmembrane transport (GO:1902600). sodium ion transmembrane transport (GO:0035725). cellular metal ion homeostasis (GO:0006875). cellular monovalent inorganic cation homeostasis (GO:0030004). export from cell (GO:0140352).	————	primary active transporter (PC00068).

HFD+PB vs ND - DOWNREGULATED							
Gene Symbol	**log2FC**	***P* value**	**Hit?**	**Molecular Function**	**Biological Function**	**Cellular Component**	**Protein Class**
Camk2b	-1.710	0.001	No	————	————	————	————
Armc8	-1.703	0.006	Yes	————	proteasome-mediated ubiquitin-dependent protein catabolic process (GO:0043161).	protein-containing complex (GO:0032991). intracellular part (GO:0044424).	————
Nedd9	-1.701	0.002	Yes	————	actin filament organization (GO:0007015). transmembrane receptor protein tyrosine kinase signaling pathway (GO:0007169). cell migration (GO:0016477). actin cytoskeleton reorganization (GO:0031532).	cytoplasm (GO:0005737). plasma membrane (GO:0005886).	————

HFD+PB vs ND - DOWNREGULATED							
Gene Symbol	**log2FC**	***P* value**	**Hit?**	**Molecular Function**	**Biological Function**	**Cellular Component**	**Protein Class**
Gopc	-1.698	0.012	Yes	————	————	————	membrane traffic protein (PC00150).
Usp32	-1.696	0.000	Yes	————	————	————	cysteine protease (PC00081).
Fam49a	-1.693	0.028	Yes	————	————	————	————
Klhl13	-1.689	0.014	Yes	————	————	midbody (GO:0030496).	————
Slc1a3	-1.680	0.012	No	————	————	————	————
Atl2	-1.679	0.040	Yes	GTP binding (GO:0005525). GTPase activity (GO:0003924).	protein homooligomerization (GO:0051260). endoplasmic reticulum organization (GO:0007029).	————	heterotrimeric G-protein (PC00117).

HFD+PB vs ND - DOWNREGULATED							
Gene Symbol	**log2FC**	***P* value**	**Hit?**	**Molecular Function**	**Biological Function**	**Cellular Component**	**Protein Class**
Rp2	-1.675	0.002	Yes	GTPase activity (GO:0003924). GTPase activator activity (GO:0005096).	post-Golgi vesicle-mediated transport (GO:0006892).	cilium (GO:0005929). intraciliary transport particle (GO:0030990). plasma membrane region (GO:0098590).	GTPase-activating protein (PC00257).
Gpr149	-1.671	0.048	Yes	G protein-coupled receptor activity (GO:0004930). neuropeptide binding (GO:0042923).	neuropeptide signaling pathway (GO:0007218).	integral component of plasma membrane (GO:0005887). plasma membrane region (GO:0098590). neuron projection (GO:0043005).	G-protein coupled receptor (PC00021).
Ctns	-1.671	0.024	Yes	L-amino acid transmembrane transporter activity (GO:0015179).	L-amino acid transport (GO:0015807). neutral amino acid transport (GO:0015804).	vacuolar membrane (GO:0005774).	amino acid transporter (PC00046).

HFD+PB vs ND - DOWNREGULATED							
Gene Symbol	**log2FC**	***P* value**	**Hit?**	**Molecular Function**	**Biological Function**	**Cellular Component**	**Protein Class**
Atp1a2	-1.668	0.039	Yes	ATPase activity (GO:0016887). ATPase-coupled transmembrane transporter activity (GO:0042626). potassium ion transmembrane transporter activity (GO:0015079). active ion transmembrane transporter activity (GO:0022853). sodium ion transmembrane transporter activity (GO:0015081).	potassium ion transmembrane transport (GO:0071805). import into cell (GO:0098657). proton transmembrane transport (GO:1902600). sodium ion transmembrane transport (GO:0035725). cellular metal ion homeostasis (GO:0006875). cellular monovalent inorganic cation homeostasis (GO:0030004). export from cell (GO:0140352).	————	primary active transporter (PC00068).

HFD+PB vs ND - DOWNREGULATED							
Gene Symbol	**log2FC**	***P* value**	**Hit?**	**Molecular Function**	**Biological Function**	**Cellular Component**	**Protein Class**
Fstl4	-1.663	0.008	Yes	————	multicellular organism development (GO:0007275). cell differentiation (GO:0030154).	————	protease inhibitor (PC00191).
Fez1	-1.662	0.000	Yes	————	————	cytoplasm (GO:0005737). plasma membrane region (GO:0098590). axon (GO:0030424).	————
Slc30a4	-1.658	0.001	No	————	————	————	————
Nrcam	-1.650	0.046	No	————	————	————	————
Cpox	-1.650	0.034	Yes	oxidoreductase activity (GO:0016491).	heme biosynthetic process (GO:0006783).	cytoplasm (GO:0005737).	oxidase (PC00175).

HFD+PB vs ND - DOWNREGULATED							
Gene Symbol	**log2FC**	***P* value**	**Hit?**	**Molecular Function**	**Biological Function**	**Cellular Component**	**Protein Class**
Tapt1	-1.638	0.026	Yes	————	maintenance of location (GO:0051235). protein localization to endoplasmic reticulum (GO:0070972). cellular process (GO:0009987).	integral component of endoplasmic reticulum membrane (GO:0030176). vacuole (GO:0005773). plasma membrane (GO:0005886).	————
Scaf8	-1.638	0.010	No	————	————	————	————

Nipbl	-1.637	0.016	Yes	chromatin binding (GO:0003682).	regulation of cellular localization (GO:0060341). regulation of protein localization (GO:0032880). chromosome condensation (GO:0030261). mitotic sister chromatid cohesion (GO:0007064). double-strand break repair via homologous recombination (GO:0000724). transcription by RNA polymerase II (GO:0006366). chromatin organization (GO:0006325). positive regulation of transcription by RNA	nuclear chromatin (GO:0000790). protein-containing complex (GO:0032991).	chromatin/chromatin-binding, or -regulatory protein (PC00077).

HFD+PB vs ND - DOWNREGULATED							
Gene Symbol	**log2FC**	***P* value**	**Hit?**	**Molecular Function**	**Biological Function**	**Cellular Component**	**Protein Class**
					polymerase II (GO:0045944). positive regulation of mitotic cell cycle (GO:0045931). establishment of protein localization to organelle (GO:0072594). positive regulation of molecular function (GO:0044093). positive regulation of organelle organization (GO:0010638). regulation of mitotic sister chromatid segregation (GO:0033047).		

HFD+PB vs ND - DOWNREGULATED							
Gene Symbol	**log2FC**	***P* value**	**Hit?**	**Molecular Function**	**Biological Function**	**Cellular Component**	**Protein Class**
Tspan12	-1.637	0.015	Yes	————	cellular response to growth factor stimulus (GO:0071363). regulation of cellular response to growth factor stimulus (GO:0090287). transmembrane receptor protein tyrosine kinase signaling pathway (GO:0007169). regulation of signal transduction (GO:0009966).	integral component of plasma membrane (GO:0005887).	————
Akap11	-1.634	0.000	No	————	————	————	————

HFD+PB vs ND - DOWNREGULATED							
Gene Symbol	**log2FC**	***P* value**	**Hit?**	**Molecular Function**	**Biological Function**	**Cellular Component**	**Protein Class**
Nsg1	-1.628	0.006	Yes	clathrin binding (GO:0030276).	cellular protein-containing complex assembly (GO:0034622). endosomal transport (GO:0016197).	endosome (GO:0005768). integral component of membrane (GO:0016021). vacuole (GO:0005773). plasma membrane (GO:0005886).	————
Yars2	-1.624	0.015	Yes	ligase activity (GO:0016874). catalytic activity, acting on a tRNA (GO:0140101).	cellular amino acid metabolic process (GO:0006520). tRNA metabolic process (GO:0006399).	cytosol (GO:0005829).	aminoacyl-tRNA synthetase (PC00047).
Pcp4	-1.621	0.000	Yes	————	————	————	————
Stmn3	-1.621	0.000	No	————	————	————	————

HFD+PB vs ND - DOWNREGULATED							
Gene Symbol	**log2FC**	***P* value**	**Hit?**	**Molecular Function**	**Biological Function**	**Cellular Component**	**Protein Class**
Usp38	-1.620	0.040	Yes	thiol-dependent ubiquitin-specific protease activity (GO:0004843). cysteine-type endopeptidase activity (GO:0004197).	protein deubiquitination (GO:0016579).	————	cysteine protease (PC00081).
Tagln3	-1.620	0.031	Yes	————	————	————	non-motor actin binding protein (PC00165).
Rhd	-1.620	0.029	Yes	ammonium transmembrane transporter activity (GO:0008519).	ammonium transport (GO:0015696). cation transmembrane transport (GO:0098655).	integral component of plasma membrane (GO:0005887).	primary active transporter (PC00068).

HFD+PB vs ND - DOWNREGULATED							
Gene Symbol	**log2FC**	***P* value**	**Hit?**	**Molecular Function**	**Biological Function**	**Cellular Component**	**Protein Class**
Mt2A	-1.614	0.001	Yes	metal ion binding (GO:0046872).	cellular zinc ion homeostasis (GO:0006882). response to cadmium ion (GO:0046686). response to toxic substance (GO:0009636). cellular response to chemical stimulus (GO:0070887). response to stress (GO:0006950).	nucleus (GO:0005634). cytoplasm (GO:0005737).	————
Schip1	-1.610	0.009	Yes	————	————	————	————
Krt10	-1.609	0.042	Yes	————	————	————	————
Slc2a13	-1.609	0.026	Yes	————	————	————	————
Marcks	-1.607	0.001	No	————	————	————	————

HFD+PB vs ND - DOWNREGULATED							
Gene Symbol	**log2FC**	***P* value**	**Hit?**	**Molecular Function**	**Biological Function**	**Cellular Component**	**Protein Class**
Adap1	-1.606	0.026	Yes	————	————	intracellular membrane-bounded organelle (GO:0043231). plasma membrane (GO:0005886).	————
Ccdc153	-1.606	0.000	Yes	————	————	————	————
Ivns1abp	-1.603	0.002	Yes	————	————	————	scaffold/adaptor protein (PC00226).
Sp1	-1.603	0.012	Yes	DNA-binding transcription factor activity, RNA polymerase II-specific (GO:0000981).	transcription by RNA polymerase II (GO:0006366). regulation of transcription by RNA polymerase II (GO:0006357).	nucleus (GO:0005634).	C2H2 zinc finger transcription factor (PC00248).
Hdac9	-1.603	0.004	Yes	————	————	————	histone modifying enzyme (PC00261).

HFD+PB vs ND - DOWNREGULATED							
Gene Symbol	**log2FC**	***P* value**	**Hit?**	**Molecular Function**	**Biological Function**	**Cellular Component**	**Protein Class**
Phyhip	-1.602	0.013	Yes	————	————	————	————
Psd	-1.599	0.000	No	————	————	————	————
Sfpq	-1.594	0.010	Yes	transcription regulatory region sequence-specific DNA binding (GO:0000976).	transcription, DNA-templated (GO:0006351). regulation of transcription, DNA-templated (GO:0006355). mRNA splicing, via spliceosome (GO:0000398).	nucleus (GO:0005634).	RNA binding protein (PC00031).
Fzd6	-1.594	0.024	Yes	transmembrane signaling receptor activity (GO:0004888). Wnt-protein binding (GO:0017147).	canonical Wnt signaling pathway (GO:0060070). non-canonical Wnt signaling pathway (GO:0035567).	integral component of membrane (GO:0016021). plasma membrane (GO:0005886).	transmembrane signal receptor (PC00197).
Bcan	-1.594	0.004	No	————	————	————	————

HFD+PB vs ND - DOWNREGULATED							
Gene Symbol	**log2FC**	***P* value**	**Hit?**	**Molecular Function**	**Biological Function**	**Cellular Component**	**Protein Class**
Stmn4	-1.594	0.001	Yes	tubulin binding (GO:0015631).	neuron projection development (GO:0031175). regulation of microtubule polymerization or depolymerization (GO:0031110). microtubule depolymerization (GO:0007019).	cytoplasm (GO:0005737). plasma membrane region (GO:0098590). neuron projection (GO:0043005).	————
Klk6	-1.594	0.006	Yes	————	————	secretory granule (GO:0030141). vacuole (GO:0005773). plasma membrane (GO:0005886).	serine protease (PC00203).
Fam204a	-1.594	0.004	Yes	————	————	————	————

HFD+PB vs ND - DOWNREGULATED							
Gene Symbol	**log2FC**	***P* value**	**Hit?**	**Molecular Function**	**Biological Function**	**Cellular Component**	**Protein Class**
Nod1	-1.594	0.043	Yes	————	intracellular signal transduction (GO:0035556).	————	scaffold/adaptor protein (PC00226).
Dync2h1	-1.590	0.001	No	————	————	————	————
Lmo4	-1.589	0.003	Yes	————	————	————	————

HFD+PB vs ND - DOWNREGULATED							
Gene Symbol	**log2FC**	***P* value**	**Hit?**	**Molecular Function**	**Biological Function**	**Cellular Component**	**Protein Class**
Tmed7	-1.586	0.034	Yes	————	endoplasmic reticulum to Golgi vesicle-mediated transport (GO:0006888). Golgi organization (GO:0007030). intracellular protein transport (GO:0006886).	COPII-coated ER to Golgi transport vesicle (GO:0030134). Golgi apparatus (GO:0005794). endoplasmic reticulum (GO:0005783). endoplasmic reticulum-Golgi intermediate compartment (GO:0005793). vacuole (GO:0005773). plasma membrane (GO:0005886).	vesicle coat protein (PC00235).

HFD+PB vs ND - DOWNREGULATED							
Gene Symbol	**log2FC**	***P* value**	**Hit?**	**Molecular Function**	**Biological Function**	**Cellular Component**	**Protein Class**
Pak1	-1.585	0.027	Yes	protein serine/threonine kinase activity (GO:0004674).	regulation of axonogenesis (GO:0050770). stress-activated protein kinase signaling cascade (GO:0031098). axonogenesis (GO:0007409). mitotic nuclear division (GO:0140014). activation of protein kinase activity (GO:0032147). signal transduction by protein phosphorylation (GO:0023014). regulation of mitotic cell cycle (GO:0007346).	cytoplasm (GO:0005737).	————

HFD+PB vs ND - DOWNREGULATED							
Gene Symbol	**log2FC**	***P* value**	**Hit?**	**Molecular Function**	**Biological Function**	**Cellular Component**	**Protein Class**
Eif5a2	-1.585	0.007	Yes	translation regulator activity (GO:0045182). RNA binding (GO:0003723).	positive regulation of translation (GO:0045727). translational elongation (GO:0006414).	————	translation initiation factor (PC00224).
Susd1	-1.583	0.001	Yes	————	————	————	extracellular matrix glycoprotein (PC00100).
Zcchc12	-1.580	0.034	Yes	nuclear receptor transcription coactivator activity (GO:0030374).	BMP signaling pathway (GO:0030509). transcription by RNA polymerase II (GO:0006366).	nuclear speck (GO:0016607).	————

HFD+PB vs ND - DOWNREGULATED							
Gene Symbol	**log2FC**	***P* value**	**Hit?**	**Molecular Function**	**Biological Function**	**Cellular Component**	**Protein Class**
Baiap2	-1.568	0.007	Yes	————	actin filament polymerization (GO:0030041). positive regulation of actin filament polymerization (GO:0030838). actin cytoskeleton reorganization (GO:0031532). actin filament bundle assembly (GO:0051017).	cytosol (GO:0005829). nucleoplasm (GO:0005654).	scaffold/adaptor protein (PC00226).
Trim23	-1.568	0.028	No	————	————	————	————

HFD+PB vs ND - DOWNREGULATED							
Gene Symbol	**log2FC**	***P* value**	**Hit?**	**Molecular Function**	**Biological Function**	**Cellular Component**	**Protein Class**
Nudt10	-1.565	0.008	Yes	nucleotide diphosphatase activity (GO:0004551).	purine ribonucleotide metabolic process (GO:0009150). nucleotide catabolic process (GO:0009166). organonitrogen compound catabolic process (GO:1901565). alcohol metabolic process (GO:0006066).	nucleus (GO:0005634). cytoplasm (GO:0005737).	phosphatase (PC00181).
Pank3	-1.562	0.001	Yes	phosphotransferase activity, alcohol group as acceptor (GO:0016773). kinase activity (GO:0016301).	purine ribonucleotide biosynthetic process (GO:0009152). coenzyme biosynthetic process (GO:0009108).	nucleus (GO:0005634). cytosol (GO:0005829).	————

HFD+PB vs ND - DOWNREGULATED							
Gene Symbol	**log2FC**	***P* value**	**Hit?**	**Molecular Function**	**Biological Function**	**Cellular Component**	**Protein Class**
Golga7	-1.560	0.000	Yes	catalytic activity, acting on a protein (GO:0140096). palmitoyltransferase activity (GO:0016409).	peptidyl-amino acid modification (GO:0018193). protein lipidation (GO:0006497). protein acylation (GO:0043543). protein targeting to membrane (GO:0006612).	transferase complex (GO:1990234).	————
C1d	-1.558	0.001	Yes	————	————	————	transcription cofactor (PC00217).

Synj1	-1.556	0.014	Yes	phosphatase activity (GO:0016791). SH3 domain binding (GO:0017124).	small molecule catabolic process (GO:0044282). vesicle budding from membrane (GO:0006900). cellular carbohydrate metabolic process (GO:0044262). synaptic vesicle endocytosis (GO:0048488). membrane invagination (GO:0010324). alcohol metabolic process (GO:0006066). phosphatidylinositol metabolic process (GO:0046488). brain development (GO:0007420).	presynapse (GO:0098793). perinuclear region of cytoplasm (GO:0048471).	phosphatase (PC00181).

HFD+PB vs ND - DOWNREGULATED							
Gene Symbol	**log2FC**	***P* value**	**Hit?**	**Molecular Function**	**Biological Function**	**Cellular Component**	**Protein Class**
					organophosphate catabolic process (GO:0046434). dephosphorylation (GO:0016311). nervous system process (GO:0050877). behavior (GO:0007610).		
Srgn	-1.550	0.017	Yes	————	————	————	————
Cwf19l2	-1.543	0.013	Yes	————	mRNA splicing, via spliceosome (GO:0000398).	post-mRNA release spliceosomal complex (GO:0071014). U5 snRNP (GO:0005682).	————
Rnf216	-1.543	0.011	Yes	————	————	————	ubiquitin-protein ligase (PC00234).

HFD+PB vs ND - DOWNREGULATED							
Gene Symbol	**log2FC**	***P* value**	**Hit?**	**Molecular Function**	**Biological Function**	**Cellular Component**	**Protein Class**
Adcyap1r1	-1.541	0.037	Yes	G protein-coupled peptide receptor activity (GO:0008528). peptide hormone binding (GO:0017046).	————	————	————
Ipo7	-1.540	0.000	Yes	————	protein import into nucleus (GO:0006606).	nuclear envelope (GO:0005635). cytosol (GO:0005829). vacuole (GO:0005773). plasma membrane (GO:0005886).	transporter (PC00227).
Ptp4a3	-1.539	0.018	Yes	————	————	nucleus (GO:0005634).	————

HFD+PB vs ND - DOWNREGULATED							
Gene Symbol	**log2FC**	***P* value**	**Hit?**	**Molecular Function**	**Biological Function**	**Cellular Component**	**Protein Class**
Stmn2	-1.535	0.003	Yes	tubulin binding (GO:0015631).	neuron projection development (GO:0031175). regulation of microtubule polymerization or depolymerization (GO:0031110). microtubule depolymerization (GO:0007019).	growth cone (GO:0030426). cytoplasm (GO:0005737). plasma membrane region (GO:0098590).	————
Csmd2	-1.535	0.002	Yes	————	————	————	————
Lrrc4b	-1.535	0.009	Yes	————	————	————	————
Scgb2b24	-1.532	0.012	Yes	————	————	————	————

HFD+PB vs ND - DOWNREGULATED							
Gene Symbol	**log2FC**	***P* value**	**Hit?**	**Molecular Function**	**Biological Function**	**Cellular Component**	**Protein Class**
Enoph1	-1.527	0.036	Yes	phosphatase activity (GO:0016791).	alpha-amino acid metabolic process (GO:1901605). sulfur compound metabolic process (GO:0006790). drug metabolic process (GO:0017144). cellular amino acid biosynthetic process (GO:0008652).	————	phosphatase (PC00181).
Faim2	-1.527	0.003	Yes	————	————	————	————
Ermn	-1.519	0.005	Yes	————	————	————	————
Azin1	-1.519	0.002	No	————	————	————	————

HFD+PB vs ND - DOWNREGULATED							
Gene Symbol	**log2FC**	***P* value**	**Hit?**	**Molecular Function**	**Biological Function**	**Cellular Component**	**Protein Class**
Sox10	-1.517	0.015	Yes	DNA-binding transcription activator activity, RNA polymerase II-specific (GO:0001228).	negative regulation of transcription by RNA polymerase II (GO:0000122). morphogenesis of an epithelium (GO:0002009). transcription by RNA polymerase II (GO:0006366). positive regulation of transcription by RNA polymerase II (GO:0045944).	————	————
Rnf111	-1.516	0.015	Yes	ubiquitin protein ligase activity (GO:0061630). SMAD binding (GO:0046332).	ubiquitin-dependent protein catabolic process (GO:0006511).	nucleus (GO:0005634). cytoplasm (GO:0005737).	————

HFD+PB vs ND - DOWNREGULATED							
Gene Symbol	**log2FC**	***P* value**	**Hit?**	**Molecular Function**	**Biological Function**	**Cellular Component**	**Protein Class**
Gramd1c	-1.513	0.000	Yes	————	————	————	————
Ngef	-1.513	0.010	No	————	————	————	————
Krt26	-1.504	0.033	Yes	————	————	————	————
Ash1l	-1.500	0.003	Yes	————	————	————	————
Baalc	-1.497	0.016	Yes	————	————	cytoplasm (GO:0005737).	————

HFD+PB vs ND - DOWNREGULATED							
Gene Symbol	**log2FC**	***P* value**	**Hit?**	**Molecular Function**	**Biological Function**	**Cellular Component**	**Protein Class**
Gng3	-1.496	0.007	Yes	protein binding (GO:0005515).	G protein-coupled receptor signaling pathway (GO:0007186).	catalytic complex (GO:1902494). leaflet of membrane bilayer (GO:0097478). plasma membrane protein complex (GO:0098797). extrinsic component of cytoplasmic side of plasma membrane (GO:0031234). cytoplasmic part (GO:0044444).	heterotrimeric G-protein (PC00117).

HFD+PB vs ND - DOWNREGULATED							
Gene Symbol	**log2FC**	***P* value**	**Hit?**	**Molecular Function**	**Biological Function**	**Cellular Component**	**Protein Class**
Ets2	-1.490	0.008	Yes	DNA-binding transcription factor activity, RNA polymerase II-specific (GO:0000981).	cell differentiation (GO:0030154). transcription by RNA polymerase II (GO:0006366). regulation of transcription by RNA polymerase II (GO:0006357).	nucleus (GO:0005634).	winged helix/forkhead transcription factor (PC00246).
LOC108348326	-1.489	0.021	Yes	ubiquitin-protein transferase activity (GO:0004842).	protein import into peroxisome matrix (GO:0016558). protein monoubiquitination (GO:0006513).	integral component of peroxisomal membrane (GO:0005779). transporter complex (GO:1990351).	transfer/carrier protein (PC00219).

HFD+PB vs ND - DOWNREGULATED							
Gene Symbol	**log2FC**	***P* value**	**Hit?**	**Molecular Function**	**Biological Function**	**Cellular Component**	**Protein Class**
Gng2	-1.488	0.001	Yes	protein binding (GO:0005515).	G protein-coupled receptor signaling pathway (GO:0007186).	catalytic complex (GO:1902494). leaflet of membrane bilayer (GO:0097478). plasma membrane protein complex (GO:0098797). extrinsic component of cytoplasmic side of plasma membrane (GO:0031234). cytoplasmic part (GO:0044444).	heterotrimeric G-protein (PC00117).
Dlgap3	-1.488	0.013	No	————	————	————	————
Syce1l	-1.488	0.007	Yes	————	————	synaptonemal complex (GO:0000795).	————
Lzts1	-1.485	0.045	Yes	————	————	————	————
Sclt1	-1.485	0.028	Yes	————	————	————	————

HFD+PB vs ND - DOWNREGULATED							
Gene Symbol	**log2FC**	***P* value**	**Hit?**	**Molecular Function**	**Biological Function**	**Cellular Component**	**Protein Class**
Mt-nd6	-1.485	0.000	Yes	————	————	mitochondrion (GO:0005739).	oxidoreductase (PC00176).
Magi2	-1.483	0.049	No	————	————	————	————
Cse1l	-1.478	0.002	Yes	transporter activity (GO:0005215).	protein import into nucleus (GO:0006606). protein export from nucleus (GO:0006611).	nuclear envelope (GO:0005635). cytosol (GO:0005829). vacuole (GO:0005773). plasma membrane (GO:0005886).	transporter (PC00227).
Med14	-1.476	0.008	Yes	transcription coregulator activity (GO:0003712).	transcription by RNA polymerase II (GO:0006366). regulation of transcription by RNA polymerase II (GO:0006357).	core mediator complex (GO:0070847). mediator complex (GO:0016592).	general transcription factor (PC00259).

HFD+PB vs ND - DOWNREGULATED							
Gene Symbol	**log2FC**	***P* value**	**Hit?**	**Molecular Function**	**Biological Function**	**Cellular Component**	**Protein Class**
Cnrip1	-1.474	0.018	Yes	G protein-coupled receptor binding (GO:0001664).	signal transduction (GO:0007165). negative regulation of signaling receptor activity (GO:2000272).	plasma membrane (GO:0005886).	————
Serpini1	-1.474	0.009	Yes	endopeptidase inhibitor activity (GO:0004866). serine-type endopeptidase activity (GO:0004252). protease binding (GO:0002020).	proteolysis (GO:0006508). cellular protein metabolic process (GO:0044267). negative regulation of endopeptidase activity (GO:0010951).	extracellular space (GO:0005615).	protease inhibitor (PC00191).
RGD1308601	-1.474	0.007	Yes	ubiquitin protein ligase activity (GO:0061630).	ubiquitin-dependent protein catabolic process (GO:0006511).	————	————
Sult4a1	-1.470	0.009	Yes	————	————	————	————
Fkbp3	-1.469	0.000	Yes	————	————	————	————

HFD+PB vs ND - DOWNREGULATED							
Gene Symbol	**log2FC**	***P* value**	**Hit?**	**Molecular Function**	**Biological Function**	**Cellular Component**	**Protein Class**
Rnase4	-1.457	0.039	Yes	ribonuclease activity (GO:0004540).	————	————	————
Hook1	-1.457	0.015	Yes	microtubule binding (GO:0008017).	cytoskeleton-dependent intracellular transport (GO:0030705). cytoplasmic microtubule organization (GO:0031122).	centrosome (GO:0005813). centriole (GO:0005814).	membrane traffic protein (PC00150).
Kcna6	-1.457	0.004	No	————	————	————	————
Prim1	-1.457	0.009	Yes	DNA-directed 5'-3' RNA polymerase activity (GO:0003899).	DNA-dependent DNA replication (GO:0006261). DNA biosynthetic process (GO:0071897). RNA biosynthetic process (GO:0032774).	————	primase (PC00189).
Cnih2	-1.452	0.001	Yes	————	————	————	membrane traffic protein (PC00150).

HFD+PB vs ND - DOWNREGULATED							
Gene Symbol	**log2FC**	***P* value**	**Hit?**	**Molecular Function**	**Biological Function**	**Cellular Component**	**Protein Class**
Mt-nd5	-1.448	0.000	Yes	————	————	————	oxidoreductase (PC00176).

Scn1b	-1.445	0.045	Yes	molecular function regulator (GO:0098772). cation channel activity (GO:0005261). sodium ion transmembrane transporter activity (GO:0015081). ion channel binding (GO:0044325).	actin filament-based process (GO:0030029). regulation of metal ion transport (GO:0010959). movement of cell or subcellular component (GO:0006928). signaling (GO:0023052). regulation of heart contraction (GO:0008016). action potential (GO:0001508). sodium ion transmembrane transport (GO:0035725). cardiac muscle contraction (GO:0060048).	integral component of plasma membrane (GO:0005887). plasma membrane protein complex (GO:0098797). cation channel complex (GO:0034703).	voltage-gated ion channel (PC00241).

HFD+PB vs ND - DOWNREGULATED							
Gene Symbol	**log2FC**	***P* value**	**Hit?**	**Molecular Function**	**Biological Function**	**Cellular Component**	**Protein Class**
					regulation of cation transmembrane transport (GO:1904062). regulation of ion transmembrane transporter activity (GO:0032412).		
Prc1	-1.438	0.036	Yes	————	————	————	non-motor microtubule binding protein (PC00166).
Tjp1	-1.437	0.014	Yes	————	————	————	tight junction (PC00214).
Ppfia3	-1.433	0.036	No	————	————	————	————
Clk1	-1.430	0.038	Yes	————	————	————	————

HFD+PB vs ND - DOWNREGULATED							
Gene Symbol	**log2FC**	***P* value**	**Hit?**	**Molecular Function**	**Biological Function**	**Cellular Component**	**Protein Class**
Tnrc6b	-1.430	0.000	Yes	————	regulation of mRNA catabolic process (GO:0061013). gene silencing by miRNA (GO:0035195). positive regulation of RNA metabolic process (GO:0051254). gene expression (GO:0010467). positive regulation of cellular catabolic process (GO:0031331). nuclear-transcribed mRNA poly (A). tail shortening (GO:0000289).	P-body (GO:0000932). nucleoplasm (GO:0005654).	RNA binding protein (PC00031).
Gtf2b	-1.418	0.045	No	————	————	————	————

HFD+PB vs ND - DOWNREGULATED							
Gene Symbol	**log2FC**	***P* value**	**Hit?**	**Molecular Function**	**Biological Function**	**Cellular Component**	**Protein Class**
Sycp3	-1.418	0.020	Yes	————	spermatid development (GO:0007286). meiotic nuclear division (GO:0140013).	synaptonemal complex (GO:0000795).	————
Gnao1	-1.413	0.004	Yes	G protein-coupled receptor binding (GO:0001664). GTPase activity (GO:0003924). protein-containing complex binding (GO:0044877).	regulation of cAMP-mediated signaling (GO:0043949). regulation of adenylate cyclase activity (GO:0045761). adenylate cyclase-modulating G protein-coupled receptor signaling pathway (GO:0007188). cAMP-mediated signaling (GO:0019933).	catalytic complex (GO:1902494). leaflet of membrane bilayer (GO:0097478). plasma membrane protein complex (GO:0098797). extrinsic component of cytoplasmic side of plasma membrane (GO:0031234).	heterotrimeric G-protein (PC00117).

Tcf7l2	-1.410	0.005	Yes	transcription regulatory region DNA binding (GO:0044212). sequence-specific DNA binding (GO:0043565). beta-catenin binding (GO:0008013).	regulation of insulin secretion (GO:0050796). positive regulation of signaling (GO:0023056). insulin secretion (GO:0030073). positive regulation of cell communication (GO:0010647). cell fate commitment (GO:0045165). glucose homeostasis (GO:0042593). canonical Wnt signaling pathway (GO:0060070). transcription by RNA polymerase II (GO:0006366).	nucleus (GO:0005634). transcription factor complex (GO:0005667).	————

HFD+PB vs ND - DOWNREGULATED							
Gene Symbol	**log2FC**	***P* value**	**Hit?**	**Molecular Function**	**Biological Function**	**Cellular Component**	**Protein Class**
					muscle structure development (GO:0061061). positive regulation of protein secretion (GO:0050714). regulation of transcription by RNA polymerase II (GO:0006357).		
Htra1	-1.408	0.030	Yes	————	————	————	serine protease (PC00203).
LOC108348175	-1.402	0.000	Yes	RNA binding (GO:0003723).	————	nucleus (GO:0005634).	RNA splicing factor (PC00148).
Mospd2	-1.395	0.041	Yes	————	————	————	————

HFD+PB vs ND - DOWNREGULATED							
Gene Symbol	**log2FC**	***P* value**	**Hit?**	**Molecular Function**	**Biological Function**	**Cellular Component**	**Protein Class**
Nckap5	-1.391	0.045	Yes	————	microtubule bundle formation (GO:0001578). microtubule depolymerization (GO:0007019).	microtubule (GO:0005874).	————
Man1c1	-1.391	0.039	Yes	hydrolase activity (GO:0016787).	glycoprotein metabolic process (GO:0009100).	extracellular space (GO:0005615). vesicle (GO:0031982). Golgi membrane (GO:0000139). endoplasmic reticulum (GO:0005783). vacuole (GO:0005773). plasma membrane (GO:0005886).	protein modifying enzyme (PC00260).

HFD+PB vs ND - DOWNREGULATED							
Gene Symbol	**log2FC**	***P* value**	**Hit?**	**Molecular Function**	**Biological Function**	**Cellular Component**	**Protein Class**
Resp18	-1.391	0.007	Yes	————	————	endoplasmic reticulum (GO:0005783). vacuole (GO:0005773). plasma membrane (GO:0005886).	————
Snrpf	-1.388	0.032	Yes	RNA binding (GO:0003723).	————	————	RNA splicing factor (PC00148).
Sec23b	-1.381	0.001	Yes	GTPase activity (GO:0003924). GTPase activator activity (GO:0005096).	COPII-coated vesicle budding (GO:0090114).	membrane coat (GO:0030117). ER to Golgi transport vesicle membrane (GO:0012507). endoplasmic reticulum part (GO:0044432). vacuole (GO:0005773). plasma membrane (GO:0005886).	vesicle coat protein (PC00235).

HFD+PB vs ND - DOWNREGULATED							
Gene Symbol	**log2FC**	***P* value**	**Hit?**	**Molecular Function**	**Biological Function**	**Cellular Component**	**Protein Class**
Zfp365	-1.378	0.025	Yes	————	————	————	————
Dhx32	-1.370	0.021	Yes	RNA binding (GO:0003723).	————	spliceosomal complex (GO:0005681).	RNA helicase (PC00032).
Ahnak	-1.367	0.010	Yes	RNA binding (GO:0003723).	RNA splicing (GO:0008380). regulation of RNA splicing (GO:0043484).	cytoplasm (GO:0005737). plasma membrane (GO:0005886).	————
Ublcp1	-1.362	0.030	No	————	————	————	————
Rammet	-1.361	0.013	Yes	————	————	————	————
Fbxo38	-1.357	0.030	Yes	————	————	————	————
Pitrm1	-1.357	0.041	Yes	————	————	————	metalloprotease (PC00153).

HFD+PB vs ND - DOWNREGULATED							
Gene Symbol	**log2FC**	***P* value**	**Hit?**	**Molecular Function**	**Biological Function**	**Cellular Component**	**Protein Class**
Cbr4	-1.354	0.002	Yes	oxidoreductase activity, acting on the CH-OH group of donors, NAD or NADP as acceptor (GO:0016616). cofactor binding (GO:0048037).	oxidation-reduction process (GO:0055114). fatty acid biosynthetic process (GO:0006633).	————	oxidoreductase (PC00176).
Nt5dc1	-1.354	0.004	Yes	5'-nucleotidase activity (GO:0008253).	————	————	nucleotide phosphatase (PC00173).
Cldn11	-1.352	0.027	No	————	————	————	————
Tbc1d5	-1.352	0.000	Yes	GTPase activity (GO:0003924). GTPase activator activity (GO:0005096). Rab GTPase binding (GO:0017137).	intracellular protein transport (GO:0006886). positive regulation of GTPase activity (GO:0043547).	————	GTPase-activating protein (PC00257).

HFD+PB vs ND - DOWNREGULATED							
Gene Symbol	**log2FC**	***P* value**	**Hit?**	**Molecular Function**	**Biological Function**	**Cellular Component**	**Protein Class**
Cherp	-1.352	0.023	Yes	————	cellular calcium ion homeostasis (GO:0006874).	perinuclear region of cytoplasm (GO:0048471).	RNA binding protein (PC00031).
Slc4a10	-1.331	0.031	Yes	solute:sodium symporter activity (GO:0015370). organic anion transmembrane transporter activity (GO:0008514).	regulation of intracellular pH (GO:0051453). organic anion transport (GO:0015711).	————	secondary carrier transporter (PC00258).
Slc44a1	-1.322	0.034	No	————	————	————	————

Hcrt	-1.318	0.043	Yes	neuropeptide hormone activity (GO:0005184). neuropeptide receptor binding (GO:0071855).	regulation of neurotransmitter secretion (GO:0046928). positive regulation of signaling (GO:0023056). positive regulation of cell communication (GO:0010647). homeostatic process (GO:0042592). positive regulation of multicellular organismal process (GO:0051240). response to starvation (GO:0042594). regulation of system process (GO:0044057).	perinuclear region of cytoplasm (GO:0048471).	————

HFD+PB vs ND - DOWNREGULATED							
Gene Symbol	**log2FC**	***P* value**	**Hit?**	**Molecular Function**	**Biological Function**	**Cellular Component**	**Protein Class**
					action potential (GO:0001508). nervous system process (GO:0050877). behavior (GO:0007610). neurotransmitter secretion (GO:0007269).		
Med24	-1.318	0.019	Yes	transcription coregulator activity (GO:0003712).	————	core mediator complex (GO:0070847). mediator complex (GO:0016592).	general transcription factor (PC00259).
Ankrd40	-1.312	0.008	Yes	————	————	————	————
Nelfa	-1.312	0.016	Yes	————	————	————	————
Crym	-1.310	0.018	No	————	————	————	————

HFD+PB vs ND - DOWNREGULATED							
Gene Symbol	**log2FC**	***P* value**	**Hit?**	**Molecular Function**	**Biological Function**	**Cellular Component**	**Protein Class**
Arih1	-1.310	0.011	Yes	ubiquitin-like protein conjugating enzyme binding (GO:0044390). ubiquitin protein ligase activity (GO:0061630).	proteasome-mediated ubiquitin-dependent protein catabolic process (GO:0043161). protein polyubiquitination (GO:0000209). positive regulation of proteasomal ubiquitin-dependent protein catabolic process (GO:0032436).	ubiquitin ligase complex (GO:0000151). cytoplasm (GO:0005737).	ubiquitin-protein ligase (PC00234).
Rbm3	-1.308	0.004	No	————	————	————	————
Tmem126a	-1.302	0.001	Yes	————	————	————	————
Khdrbs3	-1.297	0.024	No	————	————	————	————

HFD+PB vs ND - DOWNREGULATED							
Gene Symbol	**log2FC**	***P* value**	**Hit?**	**Molecular Function**	**Biological Function**	**Cellular Component**	**Protein Class**
Heatr5a	-1.294	0.041	Yes	————	vesicle budding from membrane (GO:0006900). protein localization (GO:0008104). membrane invagination (GO:0010324). endocytosis (GO:0006897). retrograde transport, endosome to Golgi (GO:0042147).	endocytic vesicle (GO:0030139). Golgi apparatus (GO:0005794). vacuole (GO:0005773). plasma membrane (GO:0005886).	————
Atat1	-1.285	0.049	Yes	peptide-lysine-N-acetyltransferase activity (GO:0061733).	internal peptidyl-lysine acetylation (GO:0018393).	————	————
Lrrc8c	-1.285	0.018	Yes	————	————	————	scaffold/adaptor protein (PC00226).

HFD+PB vs ND - DOWNREGULATED							
Gene Symbol	**log2FC**	***P* value**	**Hit?**	**Molecular Function**	**Biological Function**	**Cellular Component**	**Protein Class**
Nudcd2	-1.280	0.008	Yes	unfolded protein binding (GO:0051082).	protein folding (GO:0006457).	cytoplasm (GO:0005737).	microtubule or microtubule-binding cytoskeletal protein (PC00157).
ST7	-1.279	0.022	Yes	————	————	————	————
Syt14	-1.276	0.043	Yes	————	————	————	————
Dbndd2	-1.270	0.001	Yes	————	————	————	————
Tmem38a	-1.270	0.024	No	————	————	————	————
Strn3	-1.270	0.012	Yes	calmodulin binding (GO:0005516). protein phosphatase binding (GO:0019903). protein-containing complex binding (GO:0044877).	————	dendrite (GO:0030425). plasma membrane region (GO:0098590).	————

Syt4	-1.269	0.048	Yes	calcium ion binding (GO:0005509). SNARE binding (GO:0000149). clathrin binding (GO:0030276). calcium-dependent phospholipid binding (GO:0005544).	regulation of response to stimulus (GO:0048583). vesicle fusion to plasma membrane (GO:0099500). ammonium transport (GO:0015696). organic hydroxy compound transport (GO:0015850). drug transport (GO:0015893). response to calcium ion (GO:0051592). calcium-ion regulated exocytosis (GO:0017156). regulation of exocytosis (GO:0017157). regulation of ion transport (GO:0043269).	exocytic vesicle (GO:0070382). plasma membrane region (GO:0098590). vacuole (GO:0005773). axon (GO:0030424).	membrane trafficking regulatory protein (PC00151).

HFD+PB vs ND - DOWNREGULATED							
Gene Symbol	**log2FC**	***P* value**	**Hit?**	**Molecular Function**	**Biological Function**	**Cellular Component**	**Protein Class**
					cellular response to chemical stimulus (GO:0070887).		
Srsf2	-1.267	0.001	Yes	RNA binding (GO:0003723).	mRNA cis splicing, via spliceosome (GO:0045292). regulation of alternative mRNA splicing, via spliceosome (GO:0000381). alternative mRNA splicing, via spliceosome (GO:0000380).	cytoplasm (GO:0005737). nuclear speck (GO:0016607).	RNA splicing factor (PC00148).

HFD+PB vs ND - DOWNREGULATED							
Gene Symbol	**log2FC**	***P* value**	**Hit?**	**Molecular Function**	**Biological Function**	**Cellular Component**	**Protein Class**
Trappc8	-1.262	0.028	Yes	————	autophagosome assembly (GO:0000045). endoplasmic reticulum to Golgi vesicle-mediated transport (GO:0006888). vacuolar protein processing (GO:0006624). peroxisome organization (GO:0007031). organelle disassembly (GO:1903008). protein localization to vacuole (GO:0072665).	TRAPP complex (GO:0030008). phagophore assembly site (GO:0000407). Golgi apparatus part (GO:0044431). cytoplasmic vesicle (GO:0031410). vacuole (GO:0005773). plasma membrane (GO:0005886).	————
Cxcl14	-1.259	0.004	Yes	————	————	————	————

HFD+PB vs ND - DOWNREGULATED							
Gene Symbol	**log2FC**	***P* value**	**Hit?**	**Molecular Function**	**Biological Function**	**Cellular Component**	**Protein Class**
Eef1a2	-1.257	0.000	Yes	translation regulator activity (GO:0045182). RNA binding (GO:0003723). GTPase activity (GO:0003924).	translational elongation (GO:0006414).	————	translation factor (PC00223).
Rhot1	-1.255	0.028	Yes	GTP binding (GO:0005525). GTPase activity (GO:0003924).	organelle transport along microtubule (GO:0072384). Rho protein signal transduction (GO:0007266). regulation of mitochondrion organization (GO:0010821). mitochondrion organization (GO:0007005).	integral component of mitochondrial outer membrane (GO:0031307).	small GTPase (PC00208).
Nsf	-1.250	0.025	No	————	————	————	————
Selenos	-1.248	0.000	No	————	————	————	————

Moxd1	-1.248	0.003	Yes	copper ion binding (GO:0005507). oxidoreductase activity, acting on paired donors, with incorporation or reduction of molecular oxygen (GO:0016705). monooxygenase activity (GO:0004497).	aromatic compound catabolic process (GO:0019439). organic cyclic compound catabolic process (GO:1901361). cellular nitrogen compound biosynthetic process (GO:0044271). organic cyclic compound biosynthetic process (GO:1901362). alcohol biosynthetic process (GO:0046165). regulation of neurotransmitter levels (GO:0001505).	secretory granule membrane (GO:0030667). extracellular space (GO:0005615). vacuole (GO:0005773). plasma membrane (GO:0005886).	————

HFD+PB vs ND - DOWNREGULATED							
Gene Symbol	**log2FC**	***P* value**	**Hit?**	**Molecular Function**	**Biological Function**	**Cellular Component**	**Protein Class**
					organonitrogen compound catabolic process (GO:1901565). drug metabolic process (GO:0017144). organonitrogen compound biosynthetic process (GO:1901566). ammonium ion metabolic process (GO:0097164). aromatic compound biosynthetic process (GO:0019438).		
Ndrg1	-1.245	0.019	Yes	————	signal transduction (GO:0007165).	cytoplasm (GO:0005737).	serine protease (PC00203).
Galnt11	-1.244	0.010	No	————	————	————	————

HFD+PB vs ND - DOWNREGULATED							
Gene Symbol	**log2FC**	***P* value**	**Hit?**	**Molecular Function**	**Biological Function**	**Cellular Component**	**Protein Class**
Pllp	-1.244	0.032	Yes	structural molecule activity (GO:0005198).	myelination (GO:0042552).	integral component of membrane (GO:0016021).	membrane traffic protein (PC00150).
Qrich1	-1.243	0.028	Yes	DNA-binding transcription factor activity, RNA polymerase II-specific (GO:0000981).	regulation of cell morphogenesis (GO:0022604). cell morphogenesis (GO:0000902). transcription by RNA polymerase II (GO:0006366). regulation of transcription by RNA polymerase II (GO:0006357).	nucleus (GO:0005634).	zinc finger transcription factor (PC00244).

HFD+PB vs ND - DOWNREGULATED							
Gene Symbol	**log2FC**	***P* value**	**Hit?**	**Molecular Function**	**Biological Function**	**Cellular Component**	**Protein Class**
Usp25	-1.243	0.019	Yes	thiol-dependent ubiquitin-specific protease activity (GO:0004843). cysteine-type endopeptidase activity (GO:0004197).	protein deubiquitination (GO:0016579).	————	cysteine protease (PC00081).

HFD+PB vs ND - DOWNREGULATED							
Gene Symbol	**log2FC**	***P* value**	**Hit?**	**Molecular Function**	**Biological Function**	**Cellular Component**	**Protein Class**
Bbs9	-1.239	0.015	Yes	————	intraciliary transport involved in cilium assembly (GO:0035735). vesicle targeting, trans-Golgi to periciliary membrane compartment (GO:0097712). axoneme assembly (GO:0035082). ciliary transition zone assembly (GO:1905349). protein localization to cilium (GO:0061512).	BBSome (GO:0034464). intraciliary transport particle (GO:0030990). plasma membrane region (GO:0098590).	————
Fam216b	-1.238	0.010	Yes	————	————	————	————
Clpx	-1.236	0.020	Yes	————	————	————	————
Zfp266	-1.234	0.045	No	————	————	————	————

HFD+PB vs ND - DOWNREGULATED							
Gene Symbol	**log2FC**	***P* value**	**Hit?**	**Molecular Function**	**Biological Function**	**Cellular Component**	**Protein Class**
Socs5	-1.234	0.027	Yes	phosphotransferase activity, alcohol group as acceptor (GO:0016773). kinase activity (GO:0016301). kinase binding (GO:0019900). kinase regulator activity (GO:0019207).	phosphatidylinositol phosphorylation (GO:0046854).	phosphatidylinositol 3-kinase complex (GO:0005942).	kinase modulator (PC00140).
Nrxn2	-1.232	0.015	No	————	————	————	————
Sh3glb1	-1.228	0.002	Yes	————	————	————	————
Mt-nd4	-1.227	0.000	Yes	NADH dehydrogenase activity (GO:0003954). cofactor binding (GO:0048037).	proton transmembrane transport (GO:1902600). aerobic respiration (GO:0009060).	respiratory chain complex I (GO:0045271).	oxidoreductase (PC00176).

HFD+PB vs ND - DOWNREGULATED							
Gene Symbol	**log2FC**	***P* value**	**Hit?**	**Molecular Function**	**Biological Function**	**Cellular Component**	**Protein Class**
Slc35d1	-1.226	0.011	Yes	antiporter activity (GO:0015297). pyrimidine nucleotide-sugar transmembrane transporter activity (GO:0015165). organic anion transmembrane transporter activity (GO:0008514).	————	Golgi apparatus (GO:0005794). vacuole (GO:0005773). plasma membrane (GO:0005886).	secondary carrier transporter (PC00258).
Ndn	-1.222	0.000	Yes	————	————	————	scaffold/adaptor protein (PC00226).

HFD+PB vs ND - DOWNREGULATED							
Gene Symbol	**log2FC**	***P* value**	**Hit?**	**Molecular Function**	**Biological Function**	**Cellular Component**	**Protein Class**
Osbp	-1.216	0.003	Yes	sterol binding (GO:0032934). lipid transporter activity (GO:0005319).	————	perinuclear region of cytoplasm (GO:0048471). endoplasmic reticulum part (GO:0044432). cytosol (GO:0005829). vacuole (GO:0005773). plasma membrane (GO:0005886).	————
Cnot7	-1.214	0.008	Yes	poly (A).-specific ribonuclease activity (GO:0004535).	negative regulation of translation (GO:0017148). translational elongation (GO:0006414). nuclear-transcribed mRNA catabolic process, deadenylation-dependent decay (GO:0000288).	P-body (GO:0000932). CCR4-NOT complex (GO:0030014).	mRNA polyadenylation factor (PC00146).

HFD+PB vs ND - DOWNREGULATED							
Gene Symbol	**log2FC**	***P* value**	**Hit?**	**Molecular Function**	**Biological Function**	**Cellular Component**	**Protein Class**
Matr3	-1.211	0.001	No	————	————	————	————
Tank	-1.211	0.019	Yes	————	————	————	————
Cltrn	-1.211	0.000	Yes	————	————	————	————

Dnm1	-1.207	0.031	Yes	GTPase activity (GO:0003924). microtubule binding (GO:0008017).	establishment of protein localization to organelle (GO:0072594). membrane fusion (GO:0061025). protein-containing complex localization (GO:0031503). vesicle budding from membrane (GO:0006900). synaptic vesicle transport (GO:0048489). synaptic vesicle endocytosis (GO:0048488). protein transport (GO:0015031). regulation of synapse structure or activity (GO:0050803).	membrane coat (GO:0030117). postsynaptic density (GO:0014069). microtubule cytoskeleton (GO:0015630). mitochondrial membrane (GO:0031966). postsynaptic membrane (GO:0045211). dendritic spine (GO:0043197). cytoplasmic vesicle (GO:0031410). axon (GO:0030424).	membrane traffic protein (PC00150).

HFD+PB vs ND - DOWNREGULATED							
Gene Symbol	**log2FC**	***P* value**	**Hit?**	**Molecular Function**	**Biological Function**	**Cellular Component**	**Protein Class**
					membrane invagination (GO:0010324). receptor internalization (GO:0031623). mitochondrial fission (GO:0000266).		

Ptk2b	-1.205	0.036	Yes	protein tyrosine kinase activity (GO:0004713). signaling receptor binding (GO:0005102).	cell population proliferation (GO:0008283). peptidyl-tyrosine phosphorylation (GO:0018108). angiogenesis (GO:0001525). epidermal growth factor receptor signaling pathway (GO:0007173). cell differentiation (GO:0030154). cell adhesion (GO:0007155). regulation of cell adhesion (GO:0030155). regulation of cell population proliferation (GO:0042127).	focal adhesion (GO:0005925). leaflet of membrane bilayer (GO:0097478). dendritic spine (GO:0043197). extrinsic component of cytoplasmic side of plasma membrane (GO:0031234). plasma membrane region (GO:0098590).	————

HFD+PB vs ND - DOWNREGULATED							
Gene Symbol	**log2FC**	***P* value**	**Hit?**	**Molecular Function**	**Biological Function**	**Cellular Component**	**Protein Class**
Ctxn1	-1.204	0.003	Yes	————	————	————	————
Bok	-1.203	0.029	Yes	protein homodimerization activity (GO:0042803).	extrinsic apoptotic signaling pathway (GO:0097191). intrinsic apoptotic signaling pathway in response to DNA damage (GO:0008630).	mitochondrial outer membrane (GO:0005741).	————
Gtf2a2	-1.198	0.004	Yes	transcription coactivator activity (GO:0003713). TBP-class protein binding (GO:0017025).	RNA polymerase II preinitiation complex assembly (GO:0051123). positive regulation of DNA-binding transcription factor activity (GO:0051091). positive regulation of transcription by RNA polymerase II (GO:0045944).	RNA polymerase II transcription factor complex (GO:0090575). RNA polymerase II, holoenzyme (GO:0016591).	general transcription factor (PC00259).

HFD+PB vs ND - DOWNREGULATED							
Gene Symbol	**log2FC**	***P* value**	**Hit?**	**Molecular Function**	**Biological Function**	**Cellular Component**	**Protein Class**
Map4k4	-1.198	0.011	Yes	protein serine/threonine kinase activity (GO:0004674).	stress-activated protein kinase signaling cascade (GO:0031098). mitotic nuclear division (GO:0140014). neuron projection morphogenesis (GO:0048812). activation of protein kinase activity (GO:0032147). signal transduction by protein phosphorylation (GO:0023014). regulation of mitotic cell cycle (GO:0007346).	cytoplasm (GO:0005737).	————
Cdh13	-1.190	0.032	Yes	————	————	————	————

HFD+PB vs ND - DOWNREGULATED							
Gene Symbol	**log2FC**	***P* value**	**Hit?**	**Molecular Function**	**Biological Function**	**Cellular Component**	**Protein Class**
Mt-nd3	-1.189	0.013	Yes	————	————	————	oxidoreductase (PC00176).
Mdm1	-1.188	0.024	Yes	————	————	————	————
Ttc30b	-1.187	0.014	No	————	————	————	————
Vps13d	-1.186	0.032	Yes	————	maintenance of location (GO:0051235). protein localization to Golgi apparatus (GO:0034067). protein targeting to vacuole (GO:0006623). cellular process (GO:0009987).	extrinsic component of membrane (GO:0019898).	————

HFD+PB vs ND - DOWNREGULATED							
Gene Symbol	**log2FC**	***P* value**	**Hit?**	**Molecular Function**	**Biological Function**	**Cellular Component**	**Protein Class**
Rcan2	-1.184	0.031	Yes	protein serine/threonine phosphatase activity (GO:0004722). protein phosphatase binding (GO:0019903). protein phosphatase regulator activity (GO:0019888).	inositol phosphate-mediated signaling (GO:0048016). regulation of intracellular signal transduction (GO:1902531). calcium-mediated signaling (GO:0019722).	cytoplasm (GO:0005737).	intercellular signal molecule (PC00207).
Cox7c	-1.183	0.041	Yes	cytochrome-c oxidase activity (GO:0004129).	mitochondrial electron transport, cytochrome c to oxygen (GO:0006123). ATP synthesis coupled proton transport (GO:0015986).	————	oxidase (PC00175).
Timm9	-1.178	0.004	Yes	————	————	————	primary active transporter (PC00068).

HFD+PB vs ND - DOWNREGULATED							
Gene Symbol	**log2FC**	***P* value**	**Hit?**	**Molecular Function**	**Biological Function**	**Cellular Component**	**Protein Class**
Mpc1	-1.175	0.020	Yes	monocarboxylic acid transmembrane transporter activity (GO:0008028).	mitochondrial transmembrane transport (GO:1990542). carboxylic acid transmembrane transport (GO:1905039). monocarboxylic acid transport (GO:0015718).	integral component of mitochondrial inner membrane (GO:0031305).	————
Farp1	-1.172	0.047	Yes	Rac GTPase binding (GO:0048365). Rho guanyl-nucleotide exchange factor activity (GO:0005089).	————	————	————

Msr1	-1.171	0.003	Yes	low-density lipoprotein particle binding (GO:0030169). amyloid-beta binding (GO:0001540).	extracellular structure organization (GO:0043062). lipid storage (GO:0019915). plasma lipoprotein particle clearance (GO:0034381). regulation of localization (GO:0032879). vesicle budding from membrane (GO:0006900). membrane invagination (GO:0010324). positive regulation of biological process (GO:0048518). receptor-mediated endocytosis (GO:0006898). protein-containing complex disassembly (GO:0032984).	leaflet of membrane bilayer (GO:0097478). external side of plasma membrane (GO:0009897).	serine protease (PC00203).

HFD+PB vs ND - DOWNREGULATED							
Gene Symbol	**log2FC**	***P* value**	**Hit?**	**Molecular Function**	**Biological Function**	**Cellular Component**	**Protein Class**
Herc2	-1.170	0.027	Yes	————	————	————	guanyl-nucleotide exchange factor (PC00113).
Gtf2f2	-1.170	0.000	No	————	————	————	————
Ttyh1	-1.168	0.001	Yes	ion gated channel activity (GO:0022839). chloride channel activity (GO:0005254).	————	plasma membrane (GO:0005886).	ion channel (PC00133).
Hif1a	-1.166	0.000	No	————	————	————	————

HFD+PB vs ND - DOWNREGULATED							
Gene Symbol	**log2FC**	***P* value**	**Hit?**	**Molecular Function**	**Biological Function**	**Cellular Component**	**Protein Class**
Gpd1	-1.160	0.021	Yes	oxidoreductase activity, acting on the CH-OH group of donors, NAD or NADP as acceptor (GO:0016616).	organophosphate metabolic process (GO:0019637). carbohydrate derivative metabolic process (GO:1901135). oxidation-reduction process (GO:0055114). phosphate-containing compound metabolic process (GO:0006796).	cytosol (GO:0005829).	dehydrogenase (PC00092).
Ogn	-1.156	0.021	Yes	————	————	————	————

HFD+PB vs ND - DOWNREGULATED							
Gene Symbol	**log2FC**	***P* value**	**Hit?**	**Molecular Function**	**Biological Function**	**Cellular Component**	**Protein Class**
Caly	-1.154	0.000	Yes	clathrin binding (GO:0030276).	cellular protein-containing complex assembly (GO:0034622). endosomal transport (GO:0016197).	endosome (GO:0005768). integral component of membrane (GO:0016021). vacuole (GO:0005773). plasma membrane (GO:0005886).	————
Trafd1	-1.153	0.043	No	————	————	————	————
Rpgr	-1.153	0.034	Yes	————	————	————	————
Psip1	-1.153	0.033	No	————	————	————	————
Cbfb	-1.153	0.030	Yes	transcription coactivator activity (GO:0003713). sequence-specific DNA binding (GO:0043565).	transcription by RNA polymerase II (GO:0006366). regulation of transcription by RNA polymerase II (GO:0006357).	RNA polymerase II transcription factor complex (GO:0090575).	DNA-binding transcription factor (PC00218).

HFD+PB vs ND - DOWNREGULATED							
Gene Symbol	**log2FC**	***P* value**	**Hit?**	**Molecular Function**	**Biological Function**	**Cellular Component**	**Protein Class**
Ptma	-1.152	0.000	Yes	————	————	————	————
Tubb4a	-1.151	0.041	Yes	GTP binding (GO:0005525). structural molecule activity (GO:0005198).	mitotic nuclear division (GO:0140014). microtubule cytoskeleton organization (GO:0000226).	cytoplasm (GO:0005737). microtubule (GO:0005874).	tubulin (PC00228).
Camkv	-1.150	0.018	No	————	————	————	————

HFD+PB vs ND - DOWNREGULATED							
Gene Symbol	**log2FC**	***P* value**	**Hit?**	**Molecular Function**	**Biological Function**	**Cellular Component**	**Protein Class**
Lamb1	-1.150	0.041	Yes	integrin binding (GO:0005178). extracellular matrix structural constituent (GO:0005201).	cellular component assembly (GO:0022607). extracellular matrix organization (GO:0030198). substrate adhesion-dependent cell spreading (GO:0034446). cell migration (GO:0016477). tissue development (GO:0009888). animal organ morphogenesis (GO:0009887).	basement membrane (GO:0005604). protein-containing complex (GO:0032991).	extracellular matrix protein (PC00102).
Ptprn	-1.148	0.035	Yes	————	————	————	————

HFD+PB vs ND - DOWNREGULATED							
Gene Symbol	**log2FC**	***P* value**	**Hit?**	**Molecular Function**	**Biological Function**	**Cellular Component**	**Protein Class**
Syn1	-1.146	0.002	Yes	————	neurotransmitter secretion (GO:0007269).	synaptic vesicle membrane (GO:0030672). vacuole (GO:0005773). plasma membrane (GO:0005886).	membrane trafficking regulatory protein (PC00151).
Tmcc2	-1.145	0.021	Yes	————	————	endomembrane system (GO:0012505). vacuole (GO:0005773). plasma membrane (GO:0005886).	————
Myadm	-1.144	0.019	No	————	————	————	————

HFD+PB vs ND - DOWNREGULATED							
Gene Symbol	**log2FC**	***P* value**	**Hit?**	**Molecular Function**	**Biological Function**	**Cellular Component**	**Protein Class**
LOC103689983	-1.140	0.001	Yes	magnesium ion binding (GO:0000287). transferase activity, transferring pentosyl groups (GO:0016763).	purine ribonucleotide biosynthetic process (GO:0009152). IMP metabolic process (GO:0046040). nucleobase metabolic process (GO:0009112). pigment metabolic process (GO:0042440). nucleobase-containing small molecule biosynthetic process (GO:0034404).	————	glycosyltransferase (PC00111).

HFD+PB vs ND - DOWNREGULATED							
Gene Symbol	**log2FC**	***P* value**	**Hit?**	**Molecular Function**	**Biological Function**	**Cellular Component**	**Protein Class**
Tbc1d1	-1.135	0.026	Yes	GTPase activity (GO:0003924). GTPase activator activity (GO:0005096). Rab GTPase binding (GO:0017137).	intracellular protein transport (GO:0006886). positive regulation of GTPase activity (GO:0043547).	————	GTPase-activating protein (PC00257).
Ep400	-1.135	0.018	Yes	————	————	————	————
Nxt1	-1.135	0.042	Yes	————	protein import into nucleus (GO:0006606).	vacuole (GO:0005773). plasma membrane (GO:0005886). nuclear pore central transport channel (GO:0044613).	————

HFD+PB vs ND - DOWNREGULATED							
Gene Symbol	**log2FC**	***P* value**	**Hit?**	**Molecular Function**	**Biological Function**	**Cellular Component**	**Protein Class**
Taf4b	-1.128	0.008	Yes	DNA binding (GO:0003677). transcription factor binding (GO:0008134).	transcription by RNA polymerase II (GO:0006366). positive regulation of transcription by RNA polymerase II (GO:0045944).	transcription factor TFIID complex (GO:0005669).	general transcription factor (PC00259).
39326.000	-1.125	0.008	No	————	————	————	————

HFD+PB vs ND - DOWNREGULATED							
Gene Symbol	**log2FC**	***P* value**	**Hit?**	**Molecular Function**	**Biological Function**	**Cellular Component**	**Protein Class**
Arid1a	-1.121	0.019	Yes	nucleosome binding (GO:0031491).	positive regulation of transcription, DNA-templated (GO:0045893). ATP-dependent chromatin remodeling (GO:0043044). transcription by RNA polymerase II (GO:0006366). regulation of transcription by RNA polymerase II (GO:0006357).	ATPase complex (GO:1904949). nuclear chromatin (GO:0000790). neuron part (GO:0097458). nucleoplasm (GO:0005654).	————
Zcchc24	-1.117	0.039	No	————	————	————	————
Plekha1	-1.114	0.039	Yes	protein binding (GO:0005515).	————	cytoplasm (GO:0005737).	————
Plcl1	-1.112	0.012	No	————	————	————	————
Ldlr	-1.111	0.032	No	————	————	————	————

HFD+PB vs ND - DOWNREGULATED							
Gene Symbol	**log2FC**	***P* value**	**Hit?**	**Molecular Function**	**Biological Function**	**Cellular Component**	**Protein Class**
Col4a3bp	-1.111	0.016	Yes	phospholipid transporter activity (GO:0005548). phosphatidylinositol phosphate binding (GO:1901981). amide binding (GO:0033218).	lipid transport (GO:0006869). membrane organization (GO:0061024). intracellular transport (GO:0046907). amide transport (GO:0042886).	cytosol (GO:0005829). Golgi apparatus (GO:0005794). vacuole (GO:0005773). plasma membrane (GO:0005886).	transfer/carrier protein (PC00219).
Arf4	-1.108	0.016	Yes	GTP binding (GO:0005525).	vesicle-mediated transport (GO:0016192). intracellular protein transport (GO:0006886).	cytoplasm (GO:0005737). plasma membrane (GO:0005886).	G-protein (PC00020).

HFD+PB vs ND - DOWNREGULATED							
Gene Symbol	**log2FC**	***P* value**	**Hit?**	**Molecular Function**	**Biological Function**	**Cellular Component**	**Protein Class**
Sppl2a	-1.108	0.006	Yes	endopeptidase activity (GO:0004175).	membrane protein proteolysis (GO:0033619).	cytoplasmic side of membrane (GO:0098562). leaflet of membrane bilayer (GO:0097478). Golgi-associated vesicle membrane (GO:0030660). integral component of endoplasmic reticulum membrane (GO:0030176). lysosomal membrane (GO:0005765). plasma membrane (GO:0005886).	aspartic protease (PC00053).

HFD+PB vs ND - DOWNREGULATED							
Gene Symbol	**log2FC**	***P* value**	**Hit?**	**Molecular Function**	**Biological Function**	**Cellular Component**	**Protein Class**
Rabgap1	-1.106	0.015	Yes	GTPase activity (GO:0003924). GTPase activator activity (GO:0005096). Rab GTPase binding (GO:0017137).	intracellular protein transport (GO:0006886). positive regulation of GTPase activity (GO:0043547).	————	GTPase-activating protein (PC00257).
Hydin	-1.106	0.005	Yes	————	————	————	————

Sema4d	-1.102	0.025	Yes	receptor ligand activity (GO:0048018).	negative regulation of locomotion (GO:0040013). neural crest cell differentiation (GO:0014033). regulation of cell size (GO:0008361). negative regulation of cellular component movement (GO:0051271). negative regulation of neuron differentiation (GO:0045665). axon guidance (GO:0007411). transcription by RNA polymerase II (GO:0006366).	integral component of plasma membrane (GO:0005887). extracellular space (GO:0005615).	membrane-bound signaling molecule (PC00152).

					cell surface receptor signaling pathway (GO:0007166). positive regulation of GTPase activity (GO:0043547). bone development (GO:0060348). negative regulation of transcription by RNA polymerase II (GO:0000122). negative regulation of phosphatase activity (GO:0010923). axon extension (GO:0048675). ossification (GO:0001503).		

					regulation of axonogenesis (GO:0050770). regulation of cell growth (GO:0001558). negative regulation of response to external stimulus (GO:0032102). dephosphorylation (GO:0016311). negative regulation of cellular component organization (GO:0051129). regulation of chemotaxis (GO:0050920). cell migration (GO:0016477). positive regulation of cell migration (GO:0030335).		

HFD+PB vs ND - DOWNREGULATED							
Gene Symbol	**log2FC**	***P* value**	**Hit?**	**Molecular Function**	**Biological Function**	**Cellular Component**	**Protein Class**
Vegfa	-1.102	0.011	No	————	————	————	————

Rhob	-1.096	0.015	Yes	GTP binding (GO:0005525). protein kinase binding (GO:0019901). GTPase activity (GO:0003924).	regulation of cell shape (GO:0008360). cortical cytoskeleton organization (GO:0030865). regulation of actin cytoskeleton organization (GO:0032956). cell morphogenesis (GO:0000902). establishment or maintenance of cell polarity (GO:0007163). actin filament organization (GO:0007015). Rho protein signal transduction (GO:0007266). cell migration (GO:0016477).	cytoskeleton (GO:0005856). cell cortex (GO:0005938). intracellular membrane-bounded organelle (GO:0043231). cytoplasmic vesicle (GO:0031410). cell projection (GO:0042995). plasma membrane (GO:0005886).	small GTPase (PC00208).

HFD+PB vs ND - DOWNREGULATED							
Gene Symbol	**log2FC**	***P* value**	**Hit?**	**Molecular Function**	**Biological Function**	**Cellular Component**	**Protein Class**
Htr2c	-1.095	0.000	No	————	————	————	————
Ubqln2	-1.090	0.007	Yes	polyubiquitin modification-dependent protein binding (GO:0031593).	autophagosome assembly (GO:0000045). regulation of macroautophagy (GO:0016241). ubiquitin-dependent ERAD pathway (GO:0030433).	cytosol (GO:0005829).	————
Dock8	-1.089	0.036	Yes	————	————	————	guanyl-nucleotide exchange factor (PC00113).
LOC499219	-1.087	0.032	Yes	————	————	————	P53-like transcription factor (PC00253).
Pphln1	-1.086	0.011	Yes	————	————	————	————

HFD+PB vs ND - DOWNREGULATED							
Gene Symbol	**log2FC**	***P* value**	**Hit?**	**Molecular Function**	**Biological Function**	**Cellular Component**	**Protein Class**
Dek	-1.085	0.016	Yes	histone binding (GO:0042393).	regulation of double-strand break repair (GO:2000779). double-strand break repair (GO:0006302).	nucleus (GO:0005634).	chromatin/chromatin-binding, or -regulatory protein (PC00077).
Kcnab1	-1.084	0.007	Yes	————	————	————	————
Bcas2	-1.080	0.003	Yes	————	————	catalytic step 2 spliceosome (GO:0071013). U5 snRNP (GO:0005682). Prp19 complex (GO:0000974).	RNA splicing factor (PC00148).
Ube3a	-1.076	0.047	Yes	————	————	————	————
Hccs	-1.072	0.035	Yes	lyase activity (GO:0016829).	cellular protein modification process (GO:0006464). cytochrome complex assembly (GO:0017004).	mitochondrion (GO:0005739).	lyase (PC00144).

HFD+PB vs ND - DOWNREGULATED							
Gene Symbol	**log2FC**	***P* value**	**Hit?**	**Molecular Function**	**Biological Function**	**Cellular Component**	**Protein Class**
Rad17	-1.070	0.045	Yes	DNA binding (GO:0003677). DNA-dependent ATPase activity (GO:0008094). chromatin binding (GO:0003682).	DNA damage checkpoint (GO:0000077). DNA repair (GO:0006281). G2/M transition of mitotic cell cycle (GO:0000086). mitotic nuclear division (GO:0140014). mitotic DNA replication checkpoint (GO:0033314).	nuclear chromatin (GO:0000790).	————
Yrdc	-1.070	0.012	Yes	nucleotidyltransferase activity (GO:0016779). tRNA binding (GO:0000049).	regulation of biological quality (GO:0065008).	cytoplasm (GO:0005737).	————
Mt-atp8	-1.069	0.027	Yes	ATPase activity (GO:0016887).	————	mitochondrial proton-transporting ATP synthase complex (GO:0005753).	ATP synthase (PC00002).

HFD+PB vs ND - DOWNREGULATED							
Gene Symbol	**log2FC**	***P* value**	**Hit?**	**Molecular Function**	**Biological Function**	**Cellular Component**	**Protein Class**
Jam3	-1.068	0.001	Yes	————	————	————	————
Zfp513	-1.068	0.031	Yes	RNA polymerase II regulatory region sequence-specific DNA binding (GO:0000977).	regulation of chromatin organization (GO:1902275). histone methylation (GO:0016571). regulation of gene expression (GO:0010468). gene expression (GO:0010467). regulation of protein modification process (GO:0031399).	histone methyltransferase complex (GO:0035097).	C2H2 zinc finger transcription factor (PC00248).
Tmem212	-1.067	0.016	Yes	————	————	————	transporter (PC00227).
Dnaaf1	-1.066	0.021	Yes	————	————	————	————

Lgals3	-1.066	0.013	Yes	extracellular matrix binding (GO:0050840). protein binding (GO:0005515). protein-containing complex binding (GO:0044877).	positive chemotaxis (GO:0050918). positive regulation of calcium ion transport (GO:0051928). extrinsic apoptotic signaling pathway (GO:0097191). negative regulation of transport (GO:0051051). endocytosis (GO:0006897). vesicle budding from membrane (GO:0006900). macrophage chemotaxis (GO:0048246). calcium ion transport (GO:0006816). membrane invagination (GO:0010324).	nucleus (GO:0005634). extracellular space (GO:0005615). cytoplasm (GO:0005737). collagen-containing extracellular matrix (GO:0062023). plasma membrane part (GO:0044459).	extracellular matrix protein (PC00102).

HFD+PB vs ND - DOWNREGULATED							
Gene Symbol	**log2FC**	***P* value**	**Hit?**	**Molecular Function**	**Biological Function**	**Cellular Component**	**Protein Class**
					negative regulation of extrinsic apoptotic signaling pathway (GO:2001237). granulocyte chemotaxis (GO:0071621). regulation of endocytosis (GO:0030100). negative regulation of cellular component organization (GO:0051129).		

HFD+PB vs ND - DOWNREGULATED							
Gene Symbol	**log2FC**	***P* value**	**Hit?**	**Molecular Function**	**Biological Function**	**Cellular Component**	**Protein Class**
Actl6a	-1.063	0.029	Yes	chromatin binding (GO:0003682).	histone H4 acetylation (GO:0043967). ATP-dependent chromatin remodeling (GO:0043044). nervous system development (GO:0007399). transcription by RNA polymerase II (GO:0006366). regulation of transcription by RNA polymerase II (GO:0006357).	ATPase complex (GO:1904949). NuA4 histone acetyltransferase complex (GO:0035267). nuclear chromatin (GO:0000790).	actin and actin related protein (PC00039).
Slc6a20	-1.058	0.030	No	————	————	————	————
Atp6v1h	-1.057	0.013	Yes	————	————	————	ATP synthase (PC00002).

HFD+PB vs ND - DOWNREGULATED							
Gene Symbol	**log2FC**	***P* value**	**Hit?**	**Molecular Function**	**Biological Function**	**Cellular Component**	**Protein Class**
Tbl1x	-1.056	0.030	Yes	transcription corepressor activity (GO:0003714).	transcription by RNA polymerase II (GO:0006366). histone deacetylation (GO:0016575). regulation of transcription by RNA polymerase II (GO:0006357).	histone deacetylase complex (GO:0000118).	————
Ranbp2	-1.055	0.028	Yes	GTPase activity (GO:0003924). GTPase activator activity (GO:0005096). Ras GTPase binding (GO:0017016).	————	vacuole (GO:0005773). plasma membrane (GO:0005886). nuclear pore (GO:0005643).	scaffold/adaptor protein (PC00226).

HFD+PB vs ND - DOWNREGULATED							
Gene Symbol	**log2FC**	***P* value**	**Hit?**	**Molecular Function**	**Biological Function**	**Cellular Component**	**Protein Class**
Ddx5	-1.054	0.000	Yes	————	————	nucleus (GO:0005634). cytoplasm (GO:0005737). ribonucleoprotein complex (GO:1990904).	————
Thumpd3	-1.054	0.011	Yes	tRNA methyltransferase activity (GO:0008175). S-adenosylmethionine-dependent methyltransferase activity (GO:0008757).	tRNA methylation (GO:0030488).	————	RNA methyltransferase (PC00033).
Rtn4	-1.053	0.000	Yes	————	————	————	————
Mt-cyb	-1.051	0.000	Yes	————	————	chloroplast thylakoid membrane (GO:0009535).	————

HFD+PB vs ND - DOWNREGULATED							
Gene Symbol	**log2FC**	***P* value**	**Hit?**	**Molecular Function**	**Biological Function**	**Cellular Component**	**Protein Class**
Tubb2a	-1.051	0.013	Yes	GTP binding (GO:0005525). structural molecule activity (GO:0005198).	neuron migration (GO:0001764). mitotic nuclear division (GO:0140014). microtubule cytoskeleton organization (GO:0000226).	cytoplasm (GO:0005737). microtubule (GO:0005874).	tubulin (PC00228).
Tm6sf1	-1.050	0.045	Yes	————	————	lysosomal membrane (GO:0005765).	————
Rab21	-1.050	0.002	Yes	GTPase activity (GO:0003924).	Ras protein signal transduction (GO:0007265). intracellular protein transport (GO:0006886).	early endosome (GO:0005769). vacuole (GO:0005773). plasma membrane (GO:0005886).	————

HFD+PB vs ND - DOWNREGULATED							
Gene Symbol	**log2FC**	***P* value**	**Hit?**	**Molecular Function**	**Biological Function**	**Cellular Component**	**Protein Class**
Dynlt1	-1.049	0.017	Yes	————	————	————	microtubule or microtubule-binding cytoskeletal protein (PC00157).
Hint3	-1.045	0.031	No	————	————	————	————
Svbp	-1.045	0.018	Yes	————	protein secretion (GO:0009306). negative regulation of protein modification process (GO:0031400). protein ubiquitination (GO:0016567).	apical part of cell (GO:0045177).	————

HFD+PB vs ND - DOWNREGULATED							
Gene Symbol	**log2FC**	***P* value**	**Hit?**	**Molecular Function**	**Biological Function**	**Cellular Component**	**Protein Class**
Snx5	-1.044	0.005	Yes	phosphatidylinositol binding (GO:0035091). cytoskeletal protein binding (GO:0008092).	vesicle budding from membrane (GO:0006900). membrane invagination (GO:0010324). endocytosis (GO:0006897). retrograde transport, endosome to Golgi (GO:0042147).	endosome (GO:0005768). vacuole (GO:0005773). plasma membrane (GO:0005886).	————
Trappc2	-1.041	0.044	Yes	————	————	————	membrane traffic protein (PC00150).
S100a6	-1.041	0.001	Yes	————	————	————	calmodulin-related (PC00061).

HFD+PB vs ND - DOWNREGULATED							
Gene Symbol	**log2FC**	***P* value**	**Hit?**	**Molecular Function**	**Biological Function**	**Cellular Component**	**Protein Class**
Erlin1	-1.038	0.032	Yes	cholesterol binding (GO:0015485).	signal transduction (GO:0007165). cellular response to stress (GO:0033554). transcription by RNA polymerase II (GO:0006366). positive regulation of transcription by RNA polymerase II (GO:0045944).	endoplasmic reticulum membrane (GO:0005789). vacuole (GO:0005773). plasma membrane (GO:0005886).	————
Lrp6	-1.031	0.002	Yes	————	————	————	apolipoprotein (PC00052).
Fgf13	-1.029	0.015	Yes	————	————	————	growth factor (PC00112).
Scg5	-1.020	0.002	No	————	————	————	————
LOC680885	-1.011	0.008	Yes	————	————	————	————

HFD+PB vs ND - DOWNREGULATED							
Gene Symbol	**log2FC**	***P* value**	**Hit?**	**Molecular Function**	**Biological Function**	**Cellular Component**	**Protein Class**
Sub1	-1.006	0.001	Yes	transcription coactivator activity (GO:0003713).	positive regulation of transcription initiation from RNA polymerase II promoter (GO:0060261). transcription initiation from RNA polymerase II promoter (GO:0006367).	nucleus (GO:0005634). transcription factor complex (GO:0005667).	general transcription factor (PC00259).
Fam174a	-1.003	0.021	Yes	————	————	————	————
Txnip	-1.002	0.018	Yes	————	————	————	————

III. Deregulated genes in the HFD+PB vs HFD comparison

Table 0.8. Highly upregulated genes in HFD+PB rats when compared to HFD and their functional classification as determined by PANTHER bioinformatics.

Genes were determined to be highly deregulated if they had a log2 fold change (log2FC) > 1 and a *P* value < 0.05. "Hit" refers to whether the gene was found by PANTHER.

HFD+PB vs HFD – UPREGULATED GENES							
Gene Symbol	**log2FC**	***P* value**	**Hit?**	**Molecular Function**	**Biological Function**	**Cellular Component**	**Protein Class**
Rhbdl2	4.365	0.000	Yes	————	————	————	————
Tyk2	3.780	0.005	Yes	————	————	————	————
Slc35f5	3.537	0.002	Yes	————	————	————	secondary carrier transporter(PC00258)
Papolg	3.480	0.023	Yes	adenylyltransferase activity(GO:0070566)	mRNA polyadenylation(GO:0006378)	nucleus(GO:0005634)	mRNA polyadenylation factor(PC00146)
Col6a5	3.480	0.019	Yes	————	————	————	————

HFD+PB vs HFD – UPREGULATED GENES							
Gene Symbol	**log2FC**	***P* value**	**Hit?**	**Molecular Function**	**Biological Function**	**Cellular Component**	**Protein Class**
Tiam1	3.365	0.011	Yes	Rac GTPase binding(GO:0048365). Rho guanyl—nucleotide exchange factor activity(GO:0005089)	positive regulation of axonogenesis(GO:0050772). small GTPase mediated signal transduction(GO:0007264). axonogenesis(GO:0007409). positive regulation of GTPase activity(GO:0043547)	cytosol(GO:0005829). plasma membrane(GO:0005886)	————
Mettl27	3.365	0.016	Yes	————	————	————	methyltransferase(PC00155)
RGD1308750	3.365	0.015	Yes	mRNA binding(GO:0003729)	regulation of translation(GO:0006417). translational elongation(GO:0006414)	nucleolus(GO:0005730)	————
RGD1560608	3.239	0.041	Yes	————	————	————	————

HFD+PB vs HFD – UPREGULATED GENES							
Gene Symbol	**log2FC**	***P* value**	**Hit?**	**Molecular Function**	**Biological Function**	**Cellular Component**	**Protein Class**
Kri1	3.239	0.030	Yes	————	RNA phosphodiester bond hydrolysis, endonucleolytic(GO:0090502). maturation of SSU—rRNA from tricistronic rRNA transcript (SSU—rRNA, 5.8S rRNA, LSU—rRNA)(GO:0000462). cleavage involved in rRNA processing(GO:0000469). maturation of 5.8S rRNA from tricistronic rRNA transcript (SSU—rRNA, 5.8S rRNA, LSU—rRNA)(GO:0000466)	t—UTP complex(GO:0034455). 90S preribosome(GO:0030686)	————

Rnd1	3.239	0.040	Yes	GTP binding(GO:0005525). protein kinase binding(GO:0019901). GTPase activity(GO:0003924)	regulation of cell shape(GO:0008360). cortical cytoskeleton organization(GO:0030865). regulation of actin cytoskeleton organization(GO:0032956). cell morphogenesis(GO:0000902). establishment or maintenance of cell polarity(GO:0007163). actin filament organization(GO:0007015). Rho protein signal transduction(GO:0007266). cell migration(GO:0016477)	cytoskeleton(GO:0005856). cell cortex(GO:0005938). intracellular membrane—bounded organelle(GO:0043231). cytoplasmic vesicle(GO:0031410). cell projection(GO:0042995). plasma membrane(GO:0005886)	small GTPase(PC00208)

HFD+PB vs HFD – UPREGULATED GENES							
Gene Symbol	**log2FC**	***P* value**	**Hit?**	**Molecular Function**	**Biological Function**	**Cellular Component**	**Protein Class**
B3galt4	3.104	0.007	No	————	————	————	————
Zfp267	2.949	0.033	Yes	————	————	————	C2H2 zinc finger transcription factor(PC00248)
Syk	2.949	0.050	No	————	————	————	————
Slc36a1	2.783	0.011	Yes	amino acid transmembrane transporter activity(GO:0015171)	amino acid transmembrane transport(GO:0003333)	————	amino acid transporter(PC00046)
Ccdc17	2.783	0.013	Yes	————	————	————	————
Adamts2	2.783	0.012	Yes	————	————	————	metalloprotease(PC00153)

HFD+PB vs HFD – UPREGULATED GENES							
Gene Symbol	**log2FC**	***P* value**	**Hit?**	**Molecular Function**	**Biological Function**	**Cellular Component**	**Protein Class**
H2afx	2.689	0.001	Yes	DNA binding(GO:0003677)	transcription, DNA—templated(GO:0006351). chromatin silencing(GO:0006342). cellular response to DNA damage stimulus(GO:0006974)	nuclear chromatin(GO:0000790)	histone(PC00118)

HFD+PB vs HFD – UPREGULATED GENES							
Gene Symbol	**log2FC**	***P* value**	**Hit?**	**Molecular Function**	**Biological Function**	**Cellular Component**	**Protein Class**
Traf3ip1	2.590	0.031	Yes	————	regulation of microtubule cytoskeleton organization(GO:0070507). intraciliary transport involved in cilium assembly(GO:0035735). vesicle targeting, trans—Golgi to periciliary membrane compartment(GO:0097712). axoneme assembly(GO:0035082). ciliary transition zone assembly(GO:1905349). protein localization to cilium(GO:0061512)	centrosome(GO:0005813). centriole(GO:0005814). ciliary basal body(GO:0036064). plasma membrane region(GO:0098590). intraciliary transport particle B(GO:0030992). axoneme(GO:0005930). microtubule(GO:0005874)	————

HFD+PB vs HFD – UPREGULATED GENES							
Gene Symbol	**log2FC**	***P* value**	**Hit?**	**Molecular Function**	**Biological Function**	**Cellular Component**	**Protein Class**
B3gntl1	2.590	0.023	Yes	————	————	————	glycosyltransferase(PC00111)
Miga1	2.590	0.030	Yes	————	mitochondrial fusion(GO:0008053)	————	————
Ryr1	2.590	0.023	No	————	————	————	————
Tmem102	2.589	0.008	Yes	————	————	————	————

HFD+PB vs HFD – UPREGULATED GENES							
Gene Symbol	**log2FC**	***P* value**	**Hit?**	**Molecular Function**	**Biological Function**	**Cellular Component**	**Protein Class**
Ttc8	2.519	0.013	Yes	————	intraciliary transport involved in cilium assembly(GO:0035735). non—motile cilium assembly(GO:1905515). vesicle targeting, trans—Golgi to periciliary membrane compartment(GO:0097712). axoneme assembly(GO:0035082). ciliary transition zone assembly(GO:1905349). protein localization to cilium(GO:0061512)	BBSome(GO:0034464). ciliary basal body(GO:0036064). non—motile cilium(GO:0097730). intraciliary transport particle(GO:0030990). plasma membrane region(GO:0098590)	————
Pla2g1b	2.483	0.020	Yes	————	————	————	phospholipase(PC00186)

HFD+PB vs HFD – UPREGULATED GENES							
Gene Symbol	**log2FC**	***P* value**	**Hit?**	**Molecular Function**	**Biological Function**	**Cellular Component**	**Protein Class**
Prss36	2.445	0.013	No	————	————	————	————
AABR07072748.1	2.367	0.041	Yes	————	————	————	————
Clcnkb	2.367	0.048	No	————	————	————	————

HFD+PB vs HFD – UPREGULATED GENES							
Gene Symbol	**log2FC**	***P* value**	**Hit?**	**Molecular Function**	**Biological Function**	**Cellular Component**	**Protein Class**
Rrh	2.367	0.002	Yes	G protein—coupled receptor activity(GO:0004930)	cellular response to light stimulus(GO:0071482). response to external stimulus(GO:0009605). G protein—coupled receptor signaling pathway(GO:0007186). detection of stimulus(GO:0051606)	integral component of plasma membrane(GO:0005887). non—motile cilium(GO:0097730). ciliary part(GO:0044441). intraciliary transport particle(GO:0030990). plasma membrane region(GO:0098590). neuron projection(GO:0043005)	G—protein coupled receptor(PC00021)
Uros	2.367	0.031	Yes	hydro—lyase activity(GO:0016836)	carboxylic acid biosynthetic process(GO:0046394). heme biosynthetic process(GO:0006783)	————	hydrolase(PC00121)

HFD+PB vs HFD – UPREGULATED GENES							
Gene Symbol	**log2FC**	***P* value**	**Hit?**	**Molecular Function**	**Biological Function**	**Cellular Component**	**Protein Class**
Trpm7	2.215	0.004	No	————	————	————	————

Anxa9	2.197	0.023	Yes	phospholipase A2 activity(GO:0004623). extracellular matrix binding(GO:0050840). phosphatidylinositol—4,5—bisphosphate binding(GO:0005546). identical protein binding(GO:0042802). enzyme inhibitor activity(GO:0004857). cadherin binding(GO:0045296). protease binding(GO:0002020). Rab GTPase binding(GO:0017137).	regulation of cellular protein catabolic process(GO:1903362). positive regulation of multi—organism process(GO:0043902). negative regulation of blood coagulation(GO:0030195). positive regulation of calcium ion transport(GO:0051928). endothelial cell differentiation(GO:0045446). negative regulation of protein catabolic process(GO:0042177). zymogen activation(GO:0031638).	nucleus(GO:0005634). extracellular space(GO:0005615). cytoplasm(GO:0005737). collagen—containing extracellular matrix(GO:0062023). vesicle(GO:0031982). plasma membrane(GO:0005886)	calcium—binding protein(PC00060)

				voltage—gated calcium channel activity(GO:0005245). calcium—dependent phospholipid binding(GO:0005544)	positive regulation of multicellular organismal process(GO:0051240). intracellular sterol transport(GO:0032366). regulation of endocytosis(GO:0030100). cholesterol transport(GO:0030301). plasma lipoprotein particle clearance(GO:0034381). protein—containing complex assembly(GO:0065003). receptor—mediated endocytosis(GO:0006898).		

					positive regulation of molecular function(GO:0044093). positive regulation of signaling(GO:0023056). signaling(GO:0023052). regulation of gene expression(GO:0010468). negative regulation of molecular function(GO:0044092). protein localization to plasma membrane(GO:0072659). cell population proliferation(GO:0008283). regulation of cellular localization(GO:0060341).		

					vacuole organization(GO:0007033). positive regulation of cell population proliferation(GO:0008284). bone morphogenesis(GO:0060349). chondrocyte differentiation(GO:0002062). myeloid cell development(GO:0061515). blood coagulation(GO:0007596). cellular protein catabolic process(GO:0044257).		

					protein phosphorylation(GO:0006468). heart development(GO:0007507). response to external stimulus(GO:0009605). angiogenesis(GO:0001525). calcium ion transport(GO:0006816). positive regulation of organelle organization(GO:0010638). negative regulation of cellular catabolic process(GO:0031330). multi—organism process(GO:0051704).		

					negative regulation of cellular protein metabolic process(GO:0032269). protein—containing complex disassembly(GO:0032984). biomineral tissue development(GO:0031214). regulation of proteolysis(GO:0030162). positive regulation of cell differentiation(GO:0045597). developmental growth(GO:0048589). osteoclast differentiation(GO:0030316).		

HFD+PB vs HFD – UPREGULATED GENES							
Gene Symbol	**log2FC**	***P* value**	**Hit?**	**Molecular Function**	**Biological Function**	**Cellular Component**	**Protein Class**
					vesicle budding from membrane(GO:0006900). vesicle fusion(GO:0006906). positive regulation of protein phosphorylation(GO:0001934). membrane invagination(GO:0010324). collagen fibril organization(GO:0030199). regulation of multicellular organismal development(GO:2000026)		
Slc30a2	2.004	0.038	No	————	————	————	————
Armc6	1.870	0.003	Yes	————	————	————	————

HFD+PB vs HFD – UPREGULATED GENES							
Gene Symbol	**log2FC**	***P* value**	**Hit?**	**Molecular Function**	**Biological Function**	**Cellular Component**	**Protein Class**
Pmf1	1.827	0.005	Yes	————	chromosome segregation(GO:0007059)	condensed nuclear chromosome kinetochore(GO:0000778)	————
Cd68	1.783	0.020	Yes	————	establishment of protein localization to organelle(GO:0072594)	late endosome membrane(GO:0031902). lysosomal membrane(GO:0005765). plasma membrane(GO:0005886)	membrane trafficking regulatory protein(PC00151)
Slc39a4	1.783	0.016	No	————	————	————	————
LOC680227	1.782	0.016	No	————	————	————	————
Phf12	1.782	0.015	Yes	————	————	————	chromatin/chromatin—binding, or —regulatory protein(PC00077)

HFD+PB vs HFD – UPREGULATED GENES							
Gene Symbol	**log2FC**	***P* value**	**Hit?**	**Molecular Function**	**Biological Function**	**Cellular Component**	**Protein Class**
Tent4a	1.708	0.048	Yes	adenylyltransferase activity(GO:0070566). mRNA binding(GO:0003729)	ncRNA processing(GO:0034470). nuclear—transcribed mRNA catabolic process(GO:0000956). RNA 3'—end processing(GO:0031123)	protein—containing complex(GO:0032991). nucleolus(GO:0005730)	mRNA polyadenylation factor(PC00146)
LOC499643	1.708	0.040	Yes	————	————	————	————
Tradd	1.567	0.022	Yes	————	————	————	————
Sntb2	1.560	0.028	Yes	————	————	plasma membrane protein complex(GO:0098797). intracellular(GO:0005622)	————
Zfp106	1.548	0.008	Yes	————	————	————	————
Ppp1r13b	1.498	0.041	Yes	protein binding(GO:0005515)	————	nucleus(GO:0005634)	protein—binding activity modulator(PC00095)

HFD+PB vs HFD – UPREGULATED GENES							
Gene Symbol	**log2FC**	***P* value**	**Hit?**	**Molecular Function**	**Biological Function**	**Cellular Component**	**Protein Class**
Rnf170	1.483	0.011	Yes	————	————	————	————
Ptp4a1	1.461	0.013	Yes	————	————	nucleus(GO:0005634)	————

Timp1	1.439	0.007	Yes	endopeptidase inhibitor activity(GO:0004866). protease binding(GO:0002020). metalloendopeptidase activity(GO:0004222)	response to cytokine(GO:0034097). protein catabolic process(GO:0030163). membrane protein proteolysis(GO:0033619). cellular protein metabolic process(GO:0044267). negative regulation of endopeptidase activity(GO:0010951). negative regulation of protein catabolic process(GO:0042177). negative regulation of cellular catabolic process(GO:0031330).	extracellular space(GO:0005615). extracellular matrix(GO:0031012)	protease inhibitor(PC00191)

HFD+PB vs HFD – UPREGULATED GENES							
Gene Symbol	**log2FC**	***P* value**	**Hit?**	**Molecular Function**	**Biological Function**	**Cellular Component**	**Protein Class**
					response to hormone(GO:0009725). cellular catabolic process(GO:0044248)		
Rps6ka3	1.434	0.042	Yes	protein serine/threonine kinase activity(GO:0004674)	————	————	————
Rapgef2	1.426	0.043	Yes	————	————	————	guanyl—nucleotide exchange factor(PC00113)
Secisbp2	1.367	0.010	No	————	————	————	————
Mturn	1.367	0.033	Yes	————	————	————	————
Cebpa	1.319	0.049	No	————	————	————	————
Eloa	1.313	0.031	No	————	————	————	————
Lrp5	1.306	0.048	Yes	————	————	————	————

HFD+PB vs HFD – UPREGULATED GENES							
Gene Symbol	**log2FC**	***P* value**	**Hit?**	**Molecular Function**	**Biological Function**	**Cellular Component**	**Protein Class**
Nrep	1.268	0.033	Yes	————	axon development(GO:0061564). response to wounding(GO:0009611). transforming growth factor beta receptor signaling pathway(GO:0007179). cellular response to stress(GO:0033554). regulation of neuron differentiation(GO:0045664). regulation of transforming growth factor beta receptor signaling pathway(GO:0017015)	nucleus(GO:0005634). cytoplasm(GO:0005737)	————

HFD+PB vs HFD – UPREGULATED GENES							
Gene Symbol	**log2FC**	***P* value**	**Hit?**	**Molecular Function**	**Biological Function**	**Cellular Component**	**Protein Class**
Calhm2	1.268	0.019	Yes	cation channel activity(GO:0005261)	————	integral component of plasma membrane(GO:0005887)	————
Eed	1.252	0.020	Yes	nucleosome binding(GO:0031491). histone—lysine N—methyltransferase activity(GO:0018024)	negative regulation of transcription by RNA polymerase II(GO:0000122). transcription by RNA polymerase II(GO:0006366). chromatin silencing(GO:0006342)	histone methyltransferase complex(GO:0035097). PcG protein complex(GO:0031519)	chromatin/chromatin—binding, or —regulatory protein(PC00077)
Crabp2	1.222	6.4773812190935E—10	Yes	————	————	————	————
Sez6l	1.209	0.014	Yes	————	————	————	————
Plekhg5	1.197	0.033	Yes	————	————	————	————

HFD+PB vs HFD – UPREGULATED GENES							
Gene Symbol	**log2FC**	***P* value**	**Hit?**	**Molecular Function**	**Biological Function**	**Cellular Component**	**Protein Class**
Vps33b	1.185	0.032	Yes	————	————	————	membrane trafficking regulatory protein(PC00151)
Xbp1	1.169	0.026	No	————	————	————	————
Fam234b	1.145	0.031	Yes	————	————	————	————
Ccdc137	1.145	0.029	Yes	————	————	————	————
Stard5	1.140	0.032	Yes	————	————	————	————
RT1—Da	1.138	2.9187087063 0428E—06	Yes	————	————	————	major histocompatibility complex protein(PC00149)
Fcgr2b	1.104	0.037	Yes	————	————	————	immunoglobulin receptor superfamily(PC00124)
Laptm5	1.097	0.001	Yes	————	————	————	transporter(PC00227)

HFD+PB vs HFD – UPREGULATED GENES							
Gene Symbol	**log2FC**	***P* value**	**Hit?**	**Molecular Function**	**Biological Function**	**Cellular Component**	**Protein Class**
Cd74	1.088	1.3332991582 8914E—09	Yes	————	————	————	scaffold/adaptor protein(PC00226)
Nthl1	1.082	0.048	Yes	catalytic activity, acting on DNA(GO:0140097). hydrolase activity(GO:0016787)	base—excision repair(GO:0006284). nucleotide—excision repair, DNA incision(GO:0033683)	————	DNA glycosylase(PC00010)
Zfp426	1.082	0.044	Yes	————	————	————	————

HFD+PB vs HFD – UPREGULATED GENES							
Gene Symbol	**log2FC**	***P* value**	**Hit?**	**Molecular Function**	**Biological Function**	**Cellular Component**	**Protein Class**
Cenpv	1.072	0.031	Yes	————	chromatin remodeling(GO:0006338). membrane fission(GO:0090148). protein—DNA complex assembly(GO:0065004). regulation of chromosome organization(GO:0033044). chromatin assembly or disassembly(GO:0006333). cytokinesis(GO:0000910). DNA packaging(GO:0006323). positive regulation of cytokinesis(GO:0032467)	nucleus(GO:0005634). spindle midzone(GO:0051233). kinetochore(GO:0000776)	————

HFD+PB vs HFD – UPREGULATED GENES							
Gene Symbol	**log2FC**	***P* value**	**Hit?**	**Molecular Function**	**Biological Function**	**Cellular Component**	**Protein Class**
Frem3	1.069	0.012	Yes	————	————	————	————
Coro2b	1.064	0.000	Yes	actin filament binding(GO:0051015)	actin filament organization(GO:0007015)	————	non—motor actin binding protein(PC00165)
Ube2j1	1.063	0.036	Yes	ubiquitin—protein transferase activity(GO:0004842)	————	————	ubiquitin—protein ligase(PC00234)
Smpdl3b	1.063	0.049	Yes	phosphoric diester hydrolase activity(GO:0008081)	————	extracellular space(GO:0005615)	phosphodiesterase(PC00185)
Dusp6	1.059	0.006	Yes	MAP kinase activity(GO:0004707). protein tyrosine/serine/threonine phosphatase activity(GO:0008138)	inactivation of MAPK activity(GO:0000188). MAPK cascade(GO:0000165)	cytosol(GO:0005829)	————

HFD+PB vs HFD – UPREGULATED GENES							
Gene Symbol	**log2FC**	***P* value**	**Hit?**	**Molecular Function**	**Biological Function**	**Cellular Component**	**Protein Class**
Dnajb1	1.047	8.9858023757 2458E—11	Yes	chaperone binding(GO:0051087). unfolded protein binding(GO:0051082)	chaperone—mediated protein folding(GO:0061077)	cytosol(GO:0005829)	————
Enah	1.045	0.050	Yes	SH3 domain binding(GO:0017124)	cell motility(GO:0048870). actin polymerization or depolymerization(GO:0008154). axon guidance(GO:0007411)	————	scaffold/adaptor protein(PC00226)
RT1—Db1	1.029	3.9155347456 7097E—08	No	————	————	————	————

HFD+PB vs HFD – UPREGULATED GENES							
Gene Symbol	**log2FC**	***P* value**	**Hit?**	**Molecular Function**	**Biological Function**	**Cellular Component**	**Protein Class**
Lyar	1.005	0.026	Yes	DNA binding(GO:0003677)	negative regulation of transcription by RNA polymerase II(GO:0000122). transcription by RNA polymerase II(GO:0006366). rRNA processing(GO:0006364)	nucleolus(GO:0005730)	RNA processing factor(PC00147)

Table 0.9. Highly downregulated genes in HFD+PB rats when compared to HFD and their functional classification as determined by PANTHER bioinformatics.

Genes were determined to be highly deregulated if they had a log2 fold change (log2FC) < -1 and a *P* value < 0.05. "Hit" refers to whether the gene was found by PANTHER.

HFD+PB vs HFD – DOWNREGULATED GENES							
Gene Symbol	**log2FC**	***P* value**	**Hit?**	**Molecular Function**	**Biological Function**	**Cellular Component**	**Protein Class**
Cga	-4.973	0.020	Yes	————	extracellular space(GO:0005615). protein—containing complex(GO:0032991)	————	cellular aromatic compound metabolic process(GO:0006725). regulation of lipid biosynthetic process(GO:0046890). positive regulation of biosynthetic process(GO:0009891). cellular modified amino acid metabolic process(GO:0006575). steroid biosynthetic process(GO:0006694). hormone metabolic process(GO:0042445). organic hydroxy compound metabolic process(GO:1901615)

HFD+PB vs HFD – DOWNREGULATED GENES							
Gene Symbol	**log2FC**	***P* value**	**Hit?**	**Molecular Function**	**Biological Function**	**Cellular Component**	**Protein Class**
Cit	-4.607	0.001	Yes	non—receptor serine/threonine protein kinase(PC00167)	cytoskeleton(GO:0005856). cytoplasm(GO:0005737)	————	actomyosin structure organization(GO:0031032). peptidyl—threonine phosphorylation(GO:0018107)
Vwa1	-4.303	0.005	No	————	————	————	————
Pinlyp	-4.215	0.002	Yes	heterotrimeric G—protein(PC00117)	catalytic complex(GO:1902494). leaflet of membrane bilayer(GO:0097478). plasma membrane protein complex(GO:0098797). extrinsic component of cytoplasmic side of plasma membrane(GO:0031234). cytoplasmic part(GO:0044444)	————	G protein—coupled receptor signaling pathway(GO:0007186)

HFD+PB vs HFD – DOWNREGULATED GENES							
Gene Symbol	**log2FC**	***P* value**	**Hit?**	**Molecular Function**	**Biological Function**	**Cellular Component**	**Protein Class**
Tbc1d8b	-4.215	0.023	Yes	————	————	————	————
Ptprz1	-4.215	0.029	No	————	————	————	————
Gjb2	-4.122	0.008	Yes	gap junction(PC00105)	————	————	————
Fam84a	-4.022	0.014	Yes	————	————	————	————
Jakmip1	-4.022	0.016	Yes	————	————	————	————
Amot	-4.022	0.017	Yes	————	apical junction complex(GO:0043296). cytoplasmic vesicle(GO:0031410). plasma membrane(GO:0005886)	————	angiogenesis(GO:0001525). establishment of cell polarity(GO:0030010). regulation of cell migration(GO:0030334). actin cytoskeleton organization(GO:0030036). cell migration(GO:0016477). intracellular signal transduction(GO:0035556)

HFD+PB vs HFD – DOWNREGULATED GENES							
Gene Symbol	**log2FC**	***P* value**	**Hit?**	**Molecular Function**	**Biological Function**	**Cellular Component**	**Protein Class**
Mfap2	-4.022	0.014	Yes	————	————	————	————
Nap1l5	-3.990	0.000	Yes	chromatin/chromatin—binding, or —regulatory protein(PC00077)	————	————	————

HFD+PB vs HFD – DOWNREGULATED GENES							
Gene Symbol	**log2FC**	***P* value**	**Hit?**	**Molecular Function**	**Biological Function**	**Cellular Component**	**Protein Class**
Slc32a1	-3.973	0.001	Yes	————	BBSome(GO:0034464). intraciliary transport particle(GO:0030990). plasma membrane region(GO:0098590)	————	intraciliary transport involved in cilium assembly(GO:0035735). vesicle targeting, trans—Golgi to periciliary membrane compartment(GO:0097712). axoneme assembly(GO:0035082). ciliary transition zone assembly(GO:1905349). protein localization to cilium(GO:0061512)

HFD+PB vs HFD – DOWNREGULATED GENES							
Gene Symbol	**log2FC**	***P* value**	**Hit?**	**Molecular Function**	**Biological Function**	**Cellular Component**	**Protein Class**
Trmt13	-3.916	0.023	Yes	methyltransferase(PC00155)	mitochondrion(GO:0005739)	————	cellular protein modification process(GO:0006464). tRNA modification(GO:0006400)
Gap43	-3.803	0.000	Yes	————	postsynaptic density(GO:0014069). cytoplasm(GO:0005737). plasma membrane(GO:0005886)	————	wound healing(GO:0042060). axon guidance(GO:0007411). cellular response to stress(GO:0033554). developmental growth(GO:0048589). tissue development(GO:0009888)

HFD+PB vs HFD – DOWNREGULATED GENES							
Gene Symbol	**log2FC**	***P* value**	**Hit?**	**Molecular Function**	**Biological Function**	**Cellular Component**	**Protein Class**
Ldb2	-3.800	0.046	Yes	transcription cofactor(PC00217)	nucleus(GO:0005634). transcription factor complex(GO:0005667)	————	negative regulation of transcription by RNA polymerase II(GO:0000122). multicellular organism development(GO:0007275). transcription by RNA polymerase II(GO:0006366). positive regulation of transcription by RNA polymerase II(GO:0045944)
Zfp92	-3.800	0.015	Yes	chaperone(PC00072)	————	————	————
Chia	-3.800	0.040	No	————	————	————	————
Rab40b	-3.678	0.003	Yes	protein—binding activity modulator(PC00095)	nucleus(GO:0005634)	————	transcription by RNA polymerase II(GO:0006366). regulation of transcription by RNA polymerase II(GO:0006357)

HFD+PB vs HFD – DOWNREGULATED GENES							
Gene Symbol	**log2FC**	***P* value**	**Hit?**	**Molecular Function**	**Biological Function**	**Cellular Component**	**Protein Class**
Agt	-3.677	0.001	Yes	decarboxylase(PC00089)	————	————	————
Svop	-3.675	0.047	Yes	————	————	————	————
Fgf12	-3.675	0.038	Yes	growth factor(PC00112)	————	————	————
Hnf1b	-3.675	0.014	Yes	DNA—binding transcription factor(PC00218)	nucleus(GO:0005634)	————	positive regulation of transcription, DNA—templated(GO:0045893). transcription by RNA polymerase II(GO:0006366). regulation of transcription by RNA polymerase II(GO:0006357)
Pomc	-3.594	0.001	No	————	————	————	————
Slc13a3	-3.540	0.009	No	————	————	————	————

HFD+PB vs HFD – DOWNREGULATED GENES							
Gene Symbol	**log2FC**	***P* value**	**Hit?**	**Molecular Function**	**Biological Function**	**Cellular Component**	**Protein Class**
Mkrn2os	-3.537	0.019	Yes	small GTPase(PC00208)	membrane protein complex(GO:0098796). nucleus(GO:0005634). endosomal part(GO:0044440). vacuolar membrane(GO:0005774). plasma membrane(GO:0005886). lysosome(GO:0005764)	————	autophagy(GO:0006914). regulation of autophagy(GO:0010506). response to amino acid(GO:0043200). TOR signaling(GO:0031929). cellular response to starvation(GO:0009267). cellular response to organonitrogen compound(GO:0071417). cellular response to oxygen—containing compound(GO:1901701). positive regulation of TOR signaling(GO:0032008)

HFD+PB vs HFD – DOWNREGULATED GENES							
Gene Symbol	**log2FC**	***P* value**	**Hit?**	**Molecular Function**	**Biological Function**	**Cellular Component**	**Protein Class**
Ncam1	-3.504	0.000	No	————	————	————	————
Btbd17	-3.466	0.008	Yes	————	————	————	————
Dclk3	-3.466	0.013	Yes	primase(PC00189)	————	————	DNA—dependent DNA replication(GO:0006261). DNA biosynthetic process(GO:0071897). RNA biosynthetic process(GO:0032774)
Akap1	-3.439	0.000	No	————	————	————	————
Rit2	-3.419	0.000	Yes	phosphodiesterase(PC00185)	cytoplasm(GO:0005737)	————	————
Crlf1	-3.410	0.000	Yes	————	————	————	————
Snca	-3.388	0.034	Yes	membrane trafficking regulatory protein(PC00151)	————	————	————
Thrsp	-3.387	0.001	No	————	————	————	————

Tril	-3.347	0.000	Yes	basic leucine zipper transcription factor(PC00056)	transcription factor complex(GO:0005667). nuclear chromatin(GO:0000790). nucleoplasm(GO:0005654)	————	cell population proliferation(GO:0008283). response to cytokine(GO:0034097). response to radiation(GO:0009314). transcription by RNA polymerase II(GO:0006366). positive regulation of cell differentiation(GO:0045597). response to organic cyclic compound(GO:0014070). positive regulation of transcription by RNA polymerase II(GO:0045944). cell cycle(GO:0007049).

							regulation of cell population proliferation(GO:0042127). response to mechanical stimulus(GO:0009612). negative regulation of transcription by RNA polymerase II(GO:0000122). response to drug(GO:0042493). cell differentiation(GO:0030154). cellular response to hormone stimulus(GO:0032870). response to lipopolysaccharide(GO:0032496).

HFD+PB vs HFD – DOWNREGULATED GENES							
Gene Symbol	**log2FC**	***P* value**	**Hit?**	**Molecular Function**	**Biological Function**	**Cellular Component**	**Protein Class**
							regulation of cell cycle(GO:0051726). response to organonitrogen compound(GO:0010243)
Lpar1	-3.306	0.023	Yes	lyase(PC00144)	————	————	————
Wasf1	-3.306	0.036	Yes	nucleotide kinase(PC00172)	————	————	————

HFD+PB vs HFD – DOWNREGULATED GENES							
Gene Symbol	**log2FC**	***P* value**	**Hit?**	**Molecular Function**	**Biological Function**	**Cellular Component**	**Protein Class**
Gpr37	-3.218	0.002	Yes	————	receptor complex(GO:0043235). plasma membrane(GO:0005886)	————	adenylate cyclase—inhibiting G protein—coupled receptor signaling pathway(GO:0007193). MAPK cascade(GO:0000165). negative regulation of adenylate cyclase activity(GO:0007194). positive regulation of MAPK cascade(GO:0043410). negative regulation of cAMP—mediated signaling(GO:0043951). cAMP—mediated signaling(GO:0019933)
Nrip1	-3.218	0.017	Yes	————	————	————	————

Usp18	-3.218	0.024	Yes	membrane traffic protein(PC00150)	membrane coat(GO:0030117). postsynaptic density(GO:0014069). microtubule cytoskeleton(GO:0015630). mitochondrial membrane(GO:0031966). postsynaptic membrane(GO:0045211). dendritic spine(GO:0043197). cytoplasmic vesicle(GO:0031410). axon(GO:0030424)	————	establishment of protein localization to organelle(GO:0072594). membrane fusion(GO:0061025). protein—containing complex localization(GO:0031503). vesicle budding from membrane(GO:0006900). synaptic vesicle transport(GO:0048489). synaptic vesicle endocytosis(GO:0048488). protein transport(GO:0015031).

HFD+PB vs HFD – DOWNREGULATED GENES							
Gene Symbol	**log2FC**	***P* value**	**Hit?**	**Molecular Function**	**Biological Function**	**Cellular Component**	**Protein Class**
							regulation of synapse structure or activity(GO:0050803). membrane invagination(GO:0010324). receptor internalization(GO:0031623). mitochondrial fission(GO:0000266)
LOC103690108	-3.218	0.017	Yes	translation release factor(PC00225)	mitochondrion(GO:0005739)	————	translational termination(GO:0006415). mitochondrial translation(GO:0032543). translational elongation(GO:0006414)

HFD+PB vs HFD – DOWNREGULATED GENES							
Gene Symbol	**log2FC**	***P* value**	**Hit?**	**Molecular Function**	**Biological Function**	**Cellular Component**	**Protein Class**
Rab3b	-3.181	0.000	Yes	————	endosome(GO:0005768). synaptic vesicle(GO:0008021). vacuole(GO:0005773). plasma membrane(GO:0005886)	————	vesicle fusion to plasma membrane(GO:0099500). organelle localization(GO:0051640). regulation of exocytosis(GO:0017157). protein secretion(GO:0009306). protein localization to plasma membrane(GO:0072659)
Rassf5	-3.125	0.024	Yes	scaffold/adaptor protein(PC00226)	————	————	————
Arhgap21	-3.125	0.002	Yes	————	————	————	————
Grin2b	-3.105	0.001	No	————	————	————	————

HFD+PB vs HFD – DOWNREGULATED GENES							
Gene Symbol	**log2FC**	***P* value**	**Hit?**	**Molecular Function**	**Biological Function**	**Cellular Component**	**Protein Class**
Edil3	-3.092	0.045	Yes	ion channel(PC00133)	plasma membrane(GO:0005886)	————	————
Icam5	-3.092	0.010	Yes	————	————	————	————
Fam131b	-3.066	0.000	No	————	————	————	————
Clcn2	-3.026	0.021	Yes	————	integral component of plasma membrane(GO:0005887)	————	————
Gpr88	-3.026	0.034	Yes	————	————	————	————

HFD+PB vs HFD – DOWNREGULATED GENES							
Gene Symbol	**log2FC**	***P* value**	**Hit?**	**Molecular Function**	**Biological Function**	**Cellular Component**	**Protein Class**
Etnk2	-3.026	0.019	Yes	————	ciliary basal body(GO:0036064). ciliary base(GO:0097546). plasma membrane region(GO:0098590). ciliary transition fiber(GO:0097539). intraciliary transport particle B(GO:0030992). ciliary transition zone(GO:0035869)	————	intraciliary transport involved in cilium assembly(GO:0035735). vesicle targeting, trans—Golgi to periciliary membrane compartment(GO:0097712). axoneme assembly(GO:0035082). ciliary transition zone assembly(GO:1905349). protein localization to cilium(GO:0061512)
Hnmt	-3.026	0.023	No	————	————	————	————
Rbfox1	-3.025	0.000	Yes	RNA splicing factor(PC00148)	————	————	nervous system development(GO:0007399)

HFD+PB vs HFD – DOWNREGULATED GENES							
Gene Symbol	**log2FC**	***P* value**	**Hit?**	**Molecular Function**	**Biological Function**	**Cellular Component**	**Protein Class**
Gspt2	-3.025	0.004	Yes	tubulin(PC00228)	cytoplasm(GO:0005737). microtubule(GO:0005874)	————	mitotic nuclear division(GO:0140014). microtubule cytoskeleton organization(GO:0000226)
Gjb6	-2.995	0.000	Yes	————	————	————	————
Ak5	-2.954	0.009	Yes	RNA splicing factor(PC00148)	mRNA cleavage factor complex(GO:0005849)	————	mRNA processing(GO:0006397)
Tmem59l	-2.943	0.000	No	————	————	————	————

Sema4f	-2.919	0.032	Yes	membrane—bound signaling molecule(PC00152)	integral component of plasma membrane(GO:0005887). extracellular space(GO:0005615)	————	negative regulation of locomotion(GO:0040013). neural crest cell differentiation(GO:0014033). regulation of cell size(GO:0008361). negative regulation of cellular component movement(GO:0051271). negative regulation of neuron differentiation(GO:0045665). axon guidance(GO:0007411). cell surface receptor signaling pathway(GO:0007166).

							axon extension(GO:0048675). regulation of axonogenesis(GO:0050770). regulation of cell growth(GO:0001558). negative regulation of response to external stimulus(GO:0032102). negative regulation of cellular component organization(GO:0051129). regulation of chemotaxis(GO:0050920). cell migration(GO:0016477).

HFD+PB vs HFD – DOWNREGULATED GENES							
Gene Symbol	**log2FC**	***P* value**	**Hit?**	**Molecular Function**	**Biological Function**	**Cellular Component**	**Protein Class**
							positive regulation of cell migration(GO:0030335)
Cdkn2c	-2.919	0.037	Yes	————	————	————	————
Tcea3	-2.919	0.023	Yes	————	plasma membrane(GO:0005886)	————	————
Dhx57	-2.919	0.044	Yes	————	————	————	————
Kcnmb4	-2.919	0.031	Yes	GTPase—activating protein(PC00257)	————	————	intracellular protein transport(GO:0006886). positive regulation of GTPase activity(GO:0043547)
Scamp5	-2.919	0.025	No	————	————	————	————

HFD+PB vs HFD – DOWNREGULATED GENES							
Gene Symbol	**log2FC**	***P* value**	**Hit?**	**Molecular Function**	**Biological Function**	**Cellular Component**	**Protein Class**
Dab1	-2.880	0.013	Yes	scaffold/adaptor protein(PC00226)	cytoplasm(GO:0005737)	————	neuron migration(GO:0001764). central nervous system development(GO:0007417). animal organ development(GO:0048513)
Hmgxb4	-2.880	0.012	Yes	————	————	————	————
Gng8	-2.880	0.018	Yes	membrane traffic protein(PC00150)	integral component of membrane(GO:0016021)	————	myelination(GO:0042552)
Gad2	-2.880	0.011	Yes	homeodomain transcription factor(PC00119)	nucleus(GO:0005634)	————	cell differentiation(GO:0030154). transcription by RNA polymerase II(GO:0006366). positive regulation of transcription by RNA polymerase II(GO:0045944)

HFD+PB vs HFD – DOWNREGULATED GENES							
Gene Symbol	**log2FC**	***P* value**	**Hit?**	**Molecular Function**	**Biological Function**	**Cellular Component**	**Protein Class**
Sntn	-2.880	0.011	Yes	transmembrane signal receptor(PC00197)	membrane protein complex(GO:0098796). extracellular space(GO:0005615). integral component of membrane(GO:0016021). receptor complex(GO:0043235). extracellular matrix(GO:0031012)	————	toll—like receptor signaling pathway(GO:0002224). innate immune response(GO:0045087). cytokine production(GO:0001816). immune effector process(GO:0002252). regulation of cytokine production(GO:0001817)
Frrs1l	-2.880	0.013	Yes	ubiquitin—protein ligase(PC00234)	————	————	————
Mmrn2	-2.803	0.036	Yes	ubiquitin—protein ligase(PC00234)	————	————	————
Mical1	-2.802	0.007	Yes	————	————	————	————

HFD+PB vs HFD – DOWNREGULATED GENES							
Gene Symbol	**log2FC**	***P* value**	**Hit?**	**Molecular Function**	**Biological Function**	**Cellular Component**	**Protein Class**
LOC100911402	-2.742	0.026	Yes	————	endosome(GO:0005768). integral component of membrane(GO:0016021). vacuole(GO:0005773). plasma membrane(GO:0005886)	————	cellular protein—containing complex assembly(GO:0034622). endosomal transport(GO:0016197)
Resp18	-2.730	0.000	Yes	————	————	————	————
Mpp3	-2.720	0.021	Yes	————	cytoplasmic vesicle(GO:0031410). endoplasmic reticulum(GO:0005783). vacuole(GO:0005773). plasma membrane(GO:0005886)	————	regulation of response to stress(GO:0080134). response to osmotic stress(GO:0006970)
Cdca7	-2.678	0.043	Yes	————	nucleus(GO:0005634)	————	————

HFD+PB vs HFD – DOWNREGULATED GENES							
Gene Symbol	**log2FC**	***P* value**	**Hit?**	**Molecular Function**	**Biological Function**	**Cellular Component**	**Protein Class**
Lgi4	-2.677	0.001	Yes	immunoglobulin superfamily cell adhesion molecule(PC00125)	plasma membrane(GO:0005886)	————	cell adhesion(GO:0007155)
Mlc1	-2.656	0.012	Yes	serine protease(PC00203)	secretory granule(GO:0030141). vacuole(GO:0005773). plasma membrane(GO:0005886)	————	————
RGD1308544	-2.651	0.005	Yes	————	mitochondrial membrane part(GO:0044455). extrinsic component of membrane(GO:0019898). mitochondrial inner membrane(GO:0005743)	————	ubiquinone biosynthetic process(GO:0006744)
Vsnl1	-2.642	0.000	Yes	————	————	————	————

HFD+PB vs HFD – DOWNREGULATED GENES							
Gene Symbol	**log2FC**	***P* value**	**Hit?**	**Molecular Function**	**Biological Function**	**Cellular Component**	**Protein Class**
Lgr4	-2.632	0.021	Yes	————	————	————	axon guidance(GO:0007411)
Peli1	-2.632	0.037	Yes	————	————	————	protein polyubiquitination(GO:0000209). cell surface receptor signaling pathway(GO:0007166)
Adamts17	-2.632	0.028	Yes	protease inhibitor(PC00191)	extracellular space(GO:0005615)	————	proteolysis(GO:0006508). cellular protein metabolic process(GO:0044267). negative regulation of endopeptidase activity(GO:0010951)

HFD+PB vs HFD – DOWNREGULATED GENES							
Gene Symbol	**log2FC**	***P* value**	**Hit?**	**Molecular Function**	**Biological Function**	**Cellular Component**	**Protein Class**
Tubb3	-2.627	0.000	Yes	————	cytoplasm(GO:0005737). plasma membrane region(GO:0098590). neuron projection(GO:0043005)	————	neuron projection development(GO:0031175). regulation of microtubule polymerization or depolymerization(GO:0031110). microtubule depolymerization(GO:0007019)
Rgs4	-2.620	0.001	Yes	GTPase—activating protein(PC00257)	————	————	————
Tial1	-2.611	0.012	Yes	scaffold/adaptor protein(PC00226)	————	————	————
Ttc9b	-2.603	0.001	Yes	————	————	————	————

Fsd1	-2.596	0.010	Yes	————	nucleus(GO:0005634). transcription factor complex(GO:0005667)	————	regulation of insulin secretion(GO:0050796). positive regulation of signaling(GO:0023056). insulin secretion(GO:0030073). positive regulation of cell communication(GO:0010647). cell fate commitment(GO:0045165). glucose homeostasis(GO:0042593). canonical Wnt signaling pathway(GO:0060070). transcription by RNA polymerase II(GO:0006366).

HFD+PB vs HFD – DOWNREGULATED GENES							
Gene Symbol	**log2FC**	***P* value**	**Hit?**	**Molecular Function**	**Biological Function**	**Cellular Component**	**Protein Class**
							muscle structure development(GO:0061061). positive regulation of protein secretion(GO:0050714). regulation of transcription by RNA polymerase II(GO:0006357)
Ccl9	-2.540	0.048	Yes	RNA methyltransferase(PC00033)	cytoplasm(GO:0005737)	————	tRNA methylation(GO:0030488)
Serpinb6b	-2.539	0.028	Yes	————	————	————	leukocyte migration(GO:0050900). leukocyte cell—cell adhesion(GO:0007159)
Kif5a	-2.498	0.000	No	————	————	————	————

HFD+PB vs HFD – DOWNREGULATED GENES							
Gene Symbol	**log2FC**	***P* value**	**Hit?**	**Molecular Function**	**Biological Function**	**Cellular Component**	**Protein Class**
Itih3	-2.496	0.004	Yes	tubulin(PC00228)	cytoplasm(GO:0005737). microtubule(GO:0005874)	————	neuron migration(GO:0001764). mitotic nuclear division(GO:0140014). microtubule cytoskeleton organization(GO:0000226)

HFD+PB vs HFD – DOWNREGULATED GENES							
Gene Symbol	**log2FC**	***P* value**	**Hit?**	**Molecular Function**	**Biological Function**	**Cellular Component**	**Protein Class**
Nrsn1	-2.470	0.000	Yes	non—motor microtubule binding protein(PC00166)	dendrite(GO:0030425). cytosol(GO:0005829). plasma membrane region(GO:0098590). neuronal cell body(GO:0043025). microtubule associated complex(GO:0005875). microtubule(GO:0005874)	————	regulation of supramolecular fiber organization(GO:1902903). axonogenesis(GO:0007409). regulation of microtubule polymerization or depolymerization(GO:0031110). microtubule depolymerization(GO:0007019). dendrite development(GO:0016358)

HFD+PB vs HFD – DOWNREGULATED GENES							
Gene Symbol	**log2FC**	***P* value**	**Hit?**	**Molecular Function**	**Biological Function**	**Cellular Component**	**Protein Class**
Nedd1	-2.466	0.024	Yes	————	centrosome(GO:0005813). centriole(GO:0005814). ciliary basal body(GO:0036064). intraciliary transport particle(GO:0030990). spindle pole(GO:0000922). plasma membrane region(GO:0098590)	————	protein localization to organelle(GO:0033365)
Wdr5b	-2.439	0.028	Yes	————	histone methyltransferase complex(GO:0035097)	————	histone H3—K4 methylation(GO:0051568)
Frmd6	-2.439	0.050	Yes	————	cytoskeleton(GO:0005856)	————	actomyosin structure organization(GO:0031032)
Shoc2	-2.439	0.050	Yes	————	————	————	tRNA methylation(GO:0030488)
Prss23	-2.439	0.048	Yes	————	————	————	————

HFD+PB vs HFD – DOWNREGULATED GENES							
Gene Symbol	**log2FC**	***P* value**	**Hit?**	**Molecular Function**	**Biological Function**	**Cellular Component**	**Protein Class**
Unc5b	-2.439	0.043	Yes	————	cytoplasm(GO:0005737). plasma membrane(GO:0005886)	————	RNA splicing(GO:0008380). regulation of RNA splicing(GO:0043484)
Cck	-2.437	0.000	Yes	————	————	————	————
Ptprd	-2.419	0.019	Yes	protein phosphatase(PC00195)	————	————	protein dephosphorylation(GO:0006470). synaptic membrane adhesion(GO:0099560)

Gtdc1	-2.388	0.030	Yes	————	————	————	transcription, DNA—templated(GO:0006351). negative regulation of extrinsic apoptotic signaling pathway(GO:2001237). cell development(GO:0048468). positive regulation of neurogenesis(GO:0050769). I—kappaB kinase/NF—kappaB signaling(GO:0007249). extrinsic apoptotic signaling pathway via death domain receptors(GO:0008625). positive regulation of NF—kappaB transcription factor activity(GO:0051092)

HFD+PB vs HFD – DOWNREGULATED GENES							
Gene Symbol	**log2FC**	***P* value**	**Hit?**	**Molecular Function**	**Biological Function**	**Cellular Component**	**Protein Class**
Enpp4	-2.387	0.018	Yes	nucleotide phosphatase(PC00173)	————	————	————
Nfyb	-2.387	0.007	Yes	————	————	————	————
Matk	-2.387	0.013	Yes	————	————	————	————
Chgb	-2.377	0.001	Yes	————	cytoplasm(GO:0005737)	————	organic substance catabolic process(GO:1901575). phosphorus metabolic process(GO:0006793). cellular catabolic process(GO:0044248). oxoacid metabolic process(GO:0043436)
Tubb2b	-2.375	0.001	Yes	G—protein coupled receptor(PC00021)	————	————	————
Omg	-2.355	0.027	Yes	————	midbody(GO:0030496)	————	————

HFD+PB vs HFD – DOWNREGULATED GENES							
Gene Symbol	**log2FC**	***P* value**	**Hit?**	**Molecular Function**	**Biological Function**	**Cellular Component**	**Protein Class**
Ttc26	-2.355	0.021	Yes	————	intracellular membrane—bounded organelle(GO:0043231). cytosol(GO:0005829)	————	————
Nptxr	-2.353	0.012	No	————	————	————	————
Ugt8	-2.333	0.047	Yes	————	intracellular membrane—bounded organelle(GO:0043231)	————	————

HFD+PB vs HFD – DOWNREGULATED GENES							
Gene Symbol	**log2FC**	***P* value**	**Hit?**	**Molecular Function**	**Biological Function**	**Cellular Component**	**Protein Class**
Tspan2	-2.333	0.021	Yes	small GTPase(PC00208)	————	————	vesicle budding from membrane(GO:0006900). cell projection assembly(GO:0030031). membrane invagination(GO:0010324). Rho protein signal transduction(GO:0007266). endocytosis(GO:0006897). cell migration(GO:0016477)
Smyd4	-2.333	0.012	Yes	————	nucleus(GO:0005634)	————	————
Elavl2	-2.333	0.008	No	————	————	————	————
Stmn3	-2.322	0.000	No	————	————	————	————
Wfdc1	-2.317	0.009	Yes	————	————	————	————
Mgst2	-2.306	0.035	Yes	extracellular matrix glycoprotein(PC00100)	————	————	————

HFD+PB vs HFD – DOWNREGULATED GENES							
Gene Symbol	**log2FC**	***P* value**	**Hit?**	**Molecular Function**	**Biological Function**	**Cellular Component**	**Protein Class**
Mal	-2.305	0.024	Yes	scaffold/adaptor protein(PC00226)	————	————	————
Cox18	-2.288	0.017	Yes	transporter(PC00227)	integral component of mitochondrial inner membrane(GO:0031305)	————	mitochondrial respiratory chain complex IV assembly(GO:0033617). protein insertion into mitochondrial inner membrane(GO:0045039)
Fastkd3	-2.288	0.024	Yes	G—protein coupled receptor(PC00021)	integral component of plasma membrane(GO:0005887)	————	cellular response to light stimulus(GO:0071482). response to external stimulus(GO:0009605). G protein—coupled receptor signaling pathway(GO:0007186). detection of stimulus(GO:0051606)

HFD+PB vs HFD – DOWNREGULATED GENES							
Gene Symbol	**log2FC**	***P* value**	**Hit?**	**Molecular Function**	**Biological Function**	**Cellular Component**	**Protein Class**
Crnkl1	-2.288	0.014	No	————	————	————	————
Ptprn	-2.270	0.000	Yes	————	extracellular space(GO:0005615). plasma membrane region(GO:0098590). axon(GO:0030424)	————	digestion(GO:0007586)
Cplx1	-2.259	0.000	Yes	————	terminal bouton(GO:0043195). SNARE complex(GO:0031201). plasma membrane region(GO:0098590)	————	regulation of neurotransmitter secretion(GO:0046928). vesicle fusion to plasma membrane(GO:0099500). synaptic vesicle exocytosis(GO:0016079)
Syngr3	-2.253	0.002	Yes	transporter(PC00227)	————	————	————
Fn1	-2.218	0.046	No	————	————	————	————
Apod	-2.212	0.010	No	————	————	————	————

HFD+PB vs HFD – DOWNREGULATED GENES							
Gene Symbol	**log2FC**	***P* value**	**Hit?**	**Molecular Function**	**Biological Function**	**Cellular Component**	**Protein Class**
Nefl	-2.193	0.000	Yes	————	————	————	————
Dtna	-2.165	0.025	Yes	————	————	————	————
Glmn	-2.144	0.039	Yes	ubiquitin—protein ligase(PC00234)	cytoplasm(GO:0005737)	————	————
Slf2	-2.144	0.045	Yes	————	————	————	————
Mbp	-2.139	0.027	Yes	protease inhibitor(PC00191)	extracellular space(GO:0005615). cytoplasm(GO:0005737)	————	proteolysis(GO:0006508). cellular protein metabolic process(GO:0044267). negative regulation of endopeptidase activity(GO:0010951)

HFD+PB vs HFD – DOWNREGULATED GENES							
Gene Symbol	**log2FC**	***P* value**	**Hit?**	**Molecular Function**	**Biological Function**	**Cellular Component**	**Protein Class**
Grin1	-2.125	0.004	Yes	————	growth cone(GO:0030426). cytoplasm(GO:0005737). plasma membrane region(GO:0098590)	————	neuron projection development(GO:0031175). regulation of microtubule polymerization or depolymerization(GO:0031110). microtubule depolymerization(GO:0007019)
Apba2	-2.124	0.022	Yes	————	————	————	————

HFD+PB vs HFD – DOWNREGULATED GENES							
Gene Symbol	**log2FC**	***P* value**	**Hit?**	**Molecular Function**	**Biological Function**	**Cellular Component**	**Protein Class**
Atp1a2	-2.122	0.005	Yes	primary active transporter(PC00068)	————	————	potassium ion transmembrane transport(GO:0071805). import into cell(GO:0098657). proton transmembrane transport(GO:1902600). sodium ion transmembrane transport(GO:0035725). cellular metal ion homeostasis(GO:0006875). cellular monovalent inorganic cation homeostasis(GO:0030004). export from cell(GO:0140352)
Disp2	-2.111	0.020	Yes	————	————	————	————

HFD+PB vs HFD – DOWNREGULATED GENES							
Gene Symbol	**log2FC**	***P* value**	**Hit?**	**Molecular Function**	**Biological Function**	**Cellular Component**	**Protein Class**
Mmd2	-2.109	0.020	Yes	G—protein coupled receptor(PC00021)	————	————	————
Stx1b	-2.100	0.001	Yes	myelin protein(PC00161)	cortical actin cytoskeleton(GO:0030864)	————	————
Stmn2	-2.097	0.000	Yes	nucleotide kinase(PC00172)	mitochondrion(GO:0005739)	————	————
Foxp2	-2.092	0.022	Yes	————	intracellular membrane—bounded organelle(GO:0043231). plasma membrane(GO:0005886)	————	————
Olig1	-2.078	0.000	No	————	————	————	————
Tagln3	-2.066	0.006	Yes	————	————	————	————

Pak1	-2.066	0.001	Yes	cytokine(PC00083)	extracellular space(GO:0005615)	————	ERK1 and ERK2 cascade(GO:0070371). inflammatory response(GO:0006954). G protein—coupled receptor signaling pathway(GO:0007186). chemokine—mediated signaling pathway(GO:0070098). innate immune response(GO:0045087). positive regulation of ERK1 and ERK2 cascade(GO:0070374). response to interleukin—1(GO:0070555).

HFD+PB vs HFD – DOWNREGULATED GENES							
Gene Symbol	**log2FC**	***P* value**	**Hit?**	**Molecular Function**	**Biological Function**	**Cellular Component**	**Protein Class**
							cellular response to tumor necrosis factor(GO:0071356). granulocyte chemotaxis(GO:0071621). lymphocyte migration(GO:0072676). positive regulation of GTPase activity(GO:0043547)

HFD+PB vs HFD – DOWNREGULATED GENES							
Gene Symbol	**log2FC**	***P* value**	**Hit?**	**Molecular Function**	**Biological Function**	**Cellular Component**	**Protein Class**
Begain	-2.066	0.045	Yes	————	————	————	chemical synaptic transmission, postsynaptic(GO:0099565). modulation of chemical synaptic transmission(GO:0050804). regulation of system process(GO:0044057). regulation of signaling receptor activity(GO:0010469)
Tbc1d25	-2.066	0.036	Yes	GTPase—activating protein(PC00257)	————	————	intracellular protein transport(GO:0006886). positive regulation of GTPase activity(GO:0043547)
Sparcl1	-2.059	0.004	No	————	————	————	————

Rprml	-2.054	0.023	Yes	————	focal adhesion(GO:0005925). leaflet of membrane bilayer(GO:0097478). dendritic spine(GO:0043197). extrinsic component of cytoplasmic side of plasma membrane(GO:0031234). plasma membrane region(GO:0098590)	————	cell population proliferation(GO:0008283). peptidyl—tyrosine phosphorylation(GO:0018108). angiogenesis(GO:0001525). epidermal growth factor receptor signaling pathway(GO:0007173). cell differentiation(GO:0030154). cell adhesion(GO:0007155). regulation of cell adhesion(GO:0030155). regulation of cell population proliferation(GO:0042127)

HFD+PB vs HFD – DOWNREGULATED GENES							
Gene Symbol	**log2FC**	***P* value**	**Hit?**	**Molecular Function**	**Biological Function**	**Cellular Component**	**Protein Class**
Cep290	-2.054	0.020	Yes	————	voltage—gated calcium channel complex(GO:0005891)	————	synapse organization(GO:0050808). calcium ion transmembrane transport(GO:0070588). chemical synaptic transmission(GO:0007268). regulation of calcium ion transport(GO:0051924). regulation of cation transmembrane transport(GO:1904062). regulation of ion transmembrane transporter activity(GO:0032412)

HFD+PB vs HFD – DOWNREGULATED GENES							
Gene Symbol	**log2FC**	***P* value**	**Hit?**	**Molecular Function**	**Biological Function**	**Cellular Component**	**Protein Class**
Serpini1	-2.050	0.003	Yes	protease inhibitor(PC00191)	extracellular space(GO:0005615)	————	proteolysis(GO:0006508). cellular protein metabolic process(GO:0044267). negative regulation of endopeptidase activity(GO:0010951)
Sult4a1	-2.035	0.000	Yes	————	nucleus(GO:0005634). cytoplasm(GO:0005737)	————	cellular zinc ion homeostasis(GO:0006882). response to cadmium ion(GO:0046686). response to toxic substance(GO:0009636). cellular response to chemical stimulus(GO:0070887). response to stress(GO:0006950)

HFD+PB vs HFD – DOWNREGULATED GENES							
Gene Symbol	**log2FC**	***P* value**	**Hit?**	**Molecular Function**	**Biological Function**	**Cellular Component**	**Protein Class**
Bcat1	-2.031	0.000	Yes	membrane traffic protein(PC00150)	integral component of membrane(GO:0016021)	————	myelination(GO:0042552)
Synm	-2.025	0.031	Yes	————	————	————	————
S1pr5	-2.025	0.017	Yes	————	integral component of plasma membrane(GO:0005887)	————	————
Lhx2	-2.025	0.037	No	————	————	————	————
Cpped1	-2.011	0.002	Yes	RNA helicase(PC00032)	nucleus(GO:0005634)	————	————
Nudt21	-1.995	0.025	Yes	heterotrimeric G—protein(PC00117)	————	————	————
LOC100365363	-1.995	0.026	Yes	————	histone acetyltransferase complex(GO:0000123)	————	transcription by RNA polymerase II(GO:0006366). positive regulation of transcription by RNA polymerase II(GO:0045944)
Ptprr	-1.995	0.036	No	————	————	————	————

HFD+PB vs HFD – DOWNREGULATED GENES							
Gene Symbol	**log2FC**	***P* value**	**Hit?**	**Molecular Function**	**Biological Function**	**Cellular Component**	**Protein Class**
Apoc1	-1.995	0.042	No	————	————	————	————
Gad1	-1.983	0.011	Yes	decarboxylase(PC00089)	————	————	————
Cbs	-1.972	0.042	Yes	————	————	————	————
Gria2	-1.972	0.029	No	————	————	————	————
Adap1	-1.967	0.007	Yes	————	————	————	————
Scn1b	-1.960	0.001	Yes	primary active transporter(PC00068)	————	————	regulation of metal ion transport(GO:0010959). sodium ion transmembrane transport(GO:0035725). regulation of cation transmembrane transport(GO:1904062). regulation of ion transmembrane transporter activity(GO:0032412)

HFD+PB vs HFD – DOWNREGULATED GENES							
Gene Symbol	**log2FC**	***P* value**	**Hit?**	**Molecular Function**	**Biological Function**	**Cellular Component**	**Protein Class**
Rcan2	-1.959	0.000	Yes	intercellular signal molecule(PC00207)	cytoplasm(GO:0005737)	————	inositol phosphate—mediated signaling(GO:0048016). regulation of intracellular signal transduction(GO:1902531). calcium—mediated signaling(GO:0019722)
Mbtps2	-1.955	0.020	Yes	metalloprotease(PC00153)	————	————	————
Mt-nd4l	-1.955	0.017	Yes	————	————	————	————
Gng13	-1.955	0.043	Yes	metalloprotease(PC00153)	————	————	————
Adora1	-1.954	0.043	Yes	G—protein coupled receptor(PC00021)	————	————	————
Rbp4	-1.954	0.049	Yes	————	————	————	————
Ubap1l	-1.954	0.041	Yes	acetyltransferase(PC00038)	————	————	————
Ptpn5	-1.954	0.047	No	————	————	————	————

HFD+PB vs HFD – DOWNREGULATED GENES							
Gene Symbol	**log2FC**	***P* value**	**Hit?**	**Molecular Function**	**Biological Function**	**Cellular Component**	**Protein Class**
Ccdc136	-1.943	0.015	Yes	scaffold/adaptor protein(PC00226)	————	————	————

Tmem87b	-1.940	0.011	Yes	membrane trafficking regulatory protein(PC00151)	exocytic vesicle(GO:0070382). plasma membrane region(GO:0098590). vacuole(GO:0005773). axon(GO:0030424)	————	regulation of response to stimulus(GO:0048583). vesicle fusion to plasma membrane(GO:0099500). ammonium transport(GO:0015696). organic hydroxy compound transport(GO:0015850). drug transport(GO:0015893). response to calcium ion(GO:0051592). calcium—ion regulated exocytosis(GO:0017156). regulation of exocytosis(GO:0017157). regulation of ion transport(GO:0043269).

HFD+PB vs HFD – DOWNREGULATED GENES							
Gene Symbol	**log2FC**	***P* value**	**Hit?**	**Molecular Function**	**Biological Function**	**Cellular Component**	**Protein Class**
							cellular response to chemical stimulus(GO:0070887)

Vegfb	-1.940	0.018	Yes	voltage—gated ion channel(PC00241)	integral component of plasma membrane(GO:0005887). plasma membrane protein complex(GO:0098797). cation channel complex(GO:0034703)	————	actin filament—based process(GO:0030029). regulation of metal ion transport(GO:0010959). movement of cell or subcellular component(GO:0006928). signaling(GO:0023052). regulation of heart contraction(GO:0008016). action potential(GO:0001508). sodium ion transmembrane transport(GO:0035725). cardiac muscle contraction(GO:0060048).

HFD+PB vs HFD – DOWNREGULATED GENES							
Gene Symbol	**log2FC**	***P* value**	**Hit?**	**Molecular Function**	**Biological Function**	**Cellular Component**	**Protein Class**
							regulation of cation transmembrane transport(GO:1904062). regulation of ion transmembrane transporter activity(GO:0032412)
Nat8l	-1.940	0.015	Yes	translation factor(PC00223)	protein—containing complex(GO:0032991). cytoplasmic part(GO:0044444)	————	translational termination(GO:0006415). cytoplasmic translation(GO:0002181). translational elongation(GO:0006414)

HFD+PB vs HFD – DOWNREGULATED GENES							
Gene Symbol	**log2FC**	***P* value**	**Hit?**	**Molecular Function**	**Biological Function**	**Cellular Component**	**Protein Class**
Sash1	-1.934	0.045	Yes	membrane trafficking regulatory protein(PC00151)	neuromuscular junction(GO:0031594). synaptic vesicle membrane(GO:0030672). vacuole(GO:0005773). plasma membrane(GO:0005886)	————	————
Osbpl8	-1.934	0.044	Yes	————	————	————	————
Mag	-1.918	0.006	Yes	G—protein coupled receptor(PC00021)	————	————	————
Slc43a2	-1.918	0.018	Yes	————	————	————	neutral amino acid transport(GO:0015804)

HFD+PB vs HFD – DOWNREGULATED GENES							
Gene Symbol	**log2FC**	***P* value**	**Hit?**	**Molecular Function**	**Biological Function**	**Cellular Component**	**Protein Class**
Jun	-1.918	0.033	Yes	RNA binding protein(PC00031)	P—body(GO:0000932). nucleoplasm(GO:0005654)	————	regulation of mRNA catabolic process(GO:0061013). gene silencing by miRNA(GO:0035195). positive regulation of RNA metabolic process(GO:0051254). gene expression(GO:0010467). positive regulation of cellular catabolic process(GO:0031331). nuclear—transcribed mRNA poly(A) tail shortening(GO:0000289)

HFD+PB vs HFD – DOWNREGULATED GENES							
Gene Symbol	**log2FC**	***P* value**	**Hit?**	**Molecular Function**	**Biological Function**	**Cellular Component**	**Protein Class**
Vgf	-1.906	0.036	Yes	transferase(PC00220)	nuclear envelope(GO:0005635). endoplasmic reticulum(GO:0005783). vacuole(GO:0005773). plasma membrane(GO:0005886)	————	carboxylic acid biosynthetic process(GO:0046394). icosanoid metabolic process(GO:0006690)
Gja1	-1.903	0.000	Yes	gap junction(PC00105)	————	————	————
Adgrb2	-1.887	0.023	Yes	————	————	————	————
Spata18	-1.881	0.010	No	————	————	————	————
Rundc3a	-1.873	0.002	Yes	————	integral component of plasma membrane(GO:0005887)	————	cell adhesion(GO:0007155)
Mt1m	-1.870	0.026	Yes	kinase(PC00137)	————	————	————

HFD+PB vs HFD – DOWNREGULATED GENES							
Gene Symbol	**log2FC**	***P* value**	**Hit?**	**Molecular Function**	**Biological Function**	**Cellular Component**	**Protein Class**
Lypd1	-1.870	0.044	Yes	————	————	————	acetylcholine receptor signaling pathway(GO:0095500)
Kcna6	-1.867	0.000	No	————	————	————	————
Ptn	-1.864	0.002	Yes	general transcription factor(PC00259)	————	————	————
Sfxn1	-1.861	0.032	No	————	————	————	————
Uchl1	-1.851	0.000	Yes	cysteine protease(PC00081)	cytoplasm(GO:0005737)	————	protein deubiquitination(GO:0016579)
Galnt16	-1.850	0.023	Yes	glycosyltransferase(PC00111)	Golgi apparatus(GO:0005794). vacuole(GO:0005773). plasma membrane(GO:0005886)	————	————
Adcyap1r1	-1.850	0.016	Yes	————	————	————	————

HFD+PB vs HFD – DOWNREGULATED GENES							
Gene Symbol	**log2FC**	***P* value**	**Hit?**	**Molecular Function**	**Biological Function**	**Cellular Component**	**Protein Class**
Cherp	-1.850	0.001	Yes	————	mitochondrial large ribosomal subunit(GO:0005762)	————	————
Faim2	-1.850	0.000	Yes	————	ESCRT I complex(GO:0000813). vacuole(GO:0005773). plasma membrane(GO:0005886)	————	ubiquitin—dependent protein catabolic process via the multivesicular body sorting pathway(GO:0043162). multivesicular body sorting pathway(GO:0071985). protein catabolic process in the vacuole(GO:0007039)
Dhx36	-1.842	0.023	Yes	————	————	————	————
Klhl13	-1.832	0.005	Yes	GTPase—activating protein(PC00257)	————	————	————
Dlgap3	-1.803	0.007	No	————	————	————	————

HFD+PB vs HFD – DOWNREGULATED GENES							
Gene Symbol	**log2FC**	***P* value**	**Hit?**	**Molecular Function**	**Biological Function**	**Cellular Component**	**Protein Class**
Ift88	-1.802	0.039	Yes	————	centriole(GO:0005814). ciliary basal body(GO:0036064). non—motile cilium(GO:0097730). ciliary base(GO:0097546). intraciliary transport particle(GO:0030990). plasma membrane region(GO:0098590). ciliary transition fiber(GO:0097539). ciliary transition zone(GO:0035869)	————	intraciliary transport involved in cilium assembly(GO:0035735). non—motile cilium assembly(GO:1905515). vesicle targeting, trans—Golgi to periciliary membrane compartment(GO:0097712). axoneme assembly(GO:0035082). ciliary transition zone assembly(GO:1905349). protein localization to cilium(GO:0061512)
Arhgef28	-1.802	0.037	Yes	metalloprotease(PC00153)	————	————	————

HFD+PB vs HFD – DOWNREGULATED GENES							
Gene Symbol	**log2FC**	***P* value**	**Hit?**	**Molecular Function**	**Biological Function**	**Cellular Component**	**Protein Class**
Nkx6-2	-1.802	0.050	Yes	small GTPase(PC00208)	plasma membrane(GO:0005886)	————	neuron projection development(GO:0031175). Ras protein signal transduction(GO:0007265). positive regulation of neuron projection development(GO:0010976)
Zfp292	-1.802	0.038	Yes	oxidoreductase(PC00176)	————	————	————

HFD+PB vs HFD – DOWNREGULATED GENES							
Gene Symbol	**log2FC**	***P* value**	**Hit?**	**Molecular Function**	**Biological Function**	**Cellular Component**	**Protein Class**
Gng3	-1.786	0.001	Yes	SNARE protein(PC00034)	presynaptic membrane(GO:0042734). presynaptic active zone(GO:0048786). synaptic vesicle(GO:0008021). integral component of membrane(GO:0016021). SNARE complex(GO:0031201). vacuole(GO:0005773)	————	vesicle fusion to plasma membrane(GO:0099500). organelle localization(GO:0051640). synaptic vesicle exocytosis(GO:0016079). intracellular protein transport(GO:0006886)
Syt4	-1.781	0.004	Yes	tubulin(PC00228)	cytoplasm(GO:0005737). microtubule(GO:0005874)	————	mitotic nuclear division(GO:0140014). microtubule cytoskeleton organization(GO:0000226)

HFD+PB vs HFD – DOWNREGULATED GENES							
Gene Symbol	**log2FC**	***P* value**	**Hit?**	**Molecular Function**	**Biological Function**	**Cellular Component**	**Protein Class**
Cnrip1	-1.772	0.006	Yes	————	plasma membrane(GO:0005886)	————	signal transduction(GO:0007165). negative regulation of signaling receptor activity(GO:2000272)
Rap1gap	-1.762	0.018	Yes	G—protein coupled receptor(PC00021)	————	————	————
Bcan	-1.758	0.008	No	————	————	————	————
Fem1c	-1.754	0.042	Yes	————	————	————	————
RragB	-1.748	0.036	Yes	————	————	————	————
Klk6	-1.748	0.022	Yes	————	endoplasmic reticulum membrane(GO:0005789). vacuole(GO:0005773). plasma membrane(GO:0005886)	————	cellular response to cytokine stimulus(GO:0071345). defense response(GO:0006952)

HFD+PB vs HFD – DOWNREGULATED GENES							
Gene Symbol	**log2FC**	***P* value**	**Hit?**	**Molecular Function**	**Biological Function**	**Cellular Component**	**Protein Class**
Cks1b	-1.741	0.046	Yes	cysteine protease(PC00081)	————	————	protein deubiquitination(GO:0016579)
Rhoj	-1.727	0.018	Yes	————	extracellular space(GO:0005615). secretory granule(GO:0030141). vacuole(GO:0005773). plasma membrane(GO:0005886)	————	————
Sptbn2	-1.724	0.005	No	————	————	————	————
Patj	-1.723	0.000	Yes	————	————	————	————
Rasgrf1	-1.709	0.021	No	————	————	————	————

HFD+PB vs HFD – DOWNREGULATED GENES							
Gene Symbol	**log2FC**	***P* value**	**Hit?**	**Molecular Function**	**Biological Function**	**Cellular Component**	**Protein Class**
Tbc1d1	-1.703	0.010	Yes	GTPase—activating protein(PC00257)	————	————	intracellular protein transport(GO:0006886). positive regulation of GTPase activity(GO:0043547)
Togaram1	-1.703	0.042	Yes	non—motor microtubule binding protein(PC00166)	————	————	————
Tcf7l2	-1.682	0.001	Yes	————	————	————	————
Fxyd7	-1.677	0.011	Yes	————	cytosol(GO:0005829)	————	cGMP—mediated signaling(GO:0019934). positive regulation of intracellular signal transduction(GO:1902533)
Agap2	-1.673	0.001	Yes	————	————	————	————
Ndrg1	-1.665	0.004	Yes	serine protease(PC00203)	cytoplasm(GO:0005737)	————	signal transduction(GO:0007165)

HFD+PB vs HFD – DOWNREGULATED GENES							
Gene Symbol	**log2FC**	***P* value**	**Hit?**	**Molecular Function**	**Biological Function**	**Cellular Component**	**Protein Class**
Mb21d2	-1.665	0.029	Yes	————	————	————	————
Map7d2	-1.651	0.044	Yes	non—motor microtubule binding protein(PC00166)	microtubule cytoskeleton(GO:0015630)	————	microtubule cytoskeleton organization(GO:0000226)

Slc26a6	-1.651	0.044	Yes	membrane trafficking regulatory protein(PC00151)	exocytic vesicle(GO:0070382). plasma membrane region(GO:0098590). vacuole(GO:0005773). axon(GO:0030424)	————	regulation of response to stimulus(GO:0048583). vesicle fusion to plasma membrane(GO:0099500). ammonium transport(GO:0015696). organic hydroxy compound transport(GO:0015850). drug transport(GO:0015893). response to calcium ion(GO:0051592). calcium—ion regulated exocytosis(GO:0017156). regulation of exocytosis(GO:0017157). regulation of ion transport(GO:0043269).

HFD+PB vs HFD – DOWNREGULATED GENES							
Gene Symbol	**log2FC**	***P* value**	**Hit?**	**Molecular Function**	**Biological Function**	**Cellular Component**	**Protein Class**
							cellular response to chemical stimulus(GO:0070887)
Wscd1	-1.649	0.000	Yes	————	————	————	————
Cnp	-1.649	0.027	Yes	————	plasma membrane region(GO:0098590). neuronal cell body(GO:0043025). transport vesicle(GO:0030133). neuron projection(GO:0043005). vacuole(GO:0005773)	————	nervous system development(GO:0007399)
Snrpf	-1.646	0.021	Yes	RNA splicing factor(PC00148)	————	————	————
Camk2b	-1.646	0.002	No	————	————	————	————

HFD+PB vs HFD – DOWNREGULATED GENES							
Gene Symbol	**log2FC**	***P* value**	**Hit?**	**Molecular Function**	**Biological Function**	**Cellular Component**	**Protein Class**
Mtfmt	-1.642	0.006	Yes	————	————	————	————
Pitrm1	-1.633	0.047	Yes	membrane trafficking regulatory protein(PC00151)	cytoplasm(GO:0005737). dendritic spine(GO:0043197). plasma membrane region(GO:0098590)	————	chemical synaptic transmission(GO:0007268)
Slc1a3	-1.630	0.025	No	————	————	————	————
Akap11	-1.626	0.001	No	————	————	————	————

HFD+PB vs HFD – DOWNREGULATED GENES							
Gene Symbol	**log2FC**	***P* value**	**Hit?**	**Molecular Function**	**Biological Function**	**Cellular Component**	**Protein Class**
Mobp	-1.620	0.001	Yes	————	————	————	anatomical structure formation involved in morphogenesis(GO:0048646). central nervous system neuron differentiation(GO:0021953). brain development(GO:0007420). cell migration(GO:0016477)
Mtrf1	-1.616	0.049	Yes	————	————	————	————
Magi2	-1.616	0.040	No	————	————	————	————
Amn1	-1.613	0.009	Yes	nucleotide kinase(PC00172)	————	————	————
Sncb	-1.606	0.002	No	————	————	————	————
Ngef	-1.596	0.021	No	————	————	————	————

HFD+PB vs HFD – DOWNREGULATED GENES							
Gene Symbol	**log2FC**	***P* value**	**Hit?**	**Molecular Function**	**Biological Function**	**Cellular Component**	**Protein Class**
Mapk8ip2	-1.596	0.028	Yes	————	————	————	regulation of metal ion transport(GO:0010959). sodium ion transport(GO:0006814)
Trim34	-1.587	0.032	Yes	————	————	————	————
RGD1311745	-1.580	0.028	Yes	————	————	————	————
Dguok	-1.566	0.016	Yes	phosphatase modulator(PC00184)	————	————	————

HFD+PB vs HFD – DOWNREGULATED GENES							
Gene Symbol	**log2FC**	***P* value**	**Hit?**	**Molecular Function**	**Biological Function**	**Cellular Component**	**Protein Class**
Eef1a2	-1.565	0.000	Yes	phosphatase(PC00181)	————	————	small molecule catabolic process(GO:0044282). cellular carbohydrate metabolic process(GO:0044262). alcohol metabolic process(GO:0006066). organophosphate catabolic process(GO:0046434). dephosphorylation(GO:0016311)
Serpinf1	-1.563	0.006	Yes	protease inhibitor(PC00191)	extracellular space(GO:0005615)	————	proteolysis(GO:0006508). cellular protein metabolic process(GO:0044267). negative regulation of endopeptidase activity(GO:0010951)

HFD+PB vs HFD – DOWNREGULATED GENES							
Gene Symbol	**log2FC**	***P* value**	**Hit?**	**Molecular Function**	**Biological Function**	**Cellular Component**	**Protein Class**
Hcrt	-1.563	0.025	Yes	————	————	————	————
Pls3	-1.563	0.004	No	————	————	————	————
Ptp4a3	-1.556	0.029	Yes	————	nucleus(GO:0005634)	————	————
Penk	-1.547	0.005	Yes	neuropeptide(PC00162)	dendrite(GO:0030425). plasma membrane region(GO:0098590). neuronal cell body(GO:0043025). axon terminus(GO:0043679)	————	neuropeptide signaling pathway(GO:0007218). chemical synaptic transmission(GO:0007268). sensory perception(GO:0007600)

HFD+PB vs HFD – DOWNREGULATED GENES							
Gene Symbol	**log2FC**	***P* value**	**Hit?**	**Molecular Function**	**Biological Function**	**Cellular Component**	**Protein Class**
Ppp1r3b	-1.540	0.039	Yes	RNA splicing factor(PC00148)	Lsm2—8 complex(GO:0120115). catalytic step 2 spliceosome(GO:0071013). post—mRNA release spliceosomal complex(GO:0071014). U5 snRNP(GO:0005682). U2—type spliceosomal complex(GO:0005684). Prp19 complex(GO:0000974). U2 snRNP(GO:0005686). U6 snRNP(GO:0005688)	————	spliceosomal complex assembly(GO:0000245)

HFD+PB vs HFD – DOWNREGULATED GENES							
Gene Symbol	**log2FC**	***P* value**	**Hit?**	**Molecular Function**	**Biological Function**	**Cellular Component**	**Protein Class**
Prim1	-1.540	0.012	Yes	kinase activator(PC00138)	transcription factor TFIIH core complex(GO:0000439). transcription factor TFIIH holo complex(GO:0005675)	————	phosphorylation of RNA polymerase II C—terminal domain(GO:0070816). transcription by RNA polymerase II(GO:0006366). cell cycle(GO:0007049). regulation of cyclin—dependent protein serine/threonine kinase activity(GO:0000079)
Mum1	-1.540	0.040	Yes	————	————	————	activation of JUN kinase activity(GO:0007257). JUN phosphorylation(GO:0007258)
Dnm1	-1.539	0.002	Yes	oxidoreductase(PC00176)	————	————	————

HFD+PB vs HFD – DOWNREGULATED GENES							
Gene Symbol	**log2FC**	***P* value**	**Hit?**	**Molecular Function**	**Biological Function**	**Cellular Component**	**Protein Class**
S100b	-1.529	0.014	Yes	calmodulin—related(PC00061)	————	————	————
Gng2	-1.529	0.003	Yes	————	————	————	T cell mediated immunity(GO:0002456). positive regulation of adaptive immune response(GO:0002821)
Acad10	-1.523	0.030	Yes	————	SCF ubiquitin ligase complex(GO:0019005)	————	SCF—dependent proteasomal ubiquitin—dependent protein catabolic process(GO:0031146)
Pcsk6	-1.523	0.016	No	————	————	————	————

HFD+PB vs HFD – DOWNREGULATED GENES							
Gene Symbol	**log2FC**	***P* value**	**Hit?**	**Molecular Function**	**Biological Function**	**Cellular Component**	**Protein Class**
Podxl2	-1.520	0.009	Yes	————	extracellular space(GO:0005615)	————	regulation of cell growth(GO:0001558). cellular component organization(GO:0016043). cell growth(GO:0016049)
Nfasc	-1.517	0.049	Yes	lyase(PC00144)	cytoplasm(GO:0005737)	————	secondary metabolic process(GO:0019748). alpha—amino acid metabolic process(GO:1901605). sulfur compound metabolic process(GO:0006790). drug metabolic process(GO:0017144). cellular biosynthetic process(GO:0044249)

HFD+PB vs HFD – DOWNREGULATED GENES							
Gene Symbol	**log2FC**	***P* value**	**Hit?**	**Molecular Function**	**Biological Function**	**Cellular Component**	**Protein Class**
Abhd17b	-1.503	0.047	Yes	translation factor(PC00223)	————	————	translational elongation(GO:0006414)
Tubb4a	-1.499	0.008	Yes	————	————	————	————
Cnih2	-1.491	0.001	Yes	————	endoplasmic reticulum(GO:0005783). vacuole(GO:0005773). plasma membrane(GO:0005886)	————	————
Dcp1b	-1.481	0.047	Yes	mRNA capping factor(PC00145)	P—body(GO:0000932)	————	nucleic acid phosphodiester bond hydrolysis(GO:0090305). deadenylation—dependent decapping of nuclear—transcribed mRNA(GO:0000290). gene expression(GO:0010467)

HFD+PB vs HFD – DOWNREGULATED GENES							
Gene Symbol	**log2FC**	***P* value**	**Hit?**	**Molecular Function**	**Biological Function**	**Cellular Component**	**Protein Class**
Pllp	-1.481	0.012	Yes	————	————	————	————

Syt1	-1.455	0.015	Yes	membrane trafficking regulatory protein(PC00151)	secretory granule(GO:0030141). plasma membrane region(GO:0098590). synaptic vesicle membrane(GO:0030672). vacuole(GO:0005773). axon(GO:0030424)	————	ammonium transport(GO:0015696). organic hydroxy compound transport(GO:0015850). drug transport(GO:0015893). regulation of ion transport(GO:0043269). regulation of response to stimulus(GO:0048583). vesicle fusion to plasma membrane(GO:0099500). vesicle budding from membrane(GO:0006900). synaptic vesicle endocytosis(GO:0048488). response to calcium ion(GO:0051592).

HFD+PB vs HFD – DOWNREGULATED GENES							
Gene Symbol	**log2FC**	***P* value**	**Hit?**	**Molecular Function**	**Biological Function**	**Cellular Component**	**Protein Class**
							membrane invagination(GO:0010324). calcium—ion regulated exocytosis(GO:0017156). regulation of exocytosis(GO:0017157). synaptic vesicle exocytosis(GO:0016079). cellular response to chemical stimulus(GO:0070887)
Cadm3	-1.452	0.046	Yes	————	————	————	————
Phyhip	-1.452	0.038	Yes	————	————	————	————

HFD+PB vs HFD – DOWNREGULATED GENES							
Gene Symbol	**log2FC**	***P* value**	**Hit?**	**Molecular Function**	**Biological Function**	**Cellular Component**	**Protein Class**
Irgm	-1.452	0.034	Yes	C2H2 zinc finger transcription factor(PC00248)	nucleus(GO:0005634)	————	transcription by RNA polymerase II(GO:0006366). regulation of transcription by RNA polymerase II(GO:0006357)
Pdxp	-1.448	0.001	No	————	————	————	————
Clip3	-1.447	0.007	Yes	heterotrimeric G—protein(PC00117)	catalytic complex(GO:1902494). leaflet of membrane bilayer(GO:0097478). plasma membrane protein complex(GO:0098797). extrinsic component of cytoplasmic side of plasma membrane(GO:0031234). cytoplasmic part(GO:0044444)	————	G protein—coupled receptor signaling pathway(GO:0007186)

HFD+PB vs HFD – DOWNREGULATED GENES							
Gene Symbol	**log2FC**	***P* value**	**Hit?**	**Molecular Function**	**Biological Function**	**Cellular Component**	**Protein Class**
Pcp4	-1.442	0.000	Yes	————	————	————	————
RGD1309036	-1.440	0.019	No	————	————	————	————
Tmem38a	-1.433	0.007	No	————	————	————	————
Cldn11	-1.431	0.043	No	————	————	————	————

HFD+PB vs HFD – DOWNREGULATED GENES							
Gene Symbol	**log2FC**	***P* value**	**Hit?**	**Molecular Function**	**Biological Function**	**Cellular Component**	**Protein Class**
Rab6b	-1.431	0.002	Yes	————	Golgi apparatus(GO:0005794). vacuole(GO:0005773). plasma membrane(GO:0005886)	————	retrograde vesicle—mediated transport, Golgi to endoplasmic reticulum(GO:0006890). Ras protein signal transduction(GO:0007265). intra—Golgi vesicle—mediated transport(GO:0006891). intracellular protein transport(GO:0006886). retrograde transport, endosome to Golgi(GO:0042147)
Fbxo4	-1.427	0.041	Yes	transfer/carrier protein(PC00219)	————	————	————

HFD+PB vs HFD – DOWNREGULATED GENES							
Gene Symbol	**log2FC**	***P* value**	**Hit?**	**Molecular Function**	**Biological Function**	**Cellular Component**	**Protein Class**
Nelfa	-1.422	0.017	Yes	————	dendrite(GO:0030425). plasma membrane region(GO:0098590). synaptic vesicle membrane(GO:0030672). vacuole(GO:0005773). integral component of organelle membrane(GO:0031301). neuron projection terminus(GO:0044306)	————	neurotransmitter transport(GO:0006836). synaptic vesicle cycle(GO:0099504)

HFD+PB vs HFD – DOWNREGULATED GENES							
Gene Symbol	**log2FC**	***P* value**	**Hit?**	**Molecular Function**	**Biological Function**	**Cellular Component**	**Protein Class**
Tubb2a	-1.420	0.001	Yes	tubulin(PC00228)	cytoplasm(GO:0005737). microtubule(GO:0005874)	————	neuron migration(GO:0001764). mitotic nuclear division(GO:0140014). microtubule cytoskeleton organization(GO:0000226)

Ermn	-1.417	0.027	Yes	growth factor(PC00112)	extracellular space(GO:0005615)	————	positive chemotaxis(GO:0050918). sprouting angiogenesis(GO:0002040). positive regulation of leukocyte chemotaxis(GO:0002690). transmembrane receptor protein tyrosine kinase signaling pathway(GO:0007169). protein phosphorylation(GO:0006468). positive regulation of angiogenesis(GO:0045766). response to hypoxia(GO:0001666).

HFD+PB vs HFD – DOWNREGULATED GENES							
Gene Symbol	**log2FC**	***P* value**	**Hit?**	**Molecular Function**	**Biological Function**	**Cellular Component**	**Protein Class**
							cellular response to growth factor stimulus(GO:0071363). positive regulation of protein phosphorylation(GO:0001934). endothelial cell proliferation(GO:0001935). leukocyte chemotaxis(GO:0030595). myeloid leukocyte migration(GO:0097529). positive regulation of epithelial cell proliferation(GO:0050679)
Scg5	-1.409	0.000	No	————	————	————	————

HFD+PB vs HFD – DOWNREGULATED GENES							
Gene Symbol	**log2FC**	***P* value**	**Hit?**	**Molecular Function**	**Biological Function**	**Cellular Component**	**Protein Class**
Nkain4	-1.402	0.022	Yes	————	synaptonemal complex(GO:0000795)	————	————
Prune1	-1.398	0.042	Yes	————	nucleus(GO:0005634)	————	RNA splicing(GO:0008380)
Ogn	-1.398	0.030	Yes	————	————	————	————
Pkn1	-1.387	0.017	Yes	non—receptor serine/threonine protein kinase(PC00167)	————	————	peptidyl—serine phosphorylation(GO:0018105). intracellular signal transduction(GO:0035556)
C1d	-1.383	0.011	Yes	transcription cofactor(PC00217)	————	————	————
Bbs9	-1.377	0.022	Yes	————	————	————	————

Lrrc4b	-1.370	0.035	Yes	————	perinuclear region of cytoplasm(GO:0048471)	————	regulation of neurotransmitter secretion(GO:0046928). positive regulation of signaling(GO:0023056). positive regulation of cell communication(GO:0010647). homeostatic process(GO:0042592). positive regulation of multicellular organismal process(GO:0051240). response to starvation(GO:0042594). regulation of system process(GO:0044057).

HFD+PB vs HFD – DOWNREGULATED GENES							
Gene Symbol	**log2FC**	***P* value**	**Hit?**	**Molecular Function**	**Biological Function**	**Cellular Component**	**Protein Class**
							action potential(GO:0001508). nervous system process(GO:0050877). behavior(GO:0007610). neurotransmitter secretion(GO:0007269)
Recql5	-1.362	0.031	Yes	DNA helicase(PC00011)	cytoplasm(GO:0005737). chromosome(GO:0005694)	————	DNA biosynthetic process(GO:0071897). double—strand break repair via homologous recombination(GO:0000724). DNA unwinding involved in DNA replication(GO:0006268)

HFD+PB vs HFD – DOWNREGULATED GENES							
Gene Symbol	**log2FC**	***P* value**	**Hit?**	**Molecular Function**	**Biological Function**	**Cellular Component**	**Protein Class**
Nsg1	-1.362	0.047	Yes	————	endosome(GO:0005768). integral component of membrane(GO:0016021). vacuole(GO:0005773). plasma membrane(GO:0005886)	————	cellular protein—containing complex assembly(GO:0034622). endosomal transport(GO:0016197)
Tyw3	-1.362	0.035	Yes	————	————	————	————
Trafd1	-1.362	0.029	Yes	non—motor actin binding protein(PC00165)	————	————	————
Cdc42ep2	-1.355	0.043	Yes	————	nuclear part(GO:0044428). protein—containing complex(GO:0032991). chromatin(GO:0000785)	————	mitotic sister chromatid cohesion(GO:0007064)
Ly6h	-1.351	0.018	Yes	————	————	————	————

HFD+PB vs HFD – DOWNREGULATED GENES							
Gene Symbol	**log2FC**	***P* value**	**Hit?**	**Molecular Function**	**Biological Function**	**Cellular Component**	**Protein Class**
Scnm1	-1.339	0.004	Yes	————	perinuclear region of cytoplasm(GO:0048471). endoplasmic reticulum part(GO:0044432). cytosol(GO:0005829). vacuole(GO:0005773). plasma membrane(GO:0005886)	————	————
Ndrg4	-1.333	0.026	No	————	————	————	————
Syce1l	-1.333	0.042	Yes	————	nucleus(GO:0005634). cytoplasm(GO:0005737). ribonucleoprotein complex(GO:1990904)	————	————

HFD+PB vs HFD – DOWNREGULATED GENES							
Gene Symbol	**log2FC**	***P* value**	**Hit?**	**Molecular Function**	**Biological Function**	**Cellular Component**	**Protein Class**
Dbndd2	-1.329	0.002	Yes	G—protein coupled receptor(PC00021)	integral component of plasma membrane(GO:0005887)	————	regulation of cAMP—mediated signaling(GO:0043949). regulation of adenylate cyclase activity(GO:0045761). adenylate cyclase—activating G protein—coupled receptor signaling pathway(GO:0007189). activation of adenylate cyclase activity(GO:0007190)
Faim	-1.329	0.022	No	————	————	————	————
Ahnak	-1.322	0.044	Yes	————	————	————	————
Camkv	-1.319	0.004	No	————	————	————	————

HFD+PB vs HFD – DOWNREGULATED GENES							
Gene Symbol	**log2FC**	***P* value**	**Hit?**	**Molecular Function**	**Biological Function**	**Cellular Component**	**Protein Class**
Kif16b	-1.313	0.027	Yes	microtubule binding motor protein(PC00156)	microtubule associated complex(GO:0005875). microtubule(GO:0005874)	————	microtubule—based movement(GO:0007018)
Med24	-1.305	0.022	Yes	general transcription factor(PC00259)	core mediator complex(GO:0070847). mediator complex(GO:0016592)	————	————
Susd1	-1.305	0.029	Yes	voltage—gated ion channel(PC00241)	integral component of plasma membrane(GO:0005887). plasma membrane protein complex(GO:0098797). cation channel complex(GO:0034703)	————	response to calcium ion(GO:0051592). detection of chemical stimulus(GO:0009593)

HFD+PB vs HFD – DOWNREGULATED GENES							
Gene Symbol	**log2FC**	***P* value**	**Hit?**	**Molecular Function**	**Biological Function**	**Cellular Component**	**Protein Class**
Mt2A	-1.296	0.021	Yes	scaffold/adaptor protein(PC00226)	cyclin—dependent protein kinase holoenzyme complex(GO:0000307). SCF ubiquitin ligase complex(GO:0019005)	————	mitotic nuclear division(GO:0140014). positive regulation of cell cycle(GO:0045787). protein phosphorylation(GO:0006468). positive regulation of protein serine/threonine kinase activity(GO:0071902). regulation of mitotic cell cycle(GO:0007346). regulation of cyclin—dependent protein serine/threonine kinase activity(GO:0000079)

HFD+PB vs HFD – DOWNREGULATED GENES							
Gene Symbol	**log2FC**	***P* value**	**Hit?**	**Molecular Function**	**Biological Function**	**Cellular Component**	**Protein Class**
Rufy3	-1.290	0.006	Yes	————	cytoplasm(GO:0005737)	————	————
Cxcl14	-1.290	0.005	Yes	growth factor(PC00112)	————	————	————
Syt11	-1.280	0.003	Yes	cytokine(PC00083)	leaflet of membrane bilayer(GO:0097478). external side of plasma membrane(GO:0009897). receptor complex(GO:0043235)	————	————
Syn2	-1.276	0.005	No	————	————	————	————
Ncald	-1.270	0.031	Yes	————	————	————	————
Slc44a1	-1.270	0.046	No	————	————	————	————
Snapc5	-1.268	0.009	Yes	————	————	————	————
Zbtb22	-1.259	0.012	Yes	non—motor actin binding protein(PC00165)	————	————	————
Golga7	-1.258	0.016	Yes	protease inhibitor(PC00191)	————	————	————

HFD+PB vs HFD – DOWNREGULATED GENES							
Gene Symbol	**log2FC**	***P* value**	**Hit?**	**Molecular Function**	**Biological Function**	**Cellular Component**	**Protein Class**
Zc3h14	-1.250	0.048	No	————	————	————	————
Stmn1	-1.234	0.000	Yes	————	————	————	————
Fez1	-1.229	0.002	Yes	————	cytoplasm(GO:0005737). plasma membrane region(GO:0098590). axon(GO:0030424)	————	————
Cd24	-1.218	0.037	Yes	————	————	————	————
Stmn4	-1.218	0.041	Yes	————	————	————	————
Armcx3	-1.218	0.014	Yes	————	nucleus(GO:0005634). cytosol(GO:0005829)	————	DNA repair(GO:0006281). chromatin organization(GO:0006325)
Ckmt1	-1.218	0.003	No	————	————	————	————
Inpp1	-1.218	0.048	Yes	RNA binding protein(PC00031)	perinuclear region of cytoplasm(GO:0048471)	————	cellular calcium ion homeostasis(GO:0006874)
Myadm	-1.218	0.014	No	————	————	————	————

HFD+PB vs HFD – DOWNREGULATED GENES							
Gene Symbol	**log2FC**	***P* value**	**Hit?**	**Molecular Function**	**Biological Function**	**Cellular Component**	**Protein Class**
Ivns1abp	-1.218	0.022	Yes	scaffold/adaptor protein(PC00226)	————	————	————
Crym	-1.218	0.044	No	————	————	————	————
Cyp46a1	-1.218	0.019	Yes	oxygenase(PC00177)	————	————	organic cyclic compound catabolic process(GO:1901361). small molecule catabolic process(GO:0044282). lipid catabolic process(GO:0016042). cholesterol metabolic process(GO:0008203)

HFD+PB vs HFD – DOWNREGULATED GENES							
Gene Symbol	**log2FC**	***P* value**	**Hit?**	**Molecular Function**	**Biological Function**	**Cellular Component**	**Protein Class**
Caly	-1.211	0.000	Yes	————	transferase complex(GO:1990234)	————	peptidyl—amino acid modification(GO:0018193). protein lipidation(GO:0006497). protein acylation(GO:0043543). protein targeting to membrane(GO:0006612)
Apoe	-1.211	0.010	Yes	apolipoprotein(PC00052)	————	————	————
Tmcc2	-1.197	0.031	Yes	————	endomembrane system(GO:0012505). vacuole(GO:0005773). plasma membrane(GO:0005886)	————	————
Ccnh	-1.196	0.025	Yes	————	————	————	————
Tmem212	-1.195	0.006	Yes	serine protease(PC00203)	————	————	————

HFD+PB vs HFD – DOWNREGULATED GENES							
Gene Symbol	**log2FC**	***P* value**	**Hit?**	**Molecular Function**	**Biological Function**	**Cellular Component**	**Protein Class**
Syn1	-1.194	0.004	Yes	membrane trafficking regulatory protein(PC00151)	synaptic vesicle membrane(GO:0030672). vacuole(GO:0005773). plasma membrane(GO:0005886)	————	neurotransmitter secretion(GO:0007269)
Nfx1	-1.192	0.038	Yes	zinc finger transcription factor(PC00244)	nucleus(GO:0005634)	————	transcription, DNA—templated(GO:0006351). regulation of transcription, DNA—templated(GO:0006355)

HFD+PB vs HFD – DOWNREGULATED GENES							
Gene Symbol	**log2FC**	***P* value**	**Hit?**	**Molecular Function**	**Biological Function**	**Cellular Component**	**Protein Class**
Dnaaf1	-1.191	0.040	Yes	transaminase(PC00216)	mitochondrion(GO:0005739)	————	alpha—amino acid metabolic process(GO:1901605). oxidation—reduction process(GO:0055114). branched—chain amino acid biosynthetic process(GO:0009082)
Ndn	-1.181	0.000	Yes	scaffold/adaptor protein(PC00226)	————	————	————
Ptk2b	-1.169	0.045	Yes	calmodulin—related(PC00061)	————	————	————
Fam19a5	-1.169	0.032	Yes	RNA splicing factor(PC00148)	nucleus(GO:0005634)	————	————
Mau2	-1.165	0.035	Yes	transporter(PC00227)	————	————	————
Tmem126a	-1.164	0.014	Yes	————	preribosome, small subunit precursor(GO:0030688)	————	maturation of SSU—rRNA(GO:0030490)

HFD+PB vs HFD – DOWNREGULATED GENES							
Gene Symbol	**log2FC**	***P* value**	**Hit?**	**Molecular Function**	**Biological Function**	**Cellular Component**	**Protein Class**
Marcks	-1.162	0.040	Yes	————	————	————	————
Mllt11	-1.153	0.026	Yes	————	————	————	————

Ddx5	-1.140	0.000	Yes	————	cytoplasm(GO:0005737)	————	regulation of axonogenesis(GO:0050770). stress—activated protein kinase signaling cascade(GO:0031098). axonogenesis(GO:0007409). mitotic nuclear division(GO:0140014). activation of protein kinase activity(GO:0032147). signal transduction by protein phosphorylation(GO:0023014). regulation of mitotic cell cycle(GO:0007346)

HFD+PB vs HFD – DOWNREGULATED GENES							
Gene Symbol	**log2FC**	***P* value**	**Hit?**	**Molecular Function**	**Biological Function**	**Cellular Component**	**Protein Class**
Nob1	-1.138	0.010	Yes	————	integral component of membrane(GO:0016021). plasma membrane region(GO:0098590). synaptic vesicle membrane(GO:0030672). neuron projection(GO:0043005). vacuole(GO:0005773)	————	————
Ipo7	-1.137	0.034	Yes	transporter(PC00227)	nuclear envelope(GO:0005635). cytosol(GO:0005829). vacuole(GO:0005773). plasma membrane(GO:0005886)	————	protein import into nucleus(GO:0006606)
LOC691995	-1.135	0.025	No	————	————	————	————

HFD+PB vs HFD – DOWNREGULATED GENES							
Gene Symbol	**log2FC**	***P* value**	**Hit?**	**Molecular Function**	**Biological Function**	**Cellular Component**	**Protein Class**
Ate1	-1.132	0.043	Yes	————	integral component of plasma membrane(GO:0005887)	————	————
Adgrg1	-1.128	0.016	No	————	————	————	————
Nup98	-1.121	0.045	Yes	membrane traffic protein(PC00150)	————	————	————
Mrps30	-1.120	0.016	Yes	————	————	————	————
Rfxank	-1.119	0.032	Yes	scaffold/adaptor protein(PC00226)	————	————	JNK cascade(GO:0007254). regulation of JNK cascade(GO:0046328)

HFD+PB vs HFD – DOWNREGULATED GENES							
Gene Symbol	**log2FC**	***P* value**	**Hit?**	**Molecular Function**	**Biological Function**	**Cellular Component**	**Protein Class**
Mt-nd5	-1.118	0.000	Yes	————	nucleus(GO:0005634). cytoplasm(GO:0005737)	————	cellular zinc ion homeostasis(GO:0006882). response to cadmium ion(GO:0046686). response to toxic substance(GO:0009636). cellular response to chemical stimulus(GO:0070887). response to stress(GO:0006950)
Ttyh1	-1.109	0.010	Yes	————	chloroplast thylakoid membrane(GO:0009535)	————	————
Tagln2	-1.102	0.016	Yes	non—motor actin binding protein(PC00165)	————	————	————
Fkbp3	-1.093	0.000	Yes	————	————	————	————

HFD+PB vs HFD – DOWNREGULATED GENES							
Gene Symbol	**log2FC**	***P* value**	**Hit?**	**Molecular Function**	**Biological Function**	**Cellular Component**	**Protein Class**
38596.000	-1.086	0.004	No	————	————	————	————
Sec23b	-1.084	0.020	Yes	vesicle coat protein(PC00235)	membrane coat(GO:0030117). ER to Golgi transport vesicle membrane(GO:0012507). endoplasmic reticulum part(GO:0044432). vacuole(GO:0005773). plasma membrane(GO:0005886)	————	COPII—coated vesicle budding(GO:0090114)
Ptma	-1.082	0.000	Yes	protease inhibitor(PC00191)	extracellular space(GO:0005615)	————	proteolysis(GO:0006508). cellular protein metabolic process(GO:0044267). negative regulation of endopeptidase activity(GO:0010951)

HFD+PB vs HFD – DOWNREGULATED GENES							
Gene Symbol	**log2FC**	***P* value**	**Hit?**	**Molecular Function**	**Biological Function**	**Cellular Component**	**Protein Class**
Cacnb3	-1.080	0.025	Yes	————	cytoplasm(GO:0005737). plasma membrane region(GO:0098590). neuron projection(GO:0043005)	————	neuron projection development(GO:0031175). regulation of microtubule polymerization or depolymerization(GO:0031110). microtubule depolymerization(GO:0007019)

HFD+PB vs HFD – DOWNREGULATED GENES							
Gene Symbol	**log2FC**	***P* value**	**Hit?**	**Molecular Function**	**Biological Function**	**Cellular Component**	**Protein Class**
Gprasp2	-1.073	0.032	Yes	————	endosome(GO:0005768). synaptic vesicle(GO:0008021). vacuole(GO:0005773). plasma membrane(GO:0005886)	————	vesicle fusion to plasma membrane(GO:0099500). organelle localization(GO:0051640). regulation of exocytosis(GO:0017157). protein secretion(GO:0009306). protein localization to plasma membrane(GO:0072659)
Rab21	-1.071	0.011	Yes	————	early endosome(GO:0005769). vacuole(GO:0005773). plasma membrane(GO:0005886)	————	Ras protein signal transduction(GO:0007265). intracellular protein transport(GO:0006886)

HFD+PB vs HFD – DOWNREGULATED GENES							
Gene Symbol	**log2FC**	***P* value**	**Hit?**	**Molecular Function**	**Biological Function**	**Cellular Component**	**Protein Class**
Mt-cyb	-1.069	0.000	Yes	oxidoreductase(PC00176)	NADH dehydrogenase complex(GO:0030964)	————	————
Rgs9	-1.063	0.018	Yes	————	————	————	————

Osbp	-1.061	0.042	Yes	————	cytoskeleton(GO:0005856). cytoplasm(GO:0005737). plasma membrane(GO:0005886)	————	regulation of cell shape(GO:0008360). regulation of plasma membrane bounded cell projection organization(GO:0120035). regulation of cell projection assembly(GO:0060491). cell morphogenesis(GO:0000902). actin filament polymerization(GO:0030041). positive regulation of actin filament polymerization(GO:0030838).

HFD+PB vs HFD – DOWNREGULATED GENES							
Gene Symbol	**log2FC**	***P* value**	**Hit?**	**Molecular Function**	**Biological Function**	**Cellular Component**	**Protein Class**
							Rho protein signal transduction(GO:0007266). plasma membrane bounded cell projection assembly(GO:0120031). positive regulation of cell projection organization(GO:0031346)
Dnaja3	-1.057	0.037	Yes	————	————	————	————
Sv2a	-1.057	0.031	Yes	————	————	————	————
Nsmf	-1.055	0.013	No	————	————	————	————
Serpinb9	-1.046	0.024	Yes	non—receptor serine/threonine protein kinase(PC00167)	————	————	————
Trim2	-1.045	0.014	No	————	————	————	————
Eno2	-1.039	0.012	No	————	————	————	————

HFD+PB vs HFD – DOWNREGULATED GENES							
Gene Symbol	**log2FC**	***P* value**	**Hit?**	**Molecular Function**	**Biological Function**	**Cellular Component**	**Protein Class**
LOC100911625	-1.038	0.004	No	————	————	————	————
Ift74	-1.038	0.028	Yes	————	centrosome(GO:0005813). centriole(GO:0005814). cilium(GO:0005929). plasma membrane region(GO:0098590). intraciliary transport particle B(GO:0030992)	————	intraciliary transport involved in cilium assembly(GO:0035735). vesicle targeting, trans—Golgi to periciliary membrane compartment(GO:0097712). axoneme assembly(GO:0035082). ciliary transition zone assembly(GO:1905349). protein localization to cilium(GO:0061512)

HFD+PB vs HFD – DOWNREGULATED GENES							
Gene Symbol	**log2FC**	***P* value**	**Hit?**	**Molecular Function**	**Biological Function**	**Cellular Component**	**Protein Class**
Tmem135	-1.037	0.029	Yes	heterotrimeric G—protein(PC00117)	catalytic complex(GO:1902494). leaflet of membrane bilayer(GO:0097478). plasma membrane protein complex(GO:0098797). extrinsic component of cytoplasmic side of plasma membrane(GO:0031234). cytoplasmic part(GO:0044444)	————	G protein—coupled receptor signaling pathway(GO:0007186)
Coq8a	-1.035	0.047	Yes	————	————	————	————
Tnrc6b	-1.025	0.005	Yes	————	————	————	————
LOC108348175	-1.022	0.040	Yes	non—motor actin binding protein(PC00165)	————	————	————
Mcrs1	-1.016	0.011	Yes	RNA helicase(PC00032)	————	————	————

Anapc4	-1.013	0.044	Yes	————	anaphase—promoting complex(GO:0005680). nuclear periphery(GO:0034399)	————	proteasome—mediated ubiquitin—dependent protein catabolic process(GO:0043161). protein K11—linked ubiquitination(GO:0070979). regulation of mitotic cell cycle phase transition(GO:1901990). positive regulation of organelle organization(GO:0010638). metaphase/anaphase transition of mitotic cell cycle(GO:0007091). mitotic sister chromatid separation(GO:0051306).

HFD+PB vs HFD – DOWNREGULATED GENES							
Gene Symbol	**log2FC**	***P* value**	**Hit?**	**Molecular Function**	**Biological Function**	**Cellular Component**	**Protein Class**
							positive regulation of mitotic cell cycle(GO:0045931)
Gpr162	-1.009	0.039	Yes	————	————	————	————
Map3k10	-1.005	0.019	Yes	gap junction(PC00105)	————	————	————
Map1b	-1.000	0.039	Yes	serine protease(PC00203)	extracellular space(GO:0005615)	————	————